Investigation of vibrational spectrum and intramolecular hydrogen bonding in Danthron

Z.Ghasemi, M.Zahedi-Tabrizi*
Department of Chemistry, Faculty of Sciences, Alzahra University,Tehran, Iran
Email: Zahedi@alzahra.ac.ir

Keywords: 1,8-dihydroxy-9,10-anthraquinone, danthron , naphthazarin, Intramolecular hydrogen bonding , vibrational assignment, DFT.

Introduction:

Danthron (1,8-dihydroxyanthraquinone) is one of the Anthraquinone Dihydroxy derivatives(DHAQs).Dihydroxyquinones are compounds of significant chemical and biochemical interest. These molecules have important applications as a prominent family of pharmaceutically active and biologically relevant chromophores, as an analytical tool for the determination of metals, and in many aspects of electrochemistry.

Danthron is the simplest molecule showing the chromophore framework peculiar to several compounds of biological and pharmaceutical interest.

Danthron is present in some antitumor drugs as Emodin & Hypericin and the latter in doxorubicin, daunorubicin, and adriamycin [1-5].

It has been produced and widely used since the beginning of the century as a laxative.

Since Danthron exhibit two intramolecular hydrogen bond due to the resonance assisted effect it can be investigated by vibrational spectroscopy.

Materials and methods:

All reported properties were performed by using Gaussian 03 in the DFT method and using B3LYP functional and with 6-31G** and 6-311++G** basis sets. The assignment of the experimental frequencies is based on the observed band frequencies and intensity changes in the infrared and Raman spectra of the deuterated species confirmed by establishing one to one correlation between observed and theoretically calculated frequencies.

Result and discussion:

Intramolecular hydrogen bond strength (difference between cis-enol and trans-enol forms) and the geometry optimization (O…H , O…O hydrogen bond lengths and O..H–O angle bond) were calculated.

^{1}H-NMR spectra of danthron were indetified and the chemical shift of the proton for danthron computed in the gas and solution phase by using the GIAO method . The chemical shift measured from TMS is 12.43 ppm and 12.44 ppm in the gas phase and in the $CDCl_3$ solution respectively.

The calculation of vibrational frequencies and assignment of vibrational modes of danthron and it's deuterated sample were performed.

By investigation of vibrational frequencies of IR and Raman spectra and its deuterated analog we have calculated $\frac{\nu OH}{\nu OD}$ and $\frac{\lambda OH}{\lambda OD}$ that are involved in intramolecular hydrogen bond.

Conclusion:

The full optimized geometries of Danthron and naphthazarin are fully optimized at B3LYP level of theory using 6-31g** and 6-311++g** basis sets. The results of DFT calculations indicate that the intramolecular hydrogen bond strength in danthron is less than naphthazarin. According to this calculations this decrease in the hydrogen bond strength is caused by resonance effect.

Reference:

[1] R.H. Thomson, Naturally Occurring Quinones, Academic Press, New York, 1971.
[2] F. Arcamone, Doxorubicin: Anticancer Antibiotics, Academic Press, New York, 1981.
[3] W.A. Remers, The Chemistry of Antitumor Antibiotics, Wiley, New York, 1981.
[4] Y. Nonaka, M. Tsuboi, K. Nakamoto, J. Raman Spectrosc. 21 (1990) 133.
[5] D. Jancura, S. Sanchez-Cortes, E. Kocisova, A. Tinti, P. Miskovsky, A. Bertoluzza, Biospectroscopy 1 (1995) 265.

Modeling of vibrational spectra for primary alcohols: DFTcalculations

V. Hadigheh Rezvan*, A.Parchehbaf Jadid, Arezoo Fahimi boudalalou
Department of chemistry, Ardebil Branch, Islamic Azad university
Ardebil, Iran
Email: ramin5171@gmail.com

Keywords : vibrational spectra, DFT, primary alcohols, modeling

Introduction:

According to importance of molecular modeling, we have tried to modeling vibrational spectra of primary alcohols.

For doing this work, first geometries of the molecules were optimized with LSDA ,HF , B3LYP methods in combination of 6-311G (d,p) basis set.

In order to obtain relationship between theoretical & experimental stretching frequency of O-H bond in primary alcohols , we have calculated vibrational spectra of these compounds .

Methods:

The obtained data and comparation of them with experimental values showed that results of LSDA method are the best, So we obtained equations for relation between experimental and LSDA results by Excel software.

We carried out geometery optimization and frequency calculations by Gaussian 03 program .

A6, A7,……,A11

فرکانس محاسباتی

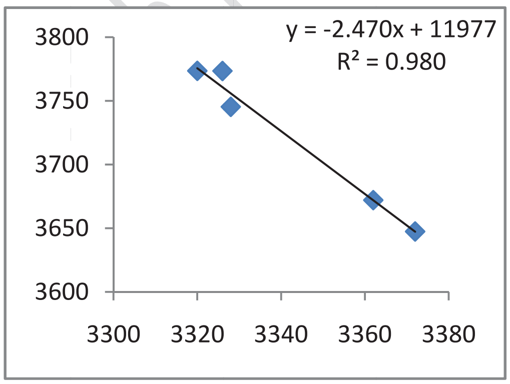

A1,A2,…..,A5

فرکانس محاسباتی

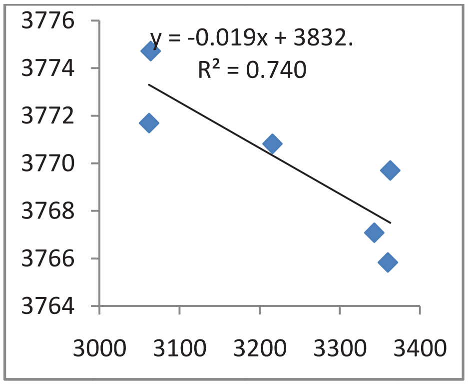

فرکانس تجربی


$R-\underset{R'}{\underset{|}{CH}}-CH_2OH$

فرکانس تجربی

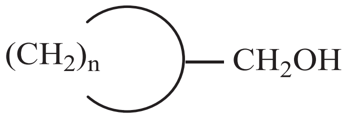

Name	molecules
A1	2,2-dichloro ethanol
A2	2,3-dichloro-1- propanol
A3	2-(isopropylamino) ethanol
A4	2-(trimethylsilyl) ethanol
A5	(+)-4-methyl-1-hexanol
A6	1-amino-1-cyclopentanem ethanol
A7	1-aziridineethanol
A8	1-methyl-3-piperidine methanol
A9	1-piperidin- ethanol
A10	2-(2-thienyl ethanol
A11	2,3-epoxy-1-propanol

Reference:

[1]FT-Raman and FT-IR spectra, ab initio and density functional studies of 2-amino-4,5-difluorobenzoic acidN. Sundaraganesan S. Ilakiamani[a] and B. Dominic Joshua.

[2] Modeling of Food Preservatives Chromatographic LipophlicityApplying Genetic Algorithm and Multiple Linear Regression Dorina Casoni and Costel Sarbu*.

A theoretical investigation on the stability of several endohedral mixed-metal nitride cluster fullerenes using DFT

M. Rahman[a], A.Shayesteh [a*]
[a] School of chemistry, College of Science, University of Tehran, Tehran, Iran
Email: shayesteh@khayam.ut.ac.ir

Key words: endohedral fullerenes, mixed-metal nitride cluster, density functional theory.

Introduction:

One of the most significant and unique characteristics of fullerenes is ability to host atoms and even small molecules in their interior.[1] Through various mechanisms such as charge transfer, endohedral metallofullerenes (EMFs) are well-known stabilizers for some chemical entities that cannot exist outside the carbon cage.[2] EMFs can be classified into four principal branches: classical EMFs, metallic carbide EMFs, metallic nitride EMFs (MNCFs) and metallic oxide EMFs.[3] Metal-nitride cluster fullerenes ($M_3N@C_{2n}$, M=metal and $68 \leq 2n \leq 96$) are the particular class of EMFs with the tri-metallic nitride cluster in carbon cage interior. NCFs have received considerable attention in the past decade because of their higher kinetic stability and improved yields in comparison with the conventional EMFs.[4] On the other hand, the carbon cage surrounds an encaged tri-metal nitride cluster which is not stable as a single molecule.[5] Most MNCFs known so far are limited to the Group III (Sc, Y, and lanthanide) of metals, but recently some new mixed-metal nitride clusterfullerenes (MMNCFs) such as $M_xSc_{3-x}N@C_{80}$ (M =Ti, Y, Ce, Nd, Gd, Tb, Dy, Er, Lu) have been synthesized.[6]

Methods:

The structure and shape of the nitride cluster, as the inner part of the metal nitride cluster fullerene, has a considerable impact on the structure of the MNCFs. In this summery, we report the results of our theoretical investigations about some MNCFs by means of DFT computations to reveal the stability of various structures of the MMNCFs such as

$TiSc_2N@C_{80}$, $VSc_2N@C_{80}$ and $CrSc_2N@C_{80}$. Geometry optimization has been done using PBE functional and def2-SVP and def2-TZVP basis sets employing ORCA quantum chemistry program package.[7-9] Visualization of the molecular orbitals and electron density iso-surfaces has been done with ChemCraft program.[10]

Result and discussion:

Many studies in the past decade have shown the rotation of M_3N cluster in the carbon cages which results in various conformers on different [6,6] and [5,6] bond types in carbon cage with close relative energies. DFT-optimized molecular structures of $TiSc_2N@C_{80}$, $VSc_2N@C_{80}$ and $CrSc_2N@C_{80}$ conformers have shown that the most stable structures, as written in Table1. are conformer **3**, **2** and **1** for $TiSc_2N@C_{80}$, $VSc_2N@C_{80}$ and $CrSc_2N@C_{80}$, respectively.

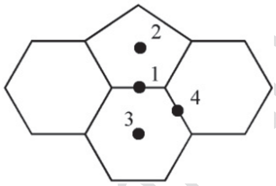

Note that **1, 2, 3** and **4** denote the various conformers obtained from the type D, corannulene, of different carbon types.[11]

Table 1. Total energies (E_h) of $TiSc_2N@C_{80}$, $VSc_2N@C_{80}$ and $CrSc_2N@C_{80}$ conformers in neutral states computed at the PBE/def2-SVP and PBE/def2-TZVP levels of theory.

		1	**2**	**3**	**4**
		def2-SVP	def2-SVP	def2-SVP	def2-SVP
	S	def2-TZVP	def2-TZVP	def2-TZVP	def2-TZVP
$TiSc_2N@C_{80}$	2	-5467.7173353	-5467.7249241	-5467.7252918	-5467.7201988
		-5471.1360187	-5471.1434945	-5471.1438078	-5471.1384494
$VSc_2N@C_{80}$	3	-5562.2368601	-5562.2393299	-5562.2233519	-5562.2332947
		-5565.6562304	-5565.6585050	-5565.6560729	-5565.6526611
$CrSc_2N@C_{80}$	4	-5662.6756108	-5662.6752996	-5662.6641499	-5562.6643804
		-5666.1182271	-5666.1178864	-5666.1073431	-5666.1076268

Conclusion:

In this work, we have performed a study of stability of different conformers of the $TiSc_2N@C_{80}$, $VSc_2N@C_{80}$ and $CrSc_2N@C_{80}$. The results of our calculations clearly show that the conformer **3**, **2** and **1** are the most energetically stable structure among the other $TiSc_2N@C_{80}$, $VSc_2N@C_{80}$ and $CrSc_2N@C_{80}$ conformers.

Reference:

[1] J. R. Heath, S. C. O. Brien, Q. Zhang, Y. Liu, R. F. Curl, H.W. Kroto, F. K. Tittel, R. E. Smalley, Lanhanum Complexes of Spheroidal Carbon Shells, J. Am. Chem. Soc. 107, 7779-7780, 1985.

[2] A. A. Popov, L. Dunsch, Electrochemistry In Cavea: Endohedral Redox Reactions of Encaged Species in Fullerenes, J. Phys. Chem. Lett. 2, 786-794, 2011.

[3] M.N. Chaur, F. Melin, A.L. Ortiz, L. Echegoyen, Chemical, Electrochemical, and Structural Properties of Endohedral Metallofullerenes, Angew. Chem. Int. Ed. 48,7514-7538, 2009.

[4] A. A. Popov, C. Chen, S. Yang, F. Lipps, L. Dunsch, Spin-Flow Vibrational Spectroscopy of Molecules with Flexible Spin Density: Electrochemistry, ESR, Cluster and Spin Dynamics, and Bonding in TiSc2N@C80, J. Acsnano. 4, 4857-4871, 2010.

[5] P.W. Fowler, D. E. Manolopoulos, An Atlas of Fullerenes, Clarendon Press, Oxford, 1995.

[6] L. Dunsch, S. Yang, Endohedral clusterfullerenes: playing with cluster and cage sizes, Phys. Chem. Chem. Phys. 9, 3067-3081, 2007.

[7] J. P. Perdew, K. Burke, M. Ernzerhof, Generalized Gradient Approximation Made Simple, Phys. Rev. Lett. 77, 3865-3868, 1996.

[8] F. Weigend, R. Ahlrichs, Balanced basis sets of split valence, triple zeta valence and quadruple zeta valence quality for H to Rn: Design and assessment of accuracy, Phys. Chem. Chem. Phys. 7, 3297-3305, 2005.

[9] F. Neese, ORCA, an ab initio, density functional and semiempirical program package, Version 2.6-35, Institute for Physical and Theoretical Chemistry: Bonn, 2007.

[10] G. A. Zhurko, ChemCraft, Version 1.5; http://www.chemcraftprog.com.

[11] S. Osuna, M. Swart, M. Sola, The reactivity of endohedral fullerenes. What can be learnt from computational studies?, Phys. Chem. Chem. Phys. 13, 3585-3603, 2011.

Mixed Micellization of Gemini Surfactants and Conventional Surfactants: A Monte Carlo Simulation

Zahra Khodadadi*[,a], Hussein Gharibi[a], S. Morteza Mousavi-Khoshdel[b] and S. Majid Hashemianzadeh[b]

[a] Department of Physical Chemistry, Tarbiat Modarres University, Tehran, Iran
[b] Molecular Simulation Research Laboratory, Department of Chemistry, Iran University of Science and Technology, Tehran, Iran
Email:za_khd@yahoo.com

Key words: Monte Carlo, Gemini Surfactant, Synergism

Introduction:

In recent years, novel surfactants such as Gemini have attracted much attention because of their unique properties similar low CMC values and their stronger efficacy in decreasing the surface tension of water. Gemini is special kind of surfactants made up of two identical amphiphilic moieties connected by a spacer [1]. Because of their high cost, Gemini surfactants are likely to be used in combination with conventional surfactants. Gemini surfactants when mixed with single chain surfactants showed synergistic mixing behavior [2-3].

The objectives of this study were the investigation a lattice model of mixed micellization of Gemini and conventional surfactants.

Simulation Method:

This model consists of linear surfactant molecules on a three-dimensional $100 \times 100 \times 100$ cubic lattice. Each of the molecules of water can occupy a single lattice site. A surfactant occupies several lattice sites. A single-chain surfactant can be described by the symbol H_iT_j where T denotes tail and H denotes the head of the surfactants. i, j are integers symbolizing the lengths of the head and tail, respectively, in units of lattice sites. The microscopic lattice model of a Gemini surfactant can be represented by the symbol $T_jH_iS_nH_iT_j$ where n does the number of lattice sites constituting the spacer represented by the symbol *S*. The total energy of the system divided by $k_B T$ is:

$$E_{Total} = \sum_{mn} N_{mn} E_{mn}$$

where Nmn is the total number of mn pairs in the system, E_{mn} interaction energy, k_B is the Boltzmann constant, and T is the temperature. The only type of move used to modify the configuration was the reptation move. The trial configuration was accepted or rejected according to Metropolis algorithm.

Results and discussion:

Figure1 shows the composition dependence of CMC of ionic Gemini surfactant/non-ionic conventional mixtures ($T_5H_1S_4H_1T_5/H_4T_4$). The mixture has been shown synergism, i.e., where the CMC's of some mixed (CMC_M) lower than the CMC's of the pure surfactants.

The excess Gibbs free energy (G^E) versus the volume fraction of $T_5H_1S_4H_1T_5$ in the mixed micelles is shown in Figure2. It is obvious from the plots that the excess Gibbs free energy is not symmetric with respect to the mole fraction, while in regular solution theory, excess Gibbs free energy is symmetric and reaches a minimum when the mole fraction of surfactant is 0.5.

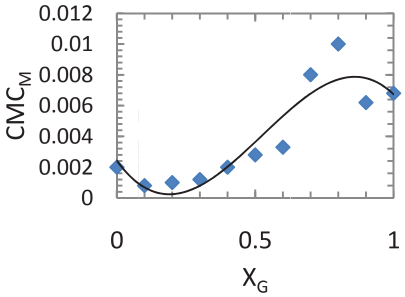

FIG. 1. Variation of the CMC_M of the $T_5H_1S_4H_1T_5/H_4T_4$ mixture with the Gemini surfactant volume fraction (*X_G*). The solid line is guides to the eyes.

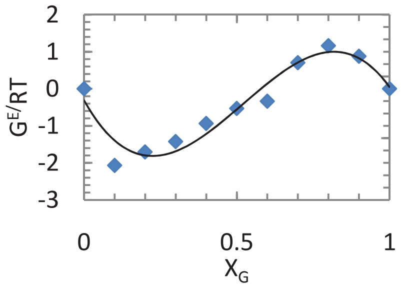

FIG. 2. Excess Gibbs free energy as a function of volume fraction of Gemini surfactant in mixed micelles (*X_G*) $T_5H_1S_4H_1T_5/H_4T_4$ mixture. The solid line is guides to the eyes.

Conclusion:

We have studied a binary mixture of ionic Gemini surfactants and nonionic surfactant by measuring the CMC of the mixtures and excess Gibbs free energy of the mixed micelles as a function of the mixture composition. Synergism in micelle formation (presence of a minimum in the CMC vs composition plot) has been observed for mixture.

References:

[1] Y. Shang, Y. Xu, H. Liu, Y. Hu. ,Journal of Dispersion Science and Technology 27 (2006) 105-108.

[2] M.J. Rosen, T. Gao, Y. Nakatsuji. ,Colloids and Surfaces A: Physicochemical and Engineering Aspects 88 (1994) 1-11.

[3] M.J. Rosen, D.S. Murphy., Journal of Colloid and Interface Science 110 (1986) 224-236.

Theoretical study of five different porphyrins as sensitized dyes on TiO_2 nanostructure solar cells

F. Farshidnian[a*], R. Rahimi[b], M. Rabbani[b], Arash Jabbari[a]
[a]Department of Chemistry, Islamic Azad University, Saveh Branch, Saveh, Iran
[b]Department of Chemistry, Iran University of Science and Technology, Narmak, Tehran, Iran
Email: F.farshidnia@gmail.com

Key words: Solar cells, Porphyrin, optical absorption, Theoretical study.

Introduction:

In recent year's different porphyrins, have been used as photo-sensitizers for polycrystalline TiO_2 in order to enhance the visible light-sensitivity of the TiO_2 matrix and thereby increases its photocatalytic activity. Type of Functional group substituted in porphyrins plays a critical role in the photocatalytic processes of the porphyrin–TiO_2 system. Since lots of sensitizers with carboxyl acid group as anchoring group to the surface of the TiO_2 nanoparticles have been proved efficient to inject excited electron to the conductive band of TiO_2, in which case the carboxyl acid group is a donor and the TiO_2 is an acceptor, those sensitizer candidates which can transport electron from the other part of the sensitizer to the carboxyl acid group are thus rationally considered promising to be able to inject excited electrons to the conduction band of the TiO_2 particles [1-3]. In this study, we have carried out Density Functional Theory (DFT) and Time Dependent DFT (TDDFT) calculations in solution of the geometry, electronic structure and optical absorption spectra of TCPP, TSPP, TBP, TMPP and TBMCPP sensitizers.

Methods:

The GAUSSIAN 09W package was used to perform geometry optimizations and time-dependent calculations (B3LYP/6-311G(d)) for TCPP, TSPP, TBP, TMPP and TBMCPP. The geometries of were first optimized in vacuum using density functional 6-311G(d) method.

Solvation effects were included by means of the Conductor-like polarizable continuum model (C-PCM) in the dichloromethane solvent. Natural bond orbital (NBO) analysis was also conducted on optimized geometries with the NBO program included in the Gaussian program package. The molecular orbital energy levels were compared for screening of the sensitizer candidates for DSSCs. The electronic absorption spectra of the TCPP, TSPP, TBP, TMPP and TBMCPP were calculated using the time-dependent density functional theory (TDDFT) method in the solvent. All the calculations were performed using the Gaussian09 program.

Result and discussion:

The charge transfer orientation is associated with the distribution of the highest occupied molecular orbital (HOMO) and the lowest unoccupied molecular orbital (LUMO) of the sensitizer. The smaller HOMO–LUMO gap indicates the higher photo-to-electric conversion efficiency. This trend can be explained as follows. Let us suppose that the HOMO of the sensitizer is lower enough than the redox potential of the electrolyte and the LUMO is higher enough than the conduction band of the TiO_2 particle, which indicates the open circuit voltage V_{oc} of the solar cell will not be influenced by the HOMO, LUMO variations. With the HOMO–LUMO gap decrease, more photons at the longer-wavelength side would be absorbed to excite the electrons into the unoccupied molecular orbital, which increases the short circuit current density J_{sc} and further the conversion efficiency η of the solar cell. The calculated wavelengthes, oscillator strengthes and transition energies for the most relevant transitions of the electronic absorption bands of TCPP, TSPP, TBP, TMPP and TBMCPP in the solvent were obtained through TDDFT calculations.

Conclusion:

The electronic and spectroscopic properties of TCPP, TSPP, TBP, TMPP and TBMCPP have been investigated by means of DFT/TDDFT calculations. From the orbital analysis and the orbital spatial orientation of HOMO and LUMO for TCPP, TSPP, TBP, TMPP and TBMCPP, the result shows that TSPP seems to provide higher photo-to-electric conversion efficiencies.

Reference:

[1] Kusama H et al.“TiO_2 band shift by nitrogen-Containing heterocycles in dye-sensitized solar cells: a periodic density functional theory study”. Langmuir 2008;24:4411–9.

[2] Gratzel M. “Solar energy conversion by dye-sensitized photovoltaic cells”. Inorg Chem 2005;44:6841–51.

[3] Wang C et al. “Novel mesosubstituted porphyrins: synthesis, characterization and photocatalytic activity of their TiO_2-based composites”. Dyes Pigm 2009;80:321–8.

Theoretical Study of Phe a, phe b and Phe a-Phe b Chlorophyllous molecules for Dye sensitized solar cells (DSSCs)

R. Rahimi[a], F. Farshidnian[b*], M. Rabbani[a]
[a]Department of Chemistry, Iran University of Science and Technology, Narmak, Tehran, Iran
[b]Department of Chemistry, Islamic Azad University, Saveh Branch, Saveh, Iran
Email: F.farshidnia@gmail.com

Key words: Chlorophyllous, Theoretical Study, DFT, Dye sensitized solar cells.

Introduction:

Natural photosynthetic systems have evolved over billions of years, and they can therefore provide hints regarding some possible strategies for improving the performance of organic photovoltaic systems such as dye-sensitized solar cells (DSSCs). Chlorophylls (Chls) play a fundamental role in photosynthesis. They are the molecular species that are responsible for both light energy capture and its conversion into an electrochemical gradient. Dye sensitized solar cells (DSSCs) are currently attracting widespread academic and commercial interest for the conversion of sunlight into electricity because of their low cost and high DSSCs are similar to natural photosynthesis in the initial processes involving in light-harvesting and charge separation [1-3]. To gain a better understanding of the role of the sensitizer, particularly of its electronic structure and excited-state properties in the efficiency of dye-sensitized solar cell devices, we have carried out Density Functional Theory (DFT) and Time Dependent DFT (TDDFT) calculations in solution of the geometry, electronic structure and optical absorption spectra of a Phe a, phe b and cople of Phe a-Phe b Chlorophyllous sensitizers.

Methods:

The GAUSSIAN 09W package was used to perform geometry optimizations and time-dependent calculations (B3LYP/6-311G(d)) for Phe a, phe b and Phe a-Phe b Chlorophyllous.

Percentage compositions of molecular orbitals were calculated using the NBO program. The geometries of Phe a, phe b and Phe a-Phe b were first optimized in vacuum using density functional B3LYP/6-311G(d) method. The electronic absorption spectra of the Phe a, phe b and Phe a-Phe b Chlorophyllous were calculated using the time-dependent density functional theory (TDDFT) method in the solvent. All the calculations were performed using the Gaussian09 program.

Results and discussion:

The HOMO and LUMO for Phe a are located at -5.377 and -2.978 eV, respectively. The energy gap between the HOMO and the LUMO is 2.398 eV for Phe a. The energy gaps of the other molecules are all smaller than that of Phe a. The order of the energy gaps is Phe a-Phe b> Phe b> Phe a. the smaller HOMO–LUMO gap indicates the higher photo-to-electric conversion efficiency. The HOMO of the sensitizer is lower enough than the redox potential of the electrolyte and the LUMO is higher enough than the conduction band of the TiO_2 particle, which indicates the open circuit voltage V_{oc} of the solar cell will not be influenced by the HOMO, LUMO variations. With the HOMO–LUMO gap decrease, more photons at the longer-wavelength side would be absorbed to excite the electrons into the unoccupied molecular orbital, which increases the short circuit current density J_{sc} and further the conversion efficiency η of the solar cell. The calculated wavelengthes, oscillator strengthes and transition energies for the most relevant transitions of the electronic absorption bands of Phe a, phe b and Phe a-Phe b in the solvent were obtained through TDDFT calculations. The Chls show a series of bands between 350 and 650 nm due to π-π^* absorptions of the conjugated macrocycle.

Conclusions:

When the sensitizers absorb light energy, it injects electron into the conduction band of the semiconductor. The results from the orbital analysis and the orbital spatial orientation of HOMO and LUMO for Phe a, phe b and Phe a-Phe b, show that couple of Phe a-Phe b seems to provide higher photo-to-electric conversion efficiencies.

Reference:

[1] Ruili Wang et al. “Density functional theory based calculations of the vibrational properties of chlorophyll-a” Vibrational Spectroscopy 44 (2007) 357–368

[2] Xiao-Feng Wanget al. ‘Significant enhancement in the power-conversion efficiency of chlorophyll co-sensitized solar cells by mimicking the principles of natural photosynthetic light-harvesting complexes”, Biosensors and Bioelectronics 25 (2010) 1970–1976

[3] Wang C et al. “Novel mesosubstituted porphyrins: synthesis, characterization and photocatalytic activity of their TiO2-based composites”, Dyes Pigm 80 (2009) 321–328.

DFT study on the electronic properties of the nanodiamond (C_{24}) with doxorubicin drug

D. Farmanzadeh*, R. Mohsseni Ahangar
Faculty of Chemistry, University ofMazandaran, Babolsar, Islamic Republic of Iran
Email: d.farmanzad@umz.ac.ir

Key words: Nanodiamonds, Doxorubicin, DFT, Electronic properties.

Introduction:

The applications of nanodiamond (ND) in drug delivery, bioactive surface coatings, and biolabeling have become a focus point of interests owing to the remarkable properties of the nanodiamond [1]. NDs are promising next generation nanocarriers with demonstrated therapeutic potential. As uniquely biocompatible, scalable and chemically flexible nanoparticles, NDs are an ideal candidate for translating basic technologies into clinical therapies [2]. NDs are carbon nanoparticles and can deliver a wide range of therapeutics, including small molecules, proteins, and nucleic acids [3]. In this study, we investigate the effect of hydrogen capped and without hydrogen capped of truncated octahedral ND (C_{24}) and its complexes with the doxorubicin (DOX) drug on the electronic properties.

Computational Methods:

The geometry optimization and electronic properties calculations were performed at the Becke's three parameter hybrid method with LYP correlation (B3LYP) level of DFT with 6-31G* basis set for all atoms using Gaussian 03 program package.

Result and discussion:

The geometry of all studied molecules, C_{24}, $C_{24}H_{24}$, DOX, C_{24}- DOX and $C_{24}H_{24}$- DOX are optimized and the obtained optimized structures of the C_{24} and DOX are visualized in Fig. 1.

The calculated values of the highest occupied molecular orbital (HOMO), the lowest unoccupied molecular orbital (LUMO), the HLG (HLG =E_{LUMO} - E_{HOMO}), dipole moment and electronic energy of C_{24}, $C_{24}H_{24}$, DOX, C_{24} - DOX and $C_{24}H_{24}$- DOX are reported in Table 1. It can be seen from Table 1 that, the C_{24}- DOX complex has a minimum value of HLG in comparison with other species whereas its dipole moment (μ) is maximum.

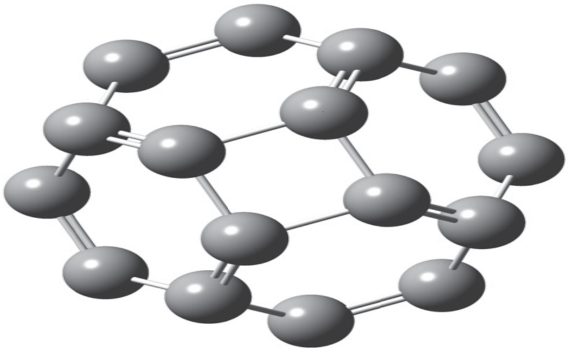

Figure 1: Optimized structure of C_{24}

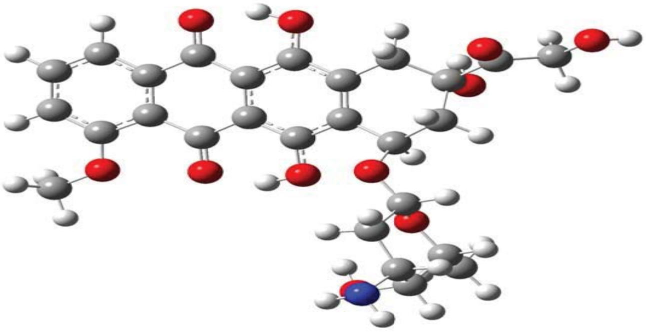

Figure 2: Optimized structure of DOX

Table 1: Calculated HOMO, LUMO energy, HLG, Electronic energy (in eV) and Dipole moment (in Debye).

	HOMO	LUMO	HLG	Electronic energy	Dipole moment
C_{24}	−5.90	−3.36	2.51	-24865.8	0.0
$C_{24}H_{24}$	−6.11	0.70	6.82	-25274.0	0.0
DOX	−5.71	−2.86	2.85	-52477.6	5.58
C_{24}-DOX	−5.51	−3.11	2.40	-80430.1	7.56
$C_{24}H_{24}$-DOX	−5.75	−2.90	2.85	-80803.5	7.47

Conclusion:

In summary, based on calculated HLG and electronic dipole moment values in this study, the C_{24}- DOX complex is reactive in comparison with the C_{24}, $C_{24}H_{24}$, DOX, and $C_{24}H_{24}$- DOX species. Also the obtained results show that capping of C_{24} with hydrogen influence on the HOMO and LUMO energies and electronic properties.

Reference:

[1] W. Siang Yeap, S. Chen, and K.Ping Loh; "Detonation nanodiamond: an organic platform for the suzukicoupling of organic molecules"; American Chemical Society; 25, 185, 2009.

[2] M. Chen,"Nanodiamond platforms for therapeutic applications"; Senior Honors Thesis Program in Biological Sciences Northwestern University; 2010.

[3] E.K. Chow, X-Q Zhang, M. Chen, R. Lam, E. Robinson, H. Huang, D. Schaffer, E. Osawa, A. Goga and D. Ho, "Nanodiamond therapeutic delivery agents mediate enhanced chemoresistant tumor treatment"; Science Translational Medicine; 3, 73, 2011.

Some thermodynamic properties of fluid SF_6 using a new HFD-like potential including three-body interactions: The inversion method and molecular dynamics simulation

Somayeh Naghipour Borj* and Mohsen Abbaspour
Department of Chemistry, Hakim Sabzevari University, Sabzevar, Iran
*E-mail Address: somayeh5naghipour60@gmail.com

Keywords: Potential energy function; Three body interactions; Molecular dynamics simulation; second virial coefficient; Transport properties.

Introduction:

Sulfur hexafluoride (SF_6) is a highly stable, nontoxic, nonpolar, symmetrically shaped chemical compound which is widely used in several industrial applications. For its thermophysical properties, it is also used to improve the thermal insulation of double glazed windows and as an inert solvent for chemical reactions in supercritical fluids [1].

The purpose of the present paper is to determine an accurate sulfur hexafluoride pair-potential energy function via the inversion of the reduced viscosity collision integrals at zero pressure. The second virial coefficient and some transport properties of sulfur hexafluoride have been also calculated using the obtained pair-potential at wide ranges of temperatures.

The MD simulation has been also performed to obtain some thermodynamic, structural, and transport, properties of fluid sulfur hexafluoride at different temperatures and densities using the calculated pair-potential.

To take three-body forces into account, an extended mean-field term of Hauschild and Prausnitz [2] has been used with the two-body potential of SF_6. The MD simulation of sulfur hexafluoride has been also used to determine a new equation of state.

Results and discussion:

The calculated inversion potential of sulfur hexafluoride at zero pressure were in very good agreement with the potential of Goharshadi et al. [3] and the ab initio potential of Dellis and Samios [4].

Our calculated values of second virial coefficient, viscosity, self-diffusion coefficient of SF_6 were also in good agreement with the experimental data .

Our results of pressure for fluid SF_6 in the NVT ensemble have been compared at different temperatures (in the liquid state, vapor, and supercritical region) and different densities with the experimental data. The results indicated that the three-body potential has improved the results and make them closer to the experiment.

The MD simulation has been also used to determine sulfur hexafluoride EOS using the total (two-body plus three-body) potential in good agreement with the NIST EOS [5].

The calculated reduced self-diffusion coefficient and radial distribution function for liquid sulfur hexafluoride using our potentials have been also shown good agreement with the experimental values.

Conclusions :

The new pair-potential energy function of sulfur hexafluoride has been determined via the inversion of reduced viscosity collision integrals at zero pressure and fitted to obtain a HFD-like potential form. The pair-potential reproduces the second virial coefficient, viscosity, and self-diffusion coefficient of sulfur hexafluoride in a good accordance with experimental data over wide ranges of temperatures.

The MD simulation has been also performed to obtain pressure, self-diffusion coefficient, and radial distribution function of fluid sulfur hexafluoride at different temperatures and densities using the calculated HFD-like pair-potential. To take higher-body forces into account, three-body potential of Hauschild and Prausnitz [2] extended as a function of density and temperature and used with the two-body HFD-like potential of SF_6 to improve the prediction of the calculated properties without requiring an expensive three-body calculation.

It is concluded that the three-body potential of Hauschild and Prausnitz [2] has improved the pressure and self-diffusion results and make them closer to the experiment. The MD simulation of sulfur hexafluoride has been also used to determine a new equation of state in good overall agreement with the literature EOS.

References

[1] A. Boushehri, L.A. Viehland, E.A. Mason, Chem. Phys. 28 (1978) 313-318.
[2] T. Hauschild, J.M. Prausnitz, Mol. Simul. 11 (1993) 177-185.
[3] E.K. Goharshadi, M. Nahali, M. Baherololoom, Indian J. Chem. A 44 (2005)
[4] D. Dellis, J. Samios, Fluid Phase Equilib. 291 (2010) 81-89.
[5] NIST Chemistry Webbook. <http://webbook.nist.gov/chemistry/fluid>.

Many-Body effects in some thermodynamic properties of CF4, CF4-Ar, and CF4-CH4 using HFD-like potentials from molecular dynamics simulation

Mohsen Abbaspour, Maryam Sheykh, and Somayeh Naghipour Borj*
Department of Chemistry, Hakim Sabzevari University, Sabzevar, Iran
*E-mail Address: somayeh5naghipour60@gmail.com

Keywords: HFD-like potential; Many-body interaction; Molecular dynamics simulation; Equation of state; Self-diffusion coefficient.

Introduction:

Theoretical calculations and computer simulations, usually applied for the prediction of bulk properties, still prefer small, highly symmetric molecules, like CF4, for their investigations.

The purpose of the present paper is to perform Molecular dynamics (MD) simulation to obtain pressure and self-diffusion coefficient of fluid carbon tetrafluoride using the two-body HFD-like potential of Goharshadi et al. [1]. We have also obtained pressure of CF4-Ar and CF4-CH4 fluid mixtures at a given temperature and different densities using the ab initio potential of Vayner et al. [2] and the inversion potential of Clifford et al. [3], respectively. To take many-body forces into account, three-body potential of Hauschild and Prausnitz [4] has been used with the two-body potentials of these systems. The MD simulation of carbon tetrafluoride has been also used to determine a new equation of state.

Results and discussion:

Our results of reduced pressure for fluid carbon tetrafluoride in the NVT ensemble have been compared at different temperatures (in the liquid state, vapor, and supercritical region) and different densities with the experimental data [5]. The results indicated that the three-body potential has improved the results and make them closer to the experiment. It is also expected and shown that the different potentials represent smaller deviations at lower densities and higher temperatures.

The MD simulation has been used to determine carbon tetrafluoride EOS using the total (two-body plius three-body) potential. The new EOS shows a good agreement with that of NIST [5] at four different reduced temperatures.

The calculated reduced self-diffusion coefficient of carbon tetrafluoride from the time-dependent mean-square displacement using the two and total potentials were also in good agreement with the experimental values of Khoury and Kobayashi [6] obtained by the pulsed nuclear magnetic resonance method. It also shown that the three-body potential of Hauschild and Prausnitz has very small contribution to the self-diffusion but improves the simulated values to give better agreement with the experiment.

We have compared our simulated pressure results of CF_4-Ar and CF_4-CH_4 mixtures at constant temperature in the NVT ensemble and three different molar fractions and different densities using the two-body and total potentials with the experiment. The results indicated that the three-body potential has improved the results and make them closer to the experiment. It is also shown that the improvement in agreement is mostly at high densities.

Conclusions:

The MD simulation has been performed to obtain pressure of CF4 and CF4-Ar and CF4-CH4 mixtures using the two-body HFD-like potentials. To take many-body forces into account, three-body potential of Hauschild and Prausnitz [4] has been used with the two-body potentials. The MD simulation has been also used to determine a new equation of state which may be used as a reference for fluid carbon tetrafluoride.

We have also simulated self-diffusion coefficient of fluid carbon tetrafluoride using two-body and total potentials in good agreement with the experiment. The results indicated that the three-body potential of Hauschild and Prausnitz has very small contribution to the self-diffusion but improves the simulated values to give better agreement with the experiment.

References:

[1] E.K. Goharshadi, M. Abbaspour, A. Morsali, Ind. Eng. Chem. Res. 42 (2003) 2256

[2] G. Vayner, Y. Alexeev, J. Wang, T.L. Windus, W.L. Hase, J. Phys. Chem. A 110 (2006) 3174.

[3] A.A. Clifford, E. Dickinson, G.P. Matthews, E.B. Smith, J. Chem. Soc. Farad. Trans. 1 72 (1976) 2917.

[4] T. Hauschild, J.M. Prausnitz, Mol. Simul. 11 (1993) 177.

[5] NIST Chemistry Webbook. Available at http://webbook.nist.gov/chemistry/fluid.

[6] F. Khoury, R. Kobayashi, J. Chem. Phys. 55 (1971) 2439-2445.

Drastic influence of the intramolecular cation-π interaction on the basicity of selected amines: AIM and NBO analysis

Somayyeh Kheirjou, Ramin Kheirjou and Alireza Fattahi *
Department of Chemistry, Sharif University of Technology, P.O. Box: 11365-9516, Tehran, Iran
*Corresponding author: fattahi@sharif.edu

Abstract:

In this study, drastic influence of the intramolecular cation-π interaction on the basicity of selected amines has been considered. The optimized minimum-energy geometries of different studied amines and their protonated structures were determined by using DFT calculations at the B3LYP/6-311++G(d,p) level of theory. All gas phase computations were performed at level MP2/6-311++G(d,p)//(B3LYP/6-31+G(d). Solvation was included in the calculations using the polarized continuum model (PCM). Structure optimization in solution phase was performed using the structures optimized in gas phase at the HF/6-31G(d,p) level of theory. Geometry optimizations indicate that the most stable structures are stabilized by intramolecular cation-π interaction. The proton affinity (PA) of selected amines is controlled by the strength of intramolecular cation-π interaction of ammuniom with aromatic group. These cation-π interactions strongly influence the basicity of amines. The highest PA value among the studied amines was found to be 229.3 kcal/mol for para methoxy benzene butanamine. This is comparable with proton affinity of HMPA. The solution phase calculations were carried out in aqueous solution. Natural bond orbital (NBO) analysis was performed to calculate the charge transfers and the second-order interaction energies (E (2)) between the donor and acceptor. Quantum theory of atoms in molecules (QTAIM) was also applied to determine the nature of cation-π interaction. QTAIM studies showed that the intramolecular cation-π interaction in these structures is electrostatic (closed-shell) interactions.

Keywords: Basicity, Cation-π interaction, DFT, Natural bonding orbital (NBO), Quantum theory of atoms in molecules (QTAIM)

Influence of boron atom on the acidity of alcohol in both gas phase and solution phase, A DFT study

Somayyeh Kheirjou, Ramin Kheirjou and Alireza Fattahi *
Department of Chemistry, Sharif University of Technology, P.O. Box: 11365-9516, Tehran, Iran
*Corresponding author: fattahi@sharif.edu

Abstract:

In this study, the drastic influence of the boron atom on the acidity of alcohol has been considered. The calculated $\Delta H_{acidity}$ (320.9 - 338.1 kcal/mol) and pK_a range of boron containing alcohol (-0.1 – 9.4) indicate that the boration of alcohol leads to considerable enhancement of its acidity. For instance, we have obtained the $\Delta H_{acidity}$ values 338.1, 335.2 kcal/mol and the pK_a values 4.12, 2.81 for BH_2CH_2OH, BF_2CH_2OH alcohols, respectively, which are much smaller than that of CH_3OH (with $\Delta H_{acidity}$ = 374.9 kcal/mol and pK_a = 15). The increase in acidity of boronated alcohol can be related to the stabilization of alkoxy ion due to overlap of unoccupied orbital of boron atom with the electron pairs of negative oxygen. All gas phase computations were performed at level MP2/6-311++G(d,p)//(B3LYP/6-31+G(d). The primary results indicate that the presence of boron atom in an alcohol might make it as acidic as nitric acid. The geometry optimization of studied structures was performed with DFT computation and optimized structures were used to carry out Natural Bond Orbital (NBO) analysis. NBO analysis revealed that the increase in acidity of boron-containing alcohols is due to the charge transfer from the negative oxygen (in deprotanated structure) to the empty orbital of $-BH_2$ and $-BF_2$. Quantum theory of atoms in molecules (QTAIM) was also applied to determine the nature of bonds formed in the deprotonated structure.

Keywords: Acidity, Boron atom, pK_a, DFT, Natural bonding orbital (NBO), Quantum theory of atoms in molecules (QTAIM)

Quantum mechanical study of antioxidant ability of rutin (vitamin p) against heme

Mina Ghiasi *[a] , Afsaneh Azadnia [a] and Mansour Zahedi [b]

[a] Department of Chemistry, Faculty of Science, Alzahra University, 19835-389, Vanak, Tehran, Iran.
ghiasi@alzahra.ac.ir
Tel: +982188044051-9(2608)
[b] Department of Chemistry, Faculty of Science, Shahid Beheshti University, G. C., Evin, 19839-63113, Tehran, Iran.

Key word: Heme, Vitamin P, QM calculation, Bond Dissociation Enthalpy

Introduction:

Hemoglobin (Hb) is the major heme protein of red blood cells (RBC) which is responsible for the transport of oxygen to tissue, Figure 1A. In vitro, Fe(II)Hb undergoes slow Auto-oxidation to give Fe(III)Hb (methemoglobin, metHb) and superoxide [1]. Flavonoids belong to a group of natural substances with variable phenolic structures. They have been extensively studied for their capacity to inhibit radical reactions in chemical and biological systems. Rutin (vitamin p), Figure 1B, is one of the most important bioflavonoid with antioxidant activity in vivo and in vitro [2]. Here, a systematic study of several interactions and arrangements between rutin, corresponding radical of rutin and methemoglobin ($Fe^{III}Hb$) have been undertaken, Figure 2. Density Functional Theory (DFT) calculations by using B3LYP/6-31G* method were employed to calculate interaction energies, electronic states, and geometrical arrangements for the complex between the methemoglobin and rutin.

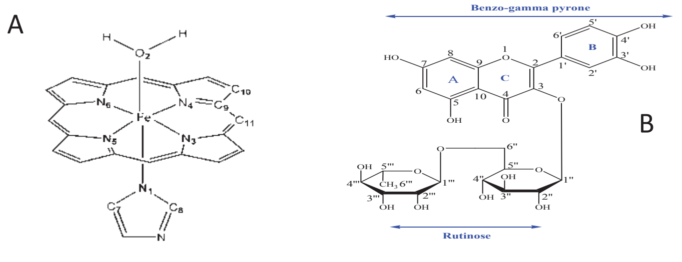

Figure 1. Presentation of the model system of Heme (A), and Rutin (B).

Computational details:

All calculations were performed using the Gaussian 2003 software. The geometries of both rutin and the heme group were fully optimized using the B3LYP/6-31G* method. Restricted formalism were applied to all close-shell systems. For the heme group, rutin's radical and the heme-rutin complex, calculations were performed with the unrestricted formalism (UB3LYP).

Conclusion:

Since the study of flavonoids and heme is complex because of the heterogeneity of the different molecular structures and the scarcity of data on bioavailability, insufficient methods are available to measure oxidative damage in vivo. So there is a need to improve theoretical techniques to allow collection of more data about structural details of products in the oxidation process.

The molecular properties which we used to investigate a possible antioxidant mechanism of rutin was the spin density distribution of the radical formed after omission of a hydrogen atom. Theoretical results confirm the important role of the B-ring and sheds light on the role of the 3'-OH and 4'-OH groups in the antioxidant properties of rutin. Rutin molecule can connected to iron ion in metHb from two positions, O2′′′ and O4′. Calculated results indicate that the released energy when rutin interacts with metHb from O2′′′ position is higher than O4′. Also, if the rutin radical exists in the media, the interaction between metHb and rutin radical (RR) leads to the complex metHb-RR, Figure 2. Calculation of net atomic charges shows the average charge on the iron ion in the metHb decrease to 1.5 in all various complexes. It can be concluded that rutin has a beneficial effect against oxidative damage of hemoglobin and red blood cells.

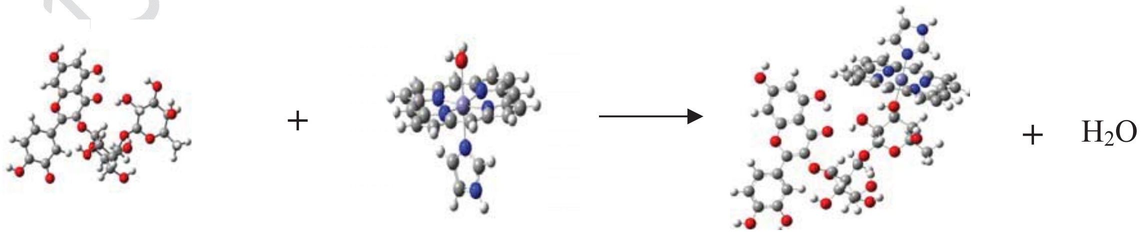

Figure 2. The reaction path between the vitamin P and heme.

References:

[1] P.M.Aron etal. ; " Flavan-3-ols: nature, occurrence and biological activity" ; J. Mol. Nutr. Food Res; 52,79-104,2008.

[2] M.Ghiasi etal . ; "Quantum mechanical study of antioxidative ability and antioxidative mechanism of rutin (vitamin P) in solution " ; Carbohyd. Res ; 346 ,739-744,2011.

Theoretical investigation of the interactions between Li atom and elements from first to fourth rows of periodic table

M. Mehraean[a]
a Department of Chemistry, Zanjan University, Zanjan, Iran.
E-mail: laleh.mehraeen@gmail.com

Keywords: Lithium bond, AIM analysis, B3LYP calculation, organolithium compounds

Introduction:

The organolithium compounds with their special bond properties have critical role in organic synthesis [1]. Also there has been a great deal of interest in study of lithium bond [90-93]. However, according to our knowledge, there is rare information about the nature of lithium bond. In this paper, the bond nature of dimmer complexes containing lithium and elements from first to fourth rows of periodic table are studied using the ab initio and atom in molecule (AIM) methods.

Methods:

First all the structures optimized at B3LYP/6-311++G (3df, 3pd) level of theory using G098W program package. Then, quantum theories of AIM method have been applied to analyze the intermolecular interactions.

Result and discussion:

Except lithium dimmers of noble gases, lithium dimmers of first to fourth row elements of periodic table make cyclic structures. The bond length of Li atom with noble gases are longer than the bond length of Li atom with other elements of first to fourth rows elements of periodic table. In order to obtain information about the nature of Lithium bond, AIM theory was used to analyze the bonding characteristic, which based on a topological analysis of electron density (ρ_c) and Laplacian ($\nabla^2\rho_c$), providing a universally applicable tool for the classification of the bonding interactions. The obtained charge electron density results, ρ, at one of bond critical points (BCPs) for lithium dimmers of second and fourth rows elements of periodic table are shown in figures A and B briefly. According to our investigation and as could be seen in these figures, there are no BCPs between He, Kr, Na and Br elements with Li atom. Also the less charge electron density at (BCPs) relates to Li dimmers of Ne and Ar elements. According to AIM analysis we have three types of interactions at bond critical points: a) ionic interaction: charge density is lower than 0.2eau^{-3} and laplacian of charge density and Hamiltonian are positive b) covalent interaction: charge density is greater than0.2 eau^{-3} and laplacian of charge density and Hamiltonian are negative c) intermediate of ionic and covalent interactions: charge density is lower than 0.2 eau^{-3} and laplacian of charge density and Hamiltonian are negative.

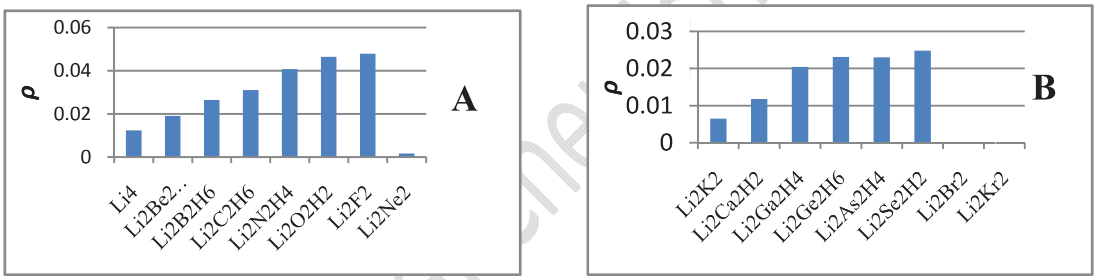

Figure 1: The charge electron density of **A)** Li dimmers of second row and **B)** Li dimmers of fourth row elements of periodic table.

Conclusion:

According to AIM the interaction between Li atom with H, C, N, O, S, Se, F and Cl atoms are ionic, interaction between Li atom with K, Be, Mg, Ca, B, Al, Ga, Si, Ge, P and As are intermediate of ionic and covalent interactions and the interaction of Li atom with the other atoms of first to fourth rows elements of periodic table are covalent.

Parametric structures show that the bond length of Li atom with He atom is longer than the bond length of Li atom with the other elements of first to fourth rows elements of periodic table.

Reference:

[1] Henry Gilman and etal; "The Analysis of Organolithium Compounds" ; Journal of organometallic chemistry; 2,447-454, 1964.

[2] R. Ponec and etal; "On the Nature of C−Li Bonding in Lithiated Hydrocarbons and Lithiocarbons"; *J. Phys. Chem. A*; *106* (6), 1019-1025, 2002.

[3] A. B. Sannigrahi and etal; "The lithium bond reexamined"; *Chem. Rev.*; *90* (6), 1061-1076, 1990.

A Density Functional Theory (DFT/B3LYP) Investigation of Charged Thiophene Oligomers

H. Shirani IL Beigi* [a] , H. Pourmohammad [b], F. Hosseini [c],

[a]Young researchers club, Department of Chemistry, Islamic Azad University, Toyserkan Branch, Toyserkan, Iran
Email: shiranihossein@gmail.com
[b] Department of Chemistry, Ardabil branch, Islamic Azad University, Ardabil, Iran
[c]Department of Chemistry, Guilan University, Rasht, Iran.

Abstract:

Calculations were performed with the Gaussian 98 program. The basis sets correspond to those implemented in the software. The geometries of the isolated bi-, ter-, and quaterthiophene cations were optimized with MP2 at the 6-311++G** level and the relaxed structures used for the calculations of the dimers. The π-stacking of oxidized thiophene oligomers is investigated using extensive ab-initio quantum chemistry methods. Dimers of singly-charged oligothiophenes are found to be unstable in the gas phase, but can be stabilized as bound dications in the singlet state by a polarizable solvent such as acetonitrile. Our calculations provide a detailed description of the mechanisms and the energetics involved in the dimerization phenomenon and highlights the role and importance of the environment in the stabilization of the stacks. The need for accurate treatments of electronic correlations and of solvation effects for a realistic description of these materials is underscored.

Introduction:

[2] Applications run from light-emitting diodes [2a] to1 thin film transistors [2b] and sensing and actuating materials. [2c] The characterization of the electronic structure for the ground and excited states, of the thermodynamical stability, and of charge transport mechanisms such as interchain hopping [1c,f] are essential to engineer thiophene-based devices. Experimental

evidence has long accumulated suggesting reversible dimerization in assemblies of oxidized oligothiophenes.[1a-e] The formation of such aggregates of two or more cations due to π-π interactions—so called π-stacking—is fundamental in determining equilibrium geometries and conductivities in solution or in the solid state.[1c] In the dimerization of cation radicals, intermolecular attraction forces must overcome Coulombic repulsion, and the net outcome is the result of a delicate balance also dependent on the length of the oligomer and the polarity of the surrounding medium.[1b,c] The pairing of charged (anion) radicals was first reported for diphenylethylene[3a] and for tetracyanoquinodimethane[3b] (TCNQ) four decades ago, and the dimerization of cationic and anionic species in solution and in the solid state has been extensively studied ever since.[3c-f]

Computational Approach:

Hartree-Fock and MP2 Calculations. Unrestricted Hartree-Fock calculations have been performed for the bithiophene dimer employing the 6-311+G (d,p) basis set. For distances shorter than 4.0 Å, the closed-shell wavefunction is found to be unstable. For the second-order Møller-Plesset perturbation (MP2) method we used three different basis sets: 6-311+G(d,p), 6-311G(d), and 6-31G*(0.25).

Results and Discussion:

results were obtained at selected geometries with the 6-31G*(0.25) basis and are shown in Table 1. As expected, the interaction energies turn out to be higher than in bithiophenes (in about 15 kcal/mol), since the π-π stabilization is weaker and the Coulombic repulsion localized in a smaller region. More importantly, the calculations exhibit only minor differences between MP2 and MP4 values.depicts the orbitals involved in the CASSCF(6,4) calculations, which were picked in view of their π symmetry. Inspection of the occupation numbers reveals a significant departure from 0 or 2 only on the HOMO and the LUMO (see Table 2). The frontier orbitals are also the ones that show some changes in the occupations when the separation between monomers is increased. All other occupation numbers remain close to 1.9-2.0 or 0.1-0.0, with negligible variation as a function of distance. Such a small variation supports our use of a single-determinant approach to obtain the energy binding curves.

Table 1:MP2 and MP4 interaction energies for two singly-charged monothiophene cations obtained at different separations with the 6-31G*(0.25) basis.

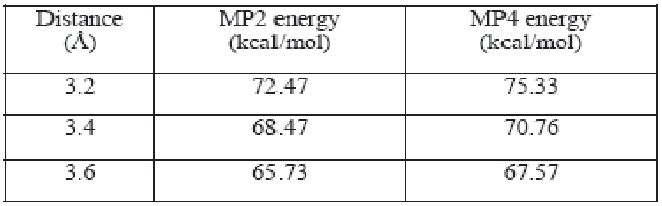

Distance (Å)	MP2 energy (kcal/mol)	MP4 energy (kcal/mol)
3.2	72.47	75.33
3.4	68.47	70.76
3.6	65.73	67.57

Table 2: Occupation numbers of the natural orbitals in the CASSCF calculations.

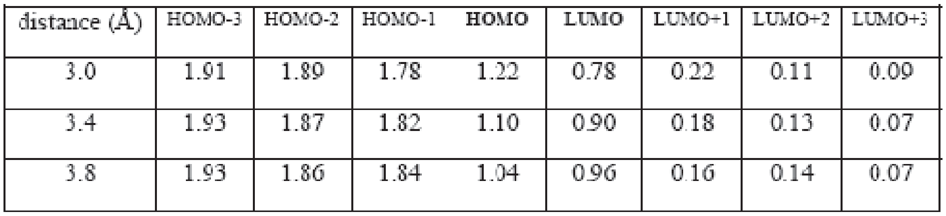

distance (Å)	HOMO-3	HOMO-2	HOMO-1	HOMO	LUMO	LUMO+1	LUMO+2	LUMO+3
3.0	1.91	1.89	1.78	1.22	0.78	0.22	0.11	0.09
3.4	1.93	1.87	1.82	1.10	0.90	0.18	0.13	0.07
3.8	1.93	1.86	1.84	1.04	0.96	0.16	0.14	0.07

Conclusions :

We presented here accurate ab-initio calculations on oxidized oligothiophene dimers, both in vacuum and in solution, using several quantum-chemistry approaches. Our results do not support the existence of stable or metastable dimers for small oligomers in vacuum; π-π interactions between singly oxidized oligothiophenes are not strong enough to overcome the Coulombic repulsion. In a polarizable solvent (acetonitrile) we found stable doubly-charged π-dimers for both bi- and terthiophenes, with binding energies comparable to experimental findings. These results highlight the delicate balance between electrostatic and correlation effects in determining the structural and electronic stability of these systems..

References:

[1]Vosko, S. H.; Wilk, L.; Nusair, M. *Canadian J. Phys.* **1980**, *58*, 1200 [2] K. Kadirvelu, M. Palanival, , S. Rajeswari, *Bioresource Technology,* (2000),74, 263- 265

[2] Boys, S. F.; Bernardi, F. *Mol. Phys.* **1970**, *19*, 553.

[3] Brocks, G.; *J. Chem. Phys.* **2000**, *112*, 5353.

[4] Tsuzuki, S.; Honda, K.; Azumi, R. *J. Am. Chem. Soc.* **2002**, *124*, 12200.

Energy barriers against methane rotation on a graphene sheet

Seyyedeh Mozhgan Seyyed Talebi [*a] , Javad Beheshtian[b] and Mehdi Neek-Amal[a]
[a]Department of Physics, Shahid Rajaee University, Lavizan, Tehran, Iran
[b]Department of Chemistry, Shahid Rajaee University, Lavizan, Tehran, Iran
(E-mail: neekamal@srttu.edu)

Keywords: Graphene, DFT, Adsorption, Energy barrier, Energy surface.

Introduction:

Natural gases as an environmentally friendly energy source and bulk transportation fuels are considered to be one of the best substitutes for fossil fuels in the future. Methane is one of the major components of natural gases therefore the adsorption behavior of methane in confined pores is of practical and theoretical interest [1]. In the past few years, new generation of gas sensors have been demonstrated using graphene-based structures and theoretical studies of gas molecular adsorption on the graphene surface have been reported [2]. In this process, the van der Waals interaction between a methane molecule and a graphene sheet is studied in molecular mechanics method which is compared with those predicted from density function theory. We found that the continuum approach eliminates the atomistic features of the energy surface.

Methods:

There are two configurations for methane molecule (CH_4) onto graphene sheet, i), when 1H is placed near the graphene (A-configuration) and ii), when 3H are placed near the graphene (B-configuration). In molecular mechanics study, the LJ potential provides both the general repulsive and attractive nature of the interaction between methane deposited onto graphene sheet. In the DFT study, as a model of graphene, we considered a graphene sheet composed of 37 benzene rings. The edge carbon atoms of graphene were terminated by hydrogen atom. First, the structure of the graphene was fully optimized at the X3LYP/6-31G* level of theory, and then the adsorption energy of methane in two configuration were obtained by the DFT calculations. The X3LYP functional is selected since it seems to give a better description of interactions [3].

Results and Discussion:

To calculate the dependency of the interaction energy on the orientation of methane, we calculate the adsorption energy versus height for these configurations and compared them.

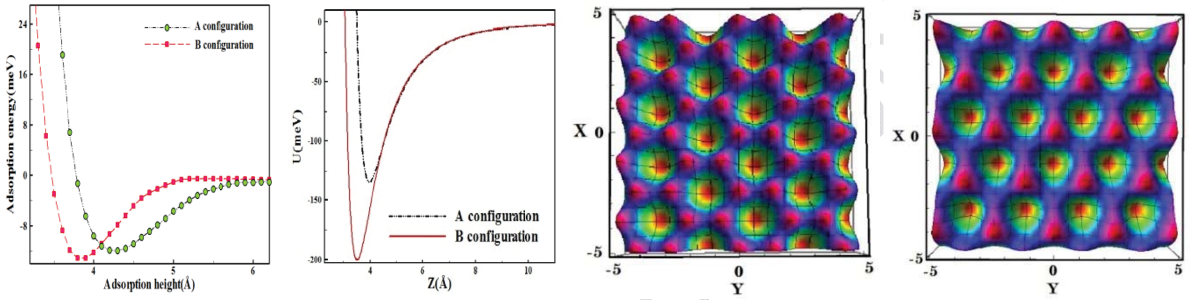

Fig1. The DFT (a) and molecular mechanics results (b) of Adsorption energy between methane and graphene for two configurations. The energy surface for A-configuration(c) and B-configuration (d).

As seen from Figure 1, The B-configuration of methane molecules near the graphene surface is more stable than A-configuration. Therefore, methane molecule prefers to be placed in the B-configuration rather than the A-configuration.

The magnitude of corrugation of the potential energy (which is energy barrier) decreases rapidly with increase of height.

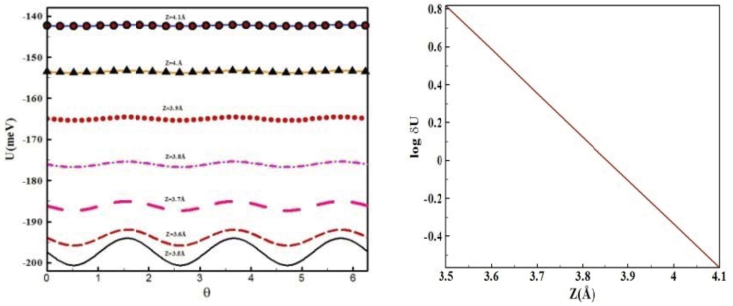

Fig.2. Energy barriers for B-configuration

Conclusions:

We studied the adsorption of methane molecules onto graphene surface for two configurations. In this study the molecular mechanics results compared to those found from DFT calculations. We find out that DFT results are in agreement with those predicted from the molecular mechanics results. The energy surface of graphene due to the vdW interaction with a methane molecule is calculated. Moreover, the energy barriers of graphene are calculated and it is found that they decrease rapidly with increasing in the vertical distances.

References:

[1] Schedin, F.;Geim, A. K.; Morozov, S. V.; Hill, E. H.; Blake, P.; Katsnelson, M. I.; Novoselov, K. S. Nat. Mater. **8** (2007) 652.

[2] R. Arsat, M. Breedon, M. Shafiei, P. G. Spizziri, S. Gilje, R.B. Kaner, K. Kalantar-zadeh, W.Wlodarski, Chemical Physics Letters.**467** (2009) 344-347.

[3] X. Xu, W.A. Goddard III, Proc. Natl. Acad. Sci. USA **101** (2004) 2673.

Tautomerism and Minimum Polarizability Principle

S.M.Alavi , .
Shahed Baharan pre university and high school, Dezfull, Iran
Email: seyedehmaryamalavi@yahoo.com

Key words: Tautomer, Stability, Computational Chemistry, Minimum Polarizability Principle

Introduction:

Computational chemistry is a branch of quantum chemistry which is related to analyzing, reviewing and measuring some systems properties that they can't be measured directly, so it uses math and statistics and it branches in two: Molecular Mechanics Theory and Electronic Structure Theory. In this research, we tried to review some of the molecules which are tautomered for each other and according to the acquired energy (zero point energy), select their stability from and review the Minimum Polarizability Principle. This principle states that the system goes along a status in order to reach the minimum polarizability. So, according to this principle, any molecule which has the least polarizability, it would have the maximum stability.

Materials and Methods:

In computational chemistry the following four different methods are manipulated:

1- Molecular mechanics method
2- 2- Semi- empirical method
3- Ab initio method
4- Density Function theory (DFT) method

In this research, calculations were followed through several methods and they were compared to each other.

In this research in order to review the information, CNDO method, semi-empirical methods, HF (Hartree-Fock) method from Ab initio approaches and B3LYP from density function theory methods were followed.

It's necessary to mention that the various basis sets were also changed in order to specify the best method and the basis set. 6-31G** and 6-311++G** from the basis sets were used in B3LYP and HF methods.

Polarizability is defined as measuring electronic density changes in an electronic field, e.g.:

$$\propto = -\left(\frac{\partial^2 E}{\partial F_a \partial F_b}\right) \qquad a, b = x, y, z$$

To calculate that, the following relation is used: $\propto = \frac{1}{3}(\propto_{xx} + \propto_{yy} + \propto_{zz})$

Apparatuses:

In order to achieve the required result, Hyper Chem. and Gaussian softwares were used. The first software draws the molecule and optimizes that and then that molecule coordinates enter Gaussian software to draw its precise structure bond length and its several minimums.

Results and discussion:

The achieved results in HF method didn't have great changes through a change in the basis set and this approach has very little mismatch with the minimum polarizability principle.

In the B3LYP method the number of breechings the principle was too much but there wasn't too much change in the results when the basis set changed.

Conclusion:

In determining the stability of the tautomers through calculating zero point energy (ZPE), there is too much discrepancy among the methods. Yet, in one of the method with various basis set the discrepancy would be very low (4%).

In reviewing the Minimum Polarization Principle, CNDO method has no workability because it doesn't calculate polarizability matrix elements.

HF method was very proper and it had the minimum error. B3LYP method also has an acceptable error. The change in the basis set does have any important influence in accordance with MPP principle.

Despite of the fact that the accuracy increases through shifting from CNDO to B3LYP, because all the quantomic functions are not considered and specific approximations are used, then, there's still error possibility.

Reference:

[1] Y .L .Zhong, Z .Z .Yang, Internatinal Journal of Quantum chemistry, 106 (2006) 1723.
[2] A .Alparone, A .Millefiori & S .Millefiori, J. Phys. chem., 312(2005)261.
[3] C. Banwell, Fundamentals of Molecuular Spectroscopy, Translated by Dr. hasan pour & Dr. Eslampour, 98 (1379).

QSPR Calculation of Density of Som Organic Compounds Use of Multiple Linear Regression (MLR) Method

M. Rahimi*, H. Farahbakhsh, A. Javadimanesh
Department of Chemistry, Faculty of Basic Sciences, Shahrood Branch, Islamic Azad University, Shahrood, Iran
Email: mehdi.rahimi1985@gmail.com

Abstract:

The standard density of 51 compounds, were drawn into the Hyperchem program and optimized using semi-empirical AM1 method and predicted using multiple linear regression (MLR). The obtained multivariate linear five descriptors model by MLR has correlation coefficient. All molecular descriptors which have entered in this model are calculated from chemical structure of any molecule. As a result, application of this model for any compound is easy and accurate ($R^2 = 0.911$).

Key word: *QSPR, Density, AM1 method,MLR.*

Introduction:

Physical and thermodynamic properties data of compounds are needed in the design and operation of industrial chemical processes[1]. QSPRs have emerged in the last decades as a useful tool for predicting physicovhemical, biological and pharmacological properties of molecules, specially in those cases where there are no available experimental data corresponding to such properties [2,3]. The aim of this work is construction an accurate quantitative relationship between the molecular structure and the retention indices by stepwise-MLR.

Method:

The QSPR study of density was performed in four fundamental stages. The descriptive power of the model was characterized by use of the statistical data multiple correlation coefficient (R). The data set of the density's was taken from the values reported by J.A. *et al.*[4]. The prediction set of 12 compounds was selected randomly from the original 51 of organic molecules with the remaining molecules constituting the training set. The accuracy of the proposed MLR model was illustrated using the following evaluation techniques: leave-one-out and leave-group-out cross-validation procedures, validation through an external test set.

Results and discussion:

For regression analysis, data set was separated into two groups: training and test sets. The molecules included in these sets were selected randomly. The training set, consisted of 39 molecules, was used for the model generation using the SPSS software package. The prediction set, consisted of 12 molecules, was used to evaluate the generated model. A small number of molecular descriptors (AMW, IDDE, Mor04m, Mor14u, Mor10u) proposed were used to establish a QSPR model. A reliable MLR model is one that has high R^2 and least number of descriptors. In addition to these, the model should have a high predictive ability. Consequently, among different models, the best model was chosen:

$$\mathbf{D}= 0.471(\pm 0.068) + 0.06(\pm 0.006)\mathrm{AMW} + 0.082(\pm 0.013)\mathrm{IDDE} + 0.136(\pm 0.029)\mathrm{Mor04m} + 0.094(\pm 0.03)\mathrm{Mor14u} + 0.094(\pm 0.03)\mathrm{Mor10u} \qquad (1)$$

$$N = 51,\ R^2= 0.911,\ \mathrm{RMSEP} = 0.1937,\ \mathrm{SEP}= 0.2023,\ Q^2_{\mathrm{LOO}} = 0.902,\ Q^2_{\mathrm{LGO}} = 0.892$$

The proposed method, due to the high predictive ability and simplicity could be a useful aid to the costly and time consuming experiments for determining the density of organic compounds.

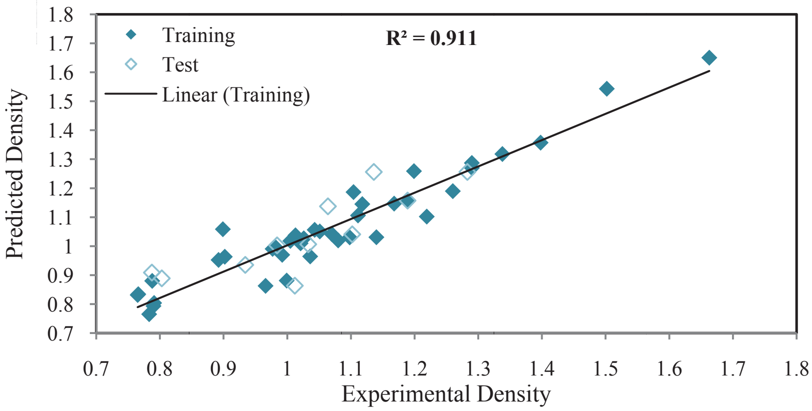

Fig.1. The predicted densityvalues by the MLR modeling vs. the experimental density values.

Conclusion:

The QSPR method by the stepwise-MLR analysis was followed to develop a model for predicting the densityof some organic compounds. In this present study, a simple five descriptors linear model was presented. This model was the result of a QSPR study on the density of 51 organic compounds. Also the simplicity of the use of it is one of the advantages of this model. All molecular descriptors of this model can be easily calculated from the chemical structure of a molecule.

References:

[1] S.W. Benson, *Thermochemical Kinetics*, Wiley, New York, (1968).
[2] W.A. Sexton, Chemical Constitution and Biological Activity, New York, (1950).
[3] C. Hansch, *Acc. Chem. Res.*, 2 (1969) 232.
[4] J.A. Dean, *Lang's Handbook of Chemistry*,McGRAW-HILL (1999).

An Improved QSPR Study of Δ_fG^0 of Some Organic Molecules Based on AM1 Calculation

M. Rahimi*, H. Farahbakhsh, A. Javadimanesh
Department of Chemistry, Faculty of Basic Sciences, Shahrood Branch, Islamic Azad University, Shahrood, Iran
Email: mehdi.rahimi1985@gmail.com

Abstract:

This work is a part of our comprehensive investigation to correlate the experimental and calculated Gibbs energies of formation and report the results of a representative set of 25 organic molecules through the application of QSPR theory. The structures of all organic molecules were drawn into the Hyperchem program and optimized using semi-empirical AM1 method. Then molecular descriptors were calculated for each compound by the Dragon software on the minimal energy conformations. The stepwise SPSS was used for the selection of the variables that resulted in the best fitted models. Some possible extensions of this study are discussed.

Key word: Gibbs energy, Hyperchem, AM1 method, QSPR.

Introduction:

Quantitative structure property relationships (QSPRs), mathematical equations relating chemical properties such as acidity, electrochemistry, reactivity and chromatographic behavior to a wide variety of structural, topological and geometrical features of the molecules have been widely used in the field of chromatographicsciences [1-3]. In this work we used the stepwise method for variable selection in MLR.

Method:

The data set of the Δ_fG^0's was taken from the values reported by J.A. *et al.*[4]. The data set was split into a training set and a prediction set. The prediction set of 6 compounds was selected randomly from the original 25 of organic molecules with the remaining molecules constituting the training set. Molecular descriptors are defined as numerical characteristics associated with chemical structures. The molecular descriptor is the final result of a logic and mathematical procedure which transforms chemical information encoded within a symbolic representation of a molecule into a useful number applied to correlate physical properties [5-7].The accuracy of the proposed MLR model was illustrated using the following evaluation techniques: leave-one-out and leave-group-out cross-validation procedures, validation through an external test set.

Results and discussion:

After regression analysis, a few suitable models were obtained among which the best model was selected and presented in Eq. (1). A small number of molecular descriptors (nHAcc, PCR, PJI2, IC0) proposed were used to establish a QSPR model. MLR analysis provided a useful equation that can be used to predict the Δ_fG^0 of organic molecules based upon these parameters. The best equation obtained for the Δ_fG^0 of the organic molecules is:

$$\mathbf{\Delta_fG^0} = -274.721(\pm 36.647) - 195.589(\pm 4.887)\text{piPC03} + 197.383(\pm 28.652)\text{nHDon} - 108.384(\pm 15.611)\text{Mor29e} + 74.824(\pm 15.273)\text{Mor32m} \qquad (1)$$

$$N = 25,\ R^2 = 0.9925,\ Q^2_{LOO} = 0.9911,\ Q^2_{LGO} = 0.9916$$

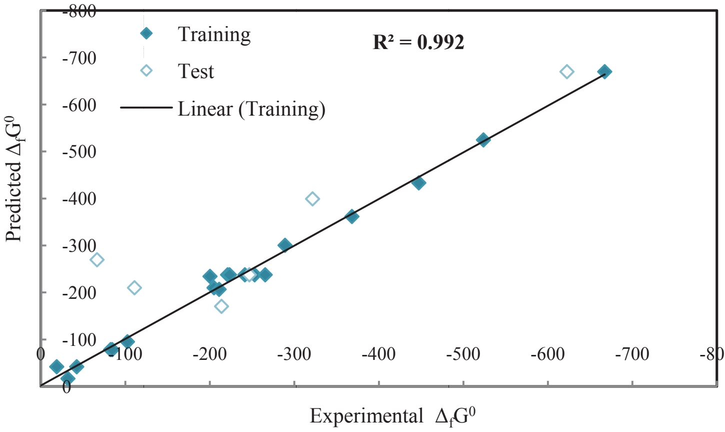

Fig.1. The predicted Δ_fG^0values by the MLR modeling vs. the experimental Δ_fG^0 values.

The results illustrated once more that the linear MLR technique combined with a successful variable selection procedure is adequate to generate an efficient QSPR model for predicting the Δ_fG^0 of organic molecules. The proposed method, due to the high predictive ability and simplicity could be a useful aid to the costly and time consuming experiments for determining the Gibbs energies of formation of organic moleculess.

Conclusion:

The QSPR method by the stepwise-MLR analysis was followed to develop a model for predicting the Gibbs energies of formation of organic molecules. The QSPR model with simply calculated molecular descriptors could be employed to estimate the Δ_fG^0 for new molecules, even in the absence of the standard candidates.

References:

[1] T.B. Aczek, R. Kaliszan, K. Novotna and P. Jandera, *J.Chromatogr A*, 1075, 109 (2005).
[2] S. Riahi, M.F. Mousavi and M. Shamsipur, *Talanta*, 69, 736 (2006).
[3] P. Ghosh, B. Chawla, P.V. Joshi and S.B. Jaffe, *Energy Fuels*, 20, 609 (2006).
[4] J.A. Dean, *Lang's Handbook of Chemistry*, McGRAW-HILL (1999).
[5] R. Todeschini and V. Consonni, *Handbook of molecular descriptors*, Wiley-VCH, Weinheim (2000).
[6] L.B. Kier and L.H. Hall, *Molecular Connectivity in Structure-Activity Analysis*, RSP-Wiley, Chichetster, UK, (1986).
[7] J. Galvez, R. Garcia, M.T. Salabert and R. Soler, *J. Chem. Inf. Comp. Sci.*, 34, 520 (1994).

A Theoretical Study on the C_2H_2 + NO reaction

F.karami*, M.Vahedpour, K.Shayan
Department of Chemistry, University of Zanjan, Zanjan, Iran
E-mail: f_karami1388@yahoo.com

Key words: Theoretical study, oxidation of acetylene, NO reduction, gas phase reactions

Introduction:

Acetylene is a hydrocarbon and the simplest alkyne. This colorless gas is widely used as a fuel and a chemical building block. It is unstable in pure form and thus is usually handled as a solution. Like other hydrocarbons, alkynes are generally hydrophobic but tend to be more reactive. As an alkyne, acetylene is unsaturated because its two carbon atoms are bonded together in a triple bond. Acetylene is a linear symmetrical molecule, the triple bond is very strong with a bond strength of 839 kJ/mol. Today acetylene is mainly manufactured by the partial combustion of methane or appears as a side product in the ethylene stream from cracking of hydrocarbons. Reactions of alkynes with oxidizing agents such as ozone usually result in cleavage of the triple-bond to give carboxylic acid products. In general equation for this kind of transformation, atomic oxygen is produced. Also, nitrogen oxides (NO_x) play an important role in troposphere chemistry because nitrogen oxides (NO_x) are responsible for acid rain.

In this work, we are initiating a systematic study on the reaction of acetylene with nitric oxide based on quantum theories to obtain the details of the reaction mechanism on the doublet potential energy surfaces [1-3].

Theoretical methods:

All geometry optimizations were carried out with hybrid density functional B3LYP approach in connection with the 6-311++G (3df-3pd) basis set. Single point energy is performed for all species at the CCSD (T) level with the B3LYP optimized geometries. All the calculations were performed with the GAUSSSIAN 03 program.

Result and discussion:

In this study we have investigated thermodynamic and kinetic of the C_2H_2 and NO reaction. In spite of numerous attempts, no stable collision complex has been found on the doublet potential energy surface. The first step, reactants C_2H_2+NO are directly transformed to IN1 via TS1 with energy barrier of 14.07 kcal/mol. The IN1 can to convert into IN2 through TS2 with energy barrier of 77.26 kcal/mol. The intermediate IN2 is converted into IN3 via TS3 by O-H bond formation. The energy barrier for IN2 →IN3 conversion is 16.02 kcal/mol. Figure 1 shows that the energy of IN3 is -53.69 kcal/mol lower than the original reactants, so IN3 is most stable intermediate in comparison with others. Finally, the conversion IN3 →P (NCCH2O) transact with TS4 with energy barrier of 46.31 kcal/mol. The structure of transition state TS4 was found hydrogen shift. The Gibbs free energy for this reaction has been obtained -227.96 kcal/mol.

Table1: The total energies and relative energies (in the parenthesis) values for C_2H_2+NO reaction

Species	B3LYP	CCSD(T)	Species	B3LYP	CCSD(T)
C_2H_2+NO	-207.2724(0.00)	-206.9047	TS3	-207.2683(22.331)	-206.8625
TS1	-207.2853(14.070)	-206.8851	IN3	-207.3579(-53.699)	-206.9934
IN1	-207.3722(-40.323)	-206.9709	TS4	-207.1524 (75.289)	-206.9151
TS2	-207.2431(36.935)	-206.8408	P(NCCH2O)	-207.3265(-33.929)	-206.9629
IN2	-207.2980(6.307)	-206.8959			

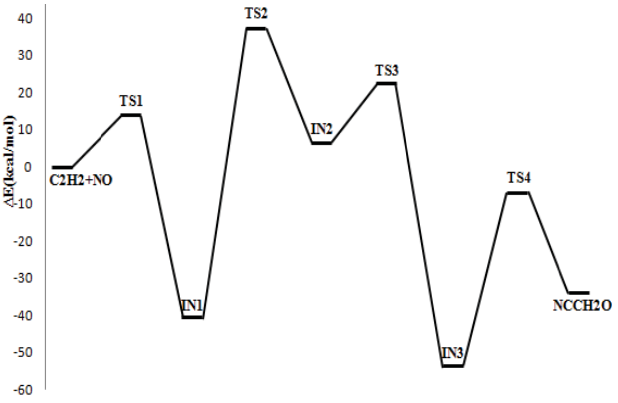

Fig.1. Potential energy profile of the C_2H_2+NO reaction at the B3LYP level

Conclusion:

Details of the reaction pathway of C_2H_2+NO on the doublet potential energy surfaces have been characterized at the CCSD(T)//B3LYP/6-311++G(3df, 3pd) level. The calculated results reveal which this channel is feasible thermodynamic pathway for produce P which is more stable product. The low energy of transition state show the reaction is feasible in kinetic approaches.

Reference:

[1] R.H.Petrucci and etal; "General Chemistry"; Prentice-Hall;2 2002
[2] P. Pässler and etal; "Acetylene in Ullmann's Encyclopedia of Industrial Chemistry" Wiley-VCH, Weinheim, 2008.
[3] P. Dagaut and etal; "Experimental and kinetic modeling of nitric oxide reduction by acetylene in an atmospheric pressure jet-stirred reactor"; Fuel; 78, 1245–1252, 1999.

A quantum chemical study on the structural and electronic properties of (2, 6-Dichloro-benzylidene)-(2, 4-dichloro-phenyl) – amine

A. soltani[a], F. Ghari [b]*, E. Tazikeh Lemeski[b], S. M. Vahdat[b]
[a]Young Researchers Club, Gorgan Branch, Islamic Azad University, Gorgan, Iran
[b]Department of Chemistry, Ayatollah amoli Branch, Islamic Azad University, Amol, Iran
[c]Department of Chemistry, Gorgan Branch, Islamic Azad University, Gorgan, Iran
Email: fereshteh_ghari@yahoo.com

Key words: DBDPA, DFT, HOMO-LUMO, Quantum molecular descriptors

Introduction:

Schiff-base compounds are typically formed by condensation of a primary amine and an aldehyde, they are used as substrates in the preparation of a number of transitionmetal complexes they have good catalysis ability and are suitable for generation of supramolecular structures [1-2]. In this paper, we have studied the electronic properties of the (2, 6-Dichloro-benzylidene)-(2, 4-dichloro-phenyl)- amine (DBDPA) compound was also performed at B3LYP/6-31G* level.

Computational details:

The DFT computation has been performed via Gaussian 03[3] program package at the B3LYP method with standard 6-31G* basis set for geometry optimization of the title. The electrophilicity concept was stated initially in 1999 by Parr et al. μ is defined according to the following equation: $\mu = (E_{HOMO}+E_{LUMO})/2$. $\eta = (E_{LUMO} - E_{HOMO})/2$. S and ω are defined as the following equations, respectively [4]. $S=1/2\eta$, $\omega = (\mu^2/2\ \eta)$, $\Delta N_{max}=-\mu/\eta$.

Results and Discussion:

The HOMO represents the ability to donate an electron and LUMO as an electron acceptor that are main orbitals taking part in chemical stability [4]. The HOMO and LUMO energy gap and quantum molecular descriptors computed by DFT/B3LYP in different basis sets are summarized in Table 1.

Table 1 Quantum molecular descriptors of DBDPA in gas phase.

System	$-E_{HOMO}$/eV	$-E_{LUMO}$ /eV	Gap/eV	μ/eV	η/eV	ω /eV	S /eV	ΔN_{max}/a.u.
DBDPA	6.05	1.99	4.11	-4.02	2.03	3.98	0.25	1.98

Increasing the hardness and decreasing the softness will due to the increase of stability and the decrease in reactivity of the complex. The electrophilicity index indicates the energy lowering of a ligand due to maximum flow of electron from donor to acceptor complexes and provides information about structural stability [4].

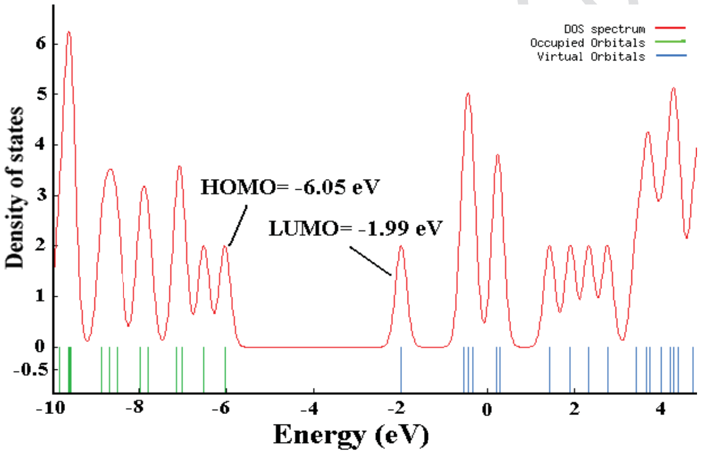

Fig.1. Total density of states (DOS) for BDPMP complex.

Conclusion:

In this present investigation the electronic properties and the HOMO- LUMO energy gap analysis of the BDPMP have been studied using ab initio DFT/B3LYP/6-31G* computation.

Reference:

[1] A. D. Khalaji, G. Grivani, S. J. Akerdi, H. Mighani, Struct Chem 21 (2010) 995.

[2] A. D. Khalaji, M.Weil, G. Grivani, S. J. Akerdi, Monatsh Chem141 (2010) 539.

[3] M.J. Frisch et al., Gaussian 03, Revision B03, Gaussian Inc., Pittsburgh, PA, 2003.

[4] Nabanita Saikia, Ramesh C. Deka, Comput. Theo. Chem. 964 (2011) 257.

NBO Analysis of Fe (III)-salen and Fe (III)-salen-like complexes as potent anticancer agents

Z. Ghanbari[a*], M. Izadyar[a], M. R. Housaindokht[b]
a) Department of Chemistry, Faculty of sciences, Ferdowsi University of Mashhad, Mashhad, Iran
b)Institute of Biotechnology, Ferdowsi University of Mashhad, Mashhad – Iran
E-mail address:Zahraghanbari10@gmail.com

Keywords: Natural Bond Orbitals (NBO); DFT; Metal Complex; Fe (III)-salen; Anticancer

Introduction:

Since introduce cis-platin as antitumor drug, metal-ligand compounds have been extensively studied due to their reactive roles in biological processes. From among Metallic Complexes, iron (III) complexes with coordinated salen where Salen is (bis(salicylidine)ethylenediamine) ligands are subject of study for their desirable antitumor features.Molecules possessing the ability to bind and cleave double stranded DNA under physiological conditions are important as anticancer agents in medicine. The interaction of DNA with Fe(III)-salen can be interpreted in the term of electrostatic binding between the $Fe(Salen)^+$ cation and the phosphate groups of DNA. Moreover these complexes showed the ability to cleave DNA via redox processes [1]. Fe(III)-salen produces free radicals in the presence of reducing agent dithiothreitol (DTT)or H_2O_2 and induces DNA damage in a redox process. Anyhow the results confirmed formation of $Fe(Salen)^+$ with stability constant (7.1×10^{25} M^{-1}).. In this article, what we considered has been searching relation of chemical structure of compounds to their antitumor activity.

Computational details:

DFT calculations, at B3LYP level in gas phase, have been performed on these structures. All computations were performed using the Gaussian 03 and AIM software [2]. Natural bond orbital(NBO), atoms in molecule (AIM), surface of the electrostatic potential on the electron density surface were used in order to interpret antitumor activity of these complexes. For this purpose, substitutes on Salen ligand and replace of chloride ligand with N-Heterocyclic ligands were studied. With this replaces Anti-Tumor activity will be changed in a wide range. NBO analysis is used for characterization of electronic structure of the complexes, too.

Results and discussion:

Computed charge distribution in these complexes indicates that the oxygen atoms have a significantly higher negative charge than nitrogen atoms in imino-group.The smaller positive charge of Fe atoms indicated that the covalent contribution in the Fe-ligand bond. Also it can be seen, there is a covalent contribution from the metal-ligand interaction with major participation of 3d atomic orbital for Fe atom. The study of the influence of the Cl ligand change to heterocyclic N-donor ligands showsthat in more cases heterocyclic N-donor ligands, increase antitumor activity. The squares of polarization coefficients confirmed that there is a good relation between antitumor activity and natural iconicity parameter of Fe(salen) with Cl or heterocyclic N-donor ligands bond. Natural iconicity parameter increasing, causes antitumor activity increasing, which confirmsthe formation of $Fe(Salen)^+$cation. On the other hand the concept of the Laplacian of the electronic charge density $\nabla^2\rho(r)$ can be used in order to determine the region in which the electronic charge is locally depleted or concentrated. More local concentration of charge for Cl ligand in bond critical point showed that its separation is more difficult. Surface of the electrostatic potential on the electron density surface reveals the nucleophilic and electrophilic regions of a molecule. The aromaticity growth of D-Amino bridges will lead to increase in Anti-Tumor feature and the electrostatic potential of the center will be more positive.

Fig1.

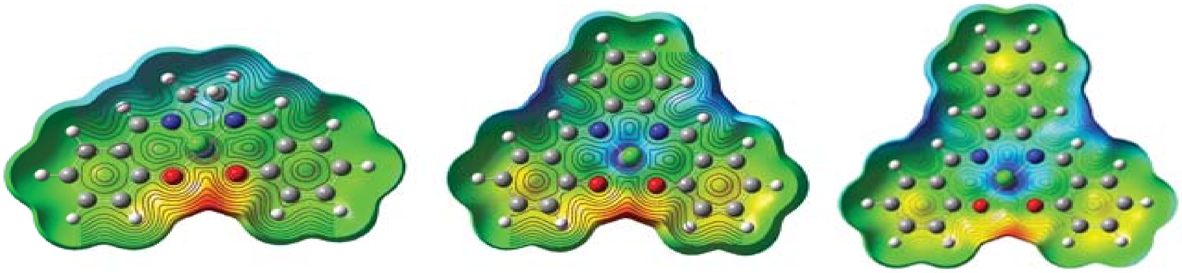

Central metal alternationwill cause to change the antitumor activity in a wide range and it can be interpret using the hard-soft acid/base (HSAB) theory and HOMO-LUMO energies.

References:

[1]A.Silvestri, G. Barone, G.Ruisi, M. T. Lo Giudice, S.Tumminello, Journal of Inorganic Biochemistry 98 (2004) 589–594.

[2]Gaussian 03, Revision C.02, Gaussian, Inc., Wallingford, CT, 2004.

[3]E. D. Glendening, C.R. Landis, F. Weinhold, WIREs Comput Mol Sci 2012, 2: 1–42 doi: 10.1002/wcms.51.

Effect of Cu insertion on the structure and electronic properties of small Rh clusters: A DFT study

A. Arab[a*], F. Gobal[b], M. Nahali[b]
[a]Department of Physical Chemistry, Faculty of Chemistry, Semnan University, Semnan, Iran
[b]Department of Chemistry, Sharif University of Technology, Tehran, Iran
Email: r.arab2010@gmail.com

Keywords: Rh-Cu clusters, DFT, structure, stability, chemical hardness

Introduction:

Studies of small clusters by DFT methods have received a good deal of attentions in the past decade because of their unique catalytic properties [1, 2]. Much attention has been paid to theoretical study of monometallic clusters while bimetallic clusters and their application in catalytic reactions are less theoretically studied [2]. Usually the catalytic activities of bimetallic surfaces are higher than monometallic surfaces because of both structural and electronic effects [2]. In the present study we employed B3PW91 method to investigate the structure and energetic of Rh_xCu_{4-x} (x= 0-4) small clusters. Also, effect of Cu insertion on the stability and the tendency to exchange electron of clusters were explained on the basis of the calculated parameters such as binding energy (BE), ionization potential (IP), electron affinity (EA), and chemical hardness.

Methods:

All calculations including optimization of structures, charge distributions, and vibrational frequencies of clusters were carried out by DFT. The B3PW91 hybrid density functional method has been used in this study. B3PW91 hybrid functional exploits a combination of B3 exchange functional [3] and PW91 correlation functional [4, 5]. Also, we have improved the accuracy of the calculations using modified LANL2DZ basis set. The natural bond orbital

(NBO) charges and the corresponding dipole moments of clusters were calculated by GENNBO 5.0 program [6].

Results and discussion:

Fig. 1 presents the variation of the global (chemical) hardness of the most stable structure of clusters against copper percentage. As can be seen in the figure with increasing copper content the chemical hardness decreases to a minimum at 75% copper content. Therefore, the cluster with 75% copper content has the maximum softness among these clusters. It means that $RhCu_3$ cluster has maximum tendency to exchange electrons.

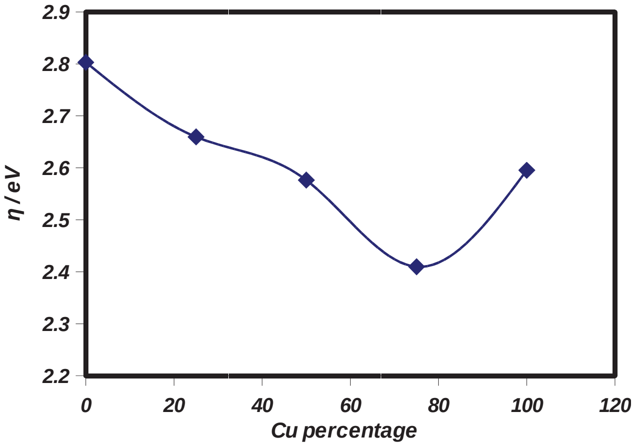

Fig. 1. The variation of the global hardness of the most stable structures of clusters against copper percentage.

Conclusions:

DFT calculations showed that with increasing the copper content of clusters the structure, binding energies, chemical hardness and dipole moment of clusters change significantly. For example, calculation of binding energies indicated that higher copper content has detrimental effect on the stability of clusters while the calculated chemical hardness shows a minimum at 75% copper content corresponds to the maximum softness.

References:

[1] G. Lv, F. Wei, H. Jiang, Y. Zhou, X. Wang, J. Mol. Struct: THEOCHEM 915 (2009) 98-104.

[2] I. Efremenko, M. Sheintuch, Chem. Phys. Lett. 401 (2005) 232-240.

[3] A.D. Becke, J. Chem. Phys. 98 (1993) 1372-1377.

[4] J.P. Perdew, J.A. Chevary, S.H. Vosko, K.A. Jackson, M.R. Pederson, D. J. Singh, C. Fiolhais, Phys. Rev. B. 46 (1992) 6671-6687.

[5] J.P. Perdew, Y. Wang, Phys. Rev. B 45 (1992) 13244-13249.

[6] E.D. Glendening, J.K. Badenhoop, A.E. Reed, J.E. Carpenter, J.A. Bohmann, C.M. Morales, F. Weinhold, Theoretical Chemistry Institute, University of Wisconsin, Madison (2001).

Study of Hydrogen RDF on C20, C19B and C19Si Fullerene Nanocages at Different Temperatures and Pressures

[1]P.Nazari , [1]B. Hasani , [1]F.R.Nikmaram*, [2]S.M.Mousavi Khoshdel,[3]S.Ketabi
[1]Department of Chemistry, Faculty of science, Islamic Azad University Shahr-e-REY Branch,Tehran, IRAN
[2]Molecular Simulation Research Laboratory, Departments of Chemistry, Iran University of Science and Technology (IUST),Tehran, Iran
[3]Department of Chemistry, East Tehran Branch (Ghiamdasht),Islamic Azad University,Tehran, Iran
*NIKMARAM88@IAUSR.AC.IR

Abstract:

In this work, H_2 adsorption on $C_{20\ (cage)}$, $C_{19}B_{\ (cage)}$ and $C_{19}Si_{\ (cage)}$ fullerene clusters have been investigated at the different temperatures (273, 298, 320, and 400 k) for the pressure range between 1 and 30 MPa, using (N,V,T) Monte Carlo simulation by Lennard -Jones(LJ) potential. The effects of the temperature and pressure on the adsorption phenomena are examined. We consider a cubic simulation box (50.0 Å, 50.0 Å, 50.0 Å) contains one fullerene cluster and H_2 molecules. For every calculation, 10^7 configurations were generated. The initial configurations were discarded to guarantee equilibration, whereas the remaining configurations were used to average the desired ensemble properties. The aim of present work is presentation and comparison of the Gravimetric storage capacity (absolute value adsorption per mass of adsorbent, ρ_w) and Radial Distribution Function (RDF) parameters for the clusters at the different temperatures and pressures. The gravimetric storage capacities on the basis of hydrogen adsorption are comparable for structures. The maximum RDF at 3Å and 273 k, on 25 MPa for C20, 20 MPa for C19Si and 30 MPa for C19B are 0.01607, 0.01906, and 0.02018, respectively.

Key words: Boron, Silicon, C20 Fullerene, Nanocage, H2 Adsorption, Monte Carlo

Introduction:

Pure hydrogen may be the final destination in the evolution of fuel usage from coal to petroleum to natural gas, which has followed a trail of increasing hydrogen content [1]. A major bottleneck for the hydrogen vehicle is the problem of hydrogen storage. Hydrogen has been recognized as an ideal energy carrier with heating value three times higher than petroleum[2]. However, several studies have been performed to meet the goals of U.S. Department of Energy (DOE) Hydrogen plan, 6.5 wt%, most of them have failed to approach the proposed target.

Recently, considerable attention has been driven to porous materials such as clathrates, zeolites, carbon nanotubes, and fullerenes as possible materials for hydrogen storage. C_{20} is regarded as the smallest experimentally synthesized carbon fullerene with 12 pentagons [3].

Boron- and silicon-doped carbon clusters of the type B_mC_n (m = 1−4) and Si_mC_n (m = 1, 2) have been produced via the laser-vaporization cluster beam technique [4].

Model and Simulation Details:

In this work, H_2 adsorption on $C_{20\ (cage)}$ and $C_{19}Si_{\ (Cage)}$ and $C_{19}B_{\ (cage)}$ fullerene clusters have been investigated at the different temperatures (273, 298,320, and 400 k) for the pressure range between 1 and 30 MPa, using (N,V,T) Monte Carlo simulation by Lennard -Jones(LJ) potential. The effects of the temperature and pressure on the adsorption phenomena are examined. We consider a cubic simulation box (50.0 Å, 50.0 Å, 50.0 Å) contains one fullerene cluster and H_2 molecules, fig1. For every calculation, 10^7 configurations were generated. The initial configurations were discarded to guarantee equilibration, whereas the remaining configurations were used to average the desired ensemble properties.

Results and Conclusion:

The aim of present work is presentation and comparison of the Gravimetric storage capacity (absolute value adsorption per mass of adsorbent, ρ_w) and Radial Distribution Function (RDF) parameters for the clusters,fig2. The gravimetric storage capacities on the basis of hydrogen absorption are comparable for all three structures. The maximum RDF at 3Å and 273 k, on 25 MPa for C20, 20 MPa for C19Si and 30 MPa for C19B are 0.01607, 0.01906, and 0.02018 , respectively.

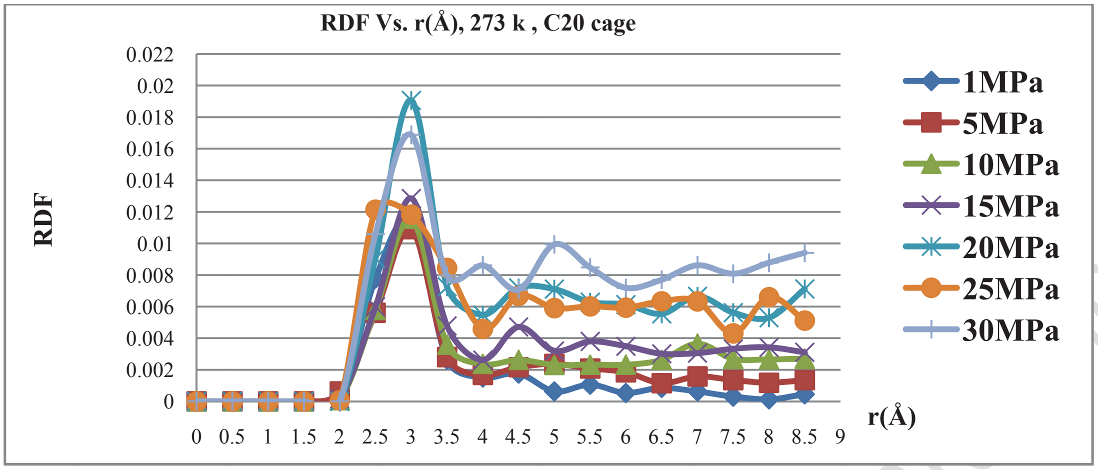
RDF Vs. r(Å), 273 k , C20 cage

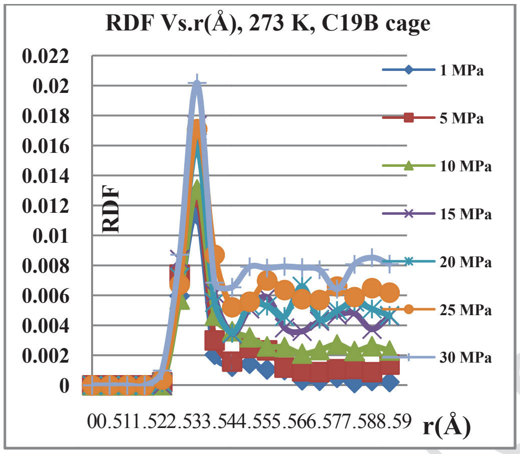
RDF Vs.r(Å), 273 K, C19B cage

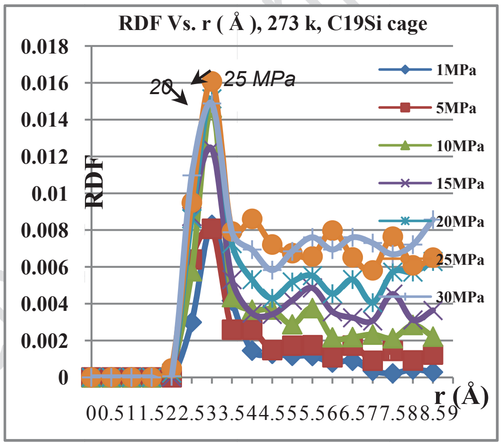
RDF Vs. r (Å), 273 k, C19Si cage

Reference:

[1] Zhou, L.Progress and Problems in Hydrogen Storage Methods Renewable Sustainable Energy Rev. 9, 395– 408, 2005.

[2] .Zhou, L. Renewable and Sustainable Energy Reviews 9, 395-408,2005.

[3] H. Prinzbach et al., Nature 407, 60,2000.

[4] Takumi Kimura, Toshiki Sugai and Hisanori Shinohara, Department of Chemistry, Nagoya University, Nagoya 464, Japan

Dynamic ^{1}H NMR and Theoretical Study of Carbon-Carbon Double Bond Rotational Energy Barrier in Stable Phosphorus Ylide Drived from Triethyl phosphate

Malihe Fazilatkhah, S. Mostafa Habibi*, Marziye Mohammadi , Elham Aghdaei ,Fatme Ghodsi

Department of Chemistry, The University of Sistan and Baluchestan, P. O. Box 98135-674,Zahedan, Iran

* corresponding author Sayyed Mostafa Habibi Khorassani, Department of Chemistry, The University of Sistan and Baluchestan, P. O. Box 98135-674, Zahedan, Iran; E-mail address: smhabibius@yahoo.com

Abstract:

The ^{1}H NMR spectrum of this compound exhibited dynamic effect that is attributed to restricted rotation around the carbon-carbon double bond. Activation and kinetic parameters including $\Delta H^{\neq}$, $\Delta G^{\neq}$, $\Delta S^{\neq}$ and E_a were determined in accord with dynamic ^{1}H NMR data. In addition, theoretical studies were investigated using *ab intio* method at HF/6-31G(d,p) level of theory. Theoretical activation parameters including $\Delta H^{\neq}$, $\Delta G^{\neq}$, $\Delta S^{\neq}$ and kinetic parameter involving E_a were recognized at 298 K. They were in a good agreement with the experimental data.

Keywords: Dynamic ^{1}H NMR, HF/6-31G(d,p) Level of Theory,Rotational Energy Barrier

Introduction:

The synthesis of phosphorus ylides is important in organic chemistry because of their application in the synthesis of organic products[1-2], especially naturally occurring products with biological and pharmacological activity[3-4]. We now describe dynamic ^{1}H NMR[5-7] and also theoretical studies as a complementary investigation of rotation around the carbon-carbon double bond in compound **4.**

Results and Discussion:

In ylide 4, C_2-C_3 bond has a partial double bond character due to the conjugation between the carbonyl group of CO_2Me and $C = P^{+}(OEt)_3$ bond as shown in, Fig 1. The rotation around the partial carbon-carbon double bond in ylide **4** is fairly fast on the NMR time scale at ambient temperature. When the temperature was considerably reduced down to 5°C, we observed the two *E*-4 and *Z*-4 geometrical isomers. Investigation of such behavior in the phosphorus ylide **4** at variable temperatures (Figure 2) allowed us to calculate the rotational energy barrier ($\Delta G^{\neq}$) on the basis of ^1H NMR study for the restricted rotational process around the carbon-carbon double bond (Table 1). In order to determine theoretical rotational energy barrier in the rotational interchangeable processes of the two *Z*- and *E*-isomers in ylide 4, first their structures were optimized at HF/6-31G level of theory by Gaussian 03 program package. Then, relative energy versus dihedral angle ($O_1C_2C_3P_4$, see Figure 1) is plotted in Figure 3. As can be seen, one transition state (TS) has been appeared on plot (Figure 3). In addition other activation parameters such as $\Delta H^{\neq}$ and $\Delta S^{\neq}$ along with activation energy were calculated for the ylide 4. They are reported in Table 1. The difference between the experimental and theoretical data is relevant to the different media.

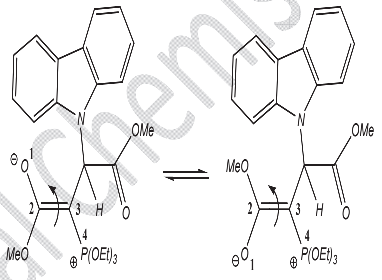

Z-4 E-4

Figure 3 The rotational interchangeable processes for the two isomers (Z and E) in the ylide 4

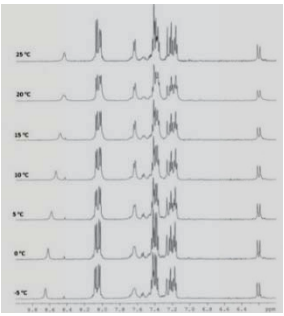

Figure 4 Performance of coalescence temperature in ^1H NMR spectrum of ylide 4.

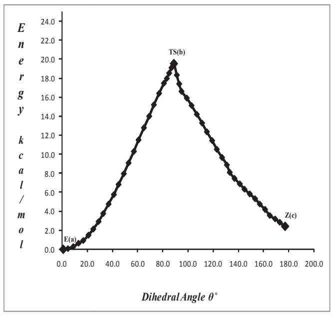

Figure 3 Relative energy in ylide 4 versus dihedral angels $O_1C_2C_3P_4$

Table 1. Selected ^{1}H chemical shifts (at 500.1 MHz, in ppm, Me_4Si) alon g with activation parameters in $CDCl_3$, for restricted rotational process around the carbon-carbon double bond(($(OEt)_3$ P–C$\neq$C–OMe).

		E_a (kcal/mol)	$\Delta S^{\neq}$ (cal/mol K)	$\Delta H^{\neq}$ (kcal/mol)	k_c (s^{-1})	$\Delta G^{\neq}$ (kcal/mol)	Δυ (Hz)	δ (ppm)	T_c (K)
Theoretical	**Process Forward** E ⟶ Z	19.39	-8.85	18.80	-	21.43	-	-	298
	Process Revert Z ⟶ E	18.85	-8.69	18.26	-	20.85	-	-	298
Experimental		15.98	-0.055	15.36	15.54	15.38	7.0	6.20, 6.21	291

Conclusion:

Dynamic ^{1}H NMR study of compound **4** confirmed a restricted rotation around the carbon-carbon double bond. Herein, the theoretical thermodynamic values from *ab intio* method at HF/6-31G(d,p) level of theory were in consistent with the experimental data. Although, there is a difference between theoretical thermodynamic values and those obtained experimentally by ^{1}H NMR, it is not unexpected, because of the different media. In experimental methods (^{1}H NMR) all thermodynamic data were obtained in solvent media ($CDCl_3$), but in theoretical method all parameters emerge from theoretical calculation in gas phase.

References:

[1]Maghsoodlou, M. T.; Hazeri, N.; Habibi-Khorassani, S. M.; Kakaei, R.; Nassiri, M. Phosphorus, Sulfur Silicon Relat. Elem. **2006**, 181, 25-30.

[2] Yavari, I.; Hazeri, N.; Maghsoodlou, M. T.; Souri, S. J. Mol Cat A **2006**, 264, 313.

[3] Yi-Yin, K.; Yu-Jin, L; Jian-Hong, J;Wei-Jian, S.; Liang, H.; Jian-Rong,G.*Tetrahedron lett.* **2009**, 50,1389-1391.

[4] Yavari, I.; Hossaini, Z.; Sabbaghan, M. *Tetrahedron Lett*. **2006**, 47, 6037-6040.

[5] Habibi-Khorasani, S. M.; Maghsoodlou, M. T.; Ebrahimi, A.; Farahani Vasheghani, F.; Mosaddeg, E.; Kazemain, M.A. TETRAHEDRON LETTERS **2009**, 50(26), 3621.

[6] Yavari, I.; Maghsoodlou, M.T.; J Chem Res 1998, (S), 386.

[7] Cervinka, O. In Roppoport, Z. Eds., The Chemistry of Enamines, Wiley: New York, 1994; Part 1. P 219.

theoretical investigation of 4-nitroacetanilide from the reaction between trialkyl phosphite and dimethyl acetylenedicarboxylate

F.Ghodsi; S. M. Habibi-Khorassani*
Department of Chemistry,The University of Sistan and Baluchestan, Zahedan, Iran.
E-mail:sm_habibikh@yahoo.com

Keywords: NH-containing heterocyclics; AIM; NMR; ab initio

Introduction:

Organophosphorus compounds are synthetic targets of interest, not least because of their value for a variety of industrial, biological, and chemical synthetic uses [1]. The physical properties and chemical reactivity of phosphonato esters interlink many areas in chemistry and biology.[2] The preparation of phosphonat0 ester compounds having two chiral centers via a one-pot reaction methodology is well-established.[3]. We now describe theoretical studies as a complementary investigation of stability compound **4a** (Figure 1).

Methods:

Quantum mechanical calculation has been performed using the Gaussian 03 and AIM2000 program packages.

Result and discussion:

The relative stabilization energies for both isomers for compounds**4a** have been calculated at the HF/6-31G(d,p) and B3LYP/6-311G(d,p) levels. The results are accumulated in Table 1. In addition, $J_{x\text{-}y}$, the values of proton and carbon coupling constants, and also chemical shifts (δ^{H}_{iso}, δ^{C}_{iso}) have been calculated at the mentioned level using the SPINSPIN keyword.

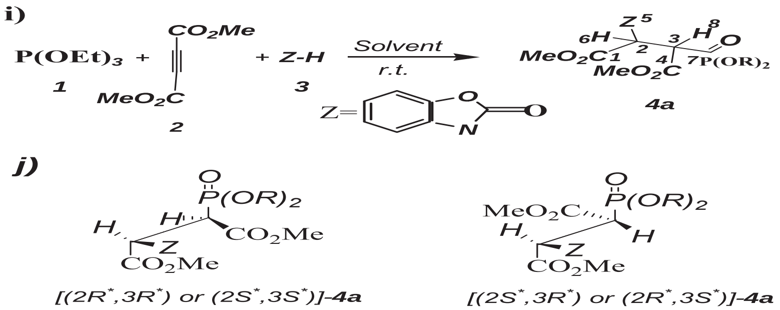

Figure 1. i) Synthesis of β-aminophosphonato esters **4a. j)** Two diastereomers with stereogenic centres **4a**.

Table 1.The relative energy (kcal/mol) between the two possible configurations 4a [(2S*, 3S*) or (2R*, 3R*)] or [(2S*, 3R*) or (2R*, 3S*)] obtained at the HF/6-31G(d,p) and B3LYP /6-311++G(d,p) levels.

compound	Configuration of 4a-	HF	B3LYP
4a	(2S*,3S*) or (2R*,3R*)-4d	5.3	4.6
4a	(2S*,3R*) or (2R*,3S*)-4d	0.0	0.0

Table 2. The values of ρ, $\nabla^2\rho$ and Hamiltonian -H(r) for both the configuration **4a** calculated at the BCP

[(2S*,3S*) or (2R*,3R*)]	$\rho\times10^3$	$\nabla^2\rho\times10^3$	$-H(r)\times10^4$	[(2S*,3R*) or (2R*,3S*)]	$\rho\times10^3$	$\nabla^2\rho\times10^3$	$-H(r)\times10^4$
1	5.0	19.0	7.4	1	8.7	36.0	13.2
2	2.4	8.1	4.3	2	4.2	18.1	8.8
3	8.7	37.2	13.8	3	10.1	35.3	3.9
4	4.2	19.5	9.5				
5	3.7	16.8	8.8				

Table 3. Selected ^{1}H NMR chemical shifts (δ in ppm) and coupling constants (*J* in Hz) for some functional groups in the [(2S*,3R*) or (2R*,3S*)] **4a** isomer

Groups	δ^H(ppm)	J_{PH}(HZ)	J_{HH}(Hz)
6H, t, 2OCH$_2$ CH$_3$	1.1^a(1.5)^b		
6H, 2s, 2OCH$_3$	3.7(3.5),3.8(3.7)		
1H, dd, P-CH	4.2(3.7)		11.5(12.7)
1H, dd, CH-CH-P	5.4(4.7)	5.7(5.8)	11.5(12.7)
4H, m, Ar	7.1-7.3(7.4-7.5)		

[a] Experimental data in accord with the 1H NMR spectroscopy

[b]: Theoretical data

Table 4 .Selected ^{13}C NMR chemical shifts (δ in ppm) and coupling constants (*J* in Hz) for some functional groups in the [(2S*, 3R*) or (2R*, 3S*)] **4a** isomer

Groups	δ^c(ppm)	J_{Pc}(Hz)
2d, 2OCH$_2$ CH$_3$	**15.9^a (17.1)^{b}16.0^a(17.8)^b**	
d, P-CH	**43.8 (40.2)**	
2s, 2OCH$_3$	**53.2(48.0)53.6(48.0)**	
d, P-C-C	**53.7(49.4)**	
2d, POCH$_2$ CH$_3$	**63.3(55.2),63.5(55.7)**	**6.9(7.4)**
4s, C$_6$H$_4$	**109.2(109.0),110.2(111.3),122.8(120.9),123.9(123.7)**	

[a] Experimental data in accord with the ^{13}C NMR spectroscopy

[b]Theoretical data

Conclusion:

Quantume mechanical calculation at HF and B3LYP levels of theory exhibited **4a** with [(2S*, 3R*) or (2R*, 3S*)] geometries are more stable, therfore, a lone isomers of **4a** with anti HCC H arrangment is reasonable. These results were agreement with the NMR experimental data.

References:

[1] Holmes, R. *Acc. Chem. Res*. **2004**, 37, 746-753.

[2]Yavari, I.; Hossaini, Z.; Karimi, E. *Monatsh. Chem*. **2007**, 138, 1267-1271.

[3]Maghsoodlou, M. T.; Habibi-Khorassani, S. M.; Heydari, R.; Rostami Charati, F. *J. Chem. Res*. **2006**, 364-365

Dynamic ^{1}H NMR along with Theoretical Study around the Carbon-Carbon Double Bond in the New Stable Phosphorus Ylide Derived from Hexamethyl Phosphorous Triamid

F.Ghodsi ; S.M.Habibi-Khorassani*; M. Fazilatkhah
Department of Chemistry, The University of Sistan and Baluchestan,
E-mail address: sm_habibikh@yahoo.com

Keywords: Dynamic ^{1}H NMR, solvent, Rotational energy barrier, ab initio

Introduction:

Ylides usually exist as a mixture of the two geometrical isomers (**Z** and **E**). These compounds exhibit dynamic ^{1}H NMR effect [1] that affords good information regarding the interchangeable process of rotational isomers that provide important kinetic data. We now describe theoretical studies [2] as a complementary investigation on the basis of rotation around the carbon-carbon double bond in a phosphorus ylide 4a.

Methods:

Quantum mechanical culations has been performed using the Gaussian 03 at HF and B3LYP.

Results and Discussion:

Synthesis of ylide **4a** involving the two Z- and E-geometrical isomers [3] is shown in (Figure 1). In order to determine theoretical rotational energy barrier in the rotational interchangeable processes of the two Z- and E-isomers in ylide **4a**, first their structures were optimized at HF/6-31G(d,p) and B3LYP levels of theory by Gaussian 03 program package. Then, relative energy was plotted versus dihedral angle (O1C2C3P4, see Figure 1) which is shown in Figure **2.** The plot in Figure 2 was obtained by scanning method at HF/6-31G(d,p) level of theory by Gaussian 03 and each point was fully optimized in the relevant Figure. As can be seen, only one transition state (TS) has been appeared on a maximum point of this plot (Figure 2). These results have been compared with the experimental data that was obtained by dynamic ^{1}H NMR data[14] (Table 1). For better comparison of theory and experimental, in addition to the gaseous phase, calculation performed in solution environment ($CDCl_3$) in Table **1** for the ylide **4a**. There is a good agreement between the activation energy in both theoretical and experimental data.

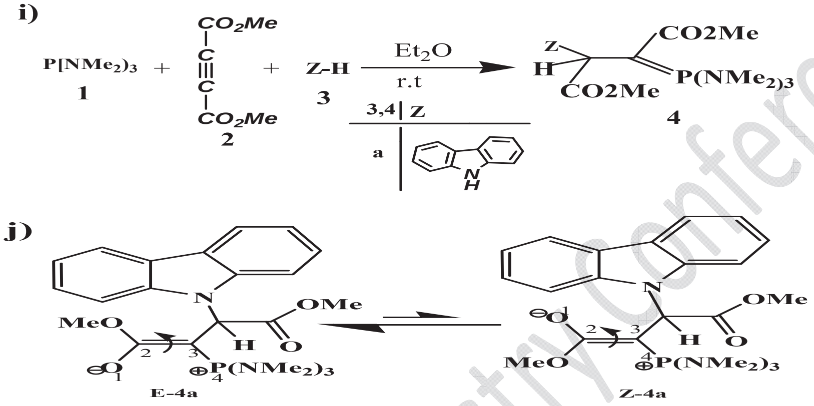

Figure 1. i) Synthesise of compound 4a. j) Interchangeable process between the two **E-4a**, **Z-4a**

Table 1. Selected ^{1}H chemical shifts (at 500.1 MHz, in ppm, Me_4Si) along with activation parameters in $CDCl_3$, for restricted rotational process around the carbon-carbon double bond $(NMe_2)_3P–C=C–OMe$) in ylide **4a**.

	E_a(kj/mol)	$\Delta S^{\#}$ (K J/mol)	$\Delta H^{\#}$ $^{\#}$(kJ/mol)	$\Delta G^{\#}$ $^{\#}$(kJ/mol)	Δ υ(Hz)	ppm(δ)	T_c (K)
Experimental[a]	76.7±1	0.028	74.1	65.5±1	25.00	5.67, 5.72	310
Theoretical[b]	42.33	-0.006	39.86	41.80	–	–	298
Theoretical[c]	42.26	-0.007	39.79	41.90	-	-	310
Theoretical[d]	39.85	-0.20	37.28	45.84	-	-	310
Theoretical[e]	34.72	-0.007	32.15	34.20	-	-	310
Theoretical[f]	33.55	-0.01	30.98	34.13			310

[a] On the basis of reports on literature[3]

[b] Data obtained using *ab initio* method at HF/6-31G(d,p) level of theory at 298 K for synthesized ylide 4a.

[c] Data obtained using *ab initio* method at HF/6-31G(d,p) level of theory at 310 K for synthesized ylide 4a.

[d] Data obtained using *ab initio* method at HF/6-31G(d,p) level of theory at 310 K for synthesized ylide 4a in ($CDCl_3$).

[e] Data obtained using *ab initio* method at B3LYP/6-31G(d,p) level of theory at 310 K for synthesized ylide 4a.

[f] Data obtained using *ab initio* method at B3LYP/6-31G(d,p) level of theory at 310 K for synthesized ylide 4a in ($CDCl_3$)

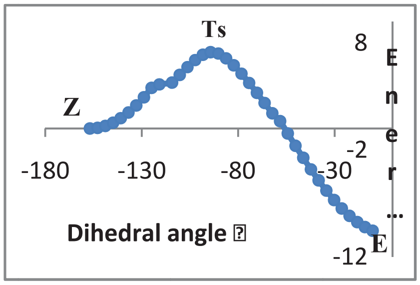

Figure 2 Relative energy in phosphorus ylide **4a** versus dihedral angels O1C2C3P4

Conclusion:

There is different between theoretical values and those obtained experimentally by ^{1}H NMR, it is not unexpected, because for huge molecular structure of ylide 4 employment of higher level of theory with basis set higher than HF/6-31G(d,p) and B3LYP/6-31G(d,p) levels is impossible. This limitation causes a small difference between both the experimental and theoretical data.

Refrences:

[1] Habibi-Khorasani, S. M.; Ebrahimi, A.; Maghsoodlou, M. T.; Same-Salari, S.; Nasiri, S.; Ghasempour, H. Magnetic Resonance in Chemistry **2011**, 49(5), 213-220.

[2] HabibiKhorassani, S. M., Ansari Fard, M., Mohammadi, M., Aghdaei, E., Shahraki, M., Hadizadeh, M., Hazeri, N., Jordan of chemistry, 7, PP. 23-32, (2012)

[3] Ziyaadini, M.; Maghsoodlou, M. T.; Hazeri. N.; Habibi-Khorassani. S.M.; Hetroatom Chem **2011**, 131-137

Linear and nonlinear optical properties of stilbazolium derivatives

M. Khedmati*[a] and N. khedmati[b]

[a]Department of Medicinal Chemistry, Faculty of pharmacy, Tabriz Medicinal University, Tabriz, Iran
Email: khedmati149@gmail.com.
[b]Department of Chemistry, Faculty of Science, Urmia University, Urmia, Iran.

Key words: Nonlinear optical properties; stilbazolium; Hartree-Fock; DFT.

Introduction:

Molecular organic materials having nonlinear optical (NLO) properties are required for applications in emerging optoelectronic and photonic technologies. NLO are useful because they allow the manipulation of laser beams, e.g., in frequency doubling or second harmonic generation (SHG), a quadratic effect. Among known NLO compounds, stilbazolium salts are particularly attractive for use in devices. Stilbazolium chromophores have been incorporated into various macroscopic structures such as Langmuir-Blodgett (LB) films, intercalated layer materials, self-assembled superlattices, inclusion complexes and guest-host and side-chain polymer films. With the sole exception of a theoretical study on the N-alkyl stilbazolium salts only N-aryl stilbazolium salts have been previously studied for their NLO properties.[1]

The present study is dedicated to perform a theoretical investigation about the linear and nonlinear optical (NLO) properties, represented as, dipole polarizability α, firsthyperpolarizability β and second hyperpolarizability γ, respectively, *trans-4′-(R)-N-methyl-4-stilbazolium* (R = Brome Br, methyl Me, Amino NH_2, Dimethylamino NMe_2, Hydroxy OH, Methoxy MeO). With this aim, we make a comparative study between the properties of these molecules to rationalize the differences in their properties in terms of the *R* group into the 1-methyl-4-styryl-pyridinium.

Computational details:

The linear and nonlinear optical (NLO) calculations were performed with the GAUSSIAN 03W software package[2], using Hartree-Fock (HF) and DFT(B3LYP) combined with the standard STO-3 G, 3-21 G, 6-31+G(d), 6-311++G(d,p) basis set. All the calculations are performed by using the Gaussian 03W program package on a personal computer.

Results and Discussion:

Static dipolar polarizability and firsthyperpolarizability in gas phase useing HF and B3LYP method (Fig. 1-4) indicate α and β values increase as the electron-accepting ability of R groups increases. Additionally, the high curve (6-31 G/SCRF) shows α and β values in methanol solvent. Fig 5 also displays the change β values with the substituent in the banzen solfunat as polar solvent. These data indicate that the dipole polarizability of this molecule is influenced by the nature of solvent. In particular, in the solvent of high polarity the α increases, while in the low polarizability solvent as THF, this property decreases [3]. Little discrepancies there exists between the theoretical values obtained with different basis sets results and the experimental ones. These differences are due to the electrostatic interactions that are present in the liquid phase and are not considered in the gas phase theoretical calculations.The differences between these β values and the corresponding experimental data are in agreement with the results of Duan et al.[4] Second hyperpolarizability (γ) were also calculated as can observe in Table 1. These results shown that the molecule presents larger second hyperpolarizability, have larger firsthyperpolarizability (β) too.

Conclusions:

We have presented a theoretical study of the linear (α) and nonlinear (β, γ) static optical properties of stilbazolium derivatives. The α and β static properties were calculated at *ab initio* HF and DFT methods with the B3LYP approaches and comparison between their properties was done. The effect of solvent polarizity on α and β values is studied. The results showed good agreement between the experimental and theoretical data that indicating the validity of the DFT and HF levels of theory and basis applied to stilbazolium molecule optical properties data.

Reference:

[1] B. J. Coe etal.; *Adv. Funkt. Mater*. 12, 109-116, 2002.

[2] Gaussian Inc., *Gaussian 03 program*, Gaussian Inc., Wallingford, 2004.

[3] L. Chmurzynski., *Molecules* 2, 169 ,1997.

[4] X. M. Duan and etal., *J. Opt. Soc. Am. B* 17, 256,2000.

Ab initio calculations of pyridine chloroderivatives and their ^{35}Cl NQR parameters

M. Khedmati*[a] and N. khedmati[b]

[a] Department of Medicinal Chemistry, Faculty of pharmacy, Tabriz Medicinal University, Tabriz, Iran
[b]Department of Chemistry, Faculty of Science, Urmia University, Urmia, Iran.
Email: khedmati149@gmail.com.

Key words: ^{35}Cl NQR frequency; ab initio calculations; pyridine chloroderivatives; CNDO.

Introduction:

The chemistry of pyridine derivatives has been recently reviewed. Despite *p*-Cl2C6H4 molecule has been theoretically characterized [1], no report has been published so far about the corresponding NQR studies of pyridine monochloro derivatives. In the present investigation detailed quantum chemical calculations including geometrical optimization, ^{35}Cl NQR frequency and thermodynamic parameters were performed using density functional theory calculations.The theoretically calculated ^{35}Cl NQR frequency values were evaluated and compared with the available experimental and semiexperimental (Complete Neglect Of Differential Overlap, CNDO) data.

Computational details:

All the calculations are performed with the Gaussian 03W software package11,[2] using second order perturbation Møller–Plesset MP2 methods, DFT(B3LYP) and HF levels combined with the 6-31G(d), 6-31+G(d), 6-311G(d), 6-311+G(d) basis set.

Results and Discussion:

Geometrical parameters :

The labeling of atoms in (α, β, γ)–Cl-Py is given in Figure 1. The bond lengths and angles determined at the DFT level of theory are in good agreement with the X-ray data. From the theoretical values we can find that most of the optimized bond lengths are slightly longer or shorter than the experimental values at the MP2, HF and DFT levels, due to the fact that the theoretical calculations belong to isolated molecules in gaseous phase and the experimental results belong to molecule in solid state.

^{35}Cl NQR frequency:

The ^{35}Cl NQR frequency calculations were performed and the values obtained were compared with experimental and data and the CNDO data are listed in Table 1. The results showed excellent agreement between experimental and computed frequencies.[3] The best method for each derivatives have been made.

Thermodynamic Properties:

Several calculated thermodynamic parameters are presented in Table 2. The energy gap between the highest occupied (HOMO) and the lowest unoccupied (LUMO) molecular oribtals characterizes the molecular electrical transport properties because it is a measure of electron conductivity. The energy gap is largely responsible for the chemical and spectroscopic properties of the molecules. The large value of band gap reflects the chemical unactivity of the pyridine derivatives.

Conclusion:

The results showed good agreement between the experimental and theoretical data indicating the validity of the DFT level of theory and basis applied to pyridine chloroderivatives for prediction of both structural and spectroscopic data of the title compound. Estimations of the^{35}Cl NQR frequencies and thermodynamic parameters have been made. Similar calculations were also performed for pyridine molecule, and comparison between their properties was made.

Reference:

[1] S. Youssif; *Organic Chemistry*, *Arkat Foundation, Aarkivoc e- Journal*., 12, 1,2001.
[2] Gaussian Inc., *Gaussian 03 program*, Gaussian Inc., Wallingford, 2004.
[3] V.A. Kirillovich and etal; *A. Bull.Russ.Acad.Sci.Div.Chem.Sci*., 41, 846-849,1992.

Molecular dynamic simulation of Human Lysozyme: insight into the thermal stability of enzyme

R.roohizadeh[a*], M.R.Dayer[b]
[a]Department of Chemistry, Islamic Azad University,Abadan,Iran
[b]Department of Biology, Faculty of Sciences, Shahid Chamran University, Ahvaz, IRAN
Email: razieh_roohizadeh@yahoo.com

Keywords: Human Lysozyme, Molecular Dynamics, Protein Stability, Solvent Accessible Surface.

Introduction:

Understanding the dynamic of protein has been a subject of study in both theoretical and experimental biophysics[1]. Computer simulations act as a bridge between microscopic length and time scales and the macroscopic world of the laboratory. In this work, we have performed molecular dynamic simulation and component analysis of the Human Lysozyme enzyme in solution of salts and ethanol. Human lysozyme itself is a relatively simple structure made up of 130 residues.This protein is present in high concentration in various tissues and fluids including liver, articular cartilage, saliva and tears[2]. Its native structure consists of two domains: an alpha-domain that has four alpha-helices (A–D) and one 3/10 helix, and a betadomain, which consists mainly of an antiparallel betasheet and a long loop.

Materials and methods:

The building of the protein models and all their simulations are carried out with the GROMACS suite of programs, installed on ubuntu linux. The ffgmx force field is used to describe the atomic interactions. The Lysozyme coordinate used in this work was obtained from RCSB protein data bank. the protein was equilibrated in a cubic box. Energy minimization was carried out using steep integrator before running the full simulation of up to 2ns.

Apparatus:

GROMACS 3.0 is the latest release of a versatile and very well optimized package for molecular simulation. All binary files are independent of hardware endian and can be read by versions of GROMACS compiled using different floating-point precision.

Result and discussion:

In order to investigate the structural stability and optimal activity of lysozyme, we stretched protein in different environment such as variant temperature(37°,50°,63° and 70°), also we were simulated the enzyme at molar solutions containing explicit water and 0-1.5 M salt concentrates like NaCl and CaCl2, monohydric alcohol(ethanol) with 20% and 80% purity. The analyses of some important structural characteristics, such as the fluctuation, Hydrogen Bonding, RMSD, the radius of gyration (Rg) of the protein, the hydrophobicness of the residues, the solvent accessible surface area (SASA) in different temperatures and situations have been considered. We were observed, notable tips about optimal condition that decrease number of hydrogen bonding between lysozyme molecule as much 5-6%, significant emersion of hydrophobic forces on protein surface, 65% increase in gyration radius which is swelling like state of lysozyme and in more time and vast fluctuation in atoms that contact with solvent or flexibility change induced by hydration. Of course for access to optimal condition, these properties have been compared with 37°c simulation

Conclusion:

We would demonstrate without salt, thermal activity of lysozyme is 50°C. This result is also in very good accordance with the experimental data available. In the present of either NaCl and CaCl2, enzyme optimal activity is transferred to another temperature such as at 0.5M CaCl2 and 1.5M NaCl, the stability of protein structure is significantly enhanced at 63°C. this agent, increase industry usage of human lysozyme. Finally increase ethanol until 80% plays important role in decrease of optimal temperature for activity of lysozyme and generally decreases the thermal denaturation.

Refrence:

[1] A.Ghosh and et al; "Dynamics of Lysozyme Structure Network: Probing the Process of Unfolding; Indian Institute of Science;2007

[2] M. Giampaolo and et al; "Lysozyme: A paradigmatic molecule for the investigation of protein structure, function and misfoldingB; University of Pavia Acta 357,168-172, 2005.

A comparative study of chemical shifts in 2-substitude pyrrole stable phosphorus ylide: ^{13}C and ^{1}H NMR GIAO c.s methods

Mehdi Shahraki*, Sayyed Mostafa Habibi-Khorassani, Younes Ghalandarzehi
Department of Chemistry, Faculty of Science, University of Sistan and Baluchestan, P.O.Box 98135-674,
Zahedan, Iran Email: meh_shahraki@yahoo.com

Keywords: GIAO; ^{13}C NMR; ^{1}H NMR; Ylide; Chemical shift

Theoretical calculation of NMR parameters has been under development for over three decades. Quantum theory-based calculation of NMR parameters is now a mature approach that can significantly widen the interpretative and analytical power of one of the most important spectroscopic techniques. The gauge-including atomic orbital (GIAO) method is one of the most successful approaches for calculations of chemical shifts. [1,2]

It has been shown to provide results that are often more accurate than those calculated with other approaches, at the same basis set size. In most cases, in order to take into account correlation effects, post-Hartree–Fock calculations of organic molecules have been performed using (i) Møller–Plesset perturbation methods, which are very time consuming and hence applicable only to small molecular systems, and (ii) density functional theory (DFT) methods, which usually provide significant results at a relatively low computational cost. In this regard, DFT methods have been preferred in the study of large organic molecules, metal complexes and organometallic compounds and for GIAO ^{13}C c.s. calculations. Although the general principles and algorithms for computing nuclear shielding are widely described, very few papers have been focused on a comparison among different quantum chemical models, basis sets, consistent reproduction and prediction of the experimental ^{13}C and ^{1}H chemical shifts to be applied in the study of medium–large organic compounds. [3,4]

Because of the importance of pyrrole moiety and its derivatives in biological activity and organic polymers and also its antibiotic properties, we have earlier reported synthesis of 2-

substitude pyrrole stable phosphorus ylides (Fig. 1.) from reaction between pyrrole and acetylenic esters in the presence of triphenylphosphine in a mixture of water-acetone. [5] In this work, we carried out a series of calculations at the HF and DFT (B3LYP, mPW1PBE and mPW1PW9127) levels in the same geometry optimization (HF/6-31G(d,p)) on the product, which its experimental ^{13}C and ^{1}H chemical shifts have been reported in the literature. [5] Based on the present study, we suggest that, among the methods taken into consideration, the best prediction of the experimental ^{13}C and ^{1}H values is obtained at the mpW1PBE and mPW1PW91 levels using the 6–31G(d,p) basis set. The mPW1PW91/6–31G(d,p) and mpw1PBE/6–31G(d,p) approaches have proved to be the most efficient in predicting the ^{1}H and ^{13}C chemical shifts of the product taken into consideration, respectively, displaying both the lowest mean absolute error (MAE) parameters and the highest R^2 coefficients. (See Figure) This study showed huge synthesized compound as 2-substitude pyrrole stable phosphorus ylide may be well accounted for by a low-level structure optimization followed by a higher level single-point ^{13}C and ^{1}H GIAO c.s. calculations. The DFT methods considered here showed good performance in the ^{13}C and ^{1}H c.s. calculations and usually provided a better performance than the Hartree–Fock (HF) methods. In particular, the one-parameter hybrid mPW1PW91 and mPW1PBE functional afforded the best overlap between calculated and experimental ^{1}H and ^{13}C c.s values outcomes, respectively.

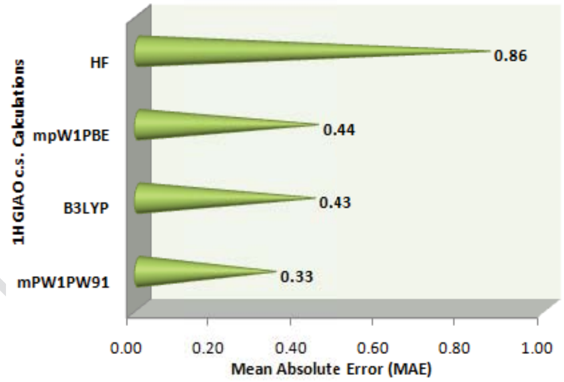

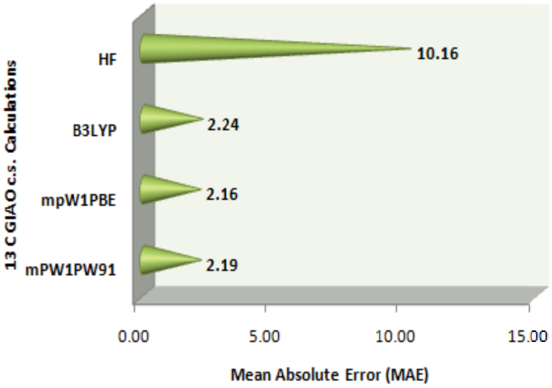

References:

[1] M. Kaupp, M. Bühl, V.G. Malkin, Calculation of NMR and EPR Parameters, Theory and Applications, Wiley-VCH, 2004.

[2] R.C. Mawhinney, G. Schreckenbach, Magn. Reson. Chem 42, 2004, 88.

[3] P. Cimino, L. Gomez-Paloma, D. Duca, R. Riccio, G. Bifulco, Magn. Reson. Chem 42, 2004, S26.

[4] Rodrigo Rotta , Álvaro Cunha Neto , Dênis Pires de Lima , Adilson Beatriz , Gil Valdo José da Silva. Journal of Molecular Structure 975, 2010, 59–62.

[5] M. T. Maghsoodlou, N. Hazeri, S. M. HabibiKhorassani, Z. Moeeni, Gh. Marandi, M. Lashkari, M. Ghasemzadeh, HR. Bijanzadeh, Journal of chemical research 2007, October, 566-568.

Theoretical Studies of Kinetics and Mechanistic investigation of the Reaction Between Triphenylphosphine, Dimethyl acetylenedicarboxylates and 3-chloroacetylacetone

O.Asheri * ,S.M.Habibi-Khorassani,M.A.Kazemian,Y.Ghalandarzehi
E-mail address: osmanasheri@yahoo.com
Department of chemistry, The University of Sistan and Baluchestan P.O.Box 98135-674,Zahedan,Iran

Keyword: Theoretical Study, Phosphorus ylides, Mechanism, Kinetics, activation parameters

Introduction:

Phosphorus ylides are reactive systems, which take part in many valuable reactions of the organic synthesis[1]. These are most often prepared by treatment of a phosphonium salt with a base. Most of the phosphonium salts are usually made from the phosphine and an alkyl halide and they are also obtained by the Michael addition of phosphorus nucleophiles to activated olefins[2].Experimental methods have many instrumental limitations such as trapping the intermediates or transition states in confirming the mechanism that reactions proceed from it. Computational methods can make confirming the mechanism easer, cheaper and exacter. Herein, we now describe a theoretical study of kinetic and mechanism of the reaction between triphenylphosphine and dialkyl acetylendicarboxylate in the presence of 3-chloroacetylacetone.

Computational methods :

Addition reaction between triphenylphosphine **1**, and dimethyl acetylenedicarboxylates **2**(**DMAD**) in the presence of 3-chloroacetylacetone **3** is shown in scheme 1 for generation **7**,**8** and **10** compounds as three possible products. All geometries of the reactants, products, intermediate and transition states (TS) involved in the reaction, were optimized at the HF/6-311G(d,p) level of theory in the gas phase. The vibrational frequencies of the species have also been calculated using the same level. The stationary points were classified as true minima if there are no imaginary vibrational frequency and Transition states were characterized by one imaginary vibrational frequency. The zero point energy (ZEP) of species was calculated with thermal correction at 298 K. All ab initio quantum calculations were carried using Gaussian03 program package[3]. The activation energies(E_a), the Arrhenius factors and rate constant were computed using Eq.(1)[a],(2)[b] and (3)[c] respectively[1], Which were derived from the transition state theory[4,5].

a : $E_a=\Delta H^{\neq}(T) + nRT$ (1)

b : $A=(ek_BT/h)\exp(\Delta S^{\neq}(T)/R)$ (2)

c: $k=(k_B.T/h)^{-\Delta n} \times \exp(\Delta H^{\neq}/RT)\times\exp(\Delta S^{\neq}/R)$ (3)

Results and discussion:

The structures of all reactants, products, intermediates and transition states optimized at HF/6-311G(d,p) level of theory. We carried out our calculations on Speculative theoretical proposed mechanism. For the step one the TS_1 energy is 29.51 and 20.54 kcal/mol higher than the energy of reactants and products, respectively. In the second step of reaction, hydrogen transfer is occurred from 3-chloroacetylacetone to dipole phosphonium ion for formation of C-H bond in intermediate namely phosphonium. In the process of proton transfer, the barrier is 33.91 kcal/mol and also the energy of TS_2 is 31.32 kcal/mol higher than products. In the third step of mechanism, the concerted reaction is started between two species ions namely phosphonium ion and 3-chloroacetylacetone ion for generating ylide. Activation energy for this step of mechanism is 9.93kcal/mol. After the third step, we were investigated two different pathway(A and B) for this reaction. Pathway A leads to structure 8 (see scheme 1). The TS_A energy is 33.97 and 27.00 kcal/mol higher than the energy of reactants and products respectively. This process is calculated to be endothermic by 6.97kcal/mol compared to the reactants, indicating that this step energetically not favorable process. Pathway B leads to structure 10 (see scheme 1). In the process of step B_1, the barrier is 21.69 kcal/mol and also the energy of TS_{B1} is 26.35 kcal/mol higher than products. The TS_{B2} energy is 7.00 and 31.68 kcal/mol higher than the energy of reactants and products respectively. This process is calculated to be exothermic by 24.68 kcal/mol compared to the reactants that implies that this step energetically favorable process. It should be noted here that all the transition states showed one imaginary frequency at same level of calculations, which implies that transition states are true.

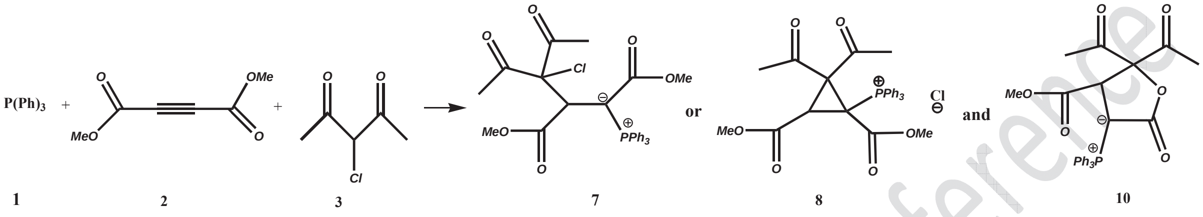

Scheme 1 Reaction between triphenylphosphine **1**, and dimethyl acetylenedicarboxylates **2**(DMAD) in the presence of 3-chloroacetylacetone **3** for generation of three possible products (7,8 and 10)

Conclusions:

Theoretical investigation of the reaction between triphenylphosphine and dimethyl acetylenedicarboxylates in the presence of C-H acid such as 3-chloroacetylacetone in the gas-phase leads to the following conclusions

1) With respect to the theoretical data, the second step of proposed mechanism (hydrogen transfer) was recognized as a rate-determining step with the energy barrier of 33.91kcal/mol.
2) In the third step of proposed mechanism, between two species ions namely phosphonium ion (I_2) and 3-chloroacetylacetone ion, we could recognize one TS due to specific structure of 3-chloroacetylacetone.
3) Pathway B that leads to the five-member ring structure energetically is favorable process in comparison with pathway A that leads to the three- member ring structure. With respect to the obtained theoretical data, this reaction will yield five member ring structure as a final product.

References:

[1]G.Marandi; M. T.Maghsoodlou; N Hazeri.;R.Heydari.; S. M .Habibi-Khorassani; A. Ebrahimi.;

S.Mollaeipoor; H .Hosseini-Mahdiabadi; M .Nassiri; R.Kabiri, Heteroatom Chem **2010**, 4, 228 – 235

[2] Habibi-Khorasani, S. M.; Ebrahimi, A.; Maghsoodlou, M. T.; S.Same-Salari; S.Nasiri, H.Ghasemp our,Magnetic Resonance in Chemistry **2011**, 49(5), 213-220.

[3] M. J .Frisch; G.W.Trucks; H. B.Schlegel;at all Gaussian, Inc, Wallingford CT, **2004.**

[4]S.Glasstone,K.J.Laider,H.Eyring,The theory of Rate Processes,McGraw-Hill,New York**. 1941**

[5]S.yamable,S.Okumoto,T.Hayashi, J.Org.Chem. 61(**1996**)6218

Chlorine Adsorption on Fullerene: A Density Functional Theory Study

H. Mehdizadeh*[a,b], M. E. Zand[a,b]
a Department of Chemistry, Payame Noor University, Shiraz, Iran
b Padidavaran Co. Fars Science and Technology Park, Shiraz, Iran
h.mehdizadeh@rocketmail.com

Introduction:

One of the most interesting discoveries of the last two decades is fullerene as a new form of carbon phase. Computational chemistry methods can be used to analysis of nano materials. Developments in electronic structure methods, in particular in density functional theory (DFT), with the continuous increase of available computing capacities to deliver unprecedented power to computational experiments on atomistic level[1,2]. Robustness of DFT makes this technique the method of choice in assisting the design and development of the next generation of devices for nanoscale applications.

The purpose of this investigation is to understand the nature of the interaction of chlorine with different sites at fullerene surface.

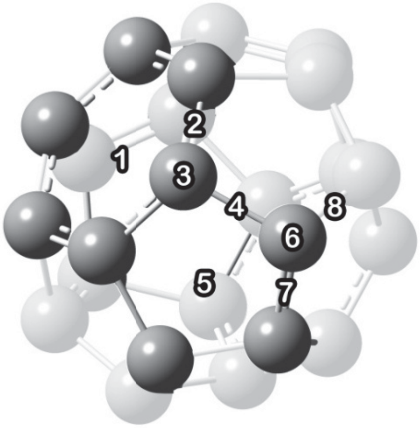

Figure 1. Labeling of C_{24} fullerene surface sites used in this study.

Methods:

Density functional theory (DFT) calculations by Gaussian09 were performed in order to optimize both fullerene and Cl_2 using the hybrid B3LYP functional with 6-311++ g** basis set without any symmetry restrictions in the singlet ground state. Calculated vibrational frequencies without imaginary frequencies ensure the stable structures. Boys-Bernardi's counterpoise procedure (CP) to correct for the basis set superposition error (BSSE) was indicated that the so-called overcorrection of the BSSE by the counterpoise method is not large.

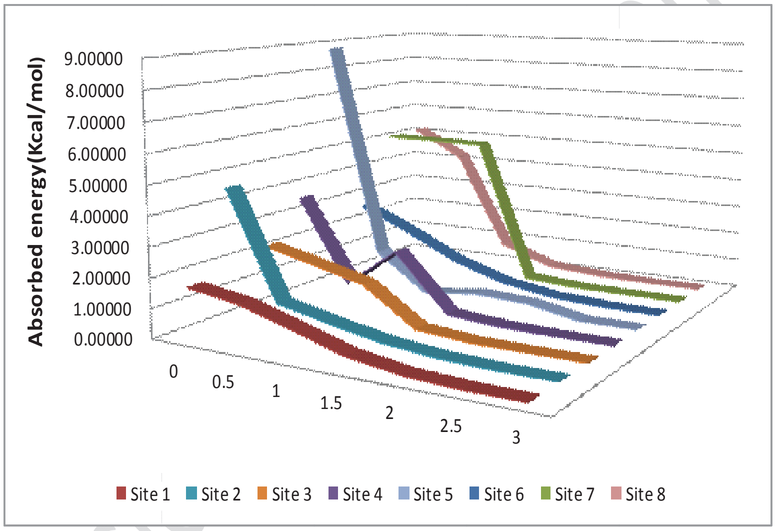

Figure 2. The graph of adsorption energy versus distance for different sites of fullerene.

Results and Discusions :

Binding energies were calculated via the difference in energy of fullerene /Cl_2 complexes from those of isolated fragments at different positions (see Figure 1), fragments were fully optimised at the B3LYP/6-311++ g** level. The Cl_2 are adsorbed vertically at different distances ranges from 0 to 3 Å as shown in Figure 2. The maximum adsorption energy is in the case of site 6. In the most stable structure the Cl_2 molecules is separated on average by 1.5 Å.

Conclusion:

From these and some detailed consideration we can conclude that fullerene is a good candidate for adsorption of CL_2 molecules. Chlorine interacts more strongly at site 5 of fullerene which is the center of a ring with five carbon atoms.

References:

[1] D.L. Klayman, Science 228 (1985) 1049.
[2]R. G.Parr and W. Yang, Density-functional theory of atoms and molecules ,Oxford Univ. Press, Oxford, 1989.

The effect of parallel external electric field on the aromaticity by density functional theory approach

Hossen Mehdizadeh*[a,b] , M. Erfan. Zand[a,b]
a Department of Chemistry, Payame Noor University, Shiraz, Iran
b Padidavaran Co. Fars Science and Technology Park, Shiraz, Iran
h.mehdizadeh@rocketmail.com

Keyword: Aromaticity, External electric field, Density Functional Theory

Introduction:

Although there is no exact quantum chemical definition, aromaticity is a widely used concept in chemistry including the theoretical chemistry community. This lack of a proper definition has led to many different perceptions of aromaticity, and many indices for its quantification have been introduced. These include structural indices, including the well-known harmonic oscillator model of aromaticity (HOMA)[1], reactivity and conceptual density functional theory (DFT)-based indices [2], and so forth. The nucleus independent chemical shifts (NICS)[3] suggests an increase of the molecular aromaticity from the outer toward the inner rings.Aromatic molecules exhibit characteristic responses with applied field. Owing to its D6h symmetry, benzene, although devoid of a permanent electric dipole moment, acquires an induced moment in the presence of an external electric field, which aligns the molecule in the direction of applied field. Of special importance in the present study, we have used NICS indices for investigation of the effect of external electric field on the aromaticity of benzene molecules.

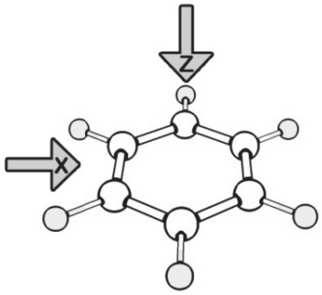

Figure 1. Orientation of field applied to benzene.

Computational method:

The influence of a uniform static external electric field on benzene molecules is studied within the density functional theory (DFT) employing the 6-311++G** basis set with B3LYP exchange-correlation prescription. All calculations have been performed in gas phase using Gaussian 09W package of program.

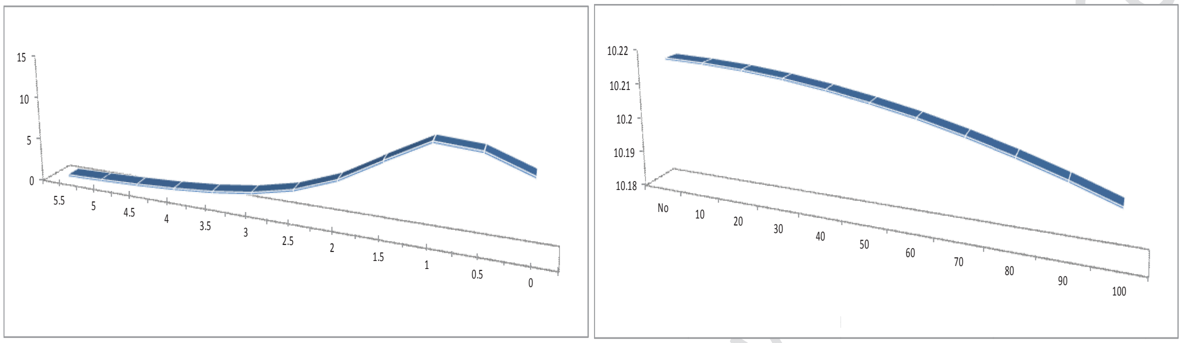

Figure 2. The aromaticity (vertical axis) as a function of field strength (write) and distance from benzene molecules (left).

Results and Discussion:

Density functional theory calculations are performed to investigate the effect of in the presence of external electric field on the aromaticity by using NICS method. We have used benzene as a model aromatic molecule. The results could be extended on a class of molecules with the same aromaticity. The strength of applied field was in the range of 10-100 V/nm. The aromaticity was obtained at different distances of benzene molecule. The obtained aromaticities ass a function of the field strength and distance from the benzene molecule are shown in Figure 2.

Conclusion:

Systematic investigations on the response of benzene molecules to an externally imposed electric field have been presented. The results show that the maximum aromaticity is occurred at the point, which is just 1Å far from the center of benzene ring. This indicates the presence of a region with high electron density which could be attributed to the delocalized p orbitals.

In addition, the aromaticity decrease as the parallel external field increases especially when the applied field is in the X direction.

These and more investigations on various properties of isolated molecules in external electric fields are hoped to be useful in understanding the characteristics of organic molecules use in molecular electronics.

References:

[1] Krygowski, T. M.; Cyranski, M. K. Chem. ReV. 2001, 101, 1355.
[2] de Proft, F.; Geerlings, P. Chem. ReV. 2001, 101 1451.
[3] Schleyer, P. v. R.; Manoharan, M.; Jiao, H.; Stahl, F. Org. Lett. 2001, 3, 3643.

Tautomerism of 6-azauracil in the gas phase and in methanol and water clusters: A theoretical study

B. Makiabadi [a*], M. Zakarianezhad[b], T. Ivazeh[b], E. Mohebbi[b]
a Department of Chemical Engineering, Sirjan University of Technology, Sirjan, Iran
b Department of Chemistry, Payame Noor University, Tehran, Iran
E-mail: bmakiabadi@sirjantech.ac.ir

Keywords: Tautomerization, 6-azauracil, Theoretical study

Introduction:

The synthesis and reactions of uracil and 6-azauracil derivatives has been the subject of great interest stemming mainly from their biological importance and the biological activity of aza analogues of uracil has been intensively investigated. [1]. Understanding the tautomeric equilibrium of nucleic acid bases is fundamental as the hydrogen bond interactions of DNA and several modeles of mutation of DNA are based on them. 6-Azauracil was formerly used as an antitumour drug. For this reason a number of biochemical works have been devoted to this compound [2]. In most of studies particular emphasis was laid on the hydration of isolated nucleic acid bases because it was proven that explicit water molecules in their first solvation shell have a clear influence in the electronic structure of the solute and in the tautomerization processes. For this reason we carried out a theoretical analysis in which the final goal was to establish the role of water and methanol molecules coordinated to the most suitable sites on four 6-azauracil tautomers in the lowering of the barriers for all the possible interconversion processes between them.

Methods:

Quantum chemical computations were carried out by employing the hybrid density functional B3LYP with the aug-cc-pVDZ basis sets with the Gaussian 03 series of programs. To take into account condensed-phase effects, single-point calculations were also performed on the gas-phase-optimized geometries using the polarizable continuum model (PCM).

Results and Discussion:

In this work, some tautomeric forms of 6-azauracil both in gas phase and in water (6-AU$(H_2O)_n$ and n=1,2,3) and methanol (6-AU$(MeOH)_n$ and n=1,2,3) clusters has been investigated theoretically. All electronic structures and energies for the reactant, transition state (TS) and product were computed at b3lyp/ aug-cc-pVDZ density functional level of theory. Results indicate that AU1 and AU5 species tautomers lie at lower and higher energy respectively. Two tautomeric structures (AU2 and AU3) in two different paths connect AU1 to AU5 (scheme 1). The solvent effect decreased the stability remains unchanged upon complexation with one, two, or three water and methanol molecules. Results indicate that all tatomerization processes are more likely to occur in solution instead of gas phase and are preferable in methanol. The relative energy profiles of the tautomerization of 6-azauracil in two water molecule is shown in scheme 2. Finally, the solvent effects as computed in a polarizable continuum were evaluated for all structures in ground and transition states. The barrier appears to be almost similar to that for the systems in gas phase but the process is thermodynamically more difficult. From the values of ΔG we calculated the rate constant of all tautomer conversions.

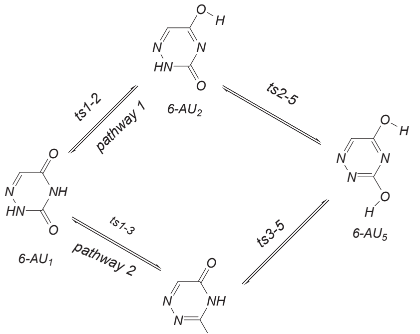

Scheme

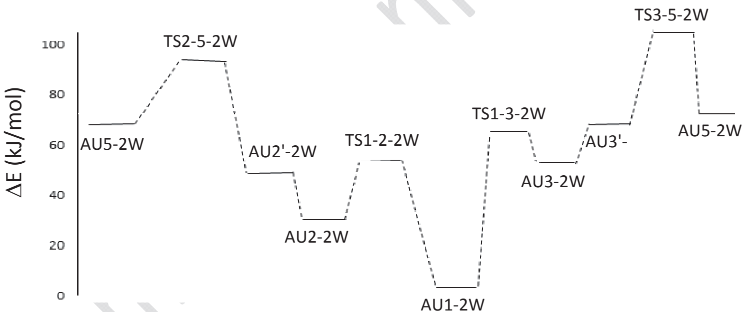

Scheme

Conclusions:

Results indicate that he keto forms of 6-AU are more stable than the enol forms both in the gas-phase and in water and methanol clusters. The order of stability of all structures remained unchanged in gas phase and in the presence of water molecules. Introduction of one and two water molecules greatly changes the picture of the whole process by progressively decreasing the energy barrier but, the priority of two parallel process remain unchanged in all pathways. Solvent establish hydrogen bonds with the bare molecule and these hydrogen bonds greatly facilitate intramolecular proton transfer process by reducing the barrier height. Furthermore, the solvent molecule facilitates the transfer of a proton by using its own hydrogen atoms.

References:

[1] H.Neunhoeffer; "Comprehensive Heterocyclic Chemistry II"; Pergamon, New York, 1996.

[2] M.Koshigami, K.Watanabe, T.Kimura, I.Yamamoto; "Central Depressant Effects of N3-Substituted 6-Azauridines in Mice"; Chem. Pharm. Bull; 39, 2597-2599, 1991.

Theoretical study on hydrated and self-assisted proton transfer mechanism in 4-methyl 2-thioimidazole

M. Zakarianezhad [a*], B. Makiabadi[b], E. Mohebbi[a], Asyeh Barkhoda[a]
a Department of Chemistry, Payame Noor University, Tehran, Iran
b Department of Chemical Engineering, Sirjan University of Technology, Sirjan, Iran
E-mail: mzakarianejad@pnu.ac.ir

Keywords: Tautomerization, 4-methyl 2-thioimidazole, Theoretical study, Proton transfer

Introduction:

The prototropic tautomerism represents one of the most important processes involved in chemistry reaction as well as in living system [1]. In particular, the thione/thiol tautomeric equilibrium, although less studied than their oxygen analogues, has attracted great experimental and theoretical interests. Among a number of physical and chemical factors that are responsible for the tautomeric equilibrium, solvation occupies one of the most important roles, because most biochemical reactions of interest occur in solution phase. 2-mercaptoimidazole and its derivatives has long been known to possess some interesting biological activities. Recently, some new 2-thioimidazole derivatives were synthesized. These new compounds show considerable antimicrobial activity against bacteria [2]. In our present work, a detail theoretical investigation is undertaken for the thione-thiol tautomerism of 4-methyl 2-mercaptoimidazole both in gas phase and in aqueous solution .

Methods:

Quantum chemical computations were carried out with the Gaussian 03 series of programs. Full geometry optimizations of stable species and transition states (TS) were performed in the gas phase by employing the hybrid density functional B3LYP with the 6-311++g(2d,2p) and aug-cc-pVDZ basis sets. Vibrational frequency calculations were carried out for all complexes at the B3LYP/6-311++g(2d,2p) and the B3LYP/aug-cc-pVDZ levels to calculate the zero point energy (ZPE). To take into account condensed-phase effects, single-point calculations were also performed on the gas-phase-optimized geometries using the polarizable continuum model (PCM) of Tomasi et al. To stablish the connection between the transition state structures and corresponding equilibrium structures, interinsic reaction coordinate (IRC) analysis was carried out at B3LYP/6-311++g(2d,2p) level of theory.

Results and Discussion:

Hydrated and self-assisted mechanism of proton transfer in this compound investigated at B3LYP/6-311++g(2d,2p) level of density functional theory. One and two explicit water molecules are considered association of in the thione-thiol tautomerism. Results indicate that the barrier height in direct proton transfer is significantly greater than self-assisted and H_2O-assisted one. Self-assisted and water-assisted proton transfer are preferable than the direct proton transfer both thermodynamically and dynamically. The binding water molecules will alter the relative thermodynamics stability of the thione/thiol tautomers. The interaction of thione tautomer with water molecules would dramatically decreases the tautomeric barrier height, but will increase the endothermicity of tautomeric reaction from thione to thiol. In all mechanism of proton transfer, binding energy of products is smaller than reactants. Thus effect of hydration and self-assisted is to favor the stability of the thione forms over than the thiols as same as the gas phase. The highest vibrational frequency in water-assisted complexes correspond to the O-H bonds of water, which are red-shift from that of isolated water.

Conclusions:

Results indicate that the hydrogen bond interaction in the self-assisted complexes is stronger than in water-assisted complexes. Direct proton transfer is more difficult than the water-assisted and self-assisted both dynamically and dynamically. The small negative value of *H(r)* shows some contribution of sharing interaction to the S···NH bond. The negative *H(r)* values for HBs increase on going from ground state to transition state and indicates that the HBs for transition states are stronger than ground states. There is an increase in the σ^* population of the N-H bond in dimers and trimers and O-H bond in W upon interaction 4-methyl 2-mercaptoimidazole.

References:

[1] A.Douhal, F.Lahmani, A.H. Zewail; "Proton-transfer reaction dynamics"; Chem. Phys. Lett.; 207, 477, 1996.

[2] M.A. Salama, L.A. Almotabacani; "SYNTHESIS AND CHEMISTRY OF SOME NEW 2-MERCAPTOIMIDAZOLE DERIVATIVES OF POSSIBLE ANTIMICROBIAL ACTIVITY" Phosphorus Sulfur and Silicon; 179, 305-319, 2004.

Theoretical study on hydrated and self-assisted proton transfer mechanism in 4-methyl 2-thioimidazole

M. Zakarianezhad [a*], B. Makiabadi[b], E. Mohebbi[a], Asyeh Barkhoda[a]
a Department of Chemistry, Payame Noor University, Tehran, Iran
b Department of Chemical Engineering, Sirjan University of Technology, Sirjan, Iran
E-mail: mzakarianejad@pnu.ac.ir

Keywords: Tautomerization, 4-methyl 2-thioimidazole, Theoretical study, Proton transfer

Introduction:

The prototropic tautomerism represents one of the most important processes involved in chemistry reaction as well as in living system [1]. In particular, the thione/thiol tautomeric equilibrium, although less studied than their oxygen analogues, has attracted great experimental and theoretical interests. Among a number of physical and chemical factors that are responsible for the tautomeric equilibrium, solvation occupies one of the most important roles, because most biochemical reactions of interest occur in solution phase. 2-mercaptoimidazole and its derivatives has long been known to possess some interesting biological activities. Recently, some new 2-thioimidazole derivatives were synthesized. These new compounds show considerable antimicrobial activity against bacteria [2]. In our present work, a detail theoretical investigation is undertaken for the thione-thiol tautomerism of 4-methyl 2-mercaptoimidazole both in gas phase and in aqueous solution .

Methods:

Quantum chemical computations were carried out with the Gaussian 03 series of programs. Full geometry optimizations of stable species and transition states (TS) were performed in the gas phase by employing the hybrid density functional B3LYP with the 6-311++g(2d,2p) and aug-cc-pVDZ basis sets. Vibrational frequency calculations were carried out for all complexes at the B3LYP/6-311++g(2d,2p) and the B3LYP/aug-cc-pVDZ levels to calculate the zero point energy (ZPE). To take into account condensed-phase effects, single-point calculations were also performed on the gas-phase-optimized geometries using the polarizable continuum model (PCM) of Tomasi et al. To stablish the connection between the transition state structures and corresponding equilibrium structures, interinsic reaction coordinate (IRC) analysis was carried out at B3LYP/6-311++g(2d,2p) level of theory.

Results and Discussion:

Hydrated and self-assisted mechanism of proton transfer in this compound investigated at B3LYP/6-311++g(2d,2p) level of density functional theory. One and two explicit water molecules are considered association of in the thione-thiol tautomerism. Results indicate that the barrier height in direct proton transfer is significantly greater than self-assisted and H_2O-assisted one. Self-assisted and water-assisted proton transfer are preferable than the direct proton transfer both thermodynamically and dynamically. The binding water molecules will alter the relative thermodynamics stability of the thione/thiol tautomers. The interaction of thione tautomer with water molecules would dramatically decreases the tautomeric barrier height, but will increase the endothermicity of tautomeric reaction from thione to thiol. In all mechanism of proton transfer, binding energy of products is smaller than reactants. Thus effect of hydration and self-assisted is to favor the stability of the thione forms over than the thiols as same as the gas phase. The highest vibrational frequency in water-assisted complexes correspond to the O-H bonds of water, which are red-shift from that of isolated water.

Conclusions:

Results indicate that the hydrogen bond interaction in the self-assisted complexes is stronger than in water-assisted complexes. Direct proton transfer is more difficult than the water-assisted and self-assisted both dynamically and dynamically. The small negative value of *H(r)* shows some contribution of sharing interaction to the $S^{\cdots}NH$ bond. The negative *H(r)* values for HBs increase on going from ground state to transition state and indicates that the HBs for transition states are stronger than ground states. There is an increase in the σ^* population of the N-H bond in dimers and trimers and O-H bond in W upon interaction 4-methyl 2-mercaptoimidazole.

References:

[1] A.Douhal, F.Lahmani, A.H. Zewail; "Proton-transfer reaction dynamics"; Chem. Phys. Lett.; 207, 477, 1996.
[2] M.A. Salama, L.A. Almotabacani; "SYNTHESIS AND CHEMISTRY OF SOME NEW 2-MERCAPTOIMIDAZOLE DERIVATIVES OF POSSIBLE ANTIMICROBIAL ACTIVITY" Phosphorus Sulfur and Silicon; 179, 305-319, 2004.

A comparative study of carbon, boron-nitride and silicon-carbide nanotubes based on surface electrostatic potential and QTAIM analysis

Sakineh Mohammadzadeh [a], Mehdi D. Esrafili*[,b]

[a] Department of Chemistry, Tabriz Branch, Islamic Azad University, Tabriz, Iran;[b] Laboratory of Theoretical Chemistry, Department of Chemistry, University of Maragheh, Maragheh, Iran. (E-mail:esrafili@maragheh.ac.ir)

Key words: Carbon nanotube; BNNTs; SiCNTs; QTAIM; Surface electrostatic potentials.

Introduction :

Since the discovery of carbon nanotubes (CNTs) by Iijima [1], numerous studies have been conducted on novel analogous tubular structures, such as boron nitride nanotubes (BNNTs) and silicon carbide nanotubes (SiCNTs) [2]. The BNNTs and SiCNTs have many advantages over CNTs because they possess high reactivity of the exterior surface ,facilitating sidewall decoration and stability at high temperature [3]. Due to different electronegativities of their atomic counterparts, BNNTs and SiCNTs can intrinsically be excellent sensors for detecting some harmful gases, such as CO, HCN [4], and O2 [5]. On the other hand, longer bond length of Si-C (1.80 Å) than those of B-N (1.44 Å) and C-C (1.42 Å) makes the SiCNTs a more proper candidate for applications in materials storage than the BNNTs and CNTs [6].
Noncovalent interactions, such as physical adsorption, are primarily electrostatic in nature [7]. In order to promote the nanotube applications mentioned above, it is essential to characterize in detail the electrostatic potentials on their surfaces. In this contribution, we report our theoretical study of electronic structures of zigzag (6,0) CNT, BNNT and SiCNT. From the set of theories with the capability of describing local variations of bonding, the quantum theory of atoms in molecules (QTAIM) approach was also selected for the current study.

Computational aspects:

All molecular orbital calculations were were performed using Gaussian 03 program [8]. The geometries of the investigated CNT, BNNT and SiCNT were optimized at the B3LYP level employing 6-31G* basis set. B3LYP/6-31G* electrostatic potentials were then computed on the surfaces defined by ρ(r)=0.001 electrons/bohr^3. Quantum theory of atoms in molecules (QTAIM) analysis for the optimized structures was performed at B3LYP/6-31G* level of theory using AIM2000 package [9].

Results and discussion:

Figure 1 shows the computed electrostatic potential maps on the three model nanotube surfaces (CNT, BNNT and SiCNT). In the case of the CNT, the electron-donating hydrogens cause the outer carbon surfaces to become negative, but only very weakly, usually averaging -2 to -4 kcal/mol. The insides of the open tubes are negative for the wider ones (but less so than the outsides), positive for the narrower. The hydrogens are the most positive portions of the open carbon tubes, with $V_{S,max}$ around 14 kcal/mol which accounts for the increased. On the other hand, the strengths and variabilities of the inner and outer surface electrostatic potentials increase considerably in going from carbon to BN and SiC tubes.

For the all CNT, BNNT and SiCNT examined here, QTAIM analysis indicates that the charge density accumulation for the axial bonds is slightly smaller than those of zigzag ones. The evaluated $\nabla^2\rho$ values for the zigzag bonds, on the other hand, are slightly greater than that of axial bonds.

Concluding remarks:

Our results indicated that the diversity of surface electrostatic potentials, differing in patterns and in strengths, that can be achieved by varying nanotube compositions and structures. There appears to be a definite opportunity to design tubes to fulfill specific functions involving noncovalent surface interactions, e.g. trapping or sensing particular toxigens, separating components of mixtures, etc.

Figure 1- Surface electrostatic potential maps of (a) (6,0) CNT, (b) (6,0) BNNT and (a) (6,0) SiCNT.

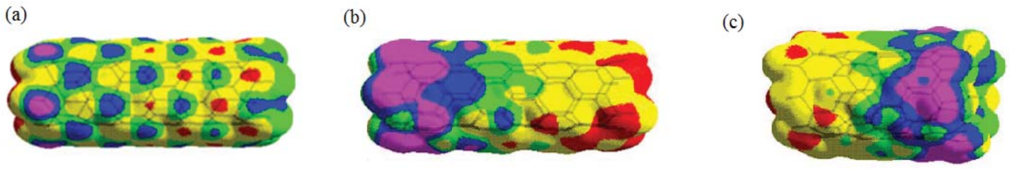

References:

[1]S. Iijima, Nature 354, 56 (1991).

[2]R. Arenala, X. Blaseb, A. Loiseaua. Mol. Phys. 59, 101 (2010).

[3]M. W. Zhao, Y. Y. Xia, F. Li, R. Q. Zhang, , Phys. Rev. B 71, 085312 (2005).

[4]M. Zhao, Y. Xia, F. Li, R.Q. Zhang, S.T. Lee, Phys. Rev. B 71, 085312 (2005).

[5]F. L. Cao, X. Y. Xu, W. Ren, C. Y. Zao, J. Phys. Chem. C 114, 970 (2010)

[6]G. Mpourmpakis, G.E. Froudakis, J. Samios, Nano Lett. 6 , 1581 (2006).

[7]G. Naray-Szabo, G.G. Ferenczy, Chem. Rev. 95, 829 (1995)

[8]M. J. Frisch, *Gaussian 03*, revision E.; Gaussian, Inc.: Wallingford, CT, 2004.

[9]F. Biegler-Konig, J. Schonbohm, and D. Bayles, J. Comput. Chem. 22 (2001) 545.

Study of Electronic and Dynamical Properties of Selenium Nanowires using Quantum Mechanics Method

F. Alavi, S. Jalili
Department of chemistry, K. N. Toosi university of technology, Tehran, Iran
email:fatemeh.s.alavi@gmail.com

keywords: electronic properties , selenium nanowires , density of states , ab-initio MD

Introduction:

The great interest in one-dimensional nanostructure such as nanotubes and nanowires is partly due to the possibility of their being used as active component in nanosize devices.

Although, carbon nanotubes and carbon nanowires are an interesting material, selenium nanowires also have special characteristics.

Selenium is an important semiconductor due to its unique properties, such as high photoconductivity, low melting point and nonlinear optical responses, so it has applications in a vast area including; xerography, photocells, photovoltaic cell, rectifiers, etc.

In this work, we calculated optical (optical conductivity), dynamical (vibrational spectra) and electronic properties (density of state, band structure and conductivity) of selenium nanowires.

Computational Methods:

All ab-initio molecular dynamic calculations were performed CPMD software within the framework of density functional theory. The generalized gradient approximation (GGA) is performed with a plane wave pseudopotential (PWP) method. For the interaction between the valance and core electrons, the ultrasoft pseudopotential is used and the Perdew-burke-Ernzerhof (PBE) functional is used to consider the exchange-correlation effect.

Results and Discussion:

We examined the electronic structure of Selenium systems in order to gain a better understanding of the nature of their bonding. Selenium nanowires have 21 atoms per unite cell in the periodic boundary conditions with hexagonal supercells. The band structure and the electronic density of state, in the energy range from -20 to 5eV for selenium nanowires are shown in fig 1.

The number of electrons in a unit cell of Se nanowires is 126, and at least 63 bands are needed to accommodate them. The energy levels are very close to each other, leading to spaghetti like band structure. The VB1 states are found to be S-like .The Fermi level is between bonding (VB2) and nonbonding (CB1) p-like states. Band gap of nanowires Se is found to be 1.2eV and thus Selenium nanowires is a semiconductor.

Figure 1.(a) electronic band structure of selenium nanowires .

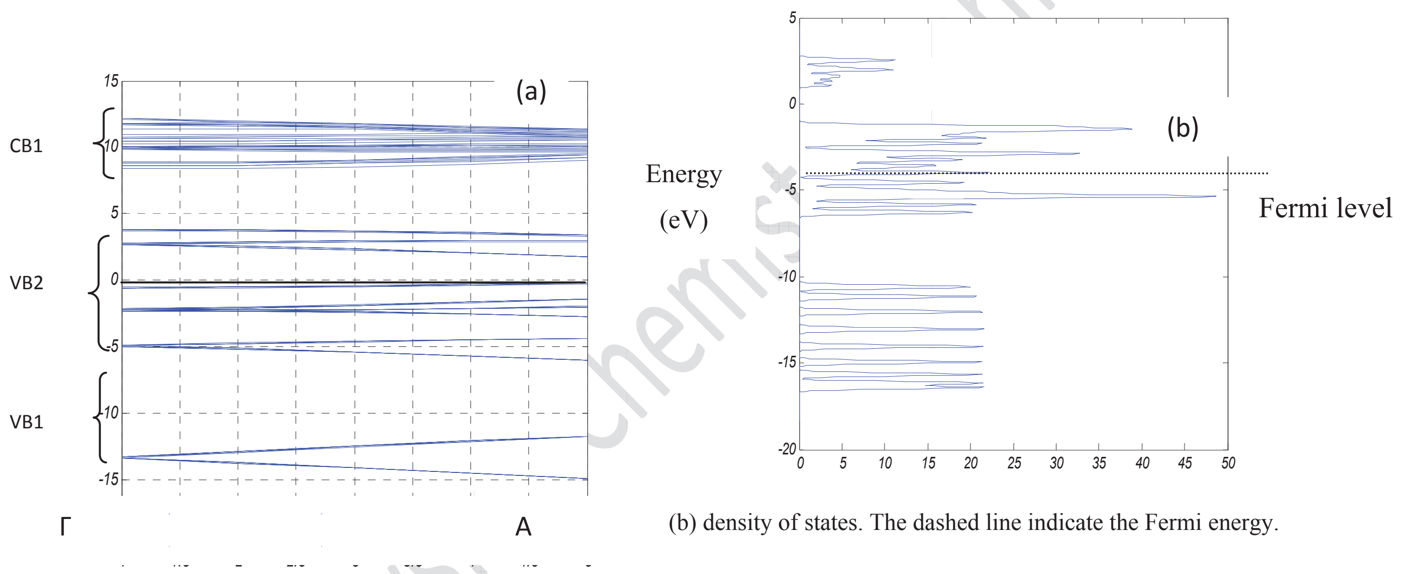

(b) density of states. The dashed line indicate the Fermi energy.

References:

[1]D. Marx , J. Hurtter ,Ab initio Molecular Dynamic;basic theory and advanced methods , 2009, Cambridge university

[2] R. Car and M. Parrinello. *Phys. Rev. Lett.*, **55**(22):2471–2474 (1985).

DOS (in arbitrary units)

Wave vector $\vec{k}$

The modeling of intermolecular potential CS2 - CS2 dimer using neuro – fuzzy methods

M. Dehestani* , M. Zbboli
Department of Chemistry, Shahid Bahonar University of Kerman, Kerman, Iran.
E-mail: dehestani2002@yahoo.com

Keywords: CS2–CS2, potential energy surface, SAPT,Fuzzy method, second virial coefficient

Introduction:

Symmetry adapted perturbation theory (SAPT) has been applied to compute the intermolecular potential energy surface (PES) of the CS2 dimer. Ab initio calculations have been performed with the aug-cc-pVDZ basis set. The model which created by fuzzy method has been used to compute second virial coefficient.

Result and discussion:

The SAPT interaction energy $\mathrm{E}_{\mathrm{int}}^{\mathrm{SAPT}}$ is calculated as follows: $\mathrm{E}_{\mathrm{int}}^{\mathrm{SAPT}} = \mathrm{E}_{\mathrm{int}}^{\mathrm{HF}} + \mathrm{E}_{\mathrm{int}}^{\mathrm{CORR}}$. We used the SAPT2 method in this study. The intermolecular potential energy of CS2 dimer is a function of four variables: R is the intermolecular distance between the centre mass of two monomers, α and β are the angles between R and the axis of the respective molecules A(CS2) and B(CS2), and a dihedral angle γ. Figure 1 shows radial dependence of the intermolecular energy surface E(R, α, β, γ).

We used 779 points to model PES in equilibrium bond length of C-S (re=2.9349 au). Our SAPT results indicate that the configuration of (α=90°, β=90°, γ=90°) is more stable than other configurations (Figure (2)).

Fuzzy method applied to create our model in MATLAB (2011a) program which expansion as:

$$E_{\mathrm{int}} = \sum_{i=1}^{11} w_i E_i \Big/ \sum_{i=1}^{11} w_i$$

$$w_i = A_{1i}(\theta_1) A_{2i}(\theta_2) A_{3i}(\theta_3) A_{4i}(R)$$

$$E_i = a_i\theta_1 + b_i\theta_2 + c_i\theta_3 + d_iR$$

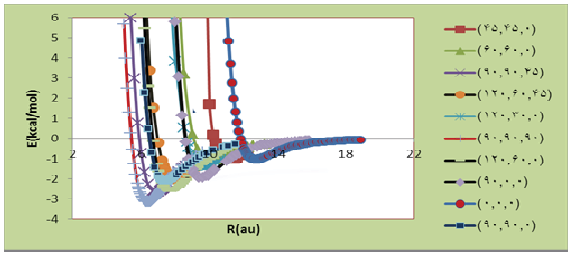

Fig (1). Radial dependence of the intermolecular energy surface

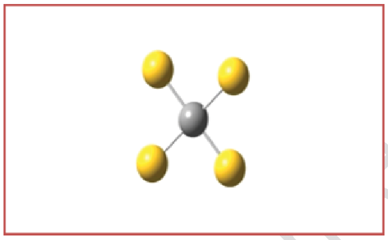

Fig (2). Configuration of (α=90°,β=90°,γ=90°)

where A_{1i}, A_{2i}, A_{3i} and A_{4i} are given by:

$$A_{1i}(\theta) = \exp[-(\theta-\mu_{\theta_i})^2/2\sigma^2_{\theta_i}] \qquad A_{2i}(\theta) = \exp[-(\theta-\mu_{\theta_2})^2/2\sigma^2_{\theta_i}]$$

$$A_{3i}(\theta) = \exp[-(\theta-\mu_{\theta_3})^2/2\sigma^2_{\theta_i}] \qquad A_{4i}(R) = \exp[-(R-\mu_{R_i})^2/2\sigma^2_{R_i}]$$

This model is used to compute the second virial coefficient. The second virial coefficients were calculated by using the classical formula:

$$B_2(T) = -N_A/4\int_0^\infty\int_0^\pi\int_0^\pi\int_0^{2\pi}\{exp[-V(R,\alpha,\beta,\Upsilon)/kT]-1\}R^2\sin\alpha\sin\beta dR\,d\alpha\,d\beta d\Upsilon$$

Where N_A is Avogadro's number and k is Boltzmann's constant.

The gaussian quadrature method was used to integrate over the angles, whereas a Romberg method, based on the trapezoidal rule, was used to integrate over the radial coordinate.

Conclusion:

As seen in Table 1, the calculated second virial coefficients have a good agreement with the experimental results

Table (1) Temperature dependence of the second virial coefficient B(T) (Experimental and Calculated values).

T(k)	Ref.(1)	Ref.(2)	This work
280.00	-930	-	-930.0
300.00	-796	-	-803.2
323.15	-	-700	-675.3
337.15	-	-605	-603.7
350.00	-567	-	-543.8

References:

[1] J. H. Dymond, E. B. Smith, The Virial Coefficients of Pure Gasesand Mixtures, Clarendon Press: Oxford, 1980.

[2] R. F. Hajjar, W. B. Kay, G. F. J. Leverett, Chem. Eng Data., 14, (1969) 377.

The effect of acidic environment on the repair process of O6 methyl guanine by cysteine

Ali Ebrahimi, Shiva Rezazadeh*
Department of Chemistry, University of Sistan and Baluchestan, Zahedan, Iran
Email: shiva_rezazadeh89@yahoo.com

Keywords: O6-methylguanine-DNA methyltransferase (MGMT), DNA damage, Cancer therapy, Methylating agent.

Introduction:

DNA damage that gives rise to aging and mutation is an important subject from the cancer therapy point of view [1]. DNA alkylation can be caused by both endogenous and exogenous DNA-damaging agents [2]. O6-methylguanine (O6mG) readily mispairs with thymine during DNA replication that causes GC → AT transversion mutation. It is known that the O6-methylguanine-DNA methyltransferase (MGMT) protein which is widely present in almost all organisms, efficiently repairs the O6mG lesions of DNA to guanine by transferring the methyl group from the O6 site of guanine to the cysteine residue (Cys145 in human MGMT) in an irreversible stoichiometric reaction [3]. This study is focused on the role of the acidic environment on the methyl transfer from O6mG to Cys145 on the repair process.

Computational details:

All structures were optimized by the Gaussian09 [4] program package using the hybrid density functional B3LYP and the 6-31+G* basis set. All stationary points verified by vibrational frequency analysis carried out at the same level of theory. All vibrational frequencies are positive for reactant and product complexes, and only one imaginary frequency is observed for transition states.

Results and discussion:

The stationary points corresponding to reactant **RC**, transition state **TS** and product **PC** have been considered along the repair mechanism of O6mG to guanine by three models. (1) Energy barrier in the presence of Cys145 is 34 kcal mol^{-1}. The most important geometrical parameters including O6C10 and S15C10 bond distances are equal to 1.45 and 4.91 Å, respectively, in **TS**. (2) The energy barrier decreases to 30 kcal mol^{-1} and the O6C10 and S15C10 bond distances change to 1.97 and 2.49 Å with the protonation of the N7 site of O6mG. (3) The protonation of both N7 and N3 sites of O6mG decreases the energy barrier of O6mG to 17 kcal mol^{-1} and changes the O6C10 and S15C10 bond distances to 2.05 and 2.56 Å. So, the O6C10 bond length increases with the protonation of O6mG and repair process is facilitated in the acidic environment.

Conclusions:

The Cys145 residue can repair O6mG to guanine in a S_N2 mechanism. The protonation of the N7 (or N3 & N7) site of O6mG, which increases the positive charge on the guanine, helps the methyl transfer from O6mG to Cys145. The energy barrier decreases considerably by the increase in the number of protonated sites.

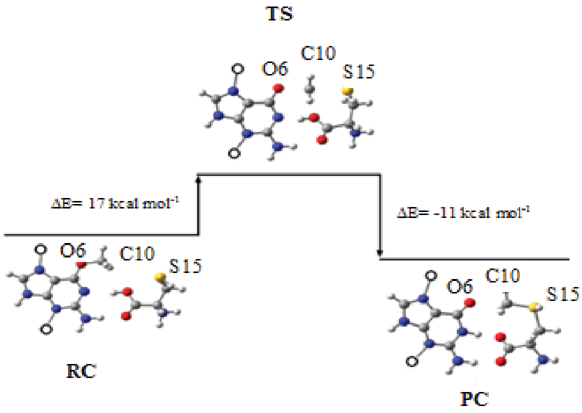

Figure 1. Repair of O6mG to guanine by Cys145; the protonated sites are shown in the guanine by hollow circles.

References:

[1] P. K. Shukla, P. C. Mishra,Phys. Chem. Chem. Phys., 11, 8191, 2009.

[2] M. D. Wyatt, D. L. Pittman, Chem. Res. Toxicol., 19, 1580, 2006.

[3] N. R. Jena, M. Bansal, Phys. Biology, 8, 1478, 2011.

[4] M. J. Frisch; et al.; Gaussian 09, Revision A.02; Gaussian Inc. Wallingford CT; 2009.

Quantum chemical computational studies on 2-[(4Methoxybenzyl)iminomethyl]phenol

Seyed NezamoddinMirsattari*, Iman Rajaie
Department of Chemistry,Islamic Azad University,Shahreza Branch,311-86145,Shahreza,Isfahan
Email: imanrajaie121@gmail.com

Key words: Density functional theory, Solvent effect, HOMO and LUMO energies,NBO.

Introduction:

The Schiff base compounds have been under investigation during recent years because of their potential applicability in many fields [1]. Investigations into the structural stability of these compounds using both experimental techniques and theoretical methods have been of interest for many years. With recent advances in computer hardware and software, it is possible to correctly describe the physico-chemical properties of molecules from first principles by various computational techniques. In recent years, density functional theory (DFT) has been a shooting star in theoretical modeling. The development of better and better exchange-correlation functionals made it possible to calculate many molecular properties with comparable accuracies to traditional correlated ab initio methods, with more favorable computational costs. In this article, we wish to report the theoretical studies on it by using DFT/B3LYP/6-31G** method. The properties of the structural geometry,conformation energies for optimized structures, molecular electrostatic potential (MEP), natural bond orbital (NBO) analysis,HOMO and LUMO energies andsolvent effects have also been taken into account by usingthe continuum model (PCM) and Onsager of five different solvent.

Computational method:

The DFT calculations with a hybrid functional B3LYP (Becke'sthree parameter hybrid functional using the LYP correlation functional) at 6-31G** basis set by the Berny method [2]were performed with the Gaussian 09W software package andGauss-view visualization program [3]. The calculated vibrational frequencies ascertained that the structures were stable (no imaginary frequencies).To determine the conformational energy profiles the optimized geometries were kept fixed, and values of the DFT energies were calculated as the functions of the torsion angles $\theta_1(C_{17}O_{16}\ C_{15}\ C_{14})$ from 0° to 360°, varied every 30°.To evaluate the energeticand dipole moments behavior of the title compound in solvent media, we carried out optimization calculations in the five kinds of solvent (chloroform,dichloroethane, ethanol, methanol,and water) by using polarizable continuum model (PCM) theory and Onsager [4]. The NBO charge distribution of the conjugated base of the molecule were also investigated.

Result and discussion:

The azomethine C=N bond distances is 1.286 Å.The C9-N8-C7 unit combining both phenyl groups hasa angle of 119.17 º[5].The optimized parameters (bond lengths and angles, and dihedralangles) of the title compound have been obtained by using theB3LYP/6-31G** methodand These results are compared with the experimental data of the title compound.These calculationsare valuable for providing insight into molecular properties ofSchiff base compounds.

Conclusion:

Density functional calculations have been performed for the title compound of 2-[(4-Methoxybenzyl) iminomethyl]- phenol and the calculated results show that B3LYP/6- 31G** method can reproduce the title compound well.The total energy of the title compound decrease with the increasing polarity of the solvent and the stability of the title compound increase in going from the gas phase to the solution phase.

Reference:

[1] H. Unver, A. Karakas, A. Elmali, J. Mol. Struct. 702 (2004) 49-054.

[2] H.B. Schlegel, J. Comput. Chem. 3 (1982) 214.

[3] R. Dennington II, T. Keith, J. Millam, GaussView, Version 4.1.2, Semichem, Inc., Shawnee Mission,KS, 2007

[4] S. Miertus, E. Scrocco, J. Tomasi, Chem. Phys. 55 (1981) 117.

[5]ChuttreePhurat,ThapongTheerawattananond and NongnujMuangsin.2-[(4-Methoxybenzyl) iminomethyl]- phenolActaCryst; E66, 3298-3303 (2010).

Comparing Anomeric Effects of halo[1,4]dioxane and halo[1,4]dithian in Solvent and Gas Phases

Y.shad[a*], S. Arshadi[b], O. Yazdani[c], S. M. Mosavi Farmad[a]
[a]Faculty of Chemistry, University of Mazandaran, Babolsar, Iran
[b]Department of chemistry, Payame Noor University, 19395-4697, I.R. of Iran
[c]Faculty of Chemistry, Razi Univercity, Kermanshah, Iran
[*]Email: h_shad_2007@yahoo.com

Keywords: Anomeric effect, Computation, Halo[1,4]dioxane, Halo[1,4]dithiane.

Introduction:

The replacement of carbon by other elements produces changes in several structural parameters such as stereo-chemical features and consequently affects the conformational characteristics of the molecule. The anomeric effect plays an important principal role in the stereo-chemical outcome by guiding the relevant electronegative substituents into an axial position [1-3]. Hence perception of the general rules that are controller of stereo-chemical effects, have great help in interpreting the properties of molecules and their reactivity.

Computational methods:

After primary design of this compounds (Fig. 1); halo-cyclohexane (Series 1), halo[1,4]dioxane (Series 1') and halo[1,4]dithiane (Series 1''), in the hyperchem software, computational method of HF/STO-3G in the Gaussian software has been used for doing primary computation of optimization. After obtaining structures with minimum energy and assurance that they are real, computation results of HF/STO-3G has been used as input for computations in theory levels of B3LYP/6-311++G**. Minimization of energy in ratio to all coordinates and without any symmetry constraints was done. Therefore structures with minimum energy were obtained. In order to perform salvation analysis of structures in series 1, 1' and 1'', their optimizations are carried out (solvents: chloroform, tetrahydrofuran and acetone), using the polarizable continuum solvation model (PCSM).

Results and discussion:

Energies (E), enthalpies (H) and free energies (G) for all series are done at the level B3LYP/6-311++G**. Using these data relative energies (E_r), enthalpies (H_r) and free energies (G_r) for all substituents (X) in gas phase are deliberate and presented in Table 1. In order to perform solvation analysis in selected solvents (chloroform; tetrahydrofuran and acetone); optimizations are carried out with polarizable continuum salvation model (PCSM) method for all series. The physical properties of the systems, such as free energies (sum of non-electrostatic and electrostatic interaction) are found. Relative free energies (G_r) for all substituents (X) in three solvents are presented in Table 2.

Table 1. Relative energies (E_r), enthalpies (H_r) and Gibbs free energies (G_r) for halo-substituted cyclohexanes (Series 1); halo-substituted 1,4-dioxane (Series 1') and halo-substituted 1,4-dithiane (Series 1") where X=F, Cl and Br [A (Axial) and E (Equterial)] & Y= C , O and S *via* B3LYP/6-311++G**. The lowest value of E, H and G for each substituent (X) is set at zero.

Halo-substituted cyclohexane (Series 1)				Halo-substituted 1,4-dioxane (Series 1')				Halo-substituted 1,4-dithiane (Series 1")			
	E_r **(kJ/Mol)**	H_r **(kJ/Mol)**	G_r **(kJ/Mol)**		E_r **(kJ/Mol)**	H_r **(kJ/Mol)**	G_r **(kJ/Mol)**		E_r **(kJ/Mol)**	H_r **(kJ/Mol)**	G_r **(kJ/Mol)**
F2E C	0.96	0.96	1.00	**F2E O**	8.95	8.95	8.87	**F2E S**	4.14	4.14	4.02
F2A C	0.00	0.00	0.00	**F2A O**	0.00	0.00	0.00	**F2A S**	0.00	0.00	0.00
Cl2A C	3.31	3.31	3.89	**Cl2E O**	7.95	7.95	7.78	**Cl2A S**	1.30	1.30	1.92
Cl2E C	0.00	0.00	0.00	**Cl2A O**	0.00	0.00	0.00	**Cl2E S**	0.00	0.00	0.00
Br2A C	3.51	3.51	4.10	**Br2E O**	9.54	9.54	9.33	**Br2A S**	2.13	2.13	2.55
Br2E C	0.00	0.00	0.00	**Br2A O**	0.00	0.00	0.00	**Br2E S**	0.00	0.00	0.00

Table 2. Relative solvation gibbs free energies (ΔG_r) calculated at the level B3LYP/6- 311++G** for structures in series 1, 1' and 1" in three solvents (chloroform, tetrahydrofuran and acetone) using the "polarizable continuum solvation model" (pcsm). The lowest Value of E, H and G for each substituent (X) is set at zero.

Chloroform	ΔG_r **(kJ/Mol)**	**Tetrahydrofuran**	ΔG_r **(kJ/Mol)**	**Acetone**	ΔG_r **(kJ/Mol)**
F2E C	0.33	**F2A C**	0.00	**F2A C**	0.04
F2A C	0.00	**F2E C**	0.00	**F2E C**	0.00
Cl2A C	3.85	**Cl2A C**	3.93	**Cl2A C**	3.97
Cl2E C	0.00	**Cl2E C**	0.00	**Cl2E C**	0.00
Br2A C	4.06	**Br2A C**	4.06	**Br2A C**	4.02
Br2E C	0.00	**Br2E C**	0.00	**Br2E C**	0.00
F2E O	9.41	**F2E O**	9.29	**F2E O**	9.54
F2A O	0.00	**F2A O**	0.00	**F2A O**	0.00
Cl2E O	9.67	**Cl2E O**	9.79	**Cl2E O**	10.46
Cl2A O	0.00	**Cl2A O**	0.00	**Cl2A O**	0.00
Br2E O	12.68	**Br2E O**	13.05	**Br2E O**	13.89
Br2A O	0.00	**Br2A O**	0.00	**Br2A O**	0.00
F2A S	0.17	**F2A S**	0.33	**F2A S**	1.80
F2E S	0.00	**F2E S**	0.00	**F2E S**	0.00
Cl2E S	0.84	**Cl2E S**	0.88	**Cl2E S**	1.17
Cl2A S	0.00	**Cl2A S**	0.00	**Cl2A S**	0.00
Br2E S	2.38	**Br2E S**	2.47	**Br2E S**	3.18
Br2A S	0.00	**Br2A S**	0.00	**Br2A S**	0.00

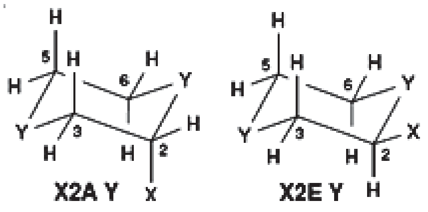

Fig. 1. Halo-substituted cyclohexane, 1,4-dioxane and 1,4-dithiane where X = F, Cl and Br [A (Axial) and E (Equatorial)] and Y = C (Series 1), O (Series 1′) and S (Series 1").

Conclusion:

In the series 1', difference between the most stable and unstablest compound is more than series 1". This result shown that anomeric effect in halo-substituted 1,4-dioxane is more than halo-substituted 1,4-dithiane. The solvation analysis illustrates that in polar solvents free solvation energy gaps are larger for series 1' in comparison to their corresponding gap of series 1 and 1". Generally, in the series 1' and 1" with increasing solvent polarity becomes larger free solvation energy gaps.

References:

[1] B.P. Prascher and A.K. Wilson, *J. Molecul. Struc. Theochem.*, **814**, 1 (2007).

[2] P.P. Graczyk and M. Mikolajczyk, *Top Stereochem.*, **21**, 159 (1994).

[3] S. Arshadi, Y. Shad, J. Emami, A.R. Bekhradnia , O. Yazdani, *Asian J. Chem*, 22, 1907 (2010).

On the nature of Mg-L interactions (L= BF, CO, N_2, NH_3 and H_2O): A symmetric-adapted perturbation theory (SAPT) study

Sirous Yourdkhani [a], Aidin. Bahrami [a], Mehdi D. Esrafili [b,*], and Nasser. L. Hadipour [a]
[a] Department of Chemistry, Tarbiat Modares University, Tehran, Iran; [b] Laboratory of Theoretical Chemistry, Department of Chemistry, University of Maragheh, Maragheh, Iran
(esrafili@maragheh.ac.ir)

Key words: Magnesium; SAPT; Mg-ligand interactions, Dispersion.

Magnesium (Mg) plays a prominent role in many structural and reactive biochemical processes. Over 300 enzymes require magnesium ions for their catalytic activity, including all enzymes utilizing [1], synthesizing adenosine triphosphate (ATP), or those that use other nucleotides to synthesize DNA and RNA [2]. Thus, an accurate and well-balanced theoretical description of the ligand binding ability and hydration of Mg(II) ions is required in order to increase our understanding of magnesium enzymology using the tools of computational quantum chemistry.

In this contribution, we report our theoretical study on geometries and electronic structures of Mg-ligand interactions. The main goal of this investigation is to provide reliable high level benchmark ab initio results for a set of 1:1 complexes in order to improve the energetic, structural, and electronic description of the ligand binding ability of a simplified chlorophyll model (Figure 1).

Computational Details:

All ab initio and DFT calculations were performed using Gaussian 03 package [3]. The geometry of the investigated various $Mg(CH_3N_2)_2L$ complexes was optimized at the MP2 level employing 6-311++G** standard basis set. The interaction energy for each complex was calculated at the HF, MP2, MP4, CCSD(T) and B3LYP levels of theory. For SAPT energy decomposition analysis, molecular integrals were first obtained with the DALTON 2.0 package [4]; SAPT partitioning was then performed using the SAPT2008 program [5].

Results and discussion:

Figure 1 shows the optimized structures for the complexes formed between Mg(CH_3N_2)$_2$ moiety and the neutral ligands (L= BF, CO, N_2, NH_3, and H_2O). From Figure 1, it is apparent that the estimated Mg–L distances are in a range of 2.127–2.711 Å which is much smaller than the sum of Van der Waals radii of corresponding counterparts. Table 1 lists the CP-corrected interaction energies obtained at the HF, MP2, MP4, CCSD(T), B3LYP, SAPT0 and SAPT methods. A more detailed analysis of these results shows that, in general, the SAPT0 and MP2 methods provide larger stabilization energy than the others. Considering the MP2 results, it is evident that the inclusion of correlation produces a stabilization of the complexes as high as 0.64-4.51 kcal/mol. As can be seen, the HF method greatly underestimates the interaction energies of the complexes and, in the cases of N_2 ligand, predicts the complex to be unbound. This indicates that dispersion must play a large role in the stabilization of Mg(CH_3N_2)$_2$–N_2 complex.

Conclusion:

Within this study, we used ab initio, DFT, and SAPT theories to investigate the nature of Mg–L interactions in a series of Mg(CH_3N_2)$_2$L complexes, where L= BF, CO, N_2, NH_3 and H_2O. Geometry optimizations indicated that estimated Mg–L distances are in a range of 2.127–2.711 Å. The MP2 and MP4 methods quite satisfactorily produce the interaction energies and are well in agreement with the CCSD(T) and SAPT results. Based on our SAPT results, the electrostatic contribution to the overall attraction energies of L= BF, CO, N_2, NH_3, and H_2O are 65%, 63%, 57%, 76%, and 76%, respectively.

Figure 1. Optimized structures of Mg(CH_3N_2)$_2$L complexes L= (a) BF, (b) CO, (c) N_2 , (d) NH_3 and (e) H_2O.

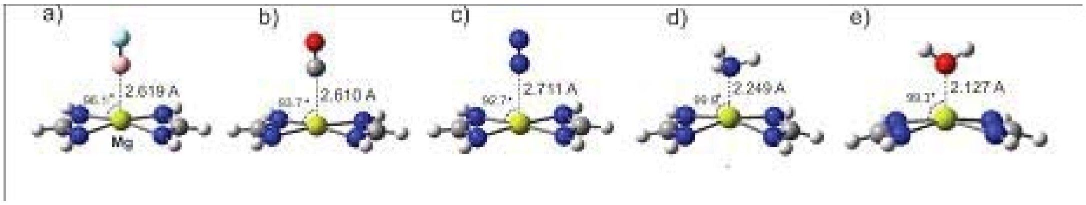

Table 1. Interaction energies and energy terms of $Mg(CH_3N_2)_2L$ (L =BF, CO, N_2, NH_3, and H_2O) complexes

Method	BF	CO	N_2	NH_3	H_2O
HF	-7.12	-2.83	+1.11	-11.41	-14.64
MP2	-8.42	-5.47	-3.40	-14.95	-15.28
MP4	-8.06	-5.41	-3.24	-14.93	-15.21
CCSD(T)	-7.88	-4.67	-2.70	-13.63	-15.14
B3LYP	-7.84	-4.26	-2.04	-13.38	-14.46
SAPT0	-9.08	-5.61	-3.65	-15.72	-17.76
SAPT	-7.70	-4.67	-2.75	-13.64	-15.45
$E_{elst}^{(10)}$	-18.23	-8.82	-3.90	-37.71	-30.72
$E_{exch}^{(10)}$	17.32	7.71	2.75	25.11	19.57
$E_{ind}^{(20)}$	-6.29	-2.46	-0.90	-6.98	-6.24
$E_{exch-ind}^{(20)}$	3.21	0.96	0.29	2.78	2.97
$\delta E_{\mathrm{int},resp}^{(HF)}$	-2.06	-0.22	0.63	5.38	2.54
$E_{disp}^{(20)}$	-3.25	-2.94	-2.64	-4.86	-3.54

References:

[1] J. F. Davis, Z. Hostomaka, Z. Hostomsky, S. R. Jordan, and D. A. Matthews. Science **252**, 88 (1991).

[2] D.E. Draper. Biophys. J. **95**, 5489 (2008).

[3] M. J. Frisch, *Gaussian 03*, revision E.; Gaussian, Inc.: Wallingford, CT, 2004.

[4] Dalton, a molecular electronic structure program, Release 2005.

[5] SAPT2008, Parallel Versions; University of Delaware and University of Warsaw, 2008.

Effect Br substitution on the structure and intramolecular hydrogen bonding strength of naphthazarin: DFT and NBO studies

R. Farahati, M. Zahedi-Tabrizi *
Department of Chemistry, Alzahra University, Tehran, Iran
Email: Zahedi@alzahra.ac.ir

Keywords: *Naphthazarin, Bromonaphthazarin, Intramolecular hydrogen bond, DFT,NBO*

Introduction:

5, 8-Dihydroxy-1, 4-naphthoquinone, commonly known as naphthazarin (hereafter NZ), is a simple model for an important group of compounds, perylenequinones, alkannin and shikonin. These are biologically active pigments obtainable from natural sources. This compound has been extensively studied theoretically and experimentally. The antitumor and antiviral activities of these compounds have attracted attentions to study the photochemical properties of NZ and its halogen substitutes [1–4].

Methods:

All calculations of the NZ (Fig. 1.) and its Br substitutions were performed using Gaussian 03 and NBO 5.0 programs. The full geometry optimization of NZ and its Br substitutions were performed with the hybrid density functional B3LYP using 6-31G** basis set. Wiberg bond orders were calculated using NBO 3.0 program implemented in Gaussian 03. The second order interaction energies (E^2), orbital population and natural steric analysis were performed at the B3LYP/6-31G** level using NBO 5.0 program, which applied the wave function information file generated by earlier version of NBO (3.0). The absolute shielding for NZ and its Br substitutions, and tetramethylsilane (TMS) have been obtained using the gauge-including atomic orbital (GIAO) method at the B3LYP/6-31G** level of theory. The predicted ^{1}H chemical shifts are derived from equation $\delta = \sigma_\circ - \sigma$, where δ is the chemical shift, σ is the absolute shielding, and $\sigma_\circ$ is the absolute shielding of TMS.

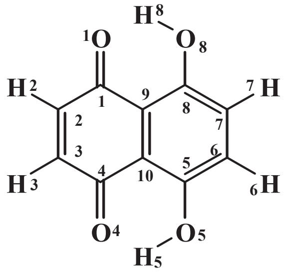

Fig.1. Numbering system and the C_{2v} structure of NZ.

Result and discussion:

Performed calculations on the 9 derivatives of NZ show that the substitution of brominein neighborhood of hydroxyl corps increases the O–H bond length, the O–H…O bond angle, ^{1}H chemical shift, and decreases the O...O and O…H bond lengths. However, the O–H bond length, the O–H…O bond angle, ^{1}H chemical shift decreased and the O...O and O…H bond lengths increased by substitution of brominein neighborhood of carbonyl corps. The geometrical parameters are in good agreement with the ^{1}H NMR results.

By natural bond orbital (NBO) method, the effect of substitution on the hydrogen bond strength, the charge distributions, steric effects, and electron delocalization in the studied compounds were investigated. The natural bond orbital analysis very well explains the calculated results of substitution of brominein atoms on the hydrogen bond strength.

Conclusion:

The geometrical parameters are in good agreement with the natural bond orbital (NBO) analysis and the proton chemical shift results.

The hydrogen bond strength increased by substitution of brominein in the vicinity of hydroxyl groups and decreased by substitution of brominein in the neighborhood of carbonyl groups.

Natural bond orbital analysis indicate that the steric effect and the electron-withdrawing effect of Br atom in neighborhood of hydroxyl group of ring increases the hydrogen bond strength, but the electron-withdrawing effect of Br in neighborhood of carbonyl decreases the hydrogen bond strength.

References:

[1] V. P. Papageorgiou, A.N. Assimopoulou, E.A. Couladouros, D. Hepworth, K.C. Nicolaou, Angew. Chem. Int. Ed. 38 (1999) 270-300.

[2] M. Zahedi-Tabrizi, S.F. Tayyari, F. Tayyari, M. Behforouz, J. Spectrochim. Acta. A. 60 (2004) 111-120.

[3] D. Z. Chen, Z. L. Hao, X. Zhao, Z. Wang, J. Mol. Struct. 803 (2007) 73-77.

[4] C.J.H. Schutte, S.O. Paul, R. Smit, J. Mol. Struct. 297 (1993) 235-241.

A theoretical study on the Gibbs free energy of the solvation of C_{60}, $H_2O@C_{60}$, $Cl^{-}@C_{60}$, $K^{+}@C_{60}$ in water, acetonitrile, CCl_4 and chloroform solutions

Fereshteh Yaghoobi, Sadegh Salehzadeh*, Mehdi Bayat
Faculty of chemistry, Bu-Ali Sina University, Hamedan, Iran.
Email: Saleh@basu.ac.ir

Key words: Theoretical study, Gibbs free energy of solvation, Solubility, Fullerene (C_{60})

Introduction:

The free Gibbs energy of solvation provides a measure of the solubility of a substance in a solvent. The more negative the energy of solvation, the higher the degree of solubility. Negative values of the solvation energy from thermodynamic consideration denote that the process is spontaneous [1]. Knowing the Gibbs free energy of solvation, for nanoparticles in octanol and water phases would greatly contribute to the understanding of nanoparticle partitioning in binary aqueous/organic systems. In recent years, the Gibbs free energy of solvation for a family of fullerene particles in octanol and water solvents through molecular dynamics simulation has been determined[2]. Following our interest in theoretical study on C_{60} molecule[3, 4]. herein we report the Gibbs free energy of solvation for C_{60}, $H_2O@C_{60}$, $Cl^{-}@C_{60}$ and $K^{+}@C_{60}$ in water, acetonitrile, CCl_4 and chloroform solutions using density functional theory.

Computational details:

Among the DFT methods, B_3LYP is used in this work. The geometries of all structures at gas phase were fully optimized at the B_3LYP/6-31G** level of theory. Solvation energies were calculated using the CPCM/UA0 at the B_3LYP/6-311++G** level of theory. Calculations were performed using the GAUSSIAN 03 program[5].

Result and discussion:

At first, the Gibbs free energy of solvation ($\Delta G^{solv)}$for theC$_{60}$was calculated in water, acetonitrile, CCl_4 and chloroform solution. ThentheΔG^{solv} valuesof the X@C$_{60}$(X= H_2O, Cl^-, K^+), in whicha neutral, anion or cation speciesis encapsulated in the C$_{60}$cavity were calculated.As it can be seen in Fig 1,the ΔG^{solv} values for the C_{60} in all studied solvents and for H_2O@C$_{60}$in water, acetonitrile and CCL$_4$were positive. However, the solvation free energyforCl^-@C$_{60}$ andK^+@C$_{60}$ systems in all above solvents had a negative value.Thus the insertion of a cation or anion in the fullerene cavity, not only in a polar solvent such as water but also in non-polar solvents such as CCL$_4$, has a significant effect on its solvation free energy.

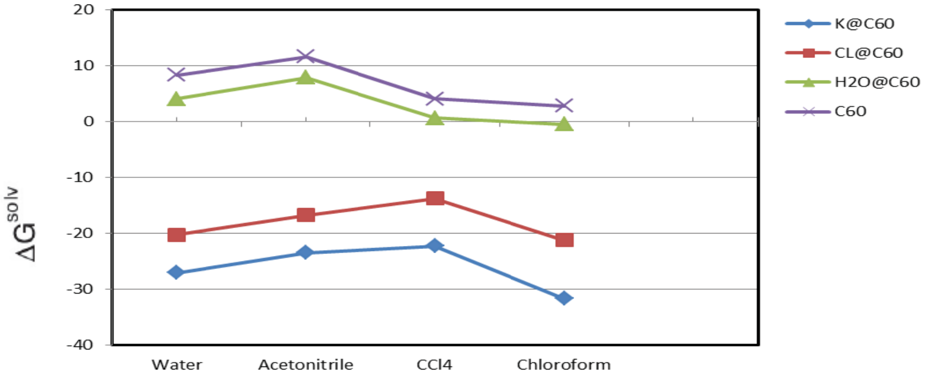

Fig1. Comparison of calculated solvation free energies

Conclusion:

The results of this work show that the C_{60} molecule has a positive value of solvation free energy in all studied solvents. However, when a Cl^- or K^+ion is encapsulated in the fullerene cavity the ΔG^{solv}will havea negative value in both the polar and non-polar solvents.An encapsulated H_2O molecule in the fullerene cavity,has also a positive effect on its free energy of solvationbut except in chloroform, the solvation free enegies have still positive values.

Reference:

[1] M. Gallo, A. Favila, D.G.-Mitnik, R.F. Smalley, Chem. Phys. Lett. 447(2007)105–109.

[2] P. S. Redmill, S. L. Capps, P.T. Cummings, C.McCabe,CARBON 47(2009)2865–2874.

[3] M. Bayat, S. Salehzadeh, J. Mol. Struct. THEOCHEM. 957 (2010) 120–125.

[4] M. Bayat, F. Yaghoobi, S. Salehzadeh, S. Hokmi, Polyhedron 30 (2011) 2809–2814.

[5] M.J. Frisch, et al; Gaussian 03, revision D.01, Gaussian, Inc., Wallingford, CT, 2004.

A theoretical study on the interaction of $HF@C_{60}$ with $[Al(H_2O)_6]^{3+}$ and $[Mg(H_2O)_6]^{2+}$ cations

Fereshteh Yaghoobi, Sadegh Salehzadeh*, Mehdi Bayat
Faculty of chemistry, Bu-Ali Sina University, Hamedan, Iran.
Email: Saleh@basu.ac.ir

Key words: Hydrated Al(III) and Mg(II) ions, Density functional theory, $HF@C_{60}$, Interaction

Introduction:

The discovery of fullerene in 1985 as a stable allotrope of carbon, with a closed cage structure attracted a lot of attention[1]. Fullerenes are capable of encapsulating small guest species such as atoms, ions and molecules inside their cavities. Soon after the discovery of C_{60}, the first such endohedral complex was reported with a lanthanum atom as the guest species[2]. The structure and stability of endohedral fullerenes has been investigated theoretically. Recently, we reported a theoretical study onthe interaction of Hydrated Al(III) and Mg(II) ionswith C_{60} andtwo other Π-systems [3].In the present work, we report a theoretical study on the interaction of HF@C60 with above hydrated metal ions.

Computational details

Among the DFT methods, B3LYP is used in this work.The geometries of the isolated $[Al(H_2O)_6]^{3+}$ and $[Mg(H_2O)_6]^{2+}$ cations, C_{60}, HF and $HF@C_{60}$molecules as well as the corresponding$\{[M(H_2O)_6]^{n+}\ldots HF@C_{60}\}$ complexes were fully optimized at theB3LYP/6-31G**level of theory. Calculations were performed using the GAUSSIAN 03 program [٣].

Results and discussion:

The optimized structures for $\{[Al(H_2O)_6]^{3+}\ldots HF@C60\}$ and $[Mg(H_2O)_6]^{2+}\ldots HF@C60\}$ complexes are shown in Fig. 1.We calculated the interaction energy for two above complexes.

The interaction energy, IE, between the $[M(H_2O)_6]^{n+}$ cations andthe HF@C_{60} studied here were calculated using Eq. (1).

$$IE=E_{\{M(H2O)6^{n+}....HF@C60\}}-(E_{M(H2O)6^{n+}}+E_{HF@C60}) \qquad (1)$$

Same asour previous work, the interaction energy for the Al complex is considerably larger than corresponding interaction energy for the Mg complex.Herein,when HF molecule is encapsulated in the fullerene cavity, the interaction energieswith hydrated metal ions are increased. Thus the interactions energies in $[M(H_2O)_6^{n+}....HF@C_{60}]$ complexes are larger than those in $[M(H_2O)_6^{n+}....C_{60}]$ complexes.

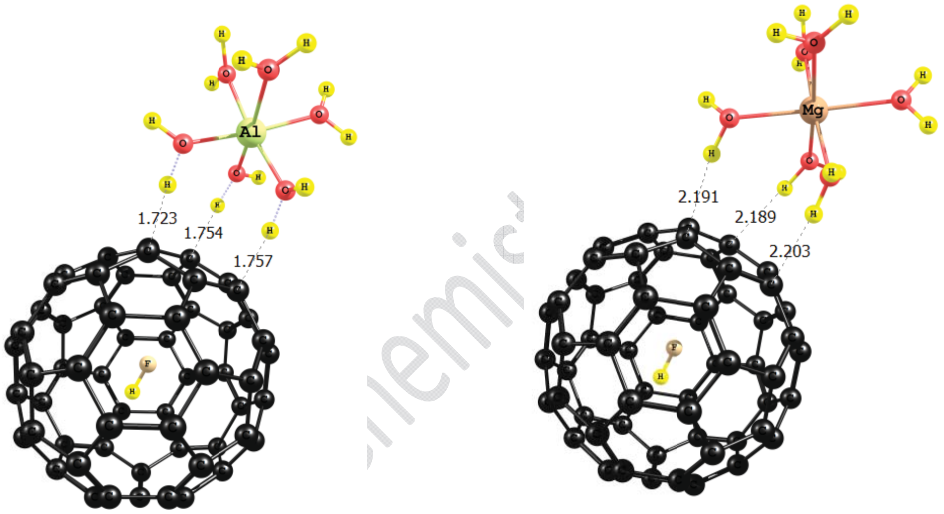

Fig1: Optimized geometries and selected bond lengths (Å) for the $\{[M(H_2O)_6]^{n+}\_\_\_ HF@C_{60}\}$ complexes (M = Al^{3+} and Mg^{2+})

Conclusion:

The results of this work show that theinsertion of HF molecule intothe fullerene molecule increases its interaction with the Al(III) and Mg(II) hydrated metal ions.

Reference:

[1] H.W. Kroto, J.R.Heath, S.C. O′Brien, R.F. Smalley, Nature 318 (1985) 162.

[2] J.R.Heath et al., J.Am. Chem. Soc.107(1985) 7779.

[3]M.J. Frisch, et al; Gaussian 03, revision D.01, Gaussian, Inc., Wallingford, CT, 2004.

Rotation around the C_3 symmetry axis in π-cation-π systems

A. Ebrahimi, R. Behazin*

Department of Chemistry, University of Sistan and Baluchestan, Zahedan, Iran

E-mail: royabehazin@yahoo.com

Keywords: Cation-π interaction, Eclipsed form, Staggered form,Rotation.

Introduction:

Noncovalent interactions such as cation-π are shown to play a crucial role in chemical and biological systems. The cation-π interactions are dominated by electrostatic and cation-induced polarizations [1]. That interaction is the strongest among the nonbonded interactions; its strength depends on the nature of aromatic systems and the kind of the cations[2]. Herein, alkali metal cations Li^+, Na^+, Be^{2+} and Mg^{2+} were sandwiched between benzene (BEN) and trifluorobenzene (TFB) in eclipsed and staggered forms (see Fig. 1).

Theoretical methods:

Both eclipsed and staggered forms of ternary complexes were optimized at the M062X/6-31+G(d) level of theory using the GAUSSIAN09 program package [3]. The topological properties of electron charge density were calculated by the atoms in molecules (AIM) method at the M062X/6-311++G(d,p) level of theory. The basis set superposition error (BSSE) correction was carried out on all optimized complexes using the counterpoise (CP) method of Boys and Bernardi at the M062X/6-31+G(d) level of theory.

(1) (2)

Figure 1. (1) eclipsed and (2) staggered forms of ternary π-M^{z+}-π complexes.

Results and discussion:

The total binding energies (ΔE) and the individual cation-π interaction energies are gathered in Table 1. As can be seen, the eclipsed forms are more stable than staggered ones by approximately -418.4 — -83.68 $Jmol^{-1}$. What is the source of higher stability of eclipsed relative to staggered form? The BEN•••M^{z+} and M^{z+}•••TFB distances decrease by the increase in the ΔE_1 and ΔE_2 values. A reverse relationship is observed between the $\sum\rho_{BCP}$ and the ΔE_1 (and the ΔE_2) values. In each case, the distance between the cation and π systems in the eclipsed form is shorter than staggered form.

Individual cation-π interactions were estimated by the electron charge density calculated at the BCPs between the atoms of π-systems and cations. Both the BEN•••M^{z+} and M^{z+}•••TFB interactions are weakened by other π-electron cloud in the ternary complex BEN-M^{z+}-TFB.

Table 1. The total binding energies of binary and ternary complexes in kJ mol^{-1}.

M^{z+}	$\Delta E_{(1)}$	$\Delta E_{(2)}$	$E_{BEN...Mz+}$	$E_{Mz+...TFB}$
Li^+	-234.43	-234.01	-170.58	-101.13
Na^+	-152.38	-152.09	-111.71	-57.28
Be^{2+}	-761.01	-760.88	-515.80	-392.34
Mg^{2+}	-517.03	-516.94	-353.67	-252.07

Conclusions:

The eclipsed form is more stable than staggered form in all cases; the highest difference between two forms corresponds to BEN-Li^+-TFB. The more stability of eclipsed form is accompanied by the longer distance between BEN and TFB by approximately 10^{-3} – 10^{-2} Å. The binding energies are in agreement with the results of geometrical parameters and AIM analysis.

References:

[1] F.B. Sayyed, C.H. Suresh,J. Phys. Chem. A, 2011, 115, 9300–9307.
[2] D. Vijay, G.N. Sastry, Chemical Physics Letters, 2010, 485, 235–242.
[3] M. J. Frisch, et al., Gaussian 09, Revision A.02; Gaussian Inc. Wallingford CT, 2009.

The mutual relationship between H-bonding and cation…π interactions in cation:(G···C) complexes

A. Ebrahimi, R. Behazin*, S. Abedini
Department of Chemistry, University of Sistan and Baluchestan, Zahedan, Iran
E-mail: royabehazin@yahoo.com

Keywords: Guanine, Cytosine, H-bonding, Cation-π interaction.

Introduction:

Noncovalent interactions, such as cation-π and H-bond interactions are shown to play an essential role in the structure of DNA and proteins, as well as in their interactions with small molecules [1]. How two important non-covalent interactions involving aromatic rings mutually influences each other is a question in understanding molecular aggregation and is a topic of wide ranging interest [2]. In this work, the mutual relationship between cation-π and H-bonding interactions in cation:(G···C) complexes (see Fig.1; ··· and : are used for the H-bond and cation-π interactions, respectively) has been considered.

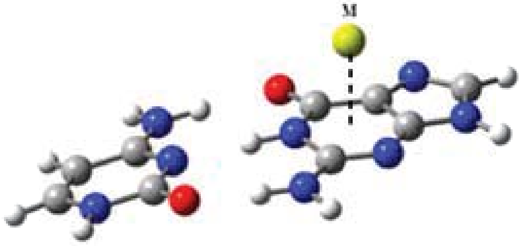

Figure 1. The interaction between cation and six membered ring of guanine in G···C complexes.

M= Li^+(**T$_1$**), Na^+(**T$_2$**), K^+(**T$_3$**), Mg^{2+}(**T$_4$**), Ca^{2+}(**T$_5$**)

Methods:

The optimization of structures have been performed by the MP2 method in conjunction with the 6-311++G(d,p) basis set using Gaussian09 program package [3]. The BSSE correction was carried out on all optimized complexes using the counterpoise (CP) method of Boys and Bernardi at the MP2/6-311++G(d,p) level of theory[4].

Results and discussion:

The binding energies calculated at the MP2/6-311++G(d,p) level for ternarycomplexes are gathered in Table1. E_{HB} and $E_{Cation\cdots\pi}$ are the binding energies for binary complexes with the structures optimized in ternary complexes (E_{HB} for the hydrogen bonded and $E_{Cation\cdots\pi}$ for the cation-π complexes).

Table 1. The total binding energies, and the individual H-bond and cation-π interaction energies in kcal/ mol.

	T_1	**T_2**	**T_3**	**T_4**	**T_5**	**D_1**	**D_2**	**D_3**	**D_4**	**D_5**
E_{Comp}	-66.25	-54.05	-50.23	-162.20	-130.9					
E_{HB}	-22.56	-23.61	-23.88	-1.39	-9.90					
$E_{Cation\cdots\pi}$	-23.73	-14.98	-11.63	-102.45	-67.26	-26.70	-17.12	-13.85	-106.6	-71.6

T and D refer to the ternary cation:(G···C) and the binary cation:guanine complexes, respectively. The binding energy of G···C base pair is equal to -27.39 kcal/ mol.

The most negative binding energy corresponds to **T_4**, due to the strong interactions with Mg^{2+}, with the highest charge/radius ratio.The trend in the total binding energies of complexes (E_{Comp}) is **T_4>T_5>T_1>T_2>T_3**. The H-bond and the cation-π interaction energies are equal to -22.56 and -23.73 kcal/mol in complex **T_1**. The H-bonding and cation-π binding energies of optimized G···C and **D_1** complexes are equal to -27.39 and -26.70 kcal/mol, respectively. Thus, the interplay of cation-π and H-bonding results in the weakening of both interactions. In the complexes **T_2** and **T_3** the trend in the changes of E_{HB} (and $E_{Cation\cdots\pi}$) are similar to the complex **T_1**; the E_{HB} and $E_{Cation\cdots\pi}$ decrease by 3.78 (2.14), 3.51 (2.22) kcal/mol in the complexes **T_2** and**T_3**, respectively. The interactions of Ca^{2+} and Mg^{2+} cations with the atoms of six membered ring are stronger than the interactions of those cations with the π system of guanine, such that the guanine misses its planarity via interaction with those cations in the complexes **T_4** and **T_5**.

Conclusions:

The interplay of H-bonding and cation-π interaction in the ternary cation:(G···C) complexes results in the weakening of both interactions, where the effect of cation-π on H-bonding is stronger. The highest change in the H-bonding and $E_{Cation\cdots\pi}$ binding energies correspond to the Li^+:(G···C) complex.

References:

[1] D. Escudero, A. Frontera, D. Quiñonero, P. M. Deyà, Chem. Phys. Letters, 2008, 456,257.
[2] A. R. Neves, P. A. Fernandes, M. J. Ramos,J. Chem. Theory Comput., 2011, 7, 2059.
[3] M. J. Frisch, et al., Gaussian 09, Revision A.02; Gaussian Inc. Wallingford CT, 2009.
[4] S. F. Boys, F. Bernardi, Mol. Phys., 1970, 19, 553.

Cocrystallization of theophylline with carboxylic acids

Ali Ebrahimi, Abolfazl Azizi*
Department of Chemistry, University of Sistan and Baluchestan, Zahedan, Iran
Email: abolfazl_azizi84@yahoo.com

Keywords: Cocrystal, Theophylline, Physicochemical properties, Stability

Introduction:

A pharmaceutical cocrystal is a solid that incorporates two neutral molecules, active pharmaceutical ingredient (API) and pharmaceutical acceptable molecule, in the crystal lattice [1]. Cocrystallization is an appropriate strategy for the improvement of physiochemical properties of pharmaceutically active molecules while retaining its molecular structure. Crystal engineering studies have previously been performed on the model pharmaceutical compound theophylline to prepare a cocrystal that is physically more stable than theophylline [2]. In the present work, the quantum mechanical calculations carried out on the cocrystals of theophylline with oxalic acid (**A**), malonic (**B**), maleic (**C**) and glutaric acid (**D**) in 1:1 ratio.

Computational details:

All structures were optimized at the B3LYP/6-311++G(d,p) level of theory [3]. Single point calculations were performed at higher levels. The topological properties of electron charge density were calculated by the atoms in molecules (AIM) method [4] using the AIM2000 program package [5].

Results and discussion:

The binding energies calculated at the B3LYP/6-311++G(d,p) level of theory are given in Table 1. According to the ΔE values, the stability of cocrystals decrease as **A** > **B** > **C** > **D**. This is similar to the trend in the size of acid molecules. By the increase in the number of carbon atoms of acid, the electron charge density increases on the carbonyl groups. Thus, electron-rich carbonyl groups make weaker hydrogen bonds when act as both donor and acceptor. A typical molecular graph obtained by the means of AIM approach on the wave functions calculated at the B3LYP/6-311++G(d,p) level of theory is shown in Figure 1. According to ρ values calculated at the bond critical points (BCPs), four H-bonds are observed in theophylline cocrystals, two strong O-H···N and two weak C-H···O bonds. As can be seen in Table 1, the highest/lowest values of $\sum\rho_{HBCP}$ corresponds to the cocrystal **A**/**D**, and the difference between those values is negligible in cocrystals **B** and **C**. So, hydrogen bonds between components in **A** are stronger than other cases, and its solubility in aqueous media is lower than others. There is a direct relationship between stabilization energies and the $\sum\rho_{HBCP}$ values.

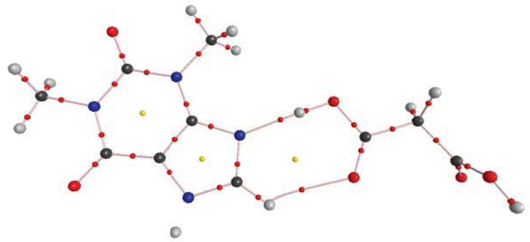

Figure 1. A sample molecular graph, in which the small red spheres and lines correspond to BCPs and bond paths, respectively

Table 1. The bending energies in kcal mol^{-1} calculated at the B3LYP/6-311++G(d,p) level and the topological properties of electron density calculated at the BCPs in the atomic unit.

	ΔE	$\sum\rho\times10^{-3}$		ΔE	$\sum\rho\times10^{-3}$
A	-11.99	0.059	**B**	-11.23	0.057
C	-11.16	0.058	**D**	-10.32	0.054

Conclusions:

The strength of the intermolecular H-bonds and therefore the stability of cocrystal decrease by the increase in the size of the acid molecule. Thus, the theophylline/oxalic acid cocrystal is more stable than other cocrystals. On the other hand, the results of AIM analysis demonstrate that the increase in the $\sum\rho_{HBCP}$ value is approximately accompanied with the increase in the stability of the cocrystals. The trend in the stability of cocrystals expected by the computational methods is in agreement with the experimental results.

Reference:

[1] P. Vishweshwar, J. A. McMahon, J. A. Bi; M. J. Zaworotko, Pharmaceutical co-crystals, J. Pharm. Sci., 95, 499-516, 2006.

[2]A. V. Trask, W. D. S. Motherwell, W. Jones, Pharmaceutical Cocrystallization: Engineering a Remedy for Theophylline Hydration, Cyst. Growth Des., 5, 1013-1021, 2005.

[3] M. J. Frish, et al., Gaussian 09 (Revision A.02), Gaussian, Inc, wallingford, CT, 2009.

[4] R. F. W. Bader, Atoms in molecules: a quantum theory, Oxford University Press, Oxford, 1990.

[5] F. W. Biegler König, J. Schönbohm, D. Bayles, AIM2000 - A program to analyze and visualize atoms in molecules, J. Comput. Chem., 22, 545-559, 2001.

The estimation of halobenzenes aromaticity using NBO calculations

Ali Ebrahimi, Najmeh Mostafavi*
Department of Chemistry, University of Sistan and Baluchestan, Zahedan, Iran
Email:mostafavi.najmeh@yahoo.com

Keywords: Aromaticity, Electrondelocalization, ATI, NBO

Introduction:

Since 140 years ago, which was introduced the concept of aromaticity by Kekule, aromaticity has been an interesting phenomenon in current chemistry. Chemists are trying to provide a clear definition and calculation for aromaticity. Although the most popular definition of aromaticity to be found in standard chemistry textbooks is electronic cyclic delocalization, but the problem is that the aromaticity is a multidimensional property and cannot be defined precisely [1]. So, different quantitative criteria including geometric, energetic and magnetic indices are used in the estimation of aromaticity. Some methods based on these criteria are average two center index (ATI), aromatic stabilization energy (ASE), and harmonic oscillator model of aromaticity (HOMA) [2]. In this work, the aromaticity of benzene ring with electron attractive substitutions has been estimated using the results of natural bond orbital (NBO) analysis. The results have been evaluated by ASE and ATI indices of aromaticity.

Methods:

All structures were optimizedat the MP2/6-31g(d,p) level of theory within the Gaussian09 program package. The NBO and the atoms in molecules (AIM) analyses have been performed by the NBO 3.1 and AIM2000 program packages. The ATI and ASE indices have been calculated as they presented by Bultinck et al. [3] and George et al [4].

Results and discussion:

Table 1 briefly represents some calculated data for fluorinated and chlorinated benzenes. As can be seen from ASE and ATI indices, aromaticity decreases by the increase in the number of electron-withdrawing substituent. The energy E^2 of $n_{(For\ Cl)}\rightarrow\pi^*$interaction decreases as the π-electron cloud is attracted by F and Cl substitutions, which is in agreement with the increase in the ASE and ATI indices. This can destroy the closed shell electron configuration of the benzene ring (increasing the occupancy of $\pi^*_{c\text{-}c}$ orbital) and decreases the stability of the ring. On the base of NBO analysis, the highest E^2 values for electron transfer from lone pair of substitution to the antibonding orbital correspond to trihalobenzenes. The fluorinated benzenes (F-Bs) become more unstable than chlorinated benzenes (Cl-Bs). The linear correlation coefficient (R) between E^2 values and the ASE index is equal to 0.98 for both F-Bs and Cl-Bs.

Table1. The ASE (kcal/mol) and ATI indices and the E^2 (kcal/mol) values calculated for benzene ring and substituted cases

Molecule	ASE	ATI	E^2	Molecule	ASE	ATI	E^2
Benzene	58.7	1.37	-	Benzene	58.7	1.37	-
Fluorobenzene	54.3	1.33	22.1	Chlorobenzene	55.1	1.34	16.1
1,3-difluorobenzene	50.6	1.29	46.8	1,3-dichlorobenzene	52.0	1.32	33.5
1,2,4-trifluorobenzene	47.9	1.28	66.4	1,2,4-trichlorobenzene	48.3	1.30	54.8

Conclusions:

With respect to the ASE and ATI indices and the E^2 values of $n_{(F\ or\ Cl)}\rightarrow\pi^*$ interaction, the aromaticity of benzene ring decreases with the increase in the number of F and Cl substitutions. In addition, there is a linier relationship between the E^2 and AES (and ATI) values. Thus, the E^2 value of $n_{(F\ or\ Cl)}\rightarrow\pi^*$ and therefore the population of $\pi^*_{c\text{-}c}$ orbital could be used as an index in the prediction of the aromaticity of substituted benzene rings.

References:

[1] N. H. Martin etal; Computed NMR shielding increments over unsaturated five-membered ring heterocycliccompounds as a measure of aromaticity;J. Mol.Graph.Mod., 27, 853-859, 2009.

[2] H. Fliegl etal, Aromatic pathways in twisted hexaphyrins, J. Phys. Chem., 114, 7153-7161,2010.

[3] P. Bultinck etal, Multicenter bond indices as a new measure of aromaticity in polycyclic aromatic hydrocarbons,J. Phys. Org. Chem., 18, 706-718, 2005.

[4] P. George etal, Comparison of various isodesmic and homodesmotic reaction heats with values derived from published ab initio molecular orbital calculations, J. Chem. Soc. Perkin Trans, 2, 1036-1047, 1977.

Molecular structure and frontier orbitals HOMO-LUMO studies of some unsymmetrical 1,4-dihydropyridine using density functional theory method

Mohammad Mobaraki Moghaddam[a], Masumeh Abdoli-Senejani[b,*]
[a] Department of Chemistry, Islamic Azad University-Saveh Branch, Saveh, Iran
[b] Department of Chemistry, Islamic Azad University-Arak Branch, Arak, Iran
E-mail: mabdoli@iau-arak.ac.ir; abdoli1356@yahoo.com

Key words:1,4-Dihydropyridines, Conformational analysis,Theoretical study,HOMO-LUMO, DFT, λ_{max}.

Introduction:

1,4-Dihydropyridines (DHPs) are very interesting compounds due to their pharmacological and biological properties [1] Structure-activity studies for some DHPs indicate that the nature and position of the substituents on the DHP ring have very important effect on their biological activities [2]. In view of the importance of the unsymmetrical nature at C_3 and C_5 positions, some new unsymmetrically substituted 1,4-dihydropyridines have been synthesized, in which a carboethoxy group (ester) and acetyl group (keto) are located on the 3- and 5- positions, respectively [3] and investigated conformational analysis of them [4].

The present study we wish to report a theoretical study on the impact of substituent of some unsymmetrical 1,4-dihydropyridine on the energy difference of the frontier orbitals HOMO-LUMO using density functional theory (DFT) B3LYP with 6-31G basis set method. In addition, parameters such as comparative heats of formation, energies of HOMO and LUMO, λ_{max}, hardness and others were investigated and analyzed for these compounds.

Computational details:

All computations using Gaussian 98 program package were carried out on a Pentium IV personal computer. The hybrid B3LYP functional with a 6-31G basis set was employed. For the each compound of the consideration were carried out the vibrational frequency calculations to characterize the minima of molecules. The starting structures were based on some known typical values of bond lengths and angles. The numbering scheme used for structural characterization of unsymmetrical 1,4-dihydropyridine is shown in figure 1. In order to calculate λ_{max} of these compounds and view the shape of frontier orbitals HOMO and LUMO, the GaussView 3.07 program was used.

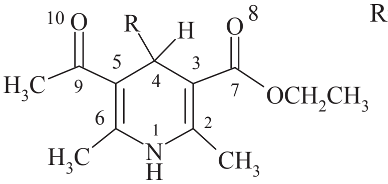

R= **a**: 2-$NO_2C_6H_4$, **b**: 3-$NO_2C_6H_4$, **c**: 3,4-$(CH_3O)_2C_6H_3$, **d:** 3-(CH_3O)-4-$(OH)C_6H_3$, **e**: C_6H_5, **f**: 4-$CH_3C_6H_4$

Figure 1

Result and discussion:

The B3LYP/6-31G computations indicate that in all compounds, the DHP ring has a flat boat conformation with a deviation of C_4 and N_1 atoms from the boat plane defined by C_2, C_3, C_5 and C_6 atoms. The aryl ring prefers an axial position on C_4 and lies above the 1,4-DHP boat. The aryl and 1,4-DHP rings are nearly perpendicular to each other. In all compounds one of the the carbonyl groups oriented trans conformation with respect to the corresponding adjacent C=C bonds of the 1,4-DHP ring.

The energies and shapes of the frontier orbitals HOMO and LUMO using density functional theory (DFT) B3LYP/6-31G method are studied. In addition, maximum wavelength and hardness of some unsymmetrical 1,4-dihydropyridine are calculated. A comparative study shows that for all compound, except **a** and **b**, the calculated λ_{max} are less than the corresponding experimental values [3]. The DFT B3LYP method is used with the larger basis sets 6-31G**and 6-31++G** to obtain the λ_{max} of one unsymmetrical 1,4-dihydropyridine with phenyl substitution in position 4. A comparative study shows that these results are in good agreement with those obtained of 6-31g method.

Conclusion:

In all B3LYP/6-optimized structures, the DHP ring has a flat boat conformation and the aryl ring prefers an axial position on C_4. The calculated λ_{max} for all compound, except **a** and **b**, are less than the corresponding experimental values. It should be noted that a detailed comparison between the gas phase (or vacuum) computational results and experimental data obtained for the solid state samples is not possible.

References:

[1] F. Friedlos, R. J. Knox, *Biochem. Pharmacol.* **1992**, *44*, 631.
[2] S. Goldman, J. Stoltefuss, *Angew. Chem. Int. Ed. Engl.* **1991**, *30,* 155.
[3] H. R. Memarian, M. Abdoli-Senejani, D. Dőpp, *Z. Naturforsch.* **2006**, *61b*, 50.
[4] H. R. Memarian, H. Sabzyan, M. Abdoli-Senejani, *J. Mol. Struct. (Theochem)* **2007**,*813*, 39.

Determination of Acidic Dissociation Constants of 5´-IMPand 5´-UMP in Water using DFT Methods

N. Motaghedia*, F. Kianib, M. Tajbakhshc, F. Ashrafia, A. Bahadorid
aDepartment of Physical chemistr University of Payam Noor, Mazandaran, Iran.
bDepartment of chemistry, Islamic Azad University, Ayatollah Amoli Branch, Amol, Iran.
cDepartment of organic Chemistry, Faculty of Chemistry, University of Mazandaran, Babolsar, Iran
dDepartment of chemistry, Islamic Azad University, Arak Branch, Arak, Iran.
*E-mail: n.motaghedi@gmail.com

Keywords: Dissociation constant, IMP, UMP, DFT method, solvation free energy

Introduction:

Derivatives of orthophosphoric acid, mainly as esters and anhydrides, are widely distributed in living systems. They are part of the so-called phosphate-sugar backbone of DNA and RNA; in the form of nucleotides they occur as coenzymes and intermediates [1]. Inosine-5'-monophosphate (IMP) is a nucleotide important monophosphate in metabolism. Uridine-5'-monophosphate (UMP) is a nucleotide that is used as a monomer in RNA. It is formed from Orotidine-5'-monophosphate in a decarboxylation reaction catalyzed by the enzyme orotidylate decarboxylase [2]. The acid-base behavior of nucleotides, nucleosides, bases, and polynucleotides is essential to deduce the speciation and the possible conformational changes with pH in solution [3]. On the other hand, during the last two decades there has been much interest in developing a methodology enabling theoretical prediction of pKa values, employing various quantum theoretical techniques. Kinds of polarizable continuum models have been applied to calculate free energy differences for cations, neutral compounds and their anions. On the basis of solvation free energies, the pKa values were obtained for the compounds in question by using thermodynamic equations; involving the combined experimental and calculated data [4]. This paper deals with the influence of factors such as the SCRF model applied, choice of a particular thermodynmic equations, atomic radii used to build a cavity in the solvent (water), optimization of geometry in water, inclusion of electron correlation, and the dimension of the basis set on the solvation free energies and on the calculated pKa values. In this study, pKa values of IMP and UMP were determined in aqueous solution by ab initio method and temperature 25°C.

Computational method:

Figure1 shows the structures of IMP and UMP and the practical numbering system adopted for performing the calculations. The initial geometries of the molecules by the semi empirical PM3 method are included in program CS Chem3D version 7.0. These geometries were optimized with the Gaussian 98 program packages using the B3LYP/6-31+G(d) methods and the default convergence criteria. To analyze the solvent effects on the specimen involved in the selected ionization reaction, the polarized continuum model (PCM) of Tomasi et al. was used [4].

Results and discussion:

The acid–base behaviour of a nucleotide is its most important physical characteristic. It determines its charge, its tautomeric structure, and thus its ability to donate and accept hydrogen bonds, which is the key feature of the base:base recognition.5 The bases are uncharged in the physiological range pH.

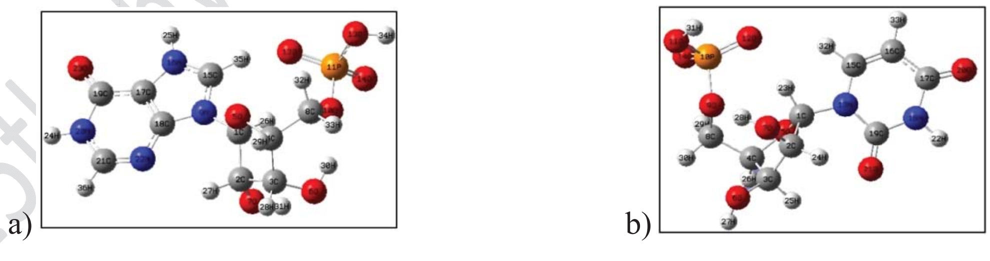

Figure 1. Optimized Structures a) IMP and b) UMP for carrying out the calculations.

Table 1. Calculated total energy using the Tomasi's method at the B3LYP/6-31+G(d) level of theory for cationic, neutral, and anionic species of IMP and UMP, water at 298.15 Ka

IMP			UMP		
Solvated Species	G0sol (Hartree)	G0sol / molecule (kJ mol-1)	Solvated Species	G0sol (Hartree)	G0sol / molecule (kJ mol-1)
H3IMP+	-15.5166 × 102	-40.33891 × 105	H2UMP	-14.9376 × 102	-39.21874 × 105
H2IMP	-15.4995 × 102	-40.69403 × 105	HUMP-	-14.9285 × 102	-39.19499 × 105
HIMP-	-15.4875 × 102	-40.59778 × 105	UMP2-	-14.9326 × 102	-39.14327 × 105
IMP2-	-15.3173 × 102	-40.21558 × 105	UMP3-	-14.7744 × 102	-39.79018 × 105
IMP3-	-15.1108 × 102	-30.67356 × 105	UMP4-	-14.5636 × 102	-38.23674 × 105
H3O+	-7.6862 × 10	-2.0180 × 105	UMP5-	-14.2919 × 102	-37.52349 × 105
H2O	-7.6434 × 10	-2.0068 × 105			

*aG*solo, total free energy in solution; *G*solo / molecule, total energy of solvated species per water molecule.

The same is true for the pentoses, where the ribose 2, 3 -diol only loses a proton above pH 12. The nucleotide phosphates lose one proton at about pH 1 . The amino bases, IMP and GMP, each becomes protonated on one of the ring nitrogens rather than on the exocyclic amino group since this does not interfere with de-localisation of the NH2 electron lone pair into the aromatic system [5-7].

Conclusion:

In order to explain the acidic dissociation constants obtained, we investigated the molecular conformations and solute-solvent interactions of the cation, anion and neutral species of IMP and UMP using ab initio and density functional theory (DFT) methods. According to the Gaussian calculations based on the quantum mechanics principals, the values of total energy and dissociation constants of IMP and UMP are investigated and the results are listed in Table 1 and 2.

Table 2. Values of pKa for the protonation of IMP obtained using the Tomasi method at the B3LYP/6-31+G(d) level of theory, at 298.15 K.*

Selected equations	IMP		UMP	
	pKa (calculated)	pKa(experimental) [8]	pKa(calculated)	pKa(experimental) [9]
H3NMP+ + H2O ⇆ H2NMP + H3O+	0.59	0.45 (I=0.1,NaClO4)	-	-
H2NMP + H2O ⇆ HNMP- + H3O+	1.49	1.30 (I=0.1,NaClO4)	0.22	-
HNMP- + H2O ⇆ NMPH-12- + H3O+	6.50	6.22 (I=0.1,NaClO4)	0.71	0.70 (I=0.1,NaClO4)
NMPH-12- + H2O ⇆ NMPH-23- +H3O+	9.30	9.02 (I=0.1,NaClO4)	5.99	6.15 (I=0.1,NaClO4)
NMPH-23- + H2O ⇆ NMPH-34- + H3O+	-	-	9.50	9.45 (I=0.1,NaClO4)
NMPH-34- + H2O ⇆ NMPH-45- + H3O+	-	-	12.3	-

*N represents nucleosides of inosine and guanosine.

References:

[1] H. Sigel et al.; J. Am. Chem. Soc.; 116 , 2958–2971, 1994.

[2] J.M. Berg and et al.; "Biochemistry"; W. H. Freeman; 2006.

[3] D..E..Metzler; "Biochemistry: The Chemical Reaction Living Cells"; Academic Press; 2001.

[4] F. Kiani et al.; J. Chem. Eng. Data; 55, 2732–2740, 2010.

[5] M. Blackburn et al.; "Nucleic Acids in Chemistry and Biology"; RSC; 2006.

[6] A. Shamel et al.; J. Chem. Eng. Data; 55, 5176–518, 2010.

[7] F. Gharib et al.; Can. J. Chem.; 84,1534-1540,2006.

[8] H. Sigel H et al.; J. Am. Chem. Soc.;116, 2958, 1994.

[9] S. S. Massoud et al., Inorg. Chem.; 27, 1447, 1988.

Nitrogen-Containing Heterocyclic Compounds Amination: DFT Energy Level alignment

Afsaneh Amiri[a,*], Milad Nouraliei[b], Nahid Atyabi [a], Zahra Hasanzadeh[a], Simin Tadayon[a]
[a]Department of Chemistry, Islamic Azad University, Center Tehran Branch, Tehran, Iran.
[b]Young Researchers Club,Central Tehran Branch, Islamic Azad University , Tehran, Iran.
Email: afsaamiri@gmail.com

Keywords: Nitrogen-Containing Heterocyclic, Amination, DFT

Introduction:

Salts containing *N*-amino cations derived from nitrogen-containing heteroaromatic compounds are widely used as reagents for amination of arenes [1] and for the synthesis of various heterocyclic compounds through the corresponding imines [2]. Compounds possessing an *N*-aminopyridinium fragment were proposed as components of photo thermo graphic elements [3], The goal of the present work was to reveal factors determining the reactivity of nitrogen-containing heteroaromatic compounds by using sodium in liquid ammonia. The mechanism of this reaction is also known as S_NH reactions. This study research purpose is the reaction energy levels alignment by quantum mechanics calculations in B3LYP/6-311+G^{**} level of theory.

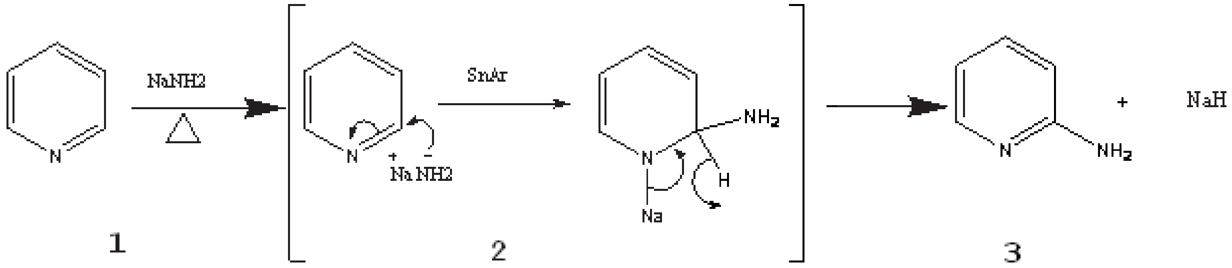

Computational Method:

All calculations reported here were performed with the Gaussian03 computer software package [4]. After all geometry optimizations were performed, analytical vibration frequencies were calculated at the same level to determine the nature of the located stationary points. Due to the nature of interacting species in the system and the absence of weak interactions, all calculations were performed on all reactants, products, and transition states using B3LYP/6-311+G**

method was performed to identify the equilibrium structures (ES) and transition states (TS) during the synthesis of pyridine derivatives. Characteristics and geometries of transition states (TS) were confirmed by the existence of only one imaginary frequency corresponding to the expected transition vector. Calculations involving an ammonia solvent were conducted using the Self-Consistent Reaction Field (SCRF) method with the Isodensity Polarized Continuum Model (IPCM) at the same level of theory.

Result and discussion:

In order to differentiate the obtained structures, we used the sum of their electronic and thermal enthalpies (SETE). The activation energy barriers calculated, Ea, as a difference between the

SETE of the TS and that of the sum of the reagents, and enthalpy ΔH as a difference between the SETE of products and SETE of the reagents for each step separately by quantum mechanical calculations were performed at B3LYP/6-311+G^{**} level of theory . Table.1 summarizes the data contains Ea and ΔH (kCal/mol) calculated in liquid ammonia.

Table. 1- The activation energy barriers and enthalpies (ΔH) of the steps of the reaction in kCal/mol.

Method	**B3LYP/6-311+G****		
Structure	**1**	**2**	**3**
ZPE	0.111518	0.114616	0.109535
E_0	-466.526425	-466.493068	-466.519156
E_{ele}	-466.6379428	-466.6076841	-466.6286907
ΔE	20.9315175		

Conclusion:

Amination of nitrogen-containing heteroaromatic compounds features some specificity, which distinguishes this reaction from alkylation of the same substrates. Based on calculations of activation energy for this reaction is 20.9315175 k cal /mol. According to our calculations, we can conclude that the reaction is completely exothermic.

References:

[1] Borodkin, G.I. and Shubin, V.G., *Russ. J. Org. Chem*. **2005**, vol. 41, 473.

[2] Yao, G., Haque, S., Sha, L., Kumaravel, G., Wang, J.,Engler, T.M., Whalley, E.T., Conlon, P.R., Chang, H., Kiesman, W.F., and Petter, R., *Bioorg. Med. Chem. Lett*., **2005**, vol. 15, 511.

[3] [16] Z. Yao, X. Gao, P. Ren, Daxue Huaxue 16 , **2001**, 48.

[4] M. j. Frisch et al. *GAUSSIAN 03*, Revision C. 01, Gaussian Inc.,Wallingford. CT, **2004**.

Structures and Electronic Properties of Aluminium Nanowires Encapsulated in Single-walled Boron Nitride H-capped and open end Nanotube

J.J. Sardroodi, Sadeq Afshari*, Jafar Azamat
Faculty of Science, Shahid Madani University of Azarbayjan, Tabriz, Iran
sadeq.afshari@gmail.com

Introduction:

Boron nitride (BN) nanotubes have attracted much attention in recent years due to their unique structures and semiconductive properties[1,2] . Similar to carbon nanotubes in atomic structure, BN nanotubes with quasi-one-dimensional nanostructures and hollow interiors are very promising potential for applications in nanoelectronic devices and cold electron emitters. Nanotubes filled with chosen materials can lead to one-dimensional nanostructures with exciting new applications. Lots of investigations have focused on hollow interior of carbon nanotubes [3,4] , and have proved that materials encapsulated in single-walled carbon nanotubes show novel properties quite direrent from their bulk counterpart for their dimensional nature and the nanoscale structures. Nowadays, molecular simulations are well suited to study the nanowires embedded in nanotubes[3] . So we discussed the structures and electronic properties using density functional theory (DFT) of Aluminium nanowires encapsulated in single-wall BN nanotubes. The results in this paper are helpful for better understanding of the electronic transport behavior of Al under confinement of single-walled BN nanotubes. From the DOSs, it can be seen the Al nanowires are conductive in nano-scale.

Modeling Method:

The DFT based calculations were performed using OpenMX 3.5 package [5]. Local density approximation (LDA) to the exchange-correlation potential was used. We considered Aluminium nanowires Encapsulated in Boron Nitride nanotube (5, 5) H-capped and open end, which contain 10 Boron, 10 Nitride and 1 Aluminium atoms per unit cell when open end.

Results and Discussion:

The structure and electronic properties of armchair boron nitride nanotubes have been investigated as a function of tube diameter using density functional theory. The length of nanotube is differ with two model, one, the nanotube is capped bye Hydrogens and other model that is the open end nanotube and have infinite length. The variation in structural parameters is analyzed based on atomic charges of Mulliken and bond length of Al-Al and the other bonds. A topological analysis for charge density (ρ), and its second derivative ($\nabla^2\rho$) for bonds have been performed using atoms in molecules (AIM) theory. Finally, the analysis of the charge distribution and charge transfer processes have been studied using density of states (DOS) and the NBO partitioning scheme, which helps us to understand the interactions inside the boron nitride nanotubes which are responsible for the stabilization of the armchair boron nitride nanotubes.

Conclusion:

The density of states and structure properties using density functional theory of optimized nanowires were also obtained. The maximum DOS values of a single chain nanowire appear to be an approximate proportional relation. The DOS curve of the single Al chain is quite different from that of the chain embedded in a BN nanotube.

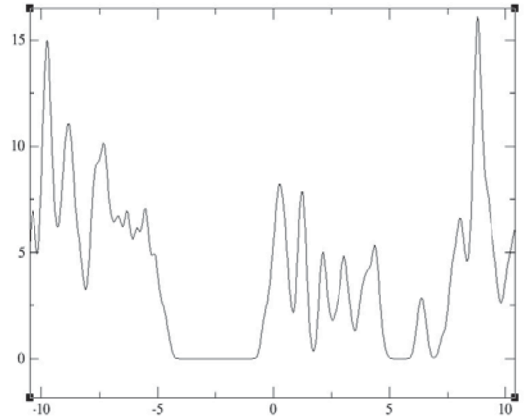

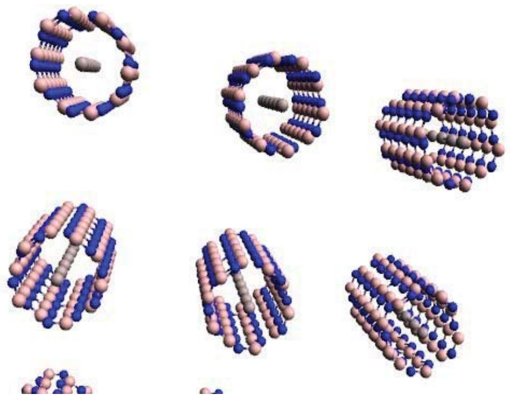

References:

[1]H.J. Xiang, J.L. Yang, J.G. Hou and Q.S. Zhu: Phys. Rev. B, 2003, 68, 035427.

[2] S.M. Hou, Z.Y. Shen, J.X. Zhang, X.Y. Zhao and Z.Q. Xue: Chem. Phys. Lett., 2004, 393,179.

[3] W.Y. Choi, J.W. Kang and H.J. Hwang: Phys. Rev. B, 2003, 68, 193405.

[4] M. Weissmann, C.C. Fu: Phys. Rev. B, 2006, 73, 125435.

[5] T. Ozaki, User's Manual of OpenMX Version 3.5 (2011).

[6] C. Hartwigsen, S. Goedecker and J. Hutter: Phys. Rev. B, 1998, 58, 3641.

Hybrid density functional theory study and nuclear magnetic resonance analysis of the decomposition reaction of but-3-en-1-ol and its analogs containing S and Se

Somayye Rafiei,[1] Seiedeh Negar Mousavi[1], Hooriye Yahyayi[2] and Davood Nori-Shargh[1]
Chemistry Department, Science Faculty, Arak Branch, Islamic Azad University, Arak, Iran
Chemistry Department, Zanjan Branch, Islamic Azad University, Zanjan, Iran
Email: rafieisomayeh@yahoo.com

Keywords: NICS, NBO, but-3-en-1-ol

Introduction:

The aromatic character of the ground and transition state structures of chemical compounds may affect the corresponding reaction barrier heights. In order to estimate the aromatic characters of chemical compounds, we may use nucleus-independent chemical shift (NICS) values.[1,2] In this work, we have calculated the thermal decomposition reaction barrier heights of but-3-en-1-ol (**1**) and its analogs containing S (**2**) and Se (**3**) to their corresponding alkene compounds by means of hybrid density functional theory based method (B3LYP/6-311+G**), natural bond orbital (NBO) and nuclear magnetic resonance (NMR) interpretations.[3,4]

Computational details:

We used the GIAO-B3LYP/6-311+G**//B3LYP/6-311+G** method in order to calculate the NICS values.[3,4] The experimental values of the NMR chemical shifts were vibrational average, whereas the computational results correspond to a fixed geometry at 0 K. NMR chemical shifts are not too sensitive to the optimized geometry.[35] The quantitative relationship between the aromatic character of the transition state structures of the thermal decomposition reaction of but-3-en-1-ol (**1**) and its analogs containing S (**2**) and Se (**3**) to their corresponding alkene compounds is demonstrated by their nucleus-independent chemical shift (NICS) values.[1,2]

Results and Discussion:

Hybrid-density functional theory (B3LYP/Def2-TZVPP) based method and NMR interpretation were used to study the thermal decomposition reaction of but-3-en-1-ol (**1**) and its analogs containing S (**2**) and Se (**3**) to their corresponding alkene compounds. The results obtained showed that the corresponding barrier heights of the thermal decomposition reaction of but-3-en-1-ol (**1**) and its analogs containing S (**2**) and Se (**3**) to their corresponding alkene compounds decreases from compound **1** to compound **3**. Importantly, the NMR analysis revealed that the NICS values of the transition state structures of compounds **1-3** increase from compound **1** to compound **3**. This fact reasonably explains the decrease of the corresponding barrier heights of the thermal decomposition reaction from compound **1** to compound **3**.

Conclusion:

The results obtained showed that the NICS values of the transition state structures of compounds **1-3** increase from compound **1** to compound **3**. The decrease of the corresponding barrier heights of the thermal decomposition reaction of but-3-en-1-ol (**1**) and its analogs containing S (**2**) and Se (**3**) to their corresponding alkene compounds can be explained by the increase of the NICS values of the transition state structures from compound **1** to compound **3**.

References:

[1]Schleyer, P. v. R.; Maerker, C.; Dransfeld, A.; Jiao, H.; Hommes, N. J. v. E. *J. Am. Chem. Soc.* **1996,** *118*, 6317–6318.

[2]Nyul´aszi, L.; Schleyer, P. v. R. *J. Am. Chem. Soc.* 1999, *121*, 6872–6875.Chen, Z.;Wannere, C. S.; Corminboeuf, C.; Puchta, R.; Schleyer, P. v. R. *Chem. Rev.* 2005, *105*, 3842–3888.

[3]M.J. Frisch, et al, Gaussian 03, Revision B.03, Gaussian, Inc., Wallingford CT, 2004.

[4]E.D. Glendening, J.K. Badenhoop, A.E. Reed, J.E. Carpenter, J.A. Bohmann, C.M. Morales, F. Weinhold, Theoretical Chemistry Institute, University of Wisconsin, Madison, WI, 2004. NBO Version 5.G.

A theory of mode of action of Glycyrrhizin and Glycyrrhetinic Acid as DNA and RNA binding agents using automated flexible ligand docking

Mahyar bonsaii[a], Firouzeh Manouchehri[b], Fahimeh Gholami Troujeni[a], Narjes Namdar Baboli[b], Khodayar Gholivand[c]*
a Department of Chemistry, Islamic Azad University, North Tehran Branch, Tehran, Iran
b Department of Chemistry, Islamic Azad University, Central Tehran Branch, Tehran, Iran
c Department of Chemistry, Tarbiat Modares University, Tehran, Iran
Email: Mahyar.bon@gmail.com

Key words: Docking, DNA, RNA, Glycyrrhizin, Glycyrrhetinic acid.

Introduction:

Glycyrrhizin is a well-known pharmacologically bioactive natural glycoside. Glycyrrhizin (GL) has been widely used as a therapeutic agent for chronic active liver diseases. Glycyrrhetinic acid (GA) is an aglycone and an active metabolite of Glycyrrhizin. In this study Fourier transform infrared (FTIR) and UV–visible spectroscopic methods were used to determine the ligand binding modes, the binding constants, and the stability of ligands –DNA, –RNA complexes in aqueous solution. Spectroscopic evidence showed that GL and GA bind DNA and RNA via G and A–T (A–U) base pairs as well as the backbone phosphate group with overall binding constants of $K_{GL–DNA}=5.7x10^3$ M^{-1} ($\Delta G_{binding}$= -5.12 kcal/mol), $K_{GA–DNA}=5.1x10^3$ M^{-1} ($\Delta G_{binding}$= -5.06 kcal/mol), $K_{GL–RNA}=3.03\times10^3$ M^{-1} ($\Delta G_{binding}$= -4.74 kcal/mol) and $K_{GA–RNA}=2.71\times10^3$ M^{-1} ($\Delta G_{binding}$= -4.67 kcal/mol). The affinity of ligands–DNA and –RNA binding is in the order of GL > GA. DNA remains in the B-family structure and RNA remains in the A-family structure, while biopolymer aggregation occurred at high ligand concentrations [1, 2]. We docked GL and GA onto the oligonucleotide extracted from the crystal structures. For every individual model, the correlation between calculated binding and experimental values were analyzed to come across most satisfying model. To determine the preferred binding sites on DNA and RNA.

Materials and methods:

The crystal structures of DNA (RNA)–ligand complex was selected from Protein Data Bank. the docking studies were performed by AutoDock 4.2.3 software. In AutoDock, the overall docking energy of a given ligand molecule in its active site is expressed as follows:

$$\Delta G = \Delta G_{vdW} \sum_{i,j} \left(\frac{A_{ij}}{r_{ij}^{12}} - \frac{B_{ij}}{r_{ij}^{6}} \right) + \Delta G_{hbond} \sum_{i,j} \left(\frac{C_{ij}}{r_{ij}^{12}} - \frac{D_{ij}}{r_{ij}^{10}} + E_{hbond} \right) + \Delta G_{elec} \sum_{i,j} \frac{q_i - q_j}{\varepsilon\left(r_{ij}\right) r_{ij}} + \Delta G_{tor} N_{tor} + \Delta G_{sol} \sum_{i_c,j} S_i V_j e^{\left(-r_{ij}^2/2\sigma^2\right)}$$

ΔG_{vdW}, ΔG_{hbond}, ΔG_{elec}, ΔG_{tor}, and ΔG_{sol} are free energy coefficients of van der Waals, hydrogen bond, electrostatic interactions, torsional term, and desolvation energy of oligonucleotide–ligand complex, respectively. r_{ij}, A_{ij}, B_{ij}, C_{ij}, and D_{ij} represent the interatomic distance, the depths of energy well, and the equilibrium separations between the two atoms, respectively. The first three terms are in vacuo force field energies for intermolecular interactions. The fourth term accounts for the internal steric energy of the ligand molecule [3].

Result and discussion:

Data derived from GL, GA, DNA and RNA docking shows different mood energy interactions. The structure that had the most compatibility with the FTIR results was selected. The selected docking data show minor groove binding into DNA with a greater tendency to A. Most known minor groove–binding drugs preferably recognize A-T sequences. However, minor groove binders are designed to have interaction with G-C pairs. We also obtained similar results on RNA. The dockings results are shown in Fig. 1.

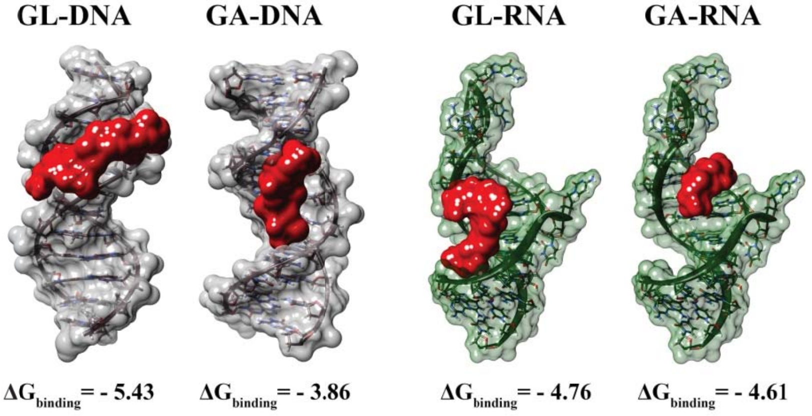

Fig. 1. Docking structure between GL, GA, DNA and RNA

Conclusion:

These compounds bind to minor groove, but with a different mechanism than what is usually knew.

Reference:

[1] Nafisi, S., Bonsaii, M., Manouchehri, F., & Abdi, K.; "Interaction of Glycyrrhizin and Glycyrrhetinic Acid with DNA"; DNA and Cell Biology; 31(1), 114-121, 2012.

[2] Nafisi, S., Manouchehri, F., & Bonsaii, M.; "Study on the interaction of glycyrrhizin and glycyrrhetinic acid with RNA" Photochemistry and Photobiology B : Biology; 111, 27-34, 2012.

[3] Nafisi, S., Bonsaii, M., Alexis, V., & Glick, J.; "Binding of 2-Acetylaminofluorene to DNA"; DNA and Cell Biology; 30(11), 955-962, 2011.

Synthesis and molecular dynamic simulation of methyl octanoate and methyl perfluorooctanoate

M. Abbaspour, M. Jafary*,E. Rezaei Seresht
Department of chemistry, Hakim sabzevari university, Sabzevar, Iran
*Email: majid_jafary@yahoo.com

Key words: Organofluorines, MD Simulation

Introduction:

Fluorine is the element of extremes, and many fluorinated organic compounds exhibit extreme and sometimes even bizarre behavior. A large number of polymers, liquid crystals, pharmaceutical and other advanced materials owe their unique property profile to the influence of fluorinated structures. Perfluoroesters are used as a precursor of perfluoroamides and perfluoroamides has applications such as battery electrolyte, pharmaceutical [1-5].

In this paper we have synthesized methyl perfluorooctanoate and then performed molecular dynamics (MD) simulation to calculate density and enthalpy of methyl octanoate and methyl perfluorooctanoate at 300 K and 350 K. We have also compared the effects of presence of fluorine in the molecule.

Methods:

Perfluorooctanoic acid introduced with thionyl chloride with catalytic amount of pyridine and product (perfluorooctanoyl chloride) after purification, react with methanol and pyridine to give methyl perfluorooctanoate. density of synthesized methyl perfluorooctanoate measured with a micropycnometer.

We have also performed MD simulation using DL_POLY 4.03 with 512 molecules with time step 0.001 picosecond and 500000 steps used.

Results and discussion:

there is an agreement between IR and ^{1}HNMR spectra of final product with methyl perfluorooctanoate spectra.

The MD simulation performed for methyl octanoate and methyl perfluorooctanoate to simulate the density and enthalpy at two temperatures (350 and 350 K). In order to use the optimized structure in the simulation, the Gaussian 09 has been used to calculate the charge of each atom and to optimize the molecules.

Although the density results showed a good accordance with the measured result; but the results of enthalpy did not show very good agreement which may be due to the kind of the force field used in the simulation. We have also shown that the enthalpy of methyl perfluorooctanoate has increased in comparison with methyl octanoate system. The enthalpy change for both methyl octanoate and methyl perfluorooctanoate between 300 and 350 K are approximately the same.

Conclusion:

The MD simulation performed for methyl octanoate and methyl perfluorooctanoate to simulate the density and enthaly at two temperatures (350 and 350 K). The results indicated the increase in enthalpy of methyl perfluorooctanoate relative to methyl octanoate system.

References:

[1] R. D. Chambers, Fluorine in Organic Chemistry, G. Olah, ed., Wiley Interscience, New york, 1973.

[2] M. Hudlicky, Chemistry of Organic Fluorine Compounds – A Laboratory Manual, Ellis HorwoodLtd, John Wiley and Sons, 1976.

[3] R. E. Banks, Preparation, Properties and Industrial Applications of Organofluorine Compounds, Ellis Horwood Ltd, John Wiley and Sons, 1982.

[4] I. C. Knunyants, G. G. Yakobson, Syntheses of Fluoroorganic Compounds, Springer, 1985.

[5] R. E. Banks, D. W. A. Sharp, J. C. Tatlow, Fluorine – The First Hundred Years (1886-1986), Elsevier Sequoia, New York, 1986.

Study of the transverse electric field effects on elastic modulus of nanotubes by density functional theory

A. Khorsandi[a]*, S.M. Mousavi-Khoshdel [a], S.M. Hashemianzadeh [a]
[a] Molecular Simulation Research Laboratory, Department of Chemistry, Iran University of Science and Technology, Hengam-Narmak , Tehran, Iran
Email: amin_khorsandi@chem.iust.ac.ir

Key words: Density functional theory, Young' modulus, Poisson's ratio, Electric field, Nanotubes.

Introduction:

The mechanical properties of nanotubes such as carbon nanotubes and boron nitride nanotubes have been the subject of many researches in the nanotechnology field. The theoretical approaches as well as experimental studies have been applied at the same. In fact, the elastic properties have been investigated using theoretically approaches based on continuum mechanics, molecular mechanics, molecular dynamics, tight-binding and ab initio quantum mechanical approaches. The main objective of these studies, have been focused on relation between size and chirality of nanotubes and elastic moduli. In this paper the effects of electrical field on the mechanical properties of nanotubes are studied. Thus, from the chemical perspective, changes in chemical properties are considered as justifications for deviations in the mechanical response of nanotubes.

Computational methods:

In this paper mechanical property of carbon, boron nitride and silicon carbide nanotubes in two conditions (with and without electric field) are investigated. For this purpose, six nanotubes such as CC(7,7), CC(12,0), BN(7,7), BN(12,0), SiC(6,6) and SiC(10,0) are selected whose diameters are about 1nm. It should be noted that the implemented mechanical loading is in-plane pure shear. At first, the optimization of nanotubes is performed in the Gaussian 09 software. Afterward, the strain enery as a result of mechanical loading is calculated. Based upon the obtained numerical results of the deformed nanotubes, an elliptic function is used to estimate the overall deformation relation. With regrad to the Green strain theory, the displacement of each particle is well defined by the conversion matrix transformed the initial circular shape of nantube to the final elliptical shape. The classical continuum theory is employed to estimate the relation of implemented strain energy and strain of nanotubes. Having employed the evolutionary genetic algorithm to achieve an accurate estimation on the fitting of energy function of elasticity theory with the obtained deformations from density functional theory.

In the second part, the nanotubes are exposed to the transverse electric field about 200 a.u to study the posible effects of electical field on the chemical properties of nanotubes and the consequent changes on the mechanical response of nanotubes. Thus, the density functional theory is used to assess deformations of nanotubes under electrical loading conditions. Moreover a comparison is performed to clarify the influences of electrical loading on the elastic modulus of nanotubes.

Result and discussion:

The obtained young' modulus is reported in below table.

	Young' modulus(GPa)			
Nanotubes	**E_y , E=0 a.u**	**Ey , E=200 a.u**	**E_x , E=0 a.u**	**E_x , E = 200 a.u**
C(7,7)	144.20	236,09	98.70	175,75
C(12,0)	134.39	206.50	103.89	172.10
BN(7,7)	154.19	252.07	140.5	229.88
BN(12,0)	184.39	280.30	162.89	247.90
SiC(6,6)	32.30	64.79	29.42	57,67
SiC(10,0)	29.91	65.33	24.10	52.8

Increasing young's modulus of nanotubes under transverse electric field in comparison with similar nanotubes which is not exposed to electric field depicted that electrical field has considerable effect on the mechanical properties of nanotubes. Indeed the electric field by modulation of band gap and state degeneracy and finally delocalization energy significantly increase the stiffness of nanotubes.

Conclusion:

In this paper the effect of transverse electric field on the elastic properties of nanotubes was investigated by using density functional theory and mechanical continuum approach. The obtained numerical results depicted that total stiffness of nanotubes follow increasing trend in the presence transverse electric field.

Reference:

[1] S. Azadi and R. Moradian, "First principle study of unzipped boron nitride nanotubes," *Physics Letters* A, vol. 374, pp. 605-609, 2010

[2] K. U. k. P. A. Gowri Sanka, "Mechanical and Electrical Properties of Single Walled Carbon Nanotubes: A Computational Study," *European Journal of Scientific Research* vol. 60, pp. 324-340, 2011.

[3] J. D. Biao Kan , Ningyi Yuan , Junxiong Wang , Zhigang Chen , Xiaoshuang Chen, "Transverse electric field–induced deformation of armchair single-walled carbon nanotube," *Nanoscale Res Lett* vol. 5, pp. 1144–1149, 2010.

[4] T. Oku, et al., "Electronic and optical properties of boron nitride nanotubes," *Journal of Physics and Chemistry of Solids*, vol. 69, pp. 1228-1231, 2008.

The AIM Analysis of Isomers of FOX-7

J. Najafpour , B.SHaikh ,F.R.Nikmaram*
Department of Chemistry, Faculty of science, Islamic Azad University Shahr-e-REY Branch,Tehran, IRAN
*NIKMARAM88@IAUSR.AC.IR

Key words: FOX-7, QTAIM, isomers, hydrogen bonding

Introduction:

Since FOX-7 (1,1-diamino-2,2-dinitroethylene) (Fig1) is a relatively new energetic material, little is known about its physical and chemical properties. Therefore, first-principles quantum chemical calculations are used to predict the energies of three type of isomers of FOX-7.Under gentle heating (thermolysis) is likely to cause hydrogen transfer between molecules, producing highly reactive chemical species. Conversely, rupture of a C-nitro bond (resulting in the production of NO2) requires a large amount of energy, suggesting that this reaction is more likely to occur when the explosive has been subjected to shock or impact. As shown in Figure 1, the FOX-7 molecule consists of nitro (-NO2) and amino (-NH2) functional groups attached to a carbon (C-C) backbone. The close proximity of amino hydrogens to nitro oxygens has prompted speculation that the stability of FOX-7 is due to hydrogen bonding within the molecule [1,2]. However, part of the increased stability can be attributed to other electronic effects. It is well known that the presence of amino groups tends to desensitise nitroaromatic molecules to shock or impact initiation.

Computational methods:

In this study, we report new quantum chemical calculations for geometry optimization using Density Functional Theory (DFT) method with the exchange correlation potential that is constructed from Becke’s three parameter formula for exchange (B3) [3], along with the Lee-Yang-Parr parameterization for correlation (LYP) [4].These calculations were performed within a valence double-zeta basis set augmented with both diffuse and polarization functions (aug-cc-pVDZ). The major classification of bonded interactions [5,6], in the framework of QTAIM has been proposed based on the sign of Laplacian of electron density($\nabla^2\rho_b$) and total energy density (H_b) evaluated at the Bond Critical Points (BCPs). H_b is sum of the kinetic energy density (G_b) and electronic potential energy density (V_b) at a BCP. The AIM analysis for the optimized structures (Fig. 2) has been performed to obtain the topological properties of the bonds. As is known, $\nabla^2\rho_b$ identifies whether the charge of the region is shared interactions($\nabla^2\rho_b > 0$ and/or $H_b > 0$) or closed shell interactions ($\nabla^2\rho_b < 0$ and/or $H_b < 0$). The former characterizes shared interactions (covalent bonds), where the electron density concentrates in the inter nuclear region, whereas the latter is typically associated with interactions between closed-shell systems (ionic bonds, hydrogen bonds, and vander waals molecules).

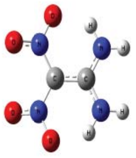

Fig 1: FOX-7 (1,1-diamino-2,2-dinitroethylene)

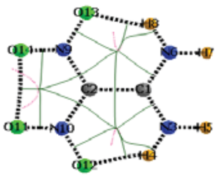

Fig2 ,a:Isomer1

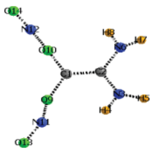

Fig2,*b:Isomer2*

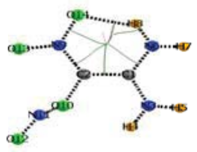

Fig2,c:Isomer3

	Bond	ρ_b	$\frac{1}{4}\nabla^2\rho_b$	G_b	V_b	H_b
Isomer1	O13-H8	1.87E-02	-2.99E-02	2.68E-02	-2.37E-02	3.09E-03
	O14-O11	2.53E-02	-3.03E-02	3.20E-02	-3.37E-02	-1.69E-03
	O12-H4	5.08E-02	-3.74E-02	5.26E-02	-6.79E-02	-1.52E-02
Isomer2	C1-O10	2.41E-01	4.83E-02	2.01E-01	-4.51E-01	-2.50E-01
	N11-O9	2.30E-01	-3.95E-02	1.52E-01	-2.65E-01	-1.13E-01
	O13-N11	4.99E-01	3.26E-01	3.61E-01	-1.05E+00	-6.87E-01
Isomer3	C2-O10	2.48E-01	5.16E-02	2.02E-01	-4.56E-01	-2.54E-01
	N11-O10	2.24E-01	-4.38E-02	1.49E-01	-2.54E-01	-1.05E-01
	N11-O12	5.09E-01	3.43E-01	3.69E-01	-1.08E+00	-7.12E-01

Conclusion:

The comparison of the $\nabla^2\rho_b$ and H_b values denotes that the most of bonded interactions are covalent and there are two hydrogen bonds O-H in the molecule.

References:

[1] (a) Östmark, H., Langlet, A., Bergman, H., Wingborg, N., Wellmar, U., and Bemm,U. (1998), .FOX-7 .A new explosive with low sensitivity and high performance,.*Proc. Eleventh (Int.) Det. Symp. Preprints*, 18-21. (b) Latypov, N.V., Bergman, J.,Langlet, A., Wellmar, U., Bemm, U. (1998), .Synthesis and reactions of 1,1-diamino-2,2-dinitroethylene,. *Tetrahedron* **54**, 11525-11536.

[2] Bemm, U., and Östmark, H. (1998), .1,1-Diamino-2,2-dinitroethylene: a novelenergetic material with infinite layers in two dimensions,. *Acta Crystallographica* C54, 1997-1999[8] Becke A.D., Density-Functional Thermochemistry. III.

[3]The Role of Exact Exchange, J. Chem. Phys., 98,p. 5648 (1993).

[4] Lee C., Yang W., Parr R.G., Development of the Colle-Salvetti Correlation-Energy Formula into a Functional of the Electron Density, Phys. Rev. B, 37,p. 785 (1988).

[5] Popelier P.L.A., “Atoms in Molecules: An Introduction”, Prentice Hall, England, (2000).

[6] Gillespie R.G., Popelier P.L.A., “Chemical Bonding and Molecular Geometry” Oxford University Press,New York, (2001).

On the effect of substituents on the Nature of the C≡C Bond in R_3E-C≡C-ER_3 (E=Pb; R=H, F, Cl) compounds

M. Hatami*[a], H. Keypour[b], M. Bayat.[c]
[a] Hamedan Technology University, Hamedan, Iran
[b, c] Faculty of Chemistry, Bu-Ali Sina University, Hamedan, Iran
Email: mmhzl1359@yahoo.com

Key words: DFT Study, Bonding analysis, Interaction energy, NBO Analysis, Bond Order, the Nature of Bond.

Introduction:

Carbon-carbon double and triple bonds have played an important role in many fields of chemistry. For many years, the synthesis of double and triple bonds between heavier Group 14 elements has attracted special interest in main group chemistry [1]. Since the first isolation of a stable disilene (R_2-Si=Si-R_2) in 1981, a variety of synthetic methods have been developed for the silicon and germanium analogues of alkenes [2]. In contrast to the remarkable progress in doubly bonded compounds, no stable compound featuring triple bonding between heavier Group 14 elements is known up to now [3] despite great interest. Thus, it has been theoretically investigated whether the alkynes and heavier analogues of them are synthetically accessible and isolated in a stable form, by providing insight into the nature of triple bonding. In this work, we investigate the effect of substituents on the nature and bond order of the C≡C bond in molecules with general formula R_3E-C≡C-ER_3 where E=Pb and R=H, F, Cl. It is evident that variation of both E atoms and R substitutes can be influence on the interaction energy values and bond orders in the C≡C bonds in foresaid molecules.

Computational details:

The structures of all molecules in the gas phase were fully optimized at standard LanL2DZ and SDD basis sets by B3LYP, BP86 and M062X levels of theory using the Gaussian 09 set of programs. Vibrational frequency analysis, calculated at the same levels of theory, indicates that optimized structures are at the stationary points corresponding to local minima without any imaginary frequency. The natural bonding orbitals (NBO) calculations were performed using NBO 3.1 program as implemented in Gaussian 09 package at the same level.

Result and discussion:

For the studied compounds in this work we can considered two possible comformers: staggered and eclipsed. At first, the more stable conformers for each molecule thermodynamically was determined and then the effect of substituents on the nature of C≡C bonds was investigated on them. The results of B3LYP/SDD calculations showed that the more stable conformers in $C_2Pb_2H_6$, $C_2Pb_2F_6$, $C_2Pb_2Cl_6$ are eclipsed, eclipsed and uneclipsed, respectively.

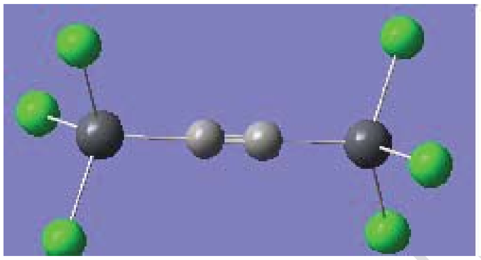

Eclipsed=3.1

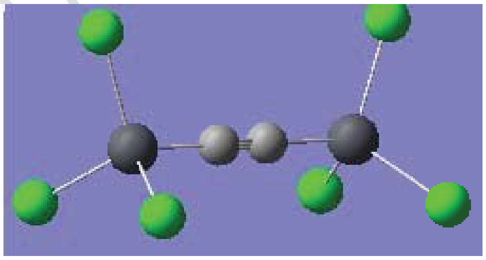

Uneclipsed=0

Conclusion:

The stability of possible conformers in molecules with general formula R_3E-C≡C-ER_3 where E=Pb and R=H, F, Cl was studied. The nature and bond order of the C≡C bond in more stable conformers were investigated theoretically.

Reference:

[1] M. Weidenbruch, Eur. J. Inorg. Chem. 1999, 373.
[2] M. Weidenbruch, S. Willms, W. Saak, Angew. Chem. Int. Ed. Engl. 1997, 36, 2503.
[3] A. Sekiguchi, S.S. Zigler, R. West, J. Am. Chem. Soc. 1986, 108, 4241.

Conformational behaviors of 2-methyl-1,3,2-dioxaphosphorinane. Ahybrid density functional theory study and natural bond orbital interpretation

Parvaneh Rahimi
Department of Chemistry, Arak Branch, Islamic Azad University, Arak, Iran

Introduction:

The stabilities of the conformations of the saturated heterocyclic compounds cannot be explained solely by steric factors. Stereoelctronic effects have significant impacts on the conformations and configurations of saturated heterocyclic compounds. The preferred geometry of the saturated heterocyclic compounds can be viewed as the result of the maximization of an interaction between the best donor lone pair and the best acceptor bond.[1-3] The most dominant conformation-controlling factor in carbohydrate compounds is known as the *anomeric effect* (*AE*).[4] The *AE* is in favor of the axial conformation of a six-membered saturated ring in opposition to the steric effect which normally leads to a preference for the equatorial conformation. Although the importance of the hyperconjugative interactions in six membered phosphorinane heterocycles has investigated,[5,6] there is no published experimental or quantitative theoretical data about the donor-acceptor delocalization effects on the conformational properties of 2-methyl-1,3,2-dioxaphosphorinane. In this work, the contributions of the total dipole moments, steric effects and the *AE* associated with the electron delocalization on the conformational and structural properties of 2-methyl-1,3,2-dioxaphosphorinane were investigated by means of hybrid density functional theory (B3LYP/6-311+G**) based method and natural bond orbital (NBO) interpretation.[7,8]

Computational details:

Hybrid density functional theory calculations were carried out using the B3LYP/6-311+G** level of theory with the GAUSSIAN 03 package of programs.[28] The main purpose of the present work was to study the impacts of the hyperconjugation, electrostatic interactions and total steric exchange energies (*TSEE*) on the conformational behaviors of 2-methyl-1,3,2-

dioxaphosphorinane. In order to estimate quantitatively the magnitude of the plausible donor-acceptor hyperconjugative interactions in the axial and equatorial conformations of 2-methyl-1,3,2-dioxaphosphorinane, we conducted NBO analyses for this compound.

Results and discussions:

Hybrid density functional theory (B3LYP/6-311+G**) based method and natural bond orbital (NBO) interpretation were used to investigate the impacts of the *anomeric effects* (*AE*) associated with the electron delocalization, dipole-dipole interactions (electrostatic model) and steric repulsions on the conformational properties of 2-methyl-1,3,2-dioxaphosphorinane. B3LYP/6-311+G** results showed the equatorial conformation of 2-methyl-1,3,2-dioxaphosphorinane is more stable than its corresponding axial conformation by about 3.03 kcal mol^{-1}. The NBO analysis of showed that the *anomeric effect* (*AE*) associated with the donor-acceptor electron delocalizations (LP→σ* and σ→σ*) is in favor of the equatorial conformation of 2-methyl-1,3,2-dioxaphosphorinane. The calculated total dipole moment value of the equatorial conformation of 2-methyl-1,3,2-dioxaphosphorinane is smaller than that of its corresponding axial conformation. Therefore, the electrostatic model associated with the dipole-dipole interactions moment seems to be sufficient to account for the more stability of the equatorial conformation of 2-methyl-1,3,2-dioxaphosphorinane compared to its corresponding axial conformation. The correlations between the *AE*, $\Delta\mu_{ax}$-$_{eq}$, Δ(*Total Steric Exchange Energies*), Wiberg Bond Indics (*WBI*), donor and acceptor orbital occupancies and energies and related off-diagonal elements (F_{ij}) have been investigated.

Conclusion:

B3LYP/6-311+G** and NBO results showed that the conformational behavior of 2-methyl-1,3,2-dioxaphosphorinane can be rationalized by means of anomeric effect and electrostatic model.

References:

[1] Epiotis, N. D.; Yates, R. L.; Larson, R. J.; Kirmayer, C. R.; Bernardi, F. *J. Am. Chem. Soc*. **1977**, 99, 8379–8388.

[2] Eliel, E. L.; Wilen, S. H. *Stereochemistry of organic compounds*, Wiley: New York, NY, 1994.

[3] Juaristi, E.; Cuevas, G. *The anomeric effect*, CRC Press, Inc: Florida, 1995.

[4] Lemieux, R. U.; Koto, S. **1974**, 30, 1933-1944.

[5] Gorenstein, D. G.; *Chem. Rev*. **1987**8, 7, 1047-1054.

[6] Wade Warrant, R. N. C.; Charles Howard Hargis, J.; Yee, K. C.; Bentrude, W. G.J. Org. Chem. **1978**, 43, 4266–4270.

[7] Frisch, M. J.; et al., *Gaussian 03,* Revision B.03, Gaussian, Inc., Wallingford CT, 2004.

[8] Glendening, E. D.; Badenhoop, J. K.; Reed, A. E.; Carpenter, J. E.; Bohmann, J. A. C.; Morales, M.; Weinhold, F. *Theoretical Chemistry Institute,* University of Wisconsin, Madison, WI, 2004. NBO Version 5.G.

A physical properties and phase diagram investigation of clay-sand system

A. Aminifar[a*], F.Khosravi [b], M.S.Abazari [a], E.Tavakoli [a]
a Department of chemistry, Faculty of sciences, Imam hossein comprehensive university, Tehran, Iran
b Department of civil engineering, Faculty of engineering, Imam hossein comprehensive university, Tehran, Iran
Email: aaminifar@hotmail.com

Key words: Phase diagram, Physical properties, Sand soil, Clay soil.

Introduction:

Many researchers are interested to study physical properties and phase diagram of metallic oxides which are constituent the soils. In our research we decided to use the prevalent clay and sand which available and manufactured in Iran to use directly. It may improve and open new view in the field of applied physical chemistry and soil science. Clay soil is hardened when fired or dried. They may also have contained variable common of water trapped in the mineral structure which is cause polar attraction. In a view of soil scientist and colloid chemist are usually preferred the size of clay between 1-2 µm respectively.

Sieving ventilation of air during of kiln it has an important rule for improving the physical properties of the clay. The melting point of clay, depend to their compositions. It seems presents of potassium oxide can lower the melting point temperature. The main composition of sand is SiO_2 , which make an unique tightness of it and enhance the melting point of sand. The microstructure of different metal oxides by variation temperatures have been studied so far and their phase diagrams CaO- MgO,CaO- MgO-SiO_2 and so on, have been reported, in condition of desification, sinteration and crystallization have also been investigated but there is not any report of this view that to measure clay and sand system so far [1-7].

Materials and methods:

Clay soil had grain size less than 0.75 mm and their liquid limit(LL) and plastic limit are equal to 40% and 14% respectively it has a density equal to 2.7 $g.cm^{-3}$. Sand soil has approximately size of 0.08-4.75 mm. In this case angle of fraction for sand is equal to 32^0 and there is no cohesive coefficient ,also sand density is equal to 2.6g.cm^{-3}.

Apparatus:

The Casagranda tool has been applied for determining the liquid limit and direct shear test has been applied for determining shear resistant of the sand soil ,on the other hand the triaxial test is suitable for clay soil. Clay and soil are dried in oven made by Yamato Company, for high temperature a special design oven made by Exciton Company had been used. [Model: EX.1200-30-6 STH, this oven is made by Iran].

Result and discussion:

The physical property of sand and clay had been report in previous section melting point of sand and clay was 1590 ^{0C} and 650 ^{0C} respectively. It seems the main compositions of clay soil are potassium oxide and calcium oxide as can observe in EDAX diagram. There is two eutectic point one eutectic point at molar concentration 65% of clay is equal to 850 ^{0C} and the eutectic point in molar concentration equal to 72% of sand is equal to 1220 ^{0C}. The lowering melting point of the clay and sand on addition of the clay and sand are on investigations.

Conclusion:

Eutectic points of clay-sand system has been measured, most of researches have been concerned diagram phase of metallic oxides of constituents of clay and sand but they haven't directly investigated clay and sand soil which we have done in this paper. It has also concluded melting point of clay is increased on adding sand soil, definitely resistance of clay in this manner is improved. By addition of clay to sand soil its melting point is decrease it my caused decreasing uses of energy in the concern industrial.

Reference:

[1] R.Krishna and etal; "CME315 Soil Mechanics Laboratory ; University of Illinois;2010
[2] www.msds.chem.ox.ac.uk,our Sand molecular formula SiO_2 silicon dioxide with Cas,

No:14808-60-7 .

[3] E.Wemer etal . ; "A review of mechanical assisted equilibrium technique and nanonugget issue" ; Chemical Geology ; 248,119-139,2008.

Boron-Substituted C_{20}Cage and Bowl Fullerene Structures;Can They be one of the options for Cl_2 Adsorbent? A DFT Study

M.Alvand, F.R.Nikmaram*, R.Ahmadi
Department of Chemistry, Faculty of science, Islamic Azad University Shahr-e-Rey Branch,
Tehran, IRAN
*NIKMARAM87@yahoo.com

Abstract:

The MPW1PW91/6-31++G** density functional calculations were used to obtain interaction energies between Cl_2 and nanostructures of C_{20}(cage), C_{20}(bowl) ,C_{20} H_{10}(bowl) , $C_{19}H_{10}B$(bowl, penta) ,$C_{19}H_{10}B$(bowl, hexa). In each case, $Cl_2$is adsorbed above the pentagonal and hexagonal sites. The charge-transfer,electronic chemical potential, ΔHLG and Adsorption energyof Cl_2molecule is considered as a measure of the ability to adsorption. All results shown thatBoron substitution in pentaposition in $C_{19}H_{10}B_{(bowl)}$ may be suitable for the adsorption of Cl_2molecule.

Key words: “Cl_2 Adsorption”, “Bowl Boron-SubstitutedC_{20}” , “DFT”

Introduction:

Gas adsorption by carbon materials is a topic of current interest. In order to exploit fullerenes one of the new forms of carbon for gas sensors. In general, the sensor systems requirea rather complex combination of materials that can selectively promote a desired charge-transfer process with efficiencies close to the thermodynamic limit[1].

For C_{20} the most stable isomer can have a ring-shape, a bowl or a fullerene structure, depending on the computational method. Experimentally , each of these C_{20} isomers can be produced under suitable reaction conditions, for example,C_{20} fullerenes from it’s perhydrogenated form, dodecahedrane,$C_{20}H_{20}$[2,3]. $C_{20}$is regarded as the smallest carbon fullerene with 12 pentagonsand bowl form of C_{20} with 6 hexagonal rings and a pentagon at center of structure; fig 1-4.In this present study, the MPW1PW91/6-31++G** density functional calculations have been carried out on some typical model systems wherein the fullerene and bowl molecules are substituted with hetero-atom like B. We have examined what type of species on carbon surfaces may be able to adsorption of Cl_2 molecule.Using NBO analysis, therelative energies, binding energies, charge - transfer, HOMO-LUMO gaps (HLG),electronic chemical potential (μ) and hardness (η), are obtained for interaction of Cl_2 and C_{20}(cage),$C_{19}B$(cage), C_{20}(bowl),C_{20} H_{10}(bowl), $C_{19}H_{10}B$ (bowl ,penta), $C_{19}H_{10}B$ (bowl, hexa, two fold) , $C_{19}H_{10}B$ (bowl ,hexa,three fold) by Gaussian 98 package. In each case, Cl_2 is adsorbed above the pentagonal and hexagonal sites (fig1,2,3).

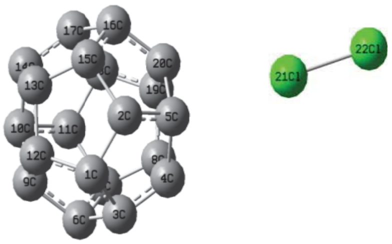

Fig1. C_{20} cage ,Cl_2

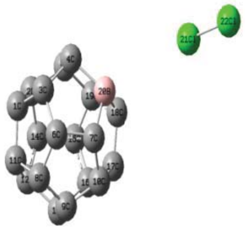

Fig2. $C_{19}B$ cage ,Cl_2

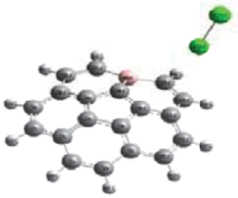

Fig3. $C_{19}H_{10}B$ (three fold ,hexa)

Results and discussions:

The Boron substitution in the bowl fullerene at hexa -three-fold position is more stable over the hexa-two-fold by0.2 Kcal/mol in energy;and$C_{19}H_{10}B$(bowl, penta) is stablethan $C_{19}H_{10}B$(bowl,hexa-three fold) by about 12.55 Kcal/mol in energy.The heteroatom substitution in the bowl fullerene may be suitable for the adsorption of Cl_2 molecule. From our results, the effects of adsorption of Cl_2 on $C_{19}H_{10}B$ (bowl, penta) with-0.309Kcal/molE_{ads} is strongerthan $C_{19}H_{10}B$(bowl ,hexa,three fold) with -0.304 Kcal/mol E_{ads}.

Increaseof electronic chemical potential 0.276 Kcal/mol, ΔHLG 0.738Kcal/mol and increase the bondlength Cl-Cl andcharge transfer;and decreaseof hardness0.253 Kcal/mol and distance of B-Clat penta position in bowl $C_{19}H_{10}B$ show that Boron substitution maybe more suitable for the Cl_2adsorption at penta position with respect to hexa position (Table1). The electronic chemical potential, hardness,adsorption energyand ΔHLG are defined as the followingequations (eq.1,2,3,4).

$$\mu = (E_{HOMO} + E_{LUMO})/2 \quad (1)$$

$$\eta = (E_{LUMO} - E_{HOMO}) / 2 \quad (2)$$

$$E_{ads} = E_{(structure,H2)} - (E_{structure} + E_{H2}) \quad (3)$$

$$\Delta HLG = HLG(structure, Cl_2) - HLG(structure) \quad (4)$$

Conclusions:

In this work, we studied the effect of Cl_2 molecule adsorption on the electronic properties of the B-C of C_{20}clusters. Our results show that theBoron substitution at penta position in the bowl $C_{19}H_{10}B$ may besuitable for the adsorption Cl_2 .

Table 1: E , E_{ads} , ΔE , HLG , Δ HLG , μ, Δμ, η of structures

Structure	E (a.u)	*E_{ads} (a.u)*	*E((Kcal/mol)*	*HLG (eV)*	*ΔHLG (eV)*	*μ (eV)*	*Δμ(e V)*	*η (eV)*
C19H10B penta	**-757/8838**	-	-	**0/134**	-	**-0/137**	-	**0/067**
C19H10B penta, Cl2	**-1675/2711**	**-0/0346**	**-920.3873**	**0/152**	**0/018**	**-0/164**	**-0/027**	**0/076**
C19H10B hexa	**-754/8637**	-	-	**0/156**	-	**-0/149**	-	**0/078**
C19H10B hexa, Cl2	**-1675/2563**	**-0/0399**	**-920.3926**	**0/1**	**-0/056**	**-0/176**	**-0/027**	**0/050**
C20H10 penta ,Cl2	**-1688/5440**	**-0/0029**	**-920.3556**	**0/11**	**-0/049**	**-0/1815**	**-0/0315**	**0/055**
C20H10 BOWL	**-768/18843**	-	-	**0/159**	-	**-0/15**	-	**0/079**
C20H10 hexa, Cl2	**-1688/5449**	**-0/0038**	**-920.3564**	**0/106**	**-0/053**	**-0/183**	**-0/033**	**0/053**
C20 cage	**-761/46787**	-	-	**0/07**	-	**-0/167**	-	**0/035**
C19B cage ,Cl2	**-1688/6242**	**- 2٠/٠٠٠٨**	**-940.3535**	**0/05**	**-0/019**	**-0/177**	**-0/011**	**0/025**
C19B cage	**-748/2707**	-	-	**0/069**	-	**-0/1665**	-	**0/034**
C20 Cage Cl2	**-1681/8206**	**-0/0001**	**-920.3528**	**0/062**	**-0/08**	**-0/177**	**-0/01**	**0/177**

References:

[1]Franco cataldo, Fullerenes:The hydrogenated fullerenes,2009

[2]Phys.Chem.Chem.Phys,2007,9,2954-2958

[3]Angew.Chem.,Int.Ed.2007,46,742-745

[4]J.Chem.Phys.1993,99,4210-4212

[5] J. Phys. Chem. Lett., 23 (2011)

[6] Theo Them. Acc(2001) 106,352-363

[7] H. Prinzbach , Nature, 407 (2000) 60

Quantum mechanical study of adsorption of CO on graphene; A Hybrid DFT calculation

Nasim Faridy sani*,[a], Mohsen Shabani[b],Mohammad Yousefi[a]
[a]Department of chemistry, Islamic Azad university, Shahre-Ray branch, Tehran, Iran
[b]Department of chemistry, Islamic Azad University, Varamin-Pishva branch, Tehran, Iran
Nasim.faridi@gmail.com

Abstract:

In this study, carbon monoxide molecule in gas phase has been adsorbed on four different positions of a four rings graphene surface (top (a,b), bridge and hollow), by using B3LYP/6-31G method. The adsorption energy has been calculated by equation (1): $E_{ads.} = E_{graphene...CO} - (E_{graphene} + E_{CO})$ (1) .It was found the bridge site is better than others for adsorption of CO. The adsorption energy is about -0.67 Kcal/mol. So, this adsorption is physical.

Key words: Graphene ,carbon monoxide ,Adsorption,B3lyp

Introduction:

Graphene was first discovered in 2004 at the Centre for Mesoscopic and Nanotechnology of the University of Manchester, UK, directed by Geim et al[1,2]. Graphene is a monolayer of carbon atoms that are tightly packed into a two-dimensional, honeycomb crystal structure [3].This extremely thin nanomaterial has shown fascinating properties and holds the promise for future carbon-based device architec- tures, owing to characteristics such as high mechanical stiffness [4]. Graphene is also a good candidate for usage as gas sensor materials to detect various molecules, ranging from gas phase molecules to some small bioactive molecules [5]. The simplest graphene-based sensor detects the conductivity change upon adsorption of analyte molecules due to the changes of charge carrier concentration in the graphene induced by adsorbed gas molecules. However, theoretical studies indicate that the pristine graphene can not meet the requirement of gas sensing applications because of the low adsorption energies of gas molecules on the graphene surfaces. In this paper, the adsorption of CO molecule in gas phaseadsorbed on pristine graphene (PG) has been investigated by performing density functional theory calculations. We aim to understand the suitable site of graphene for adsorption of CO on it and to exploit the potential applications of graphene as gas sensor [6].

Computational details:

All calculations were performed by using density functional theory (DFT)., B3LYP method, and 6-31G basis set. All computations have been performed on a personal computer using the Gaussian 03 program package and gauss view molecular visualization program. A 4 ring graphene has been selected as adsorbent. The adsorption energy has been calculated by equation (1): $E_{ads.} = E_{graphene...CO} - (E_{graphene} + E_{CO})$ (1)

Results and discussion:

To find the best site of graphene, for adsorption of CO, the gas molecule initially placed at different positions above a graphene sheet from Carbon direction of CO. After full relaxation, the most stable configurations are identified by comparing the energies of optimized configurations obtained from the different initial states. Table 1 summarizes our results. on the Fig. 1. chematic view of the energetically favorable configuration of PG adsorbed with CO adsorption energy (Ea), equilibrium graphene-molecule distance (d, defined as the distance of nearest atoms between graphene and gas molecule) and the charge transfer (Q, Mulliken charge) adsorbed on PG.

Table 1. Adsorption energy (Ea), equilibrium graphene molecule distance (d) (defined as the shortest atom-to-atom distance) and Mulliken charge (Q) of small gas molecules adsorbed on PG.

position	$E_{ads.}$(Kcal/mol)	Q(e)
CO(top a)	-0.136	-0.000986
CO(top b)	-0.183	-0.000871

CO(hallow)	-0.406	-0.001329
CO(bridge)	-0.670	-0.004759

Conclusions:

We have performed density functional theory calculations to investigate the adsorption of CO, on different positions of PG . PG shows weak adsorption energy (less than -1.0 Kcal/mol), so CO adsorbs physically. The bridge position is the best than the others. Charge transfer in bridge position is higher than others. So, the electronic properties of PG are sensitive to the adsorption of CO molecule.

References:

[1] K.S. Novoselov, A.K. Geim, S.V. Morozov, D. Jiang,Y. Zhang, S.V. Dubonos, I.V. Grigorieva, A.A. Firsov,Science 306, 666 (2004)

[2] K.S. Novoselov, D. Jiang, T.J. Booth, V.V. Khotkevich,S.V. Morozov, A.K. Geim, PNAS 102, 10451 (2005)

[3] A.K. Geim, K.S. Novoselov, Nat. Mater. 6 (2007) 183005)

[4]A.A.Balandin, S. Ghosh, W. Bao, I. Calizo, D. Teweldebrhan, F.Miao, C.N. Lau, Nano Lett. 8 (2008) 902.

[5]F. Schedin et al., Nature Mater. 6, 652 (2007).

[6] O. Leenaerts, B. Partoens, F.M. Peeters, Phys. Rev. B 77,125416 (2008).

A theoretical study on bonding and energy aspects of $[Ln(DOTA)]^-$ and $[Ln(DOTA).H_2O]^-$ complexes ($Ln=Eu^{3+}$, Ho^{3+})

Vahideh Alizadeh , Mehdi D. Esrafili *
Department of Chemistry, University of Maragheh, Maragheh, Iran
(E-mail:esrafili@maragheh.ac.ir)

Key words: DFT; Lanthanides; DOTA; water binding; NBO

Introduction:

Complexes of trivalent lanthanide ions with the cyclen derivative 1,4,7,10 tetraazacyclododecane-1,4,7,10-tetraacetate (DOTA) and related ligands are of great interest because of their use in various medical applications, such as cancer radiotherapy or magnetic resonance imaging (MRI)[1,2]. The successful use of these complexes in medical diagnosis and therapy is partially related to their high thermodynamic stability and kinetic inertness[3]. Earlier studies indicated that the Holmium and Europium complexes of DOTA show nine coordination around the metal ion with square antiprismatic geometry involving four N- and four O- donor atoms of the DOTA ligand and a coordination water molecule in a capping position [4].

The aim of the present work was the quantum chemical description of lanthanide-DOTA interactions in $[Ln(DOTA)]^-$ (Ln = Eu or Ho) complexes. The effect of water coordination to the $[Ln(DOTA)]^-$ complexes is also investigated. For this reason, we have analyzed the Ln···O and Ln···N characteristics, using the Bader's quantum theory of atoms in molecules (QTAIM) and NBO calculations. The structural and energy aspects of the complexes were also studied.

Computational Details:

All molecular orbital calculations were performed using *Gaussian 03* code [5]. Full geometry optimizations of the $[Ln(DOTA)]^-$ and $[Ln(DOTA).H_2O]^-$ ($Ln = Eu^{3+}$, Ho^{3+}) systems were performed by using the B3PW91 method and the effective core potential (ECP) of the Stuttgart group[6] . This ECP includes 46 + $4f^n$ electrons in the core, leaving the outermost 11 electrons to be treated explicitly. The use of large core ECPs has been justified by the fact that 4f orbitals do not significantly contribute to bonding because of their limited radial extension as compared to the 5d and 6s shells. C, N, O and H have been treated with an all-electron 6-311++G** basis set. NBO and QTAIM analyses were carried out using B3PW91/ECP/6-311++G** level.

Results and discussion:

The general structure of model ligands and resulting complexes are represented in Figure1. The estimated Ln–L distances are in a range of 2.29–2.76 Å which is much smaller than the sum of Van der Waals radii for Ln^{3+} and oxygen or Ln^{3+} and nitrogen, implying an attractive interaction between DOTA and Ln^{3+} cation.

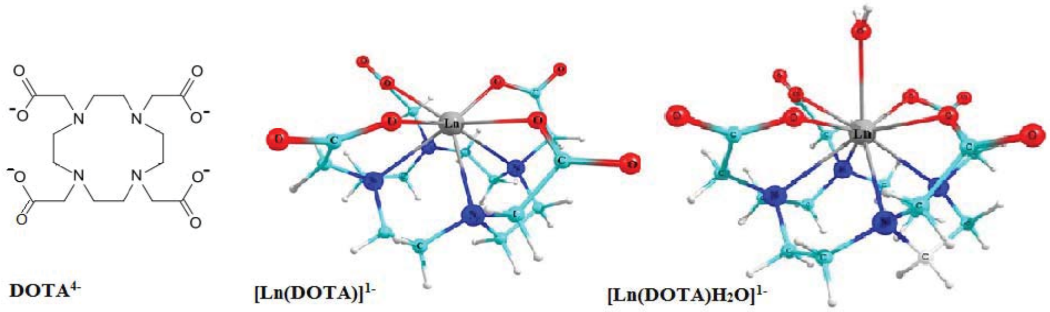

Figure 1- Molecular structure of DOTA, $[Ln(DOTA)]^-$ and $[Ln(DOTA).H_2O]^-$

From QTAIM results, it is evident that the value of Laplacian of electron density ($\nabla^2\rho_{BCP}$) and the local electronic energy density, H_{BCP} at Ln···O and Ln···N bond critical points are positive. On the basis of QTAIM results, it can be concluded that all Ln···O and Ln···N bonds of the $[Ln(DOTA)]^-$ and $[Ln(DOTA).H_2O]^-$ complexes are electrostatic in nature and as the Ln^{3+} cation involved in Ln···O and Ln...N interactions becomes harder, the interaction strength gets larger and, interestingly, more electrostatic in character. The role of water molecule coordination is also investigated by a comparison of the $[Ln(DOTA)]^-$ complexes with the $[Ln(DOTA).H_2O]^-$ ones. The mean Ln···L distances increase slightly from $[Ln(DOTA)]^-$ to

$[Ln(DOTA).H_2O]^-$ complexes. The result reveals that the addition of water molecule to the $[Ln(DOTA)]^-$ complexes leads to a marked drop in the Ln···L interaction energies due to the additional charge donation of water molecule toward the Ln and increased steric crowding around the cation.

To obtain more details on Ln-ligand interactions, the NBO analysis was performed and the results of $[Ln(DOTA).H_2O]^-$ complexes indicate that stabilizing energy $E^{(2)}$ and Fock matrix elements (F_{ij}) follow as Ln···O > Ln···Ow > Ln···N that are in agreement with QTAIM results.

References:

[1] Cutler, C. S.; Smith, C. J.; Deutsch, E. Cancer Biother. Radiopharm. 2000, 15, 531–545.

[2] The Chemistry of Contrast Agents in Medical Magnetic Resonance Imaging; Merbach, A. E., Toth, E., Eds.; Wiley: New York, 2001.

[3] Kumar, K.; Chang, C. A.; Tweedle, M. F. Inorg. Chem. 1993, 32, 587–593.

[4] Benetollo, F., Bombieri, G., Aime, S., and Botta, M., Acta. Cryst. 1999, C55, 353-356.

[5] Frisch, M.J. et al. Gaussian 03, Gaussian Inc, Pittsburgh PA, 2003.

[6] M. Dolg, H. Stoll, H. Preuss, Theor. Chim. Acta. 1993, 85, 441.

A DFT investigation on the spin–spin couplings across the hydrogen bond in non-steroidal anti-inflammatory propionic acid derivatives: Iboprofen, Naproxen and Flurbiprofen

Vahideh Alizadeh[a] , Mehdi D. Esrafili *[a]

[a] Department of Chemistry, University of Maragheh, Maragheh, Iran
(esrafili@maragheh.ac.ir)

Introduction:

Ibuprofen [(*RS*)-2-(4-(2-methylpropyl)phenyl) propanoic acid], Naproxen [(+)-(*S*)-2-(6-methoxynaphthalen-2-yl) propanoic acid] and flurbiprofen [(*RS*)-2-(2-fluorobiphenyl-4-yl)propanoic acid] (Fig. 1) are non-steroidal anti-inflammatory drugs (NSAIDs) that exhibit favorable anti-inflammatory, analgesic and antipyretic properties. The major clinical application on NSAIDs is their action as anti-inflammatory agents in muscle skeletal diseases [1].

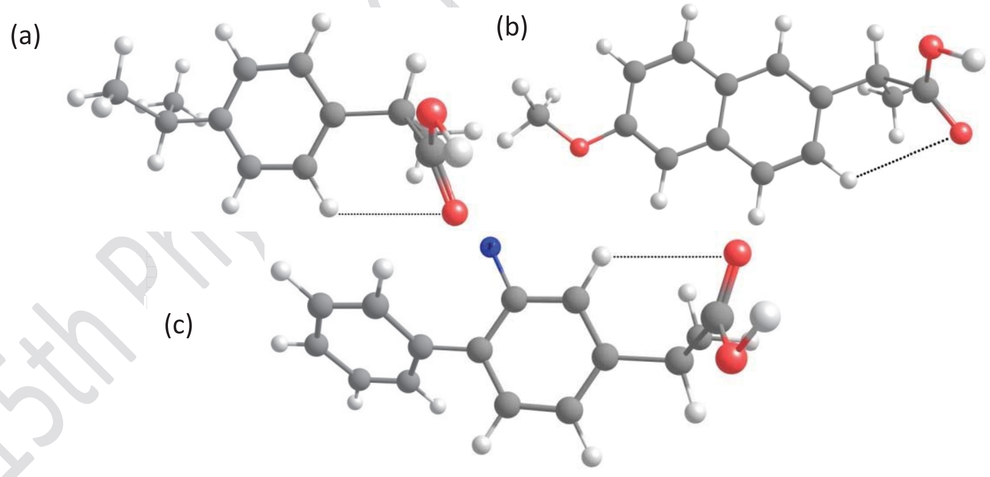

Figure 1- Molecular structure of ibuprofen (a), naproxen (b) and flurbiprofen (c)

In 2006 Jubert et al. [2] performed experimental and theoretical studies of Ibuprofen, Naproxen and Tolimetin acid in an effort to elucidate a more deeper insight on the physicochemical properties of NSAIDs. The results showed that the oxygen atoms of the

NAIDs would be the preferential sites for the electrophilic attack, among them those corresponding to the carboxylic groups. Although the study of NSAIDs is very popular, there are still many unsolved problems in the area of the theoretical study [3] for it. In this paper, we decided to study theoretically the spin–spin coupling constants to determine the conformation and the role of propionic acid to explore whether there is an intramolecular hydrogen bond or not. In addition, the Bader's quantum theory of atoms in molecules (QTAIM) has also been applied. QTAIM theory permits to follow the Lewis standpoint of a chemical reaction, to determine the electrophilic and nucleophilic zones of a molecule from the topology and topography of the Laplacian of the charge density, $\nabla^2\rho$[4].

Computational Details:

The geometry of the systems have been fully optimized at the M06-2x/pcJ-n level (n=0, 1, 2 and 3) with the Gaussian 03 facilities [5]. Hohenstein et al. have previously shown that M06-2X functional is able to describe well the noncovalent interactions in biomolecules [6]. Coupling constants were calculated at the M06-2x/ pcJ-n level. The electron density has been analyzed at the M06-2x using Gaussian 03 [5].

Result and discussion:

Propionic acid derivatives are useful molecules to test the convergence of coupling constants involving ^{17}O, ^{13}C and ^{1}H with respect to basis set size. This molecule also affords the opportunity to assess the magnitude of both one-bond and two-bond coupling constants involving these nuclides. The results indicate that $^{1}J(^{17}O,^{1}H)$ and $^{2}J(^{17}O,^{13}C)$ are dominated by Fermi Contact (FC) mechanism and confirm that $^{2}J(^{17}O,^{13}C)$ depends also on a significant PSO contribution. An evaluation of the dependence of various coupling constants on local geometry revealed that bond lengths and bond angles have the most significant influence on the coupling $^{1}J(^{17}O,^{1}H)$ and $^{2}J(^{17}O,^{13}C)$ constants; however, they also vary with the local dihedral angles. Based on QTAIM results, a reasonable correlation has been found between electron charge densities at O···H bond critical points and evaluated $^{1}J(^{17}O,^{1}H)$ constants.

Reference:

[1] A. Goodman Gilman (Ed.),ninth ed. Las Bases Farmacolo´gicas de la Terapeutica vol. II, Mc Graw Hill Interamedicana, Me´jico, 1996 pp. 661–776.

[2] A. Jubert, M. L. Legarto, N. E. Massa, L. vez, N.B. Okulik, J. Mol. Struct., 783, 2006, 34–51

[3] S.L. Carly, K. Janardan, G.J. Benjamin, E.S. Gustavo, M.R. Robert, J.H. Naomi, J. Phys. Chem. B 112, 2008, 14168–14175.

[4] R.F.W. Bader, Atoms in molecules A Quantum Theory, Oxford University Press, Oxford, 1995; P. Popelier, Atoms In Molecules. An Introduction, Prentice Hall, 2000.

[5] Frisch, M.J. et al. Gaussian 03, Gaussian Inc, Pittsburgh PA, 2003.

[6] E. G. Hohenstein, S. T. Chill, and C. D. Sherrill, J. Chem. Theory Comput. 2008, 4, 1996–2000.

A QSAR study on biological activities of polyamines as anti - alzheimer drugs

Gh .Ghasemi , H. Kefayati ,* S. Fereidoni
Department of chemistry , Islamic Azad University-Rasht Branch , Iran
Email:maedehfereidony@yahoo.com

Keywords : QSAR , Anti-Alzheimer drugs , polyamine

Introduction:

The view that Alzheimer's disease is a fatal outcome of ageing prevails over the view that it mainly affects people aged 75-95. Alzheimer's disease (AD) is a central nervous system disorder that gradually increases in severity with age resulting in memory loss, behavioral changes and a decline in thinking abilities . Connections between individual neurons are destroyed in the AD brain due to the formationof neurofibrillary tangles and senile plaques which obstruct,damage and lead to the eventual death of many neural cells. A QSAR study was performed in an attempt to explore the pharmacophore of some polyamines as anti - alzheimer agents.

Methods:

The study , which used the DFT/B3LYP methods were used to optimize the geometry of polyamines. The molecular structure of polyamines is given in (Fig1). All calculations were performed using the Gaussian 03 programs.We employed the statistic software spss (version19) , taking pIC50 as the dependent variable and every candidate descriptor calculated above as an independent variable to perform the stepwise multiple linear regression. The prediction method were made in matlab 7.1 .

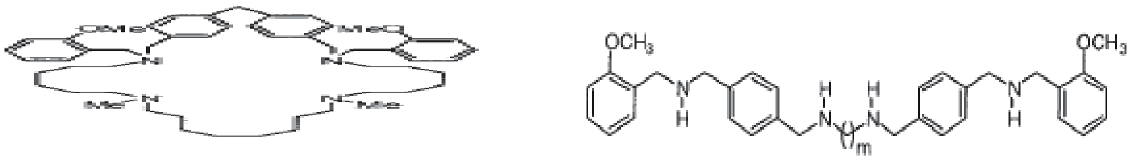

Fig1. The molecular structure of **polyamines** analogues.

Results and discussions:

In this work , we used the GA-MLR (genetic algorithm based multiple linear regressions) for variable selection .In order to calculate GA-MLR ,a program was written based on MATLAB software .A total of 1498 descriptors were initially calculated by Dragon software (version03) for the entire data set of 22 compounds .The two most descriptors which were selected by GA-MLR are as follows:NR05, XMOD. This GA selected descriptors were used as inputs for the construction of artificial neural network (ANN) model. The resulted predictions of the log(1/IC50)in gas phase is given in (table 1). The results of Intercorrelation 0.3 were much better than Intercorrelation 0.4.We have evaluated several layers ([3,1],[5,1],[7,1],[9,1],[11,1] and [2,1],[4,1],[6,1],[8,1],[10,1],[12,1]) in GA and results are shown in (Fig 2). As can be seen from this Fig2 topological and constitutional were important descriptors in our study.

Table1. Experi mental and values of log(1/IC50) using QSAR models.

Calculated (Jack-Knife)gas Intercorrelation 0.3	Calculated(Jack-Knife)gas Intercorrelation 0.4	Observed log(1/IC50)
6.0714	5.7409	6.4400
6.7428	6.3617	6.6600
6.4684	6.3300	5.6200
5.4311	6.0922	5.4800
6.6335	6.8981	6.2700
4.7272	5.7292	5.1400
6.5397	5.4581	5.8800
5.9087	5.2780	5.3600
6.4872	5.7732	6.3100
6.5298	5.9426	5.7500
6.3910	6.8655	6.2300
6.1454	6.0292	5.7900
6.2747	6.2055	6.4300
6.3197	6.0587	6.300
6.8481	6.6653	6.3500
7.0782	6.4569	6.2800
6.2858	7.1329	6.6400
4.9264	3.9551	5.3700
5.9997	6.1307	6.7700
6.1564	6.6742	6.2300
6.2865	6.4792	6.1500
6.0690	6.8670	6.4900

Table2. The statistical parameters of different constructed predicted Jack-knife model.

Method	RMSE test	RMSE train	R^2
GA-ANN Jack-knife(gas)	0.3853	0.1757	0.7825
GA-ANN(gas)	0.3920	0.2101	--

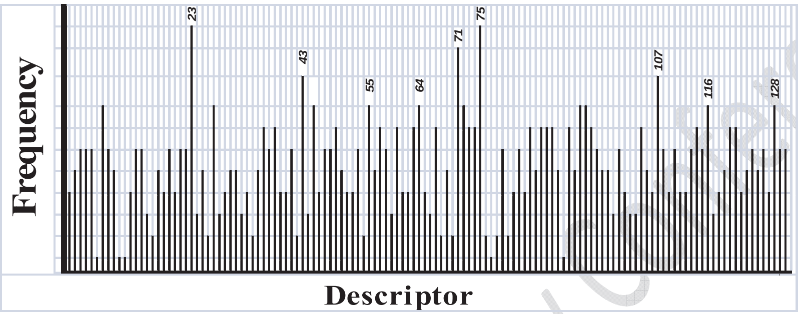

Fig2. The results of GA-ANN in gas phase.

Conclusion:

The GA is a power search technique bassed on the evolution of biological systems the selection of the best variables from. Among the available descriptors was performed by GA-MLR. We find out GA-ANN model is the favorable method toward the other statistical methods.

Refrences:

[1] Gramatica.P, Sci,2007,26:694-701 .
[2]Twamley. E , Ropacki.S, Soc,2006,12:707-735.
[3]Gharaghezi.F,Alamdari.R,Sci,2008,27:679-683.

(*E*)-3-X-Indoline-2-thiones in solution *vs.* gas phase at DFT levels

M.Z. Kassaee*, M. Koohi
Department of Chemistry, Tarbiat Modares University, P.O. Box 14115-175, Tehran, Iran
* Corresponding author. Tel.: +98 912 1000392; fax: +98 21 88006544.
E-mail: kassaeem@modares.ac.ir.

Abstract:

In this work, the structure and stability of important ligands of tyrosine kinase (**I-IV**), are compared and contrasted in gas phase *vs.* solutions (toluene, dichloromethane, methanol, water), at B3LYP/6-311++G** level of theory. The self-consistent reaction field (SCRF) is employed, at 25°C and 1atm pressure.

Key words: DFT; (*E*)-3-X-indoline-2-thione; Solvent effect; SCRF; Aromaticity; Nucleophilicity; Electrophilicity; NICS.

Introduction:

In 1998, oxoindole (**2**) was synthesised through a Wolff-Kishner like reduction of isatin (**1**) with hydrazine hydrate. In 1994, **2**was transformed into thioindole (**3**) *via* P_2S_5 and Na_2CO_3 in THF. Compound **4** was synthesized by condensation of **3** with substituted aryl aldehydes in the presence of a base (Scheme 1)[1]. Solvent effects on physical or chemical processes are employmented by means of empirical solvent parameters. The self-consistent reaction field (SCRF) theory has been relatively successful in describing the solvent effects on the molecules in solutions.

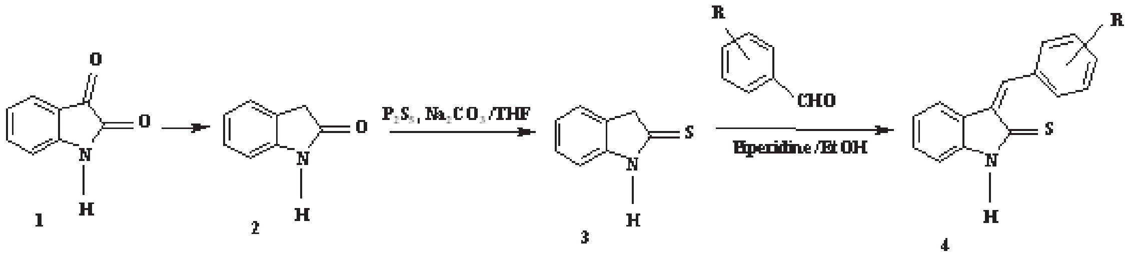

Scheme 1.

Computational methods:

The energies, thermodynamic properties, vibrational analysis, and the zero point vibrational energy (ZPVE) corrections were carried out at *ab initio* and DFT, using the Gaussian 98 program.

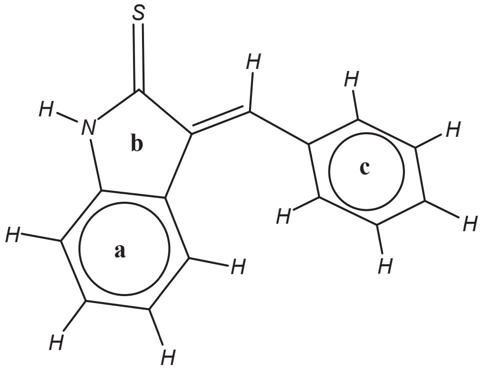

(I)

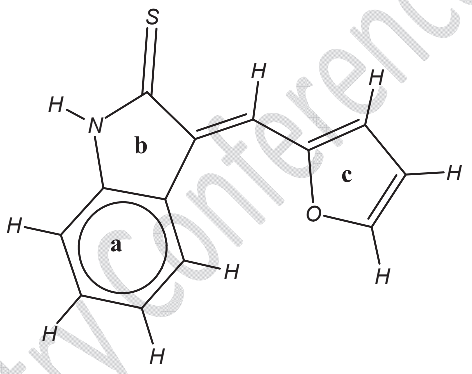

(II)

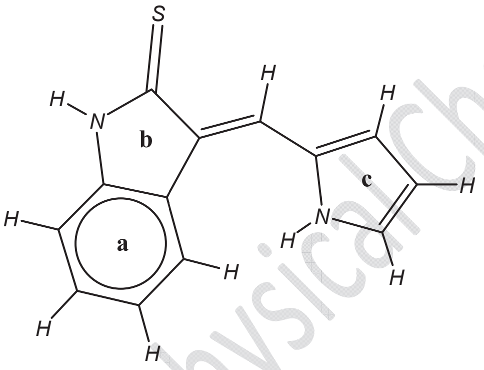

(III)

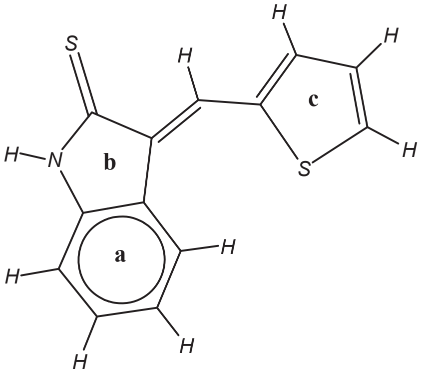

(IV)

Results and discussion:

The highest observed total free energy difference (ΔE_{l-g}) between liquid (l) and gas (g) phase relates to structure **III** in water, whereas the lowest ΔE_{l-g} is associated with **II** in toluene. Stability of each solute (**I-IV**) depends on the dielectric constant of the solvent and the possibility of hydrogen bonding. The trend encountered for the total free energy differences between l and g phase (ΔE_{l-g}) parallels the trend of media dielectric constant (€). Dipole moments (μ) of **I-IV** in solution change regularly with the increasing polarity of solvents. The trend of the LUMO – HOMO energy gaps ($\Delta E_{L\text{-}H}$) for **I-IV** immerge in the opposite direction with the trends of € and polarity of the solvent. Apparently, most Kekule´ compounds possess a full bonding resonance structure and show a well-separated $\Delta E_{L\text{-}H}$ in non-polar solvent (toluene) while, in polar solvents (CH_2Cl_2, MeOH and H_2O) have a relatively small $\Delta E_{L\text{-}H}$, which leads to the extremely high chemical reactivity.

Reference:

[1] S. Ölgen , *Arch Pharm Res.* **2006**, *29*, 1006.

Stable heavier cyclonona-3,5,7-trienylidene congeners and its halogenated derivatives, at DFT

M.Z. Kassaee*, M. Koohi
Department of Chemistry, Tarbiat Modares University, P.O. Box 14115-175, Tehran, Iran
* Corresponding author. Tel.: +98 912 1000392; fax: +98 21 88006544.
E-mail: kassaeem@modares.ac.ir.

Key words: Metallylene; Singlet–triplet energy gap; DFT; Stability.

Abstract:

In order to stabilize metallylenes enough to be isolated, some thermodynamic or kinetic stabilization of the reactive vacant *p*-orbital is required. We have already are studied the largest cyclic C_9H_{10} carbene, and divalent analogues of group 14 elements, along with the halogenated derivatives at the α,ά- or β,β́-positions of the parent divalent elements at DFT. Particularly, we show the energies of singlet and triplet states of $C_8H_{10}M$:, $C_8H_6X_4M$: and $C_8H_8X_2M$: (M = C, Si, Ge, Sn, Pb; and X = H, F, Cl, Br) as a function of the angle about the central group 14 divalent atom, to determine the angle at which the singlet and triplet states cross.

Introduction:

In recent decades, it has generally been recognized that carbenes and their heavier analogues, *i.e.*, silylenes (R_2Si:), germylenes (R_2Ge:), stannylenes (R_2Sn:), and plumbylenes (R_2Pb:) play an important role as transient intermediates. These so-called metallylenes are monomeric species of the polymetallanes. It should also be noted that the choice of the substituent "R" is of great importance in determining the isolability of "stable" metallylenes. Silylenes and to a lesser extent germylenes, have been the center of attention over the last two decades, due to the importance of these group 14 electron-deficient radicals in chemical vapor deposition, semiconductor manufacture, photonics, and aerospace industries. Radicals, ions, ion radicals of stanylenes have been suggested as intermediates in redox reactions of diazo compounds and other molecules, both in the liquid and gas phases. Metallylenes have a singlet ground state with a vacant *p*-orbital and a lone pair of valence orbitals. This extremely high reactivity must be due to their vacant p-orbitals, since 6 valence electrons is less than the 8 electrons of the "octet rule"[1].

Computational methods

Full geometry optimizations are accomplished exclusive of any symmetry constraints with gradient — corrected (DFT) using the Becke's three parameter hybrid functional (B3LYP) with correlation functional of Lee *et al.* and the 6-31+G* basis set for C, Si, and Ge and LANL2DZ basis set for Sn and Pb, employing the Gaussian 98 code.

Results and discussion:

By placing halogenated divalent elements, singlet (s)–triplet (t) energy gaps ($\Delta E_{\text{s-t}} = E_{\text{t}} - E_{\text{s}}$) appear linearly proportional to: (i) the size of the group 14 divalent element (ii) the size of the substitution (iii) the divalent angle ∠C–M–C of the triplet state involved. Unlike the $C_8H_{10}C$: carbene, which was considered as a triplet transition state, for having a negative force constant, all the scrutinized divalent species appeared as boat shaped minima with a singlet closed shell (S_{cs}). This is except for the singlet $C_8H_8F_2C$: carbene that turned out to be a three cyclic minimum through simultaneous interconversion.

Reference:

[1]Y. Mizuhata, T. Sasamori, N Tokitoh *Chem. Rev.* **2009,** *109,* 3479.

A theoretical prediction of stability of novel carbenes

M. Z. Kassaee*, B. N. Haerizade
Department of Chemistry, Tarbiat Modares University, P.O. Box 14115-175, Tehran, Iran
E-mail address: kassaeem@modares.ac.ir

Keywords: DFT, N-YHCs, NHCs, ylide, carbene

Introduction:

The first commercially available stable carbene, **I**, was synthesized in 1991 by Arduengo and co-workers [1]. This *N*-heterocyclic carbene (NHC) owed its viability to the mesomeric effects of the two neighboring nitrogen atoms plus the steric protection of the two adamantyl groups attached to them. Subsequently, diphosphino carbenes (PHC), such as **II**, were reported [7-8]. A tremendous advantage of using such NHCs is their application as ligands for transition metal complexes. Kawashima was first to prepare a free cyclic (amino) (ylidic) carbene (N-YHCs), **IV**, followed by Fürstner who reported its sulfur analogue **V**. N-YHCs are expected to have a high σ–donating ability towards transition metals, because the inductive effect of the ylide moiety is smaller than that of amino group. In addition, π-donating of the ylide carbanion to the carbenic center might stabilize a carbene, similar to the case of amino groups in NHCs.

Computational methods:

Full geometry optimizations are accomplished without any symmetry constraints by means of hybrid functional B3LYP [4] and the 6-31+G* basis set, employing the GAUSSIAN 03 code. The applied basis set is comprised of Pople's well known 6-31G* basis set and an extra plus due to the importance of diffuse functions. To obtain more accurate energetic data, single point calculations are performed at the B3LYP/6-311++G**//B3LYP/6-31+G* and B3LYP/AUG-cc-pVTZ//B3LYP/6-31+G* levels of theory. The frequency calculations are applied to characterize the structures as minima or transition states. Also, nucleus independent chemical shift (NICS) calculations are performed on optimized structures. The nucleophilicity index, *N*, which was introduced by Domingo *et al.* is calculated as $N = \Delta E_{\mathrm{HOMO(Nu)}} - \Delta E_{\mathrm{HOMO(TCNE)}}$, where tetracyanoethylene (TCNE) is chosen as the reference. The global electrophilicity, ω, is also calculated following the expression, $\omega = (\mu^2/2\eta)$, where μ is the chemical potential ($\mu = (E_{\mathrm{HOMO}} + E_{\mathrm{LUMO}}) / 2$) and η is the chemical hardness ($\eta = E_{\mathrm{HOMO}} + E_{\mathrm{LUMO}}$). Density functional calculations with the B3LYP functional are used to estimate the stability of carbenes through appropriate isodesmic reactions.

Result and discussion:

Hoffmann, Schleyer, and Schaefer have emphasized that a molecule may be called "stable" if its computed smallest vibrational frequency (υ_{min}) is at least 100 cm^{-1}. In this respect, our acyclic carbenes $\mathbf{1_C}$, $\mathbf{1_N}$, $\mathbf{1_P}$, and $\mathbf{1_S}$ may not be stable. However, cyclization stabilizes $\mathbf{2_N}$ and $\mathbf{2_S}$ by making their υ_{min} exceed 100 cm^{-1}. Ultimately, cyclization along with unsaturation stabilizes all of our cyclic unsaturated carbenes ($\mathbf{3_C}$, $\mathbf{3_N}$, $\mathbf{3_P}$, and $\mathbf{3_S}$). A better criteria for comparison of carbenes is based on $\Delta E_{\text{S-T}}$. In this sense, we may place a "stability" label on our carbenes, if their $\Delta E_{\text{S-T}}$ measure up to those of "stable carbenes" reported experimentally. Among all of our species, $\mathbf{3_N}$ is the most stable carbene for showing a rather wide gap of $\Delta E_{\text{S-T}}$ = 63.93 kcal/mol. In addition, it is more aromatic for showing a higher NICS (1) value of -9.47 ppm. Also, it demonstrates a higher υ_{min} = 216.98 cm^{-1}. Higher stability of $\mathbf{3_N}$ over $\mathbf{3_P}$, $\mathbf{3_S}$ and $\mathbf{3_C}$ could be attributed to the higher anionic character as well as the π-donating ability of immonium ylide in $\mathbf{3_N}$ which shifts the electron density more towards the carbene center than the quaternary immonium nitrogen. As a result, $C_{carbene}$–C_{ylide} bond length of $\mathbf{3_N}$ (1.38 Å) is shorter than those of the corresponding $\mathbf{3_P}$ (1.43 Å), $\mathbf{3_S}$ (1.42 Å) and obviously $\mathbf{3_C}$ (1.50 Å) (Table 3). Conversely, the shift of cross-conjugation favors the ylide side of the carbene which elongates the N–$C_{carbene}$ bond lengths of $\mathbf{3_N}$ (1.39 Å) more than those of $\mathbf{3_P}$ (1.37 Å), $\mathbf{3_S}$ (1.38 Å) and $\mathbf{3_C}$ (1.34 Å).

Conclusion:

Computations are carried out on the stability of carbenes bearing carbon, immonium, phosphorus, and sulfur ylides, with acyclic, cyclic, and unsaturated cyclic structures, at

B3LYP/6-31+G*, B3LYP/6-311++G** and B3LYP/AUG-cc-pVTZ levels. Based on the following arguments, $\mathbf{3_N}$ appears the most stable and hence the most reasonable synthetic target. (1) Among all of our species, $\mathbf{3_N}$ enjoys being the most stable carbene for showing a wider gap of $\Delta E_{S\text{-}T}$ of 63.93 kcal/mol. (2) It is highly aromatic for showing the NICS (1) value of -9.47 ppm. (3) Proper isodesmic reactions, suggest relatively highest heat of hydrogenation for $\mathbf{3_N}$ (ΔE_H = -12.82 kcal/mol). (4) Proper isodesmic reactions, suggest relatively higher *E1* value of 114.36kcal/mol for $\mathbf{3_N}$, suggesting its stability against carbene dimerizations. (5) Interestingly, $\mathbf{3_N}$ appears more nucleophilic than the NHCs reported experimentally. Moreover, immonium ylides ($\mathbf{1_N}$, $\mathbf{2_N}$, and $\mathbf{3_N}$) appear more stable than their corresponding $\mathbf{1_Y}$, $\mathbf{2_Y}$, and $\mathbf{3_Y}$, for Y= CH_2, PH_3 and SH_2. Finally, going from acyclic to the corresponding cyclic or cyclic unsaturated carbenes increases the stability of hetero-ylide carbenes.

References:

[1] A. J. Arduengo, III, R. L. Harlow, M. Kline, *J. Am. Chem. Soc.* **1991**, *113*, 361.

[2] D. Martin, A. Baceiredo, H. Gornitzka, W. W. Schoeller, G. Bertrand, *Angew. Chem.* **2005**, *117*, 1728; *Angew.Chem. Int. Ed.* **2005**, *44*, 1700.

[3] J. D. Masuda, D. Martin, C. Lyon-Saunier, A. Baceiredo, H. Gornitzka, B. Donnadieu, G. Bertrand, *Chem. Asian J.* **2007**, *2*, 178.

[4] A. D. Becke, *Phys. Rev. A*, **1988**, *38*, 3098.

Theoretical Study of Free Activation Energies of Electron Transfer Process in Nano-complexesof*meta* and *para*-Di-phenyl-methyldene-Fluorescent withFullerenes

MahnazGhiyasi* and Avat (Arman) Taherpour*
Chemistry Department, Faculty of science, Islamic Azad University Arak Branch, P.O.Box:38135-567, Arak, Iran.
avatarman.taherpour@gmail.com&ataherpour@iau-arak.ac.ir

Abstract:

In this study, the number of carbon atoms in fullerenes was used as descriptors to establish a good relationship between the structure of [*m,p*-di-phenyl-methyldene-fluorscent].[C_n] and Fullerenes C_n (n= 60, 70, 76, 82 and 86). The first to fourth free activation energies and kinetic rate constant of the electron-transfer, $\Delta G_{et(n)}^{\#}$ and $k_{et(n)}$, n=1-4 ,respectively were calculated for the complexes of and Fullerenes[*m,p*-di-phenyl-methyldene-fluoreence].[C_n].

key words: electron-transfer, electrochimecal oxidation and reduction,electrochemical properties, oxidation-potential.

Introduction:

Electrochemical Oxidation for meta and para-di-phenyl-methyldene-fluorscent derivatives leads to forming fluorenylidenedication that this dication has the anti-aromatic feature. The electrochemical properties of these compounds were also studied in detail structural change energy based on theory Marcos is expressed. A kind of very strong linear relationship has been calculated between oxidation-potential for this dication and nucleus independent chemical shift (NICS).

Mathematical method:the number of carbon atoms of these fullerenes (C_n) was utilized as a structural index for the compounds. Free energy data of electron-transfer are calculated, and after that kinetics of this process dealt with. Several valuable properties of the fullerenes can be calculated. Calculations are presented for the four reduction potentials (${}^{Red}E_1$ to ${}^{Red}E_4$) of fullerenes C_n. The relationship between the number of carbon atoms and the free energies of electron transfer ($\Delta G_{et(1)}$ to $\Delta G_{et(4)}$) are assessed using the electron transfer equation for [m,p-di-phenyl-methyldene-fluorscent].[C_n].these results and complexes resulting from them have not been reported and synthesized before.

Methods:

In this study, completed values calculated By Microsoft office excell 2007 and program matlab.

Results and Discussion:

By the use of the equations which obtained in this modeling, it is possible to calculate the values of $\Delta G_{et(1)}^{\#}$ to $\Delta G_{et(4)}^{\#}$ of [m,p-di-phenyl-methyldene-fluorscent].[C_n]](M=H and Zn) complexes. The $\Delta G_{et(n)}^{\#}$ (n=1-4) for [m,p-di-phenyl-methyldene-fluorscent].[C_n] complexes (C_n=C_{60}-C_{300})are predicted by using the appropriate equations. By utilizing these results, the electron transfer energies of$\Delta G_{et(n)}^{\#}$ (n=1-4) of the complexes between m,p-Di-phenyl-methyldene-fluorscent acid derivatives with fullerenes (C_n=C_{60}-C_{300})were approximated. The calculated values of the free electron-transfer energies of $\Delta G_{et(n)}^{\#}$ (n=1-4) for [R].C_n(R= di-phenyl-methyldene-fluorscentsupramolecular complexes (n = 60, 70, 76, 82 and 86) in the equations were interpreted. There was good agreement between the calculated and the predicted values. In lieu of increasing the number of carbons atoms in the fullerene structure, the values of $\Delta G_{et(n)}^{\#}$ (n=1-4) decreased.

Conclusion:

Molecular groups meta and para di phenyl methyledenefluorances and fullerenes the electro chimecal properties of this compounds were also studied in detail structural change energy based on theory marcos is expressed. By the use of the equation plang values $\lambda_{max(1)}$ of $\lambda_{max(4)}$ it is possible to calculated of meta and para di phenyl methylidenesfluoranse. The results and complexes resulting from them have not been reported an synthesized before.

References:

[1]Taherpour A. A. and Mohammadinasab E., *Full.Nanot.Carb.Nanostr.*, 18: 72–86, 2010.

[2] Jiao,H:schleyer,P.v.R;Mo,Y.McAllister,M.A:Tidwell,T.T.j.AM.chem.soc.1997,119,7075-7083.

[3] Crestini, C.; Pastorini, A.; Tagliatesta, P. J. Mol. Catal. A: Chem. 2004, 208, 195–202.

Theoretical Study of Free Activation Energies of Electron Transfer Process in Nano-complexesof*meta* and *para*-tetra Bis 3,4- tetra phenyl ethylens withFullerenes

MahnazGhiyasi* and Avat (Arman) Taherpour*
Chemistry Department, Faculty of science, Islamic Azad University Arak Branch, P.O.Box:38135-567, Arak, Iran.
avatarman.taherpour@gmail.com&ataherpour@iau-arak.ac.ir

Abstract:

In this study, the number of carbon atoms in fullerenes was used as descriptors to establish a good relationship between the structure of [*m,p*-di-phenyl-methyldene-fluorscent].[C_n] and Fullerenes C_n (n= 60, 70, 76, 82 and 86). The first to fourth free activation energies and kinetic rate constant of the electron-transfer, $\Delta G_{et(n)}^{\#}$ and $k_{et(n)}$, n=1-4 ,respectively were calculated for the complexes of and Fullerenes[*m,p*-Bis 3,4-tetra phenyl ethylenes].[C_n].

Key words: electron-transfer, electrochimecal oxidation and reduction,electrochemical properties, oxidation-potential.

Introduction:

Electrochemical Oxidation for meta and para-di-phenyl-methyldene-fluorscent derivatives leads to forming fluorenylidenedication that this dication has the anti-aromatic feature. The electrochemical properties of these compounds were also studied in detail structural change energy based on theory Marcos is expressed. A kind of very strong linear relationship has been calculated between oxidation-potential for this dication and nucleus independent chemical shift (NICS).

Mathematical method:the number of carbon atoms of these fullerenes (C_n) was utilized as a structural index for the compounds. Free energy data of electron-transfer are calculated, and after that kinetics of this process dealt with. Several valuable properties of the fullerenes can be calculated. Calculations are presented for the four reduction potentials (${}^{Red}E_1$ to ${}^{Red}E_4$) of fullerenes C_n. The relationship between the number of carbon atoms and the free energies of electron transfer ($\Delta G_{et(1)}$ to $\Delta G_{et(4)}$) are assessed using the electron transfer equation for [m,p-tetra phenyl-ethylenes].[C_n].these results and complexes resulting from them have not been reported and synthesized before.

Methods:

In this study, completed values calculated By Microsoft office exclle 2007 and program matlabe.

Results and Discussion:

By the use of the equations which obtained in this modeling, it is possible to calculate the values of$\Delta G_{et(1)}^{\#}$ to$\Delta G_{et(4)}^{\#}$ of [m,p-di-phenyl-methyldene-fluorscent].[C_n]](M=H and Zn) complexes. The $\Delta G_{et(n)}^{\#}$ (n=1-4) for [m,p-Bis 3,4- tetra phenyl ethylnes].[C_n] complexes (C_n=C_{60}-C_{300})are predicted by using the appropriate equations. By utilizing these results, the electron transfer energies of $\Delta G_{et(n)}^{\#}$ (n=1-4) of the complexes between m,p-Di-phenyl-methyldene-fluorscent acid derivatives with fullerenes (C_n=C_{60}-C_{300})were approximated. The calculated values of the free electron-transfer energies of$\Delta G_{et(n)}^{\#}$ (n=1-4) for [R].C_n(R= Bis 3,4- tetra phenyl-ethylenes-fluorscentsupramolecular complexes (n = 60, 70, 76, 82 and 86) in the equations were interpreted. There was good agreement between the calculated and the predicted values. In lieu of increasing the number of carbons atoms in the fullerene structure, the values of $\Delta G_{et(n)}^{\#}$ (n=1-4) decreased.

Conclusion:

Molecular groups meta and paraBis – 3,4 – substituted phenyl Ethylenes and fullerenes the electrochemical properties of these compounds were also studied in detail structural change energy based on theory marcos is expressed. By the use of the equation plang values $\lambda_{max(1)}$ of $\lambda_{max(4)}$ it is possible to calculated of meta and paraBis – 3, 4 – substituted phenyl Ethylenes.

References:

[1]Taherpour A. A. and Mohammadinasab E., *Full.Nanot.Carb.Nanostr.*, 18: 72–86, 2010.

[2]Jiao,H:schleyer,P.v.R;Mo,Y.McAllister,M.A:Tidwell,T.T.j.AM.chem.soc.1997,119,7075-7083.

[3] Crestini, C.; Pastorini, A.; Tagliatesta, P. J. Mol. Catal. A: Chem. 2004, 208, 195–202.

QSAR investigation on quinolizidinyl derivatives in Alzheimer's disease

Ghasem Ghasemi[a], Satar Arshadi[b], Alireza Nemati Rashtehroodi[c ,*]
[a] Department of Chemistry, Islamic Azad University, Rasht Branch, Rasht, Iran
[b] Department of Chemistry, Payame Noor University, Behshahr Branch, Behshahr, Iran
[c] Department of Chemistry, Payame Noor University, Sari Branch, Sari, Iran
E-mail: Mr.alireza.nemati@gmail.com;

Keywords: Alzheimer's disease, Quinolizidinyl derivatives, Genetic algorithm, QSAR.

Introduction:

Alzheimer's disease (AD) is a debilitating illness with unmet medical needs. The number of people afflicted with the disease worldwide is expected to triple by the year 2050. The multifactorial pathogenesis of AD includes accumulation of aggregates of β-amyloid (Aβ) and tau protein and loss of cholinergic neurons, with consequent deficit of the neurotransmitter acetylcholine (ACh) [1]. In advancing AD, AChE levels in the brain are declining, but a progressive increase (up to 90%) of butyrylcholinesterase (BChE, EC. 3.1.1.8) is observed, which too is able, even if at lower rate, to hydrolyze Ach [2].

Computational details:

The structures of the quinolizidinyl derivatives used in this study [3]. The 3D structures of the molecules were generated using the built optimum option of Hyperchem software (version8.0). ChemOffice and Dragon (version 3.0) programs were employed to calculate the molecular descriptors. Then, Unscrambler (version 9.7) program was used statistical methods and analyses data. All calculations were performed using Gaussian 03 program series employing DFT methods. Geometry optimization of compounds was carried out by B3LYP method employing 6–31G basis set. In this study, the independent variables were molecular descriptors and the dependent variables were the actual half maximal inhibitory concentration (IC50) values.

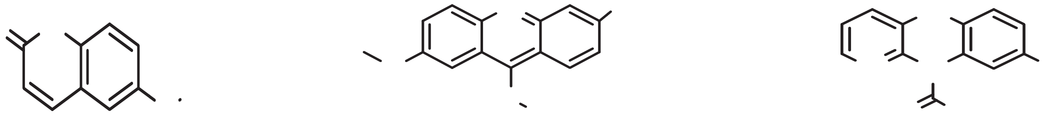

Figure.1 The molecular structure of quinolizidinyl derivatives.

Results and Discussion:

The efficiency of the QSAR model to predict log (IC50) value was also estimated using the internal cross-validation method, this resulted predictions of the log (1/IC50) using Jack–Knife model and PLS method in gas phase is given in Table 1.

Table 1 Experimental and predicted values of log (1/IC50) using Jack–Knife model and PLS method.

Observed		Predicted Jack–Knife		Predicted PLS	
A	B	A	B	A	B
1.531	1.653	1.3446	1.2755	1.813	1.170
1.653	1.653	1.6205	1.5124	1.981	1.861
0.854	1.690	0.8189	1.5678	1.004	1.565
1.591	1.477	1.6168	1.4055	1.467	1.700
1.771	1.505	1.6468	1.6393	1.621	1.448
1.568	1.672	1.6330	1.6259	1.384	1.292
1.699	1.602	1.6081	1.7428	1.311	1.450
1.740	1.672	1.6329	1.6191	1.572	1.108
0.919	0.833	1.5969	1.0209	1.582	0.981
1.634	0.756	1.6664	0.8619	1.666	0.932
0.845	1.532	1.4889	1.7720	1.500	1.424
1.623	1.623	1.7952	1.2527	1.738	1.862
1.763	1.462	1.5337	1.6348	1.523	1.526
1.663	1.690	1.7050	1.2884	1.623	1.107
0.919	0.863	1.4275	1.2297	1.412	0.804
1.613	-0.076	1.8171	-0.2344	1.353	0.381
1.653	-0.658	1.3276	-0.2886	1.284	0.121
1.681	1.756	1.4496	1.2188	1.564	0.663
0.949	0.820	1.1438	0.7352	1.119	0.244
0.826	-0.456	1.2082	-0.6694	1.282	0.109
1.544	0.0790	1.2650	-0.1312	1.294	0.347

The selected descriptors through these methods were used to construct some linear and non-linear models by using MLR and ANN methods. The seven most significant descriptors which were selected by GA are as follows: HOMT, D/Dr06, Mor28p, R2e, R8u+, nDB, R7v+.

Based on the types of variable selection method and also the types of the feature mapping technique, these models can be shown as MLR-ANN, GA-MLR, GA-PLS, and GA-ANN. It revealed that the GA–ANN model was much better than other models is given in Table 2.

Table 2 The statistical parameters of different constructed QSAR models.

Method	RMSE test	RMSE train	R^2
GA–ANN Jack–Knife (gas)	0.2165	0.1406	0.8969
GA–ANN (gas) cross validation	0.4772	0.1406	-

Conclusion:

In the present study, two linear and non-linear variable selection methods were used to select the most significant descriptors, and the MLR, PLS, ANN and GA were used to construct a quantitative relation between the activities quinolizidinyl derivatives and their calculated descriptors. ANN has been successfully used for finding a QSAR model for quinolizidinyl derivatives. It provides the best results among those we have tested.

References:

[1] R. Jakob-Roetne, H. Jacobsen, Angew. Chem. Int. Ed. 48 (2009) 3030-3059.
[2] M. M. Mesulam, A. Guillozet, P. Shaw, B. Quinn. Neurobiol. Dis. 9 (2002) 88-93.
[3] A. Carotti, B. Tasso, F. Sparatore, V. Boido, J. Med. Chem. 46 (2011) 2170-2184.

Configurational properties of 1,2-propadiene, 1-germa-1,2-propadiene, 1.2-digerma-1,2-propadiene and 1,2,3-trigerma-1,2-propadiene. A hybrid density functional theory study and natural bond orbital interpretation

Abbas Ghorbani*[1],Hooriye Yahyayi[2] and SeiedehNegar Mousavi[1]
[1]ChemistryDepartment, Islamic Azad University, Arak Branch, Arak, Iran
[2]Chemistry Department, Islamic Azad University,Zanjan Branch,Zanjan, Iran
Email: ghorbaniabbas30@yahoo.com

Keywords:DFT, NBO, germapropadiene

Introduction:

Cummulenes ($H_2C_nH_2$; n>2) and the corresponding cummulenecarbenes (CnH2; n>2) present important reaction intermediates in combustion flames,[1]chemical vapor deposition,[2] and in interstellar environments.[3]Whereas all cummulenecarbenes hold a C_2 symmetry and depict $^1A_1$ electronic ground states, the situation for the cummulenes is more complex.[4] Here, molecules having an even number of carbon atoms belong to the D_{2h} point group, whereas an odd number of carbon atoms dictate an inherent D_{2d} symmetry.[5]This correlates with ^1A_g and $^1A_1$ electronic ground states of the even and odd-numbered cummulenes, respectively. The structures of the cummulenes also correlate with recent studies of ^{13}C nuclear magnetic resonance (NMR) paramagnetic shielding constants. Due to their unique electronic structure, cummulenes hold also important technical potential as elements for molecular machines the cationic forms serve as models for molecular wires.[6]There is much published data about carbon cummulenes, there is no sufficient information about their analogs containing Ge atoms. For this purpose the ground and transition state structures of 1,2-propadiene(**1**),1-germa-1,2-propadiene(**2**),1,2-digerma-1,2-propadiene(**3**)and1,2,3-trigerma-1,2 propadiene(**4**) have been optimized by density functional theory (DFT) based method, at B3LYP/6-31G* level of theory, using the GAUSSIAN 03 package of programs.[7]The B3LYP functional method combines Becke's three-parameter exchange function with the correlation function of

Lee et al. Also, NBO (natural bond orbital) analysis was used to investigate the nature of the bonds in compounds **1–4**.[8]

Computational Methods:

DFT calculations were carried out using B3LYP/6-311+G**and unrestricted B3LYP/6-311+G** (e.g., UB3LYP/6-311+G**) levels of theory for ground and transition state structures, respectively, with the GAUSSIAN 03 package of programs. Manually constructed appropriate Z-matrix files of initial geometries of the compounds **1-4** were used as input files for optimization at the B3LYP/6-311+G** level of theory. Energy minimum molecular geometries were located by minimizing the energy, with respect to all geometrical coordinates without imposing any symmetry constraints.An NBO analysis was then performed for the ground and transition statestructures of compounds **1-4** by the NBO 5.G program contained in the PC-GAMESS interface.8

Results and Discussion:

In this work,the configurational properties of 1,2-propadiene(**1**),1-germa-1,2-propadiene(**2**), 1,2-digerma-1,2-propadiene(**3**) and 1,2,3-trigerma-1,2-propadiene(**4**) have been investigated by means of hybrid density functional theory based method (B3LYP/6-311++G**) an natural bond orbital (NBO) interpretation. The results obtained showed that the stabilization energies associated with $\sigma_{M1\text{-}H}\rightarrow\pi^*_{M2=M3}$allylic electron delocalization decreases from compound **1** to compound **4**. The decrease of the $\sigma_{M1\text{-}H}\rightarrow\pi^*_{M2=M3}$allylic electron delocalization increases the overall energy of the ground state structures, therefore, this fact reasonably explain the decrease of the energy gaps between the ground and transition state structures (i.e. the mutual interconversion barrier height). Bosed on the results obtained at the B3LYP/6-311++G** level of theory, the energy gap between HOMO-LUMO orbitals decreases from compound **1** to compound **4**. Also, the results showed that the energy required for the mutual interconversion process decreases by the increase of the average double bond and the Ge atom numbers.

Conclusion:

The results obtained showed that by the decrease of the$\sigma_{M1\text{-}H}\rightarrow\pi^*_{M2=M3}$allylic electron delocalizationin the ground state structures, the corresponding mutual interconversion barrier height decreases from compound **1** to compound **4**. In addition, the barrier height of the mutual interconversion process decreases by the decrease of energy gaps between HOMO-LUMO orbitals and also by the increase of the average double bond ($\bar{d}$) and the Ge atom numbers.

References:

[1] C. Hallin, I. G. Ivanov, T. Egilsson, A. Henry, O. Kordina, E. Janzen, Journal of Crystal Growth,**183**,163 (1998).

[2] P. M. Woods, T. J. Millar, E. Herbst, A. A. Zijlstra, Astronomy and Astrophysics 402, 189 (2003).

[3]U. Moelder, P. Burk, I. A. Koppel, THEOCHEM. 712, 81 (2004).

[4]H. Lee. Woodcock, H. F. Schaefer, P. R. Schreiner, J. Phys. Chem. A 106, 11923 (2002).

[5]R. Zahradnik, M. Srnec, Z. Havlas, Collection of Czechoslovak Chemical Communications **70**, 559 (2005).

[6]Nori-Shargh, D., Deyhimi, F., Boggs, J. E., Jameh-Bozorghi S., Shakibazadeh, R., *J. Phys. Org. Chem*. 2007; 20: 355–364.

[7]M.J. Frisch, et al, Gaussian 03, Revision B.03, Gaussian, Inc., Wallingford CT, 2004.

[8]E.D. Glendening, J.K. Badenhoop, A.E. Reed, J.E. Carpenter, J.A. Bohmann, C.M. Morales, F. Weinhold, Theoretical Chemistry Institute, University of Wisconsin, Madison, WI, 2004. NBO Version 5.G.

Theoretical Studies on Complete Gas-Phase Proton Microaffinity Analysis of Three Linear Aliphatic Hexaamine Ligands

Yasin Gholiee[a], Sadegh Salehzadeh[*,a], Shiva Khodaveisi[b], Marzieh Bayat[b], Mehdi Rezaei Sameti[b], Mehdi Bayat[a].
[a] Faculty of Chemistry, Bu-Ali Sina University, Hamedan, Iran (Email: Saleh@basu.ac.ir)
[b] Department of Chemistry, Faculty of Science, Malayer University ,Malayer, Iran

Key words: Theoretical Study, Proton Microaffinity, Proton Macroaffinity, Polyamines.

Introduction:

Multidentate amine ligands have played an important role in the development of synthetic, structural and stereochemical aspects of coordination chemistry[1]. Polyamines in their protonated states form complexes with anions in aqueous solution. In latter complexation process, polyamines are at least tetra-protonated and contain six or more nitrogen atoms. Recently we introduced three new defined proton affinities for polybasic molecules in the gas phase: proton microaffinity, proton macroaffinity and proton overallaffinity[2-4]. We showed that there is a good correlation between the calculated gas-phase proton macroaffinities of some polyamine ligands with corresponding protonation macroconstants in solution[3] . Herein we want to report a theoretical study on complete gas phase proton microaffinities of three linear hexaamine ligands with general formula $H_2N(CH_2)_nNH(CH_2)_nNH(CH_2)_m NH(CH_2)_nNH(CH_2)_nNH_2$; where n=m=2 (22222-Hex); n=3, m=2 (33233-Hex) and n=m=3 (33333-Hex).

Computational details:

The geometries of all species in the gas-phase were fully optimized at DFT (B3LYP and BP86) level of theory using the GAUSSIAN 09 set of programs. The standard 6-31G** basis set was used for all calculations. Vibrational frequency analyses, calculated at the same level of theory, indicate that optimized structures are at the stationary points corresponding to local minima without any imaginary frequency.

Result and discussion:

After calculation of proton microaffinities (Fig.1), the proton macroaffinities and proton overallaffinty for studied molecules were calculated using Eqs. (1) and (2) [2,3].

$$\overline{PA}_n = \frac{\sum_{j=1}^{l}\sum_{i=1}^{m} PA_{n,i}\times R_{n,j}\times S_{n,j}}{\sum_{j=1}^{l}\sum_{i=1}^{m} R_{n,j}\times S_{n,j}} \qquad \text{Eq (1)} \qquad \text{where} \qquad R_{n,j} = \sum_{j=1}^{K} R_{n-1,j}\times S_{n-1,j}$$

$$\overline{PA}_{ov} = \sum_{n=1}^{m}\overline{PA}_n \qquad \text{Eq (2)}$$

The results show that the variations of proton macroaffinities of all molecules is similar to variations of their protonation macroconstants in solution.

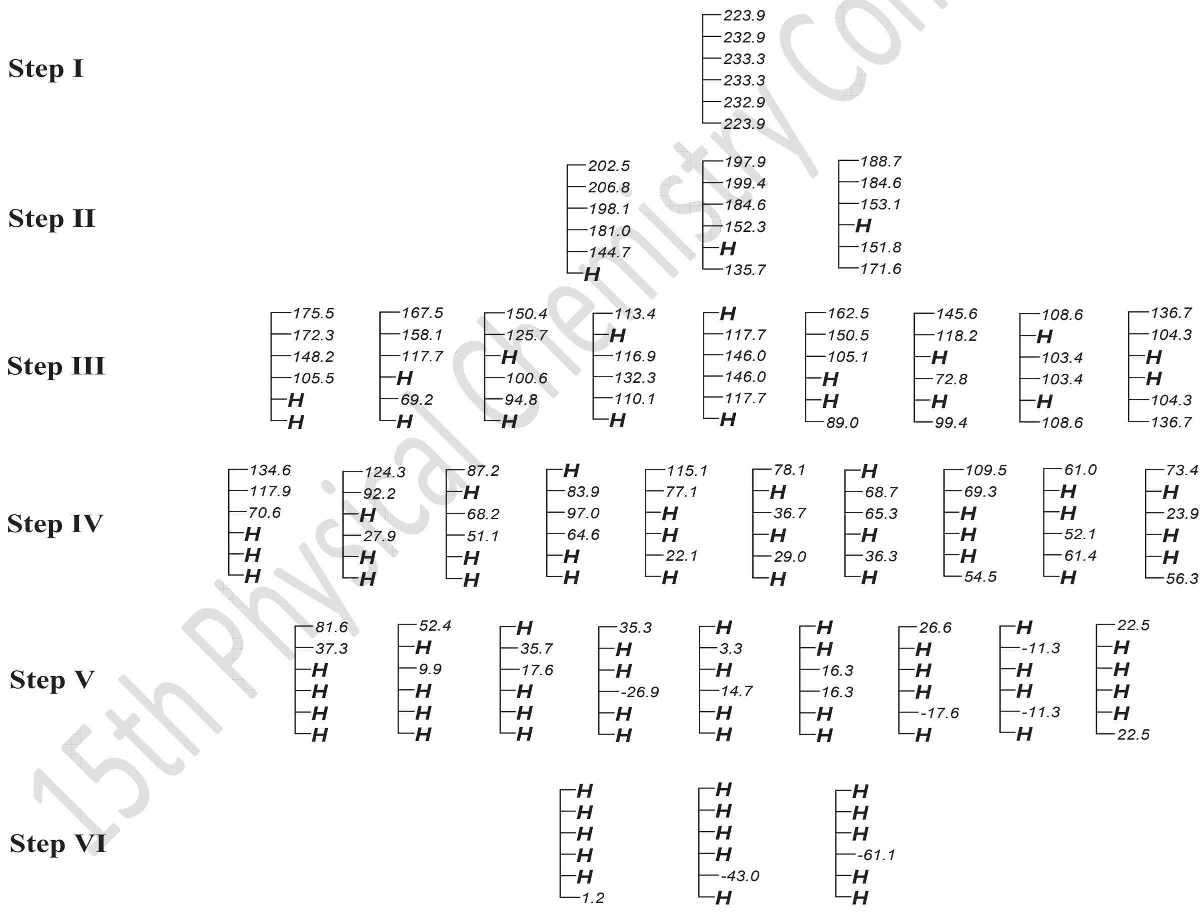

Fig 1. Illustration of full protonation steps of 22222-Hex. Numbers show the proton microaffinity of each site (kcal/mol).

Conclusion:

The reliable theoretical calculation of the gas-phase proton macroaffinities and proton overallaffinities of linear hexaamine ligands according to the complete proton microaffinity analysis is potentially possible.

References:

[1] P.D. Beer, P.A. Gale, Angew. Chem., Int. Ed. 2001, 40, 487.
[2] S. Salehzadeh, M. Bayat, Chem. Phys. Lett. 2006, 427, 455.
[3] S. Salehzadeh, M. Bayat, M. Hashemi, J. Phys. Chem. A 2007, 111, 8188-8192.
[4] S.Salehzadeh, M.Bayat, M. D. Ward , J. Phys. Chem. A 2008, 112, 4090-4094.

Theoretical Study on the Nature of C≡C Bond in R_3E-C≡C-ER_3 (E=C, Si; R=H, F, Cl) Compounds

Mehdi Bayat[*,a], Yasin Gholiee[a], Zeinab Solgi[b], Mehdi Rezaei Sameti[b], Sadegh Salehzadeh[a]
[a] Faculty of Chemistry, Bu-Ali Sina University, Hamedan, Iran (Email:mehdi806@gmail.com)
[b] Department of Chemistry, Faculty of Science, Malayer University, Malayer, Iran

Key words: Theoretical Study, Bonding analysis, Interaction energy, NBO Analysis, Bond Order, the Nature of Bond.

Introduction:

Carbon-carbon double and triple bonds have played an important role in many fields of chemistry. For many years, the synthesis of double and triple bonds between heavier Group 14 elements has attracted special interest in main group chemistry [1]. Since the first isolation of a stable disilene (R_2-Si=Si-R_2) in 1981, a variety of synthetic methods have been developed for the silicon and germanium analogues of alkenes [2]. In contrast to the remarkable progress in doubly bonded compounds, no stable compound featuring triple bonding between heavier Group 14 elements is known up to now [3] despite great interest. Thus, it has been theoretically investigated whether the alkynes and heavier analogues of them are synthetically accessible and isolated in a stable form, by providing insight into the nature of triple bonding. In this work, we investigate the effect of substituents on the nature, interaction energy values and bond order of the C≡C bond in molecules with general formula R_3E-C≡C-ER_3 where E=C, Si and R=H, F, Cl. It is evident that variation of E atoms and R substitutes affects both the interaction energy values and bond orders in the C≡C bonds in the present molecules.

Computational details:

The structures of all molecules in the gas phase were fully optimized at standard 3-21G*, 6-31G*, 6-31+G* and 6-31++G** basis sets by HF, BLYP, B3LYP and BP86 levels of theory using the Gaussian 09 set of programs. The natural bonding orbitals (NBO) calculations were performed using NBO 3.1 program as implemented in Gaussian 09 package at the same level.

Result and discussion:

There are two possible conformers for each studied compound in this work: staggered and eclipsed. At first, for each molecule the more stable conformer was determined based on their electronic energies and then the effect of substituents on the nature of C≡C bonds was investigated. The results of BP86/6-31+G* calculations showed that the more stable conformers in C_4H_6, C_4Cl_6 and C_4F_6 (where E=C) are eclipsed, eclipsed and staggered, respectively. The trend for C≡C bond orders in the latter compounds obtained from NBO analysis at the same level of theory is as follow:

C_4H_6 *(2.780)* > C_4F_6 *(2.756)* > C_4Cl_6 *(2.605)*

Also the similar trend for the interaction energy in these compounds between two R_3CC fragments with spin multiplicity of 4 is as follow:

C_4H_6 *(-271.5)* > C_4F_6 *(-259.5)* > C_4Cl_6 *(-255.7)*

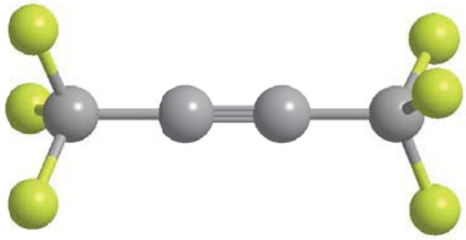

Conclusion:

The results show that the electron withdrawing halogen atoms decrease both the C≡C bond orders and interaction energy between two R_3CC fragments.

References:

[1] M. Weidenbruch, Eur. J. Inorg. Chem. 1999, 373.
[2] M. Weidenbruch, S. Willms, W. Saak, Angew. Chem. Int. Ed. Engl. 1997, 36, 2503.
[3] A. Sekiguchi, S.S. Zigler, R. West, J. Am. Chem. Soc. 1986, 108, 4241.

The anomeric effect in α-halo-*O*-oxime ethers; effects of different substitutions with different electronic properties

A-R. Nekoei*, M. Vatanparast, M. N. Soltani Rad
Department of Chemistry, Shiraz University of Technology, Shiraz 71557-313, Iran
Email: nekoei@sutech.ac.ir

Keywords: anomeric effect, α-halo-*O*-oxime ether, substitution effect, DFT, NBO

Introduction:

The anomeric effect explains the preference of the gauche conformer over the anti conformer in an R–Y–CH_2–X (Y=O, N or S; X=O, N, halogen, etc) fragment [1]. One explanation for the validity of the anomeric effect is hyperconjugation model, in which the overlap between a nonbonding electron pair on the Y atom and the vacant σ^* orbital of the C–X bond is responsible for the anomeric effect [2]. Thus the hyperconjugation causes strengthening the Y-C bond and weakening the C-X bond. Investigation the influences of various substitutions (with different electronic properties such as electron-withdrawing and electron-donating) in different oxime positions (R^1 and R^2 positions, see Fig. 1) on the anomeric effect in α-chloro-*O*-oxime ethers (ACOEs, as representative for their halo-substituted analogues) is the purpose of this paper. Various parameters associated with the anomeric effect have been analyzed.

Methods:

All calculations have been performed by density functional theory (DFT) at B3LYP/6-31G** and B3LYP/6-31G** levels using GAUSSIAN 03 program package [3]. Also, the NBO analyses have been carried out with NBO 3.1 package [4].

Results and discussion:

The optimization calculations for all conformations of the target molecules show that for all most stable forms the C–Cl bond is in the gauche position related to the N–O bond. Thus, all presented data will be related to the most stable gauche conformers. The calculated results for the selected bond lengths and atomic natural charges for all studied ACOE compounds are summarized in Table 1. By comparing these results, it is concluded that the C–Cl and O–C bond lengths increase and decrease, respectively, by increasing the electron-donating strength of substitutions in both R^1 and R^2 positions, which is an evidence for enhancement in the anomeric effect. Also the results of atomic natural charge calculations show that increasing the electron-donating character of R^1 and/or R^2 substitutions leads to more negative charge on oxygen atom. It results in more overlap between the nonbonding electron pair on the O atom and the vacant σ^* orbital of the C–Cl bond that is responsible for the anomeric effect. For more detailed study on the anomeric effect in the target molecules, the calculated donor-acceptor orbital interaction (charge transfer from $n_{(O)}$ to $\sigma^*_{(C-Cl)}$, which is directly related to the anomeric effect) energies are also summarized in Table 1. As it is evident from this table, by increasing the electron-donating strength of R^1 and/or R^2 substitutions, the interaction between nonbonding electron pair on the O atom and the vacant σ^* orbital of the C–Cl bond increases, which leads to enhancement in the anomeric effect.

Conclusion:

All results of bond lengths, atomic natural charges and charge transfer energies show that more electron donating character of R^1 and/or R^2 substitutions in ACOE compounds leads to more anomeric effect and less strong C–X bond.

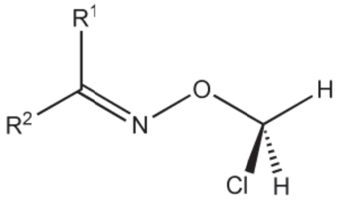

Fig. 1: The gauche conformer of ACOEs

Table 1: Selected bond lengths (Å), atomic natural charges (e), and second order perturbation energies for charge transfer ($E^{(2)}$ in kcal/mol), all calculated at B3LYP/6-311G** level of theory.

ACOE		**Bond Length**			**NBO Charge**			**$E^{(2)}$**
R^1	R^2	*C-Cl*	*O-C*	*C-N*	*Cl*	*O*	*N*	$n_{(O)}\rightarrow\sigma^*_{(C-Cl)}$
CF_3	CF_3	1.811	1.403	1.272	-0.077	-0.371	-0.072	14.38
Me	CF_3	1.828	1.389	1.273	-0.107	-0.399	-0.129	16.91
CF_3	Me	1.830	1.387	1.274	-0.110	-0.392	-0.132	17.27
t-But	Me	1.848	1.375	1.280	-0.139	-0.423	-0.194	19.84
Et	Me	1.850	1.374	1.277	-0.143	-0.421	-0.187	20.24
Me	Et	1.850	1.374	1.277	-0.142	-0.417	-0.187	20.19
Me	Me	1.850	1.374	1.277	-0.143	-0.417	-0.187	20.22
Et	Et	1.850	1.373	1.277	-0.144	-0.421	-0.188	20.30
Me	t-But	1.851	1.373	1.277	-0.143	-0.416	-0.195	20.27
Me	OCH_3	1.854	1.371	1.281	-0.149	-0.409	-0.281	20.90
OCH_3	Me	1.858	1.370	1.282	-0.154	-0.420	-0.267	21.17
$NHCH_3$	Me	1.862	1.366	1.294	-0.163	-0.444	-0.268	22.05
Me	$N(CH_3)_2$	1.863	1.366	1.294	-0.162	-0.416	-0.274	22.06
Me	$NHCH_3$	1.868	1.364	1.291	-0.169	-0.416	-0.282	22.68
$N(CH_3)_2$	Me	1.874	1.361	1.296	-0.177	-0.421	-0.277	23.35
$NHCH_3$	$NHCH_3$	1.877	1.359	1.304	-0.181	-0.435	-0.337	23.93

References:

[1]K. Omoto, K. Marusaki, H. Hirao, M. Imade, H. Fujimoto, *J. Phys. Chem*. 104A (**2000)** 6499.

[2]C. Romers, C. Altona, H. R. Buys, E. Havinga. *Top. Stereochem.* 4 **(1969)** 39.

[3]Gaussian 03, Revision B.03, M. J. Frisch, et. al., Gaussian Inc., Pittsburgh PA (**2003**).

[4] NBO 3.1, E. D. Glendening, A. E. Reed, J. E. Carpenter, F. Weinhold.

Comparing the anomeric effect in α-haloether and α-halo-*O*-oxime ether compounds; DFT and NBO studies

A-R. Nekoei*, M. Vatanparast, M. N. Soltani Rad
Department of Chemistry, Shiraz University of Technology, Shiraz 71557-313, Iran
Email: nekoei@sutech.ac.ir

Keywords: anomeric effect, α-haloether, α-halo-*O*-oxime ether, DFT, NBO

Introduction:

The anomeric effect is described as the preference of an electronegative substituent at C-l of a pyranosides ring to undertake the axial rather than equatorial orientation [1]. Two explanation have been proposed to be responsible for the anomeric effect; unfavorable interaction between lone pairs of the oxygen and the dipole of the C–X bond of a pyranoside, and another explanation, the overlap between a nonbonding electron pair on the oxygen atom and the vacant σ^* orbital of the C–X bond [2]. The anomeric effect may also be extended to the so-called "generalized anomeric effect" which defines the preference for the gauche conformer over the anti conformer in an R–Y–CH_2–X (Y=O, N or S; X=O, N, halogen, etc) fragment [3]. In the present study, using density functional theory (DFT), the anomeric effects in α-chloroether (ACE) and α-chloro-*O*-oxime (ACOE) ether compounds (Fig. 1), as representatives for their all halo-substituted analogue, have been compared. Different R groups with different electronic properties such as electron-withdrawing, electron-donating and electron-supplying have been employed for studying their influences on interactions that are responsible for anomeric effect.

Methods:

Gaussian 03W [4] and NBO 3.1 [5] programs, employing B3LYP level of density functional theory (DFT), using variety of basis sets have been used for different analyses in this work.

Results and discussion:

The calculated results for the selected bond lengths, Wiberg bond orders, atomic natural charges and donor-acceptor orbital interaction energies for ACE and ACOE compounds are summarized in Table 1. Charge transfer analysis shows that the lone pair of oxygen atom in ACOE molecules leans toward the N atom, therefore their O-C bond length is longer than the corresponding value in ACE molecules. As the result of this electron charge dispersion, the C-Cl bond lengths are shorter and stronger in ACOE compounds than classic ACE. These results are in the best agreement with the calculated donor-acceptor orbital interaction energies and atomic natural charges in Table 1. This Table shows the energy for $n_{(O)}$ to $\sigma^*_{(C-X)}$ orbital interaction in ACEs and ACOEs, which is directly related to the anomeric effect. It is obvious that the anomeric effect is significantly reduced in ACOE compounds. Instead, another notable interaction of type $n_{(O)}$ to $\pi^*_{(C-N)}$ is detected in ACOE molecules, which is absent in ACE compounds. All these data suggest that there is an electron delocalization from O atom toward R functional groups in ACOEs (which is confirmed by tabled atomic natural charges). Comparison between calculated data of ACOE molecules with different R substitutions shows that the phenyl influence on reducing anomeric effect is more than that of methyl group but less than that of CF_3 group.

Conclusion:

The anomeric effect in ACEs is verified to be more than ACOEs. Therefore in many reactions that these compounds play the role of intermediates, the latter is more stable in present of the nucleophile molecules. Also, the electronic properties of R groups influence the anomeric effect.

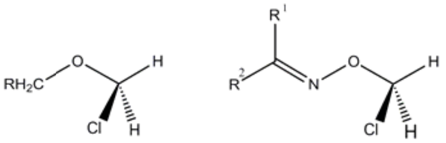

ACE ACOE

Fig. 1: Different studied ethers

Table 1: Selected bond lengths (Å), Wiberg bond orders (WBO), atomic natural charges (e), and second order perturbation energies for charge transfer ($E^{(2)}$ in kcal/mol), all calculated at B3LYP/6-311G** level of theory.

	Bond Length			**WBO**			**NBO Charge**			**$E^{(2)}$**	
ACOE	*C-Cl*	*O-C*	*N/C-O*^{a}	*C-Cl*	*O-C*	*N-O*	*C*	*N*	*O*	$n_{(O)}\rightarrow\sigma^*_{(C-Cl)}$	$n_{(O)}\rightarrow\pi^*_{(C-N)}$
$R^1=R^2=CF_3$	1.811	1.403	1.376	1.004	0.925	1.041	0.03	-0.072	-0.371	14.38	22.66
$R^1=CH_3$, $R^2=CF_3$	1.830	1.387	1.401	0.979	0.955	0.994	0.166	-0.129	-0.399	16.91	16.58
$R^1=CH_3$, $R^2=Ph$	1.845	1.377	1.416	0.954	0.98	0.971	0.266	-0.176	-0.407	19.32	13.46
$R^1=R^2=CH_3$	1.850	1.374	1.427	0.947	0.989	0.956	0.29	-0.187	-0.417	20.22	12.29
ACE											
$R=CF_3$	1.851	1.372	1.416	0.95	0.988	0.911			-0.536	20.56	
$R=CH_3$	1.871	1.361	1.438	0.923	1.02	0.875			-0.548	23.77	

[a]: N-O bond length for ACOEs and C-O bond length for ACEs.

References:

[1]J. T. Edward. *Chem. Ind. (London),* (**1955**) 1102.

[2]C.L. Perrin, K. B. Armstrong, M.A. Fabian, *J. Am. Chem. Soc.*116 (**1994**) 715

[3]A. J. Kirby, "The anomeric and related stereoelectronic effects at oxygen", Springer Verlag, Berlin (**1983**).

[4]Gaussian 03, Revision B.03, M. J. Frisch, et. al., Gaussian Inc., Pittsburgh PA (**2003**).

[5] NBO 3.1, E. D. Glendening, A. E. Reed, J. E. Carpenter, F. Weinhold.

Dynamic Behavior of Boron Nitride Nanotube and Surfactant Complexes Mediated Molecular Dynamic Stimulation

M. Foroutan*, M. Fatemi
Department of Physical Chemistry, School of Chemistry, College of Science, University of Tehran, Tehran, Iran,
m.fatemi@khayam.ut.ac.ir

Keywords: Molecular Dynamics (MD) Simulation, Boron Nitride Nanotube (BNNT), Triton X100 (TX100) Surfactant, Carbon Nanotube CNT.

Introduction:

We used a molecular dynamics (MD) simulation approach to probe the behaviors of the BNNT with Triton X100 surfactant. So we assess nanotubes in different temperatures and diameter. The comparison of our results for BNNT-TX100 composities with those of the similar carbon nanotube CNT-TX100 composites, disclose that the BNNT-TX100 interactions are much stronger, which is the most significant result of this process.

Computational Procedure:

MD simulations were first carried out on a (5, 5) armchair CNT and (5, 5) armchair BNNT with a interacting with individual molecules of TX100. Using the AMBER99[1] force field and a canonical ensemble (constant NVT), the velocity form of Verlet algorithm method and the Nose-Hoover thermostat algorithm were used to integrate the equations of motion with a time step of 1.0 fs. Non-bonded van-der-Waals interactions were modeled by a Lennard-Jones potential with a cut-off distance of 1.2 nm. Our simulation is related to the behavior of the TX100 when they are close to the nanotubes in an “ideal” poor solvent.

Results and Discussion:

Figure 1 and 2 represent the snapshots of nanotubes wrapped by the TX100. Figure 3 represents the interaction energy for (5,5) nanotubes with TX100, as a function of simulation time.the interaction energies for BNNT_TX100 are much higher than those for the corresponding CNT-TX100, due to the large contribution of electrostatic interactions and π-π nature[2]. The stronger interfacial binding of TX100 to BNNTs is caused by the polarization of BNNTs [3], which directly gives rise to the strong electrostatic interactions between them. As Table 1 shows; with an increase in nanotube diameter, the interaction energy is increased, because the surface contact area between them increases accordingly. As Figure 4 shows; the attractive interaction of the TX100 with the nanotubes increasing only slightly with increasing temperature. Thus, the temperature dependence of the interaction energies can be considered negligible.

Conclusion:

Our work demonstrated that the composite materials of BNNTs and TX100 have a potential application in the preparation of fibers with mechanical strength much higher than that of composite materials of CNTs and TX100 So the BNNTs could be more efficient nanofillers than the CNTs for nanocomposite reinforcement applications.

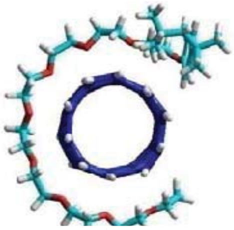

Fig.1: snapshot of (5, 5) CNT wrapping by TX100.

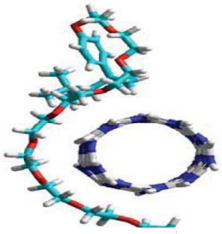

Fig. 2: snapshot of (5, 5) BNNT wrapping by TX100.

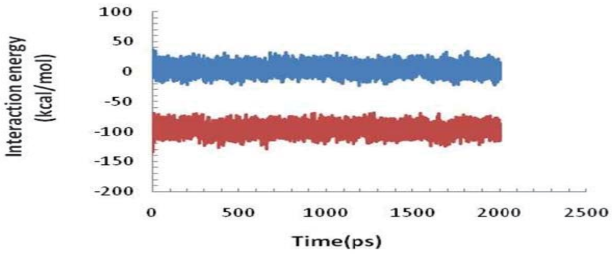

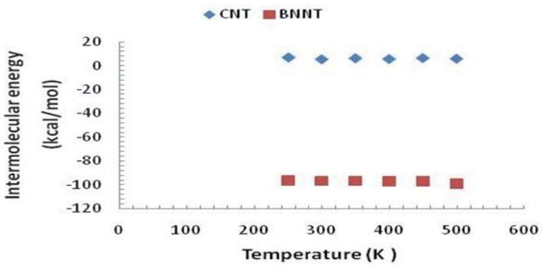

Fig.3: Interaction energy evolution for (5, 5) CNT-TX 100 and (5, 5) BNNT-TX100 composites respectively at 300 K.

Fig.4: Interaction energy of (5, 5) nanotube-TX100 composites as a function of temperature.

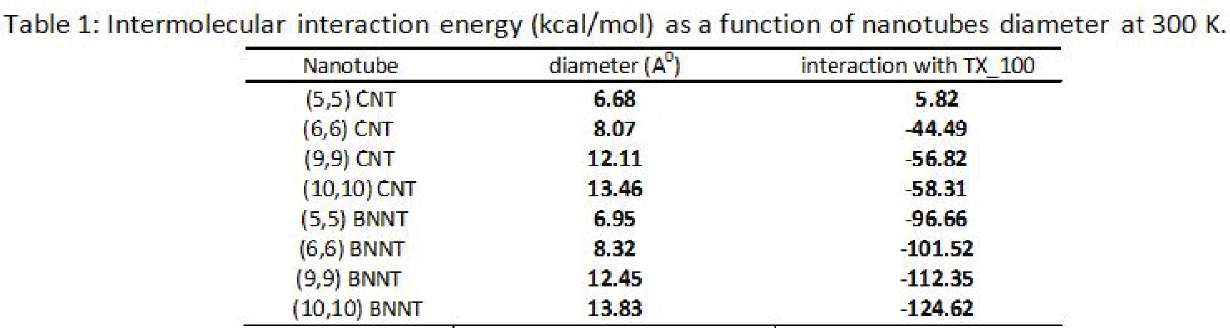

Table 1: Intermolecular interaction energy (kcal/mol) as a function of nanotubes diameter at 300 K.

Nanotube	diameter (A^0)	interaction with TX_100
(5,5) CNT	**6.68**	**5.82**
(6,6) CNT	**8.07**	**-44.49**
(9,9) CNT	**12.11**	**-56.82**
(10,10) CNT	**13.46**	**-58.31**
(5,5) BNNT	**6.95**	**-96.66**
(6,6) BNNT	**8.32**	**-101.52**
(9,9) BNNT	**12.45**	**-112.35**
(10,10) BNNT	**13.83**	**-124.62**

Reference:

[1]N.L. Allinger.; Y.H. Yuh.; J.H. Lii.; J. Am. Chem. Soc.**1989**, 111, 8551.

[2]Chen, R. J.; Zhang, Y.; Wang, D.; Dai, H. J. Am. Chem. Soc. **2001**,123, 3838.

[3]Won, C. Y.; Aluru, N. R. J. Phys. Chem. C **2008**, 112, 1812.

Seperation of Co2,So2 from Ch4 in AIN (Aluminium Nitride Nanotube)

S. Yahyazade[1], M. Hashemiyanzade
[1]MasterStudentfrom Iran University of Science&Technology(IUST), HengamSt,Tehran
[2]Dr.SeyedMajidHashemianzadehfrom Iran University of Science&Technology(IUST),HengamSt,Tehran
E-mail: Sahar310@gmail.com

Keywords : Gas Separation, Aluminium Nitride Nanotube.

Aseparation process, or simply a separation, is any mass transfer process used to convert a mixture of substances into two or more distinct product mixtures, at least one of which is enriched in one or more of the mixture's constituents. In some cases, a separation may fully divide the mixture into its pure constituents. Separations are carried out based on differences in chemical properties such as size, shape, mass, or chemical affinity between the constituents of a mixture, and are often classified according to the particular differences they use to achieve separation. In the case that no single difference can be used to accomplish a desired separation, multiple processes will often be performed in combination to achieve the desired end.

Barring a few exceptions, almost every element or compound is naturally found in an impure state. Often these impure raw materials must be separated into their purified components before they can be put to productive use, making separation processes essential for the modern industrial economy. In some cases these separations require total purification, as in the electrolysis refining of bauxite ore for aluminum metal, but a good example of an incomplete separation process is oil refining. Crude oil occurs naturally as a mixture of various hydrocarbons and impurities. The refining process splits this mixture into other, more valuable mixtures such as natural gas, gasoline and chemical feedstocks, none of which are pure substances, but each of which must be separated from the raw crude. In both these cases a series of separations is necessary to obtain the desired end products. In the case of oil refining, crude is subjected to a long series of individual distillation steps, each of which produces a different product or intermediate thus the separation of $CO_2/CH_4/SO_2$ gas mixture is still the subject of intensive fundamental and industrial research.

In this work the separation of Co2 and SO_2 from CH_4 was simulated by using AIN(aluminum Nitride Nanotube) and has been investigated computationally.

References:

[1] G.E. Ioannatos, X.E. Verykios, H2 storage on single- and multi-walled carbon nanotubes, International J. Hydrogen Energy 35 (2010).

[2]George P.Lithoxoosa,b,AnastasiosLabropoulosc,Loukas D. Peristerasb, Nikolaos Kanellopoulosc, JannisSamiosd, Ioannis G. Economoua,Adsorption of N2, CH4, CO and CO2 gases in single walled carbon nanotubes, Elsevier (2010)

[3] ZHU Yujun, ZHOU Jianhai, HU Jun , LIU Honglai and HU Ying ,Computer Simulation of Adsorption and Separation of CO2/CH4 in Modified COF-102. Chinese Journal of Chemical Engineering, (2011)

[4] Xu, Q., Liu, D.H., Yang, Q.Y., Zhong, C.L., Mi, J.G., “Li-modifiedmetal-organic frameworks for CO2/CH4 separation: a route toachieving high adsorption selectivity”, J. Mater. Chem.(2010).

[5]RainaWanbayor, VithayaRuangpornvisuti∗Adsorption of CO, H2, N2O, NH3 and CH4 on the anatase TiO2 (001) and (101)surfaces and their competitive adsorption predicted by periodic DFT calculations, Elsevier (2010)

[6] Y.S. Bae, R.Q. Snurr, Molecular simulations of very high pressure hydrogenstorage using metal–organic frameworks, MicroporousMesoporous Mater, (2010).

[7] V. Goetz, O. Pupier, A. Guillot, Adsorption , (2006).

A DFT study on the fluorinated derivatives of boron, aluminium, and nitrogen substituted cyclic carbenes

J. Amani*, S.M. Musavi, F. Gharehhasanloo,
Department of chemistry, Shahr-e-Qods Branch, Islamic Azad University, Tehran, Iran
amani@shahryariau.ac.ir

Key words: Cyclic carbene, Heat of hydrogenation, $\Delta E_{\text{HOMO-LUMO}}$, Aromaticity, DFT

Introduction:

Cyclic carbenes have been stimulated many chemists, in the recent years, both experimentally and computationally. The effects of introduction of heteroatoms into the cyclic carbenes backbone and the σ-donor and π-acceptor abilities of different substituents have been studied on the cyclic carbenes to improve the ligand properties of these systems [1, 2].

Methods:

Geometry optimizations are carried out at their singlet and triplet electronic states of carbenes using Gaussian 03 program package via MP_2/6-311++G**//6-31+G* level of theory. Also, nucleus independent chemical shift values (NICS) are calculated at the B_3LYP/6-311++G** and NBO population data is calculated at the MP_2/6-311++G** level.

Results and discussion:

In this study some novel fluorinated boron, aluminium, and nitrogen cyclic carbenes are investigated (Scheme 1). Our structures divided into three series containing four, five and six membered-ring carbenes with different heteroatom positions (**1a-c, 2a-c**, and **3a-c**, respectively).

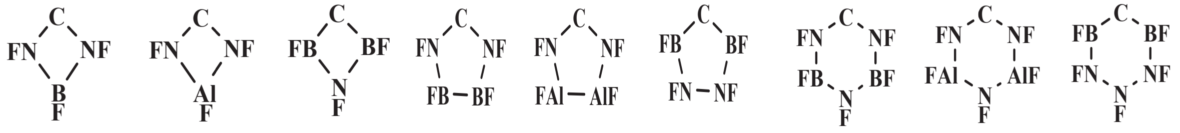

1-a 1-b 1-c 2-a 2-b 2-c 3-a 3-b 3-c

Scheme 1.

In the four membered-ring carbenes, series **1**, all the carbenes are singlet in ground state except for **1-c** that its triplet state is 25.7 kcal/mol lower in energy than the corresponding singlet one. According to Table 1, the ΔE_H is less negative for **1-b** while the highest amount of $\Delta E_{HOMO-LUMO}$ is obtained for **1-a**. In series **2**, all the carbenes are singlet ground state except for **2-c** that its triplet state is 38.5 kcal/mol lower in energy than the corresponding singlet one. In this series, ΔE_H is less negative for **2-b** and **2-c** has the highest amount of $\Delta E_{HOMO-LUMO}$. In the six membered-ring carbenes, **3-c** is the only triplet ground state carbene (with 37.4kcal/mol lower in energy than its singlet). The heat of hydrogenation is less negative for **3-b** and also the highest amount of $\Delta E_{HOMO-LUMO}$ is obtained for **3-a**.

The aromaticity of the carbenes appears very different and amazing based on the NICS values (Table 1). However, the nonplanarity of structures may justify such inconsistencies. In series **1**, **1-a** and **1-c** are aromatic (NICS (1) $_{zz}$ = -7.9 and -13.4 ppm respectively); while **1-b** is rather antiaromatic (NICS (1) $_{zz}$ = 5.3 ppm). In series **2**, **2-c** is non-aromatic (NICS (1) $_{zz}$ = -3.5 ppm) while **2-a** and **2-b** are antiaromatic (NICS (1) $_{zz}$ = 11.2 and 9.0 ppm, respectively). Finally, in series **3**, **3-a** and **3-c** are aromatic (NICS (1) $_{zz}$ = -6.6 and -6.1 ppm, respectively); while **3-b** is non-aromatic (NICS (1) $_{zz}$ = -0.8 ppm). The stabilization effect of the aluminium with fluorine substituted on the singlet cyclic carbenes is increased with increasing the size of the ring, but in the boron with fluorine substituted analogous the trend is reversed.

Table 1. Calculated thermodynamic data (kcal/mol) for **1-3 a**, **b**, **c**.

Structure	E_s	E_t	ΔE_{s-t}	ΔE_H	ΔE_{H-L}(ev)	NICS(1)$_{zz}$ (ppm)	
						singlet	triplet
1-a	-294736.4	-294669.6	66.8	-58.4	14.6	-7.9	-12.4
1-b	-431073.7	-431053.8	19.9	-40.6	11.4	5.3	-0.6
1-c	-276127.5	-276153.3	-25.7	-105.1	14.0	-13.4	1.2
2-a	-372711.2	-372672.9	38.3	-46.2	12.2	11.2	1.5
2-b	-654369.6	-645340.5	29.0	-36.6	9.5	9.0	-2.9
2-c	-372643.5	-372682.0	-38.5	-113.0	14.2	-3.5	1.1
3-a	-469311.1	-469274.3	36.8	-33.2	14.5	-6.6	-1.2
3-b	-741951.0	-741899.8	51.1	-23.4	11.6	-0.8	-4.8

3-c	-469173.1	-469210.5	-37.4	-150.6	11.2	-6.1	0.4

Conclusions:

All cyclic carbene attached to nitrogen atoms are singlet while those attached to boron atoms appear triplet ground state. Going from series **1** to **3** the kinetic stability of carbenes is increased gradually. Inconsistent aromaticity results denoting aromatic, antiaromatic and nonaromatic carbenes are found based on NICS values.

References:

[1] A.J. Arduengo, H.V.R. Dias. R.L. Harlow, Kline. M. J. Am. Chem. Soc. 1992, 114, 5530.
[2] P. Pérez, E. Chamorro. THEOCHEM. 2010, 943, 110.

A DFT study on the mechanism of Gold-catalyzed methanolysis of 1, 5 enynes

A.Ariafard[a,c*], M.Ostadebrahim[b], B.Yates[c]
a Central Tehran Branch, Islamic Azad University, Shahrak Gharb, Tehran, Iran
b University, Shahr-e-Rey Branch, Tehran, Iran
c School of Chemistry, University of Tasmania, PrivateBag 75, Hobart TAS7001, Australia
Email: ariafard@yahoo.com

Key words: 1, 5 enyne, MeOH, Au(I), Carbon atom , Bicyclic intermediate.

Introduction:

Gold salts and complexes have emerged in the past few years as the most powerful catalysts for electrophilic activation of alkynes toward a variety of nucleophiles.[1] For example, Toste et al showed that 1,5 enyne **I** reacts with MeOH in the presence of Au(I) to give methoxycyclization product **II** (Scheme1). Kozmin et al subsequently reported that the interamolecular hydroxycyclization of 1,5 enynes with tethered nucleophiles by Au(I) (or Au(III)) takes place in a similar manner. Another interesting type of the methoxycyclization products (**IV**) were found by Gagosz et al via the Au (I)-catalyzed reaction of MeOH with the 1,5 enynes **III** having two methyl substituents at Cf. The intermediate **V** was proposed to be responsible for the formation of both the products **II** and **IV** ;the attack of methanol at Ce gives **II** while that at Cf gives **IV**.

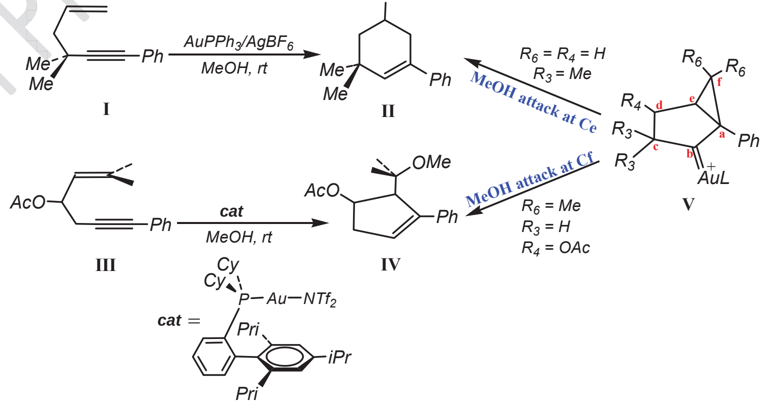

Scheme 1

Methods:

Gaussian 09 was used to fully optimize all the structures reported in this study at the B3LYP level of density functional theory (DFT). The effective core potential of Hay and Wadt with a double-ξ valence basis set (LANL2DZ) was chosen to describe Au. The 6-31G (d) basis set was used for other atoms. To further refine the energies obtained from the B3LYP calculations, we carried out single-point energy calculations for all the structures with a larger basis set at the B3LYP level. These utilizes the quadruple-ζ valence def2-QZVP basis set on Au and the 6-311+G (2d,p) basis set on other atoms. we have Gibbs free energies obtained from the B3LYP calculations in dichloromethane throughout the paper unless otherwise stated.

Result and discussion:

As stated in the Introduction, the attack of methanol on the bicyclic intermediate **V** can take place at either Ce (pathway 1) or Cf (pathway 2). This step is calculated to be rate limiting step for both these pathways. In pathway 1, our calculations show that the MeOH attack onto Ce in bicyclic intermediate (**VI**) through transition structure I_TS giving product **VII (**Scheme2).In contrast the MeOH attack onto Cf in **VI** (pathway 2) by passing transition structure I′_TS, leads to formation of **VII**′. Our the calculations results have demonstrated that MeOH attack via pathway 1 is the kinetically more favorable than the pathway 2.

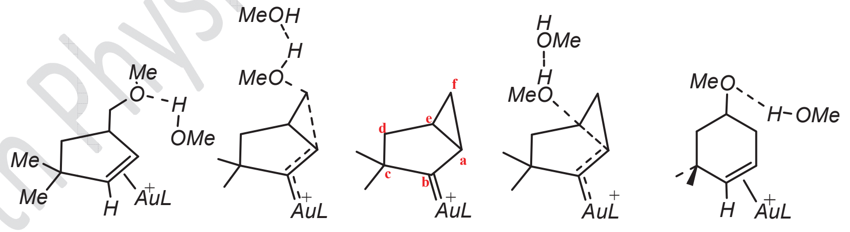

VII **I_TS** **VI** **I′_TS** **VII′**

Scheme 2

Conclusion:

Our the calculations results is consistent with the experimental data Toste that the reaction of 1,5 enyne **I** with methanol leads to the formation of product **II** (Scheme 1). However, as demonstrated by Gagosz et al, the substitution of the hydrogen atoms at Cf with methyl groups results in a change in the regioselectivity reaction. In such a case methanol prefers to attack at Ce and not Cf.

Reference:

[1] E. Jimenez- Nunez; A. M. Echavarren. *Chem. Rev*. 2008.
[2] D. Gorin; B. Sherry; D. Toste. *Chem.Rev*. 2008.
[3] L.Zhang; J.Sun; S.Kozmin. A. *Ad*V. *Synth. Catal.* 2006.
[4] A. Buzas; F. Istrate; F. Gagosz. *Angew. Chem. Int. Ed.* 2007.

A novel interaction between Protein Z and Z-dependent Protease Inhibitor complex.

S. Falsafi-Zadeh[a], Z. Karimi[a*], B. Keikhaei[b], H. Galehdari[c].
a Bioinformatics unit, Department of Genetics, Shahid Chamran University, Ahvaz, Iran.
b Research Center for Thalassemia and Hemoglobinopathy-Ahvaz Jundishapur University of Medical Sciences.
c Department of Genetics, Shahid Chamran University, Ahvaz, Iran.
Email: z.karimi20@yahoo.com

Key words: Molecular Dynamics (MD), Protein Z, Protein Z-dependent protease inhibitor**,**

Introduction:

Protein Z (PZ) is a multi domain VKD dependent protein which contains GLA, EGF1, 2 and SP domain. PZ has a cofactor role as mediating inhibition of the Factor X (FX) by the Z-dependent protease inhibitor (ZPI) in the presence of Ca^{2+} ions and phospholipids [1]. PZ circulates in plasma in a complex with ZPI. In the previous studies, interaction between PZ and ZPI has been found and involves ionic and hydrogen bond interactions between Glu-244, His-250, Arg-350, Gln-357, His-210, Arg-298, Arg-212, and Glu-219 from protein Z with Lys-239, Asp-238, Asn-261, Asp-74, Asp-293, Thr-296, and Lys-68 from ZPI. In the summery, they showed that PZ bind to ZPI with SP domain (residues 135-360). But our results show that PZ can bind to ZPI with EGF2 domain as well as SP domain [2].

Materials and Methods:

In our previous study, we have modeled complete complex of PZZPI by adding GLA domain to crystal structure PZZPI GLA domain less (3H5C.pdb with resolution 3.26Å) using visual molecular dynamic (VMD) [3, 4]. Complete complex of PZ and ZPI with 11 Ca^{2+} ions was solvated in a water box with 120, 130, 137Å dimensions which contains 57113 water molecules (TIP3W), 183368 atoms. We neutralized system with 12 Na+ and 14 Cl- ions neutralized and utilized cutoff of 12 Å for short-range non-bonded interactions. We initially performed energy minimization for two systems in 10000 step in 20ps.All simulation was performed at NPT at 310k and a pressure of 1 atm and set 2fs for time step. The MD simulation was carried out for 100ns using NAMD Version 2.7 and Charmm 27 force field [5, 6].

Apparatus:

Our system has been run by Illinois university of Urbana Champaign at Texas Advanced Computing Center (TCC).

Result and discussion:

We have found that PZ can bind to ZPI with EGF2 domain with hydrophobic interaction between residues Tyr 240(chain Z) with Pro91 (chain P) and Met 285(chain Z)-Leu 102(chain P) and this interactions remain during simulation.

Contact area of each interaction is 42.3 and 20.8 respectively. Also we calculated distance between center mass of side-chain of tyr240 to Pro91 and Met285 to Leu102 (attach file). Average distance between Tyr240-Pro91 and Met285-Leu102 is 5 Å and 5.6 Å respectively, and it is acceptable for hydrophobic interaction because the default of hydrophobic interaction has been determined 5Å.

Conclusion:

Also our result would be confirmed because Prof.Rezaie et al made a chimera of PZ and FX [7] which PZ/FX chimera (N-terminus of PZ and light chain of FX) bound to ZPI weaker than wild-type, possibly suggesting and supporting our hypothesis that EGF2 interaction with ZPI is may also contribute to the binding affinity.

Our result show that Arg298 and Asp 214 (from PZ) and Lys 68 (from ZPI) have key role in interaction PZ and ZPI because of participating in both H-bond and salt bridge bonds.

Reference:

[1] Han, X., R. Fiehler, and G.J. Broze, Jr., Isolation of a protein Z-dependent plasma protease inhibitor. Proc Natl Acad Sci U S A, 1998. **95**(16): p. 9250-5.

[2]Huang, X., et al., Basis for the specificity and activation of the serpin protein Z-dependent proteinase inhibitor (ZPI) as an inhibitor of membrane-associated factor Xa. J Biol Chem, 2010. **285**(26): p. 20399-409.

[3]Lee, C.J., et al., A proposed structural model of human protein Z. J Thromb Haemost, 2007. **5**(7): p. 1558-61.

[4] Humphrey, W., A. Dalke, and K. Schulten, VMD: visual molecular dynamics. J Mol Graph, 1996. **14**(1): p. 33-8, 27-8.

[5]Phillips, J.C., et al., Scalable molecular dynamics with NAMD. J Comput Chem, 2005. **26**(16): p. 1781-802.

[6]MacKerell, A.D., et al., All-Atom Empirical Potential for Molecular Modeling and Dynamics Studies of Proteins†. The Journal of Physical Chemistry B, 1998. **102**(18): p. 3586-3616.

[7] Rezaie, A.R., et al., Protein Z-dependent protease inhibitor binds to the C-terminal domain of protein Z. J Biol Chem, 2008. **283**(29): p. 19922-6.

Theoretical study on the mechanism of the reaction of 1, 5 enynes having a Si atom with nucleophiles catalyzed by Gold complexes

E. Asadollah[a], A. Ariafard[a,b*], B. F. Yates[b]
a Central Tehran Branch, Islamic Azad University, Shahrak Gharb, Tehran, Iran
b School of Chemistry, University of Tasmania, Privatebag 75, Hobart TAS7001, Australia, and Department of Chemistry, Faculty of Science
Email: ariafard@yahoo.com

Key words: Gold, Enyne, Silicon atom, Alcohol.

Introduction:

Gold (I) complexes are capable catalysts for activating enynes towards reaction with alcohols. For Example, the experimental data's Toste showed that the reaction of 1, 5 enynes containing a silicon atom at the 3-position (see **I**) with alcohols in presence of Au (I) complexes, the products **II** and **III** are formed. In such a case Toste investigated that, depending on nature of heteronucleophiles, different products are formed. When the heteronucleophile is PhOH, product **II** is formed and when the heteronucleophie is MeOH product **III** is formed (scheme 1). [1]

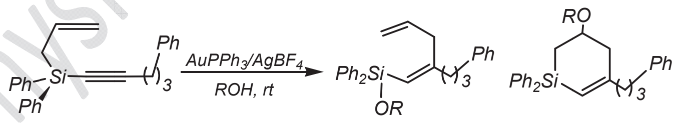

I **II** **III**

Scheme 1

At the same time Park and Lee observed that Au (I)-catalyzed reaction of 1, 5 enynes **IV** with ^{i}PrOH affords **V** (scheme 2). [2]

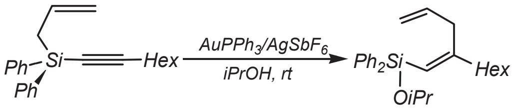

IV **V**

Scheme 2

Computational details:

Gaussian 09 was used to fully optimize all the structures reported in this paper at the B3LYP level of density functional theory (DFT). The effective core potential of Hay and Wadt with a double-ξ valence basis set (LANL2DZ) was chosen to describe Au. The 6-31G (d) basis set was used for other atoms. To further refine the energies obtained from the B3LYP calculations, we carried out single-point energy calculations for all the structures with a larger basis set at the B3LYP and M06 levels. These utilizes the quadruple-ζ valence def2-QZVP basis set on Au and the 6-311+G (2d, p) basis set on other atoms.

Result and discussion:

In this study we investigate the reaction mechanism of Au (I)-catalyzed alcoholysis of the 1, 5 enynes. Our calculations showed that the alcoholysis reaction **VI** in presence of AuL^+ with two MeOH molecules, leads to formation of **VII**. In contrast, this reaction is done with four MeOH molecules and it forms **VIII**. These results are consistent with the experimental data's Toste, Park and Lee.We performed additional calculations using PhOH as a nucleophile. Consistent with the experimental observations, we found that the nucleophilic attack of PhOH at Si only leads to formation of **IX** (scheme 3).

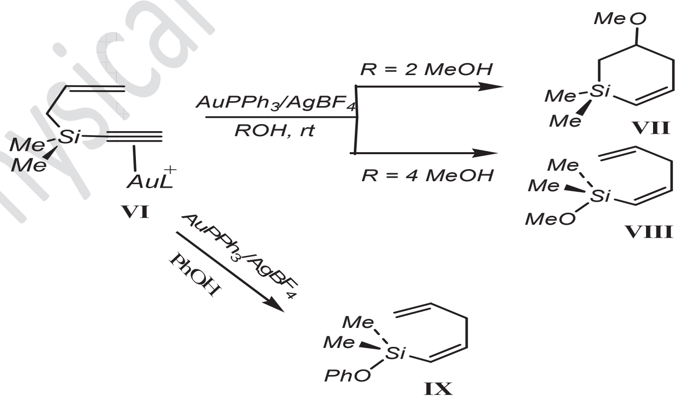

Scheme 3

Conclusion:

Our calculations results show that in reaction of 1, 5enynes with alcohols in presence of Au (I) complexes, depending on the nature of nucleophiles, different products are formed.

Reference:

[1] Y. Horino; M. R. Luzung; F. D. Toste*; J. Chem. Soc*. 2006.

[2] S. Park; D. Lee; *J. Chem. Soc*. 2006.

Relation between the substituent effect and aromaticity in imidazole derivatives: a comparative study

Alireza Najafi Chermahini*[a], Behzad Hosseinzadeh[a], Alireza Salimi beni[a], Abbas Teimouri[b]
[a]Department of Chemistry, Yasouj University, Yasouj, Iran
[b]Department of Chemistry Payame Noor University(PNU), Isfahan, Iran
E-mail: najafi@mail.yu.ac.ir, najafy@gmail.com

Keywords: Aromaticity; NICS; NBO, HOMA, Imidazoles

Introduction:

Aromaticity is one of the key concepts in chemistry which is studied time to time, by both experimental and theoretical chemists [1,2]. Numerous methods have been developed for the measurement of the extent of aromaticity since Kekule′ first introduced the concept 147 years ago, but no single measure has gained universal acceptance. Part of the problem is that aromaticity is a multidimensional property, composed of geometrical, energetic and magnetic components, whereas most measures focus on only one aspect [3]. The imidazole ring system is the most important substructures found in a large number of natural products and pharmacologically active compound systems. Compounds containing imidazole moiety have many pharmacological properties and play important roles in biochemical processes. [4]. energies and aromaticity of a series of R substituted imidazoles [R = NH_2, OH, H, CH_3, F, Cl, CN NO, NO_2], their anions and protonated forms in the gas phase have been calculated with the DFT/B3LYP and MP2 methods at the 6-311++G(d,p) level. We have analyzed the change of local aromaticity using several aromaticity indicators (Pozharsky Index, HOMA, NICS and pEDA) and found a considerable ring aromaticity for imidazoles, imidazolate anions and their protonated forms. In each class anion forms have the most aromaticity and in neutral forms,1-H imidazoles have less aromaticity character. The results of calculated aromaticities of imidazole derivatives substituted at 2 position using various scales presented in Table 1,2 and 3.

Table 1

Calculated HOMA, AI, NICS(0) and NICS(1) indices of neutral form 2-R imidazol derivatives calculated at b3lyp/6-31++G(d,p)

	HOMA		A		NICS (0)		NICS (1)		pEDA	
	DFT	MP2	DFT	MP2	DFT	MP2	DFT	MP2	DFT	MP2
NO_2	0.92	0.93	55.05	57.28	-12.62	-13.41	-10.46	-10.55	-0.125	-0.101
NO	0.95	0.95	62.38	68.33	-11.91	-13.38	-10.20	-11.01	-0.208	-0.121
CN	0.91	0.92	53.51	61.08	-13.61	- 14.19	-11.00	-10.93	-0.078	-0.059
F	0.79	0.85	30.58	39.99	-12.97	- 13.76	-9.73	-9.44	0.045	0.031
Cl	0.83	0.88	38.29	48.77	-12.56	-13.28	-10.10	-9.95	0.042	0.041
H	0.86	0.89	44.18	53.70	-13.21	-14.01	-10.82	-11.07	-0.029	-0.040
CH_3	0.84	0.89	42.63	53.15	-12.06	-12.85	-9.62	-9.89	-0.014	-0.029
OH	0.79	0.85	31.53	41.35	-12.01	-12.85	-8.61	-8.99	-0.016	0.022
SH	0.86	0.91	45.85	56.85	-12.30	-13.17	-10.13	-10.55	0.006	0.202
NH_2	0.80	0.87	35.16	47.47	-11.50	-12.73	-8.64	-9.55	0.071	0.015

Table 2.

Calculated HOMA, A, NICS(0) and NICS(1) indices of anion form 2-R imidazol derivatives calculated at b3lyp/6-31++G(d,p)

	HOMA		A		NICS (0)		NICS (1)		pEDA	
	DFT	MP2	DFT	MP2	DFT	MP2	DFT	MP2	DFT	MP2
NO_2	0.98	0.94	87.18	75.45	-10.15	-11.03	-10.39	-10.34	-0.240	-0.135
NO	0.92	0.92	74.77	75.14	-8.04	-9.36	-9.66	-10.12	-0.367	-0.163
CN	0.96	0.93	79.95	76.16	-12.16	-12.40	-11.33	-11.19	-0.370	-0.094
F	0.90	0.91	51.94	56.88	-11.48	-11.92	-9.77	-9.71	0.013	-0.012
Cl	0.93	0.92	57.98	62.51	-11.59	-11.75	-10.10	-9.98	0.004	-0.013
H	0.94	0.92	66.23	68.76	-11.83	-12.27	-10.90	-11.05	-0.043	-0.052
CH_3	0.93	0.92	65.42	68.97	-10.51	-10.88	-10.33	-10.43	-0.047	-0.051
OH	0.90	0.90	51.64	57.36	-10.52	-11.15	-10.27	-9.53	0.040	0.034
SH	0.93	0.92	59.12	66.89	-11.18	-11.31	-9.86	-10.26	0.014	0.055
NH_2	0.91	0.91	55.69	61.16	-10.08	10.77	-9.14	-9.34	0.028	-0.017

Table 3.

Calculated HOMA, A, NICS(0) and NICS(1) indices of protonated form 2-R imidazol derivatives calculated at b3lyp/6-311++G(d,p)

	HOMA		**A**		**NICS (0)**		**NICS (1)**		**pEDA**	
	DFT	MP2	DFT	MP2	DFT	MP2	DFT	MP2	DFT	MP2
NO_2	0.89	0.92	49.29	56.57	-14.36	-15.19	-9.89	-10.40	-0.060	-0.054
NO	0.92	0.95	57.74	67.01	-13.89	-15.38	-9.92	-11.12	-0.108	-0.061
CN	0.88	0.93	51.67	62.05	-14.78	-15.62	-10.29	-10.75	-0.018	-0.028
F	0.76	0.84	30.50	40.85	-14.25	-15.30	-8.89	-9.10	0.081	0.043
Cl	0.81	0.88	39.59	50.39	-13.48	-14.51	-8.90	-9.52	0.098	0.064
H	0.84	0.90	42.20	53.46	-14.34	-15.35	-10.15	-10.78	-0.021	-0.028
CH_3	0.81	0.89	40.01	51.83	-13.33	-14.41	-9.31	-10.18	0.017	-0.002
OH	0.73	0.82	28.75	38.65	-13.28	-14.39	-8.13	-8.66	0.144	0.089
SH	0.86	0.92	47.92	59.97	-13.62	-14.63	-10.10	-10.41	0.019	0.003
NH_2	0.69	0.79	28.20	38.11	-12.33	-13.53	-7.30	-8.26	0.223	0.144

References:

[1]Katritzky, A. R.; Barczynski, P.; Musumarra, G.; Pisano, D.; Szafran, M. *J. Am. Chem. Soc.* **1989**, *111*.

[2]Cyranski, M. K.; Krygowski, T. M.; Katritzky, A. R.; Schleyer, P.v.R. *J. Org. Chem.* **2002**, *67*, 1333.

[3]Schleyer, P.V.R. *Chem. Rev.* **2001**, *101*, 1115.

[4] Ho, J. Z.; Hohareb, R. M.; Ahn, J. H.; Sim, T. B.; Rapoport, H. *J. Org. Chem.* **2003**, *68*, 109.

Existence and characterization of HO_3-CH_3OH Complex: A computational study

N.MohammadSalehi[a,*],M. Solimannejad [b]
[a] Arak University.
[b]Department of Chemistry,Arak University.
Email: setaremsalehi89@gmail.com

Key words: Hydrogen bonding, Noncovalent intermolecular, Methanol, Hydrogentrioxy radical.

Introduction:

Hydrogen bonding is the strongest noncovalent intermolecular interaction and governs many chemical and biological processes in nature [1-2]. In this paper, results of the theoretical investigations of hydrogen bonding complexes pairing CH_3OH and HO_3 moieties have been reported.

The existence of the hydrogen trioxy radical (HOOO) has several important implications in atmospheric chemistry. For example, it may act as an intermediate in key chemical reactions in the atmosphere [3].

Methods:

Calculations were performed using the Gaussian 03 system of cods [4]. Results of calculations and atoms in molecules(AIM) analysis of the studied complex have been reported at MP2 and B3LYP levels using range of basis set from 6-31G(d) to 6-311++G(2df,2pd).

Result and disscution:

Two cis and trans conformers of HO_3 radical, have been considered for interaction with CH_3OH. No significance difference is observed for pairing of CH_3OH with cis or trans conformers of HO_3.

Atoms in molecules (AIM) theory have been used to identify nature of interactions in studied complex (Table1). High stability of studied complex are elucidated base on AIM analysis that predicted partially covalent nature of interactions in local minimum located on potential energy surface of $CH_3OH.HO_3$ radical-molecule complex.

Table1.AIM Parameters for H-bond in complex between CH_3OH and HOOO

Methods and Basis set	□$_{□CP}$	Laplacian	H
B3LYP/6-311++G(2df,2pd)	0.0421	0.0931	0.8037
MP2 /6-311++G(2df,2pd)	0.0476	0.0968	0.7521

Conclusions:

There is one structure on the potential energy surface of the radical-molecule complex, just with cis conformer of HO_3. The interaction is between O of CH_3OH (Hydrogen acceptor) with H of HO_3 radical(Hydrogen donor).

Base on BSSE and D_e for studied complex, Methanol can stable HO_3 radical so much.(D_e=32.216 $Kj.mol^{-1}$).

References:

[1]G.A.Jjeffrey,W.Saenger,Hydrogen Bonding in Biological structures,Springer-Verlag, Berlin,1991.

[2]S.Scheiner, Hydrogen Bonding, A Theoretical Prespective, Oxford University Press, Oxford,1997.

[3]Murray, C.; Derro,E.L.;Sechler,T.D.;Lester,M.I.J.Phys.Chem,A,"Stability of the Hydrogen Trioxy Radical via Infrared Action Spectroscopy".2007.

[4]Frish M.J.;et al."Gaussian 03,Revision Bo2.Gaussian,Inc.",Pittsburgh.PA(2003).

A computational study of interaction between Acetylene & hypohalous acids.

N.MohammadSalehi[a,*]
[a] Arak University.
Email: setaremsalehi89@gmail.com

Key words: Noncovalent interaction, hypohalous acids, Acetylene.

Introduction:

Hypohalous acids **(HOX)** have a great influence on the stratospheric ozone concentration [1, 2]. Traces of chlorine and bromine containing molecules play important roles in many areas of atmospheric chemistry. The most notable one is polar depletion of ozone concentration [1].

In this study, calculations carried out between HOX and Acetylene. Thus the present work reports a detailed examination of the stabilities, electronic structures and vibrational frequencies of these complexes.

Methods:

Calculations were performed using the Gaussian 03 system of cods [3]. The geometries of the isolated HOX and their associated complexes were fully optimized at the MP2/ 6 - 311++ G (2d, 2p) level. The harmonic vibrational frequency calculations were performed to confirm whether the predicted structures are minima and the evaluate the zero-point vibrational energies (ZPE) corrections.

Result and discussion:

Calculations have shown the interactions between acetylene and hypohalous acids were in dimmers and trimers complexes. Dimmers and trimers complexes have two and four configurations respectively. At some of them acetylene is as hydrogen acceptor and in the other it is as hydrogen donor. The stability of structures is obtained by D_e^{cp} . Energetically, the most stablecomplexes correspond to those of bromine derivatives, followed by the chlorine, being the less stable those of the fluorine.

Atoms in molecules (AIM) theory have been used to identify nature of interactions in studied complexes.

Results of vibrational analysis show that symmetric stretching frequency of all O–H bonds that take part in interactions are shifted to red**.**

Conclusions:

A theoretical study of interaction between acetylene & hypohalous acids (HOX, X= F, Cl, Br) have been carried out by means of MP2 / 6- 311++ G (2d,2p) calculations. Two and four configurations have been characterized for 1:1 and 1:2 complexes (Ac: HOX) respectively.

Thus there is two minima for X=F and Cl and one minima for X= Br were located on the potential energy surface of the (1:1) complexes.

Twelve different structures have been obtained for the (1:2) complexes, that all of them are stable.

References:

[1] F.S. Rowland, M.J. Molina, Rev. Geophys. 13 (1975) 21.
[2] M . P. McGrath, F.S. Rowland, J. Phys. Chem. 100 (1996) 4815.
[3] E. H. Appelman, Acc. Chem. Res.6 (1973) 113.

Effect of hydration on the mechanism of proton transfer in Oxozolidinethiones

B. Makiabadi [a*], M. Zakarianezhad [b], Z. ArjmandTajaddini[b], M. Hasanpour[b]
a Department of Chemical Engineering, Sirjan University of Technology, Sirjan, Iran
bDepartment of Chemistry, Payame Noor University, Tehran, Iran
E-mail:bmakiabadi@sirjantech.ac.ir

Keywords: Oxozolidine-2-thione, Proton transfer, Tautomerization, Binding energy

Introduction:

Oxozolidinethiones (OZT) are potent goitrogens, which are not counteracted byiodine as is thiocyanate [1]. A broad range of applications in chemistry have beenreported for OZT[2]. OZT has structural formulae that can be discussed in terms of tautomerism forms. Tautomerization of thione/thiol has been of interest to chemist for a very long time. A particular type of tautomerization is H_2O-assisted, in which H_2O molecules mediate the process by serving as a bridge that connects the donor and acceptor sites. Another type of tautomerization may take place through a self-association mechanism. In this work, DFT methods were used to investigate the effect of hydration and self-association on the reaction mechanism of proton transfer in OZT.

Methods:

Geometry optimization were done using B3LYP/6-311++G(2d,2p) level of theory. Harmonic vibrational frequencies were computed to verify the nature of minima and transition states of stationary point along the tautomerization path. The AIM analysis was carried out in B3LYP/6-311++G(2d,2p) level of theory

Result and discussion:

In this work, we investigated the proton transfer via intramolecular mechanism, water-assisted and self-assisted tautomerizationin OZT.On the basis of the results obtained from our calculations, the thionecomplexes, (A), are more stable than corresponding thiols (B). Alsostability of complexesincreases with the increment of the number of S…H hydrogen bonds.Dimer AA has two S…HN H-bonds and dimmer BB, which is tautomer form of AA, has two N…H-S H-bonds. AW and BW complexes are stabilized by two S…H-O and NH…O, and two SH…O and N...H-O H-bonds, respectively. In AW2 and BW2 dimers three S…HO, O…HO and O…HN hydrogen bonds are observed. In A(B)W and A(B)W2 complexes water act simultaneously as the proton donor and proton acceptor.The results show that binding energy AW to BW and AW2 to BW2aremore than corresponding dimmers AA to BB. Thus H-bond interactions in thewater-association complexes are stronger than self-association complexes. In addition, inclusion of a water molecule to AW complex increases the binding energy.The stability of thionecomplexes decreases in the order of AW2> AW> AA> A. The barrier energy for both self-assisted and H_2O-assisted proton transfer is lower than that of the direct proton transfer. As a result, H_2O-assisted tautomerization is energetically a suitable path for proton transfer. With respect to H_2O-monommer-assist second water molecule in the binding site of AW2 reduces activation energy. Compared with A to B, decreases in the reaction energies for self-assisted and H_2O-assisted proton transfer are greater, and activation energies are also lower. Thus, it can be concluded that the direct proton transfer is more difficult than the water-assisted.The results of AIM reveal the partially covalent nature of S…HN interactions in A(B)-W complexes.

Conclusions:

The results obtained show that the thione complexes are more stable than corresponding thiols. Also the stability of complexes increases with the increment of the number of S…H hydrogen bonds.The H-bond interactions in thewater-association complexes are stronger than self-association complexes. The barrier energy for both self-assisted and H_2O-assisted proton transfer is lower than that of the direct proton transfer. As a result, H_2O-assisted tautomerization is energetically a suitable path for proton transfer.The S…HN interactions in A(B)-W complexeshave the partially covalent nature .

References:

[1] F.L. Austin, C.A. Gent, I.A. Wolff;"Enantiomeric-3-hydroxypent-4-enethionamides from thioglucosides of Crambe and Brassica seeds by action of ferrous salts;" Can. J. Chem; 46, 1507-1512, 1968.

[2] G.Jalce, M.Seck, X.Franck, R.Hocquemiller, B.Figadere;"Highly Diastereoselective Synthesis of trans-2,5-Disubstituted Tetrahydrofurans"; J. Org. Chem; 2004, 69, 3240–3241.

Tautomerism of hydrated and dehydrated barbituric acid: A theoretical study

M. Zakarianezhad[a*],B. Makiabadi[b],M. Hasanpour[a],AsyehBarkhoda[a]
aDepartment of Chemistry, Payame Noor University, Tehran, Iran
bDepartment of Chemical Engineering, Sirjan University of Technology, Sirjan, Iran
E-mail: mzakarianejad@pnu.ac.ir

Keywords: Tautomerization, Barbituric acid, Theoretical study

Introduction:

Barbituric acid contains four mobile hydrogen atoms, which are responsible for several stable tautomeric forms. The current interest in barbiturates arises from their application in medicine and as dyes in chemical industry [1].The availability of one or two functional groups in the molecules of these compounds determines different properties that they possess [2]. The aim of our theoretical investigation has been laid on finding the transition states of some ket-enoltautomeric forms of barbituric acid both in gas phase and in watermolecules.

Methods:

Quantum chemical computations were carried out with the Gaussian 03 series of programs. All calculations performed in the gas phase by employing the hybrid density functional B3LYP with the6-311++g(2d,2p) and aug-cc-pVDZbasis sets.Single-point calculations were also performed on the gas-phase-optimizedgeometries using the PCM model.

Results and Discussion:

Thirteen structures of tautomers optimized in the singlet ground states. In agreement with experiment the calculated tautomer energies indicated the most stable tautomer and the least stable one. From the value of $\Delta G^{\#}$ we calculated the rate constant (*k*) of all tautomer transition state conversion. The mechanisms examined and discussed in this work contain three structure of the first tautomrism of the barbituric acid that each one goes to same product via two competitive pathways. Results indicate that first and second pathway show easier transformation with a lower energy barrier than other one. The first water molecule coordinated to the barbituric acid structure decreased the potential surface energy of all tautomeric structure presented in reaction mechanism and also all activation paremeters in all reaction paths significantly. Although the second coordinated water molecule reduced the energy of all structures presented in tautomerization mechanism but, its effect is not significant in comparison with the first one.

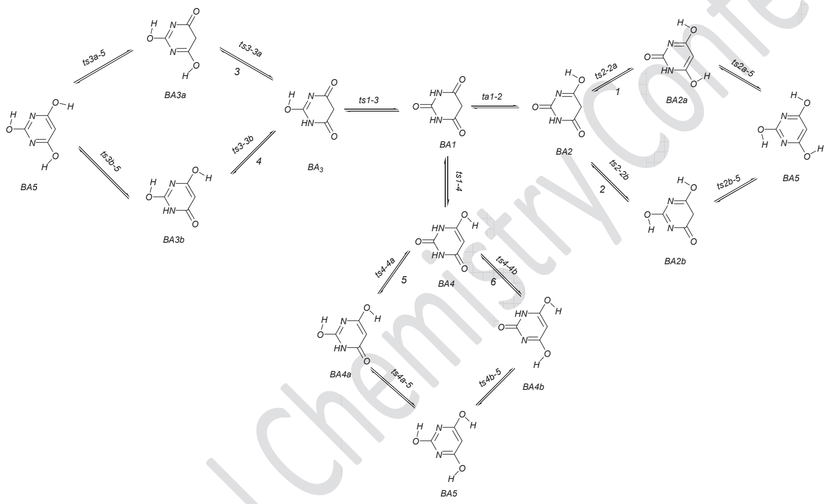

Conclusions:

Results indicate that he keto forms of BA are more stable than the enol formsboth in the gas-phase and in water. This may be because ofthe intrinsic thermodynamic preference of ketoconformation thanthe enol. The order of stability of all structures remained unchanged in gas phase and in the presence of water molecules. Introduction of one and twowater molecules greatly changes the pictureof the whole process by progressively decreasing theenergy barrier but, the priority of two parallel process remain unchanged in all pathways.Solvent establish hydrogen bondswith the bare molecule and these hydrogen bonds greatlyfacilitate intramolecular proton transfer process by reducingthe barrier height. Furthermore, the solvent moleculefacilitate the transfer of a proton by using its own hydrogenatoms. The highest barrier in parallel processes related to Ts2a-5 with221.7kJ/mol value. This barrier decreased to 191.1kJ/molin one water molecule but, is constant in the presence of two water molecules. The lowest energy barrier is related to Ts1-2with 121.7 kJ/mol value which decreased to 43.5 kJ/mol in the presence of one water molecule and increased to 56.1 kJ/molin the presence of two water molecules.

References:

[1] FWurthner, S.Yao, B.Heise, C.Tschierske; "Hydrogen bond directed formation of liquid-crystalline merocyanine dye assemblies"; Chem. Commun; 21, 2260-2263, 2001.

[2] C.Uhlmann; "Low Risk of Development of Substance Dependence for Barbiturates Prescribed as Antiepileptic Drugs"; CNS Neuroscience & Therapeutics; 15, 24-31, 2009.

Quantum mechanical study on the mechanism of Lewis acid-catalyzed ene reactions of formaldehyde

A. Morsali [a], *M. M. Heravi* [a] *and M. Najafi** [a]
[a] Faculty of Science, Department of Chemistry, Mashhad Branch, Islamic Azad University, Iran
(Email: mina.najafi66@yahoo.com)

Keywords: Mechanism, Ene reactions, Density functional theory

Introduction:

Ene reactions are additions of electrophilic double or triple bonds (enophils) to alkenes (enes) with concomitant transfer of an allylic hydrogen (Eq. (1)). Despite the synthetic value of Lewis acid-catalyzed ene reactions, a clear mechanistic understanding of these reactions has been elusive. In this work, we investigated this mechanism using the quantum mechanical approach. More specifically, for the rate determining step [1], being not very clear experimentally, a mechanism was proposed which is compatible with experimental evidence.

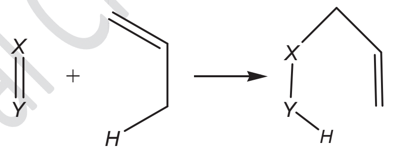

(1)

Computational details:

All of the present calculations have been performed with the B3LYP [2] hybrid density functional level using the G09 package. The 6-311++G(d,p) basis set was employed. The gas phase optimized geometries used to apply the solvent effects, where the valuable PCM [4] model was employed. We assumed that the change of the molecular geometry upon solvation has a negligible effect on the thermodynamic parameters. Thus, the optimized geometries calculated in gas phase were used. Basically, the optimized structures in solvent should be used for frequency calculations, but to reduce computational cost, optimized structures in gas phase could be used as an approximation for this purpose.

Results and discussion:

The following mechanism (Eq. 2)) for Lewis acid-catalyzed ene reactions was proposed which is compatible with experimental evidence. In this mechanism, a fast equilibrium step (with equilibrium constant K1) will result in the formation of complex I which will be converted into P during a slow process.

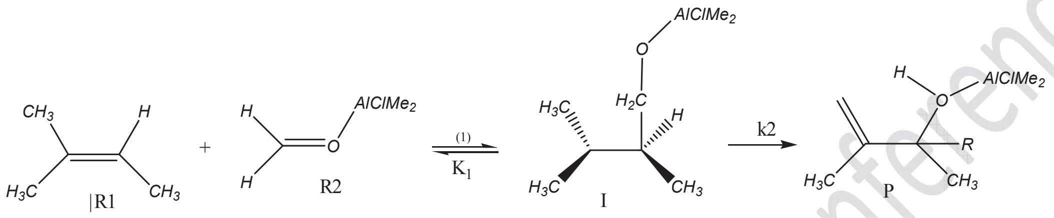

(2)

The optimized structure of transition state (TS_{RI}) obtained from step k2 has been shown in Fig. 1. By taking Solvent (Toluene) effects into consideration, $E_a = 24.3 kcal/mol$. This shows that the model presented in this research is a suitable model for the rate determining step of Lewis acid-catalyzed ene reactions.

Conclusion:

Using quantum mechanical method, Lewis acid-catalyzed ene reactions was investigated and ultimately a model was presented in which an intermediate is produced in the fast equilibrium step and in continuation is converted into product in the rate determining step.

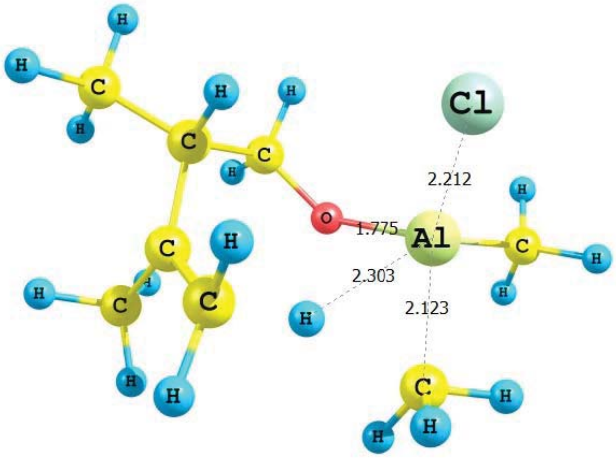

Fig 1. Optimized structure of the TS_{RI}

References:

[1] D.A. Singleton and Chao Hang, J. Org. Chem., 65 (2000) 895.

[2] A.D. Becke, Phys. Rev. A, 38 (1988) 3098.

[3] P.J. Hay, W.R. Wadt, J. Chem. Phys. 82 (1985) 299.

[4] S. Miertus, E. Scrocco, J. Tomasi, Chem. Phys. 55 (1981) 117.

Prediction of Microscopic Protonation Constants of Hematoxylin Via Computational Methods.

H.beiginejad , M.bayat[*], Y. Gholiee

Faculty of chemistry, Bu-Ali Sina University, Hamedan 65174, Iran

Corresponding Author E-mail: mehdi806@gmail.com

Key words: Hematoxylin, DFT Study, Proton microaffinity, Proton macroaffinity.

Introduction:

The acid-base properties of polybasic molecules are usually characterized in terms of macroscopic protonation constants, which are composites of the microscopic constants for the individual basic sites. Determination of microscopic protonation constants, in contrast to macroscopic protonation constants, is relatively difficult (and in some cases even impossible). More recently, a simple methodology has been reported for theoretical calculation of microscopic protonation constants of polybasic molecules in solution [1]. In latter methodology, a general thermodynamic cycle has been proposed to calculate protonation microconstants of polybasic molecules using calculated micro-ΔG values in aqueous. The protonation microconstants for Hematoxylin have not been yet measured by experimental techniques and in this work we have been calculated them theoretically.

Computational details:

The geometries of all micro species in the gas phase were fully optimized at the BP86/6-31++G** level of theory using the Gaussian 03 [2] set of programs. To calculate salvation energies, a popular continuum model of solvation, the Conductor-like Polarizable Continuum Model (CPCM) with the setting ICOMP=0, have been used at the BP86 level of theory in conjunction with above basis set. The optimized atomic radii were invoked via the solvent keyword RADII=UA0. Solvation free energies were then obtained using the SCFVAC keyword.

Result and discussion:

An aqueous solution of a tetra dentate molecule contains 2^4=16 micro species and their equilibria can be expressed in terms of 4 × 2^3 =32 micro constants. The microscopic protonation equilibria scheme of the Hematoxylin is shown in Scheme 1. The 32 microscopic protonation equilibria of Hematoxylin were calculated from the corresponding thermodynamic cycles according to the latter methodology.

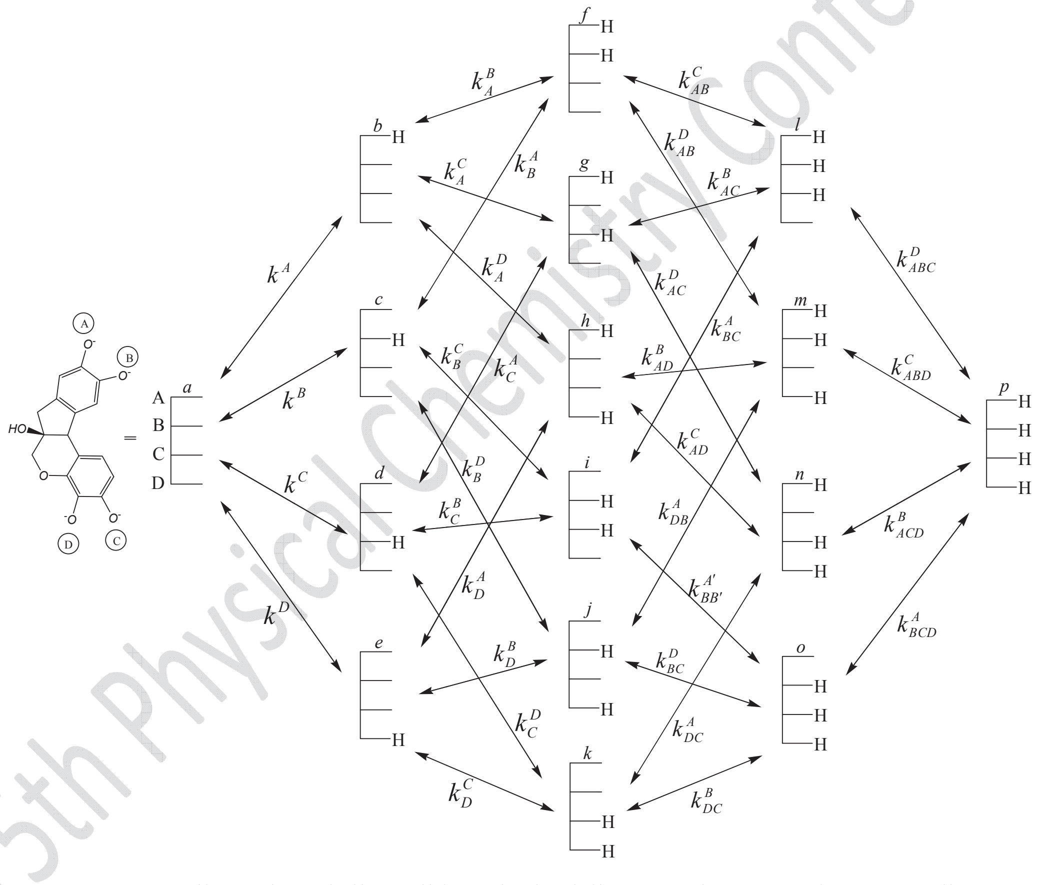

Scheme 1. Illustration of all possible paths for full protonation steps of Hematoxylin.

Conclusion:

Experimental macro constants were obtained using spectrophotometric method and DATAN software analysis, and in theoretical section all protonation microconstants of Hematoxylin molecule in aqueous solution are calculated theoretically via computational methods. There are good correlations between the protonation macro constants, calculated from latter protonation micro constants, with the experimental data at the BP86/6-31++G** levels of theory.

Reference:

[1] Salehzadeh, S.; Gholiee, Y.; Bayat, M.; International Journal of Quantum Chemistry, 111 (2011) 14, 3608–3615.
[2] M.J. Frisch, et al; Gaussian 03, revision D.01, Gaussian, Inc., Wallingford, CT, 2004.

Solid-state structures of two conformers of N-(nicotinyl) N,N´-bis(cyclopentinyl) phosphoric triamide; insights from X-ray crystallography and DFT calculations

Khodayar Gholivand*, Elham Torabi , Maryam Rajabi
Department of chemistry, Faculty of sciences tarbiat modares university, P.O. Box 14115-175 Tehran, Iran
Email: torabielham2010@gmail.com

Key words: Nicotinamide, Structural analysis, DFT, Conformation, IR spectra.

Introduction:

Phosphoric triamides have received considerable attention due to their applications as inhibitors of acetylcholinesterase and as stereoselective catalysts. The ring inversion and rotation of cyclic amines around the P–N bond provide different conformers in phosphoric triamides. In the present study two conformers of the compound $C_5H_4NC(O)NHP(O)(NC_5H_{10})_2$ are introduced. The solid-state structure of the compound was determined by X-ray crystallography and employed as a reference for quantum mechanical (QM) calculations at the DFT (B3LYP) level. We calculate geometric parameters and energy profile of the title compound in the ground state by DFT (B3LYP) methods[1].

Materials and methods:

After refluxing of PCl_5 and nicotinamide ($C_5H_4NC(O)NH_2$) in 1:1 molar ratio in CCl_4 for 6 h, solution let to get cold to the room temperature. Then formic acid was syringed drop-wise into the vigorously stirring solution in 15 min and let to stir for 6 h. Resulting white precipitate $C_5H_4NC(O)NHP(O)Cl_2$(A) ,was filtered and dried. Compound $C_5H_4NC(O)NHP(O)(NC_5H_{10})_2$ was synthesized from the reaction of precipitate A with Cyclopentyl amine in 1:4 molar ratio of nicotinamide (initiator): corresponding amine. The mentioned amine was added drop-wise to a mixture of reaction in acetonitrile (40 mL) while stirring. The temperature was not allowed to rise above 4 °C. After stirring for 8 h and then evaporating the solvent, the residue was washed with distilled H_2O. The optimization of geometry and the energy were carried out with GAUSSIAN 03 system of programs. The optimized calculation was carried out at (DFT) B3LYP/6-311+G** level without symmetry constrain.

Apparatus:

The compound and solvents for synthesis from Merck. ^1H, ^{13}C and ^{31}P NMR spectra was recorded on a Bruker (Avance DRS) 500 MHz spectrometer. ^1H, ^{13}C and ^{31}P chemical shifts were obtained in $CDCl_3$ relative to TMS and 85% H_3PO_4, respectively, as external standards. IR spectra was obtained using KBr pellets on a Shimadzu IR-60 model spectrometer. Single crystal was obtained from a mixture of C_2H_5OH/hexan at room temperature. X-ray data were collected on a Bruker SMART area detector single crystal diffractometer with graphite monochromated Mo Ka radiation (k = 0.71073 Å). The structure was refined with SHELXTL by full-matrix least-squares on F^2[2].

Result and discussion:

Two conformers (A and B) are defined in crystalline lattice. Appearing a disorder in conformer B is the result of ring inversion of one amine group. The torsion angles of O(1)–P(1)–N(4)–C(12) and O(3)–P(2)–N(8)–C(28) are -65.05° and -41.44°, which have a large different as 23.61°. But the calculated data shows -66.64° and -14.78°, respectively. The calculated energy for two conformers A and B are -838321.46 and -838322.71 kcal/mol, respectively. The conformer B is approximately 1.25 kcal/mol more stable than conformer A[3].

Conclusion:

The two conformers of the title compound can be observed in a solid phase but only one compound defined in a solution. The interesting point of the crystal structure of this molecule is the formation of two different structures due to ring inversion in one of the amine containing rings. Theoretical calculations confirm existing of the two conformers A and B with

1.25kcal/mol average different in energy. The optimized bond lengths and harmonic vibration in DFT/6-311+G** are in a good agreement with experimental IR spectra value.

Reference:

[1] Khodayar Gholivand , Hamid Reza Mahzouni , polyhedron 30 **(2011)** 61-69.
[2] Khodayar Gholivand , Hamid Reza Mahzouni , Acta Cryst. **(2011) .**B67, 238-243.
[3] Khodayar Gholivand , Ahlam Madani Alizadehgana , Sattar Arshadi , Azam Anaraki Firooz, Journal of molecular structure 791 **(2006)** 193-200 .

Investigation of Fullerene effect on reactivity of Methyldopa with NMR parameters

Roya Ahmadi[a*], Laleh Allahkaram[b], Marjan Firoozeh[a]
a Azad university Shahre -rey branch, Tehran, Iran
b Azad university Shahre -rey branch, Tehran, Iran
Email: Roya_ahmadi_chem@yahoo.com, Laleh_allahkaram@yahoo.com, Marjan.firuzeh@gmail.com

Key words: fullerene, Methyldopa, HF, Gaussian 98

Introduction:

Methyldopa is useful in the treatment of mild to moderately severe hypertension. It lowers blood pressure chiefly by reducing peripheral vascular resistance, with a variable reduction in heart rate and cardiac output. Most cardiovascular reflexes remain intact after administration of methyldopa, and blood pressure reduction is not markedly dependent on maintenance of upright posture. One potential advantage of methyldopa is that it causes reduction in renal vascular resistance.

Fullerenes, the hollow carbon cages discovered in 1985[1], have fascinated scientists. The most prominent representative of the fullerene class is C_{60}, which is the most abundant cluster in the solvent-extracted carbon soot and the smallest fullerene that satisfies the isolated pentagon rule. Since macroscopic samples of C_{60} became available in 1990[2], many applications have been suggested, particularly in the bio-area.

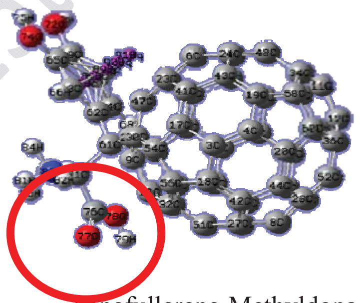

nanofullerene-Methyldopa

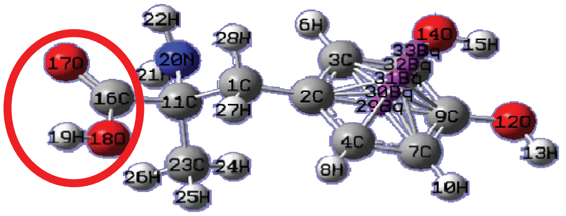

Methyldopa

Materials and methods:

All structure relating to structure of Methyldopa and nano fullerene-Methyldopa were designed primarily with use of Gauss view 4.1. In order to do final optimization, Gaussian 98 program of package HF method were used. However, for this purpose, 6-31G basis set was used.

Apparatus:

Total computations were done with use of Pentium III with processor Intel® core i3 with memory of 4 gigabytes and inside the operating system of windows SEVEN®. All computations were performed under gas phase, 1 atmosphere and 298 Kelvin temperature

Result and discussion:

In this work Methyldopa was linked to the fullerene, then compare Gap Energy, Hardness, chemical potential, dipole moment parameters between Methyldopa alone and nano- fullerene-Methyldopa. It's found that Gap Energy and Hardness were decreased in nano- fullerene but chemical potential and dipole moment were increased. In other hand compare between chemical shielding isotropy(σ_{iso}) and chemical shift(δ) in H_{79}, H_{19} (that is similar in two compound) showed that chemical shielding isotropy was decreased in acidic hydrogen of nano-fullerene-Methyldopa but chemical shift of it was increased.

Table.1

					//O C-OH		
compound	Gap Energy	Hardness	Chemical potential	dipole moment	σ_{iso}		δ
R-C_{60}-x	0.26499	0.132495	-0.146065	5.6772	H_{79}	27.8210	4.7766
R-x	0.44659	0.223295	-0.081765	4.3526	H_{19}	28.0984	4.4992

Conclusion:

The result showed that reactivity and solubility in polar solvent were increased. With increasing of chemical shift in H_{79} can find when electronic density of around H_{79} decrease, this hydrogen will be more than positive and it can easily separate in the field water (acidity). This is a support for increasing of reactivity of nano-fullerene-Methyldopa in the human body.

Reference:

[1] H.W. Kroto, J.R. Heath, S.C. O'Brien, R.F. Curl, R.E. Smalley, Nature 318 (1985) 162.
[2] W. Kra¨tschmer, L.D. Lamb, K. Fostiropoulos, D.R. Huffman.

DFT/NBO Analysis of Complexes between Nanotubes and Anti-HIV Drugs

N. Dalili Mansour*, [a] , S. Ghorbaninezhad[a]
[a]Department of Chemistry, Islamic Azad University, Rasht Branch, Rasht, Iran.
*dalili@iaurasht.ac.ir

Keywords: Nanotube, Thermodynamic Function, DFT, HIV.

Introduction :

One of the efficient drugs that has anti HIV properties, is (+)/(-) enantiomers of 2′-deoxy-3′-oxa-4′-thiocytidine (dotc) or Apricitabine (AVX754). The most common side effects of this drug are headache, nasal, congestion and muscle pain. Scientists have expressed their hope to develop the use of carbon Nanotubes to release drugs ,… . It is very important to release drug in cell without damaging healthy cells of tissue under study. It is one application of Nanotubes. To prevent of drug's side effects in use, in this work the interaction between Nanotubes and this anti-HIV drug is investigated to show if the Nanotubes are safe to deliver this drug.

Computational method :

All of the calculation were performed with a personal computer which has Intel (R) core (TM) 2 quad CPU 8400 with 4GB RAM. Geometry optimization of Nanotube (6,6) with 84 atoms and AVX754 were performed with Gaussian 03 program package at DFT level of theory , the B3LYP hybrid functional, using the standard 6-31G(d) basis set , separately. Then 4 Complexes were formed: a) Complex1 (between Nanotube and (-)dotc by forming one amine bond, b) Complex2 (between Nanotube and (-)dotc by forming one ether bond, c) Complex3 (between Nanotube and (+)dotc by forming one amine bond, d) Complex4 (between Nanotube and (+)dotc by forming one ether bond. The formed complexes were optimized by the same method and then frequency studies and NBO analysis (Natural Bond Orbital) have been also performed for optimized structures. For optimized complexes, bond lengths, bond angles, hybrid of atoms, occupancy and Mulliken charges were obtained. By frequency studies Enthalpies, Entropies, Energies and Gibbs free Energies were calculated in 298K.

AVX754

Results and discussion:

The obtained Mulliken charges in donor atoms are negative and because the s orbital share in hybrid of oxygen in complex 2 and 4 is more than the s orbital share in hybrid of nitrogen in complex 1 and 3, the bond lengths in complex 2 and 4 become less. So the ether bonds formed in these reactions are stronger than amine bonds. These results show that all of these reactions are exothermic but in all of them, the entropy decreases. So the enthalpies are assistant factors and the entropies of reactions are thermodynamically unfavorable factors in the review. The obtained formation ΔG^0 of complex 3 and 4 becomes positive in 298K. This indicates that these complexes could not be formed according to thermodynamic laws. But by decreasing temperature at least about 50K these reactions can occur. The obtained results show that hyperconjugative effects can occur by donor – acceptor interactions between lone pairs of oxygen or nitrogen atom in the drug as donor and σ^* or π^* orbitals of carbon in nanotube. These second – order perturbation energy can be shown by E^2 Term in this table. The amount of these energies causes the stability of these complexes. Also this table shows by increasing P share in The hybrid of atoms , the occupancy decreases.

Agent	ΔS/kcalmol^{-1}	ΔH/kcalmol^{-1}	ΔG^0/kcalmol^{-1}	Stability constant	Gap of HOMO & LUMO Energy/kcalmol^{-1}	$\sum E^2$
Complex1	-0.0432	-12.9374	-0.0515	1.0009	0.0687	21.4
Complex2	-0.0144	-4.1378	-0.0784	1.0001	0.0689	17.76
Complex3	-0.0153	-4.4453	0.1148	-	0.0666	21.6
Complex4	-0.0168	-4.1812	0.6947	-	0.0687	37.74

Conclusion:

- The Mulliken charges in donor atoms are negative.
- The formed bond between oxygen and carbon is stronger and has more s share in hybrid, so bond length becomes less.
- In reactions of formation of all Complexes, entropies of the reactions are thermodynamically unfavorable factors in the review.
- ΔG^{0} of formation of complexes 3 and 4 is positive. So in the follow of second law of Thermodynamic rules, these two reactions could not occur in this temperature.
- The reaction between nanotube and (+)dotc doesn't occur in the body temperature.
- All of the reactions are exothermic reactions.
- NBO analysis shows high hyperconjugations in all compounds.
- By increasing p share in hybrid, the occupancy decreases.

References :

[1] Y. Huh, J. Y. Lee, J. Cheon, Y. K. Hong, J. Y. Koo, T. J. Lee and C. J. Lee: J. Mater. Chem., 2003, 13, 2297–2300.

[2] Joint United Nations Programme on HIV/AIDS (UNAIDS) and the World Health Organization, AIDS Epidemic Update (December 1998).

[3] L. Fernandez, et al, J. THOCHEM. 882 (2007) 89-102.

Thermodynamic Functions of Complexes between Nanotubes and Anti-Cancer Drugs: A Theoretical Approach

N. Dalili Mansour[a,*], H. Kefayati[a], F. Mahboubi[a]
[a]Department of Chemistry, Islamic Azad University, Rasht Branch, Rasht, Iran
Email: dalili@iaurasht.ac.ir

Keywords: Nanotube, Hydroxycarbamide, DFT, NBO, Thermodynamic Function.

Introduction:

Hydroxycarbamide or hydroxyurea is an antineoplastic drug and has been used primarily for the treatment of myeloproliferative diseases, which has an inherent risk of transforming to acute myeloid leukemia. There has been a longstanding concern that hydroxycarbamide itself carries a leukemia risk. But large studies have shown that the risk is either absent or very small. Nevertheless, it has been a barrier for its wide use in patients with sickle-cell disease. In this work the interactions between hydroxycarbamide with a Nanotube (6,6) containing 60 carbon atoms are investigated to show if nanotube is suitable for transporting this drug and it becomes clear which site of this drug is more suitable for formation of complex between nanotube and the drug.

Computational method:

All of the calculation were performed with a personal computer which has Intel (R) core (TM) 2 quad CPU 8400 with 4GB RAM. A Nanotube (6,6) with 84 atoms is selected which reacts with Hydroxycarbamide. Hydroxycarbamide has three sites which can react with nanotube. (O_5 head: complex 1, N_1 head: complex 2 and N_4 head: complex 3) (Fig. 1) Nanotube is formed by Nanotube Modeler package [1]. The DFT Calculations have been performed using the Gaussview [2] and Gaussian 03 [3] by B3LYP method [4] and 6-31G(d) standard basis set. After optimization, the frequency calculation and NBO analysis have been performed.

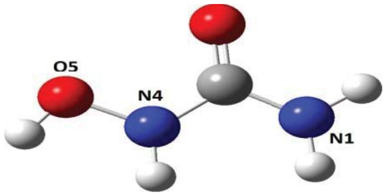

Fig. 1: Hydroxycarbamide

Results and discussion:

NBO analysis:

In this work, NBO analysis was performed by B3LYP/6-31G(d) method. Hyperconjugation may be given as a stabilizing effect that arises from an overlap between an occupied orbital when these orbitals properly oriented. This noncovalent bonding-antibonding interaction can be quantitatively described in term of the NBO approach that is expressed by means of the second – order perturbation interaction energy (E^2) .the composite between Nanotube-Hydroxycarbamide is more stable than single agents. NBO analysis shows much E^2 energy and hyper conjugation in Nanotube-Hydroxycarbamide composites from lone pair of oxygen or nitrogen atom in the drug as donor and σ^* or π^* orbitals of carbon in nanotube.

Frequency study by B3LYP/6-31G (d) Method:

These results show that ΔH^0 and $\Delta G^0$of complex1 are positive, so this reaction is endothermic and, the entropy decreases. Therefore the enthalpy and entropy are unfavorable factors for this reaction so it indicates that this complex could not be formed according to second law of thermodynamics. The obtained formation ΔG^0 of complex 2 and 3 becomes negative in 298K and the reactions are exothermic and entropies increase. So the enthalpies and entropies of these reactions are thermodynamically favorable factors. This indicates that these complexes could be formed. The obtained results can be seen in the following table:

Agent	**ΔS^0/ kcalmol^{-1}**	**ΔH^0/ kcalmol^{-1}**	**ΔG^0/ kcalmol^{-1}**	**Stability constant**	**ΣE^2 / kcalmol^{-1}**	**Gap of Energy /kcalmol^{-1}**
Complex1	-0.0134	13.9389	17.9462	-	18.81	**0.24465**
Complex2	0.0141	-15.8207	-20.0234	4.85×10^{14}	21.68	**0.24833**
Complex3	0.03280	-9.6761	-14.4553	3.95×10^{10}	18.27	**0.25127**

Conclusion:

- In the reactions of formation of all Complexes except complex1, entropies and enthalpies of the reactions are thermodynamically favorable factors.
- ΔG^0 of formation of complexes 2 & 3 are negative. So in the follow of second law of Thermodynamic rules, these two reactions could occur in this temperature. But the formation reaction of complex1 could not occur in 298 K.
- NBO analysis shows high hyper conjugations in all compounds.
- By increasing p share in hybrid, the occupancy decreases.

References:

[1] M.J.Frich,et al.,Gaussian 03, Rivision C, 02, Gaussian Inc.,Wallingford ,CT,2004.
[2] A . Frisch , A . B. Nielsen and A. J . Holder , Gaussview user Manual , Gaussion Inc(2000)
[3] M. J. Frisch. et al.,Gaussian 03 , Revision D . 0l , Gaussian Inc . Walling fordct(2004)
[4] A . D. Becke , J. chem. Phys . 98(1993)785

Quantum mechanical Investigation on the Interaction Between Nitrobenzene and Nanotube

A. Afsari[a], M. D. Ganji[a*], M. A. khalilzadeh[a], Z. Rafieepour bayaz
[a]Department of Chemistry, Islamic Azad University, Qaemshahr Branch, Mazandaran, Iran
* Corresponding Author's E-mail:ganji_md@yahoo.com (M. D. Ganji)

Keywords: nanotube, DFT, sensor, nitro benzene

Introduction:

Since their discovery, carbon nanotubes (CNTs) have received an increasing interest due to their novel properties and potential applications in chemical sensors (1), field emission displays (2), catalysis (3–7) and nano-electronic devices (8, 9). The interaction of SWNTs with chemical species is the main ingredient for many of these applications. On the other hand nitrobenzene in addition to being many used in industrial and chemical reactions is highly toxic in large quantities and prolonged exposure may cause serious damage to the central nervous system and … (10). Therefore in the present work, the adsorption of a nitrobenzene molecule on two CNTs (10, 0 zigzag) against (13, 0 zigzag) were studied and influence of nanotubes diameter on the process of absorption are reviewed.

method:

By the modeling software, nitrobenzene molecules were closed to the surface of the 10,0 nanotube in four positions. For each position, two parallel and vertical modes of nitrobenzene molecules exist. After calculation stable states were found and optimized. We employed a super cell approach in all our calculations. The structural optimizations of carbon nanotubes and nitrobenzene, And the total energy calculations for interaction between them, are carried out using the ab-initio DFT code SIESTA (11, 12) All total energy calculations were done with a double-ζ plus polarization (DZP) basis set. From the well-known expression for calculating the molecular adsorption binding energies, E ads is obtained for various cases of our study.

$$E_{ads} = E_{CNT-NitroBenzene} - E_{CNT} - E_{NitroBenzene}$$

In which E $_{(CNT\text{-}Benzene)}$ is the total energy of the CNT with an adsorbed nitrobenzene molecule, E_{CNT} the pure CNT, and $E_{NitroBenzene}$ the total energy of the isolated Nitrobenzene molecule. Naming system is as follows :

$$CNT - 10{,}0 + \text{Nitro}benzene - \ short\ as\ a\ model\ case - distanceBased\ on\ the\ \text{Å}$$

Results and discussion:

Table 1 shows the results of calculations. As is obvious, stable state for the 10,0 and 13,0 nanotube, is when a nitrobenzene molecule on the link of bevel carbon-carbon from the surface of nanotube to be lied. The imaginary axis in both the nanotube is parallel to nitrobenzene axis. Figure 1 shows the most stable adsorption state and in figure 2, two stable states of nanotubes are compared.

Table 1-Some energy of adsorption

Position	Distance(Å)	Eads(ev)
CNT-10,0+nitrobenzene-C-C-Zig-ax-par	3.3	-0.5079
CNT-10,0+nitrobenzene-C-C-par-ax-par	3.31	-0.4899
CNT-13,0+nitrobenzene-C-C-Zig-ax-par	3.33	-0.0940
CNT-13,0+Nitrobenzene-C-ax-par	3.38	-0.0930

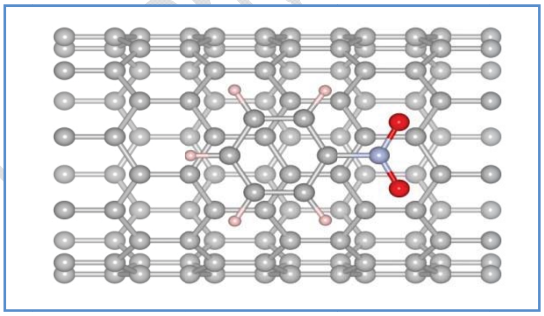

Figure5(Left): The positions of stable state- CNT-10,0+nitrobenzene-C-C-Zig-ax-par.

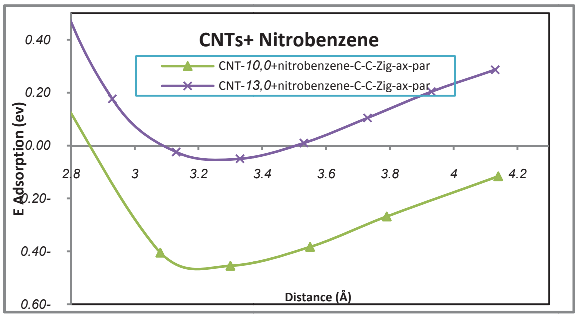

Figure2 (Right): Comparison the best positions attract for the two nanotubes

As is determined from figure 2, when nitrobenzene is very near the nanotubes, stability is very low and after being away is almost constant. Is noteworthy that less energy is possible, the system is more stable. According to this chart, Nitrobenzene adsorption on 10,0 is better than 13,0. Means Between these two CNTs, nanotube with smaller diameter is better absorber for nitrobenzene.

Conclusions:

In summary, we have investigated the interaction of nitrobenzene molecule with a (10,0) zigzag CNT and (13,0) zigzag by density functional theory-based treatments and increasing of nanotube diameter on the process of adsorption were studied. The calculation results showed that Nitrobenzene absorption is stronger with 10,0 nanotubes. Therefore, in this system the adsorb power with increasing of nanotubes diameter are decreasing.

Reference:

[1] S. Peng, K. Cho, Nano Let. 3(4) (2003) 513–517.

[2]Q. Wang, Setlur, H. A. A. Lauerhaas, J. M.J. Y.Dai, E. W Seelig, R. P. H. Chang, Appl.Phys.Lett. 72(22) (1998) 2912–2913.

[3]T. Matsumoto, T. Komatsu, K. Arai,T. Yamazaki,M. Kijima,H. Shimizu, et al, Chem Commu.(2004) 840–841.

[4] Z. Liu,X. Lin,J. Y. Lee,W. Zhang,M. Han,L. M. Gan, Langmui. 18 (2002) 4054–4060.

[5] H. Tang,J.H. Chen,Z. P. Hunag,D. Z. Wang,Z. F. Ren,L. H. Nie, et al,Carbon. 42 (2004) 191–197.

[6]S. J. Kim,Y. J. Park,E. J. Ra,K. K. Kim,K. H. An,K. H. Lee,ApplPhysLett. 90 (2007) 023114-1–3.

[7] C. L. Sun,L. C. Chen,M. C. Su,L. S. Hong,O. Chyan,C. Y. Hsu, et al,Chem Mater. 17(14) (2005) 3749–3753.

[8]P. Kim,C. M. Liber, Science. 286 (1999) 2148–2150.

[9] S. J. Tans, A. R. M. Verschueren,C. Dekker,Nature.393 (1998) 49–52.

[10] www.wikipedia.com

[11]J. M. Soler, E. Artecho, J. D. Gale, A. Garcya, J. Junqera, P. Ordejon, D. S. Portal, J.Phys.Condens.Matter.14 (2002) 2745.

[12]J. P. Perdew, K. Burke, M. Ernzerhof, Phys.Rev.Lett.77(1996)3865.

Influence of the Structural Properties of Swcnts in Phenol Adsorption: Density Functional Theory Study

A. Afsari[a], M. D. Ganji[a*], M. A. khalilzadeh[a], Z. Rafieepour bayaz
[a]Department of Chemistry, Islamic Azad University, Qaemshahr Branch, Mazandaran, Iran
* Corresponding Author's E-mail:ganji_md@yahoo.com (M. D. Ganji)

Keywords: nanotube, DFT, sensor, phenol

Introduction:

Since their discovery (1), carbon nanotubes have stimulated intense experimental and theoretical interest in their physics chemistry, and materials science. Their unique structure and properties make them proper for a variety of potential applications (2). Aromatic compounds interacting with SWNTs are of particular interest. Noncovalent sidewall SWNT functionalization with aromatic organic molecules has attracted increasing attention (3, 4). Using SWNTs as sensors for some aromatics has also been demonstrated experimentally. The other hand phenol is produced on a large scale as a precursor to many materials and useful compounds. Prolonged contact with phenol, gives the irreversible harm to humans and … (5). Therefore, a fundamental theoretical and systematic understanding of SWNT interaction with benzene derivatives, which appear as building blocks in large organic and biological systems, is necessary.

method:

In this review, first phenol on different situations has nearly nanotube surface (of 1.5Å to 5Å) and then by quantum computing density function (DFT) calculated the total energy system. Three nanotubes (6,6-10,0-10,0 with structural defect) was investigated. System energy stability is achieved by the following equation: $E_{ads} = E_{CNT-phenol} - E_{CNT} - E_{phenol}$ (1)

After obtaining the energy stability of every state, stable mode finds and it'll relax. We employed a super cell approach in all our calculations. The structural optimizations of carbon nanotubes and phenol, And the total energy calculations for interaction between them, are carried out using the ab-initio DFT code SIESTA (6, 7). Figure 1 shows the most stable state between all three nanotubes (CNT-10,0+phenol-C-Ax-Par). Naming system is as follows:

$$\text{CNT} - 6{,}6 + \text{phenol} - \text{short as a model case} - \text{distanceBased on the Å}$$

Results and discussion:

Table 1 shows the results of calculations for Stable states, And in Figure 2, three stable states of nanotubes are compared.

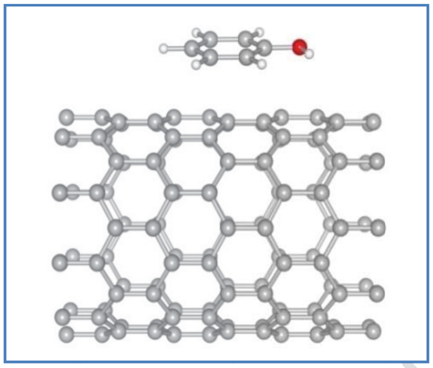

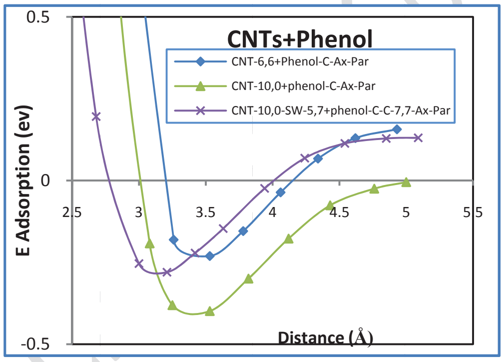

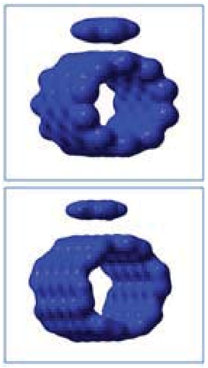

Figure6(Left): The positions of stable state- phenol on the surface of 10, 0 carbon nanotube- CNT-10,0+phenol-C-Ax-Par Figure2 (Middle): Comparison the best Scenarios attract for the two nanotubes Figure3 (Rght): Top) Charge density of CNT-10,0+phenol-C-Ax-Par-3.53. Bottom) Charge density of CNT-6, 6+Phenol-C-Ax-Par-3.53

Table 1-Some energy of adsorption

Position	**Distance(Å)**	**Eads(ev)**
CNT-10,0+phenol-C-Ax-Par	3.53	-0.4487
CNT-10,0+phenol-C-C-Ax-ax-Par	3.32	-0.4362
CNT-10,0-SW-5,7+phenol-C-C-7,7-Ax-Par	3.21	-0.2889
CNT-10,0-SW-5,7+phenol-C-C-6,5-Par-Ax-Par	3.2	-0.2564
CNT-6,6+Phenol-C-Ax-Par	3.53	-0.2505
CNT-6,6+Phenol-C-C-ax-Ax-Par	3.27	-0.2287

Charge density for the most stable and unstable systems was determined, the results are in Figure 3.

As is rich from the graph, when phenol is very near the nanotubes, stability is very low and after being away is almost constant. Is noticeable that less energy is possible, the system is more stable. According to this chart and table1, phenol adsorbed on the 10, 0 nanotube greater than the 6, 6 and 10,0 defect nanotubes. Means between these three nanotubes, 10, 0 nanotube is better sensor for phenol. As the results show Adsorption capabilities of the nanotubes are reduced due to torsion and defect in the structure.

Conclusions:

In summary, we have investigated the interaction of phenol molecule with a (10, 0) zigzag CNT, (6, 6) armchair and (10,0 defect) by density functional theory. The nanotube structures (twisting and structural defects) were studied on phenol adsorption. According to the outputs, structural defects and twisting of the nanotube will decrease the adsorption of phenol on the CNTs.

Reference:

[1] S. Iijima, *Nature.* 354 (6348) (1991) 56.

[2] M. S. Dresselhaus, G. Dresselhaus, P. C. klund, Science ofFullerenes and Carbon Nanotubes Academic, New York. (1996) .

[3] R. J. Chen, Y. Zhang, D. Wang, H. J. Dai, *J. Am. Chem. Soc.*123 (2001) 3838.

[4] X. Wang, Y. Liu, W. Qiu, D. Zhu, *J. Mater. Chem.* 12 (2002) 1636.

[5] www.wikipedia.com

[6] J. M. Soler, E. Artecho, J. D. Gale, A. Garcya, J. Junqera, P. Ordejon, D. S. Portal, *J.Phys.Condens.Matter.*14 (2002) 2745.

[7] J. P. Perdew, K. Burke, M. Ernzerhof, *Phys.Rev.Lett.* 77 (1996) 3865.

Functionalization of boron nitride nanotubes with NH_2CO and COOH functional groups

M. Zakarianezhad[a*], B. Makiabadi[b], M. Kazemi[a]
aDepartment of Chemistry, Payame Noor University, Tehran, Iran
b Department of Chemical Engineering, Sirjan University of Technology, Sirjan, Iran
E-mail:Mzakarianezhad@pnu.ac.ir

Keywords: Functionalizatian, Boron nitride nanotube, Binding energy, Electronic properties

Introduction:

BNNTs are semiconductors with a wide band gap (5.5 eV), weakly depending on the diameter, the helicity, and the number of tube walls [1]. The unusual geometric structures and unique electronic properties offer promising BNNTs applications in nanotechnology. However, the relatively large band gap and lack of solubility in solvents impose great restrictions on wider applications of BNNTs. Therefore, functionalization on the sidewalls of BN nanotubes may modify their properties. Many studies have focused on functionalization of BN nanotubes with more reactive substances [2-3]. In this paper,we have investigated structural and electronic properties of BN53zz nanotubes functionalized with NH_2CO and COOH functional groups by using DFT method and the 6-31G (d) basis set.

Methods:

For the study of interaction between NH_2CO and COOH groups with BN53zz nanotube, DFT computations were carried out using B3LYP hybrid density functional method and the 6-31G(d) basis set.In our calculations, BN53 zigzag nanotubes were chosen. The AIM and NBO analysis were carried out for the structures on the B3LYP/6-31G(d) wave functions.

Result and discussion:

We have investigated all the possible sites for adsorption of these groups on the sidewall of BN53zz nanotube. The position of COOH and NH_2CO radicals on top of the tube plays an important role ininteraction. In spite of the electroaffinity of these radicals, both of these radicals have interaction with B atom on the tube. Two types of functionalized BN53zz NT (S & P) were found in interaction of COOH and NH_2CO with BN53zz NT. In S and P structures functional groups are located onB–N bondsslanted and B–N bonds parallel to the tube axis, respectively.In the conjugation region of functional groups with nanotube, the S structures are more stable than the P structures. The results show that all of the formed complexes in the B side of tube are energetically more stable than the N side. The HOMO-LUMO gap, hardness (η), softness (S) and electrophilicity index (ω) for COOH, NH_2CO, BNNT and different configurations of functionalized BNNTs in gas phase have been calculated. Results indicate that the functionalized groups cause significant changes in the electronic properties of BNNTs. It is predicted that the conductivity of the nanotube increases upon adsorption of the COOH and NH_2CO radicals on the tube. It can be readily seen that the chemical hardness and electrophilicity index of the BNNT decrease and the chemical softness increases upon functionalization.The results obtained by natural bond orbital (NBO) analysis shows that in the S and P complexes, charge transfer take places from COOH and NH_2CO groups to nanotube. The AIM analysis was also applied to characterize the nature of B–C bond in these nanotubes. The value of $\nabla^2\rho(r)$ and H(r) at B-C BCP of all complexes show that this interaction has covalent nature.

Conclusion:

All sites on the sidewall of BN53zz nanotube were considered for adsorption NH_2CO and COOH radicals. In spite of the electroaffinity of these radicals, both of them have interaction with B in the tube. Our calculations show that after attachment of functional groups, energy gap between HOMO and LUMO orbitals decreases which would result in increase of conductivity of the nanotube upon adsorption of these groups. It can be readily seen that the chemical hardness and electrophilicity index of the BNNT decrease and the chemical softness increases upon functionalization. Complex formation leads to charge transfer from functional groups to nanotube. Also in all of complexes, B-C interactions have covalent nature.

Reference:

[1] A.Rubio, J.L.Corkill, M.L.Cohen;"Theory of graphitic boron nitride nanotubes";Phys. Rev. B; 49, 5081-5086, 1994.

[2]Y.F.Li, Z.Zhou, J.J.Zhao; "Functionalization of BN nanotubes with dichlorocarbenes" Nanotechnology; 19, 15202-15205, 2008.

[3] R.Wang, R.Zhu, D.Zhang;"Adsorption of formaldehyde molecule on the pristine and silicon-doped boron nitride nanotubes";Chem. Phys. Lett; 467, 131–135, 2008.

Molecular dynamic simulation study of structure and dynamics of asymmetrical dicationic ionic liquids

F. Gholampour* , A. Soltanabadi, S. Yeganegi,
Department of Physical Chemistry, Faculty of Chemistry, University of Mazandaran, Babolsar, Iran
Email: f_gholampour@yahoo.com

Keywords: Geminal dicationic ionic liquid, Molecular dynamic Simulation, Density, Radial distribution function, Diffusion coefficient

Introduction:

Room temperature ionic liquids (ILs) are a class of organic salts with melting points near the room temperature [1]. Geminal dicationic ILs consist of a doubly charged cation that is composed of two singly charged cations linked by an alkyl chain. They have a higher melting point, wider liquid range, and better thermal stability than the mono cationic ILs[2]. In 2010 a series of dicationic ionic liquids synthesized by Jui-Cheng et al [3] which consists imidazolium and pyridinium rings [((im_py)(Br)(Cl))] (Fig1) There have been no reports on the ab initio and molecular simulation of asymmetric dicationic ILs. This paper, for the first time, reports the molecular dynamic simulation of asymmetrical dicationic ILs (Fig 1). Densities, detailed microscopic structures, mean-square displacements (MSD) and self-diffusivities for various ion pairs have been presented.

Computational details:

Molecular dynamic simulations have been carried out on nine DILs using DL-poly 2.20 code. The simulated fluids consist of 120–180 ionic complexes. Lopes et al [4] force field was adopted for the simulations.

Results and discussion:

Densities of all DILs ((im_py)X_2, X= Cl^-, Br^- BF_4^-, NO_3^-, ntf_2^- and PF_6^-) were calculated by NPT simulations at 450 K and 1 atm and shown in Fig 2. The DIL with Cl^- has the lowest density while ntf_2^- has the highest density. We investigated the liquid structure by calculating various radial distribution functions (RDFs). The RDFs of anion and geometric center of imidazolium and pyridinium rings of cation are calculated. The simulated RDFs for the anions around geometric center of two different rings show that, anions are more accumulated around the imidazolium ring than the peridinium ring. The self-diffusion has been calculated in the time ranges of 3-8.5 ns. The calculated values of diffusion coefficients are typically one order of magnitude smaller than that of a mono cationic ILs with a comparable molar mass and it decreased by increasing the concentration of the Cl^- anion.

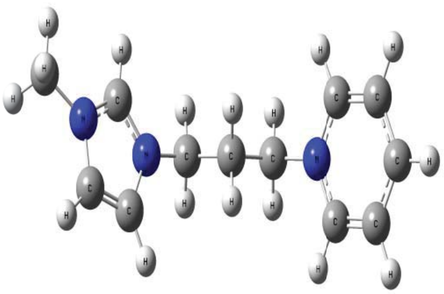

Fig. 1. Asymmetric dicationic ionic liquid.
Dicationic ionic liquid with different anions at 450K

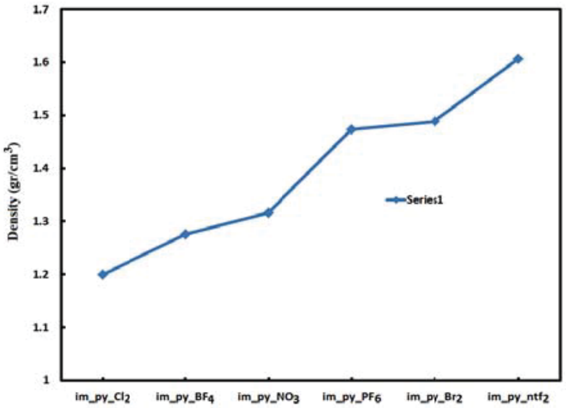

Fig. 2. Calculated density asymmetric dicationic ionic liquid.

Conclusion:

The densities, microscopic structure, mean square displacement, self-diffusion coefficients are calculated. The simulated RDFs show that anions are more accumulated around the imidazolium than the the peridinium ring. The order of the calculated values of diffusion coefficients were as Cl^-< Br^- <BF_4^- < NO_3^- < PF_6^- < ntf_2^-.

References:

[1] S. Ikegami.; ”Novel recycling system for organic synthesis via designer polymer-gel catalysts”;, H. Hamamoto , Chem. Rev; 109, 583-593,2009.

[2] X. Han etal.; “Using Geminal Dicationic Ionic Liquids as Solvents for High-Temperature Organic Reactions”; Org. Lett; 7, 4205-4208, 2005.

[3] Jui. Cheng etal.; “Synthesis and characterization of dicationic ionic liquid s that contain both hydrophilic and hydrophobic anions”; Tetrahedron, 66, 6150-6155, 2010.

[4] J. Lopes et al.; “Modeling Ionic Liquids Using a Systematic All-Atom Force Field”; J. Phys. Chem. B. 2004, 108, 2038-2047.

Enzyme molecular mechanism of O-GlcNAcase by small molecule inhibitors: A quantum mechanical approach

Mina Ghiasi* and Zohreh Hasanzadeh

[a] Department of Chemistry, Faculty of Science, Alzahra University, Vanak, Tehran, ghiasi@alzara.ac.ir, zohreh.hassanzadeh63@gmail.com

Key words: O-GlcNAc, Enzyme inhibitor, Molecular mechanism, QM calculations.

Introduction:

O-Glycoprotein 2-acetamino-2-deoxy-β-D-glucopyranosidase (O-GlcNAcase) is a member of the glycoside hydrolases family that hydrolyzes O-GlcNAc residues. O-GlcNAcase catalyzed reaction takes place through a two step mechanism, Figure 1, forming an oxazoline intermediate is a substrate-assisted catalytic process, where the 2-acetomide group is activated by an aspartate residue while departure of the aglycon leaving group is assisted by means of proton transfer from a different protonated aspartate residue [1, 2]. In this study, we have used quantum mechanical calculations for studying the catalytic mechanism used by O-GlcNAcase involving substrate-assisted catalysis.

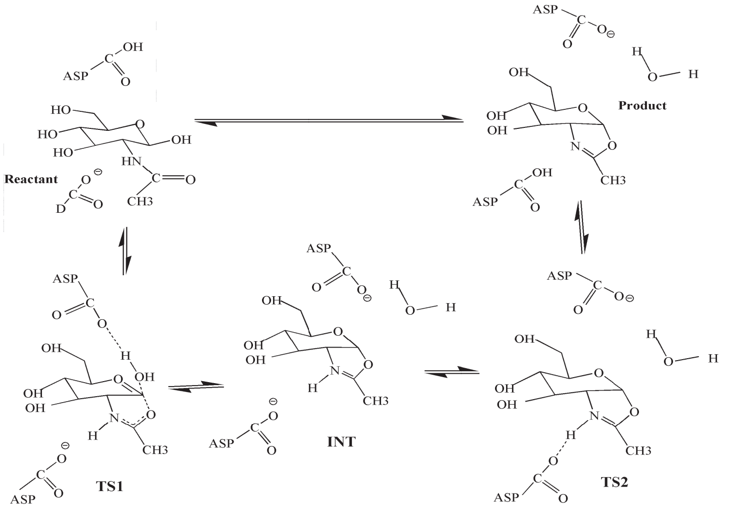

Figure 1. Proposed mechanism of the reaction catalyzed by GlcNAcase.

Computational methods:

Ab initio calculations were carried out with the Gaussian program series 2003. All geometries were fully optimized employing B3LYP/6-31G* method. QST2 method was used to search for transition state. Transition state geometry was double-checked FREQ calculations. The solvent effects on the conformational equilibrium have been investigated with a PCM method for water solvent.

Results and Discussion:

We have applied QM calculations to study the catalytic mechanism used by O-GlcNAcasa to O-GlcNAc. The energy profile indicate that the formation of the oxazoline intermediate in the O-GlcNAcase catalytic reaction takes place by means of a stepwise mechanism, Figure 2. The first step would be a cyclization of the acetamide group, which seems to be dependent on the proton transfer a conserved aspartate. From this new intermediate, a proton is transferred from the azoline ring to another conserved aspartate thus forming the oxazoline ion and departure of the aglycone (a water molecule in our model).

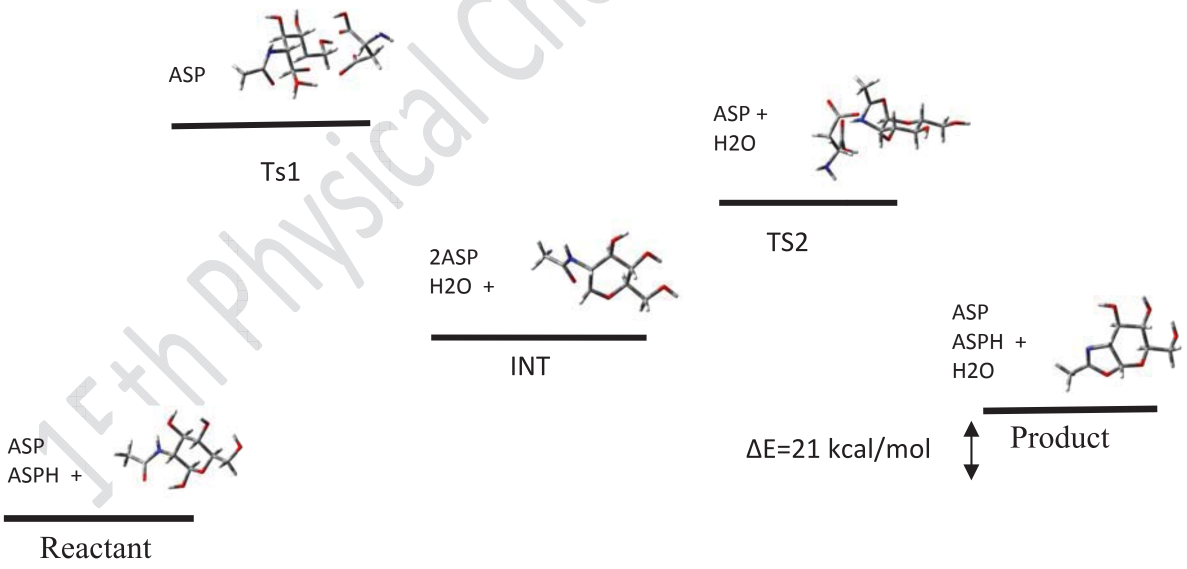

Figure 2. O-GLcNAc hydrolyzes by O-GLcNAcase in two steps mechanism.

References:

[1] D. J. vocadlo, G. J. Davies, J. Curr. Opin. Chem. Biol. 2008, 12, 539-555.

[2] M. S. Macauley, D. J. Vocadlo, Biochimica et Biophysica Acta, 2010, 1800, 107-121.

Enantiomerization energy profile of methyl propargyl ether and its analogs containing S and Se atoms. A Hybrid density functional theory study and natural bond orbital interpretation

Kamrava,[1] Seiedeh Negar Mousavi[1], Hooriye Yahyayi[2] and Davood Nori-Shargh[1]
[1]Chemistry Department, Arak Branch, Islamic Azad University, Arak, Iran
[2] Chemistry Department, Zanjan Branch, Islamic Azad University, Zanjan, Iran

Keywords: Generalized anomeric effect, ab initio, NBO, methyl propargyl ether

Introduction:

The interaction between donor and acceptor orbitals plays an important role in molecular structures, stability and reactivity[1] and it has been attracting increasing attention.[2,3] The anomeric effect (*AE*) which originally denoted the preference of electronegative substituents at the anomeric center of pyranoses for the axial conformation arises as a result of stereoelectronic interactions.[4] The generalized anomeric effect (*GAE*), is a generalization of this preference observable in acyclic compounds (such as dimethoxymethanes), as well as within rings.[4] In the *GAE*, the stereoelectronic effects cause a conformational preference for a gauche arrangement of the R-Y-C-X fragment, where Y is an atom bearing at least one lone pairs of electrons, LP, and X is an element more electronegative than C. In this work, we have studied the conformational properties of methyl propargyl ether (**1**), methyl propargyl thioether (**2**) and methyl propargyl selenoether (**3**) by means of hybrid density functional theory (B3LYP/6-311+G**) based method and natural bond orbital (NBO) interpretation .[5,6]

Computational details:

Hybrid density functional calculations were carried out using the B3LYP/Def2-TZVPP level of theory with the GAUSSIAN 03 package of programs.[5] The main purpose of the present work was to study the impacts of the stereoelectronic interaction effects, dipole-dipole interactions on the conformational properties of compounds **1-3**. An NBO analysis was then performed for the gauche and anti conformations of compounds **1-3** by the NBO 5.G program contained in the PC-GAMESS interface.[6]

Results and Discussion:

The hybrid density functional theory based method (B3LYP/6-311+G**) and natural bond orbital (NBO) analysis were used to study the impacts of the generalized anomeric effects (*GAE*) and dipole-dipole interactions on the structural and conformational properties of methyl propargyl ether (**1**), methyl propargyl thioether (**2**) and methyl propargyl selenoether (**3**). The chiral gauche conformations of all compounds studied are more stable than their corresponding anti conformations. The energy barriers of the racemization processes of the gauche conformations of compounds **1-3** *via* the plane symmetrical anti conformations are smaller than the route passing through the plane symmetrical eclipsed transition structures. The NBO analysis showed that the calculated *GAE* values decrease from compounds **1-3**. Contrary to the trend observed for the *GAE*, the calculated dipole moment differences, $\Delta(\mu_{anti}-\mu_{gauche})$, increase inversely. Consequently, the trend observed for the energy differences between the anti and gauche conformations of compounds **1-3** can be resulted from the conflict between the *GAE* and electrostatic model. The correlations between the calculated *GAE*, diploe-dipole interactions, Wiberg Bond Indics (*WBI*), orbital integrals, structural parameters and conformational behaviors of compounds **1-3** have been investigated.

Conclusion:

The results obtained showed that the *GAE* values decrease from compound **1** to compound **3** but $\Delta(\mu_{anti}-\mu_{gauche})$ increases inversely. Consequently, the conformational properties of compounds **1-3** can be controlled by the conflict between the *GAE* and electrostatic model.

Refrences:

[1]P. Deslongchamps, *Stereoelectronic Effects in Organic Chemistry*; Pergamon Press, New York, 1983.

[2]D. Nori-Shargh, H. Yahyaei, J.E. Boggs, *J. Mol. Graph. Model*. **2010**, *28*, 807-813.

[3]D. Nori-Shargh, J.E. Boggs, *J. Phys. Org. Chem*. **2010**, doi:10.1002/poc.1728.

[4]E. Juaristi, G. Cuevas, *The Anomeric Effect*; CRC Press: Boca Raton, 1995 and references therein.

[5]M.J. Frisch, et al, Gaussian 03, Revision B.03, Gaussian, Inc., Wallingford CT, 2004.

[6]E.D. Glendening, J.K. Badenhoop, A.E. Reed, J.E. Carpenter, J.A. Bohmann, C.M. Morales, F. Weinhold, Theoretical Chemistry Institute, University of Wisconsin, Madison, WI, 2004. NBO Version 5.G.

Donor-Acceptor interactions between Benzocryptand(222) and Ca^{2+} and Na^{+}

R. Behjatmanesh-Ardakani[a], M. delarami Arab[a*]
[a]Department of chemistry, Payame Noor University, PO BOX 19395-3697 Tehran, IRAN
*Email:m_delarami64@yahoo.com

Keywords: DFT, Benzocryptand, Binding energy, AIM, NBO, BCP

Introduction:

In recent years, there has been considerable research on quantum mechanical study of crown ethers. The study of interaction between alkali metal cations with crown ethers is based on Density Functional Theory (DFT) [1]. In the present work, complexation of benzocryptand with Ca^{2+} and Na^{+} has been studied. The optimized structures of these two complexes are shown in Fig 1.

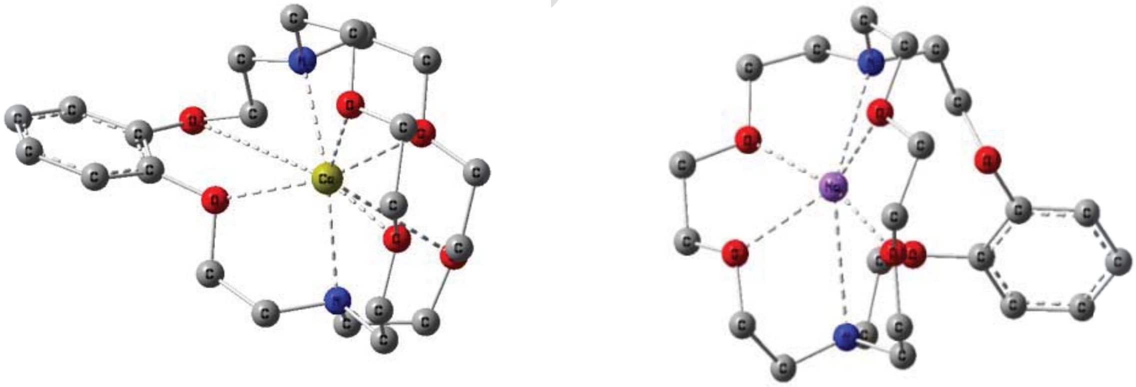

Fig 1. Optimized Structures of Ca^{2+} and Na^{+} complexes

Methods:

The molecular structures have been drawn with Gaussview 5.0 [2] program. All calculations have been performed with the Gaussian 09 [3] software using DFT method with the B3LYP/6-311G level of theory. Atoms in molecules (AIM) analyses are used to determine the presence of Bond Critical Points (BCPs) of the intramolecular bond and to evaluate their energies. The second-order perturbation energies $E^{(2)}$ obtained by Natural Bond Orbital (NBO) analysis. AIM and NBO calculations are performed using AIM2000 [4] package and version 3.1 of the NBO [5] program, respectively.

Results and discussion :

The simplest way to characterize the interaction between a crown ether and an ion is binding energy. Zero point and BSSE corrected binding energies ($\Delta E_{binding}^{ZPE+BSSE}$) for complexes of Benzocryptand with Na^+ and Ca^{2+} are -93.51 and -282.96 (Kcal/mol) respectively. Some of the topological parameters and obtained $E^{(2)}$ energies from NBO are shown in Table 1.

Table1. AIM and NBO results for studied complexes.

Bonds	**ρ(r)**	**$\nabla^2(\rho)$**	**V(r)**	**G(r)**	**H(r)**	**$\frac{\lvert V \rvert}{2G}$**	**$E^{(2)}$**
				L-Ca^{2+}			
Ca^{2+}-O25	0.0246	0.1451	-0.0242	0.0302	0.0060	0.4006	4.71
Ca^{2+}-O16	0.0233	0.1362	-0.0226	0.0283	0.0057	0.3992	4.43
				L-Na^+			
Na^+-O15	0.0166	0.1019	-0.0166	0.0210	0.0044	0.3952	3.66
Na^+-O26	0.0192	0.1232	-0.0200	0.0254	0.0054	0.3937	4.22

Conclusions:

The comparison of binding energy of Na^+ and Ca^{2+} complexes reveals that the interaction of Ca^{2+} ion with ligand is stronger. Thus, the more the charge of an ion, the stronger the binding energy. The reported $\nabla^2(\rho)$ is positive in Table 1 that shows relative reduction of electron in critical points. The results of donor-acceptor interactions are in good agreement with the experimental data.

References:

[1] Y. Zhang etal.; "DFT study of crown ether-bridged Z-stilbenes and their complexes with alkali metal cations" ; organometallic chemistry; 699, 31-38, 2012.

[2] R. Dennington etal.; GaussView 5.0, Semichem Inc., Shawnee Mission KS, 2009.

[3] M. J. Frisch etal.; Gaussian 09, Revision A.2. Gaussian, Inc; Walling ford CT, 2009.

[4] F. Biegler-König etal.; "AIM2000-A program to analyze and visualize atoms in molecules"; J. camp. Chem; 22, 545-559, 2001.

[5] D. E. Glendening etal.; NBO, version 3.1.

Introducing the Shannon – Fukui Index as a Measure of Stability in Nucleic Acida

Sulmaz boushehri*[a] , Siamak Noorizadeh[b]

[a] Islamic Azad University, Omidyeh Branch, Khoozestan, Iran (Email:sulmazboushehri@yahoo.com)

[b] Department of Chemistry, Faculty of Chemistry, Ahvaz Shahid Chamran University, Khoozestan, Iran

Keywords :Shannon - fukui Index ‹ Hirshfeld charges ‹ Basis sets ‹ Tautomery

Introduction:

Finding new quantities that can be a criterion of molecule stability is an important issue in quantum calculations. Although, numerous quantitie such as energy - polarizability - chemical potential have been introduced for this purpose, no criterion has been found that can do this in all compounds with various functional groups. The aim of this study is to evaluate a new index obtained from the combination of shannon and fukui that can best do this in biological organic systems. In this research, stability of Nucleic Acids including Thymine, Cytozine, Uracil, Adenine and Guanine is examined using the new shannon-fukui index.

Methods :

The new shannon-fukui index is defined as a combination of the shannon entropy and fukui using the following formula: $SF^{\pm} = - \Sigma F^{\pm} \ln F^{\pm}$

In this study, HF and MP_2 methods, which are Abinitio methods, and B3LYP method, which is a density functional method, are used along with 6-311++G** basis set.

Molecules and all of their tautomeric forms were drawn in Gaussview program and then were transferred to Gaussian 03 program after primary optimization. After optimization of molecule in neutral, cationic and anionic states, the positive and negative fukui values and then shannon-fukui index of all tautomeric forms of these compounds were calculated using information obtained from this program.

fukui values were calculated by use the hirshfeld charges.

Results and Discussion:

Results of calculations show that the higher the SF^- is, the more stability of compound is, that agrees with maximum entropy law (shannon is of entropy nature). Given the number of bonds in conjucated system, these results agree completely with results of evaluation of system stability. Therefore, negative Shannon-fukui index (SF^-) is an appropriate criterion for determination of the most stable form of nucleic acids.[1-6]

Among the three methods used, B3LYP has obtained better results.

References:

[1] E. Romera, P . Sánchez-Moreno, J.S. Dehesa, Chem. Phys. Lett., 414 (2005) 468.
[2] M. Alipour , A. Mohajeri , Chem. Phys , 392 (2012) 105-106.
[3] M. Solimannejad, S. Noorizadeh,M. Aarabi, Comp&Theo Chem, 976 (2011) 8-11.
[4] P. Fuentealba, R. Contreras, Modern Quantum Chemistry. A 2002.
[5] R. R. Contreras, P. Fuentealba, M. Galvan, P .Perez, Chem. Phy. Lett. 304 (1999) 405.

Density functional theory (DFT) Based Study Of Solvent Effect On $B_{10}N_{11}$ And $B_{10}N_{11}H_7$ (Gly)$_2$ Nano Structures

S. Mohajeri [*a], M. Monajjemi [a]

[a] Science and Research Branch, Islamic Azad University, Tehran, Iran

sahar_mohajeri@yahoo.com

Keywords: Density functional theory (DFT), Solvent effect, Nanocone, NMR investigation, Drug delivery.

Introduction :

An important group of nanocones is Boron nitride nanocones (BNNCs) and these Curved structures and carbon nanocones have more fascinating properties than other nano structures. Then, in general, the situation, concerning electronic and structural properties, is less focused for BN than for C cones. Recently BNNCs particles have been synthesizes [1]. Also studies of these novel systems show that they are built of conical shells and these structures are seamless [2]. A comparison between these novel systems and CNTs has led to the understanding that BNNCs have more interesting characteristics than the CNTs [3]. In the present study, we address the relative stability and NMR parameters for two kinds of BNNCs, $B_{10}N_{11}$ and $B_{10}N_{11}H_7$ (Gly) $_2$ in spread of solvents and temperatures. The results were compared to find the best solvent and temperature.

Computational Method:

The Gaussian 98 program was applied to obtain the best prediction of these structures in the electronic grand state. This program was used to study many specific properties of $B_{10}N_{11}$and $B_{10}N_{11}H_7$ (Gly) $_2$ such as thermodynamic properties, Atomic charges, Multipole moment and NMR shielding in gas phase and different solvents and temperatures. The DFT method used in this study was Becke 3 Lee-Yang-Parr (B3LYP) functional. Solvent effects on $B_{10}N_{11}$ and $B_{10}N_{11}H_7$ (Gly) $_2$ were reviewed in different solvents and six different temperatures of 298, 300, 305, 310, 315 and 320 K by using the same method and basis set. Finally the best solvent and temperature for these structures were reported. On the other hand an NMR calculation can play an important role in understanding the function of a biomolecule such as Glycine. All of the NMR shielding tensors are calculated in the basis of gauge-including atomic orbital (GAIO) method at B3LYP/3-21G level of theory not only $B_{10}N_{11}$ but also $B_{10}N_{11}H_7$ (Gly) $_2$ and the position of active sites are recognized for these two structures.

Results and Discussion:

In the present study, interaction of $B_{10}N_{11}$ nanocone with two Glycine molecules is considered. All calculations were performed to study the relative stability of $B_{10}N_{11}$ and $B_{10}N_{11}H_7$ (Gly) $_2$ especially thermodynamic properties and NMR shielding tensors in different solvents and temperatures.$B_{10}N_{11}$ nanocone was optimized in gas phase and different solvents and temperatures at the B3LYP/3-21G level of theory. Then stability of this novel structures in gas phase and the same solvents and temperatures were reviewed to obtain thermodynamic parameters. Then NMR parameters were applied for recognizing active sites of $B_{10}N_{11}$ nanocone and $B_{10}N_{11}H_7$ (Gly) $_2$ in gas phase and different solvents.

Conclusion :

The results show, $B_{10}N_{11}$ nanocone is a good detector of biological molecules such as amino acids. Finally, our results confirm the role of $B_{10}N_{11}$ nanocone as a better candidate in biological systems and drug delivery than the other nanostructures.

References:

[1] Rubio A, Corkill JL, Cohen ML (1994). Theory of graphitic boron nitride nanotubes. Phys. Rev. B. 49:5081-5084

[2] Bourgeois L, Bando Y, Han WQ, Sato T (2000). Structure of boron nitride nanoscale cones: Ordered stacking of 240 degrees and 300 degrees disclinations. Phys. Rev. B. 61: 7686-7691.

[3] Nirmala V, Kolandaivel P (2007). Structure and electronic properties of armchair boron nitride nanotubes. J. Molecular Structure: THEOCHEM. 817:137-145.

Density functional efficiency in the calculations of molecular N,N′-bis(4-hydroxy salicylidene)-diethylenetriamine

Seyed Nezamoddin Mirsattari*, Mina Abdollahi
Department of Chemistry,Islamic Azad University, Shahreza Branch, 311-86145, Shahreza, Isfahan
Email: minaa.abdolahi@yahoo.com

Keywords: Density Functional Theory, FT-IR, ^{1}H-NMR and ^{13}C-NMR Spectroscopy, SCAN.

Introduction:

Density functional theory (DFT) is the de facto standard method in computational physics and chemistry. The only unknown part of the Kohn-Sham equation is the exchange correlation functional, for which the local density approximation (LDA) is often used. DFT (with the LDA) gives pretty accurate descriptions for most cases and only fails quantitatively in rare problems, for example semiconductor band gaps, and magnetic moments in transition-metal oxides [1].

In this article, full optimization of the geometries, conformation energies for optimized structures(SCAN), natural bond orbital (NBO) analysis, vibrational frequencies, the HOMO–LUMO energy gap, solvent effects, Thermochemical stabilities and ^{1}H-NMR, ^{13}C-NMR spectroscopy were calculated by using density functional theory (DFT) method (B3LYP/ 6-31G**) [2].

Computational details:

Calculation results were obtained using the GAUSSIAN-09W software package. DFT calculations were done at the Becke-3-Lee-Yang-Parr (B3LYP) level of theory with the 6–31G(d,p) basis set [3]. To determine the conformational energy profiles the optimized geometries were kept fixed, and values of the DFT energies were calculated as the functions of the dihedral angles $\theta1(H_{46}O_{45}C_{42}C_{38})$, $\theta2(H_{17}0_{12}C_6C_3)$ from 0° to 360°, varied every 40°.

Result and discussion:

Some important information parameters (bond lengths and angles), have been listed. Bond lengths(A^0): $(C_7=N_{10})=(C_{32}=N_{29})$: 1.287; N_{21}-H_{25}: 1.019; $(O_{11}$-$H_{14})=(O_{39}$-$H_{41})$: 1.002; $(O_{12}$-$H_{17})=(O_{45}$-$H_{46})$: 0.966. Angles(^{0}): $(C_7$-N_{10}-$C_{15})=(C_{32}$-N_{29}-$C_{36})$: 119.40; C_{18}-N_{21}-C_{24}: 113.54. The IR spectra, strong bands: 1703.65 cm^{-1}(C=N).

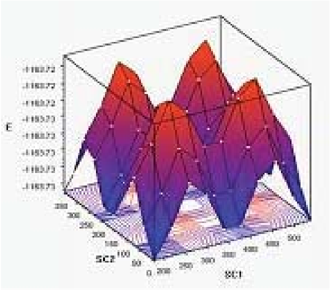

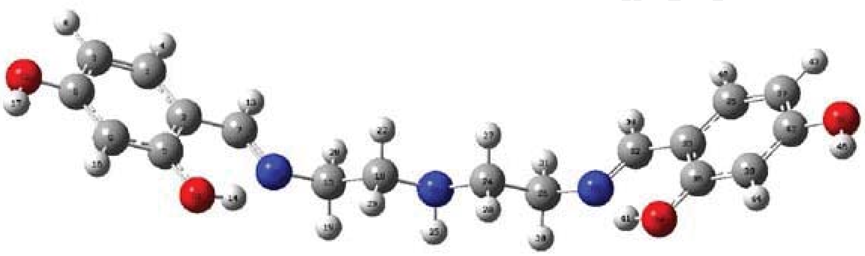

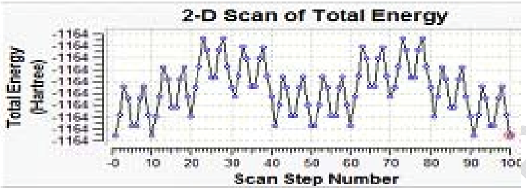

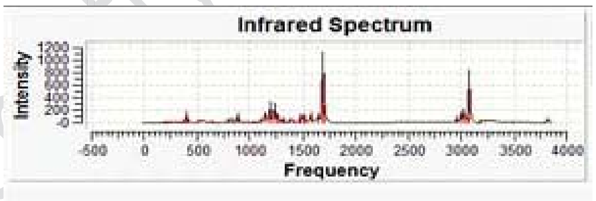

Conclusion:

Some important information such as FT- IR, ^{1}H-NMR, ^{13}C-NMR were computed and compared with experimental that has a good agreement with our experimental results. The ^{1}H and ^{13}C NMR chemical shieldings of gas phase ligand was systematically studied by the GIAO/DFT and IGAIM/DFT methods. The GIAO ^{1}H relative shift values correlate better with the experimental ones than the IGAIM, whereas the IGAIM ^{13}C relative shift values correlate better with the experimental ones than the GIAO.

Reference:

[1] R.M. Issa, M.K. Awad, F.M. Atlam; "DFT theoretical studies of antipyrine Schiff bases as corrosion inhibitors"; Materials and Corrosion; 60, 1-6, 2009.

[2] H. Tanak, M. Yavuz.; "Density functional computational studies on (E)-2-[(2- Hydroxy-5-

nitrophenyl)-iminiomethyl]-4-nitrophenolate"; J Mol Model; 16, 235–241, 2010.
[3] H. Tanak.; "Quantum chemical computational studies on 2-methyl-6-[2-(trifluoromethyl) phenyliminomethyl]phenol"; Molecular Structure; 950, 5-12, 2010.

Theoretical Study of Interaction of Schiff Base (Salpr) with Mg^{2+} Cation as a Corrosion Inhibitor

Davood Seifzadeh*, Amir Nasser Shamkhali, Hadi Basharnavaz,
Department of Applied Chemistry, Faculty of Sciences, University of Mohaghegh Ardabili, Ardabil, P. O. Box: 56199-11367, Iran
*Email: d_seifzadeh@uma.ac.ir

Keywords: DFT, corrosion, complex, thermodynamic, Mg.

Introduction:

Magnesium and its alloys are increasingly used in aerospace and automotive applications owing to their ultra lightness and high strength to weight ratio. Their density is thirds that of aluminum and one fourth that of iron. The *N*,*N*-bis(salicylidene)-2-hydroxy-1,3-propandiamine (Salpr) Schiff base is an effective inhibitor for corrosion of magnesium in 0.01 M hydrochloric acid, and the inhibition efficiency increased with increasing in the inhibitor concentration [1]. The inhibition mechanism of Salpr has not been clearly determined. One of the probable inhibition mechanisms can be the interaction of Mg^{2+} ions with Salpr ligand to form a stable complex [2-3]. In this work, we study this interaction using Density Functional Theory (DFT) to determine the thermodynamic stability of such complex. Also, partial charges of atoms in complex and free ligand are calculated to determine the active sites of these compounds.

Calculation method:

All of the calculations were performed by Firefly (PC-GAMESS) quantum chemistry package. The B3LYP hybrid functional with generalized gradient approximation (GGA) in combination with Hartree-Fock exchange is used for optimization calculations [4]. Also, the TZVP basis set was used for all calculations [5-6]. First, the structure of Salpr ligand was optimized using mentioned DFT functional and basis set. Then, the structure of $Mg(Salpr)^{2+}$ complex was optimized to calculate the formation energy of this complex as follows:

$$\Delta E_f = E_{Mg_2(Salpr)^{4+}} - 2E_{Mg^{2+}} - E_{Salpr}$$

This value can be used as a measure of thermodynamic stability of this complex. The results for structural optimization of ligand and complex and their electronic energy are given in Table 1. Also the structure of $Mg_2(Salpr)^{4+}$ complex is shown in Figure 1. Finally, the Mulliken charges of selected atoms from complex and free ligand and ΔE of HOMO and LUMO for both of complex and ligand are reported in Table 2.

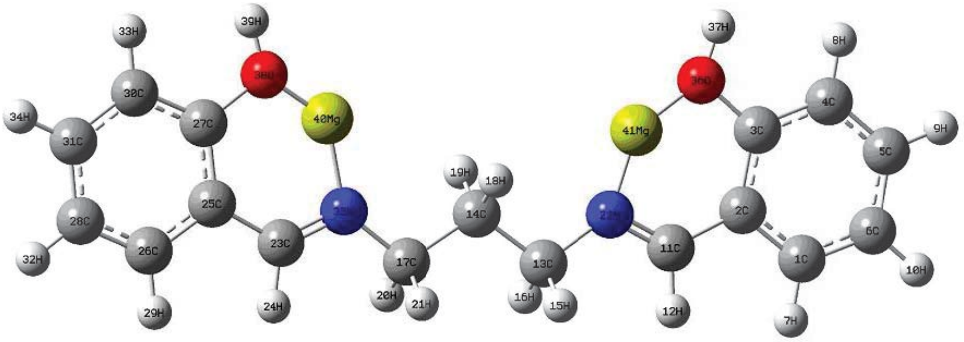

Figure 1: The optimized structure of $Mg_2(Salpr)^{4+}$ complex

Table 1: Bond lengths and electronic energies of $Mg_2(Salpr)^{4+}$ complex, and Salpr ligand. Please note that due to the symmetric structure of complex and ligand, the bond lengths of one side of mentioned molecules are reported.

Bonds (Å)	Mg40-O38	Mg40-N35	N35-C23	N35-C17	C23-C25	C17-C14	Energy(a.u.)
complex	1.92	1.98	1.34	1.52	1.44	1.55	-1317.436159643
Salpr	---	---	1.28	1.48	1.47	1.53	-918.570303570

Table2: The Mulliken charges of selected atoms from $Mg_2(Salpr)^{4+}$ complex and Salpr ligand in companion with their HOMO-LUMO energy difference.

Charge (a.u.)	Mg40	O38	N35	C23	C17	C25	$\Delta E_{HOMO-LUMO}$ (eV)
complex	1.59	-0.87	-0.76	0.24	-0.30	-0.13	2.76
Salpr	---	-0.42	-0.08	-0.05	-0.30	-0.07	4.90

Results and Discussion:

The ΔE_f of $Mg_2(Salpr)^{4+}$ complex can be calculated from the electronic energies in Table which is -1007.0 kJ/mol. This considerable negative formation energy can confirm the stability of $Mg_2(Salpr)^{4+}$ complex. Also, the change in bond lengths before and after formation of complex is a sign of chemical bond formation. By considering Table 1, the N35- C23 bond length for complex is larger than Salpr free ligand. This implies the contribution of C=N π^* orbital as a π-acceptor in the formation of chemical bond between Mg^{2+} ions and Salpr ligand. Therefore, σ-donor/ π-acceptor interaction of Salpr ligand with Mg^{2+} ions can be an explanation for large negative formation energy of $Mg_2(Salpr)^{4+}$ complex. Also, the Mulliken charges in Table 2 for complex and free ligand exhibit considerable changes which imply the charge transfer between metal ion and ligand. However, the interpretation of these charge differences is difficult due to the effect of two phenomena, the electrostatic and σ-donor/ π-acceptor interactions between metal ion and the ligand.

Conclusion:

By considering all of the mentioned results from DFT calculations, it is clear that formation of $Mg_2(Salpr)^{4+}$ complex on the Mg surface is thermodynamically favorable and the Salpr ligand can act as an inhibitor for corrosion process.

Reference:

[1] O. V. Karavaia, A. C. Bastosa, M. L. Zheludkevicha, M. G. Tarybab, S. V. Lamakab, M. G. S. Ferreira, *Electrochimica Acta* **55** (2010), 5401–5406.

[2] M. G. Hosseini, M. Ehteshamzadeh, T. Shahrabi, *Electrochimica Acta* **52** (2007), 3680–3685.

[3] H. Ashassi-Sorkhabi, B. Shabani, B. Aligholipour, D. Seifzadeh, *Appl. Surf. Sci.* **252** (2006), 4039–4047.

[4] A. D. Becke, *J. Chem. Phys.* 98 (1993), 5648-5652.

[5] A. Schaefer, H. Horn, and R. Ahlrichs, *J. Chem. Phys.*, **97** (1992) 2571-2577.

[6] A. Schaefer, C. Huber, and R. Ahlrichs, *J. Chem. Phys.*, **100** (1994) 5829-5835.

DFT study of the 1, 3 dipolar cycloadition reactions between alkyne and diazo compounds

Shahede hosseini moghaddam[a], Azita Nouri[b,*], Fateme Jafari Joneydi[c]
[a.b.c] Department of Chemistry, Islamic Azad University, Shahr-e-Qods Branch, Shahr-e-Qods, Iran
E-mail: nouria244@yahoo.com

Key words: 1,3 dipolar reactions, electrophilicity power, chemical potential ,density functional theory

Introduction:

Cycloaddition reactions are one of the most important processes in organic chemistry with both synthetic and mechanistic interest. 1, 3-dipolar cycloadditions (1, 3DC) reactions are the union of a 1,3-dipole with a dipolarophile to form a five-membered hetrocycle ring. Substituted pyrazoles are an important class of hetrocycles and have a range of biological activities. They are widely used as anti-bacteria [1],anti-diabetic [2] and anti-cancer [3]. One of the important methods for pyrazole synthesis is the 1,3-dipolar cycloaddition between a diazo compound and alkyne . In the present work, the chemical potential, μ, and global electrophilicity index, ω, are used to predict direction of charge transfer (CT) and the most favorable interaction in given 1,3-dipolar cycloadditions (Fig.1).

Computational methods:

All our calculations were carried out using the B3LYP exchange correlation functional with the standard 6-31G(d) basis set. The optimizations of equilibrium geometries of all products were obtained by full optimizations at the ground states of products. The global electrophilicity index, ω, and the chemical potential, μ, of reactants have given by: $\omega=\mu^2/2\eta$, $\eta \approx \varepsilon_L-\varepsilon_H$, $\mu \approx (\varepsilon_H-\varepsilon_L)/2$. All calculations were performed by Gussian 03 [4].

Result and discussion:

In the present work, the electronic chemical potential, μ, of reactants are used to indicate direction of charge transfer (CT) at these 1,3DC reactions. The results revealed that electronic chemical potential, μ, of the all four dipoles (2, 3, 4, 5) with values between -0.1544 a.u. and -0.1970 a.u. are lower than dipolarophile (1), -0.1033 a.u. (Table 1). So at these 13DC reactions, the charge transfer will take place from the dipolarophiles to the dipole. Also, with considering of electrophilicity power of dipolarophile, *ω*, 0.460 ev, and according to the absolute scale of electrophilicity based on the *ω* index [5] this value falls in the range of marginal electrophile (nucleophile). On the other hand, electrophilicity power of four dipoles are 2.970 ev, 2.333ev, 1.946 ev and 1.859ev for dipoles of number 4,5,3 and 2 respectively (Table 1). So these dipoles are classified as strong electrophiles. Results show that the four dipoles present a lower electrophilicity value than dipolarophile, and also have a lower chemical potential, which is the index that determines the direction of the electronic flux along these 13DC reactions. Furthermore, the most favorable interactions will take place between the less electrophilize specie 1, namely the dipolarophile in the present case, and electrophile dipole 4.

Conclusion:

The 1, 3 dipolar cycloadition reactions between same alkyne and different diazo compounds were studied using DFT methods at the B3LYP/6-31G* level. At first the electronic chemical potential, μ, of reactants are used to indicate direction of CT along these series of 1,3DCs. Then most favorable interaction was found using global electrophilicity index.

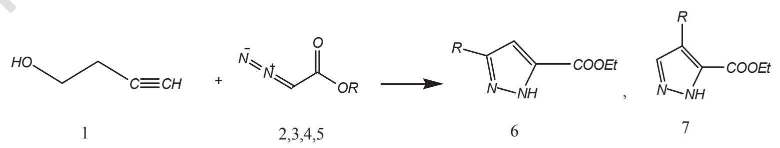

Fig.1. The considered reactions (R2=CH3, R3=C(CH3)3, R4=CN, R5=CH3CO)

Table1.Global properties of dipolarophile 1 and dipoles 2,3,4,5.

Entry	HOMO	LUMO	μ(a.u)	η(a.u)	ω(e.v)
1	-0.2614	-0.0548	-0.1033	0.3162	0.460
2	-0.2461	-0.0706	-0.1583	0.1755	1.946
3	-0.2419	-0.0668	-0.1544	0.1750	1.856
4	-0.2860	-0.1081	-0.1970	0.1779	2.970
5	-0.2632	-0.0857	-0.1745	0.1775	2.333

References:

[1] R.Jain and et al, Indian Chem. Soc. 73, 493, 1996.

[2] a) G. R .Bebernitz and et al, J. Med. Chem. 2001, 44, 2601. b) R.Soliman an et al, J. Pharm. Sci.,70, 606, 1981.

[3] a) H. Naito and et al, Chem. Pharm. Bull., 53, 153, 2005. b) A. Kreusch and et al, Med. Chem. Lett., 15, 1475, 2005.

[4] M. J. Frisch and et al, *Gaussian 03*,revision C.02; Gaussian, Inc.: Pittsburgh, PA, 2004.

[5] L.R.Domingo and et al,Tetrahedron, 58, 4417-4423, 2002.

Computational study of some selected 1,3 dipolar cycloadition reactions

Shahede hosseini moghaddam[a], Azita Nouri [b,*]

[a,b] Department of Chemistry, Islamic Azad University, Shahr-e-Qods Branch, Shahr-e-Qods, Iran

E-mail: nouria244@yahoo.com

Key words: 1, 3-dipolar cycloaddition, regioselectivity ,density functional theory

Introduction:

The 1, 3-dipolar cycloadditions (1, 3DC) first laid out by Huisgen in the 1960s. These reactions are the union of a 1,3-dipole with a dipolarophile to form a five-membered hetrocycle ring. Substituted pyrazoles are an important class of hetrocycles. In the present work, hardness, electrophilicity parameters and thermodynamic calculations are used to predict the stability sequence of regioisomer products in given 1,3-dipolar cycloadditions.At the end the chemical potential, μ, and global electrophilicity index, ω, are used to predict direction of charge transfer (CT) and the most favorable interaction in given 1,3-dipolar cycloadditions (Fig.1).

Methodology:

The DFT calculations have been performed by Guassian 03 [1] program employing B3LYP exchange-functional and 6-31G* standard basis set. The global electrophilicity index, ω, and the chemical potential, μ, of reactants have given by:

$$\omega=\mu^2/2\eta, \qquad \eta \approx \varepsilon_L-\varepsilon_H, \qquad \mu \approx (\varepsilon_H-\varepsilon_L)/2.$$

Result ans discution:

Within this work, computed total energy difference by 76.75 – 78.19 Kcal/mol and gibbs free energy difference by 58.28-59.13 Kcal/mol for all of reactions suggest that the pathway with 3-isomer product is thermodynamically the most favorable (Table 1). Thermodynamic results show that all pathways are exothermic by 70.80- 73.48 Kcal/mol. It is found that the reaction with the larges exothermicity is related to pathway2 (Fig1). Furthermore the electronic chemical potential, μ , of the all four dipolarophiles (1, 2, 3) with values between -0.1543 a.u. and -0.1970 a.u. that are lower than dipole (4). -0.1745 a.u.. So, at these 13DC reactions, the charge transfer will take place from the dipolarophile to the dipole. With considering of electrophilicity power of dipole, ω, 1.909 ev and three dipolarophiles with 0.387 ev, 0.398 ev, 0.401 ev for dipolarophiles of number 1,3 and 2 respectively, and according to the absolute scale of electrophilicity based on the ω index [2] , these dipolarophiles are classified as marginal electrophiles (nucleophiles) and dipole is classified as moderate electrophile. Results showed that the three dipolarophiles present a lower electrophilicity value than dipole, and also have a higher chemical potential, which is the index that determines the direction of the electronic flux along these 13DC reactions. Furthermore, the most favorable interactions will take place between the less electrophilize specie 1, namely the dipolarophile in the present case, and electrophile dipole 4.

Conclusion:

DFT studies were performed to investigate regioselectivity on some selected 1,3DC reactions. Results revealed that 3-isomer pathway is thermodynamically more favorable in all of reactions. Furthermore, chemical potential and global electrophilicity index were used to predict direction of charge transfer (CT) and the most favorable interaction in given 1,3-dipolar cycloadditions.

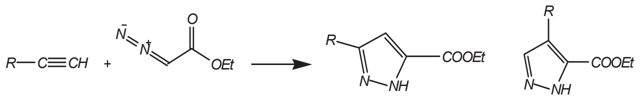

1,2,3 4 5 6

Fig.1. The considered reactions (R_1= –$CH_2CH_2CH_2OH$ **,** R_2 = –CH2-CH2-C H(CH3) –OH**,** R_3**=** –$CH_2CH_2NH_2$**)**

Table1. Relative*energies (ΔE),enthalpies (ΔH),entropies k),free energies (ΔG) energies ,in Kcal/mol (ΔS,inKcal/mol and k.computed at 25^{oc} of stationary points involved in the 13dc reactions

Entry	**Product**	**ΔE**	**ΔH**	**ΔS**	**ΔG**	**K$_{(eq)}$**
1	3-isomer	-76.75	-72.10	-46.56	-58.28	5.31 10^{42}
	4-isomer	-75.58	-70.80	-48.26	-56.41	2.25 10^{41}
2	3-isomer	-78.19	-73.48	-47.54	-59.31	3.02 10^{43}
	4-isomer	-76.86	-71.94	-50.77	-56.81	4.43 10^{41}
3	3-isomer	-77.75	-73.10	-47.52	-58.93	1.60 10^{43}
	4-isomer	-76.49	-71.74	-48.50	-57.27	9.78 10^{41}

*Relative to the corresponding reagents

Table2. Global properties of dipole 4 and dipolarophiles **1-3**

Entry	**HOMO**	**LUMO**	**μ(a.u)**	**η(a.u)**	**ω(e.v)**
1	-0.25229	-0.062940	-0.0947	0.1576	0.387
2	-0.25186	-0.06003	-0.0960	0.1559	o.401
3	-0.23289	-0.05152	-0.0907	0.1422	0.393
4	-0.24441	-0.069180	-0.1568	0.0876	1.909

References:

[1] M. J. Frisch and et al, *Gaussian 03*,revision C.02; Gaussian, Inc.: Pittsburgh, PA, 2004.

[2] L.R.Domingo and et al,Tetrahedron, 58, 4417-4423, 2002.

AQSAR Study on Biological Activities of Diketo Compounds as HIV-1 integrase inhibitors

Gh.Ghasemi,H.Kefayati,S.Bashiri*
Department of chemistry, Islamic Azad University, RashtBranch,Iran
bashiri.anita @yahoo.com

Keywords: QSAR, Diketo acid,Diketoester,Genetic algorithm,HIV-1inhibitor

Introduction:

Human immunodeficiency virus type 1 (HIV-1) is the primary cause ofacquired immuno-deficiency syndrome (AIDS) a slow,progressive and degenerative disease of the human immune system that has been one of the world's most serious health problems since 1981. In recent years, HIV-1 integrase (IN) has become an attractive target for designing anti-retroviral agents .In this work quantitative structure activity relationship (QSAR) study has been done on diketoanalogues acting as HIV-1 integrase inhibitors.Genetic algorithm(GA),artificialneural network (ANN),multiple linear regressions(MLR) were used to create the nonlinear and linear QSAR models[1-3].

Computational details:

The3D structures of the molecules were generated using the built optimum option of Hyperchemsoftware (version 8.0). Geometry optimization of compounds was carried out by B3LYP method employing 6-31G(d) basis set. All calculations were performed using Gaussian 03 program. Using Dragon (version 3.0)were employed to calculate the molecular descriptors, using MATAB for GA, ANN, MLR. In the work stepwise multiple linear regression (stepwise-MLR) and GA variable subset selection methods were used for the selection of the most relevant descriptors from all of discriptors. These descriptors would be

Steps.

used as inputs of the ANN.So,it was necessary to reduce the number of descriptors in three

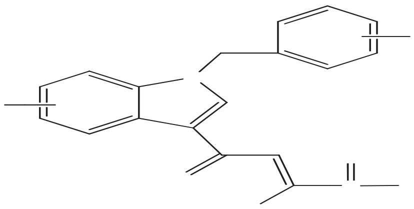

Fig 1: The molecular structure of diketo analogues.

Table2) Descriptors values for GA-MLR. model.

Molecule	X2	VAR
1	10.968	110.000
2	11.590	117.000
3	11.602	117.000
4	12.223	124.000
5	12.647	131.000
6	12.647	131.000
7	10.446	78.000
8	11.068	94.000
9	11.080	84.000
10	11.701	101.000
11	12.125	90.000
12	12.125	92.000
13	12.393	131.000
14	12.393	131.000
15	13.046	145.000
16	11.068	94.000
17	11.796	108.000
18	11.871	108.000

Table1) Experimental and predicated values of log (1/IC50) usingJack-Knife model.

Calculated (jack-knife)gas	Observed log $(1/IC_{50})$
-0.0852	0.1000
0.0892	-0.0700
0.3480	0.5200
0.0586	0.4000
-0.3128	-0.9300
-0.2926	0.0200
1.8769	1.7000
1.7756	3.7000
1.6378	2.0000
0.1361	0.7000
1.1843	0.7000
0.8227	0.8900
-0.8637	-0.6200
-0.0066	-0.3000
-0.6297	-0.0800
0.9886	0.0500
0.5155	0.9600
0.8058	0.5200

Results and discussion:

The structures of the diketo compounds used in this study are shown in Fig 1. The resulted predictions of the log (1/IC50) in gas is given in (Table 1). The selected descriptors X2, VAR were used as inputs the construction of ANN model (Table 2). Topological was important descriptor in our study. In the gas phase, the root-mean-square errors of the training set and the test set for GA-ANNmodel using Jack-knife were 0.1378,0.4512,$R^2 = 0.82$, the training and test set for GA-ANN cross validation were 0.1402 , 0.6736.

Conclusion:

In this study, two linear and non-linear variable selection methods were used to select the most significant descriptor, and the MLR, GA, ANN were used to construct a quantitative relation betweenactivitesdiketo compounds and their calculated descriptors. ANN has been successfully used for finding a QSAR model for diketo compounds.

References:

[1] Emiliani, S., Mousnier, A., Busschots, K., Maroun, M., J. Biol. Chem. 2005;280:25517–25523.
[2] Summa, V., Petrocchi, A., Bonelli, F., Crescenzi, B., J. Med. Chem. 2008;51:5843–5855.
[3] Siegal, F.P., Lopez,C., Hammer,G.S.et. al., N.Engl. J. Med. 1981;305:1431-1441.

QSAR studies on some marine natural alkaloids as anticancer agents in cancer leukemia

Ghasem Ghasemi[a], **Mohammad Zakaria** Nejad [b], Reza Gilani Far [b,*]

[a] Department of Chemistry, Islamic Azad University, Rasht Branch, Rasht, Iran
[b] Department of Chemistry, Payame Noor University, Sirjan Branch, Kerman, Iran
E-mail: re_gila@yahoo.com;

Keywords: Artificial Neural Network –Anticancer agents – Alkaloids – QSAR models.

Introduction:

Alkaloids are naturally occurring nitrogen containing biologically active heterocyclic compounds. Over the last few years, a large number of biologically important alkaloids with antiviral, antibacterial, anti-inflammatory, antimalarial, antioxidant and anticancer activities have been isolated from marine source [1]. Since ancient times nature has been a source of medicines to cure many deadly diseases. Majority of drugs in use today are either natural products (NP), their derivatives (ND), natural products mimics (NPD) or semisynthetic derivatives (SSD) [2]. The outcomes of patients age 60 years and older with acute myeloid leukemia (AML) treated with conventional cytotoxic chemotherapy remain poor, with few long-term survivors, irrespective of the induction chemotherapy provided and the intensity or duration of postremission treatment [3].

Computational details:

The 3D structures of the molecules were generated using the built optimum option of Hyperchem software (version8.0). ChemOffice and Dragon (version 3.0) programs were employed to calculate the molecular descriptors. Then, Unscrambler (version 9.7) program was used statistical methods and analyses data. All calculations were performed using

Gaussian 03 program series employing DFT methods. Geometry optimization of compounds was carried out by B3LYP method employing 6–31G (d) basis set.

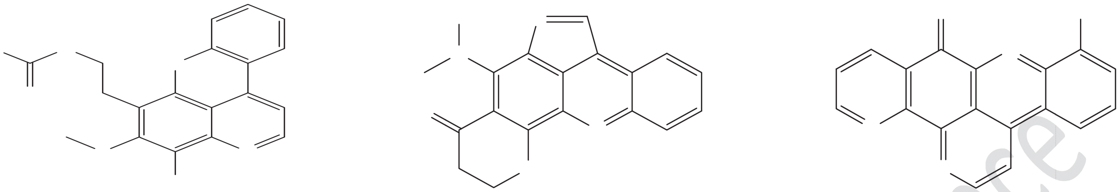

Figure 1 The molecular structure of marine natural alkaloids.

Results and discussion:

The efficiency of the QSAR model to predict log (IC50) value was also estimated using the internal cross-validation method, this resulted predictions of the log (1/IC50) using PLS, PCR and MLR methods before GA in gas phase is given in Table 1.

Table 1 Experimental and predicted values of log (1/IC50) using MLR, PCR & PLS methods.

Observed	Predicted PLS	Predicted PCR	Predicted MLR
-1.520	-0.708	-0.350	-1.220
-1.300	-1.177	-0.412	-1.525
-1.700	-0.631	-0.432	-1.699
-0.410	-0.810	-0.705	-0.421
0.000	-0.330	-0.334	0.025
0.680	0.460	-0.337	0.674
-0.300	-0.134	0.548	-0.282
-0.520	-0.742	-1.128	-0.573
1.510	1.596	-0.343	1.478
-1.430	-1.319	-1.027	-1.336
-1.000	-1.293	-0.697	-0.958
-0.520	-1.141	-0.699	-0.624
1.300	1.253	0.320	1.335
-1.240	-0.831	-0.973	-1.056
-1.160	-1.550	-1.493	-1.420
-1.220	-0.935	-0.721	-0.969
-1.100	-0.903	-0.973	-1.269
0.300	-0.220	0.253	0.288
0.630	0.318	0.629	0.608
0.590	0.692	0.471	0.543

Then, the obtained equation was used to predict log (1/IC50) values for the compounds from the corresponding test sets. Based on the types of variable selection method and also the types of the feature mapping technique, these models can be shown as MLR-ANN, GA-MLR and GA-ANN. It revealed that the GA–ANN model was much better than other models is given in Table 2.

Table 2 The statistical parameters of different constructed QSAR models.

Method	RMSE test	RMSE train	R^2
GA–ANN Jack–Knife (gas)	0.4642	0.1379	0.7935
GA–ANN (gas) cross validation	0.3889	0.1361	-

Conclusion:

The results obtained from this work indicate that the linear regression and ANN models exhibit reasonable prediction capabilities. It revealed that the GA–ANN model was much better than other models. Also, we find out MLR method is most favorable method for predict.

References:

[1] Deepak K, Diwan SR. Med. Chem. 2011, 213-268.
[2] Newman D. J. J. Med. Chem., 2008, 51, 2589.
[3] Burnett AK, Milligan D, Goldstone A. et al. Br J Haematol. 2009,145, 318-332.

Interaction energy investigation of some aromatic hydrocarbons on oxidized multiwalled carbon nanotubes

M. Dehghani[a], E. Jamalizadeh[b*], S.M.A. Hosseini[b]
Department of Chemistry, Payame Noor University (PNU), Kerman, Iran
Department of Chemistry, Faculty of Science, Shahid Bahonar University of Kerman, Kerman76175, Iran.
jamalizadeh@uk.ac.ir

Abstract:

In this work adsorption performance of benzene, toluene, ethylbenzene and p-xylene (BTEX) by NaOCl-oxidized Multiwalled carbon nanotubes (MWCNTs) is studied by using quantum chemical calculations using DFT method. Initially, location of COOH groups on the MWCNT is investigated. Then, the best adsorption site for benzene, toluene, ethylbenzene and p-xylene (BTEX) on the surface of NaOCl-oxidized Multiwalled carbon nanotubes are studied. The interaction energy between the molecules of adsorbate and NaOCl-oxidized MWCNT was calculated, which showed good consistency with adsorption parameters of experimental.

Kay word: Quantum Chemical Studies, Carbon Nanotubes, Adsorption, BTEX

Introduction:

CNTs are considered as good adsorbents owing to their large specific surface area, micropore volume, and short adsorption equilibrium time. Adsorption of aromatic compounds, such as benzene [1], polyaromatics, xylenes [2] on CNTs has been investigated experimentally or numerically. In addition, oxidized CNTs were also investigated as adsorbent. The BTEX volatile organic compounds are important industrial solvents frequently encountered as industrial contaminants endanger public health and welfare [3]. Thus, in present research work, the adsorptions of aromatic compounds on MWCNTs were untaken which mainly focus on the nature of the adsorbed molecules.

Computational methods:

To the determination of the interaction energy between the oxidized carbon nanotubes and aromatic compounds (BTEX) calculations were performed by density functional theory (DFT) method using the hybrid exchange B3LYP functional with 6-31G basis set in water solution. The Multiwalled carbon nanotube is investigated inclusive three layers with an average interlayer distance of 3.4Å [4] and with an average bond distance c-c 1.42Å [5]. The MWCNT is built with 21 carbon atoms in one, 18 carbon atoms in the second and 18 carbon atom in the third layer (Fig. 1). The best location for adsorption of COOH groups on the MWCNT is studied via optimization of the COOH/MWCNT system. After that, the adsorption of molecules on the MWCNT-COOH has been carried out which the interaction energy is given as:

$$\Delta E = E^{\alpha\cup\beta}_{CNT\ adsorbates}(\mathrm{CNT+adsorbates}) - E^{\alpha\cup\beta}_{CNT\ adsorbates}(\mathrm{CNT}) - E^{\alpha\cup\beta}_{CNT\ adsorbates}(\mathrm{adsorbates})$$

where the superscripts denote the basis set and the subscripts refer to the geometry used for energy calculation.

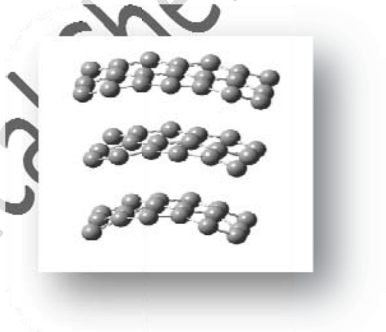

Fig 1. Structure of the oxidized MWCNT

Results and discussion:

Fig. 2. Shows the best location of COOH groups on the MWCNT. The calculated interaction energy between the molecules of adsorbate and oxidized MWCNT are represented in Table 1. The calculated equilibrium adsorption (qe) by interaction energy shows good consistency with the experimental equilibrium adsorption, Table 1.

Table 1.

Adsorbate molecules	E (au)	q_e (exp) [1]	q_e (cald)
benzene	0.04216	230.7	234.9
ethyl benzene	-0.045262	261.2	289.1
p-xylene	-0.049525	318.3	289.1
toluene	-0.004502	252.1	244.5

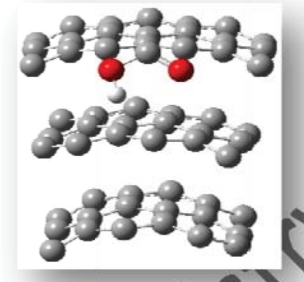

Fig. 2. Optimized structure of oxidized MWCNT

Conclusion:

The best location of COOH groups on the MWCNT is investigated. The interaction energy derived results showed that interaction energy is an efficient parameters for comparison of the adsorption parameters, which showed good consistency with adsorption parameters.

References:

[1] C.-S. Lu, F.-S. Su, S.-K. Hu, Appl. Surf. Sci. 254 (2008) 7035–7041.
[2] C.J.M. Chin, L.C. Shih, H.J. Tsai, T.K. Liu, Carbon 45 (2007) 1254–1260.
[3] Purdom PW. Environmental health. 2nd ed. New York: Academic Press; 1980.
[4]. C. S. Lu, F. S. Su, S. K. Hu, Appl. Surf. Sci. 254 (2008) 7035–7041.
[5] N. S, R C. D, Chem. Phys. Lett. 500 (2010) 65-70.

Ab initio calculation of intermolecular potentials & prediction of second virial coefficients for van der Waals complex CH_4-N_2

[a]M. Dehestani*, [b]M. Ashraf Ganjooei, [b]M. Dehghani
[a]Department of Chemistry, Shahid Bahonar University of Kerman, Kerman, Iran.
[b]Department of Chemistry, Payame Noor University of Kerman, Kerman, Iran.
E-mail: Dehestani2002@yahoo.com

Keywords: Intermolecular potential, Second virial coefficients, CH_4-N_2, SAPT

Introduction:

In this work, symmetry adapted perturbation theory (SAPT) has been performed to compute the intermolecular potential energy surface (PES) of CH_4-N_2 complex for a broad range of intermolecular separations and configurations. The parameters of (12-6) Lennard-Jones potential, ε (the depth of potential well) and σ (the distance at which the potential is zero), was estimated by fitting to the SAPT data for (12-6) Lennard-Jones potential function.

$$\boldsymbol{u(r) = 4\varepsilon\left\{\left(\frac{\sigma}{r}\right)^{12} - \left(\frac{\sigma}{r}\right)^{6}\right\}} \tag{1}$$

The obtained (12-6) Lennard-Jones potential was used to evaluate the second virial coefficients.

Computational Method:

The SAPT interaction energy is expressed as a sum of perturbative corrections. This method decomposes Hamiltonian as $H = F + W + V$, where $F = F_A + F_B$ is the sum of the Fock operators for monomer A and B, and W is the intramonomer correlation operator, and V is the intermolecular interaction operator, so the interaction energy can be represented as a double-perturbation series

$$E_{int} = \sum_{n=1}^{\infty}\sum_{j=0}^{\infty} E^{(nj)} \tag{2}$$

where the indices n and j denote the orders of perturbation in V and W, respectively [1]. The aug-cc-pVDZ basis set was used for SAPT calculations. The second virial coefficient is commonly given by the following equation

$$B_2(T) = -2\pi N_A \int_0^{\infty} (e^{-u(r)/kT} - 1)\, r^2 dr \qquad (3)$$

This equation can be written as a linear combination of four modified Bessel functions and can be evaluated for every temperature with high degree of numerical accuracy [2].

Result and Discussion:

We calculated interaction energy for 1050 points. Clearly, intermolecular potentials depend on intermolecular separations and the orientations of CH_4 and N_2 toward each other, while (12-6) Lennard-Jones only depends on the intermolecular separation. For solving this, we investigated the most stable configurations which have the deepest potential well. We calculated interaction energy for 119 points of them [3]. We obtained R^2=0.97 and ε/k =119.06 K and σ=3.32 Å. The values of the second virial coefficients obtained are presented in Figure 1 as a function of temperature. As can be shown in Table 1, the results are in good agreement with Ref. [4].

Table1. The second virial coefficients in the present study in comparison with the values of Ref. [4].

	B_2(cm^3/mol)	
T(K)	Ref. [4]	Our work
308.15	-14.76 , -17.35	-16.48
313.15	-15.60 , -15.21	-15.55
323.15	-13.80	-13.78
333.15	-11.24 , -10.24 , -12.46	-12.14

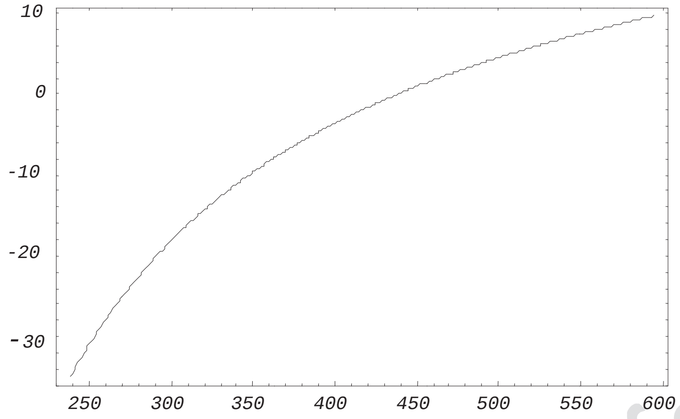

Figure 1. B_2(cm^3/mol) vs. T (K).

References:

[1] R. Moszynski, P. E. Wormer & A. van der Avoid, Symmetry adapted perturbation theory applied to the computation of intermolecular forces. In P. Jensen, & P. R. Bunker (Eds.), *Computational Molecular Spectroscopy* (pp. 69-108). New York: John wiley & Son Ltd. (2000).

[2] P. Vargas, E. Munoz, & L. Rodriguez, *Physica A ,* **290**, 92 (2000).

[3] Y. N. Kalugina, V. N. Cherepanov, M. A. Buldakov, N. Zvereva-loete, & V. Boundon, *J. Chem. Phys. ,* **131**, 134304 (2009).

[4] B. D. Ababio, P. J. Mc Elroy, & C. J. Williamson, *J. Chem. Thermodyn. ,* **33**, 413 (2001).

How the Structure of Interferon-Alpha, Responds to Temperature Change? "A Molecular Dynamics Simulation Study"

D. Mohammad-Aghaie*, M. Halvani
Department of Chemistry, Shiraz University of Technology, Shiraz, 71555-313, Iran
Corresponding author's email: d_aghaie@sutech.ac.ir

Key words: Protein, Interferon-Alpha, Molecular Dynamics Simulation

Introduction:

Interferons (IFNs) are a group of natural proteins made and released by human cells, in response to viral infection and other stimuli. They belong to the large class of glycoproteins, known as cytokines, and are named after their ability to interfere with viral replication within host cells. There are three main types of interferons, known as: alpha, beta and gamma.

Molecular dynamics (MD) simulations provide a valuable approach, to the dynamics, structure, and stability of protein systems. [1] In this study, we have simulated the interferon-alpha at four different temperatures (298, 310, 313 and 318 *K*) to investigate the response of this protein, to the temperature change. Structural analysis was performed on the output configurations, by analyzing three structural parameters. Obtained results showed the loss of stability in the two limiting temperatures, specially in 318*K*.

Method:

We have performed molecular dynamics simulations of Interferon-alpha, dissolved in water, at four different temperatures. The initial structure of interferon-alpha, taken from protein data bank (PDB ID: 1ITF) was changed to appropriate gromacs structure format. We defined a simulation box, centered the protein in it and filled the box with 12953 water molecules. Finally two Na^+ ions were added to the simulation system to make it neutral. The steepest descent algorithm was employed to run energy minimization, to ensure that the system has no steric clashes or inappropriate geometry. Two short position restrained MD simulations were conducted in NVT and NPT ensembles, each for 100 ps. Applying position restraining force on the heavy atoms of protein, allows us to equilibrate our solvent around it. Four separate MD simulations in NPT ensemble were performed on the energy minimized and equilibrated systems, at 298, 310, 313 and 318 *K,* each for 5 ns. The constant temperature and pressure simulations were performed using the Berendsen thermostat/barostat with coupling constants of 0.1 and 2 ps, respectively. We employed full periodic boundary conditions in all of the simulations. The short-range Lennard-Jones interactions were truncated at 1.0 nm, and the long range Coulombic interactions were computed using the Particle Mesh Ewald summation method. [2] Gromacs simulation package 4.5.5 [3], was used for all of the calculations and analysis of the results.

Results and discussion:

In order to study temperature effect on the structure of interferon-alpha, three structural parameters were computed and analyzed: RMSD, SASA and R_g. We examined the evolution of structures during the simulation runs, by calculating root mean square deviations (RMSD) of the trajectories, with respect to energy-minimized structure of interferon-alpha. The gyration radiuses (R_g) and solvent accessible surface areas (SASA) were also calculated. Radius of gyration is an indicator of protein structure compactness. Obvious increase of R_g and total solvent accessible surface area at 298 and 318*K*, correspond to the loss of compactness in these temperatures. Both hydrophobic and hydrophilic parts of SASA show increments. On the other hand, higher values of RMSD at these two limiting temperatures, specially 318*K,* is an evidence for reduced stability of interferon-alpha. Similar observed stabilities in temperatures 310 and 313 *K* indicates that increasing temperature for three degrees has not considerable effect on protein stability and its structural parameters. Figures 1 and 2 show the gyration radiuses and RMSD's of interferon-alpha at studied temperatures.

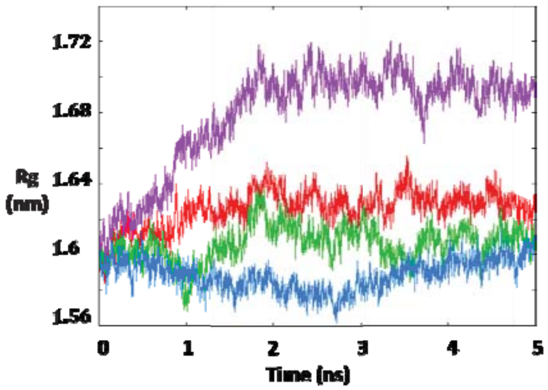

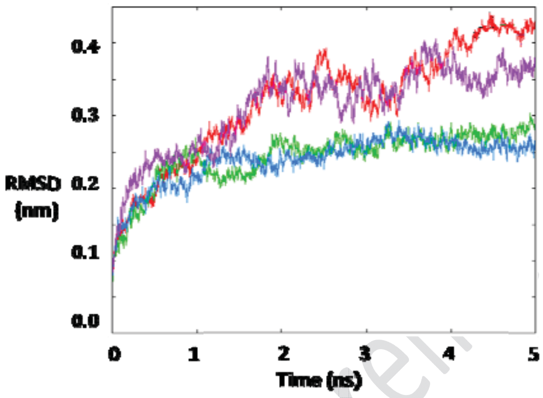

Fig. 1: Radius of gyration of interferon-alpha

Fig. 2: Root mean square deviaton of interferon-alpha

Guide to Line colors: 298*K* (**red**), 310*K* (**green**), 313*K* (**blue**) and 318*K* (**purple**)

References:

[1] Bond, P. J., Holyoake, J., Ivetac, A., Khalid, S., Sansom, M. S., *J. Struct. Biol.* 157, 593-605, 2007.

[2] Darden, T., York, D., Pedersen, L., *J. Chem. Phys.* 98, 10089–10092, 1993.

[3] Hess, B., Kutzner, C., van der Spoel, D., Lindahl, E., *J. Chem. Theor. Comp.* 4, 435–447, 2008.

Mechanism of Action of Anti-cancer drug with DNA: A theoretical approach

M. Sohanian* [a], R. Fazaeli[b] , M. Yousefi[a]

[a] Department of Chemistry, Islamic Azad UniversityShahr-e Rey Branch, Tehran, Iran

[b] *Modeling and Optimization Research Center in Science and Engineering, Islamic Azad University-South Tehran Branch, Tehran, Iran*

E-mail: merichem80@yahoo.com

Keywords: Anticancer, DNA , Platinum, Oxaliplatin

Introduction:

Oxaliplatin is one of the most successful anticancer drugs ever produced .It is believed to work by binding to DNA leading to apoptosis. Since the binding of Pt to DNA is kinetically controlled, a better understanding of this process requires the use of quantum chemical methods for probing transition states.

Methods:

Full unconstrained geometry optimization and frequency calculation for all distinct species involved the binding process of the Oxaliplatin have been carried out at the B3LYP level. The standard split valance basis set 6-31+G** was applied for C, N, O and H atoms and basis set of Hay and Wadt (LanL2DZ) was employed for Pt. The effective core potentials of Hay and Wadt with double-valance basis set (LanL2DZ) were chosen to describe Pt and polarization functions were also added for Pt(ζ = 0.993).

Reaction1

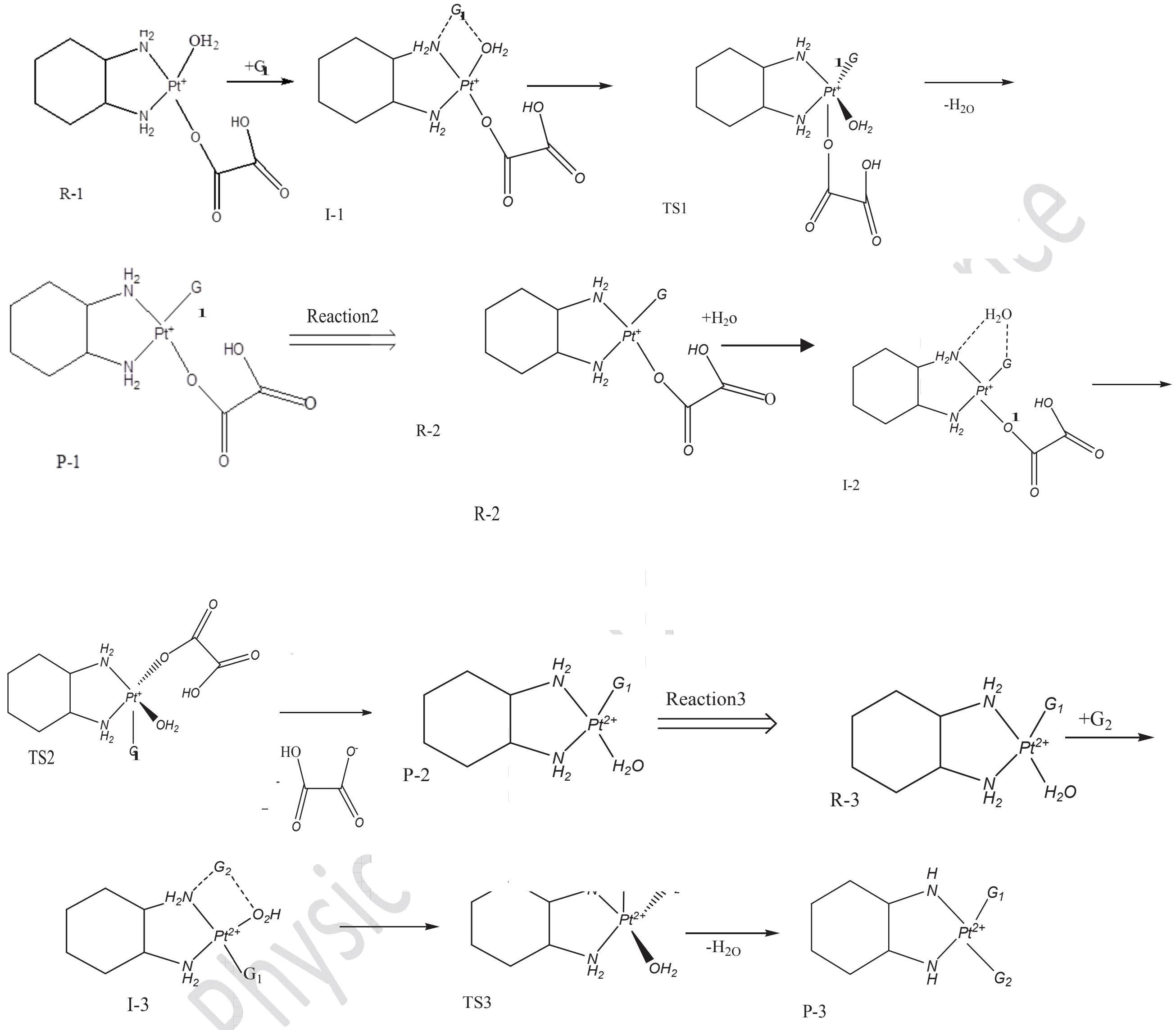

Guanine =

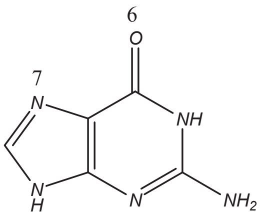

1. Reaction 1:

The first reaction is characterized by displacement of the aqua ligand of complex by the N7 of guanine via a pentacoordinated transition state. The first intermediate (I-1) is characterized by guanine to complex approach and making hydrogen bonds

1- between the aqua ligand and the O6 of G and 2-between an amine ligand and the N7 of G.

2. Reaction 2:

Reaction 2 is the step where the remaining oxalato ligand is replaced by a second water molecule.In the intermediate(I-2) the water molecule approaches the reaction center via a H-bond with an ammine hydrogen in a position transto the N7 atom. The structure found for this intermediate is quite interesting, with the hydrogen bond between oxygen O6 and another ammine hydrogen remaining at almost the same length throughout the reaction 2 pathway.

3. Reaction 3:

Reaction 3 corresponds to the final stage of the formation of bi-functional DNA–Pt adducts with the coordination of the platinum atom to the second guanine. This process involves the replacement of the aqua ligand by the adjacent guanine through coordination at the N7 site. For this reaction, labels G1 (for the guanine bound to Pt in reaction 1) and G2 (for the second guanine) have been used.

The intermediate (I-3) has two hydrogen bonds between $[Pt(NH_2)(H_2O)(G1)]^{2+}$adduct and G2 (O6 _ _ _ HOH and N7. . .HNH_2) .

Conclusions:

A detailed study of the binding of oxaliplatin aqua species with the DNA purine base guanine was performed under a quantum mechanical description using HF and density functional levels of theory.

Finally, the study report provides a molecular view of the important processes in the interaction of oxaliplatin with DNA. The structural features reported for the intermediates and transition states might be useful to design new molecules capable of binding to DNA more rapidly and consequently exhibit novel biological properties.

References:

[1] Maria Fatima et al, J. Phys. Chem. B (2009) 113, 831-838.

[2] Johan Raber et al, Molecular Physics, (2004) 102, 2537-2544.

Interaction of CO with SiCnanocluster surface

Elham Zarorati,Javad Beheshtian*
Department of Chemistry, ShahidRajaee Teacher Training University, P.O. Box 16875-163, Tehran, Iran
j.beheshtian@Gmail.com

Keywords: Carbon Silicon nanocluster, Density functional theory, Adsorption, CO.

Introduction:

Silicon carbide(SiC) is a compound of silicon and carbon with a chemical formula SiC.SiC nanomaterials may be promising semiconductors for preparation of nanoelectronic devices for high-temperature, high-power, and high-frequency applications[1].When the concentration of Carbonmonoxide(CO) increases, it is dangerous for human body.There areseveral theoretical studieson CO adsorption on various surfaces [2-3].We performed DFT calculations to study adsorption of CO on $Si_{16}C_{16}$ and $Si_{24}C_{24}$fullerene-like nanoclusters and investigated corresponding different electronic properties.

Computational methods:

All calculations were performed using DFT within M062Xlevel calculationwhich has been widely used in the nanostructure studies.The basis set were set to be 6-311G** for the optimization, frontier molecular orbital (FMO) analyses, and energy calculations.The adsorption energy of CO molecule on the pure Si_nC_n cluster obtained using the following equation:

$$E_{ads}=E\ (Si_nC_n/CO) - E\ (Si_nC_n) - E\ (CO)$$

,where E (Si_nC_n/CO) is the total energy of Si_nC_n/CO complex and E (Si_nC_n) or E (CO) is the energy of an isolated Si_nC_nor COmolecule, respectively.All calculations were implemented in GAUSSIAN 09 package.

Results:

We carried out full structural optimization of the $Si_{16}C_{16}$ and $Si_{24}C_{24}$ nanoclusters with CO gas molecule to examine the energetic, structural, and electronic properties. To find the most favorable adsorption configurations, the adsorbate is placed at different positions freely above the cluster surface having different orientations.In Fig.1 we demonstrate those structures for $Si_{16}C_{16}$ and $Si_{24}C_{24}$ respectively, which are labled by A1-A4 and B1-B4.

More details are listed in Table1. The highest energiesare related to A2 and A3 and lowest energy is related to A1.

The highest occupied molecular orbital (HOMO) and the lowest unoccupied molecular orbital (LUMO) for $Si_{16}C_{16}$ and A2 isshown in Fig2.a.

The total electronic density of states (DOS) analysis was performed using GaussSum programto verify the effects of the adsorption of CO molecule for the nanocluster electronic properties. The DOSfor the$Si_{16}C_{16}$ structure is shown in Fig 2.band for the A2 structure is shown in Fig 2.C.

Table.1 The adsorption energy (E_{ads}) of CO on the $Si_{16}C_{16}$ and $Si_{24}C_{24}$ nanoclusters, Mulliken charge transfer (the charge on the molecule after its adsorption(Q_T) on the cluster), and the change of $Si_{16}C_{16}$ and $Si_{24}C_{24}$ HOMO–LUMO gap(ΔE_g) upon the adsorption process.

Configuration	E_{ads}(kJ/mol)	ΔE_{gap}(ev)	Q_T(e)
A1	-11.57	1.95	-0.101
A2	-60.77	2.22	0.111
A3	-60.77	2.22	0.111
A4	-32.8	2.19	0.039
B1	-19.29	1.82	-0.15
B2	-29.9	2.06	0.031
B3	-48.23	2.09	0.103
B4	-30.97	2.09	0.033

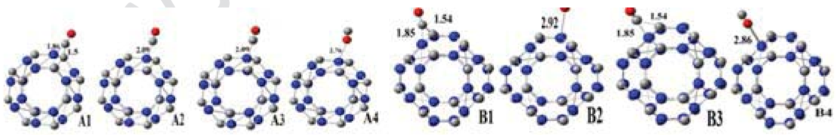

Fig.1 Optimized structures CO/ $Si_{16}C_{16}$ and $Si_{24}C_{24}$ complexes. Distances are in A °unit.

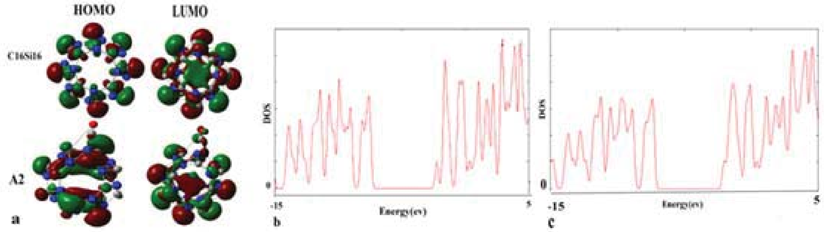

Fig.2 a HOMO and LUMO of optimized $Si_{16}C_{16}$ and $Si_{16}C_{16}$-CO nano-cages . **b** DOS plot for the $Si_{16}C_{16}$ structur .**c** DOS plot for the A2 structur.

With respect to data, it can be inferred that $Si_{16}C_{16}$ and $Si_{24}C_{24}$ nano-cages play the role of gas sensor device in the presence of CO molecule.

Reference:

[1] M.N.Huda and A.K.Ray, "Novel silicon-carbon fullerene cage " Eur. Phys. J. D 31. 63-68(2004)

[2] J. Beheshtian, Z. Bagheri, M. Kamfiroozi, A. Ahmadi, " A theoretical study of CO adsorption on aluminum nitride nanotubes" StructChem,(2011)

[3] K. Azizi, S. MajidHashemianzadeh, Sh. Bahramifar,"Density functional theory study of carbon monoxide adsorption on the inside and outside of the armchair single-walled carbon nanotubes", Current Applied Physics 11 (2011) 776-782

A Theoretical Appruach to the Gibberellic Acid (GA) Effect on Monoterpene Distribution in Rubus Caesius

Nader Zabarjad Shiraz*, Alireza Feyzbakhsh, Nasim Etemad
Department of Chemistry, Islamic Azad University, Central Tehran Branch, Tehran
*zabarjad_sh@yahoo.com

Key words: Gibberellic acid, Rubus Caesius, Ab initio, Hormone treatment

Introduction:

Growth and development of many plants regulated by the activity of plant hormones [1, 2]. Experimental studies showed that treatment of Rubus caesius by Gibberllic acid (GA, **1**) had significant effect on monoterpene composition; so that, in the presence of GA, concentration of cineole (**6**) decreased (0.34% to trace), instead the concentration of terpinolene (**3**) increased (3.53 to 5.02%). In terms of biosynthesis of monoterpenes, they derive from terpinyl cation **2** (Scheme 1). GA could interact with **2** and lead to perturbation of the product composition. In this study we try to report the effect of GA on monoterpene compotion in Rubus caesius theoretically.

Calculation method:

The structures of extracted monoterpenoids (**2-6**) (Scheme 1) were optimized at HF/6-31G* level of theory using Guassian 98 software. In next step the structure of adduct **7**, resulted from the interaction of hormone **1** and intermediate **2** were optimized at the same level of theory (Scheme 2). Heats of formations of molecules **1-7** were summarized in Table 1.

Result and discussion:

Comparison of heat of formation of adduct **7** with intermediate **2** and **1** show that, adduct **7** was 19 kcal/mol more stable than separated molecules (**1** and **2**). This could be the reason that stabilization of adduct **7** may be a struggle to intermediate **2** to rearrange to α-terpineol **4**. In other word stabilization of carbocation provided facility to deprotonation of **2** and production of terpinolene **3**.

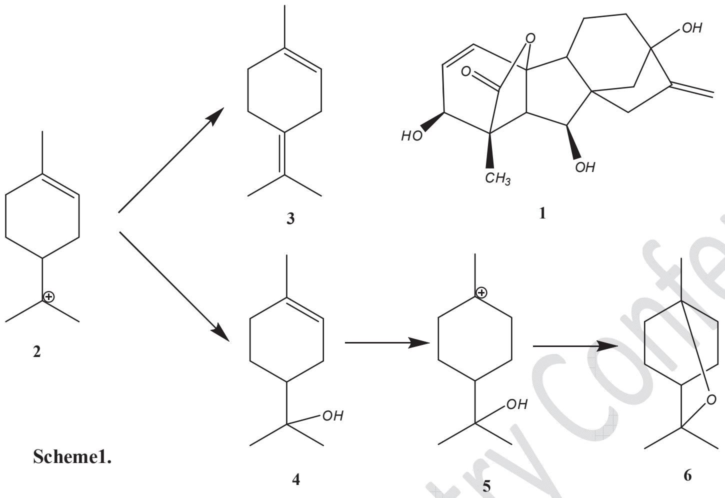

Scheme1.

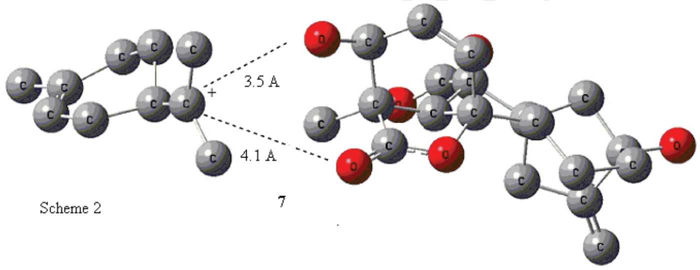

Scheme 2

Table1.

Comp.	HF(Hartree)
1	-1181.4344763
2	-388.3138745
3	-387.98718722
4	-464.0063462
5	-464.3418975
6	-464.0296332
7	-1569.77878051

Reference:

[1]Lis Balchin M. *Acta Hovticul Furae,* 1996, 426, 13-30.

[2]Eid M. N. A and Ahmed S. S. *Egypt. J. Hort.,* 1976, 3, 83-87 .

Experimental and theoretical study of a new diazaphospholane compound: $(ClCH_2CH_2)_2NPO[HN(CH_2)_2NC(O)C_6H_4(p\text{-}NO_2)]$

H. Mostaanzadeh[a*],A. Abbasi[a], F. Hajizadeh[a], T. Koval[b], M. Dusek[b]
a Department of chemistry, Faculty of sciences, University of qom, Qom, Iran
b Institute of Physics of the ASCR, v.v.i., Na Slovance 2, 182 21 Praha 8, Czech Republic
Email: hmostaan@yahoo.com

Key words: Diazaphospholane, Structural analysis, Theoretical calculation, Vibrational spectra

Introduction:

Cyclophosphamides and structurally related analogues were studied in different areas of chemistry: urease inhibitors, ashless antioxidant, antirust and antiwear additives for lubricating oiland anticancer drugs. One class of the most important derivatives of cyclophosphamide are 1,3,2-diazaphospholane ring systems that are playing a key role in cancer chemotherapy [1-3].The knowledge of the conformational properties of cyclophosphamides should be beneficial to a detailed understanding of the pharmacological effects of these compounds.

Experimental:

$(p\text{-}NO_2\text{-}C_6H_4)C(O)N(H)P(O)Cl_2$ was prepared from the reaction of phosphorus pentachloride with 4-nitrobenzamide and formic acid treatment. To a stirring dry acetonitrile solution (20 ml) of 4-nitrobenzoyl phosphoramidic dichloride, a solution of bis(2-chloroethyl) amine was added dropwise at 268K. After 8 hours stirring, the product was filtered off and then washed with distilled water. The single crystal of the final product was analyzed with X-ray diffractometer.For this measurement the four-cycle diffractometer Gemini equipped with CCD detector Atlas and the graphite monochromated Cu Kα radiation (λ = 1.54184Å) was used. The Infrared (IR) spectrum of this compound was recorded on a Shimadzu model IR-60 spectrometer.

Result and discussion:

In reaction of 4-nitrobenzoyl phosphoramidic dichloride with bis (2-chloroethyl) amine we had expected to obtain the phosphoric triamide compound **a** (Fig. 1-a) but due to the intramolecular nucleophilic attack of one of the terminal carbons of the chloroethyl substituted (-CH_2CH_2Cl) to the amidic nitrogen group (-CONH-) we got the diazaphospholane compound **b** (Fig 1-b) and released HCl gas.

We used *ab initio* calculation in order to better understanding these results. The molecular geometry and vibrational frequencies of the compounds in the ground state have been calculated using the density functional theory (DFT) method of the calculation. The theoretical model that is used here was B3LYP/6-31G(d,p) that implemented in Gaussian 03 package. The calculated Gibbs free energy of these compounds (**a** and **b)** predict that **b** is more stable than **a** in agreement with our experimental results. The calculated vibrational spectrum of **b** has better agreement than **a** with the observed IR spectral data. Furthermore the molecular geometry (the optimized bond lengths and bond angles) of **b** in the ground state is much closer to the data obtained from X-ray crystallography.

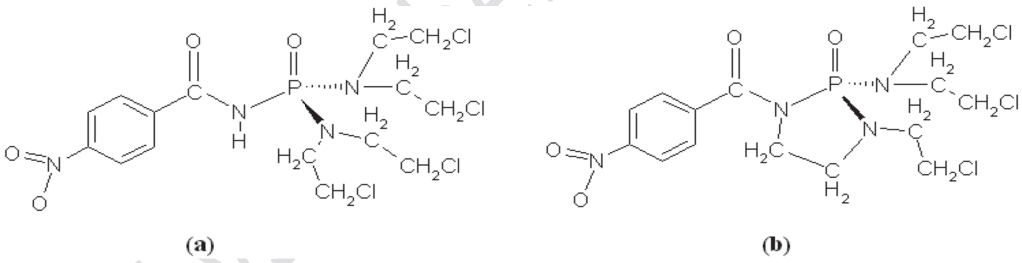

Fig.1 The molecular structures of the phosphoric triamide compound (a) and the diazaphospholane compound (b).

Reference:

[1] M. D. Swerdloff, J. F. Kolc, M. M. Rogic, L.L. Hendrikson; U.S. Patent; 4, 517, 007,1985.
[2] D. Abbott, H. Slamon, R. Sattergood; Brit. Patent; 1, 558, 462, 1980.
[3] G. Zon; Med. Chem; **19**, 205, 1982.

Molecular dynamic simulation study on native and glycated form of myoglobin

J. Alizadeh[a],A.Ebrahim-Habibi[b*], A.Shayesteh[a]
[a]School of chemistry, College of sciences, University of Tehran, Tehran, Iran
[b]Endocrinology and Metabolism Research Center, Tehran University of Medical Sciences, Tehran, Iran
Email:aehabibi@tums.ac.ir

Key words: myoglobin, glycated myoglobin, molecular dynamic simulation, potential energy

Introduction:

The prevalence of diabetes has reached epidemic proportions worldwide. Diabetes mellitus is a chronic metabolic disorder characterized by rise in blood glucose level called "hyperglycemia"[1]. Increased glucose concentration in diabetes mellitus causes glycation of several proteins like hemoglobin and myoglobin, leading to change in their properties.These heme-containing proteins are involved in the storage and transfer of oxygen within blood and muscle cells [2]. Poor blood glucose control increases the risk of heart attack, kidney failure, blindness etc. The preferential glycation sites of hemoglobin have been detected, while there have been few structural studies on myoglobin [3]. In this study we intent to discuss the impact of N-terminal glycation of myoglobin on the stability of its secondary structure.

Materials and methods:

In this study the crystallography elucidated structure of myoglobin (Mb) was used and the same Molecular Dynamics Simulation (MDS) procedure was used. This protein is composed of 149 amino acid residues. The protein structure protonation state was adjusted at pH=7.5 using the biopolymer module of MOE.2010.10 (Molecular Operating Environment, Chemical Computing Group Inc., Montreal Canada), and positioned into a periodic box of 10*10*10Å. 5876 water molecules were added and the system was minimized using the MMFF94x force field. MDS of this system was carried out on MOE software. Simulations were performed using the NPA(Nose-Poincare-Anderson)Hamiltonian equation of motion, with a temperature of 300 K, sample time of 1 ps, time steps of 0.002 ps for a total duration of 1 ns. Glycated myoglobin (GMb) was prepared by attaching a glucose molecule.

Result and discussion:

Results of the MDS include the followings: the potential energy of the system, the kinetic energy of atoms and root-mean-square deviation (RMSD). Mb and GMb structures were sampled at 1 ns time intervals. Their potential energies were extracted and visualized in the charts shown below. The comparison of these charts shows that GMb is more stable than Mb during the MDS time intervals.

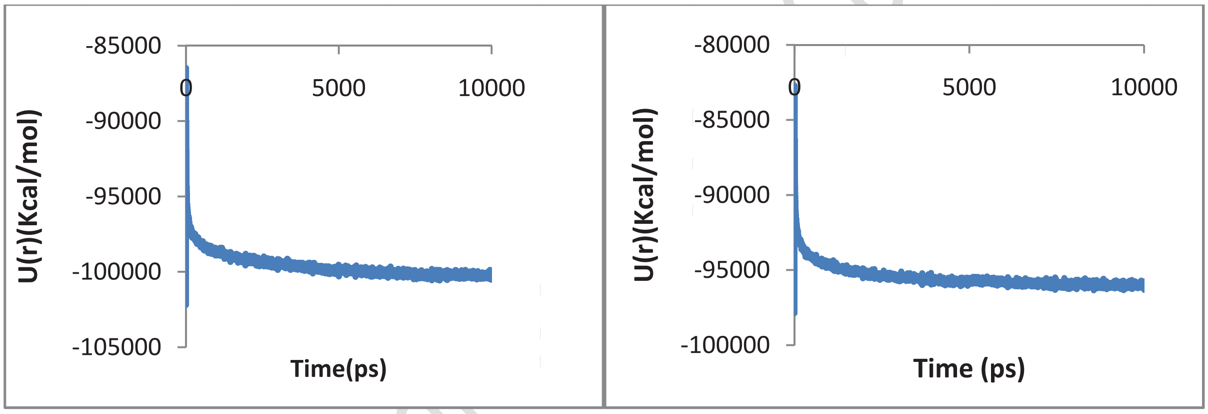

(a) (b)

Figure 1. The potential energy of the atomic system of GMb (a) and Mb (b).

Work in progress:

In this study we have obtained the potential energy of GMb and Mb. The comparison of their energy charts reveals the energeticstability of GMb. In order to specifically determine the effect of N-terminal glycation of Mb, glycine atoms of the native protein and glycated glycine atoms of the GMb will be selected and their potential energies and the interaction potential energies between the selected and unselected atomswill be compared.

References:

[1]C. M.Sultanpur, D.Kumar, S.V. Kumar, IJPSRR (2010) 3,119-122.

[2]A.Roy , R. Sil , A.S.Chakraborti, Mol.Cell.Biochem (2010) 338,105-114.

[3] M.C. De Rosa , M.T.Sanna , I.Messana , M.Castagnola , A.Galtieri , E.Tellone , R.Scatena, B.Botta ,M.Botta ,B.Giardina, BiophysChem(1998)72,323-335

Synthesis, physico-chemical properties and theoretical calculation of [1-(2-chlorophenyl)-3-(*P*-methyl phenyl)triazene] as a new asymmetric triazene

F.Younesian [a] ,H.Bagheri Sadeghi [a], M.K.Rofouei [b*]
[a]Department of Chemistry, Islamic Azad University, Tehran Central Branch, Tehran, Iran
[b]Faculty of Chemistry, Tarbiat Moallem University, Tehran, Iran
Email: (fr_younesian@yahoo.com)

Keywords: 1-(2-chlorophenyl)-3-(P-methyl phenyl)triazene, IR, Raman, NMR, DFT,HF

Introduction:

Triazenes are compounds characterized by having N=N-N functional group, referred to as the triazeno moiety. Triazenes are examples of photo chromic materials that one possible photo chromic organic materials is commercial usage in ophthalmic lenses. Triazenes represent photo chromic organic materials bas on cis-trans isomerization of nitrogen- containing double bonds. Photo chromic materials of this type are of interest for potential applications, among others, in molecular devices.

Triazene compounds have been studied for over 130 years concerning their interesting structural, anticancer, and reactivity properties. They have been used in medical, and as organometalic ligands [1-2].

Materials and Methods:

At first the [1-(2-chlorophenyl)-3-(*P*-methyl phenyl)triazene] is synthesized then molecular structure of the CPMT in the ground state is computed by performing both HF and DFT (B3LYP) with 6-311++G(d,P) basis set.

HF/DFT calculations for CPMT are performed using Gaussian 03 W[13] program package on Workstion Intel ® 2 Quad CPU Q9550 GHz processor (4Cpus) with 4 GB RAM under windows XP operating system without any constrain on the geometry.

Apparatus:

Melting point was determined by Gallenkamp melting point apparatus. Elemental analyses were performed with Perkin-Elmer 2400 series II. ^{1}H NMR and ^{13}C NMR spectra were recorded with Bruker Avancee 300 spectrometer with the processing software XWINNMR version 3.1.chemical shifts are reported on δ scale relative to TMS. FT-IR spectra were measured by Perkin-Elmer spectra RXI. FT-IR spectrometer in the frequency range of 4000-400 cm^{-1} using KBr discs. The IR spectra were recorded at room temperature at the spectral resolution of 1 cm^{-1}. The Raman spectra were recorded with Almega Thermo Nicolet Dispersive Raman Spectrometer. The spectra range were 4200-100 cm^{-1}. 32 scans were accumulated at 4-1 cm^{-1} resolution using a laser power of 100 mW at room temperature single.

Results and discussion:

The aim of this work is to synthesize and characterize 1-(2-chlorophenyl)-3-(*P*-methyl phenyl)triazene and perform computation and analysis. In this work, we will report a combined experimental and theoretical study on molecular structure and spectroscopic (FT-IR, Raman,^{1}H NMR, ^{13}C NMR) of 1-(2-chlorophenyl)-3-(*P*-methyl phenyl)triazene.

Conclusion:

Literature survey reveals that to the best of our knowledge the Synthesis of 1-(2-chlorophenyl)-3-(*P*-methyl phenyl)triazene has not been reported. In this work, we will report a combined experimental and theoretical study on molecular structure and spectroscopic (FT-IR, Raman,^{1}H NMR, ^{13}C NMR) of 1-(2-chlorophenyl)-3-(*P*-methyl phenyl)triazene. The optimized geometry, harmonic vibrational frequencies, infrared intensities and Raman scattering activities were calculated by HF and B3LYP methods with 6-311++G(d,p) basis set. The thermodynamic functions of the title compound were performed at same level. A detailed interpretation of the Infrared, Raman and NMR spectra of title compound was reported. Analysis of the experimental NMR chemical shifts was supported by quantum chemical calculation (B3LYP and HF) and HOSE code fragment based prediction tool (ACD/NMR). The theoretical results showed very good agreement with the experimental values.

References:

[1]M.K.Rofouei , N. Sohrabi, M. Shamsipur, E. Fereyduni, S. Ayyappan, N. Sundaraganesan**.** Spectrochimica Acta Part A: Molecular and Biomolecular Spectroscopy, Volume 76, Issue 2, July 2010, Pages 182-190

[2] E. Fereyduni, M.K. Rofouei, M. Kamaee, S. Ramalingam, S.M. Sharifkhani. Spectrochimica Acta Part A: Molecular and Biomolecular Spectroscopy, Volume 90, May 2012, Pages 193-201

Structural characteristics of a damaged DNA

S. Jalili, B. Mehrazma*
Department of Chemistry, Faculty of Science, K.N. Toosi University of Technology, Tehran, Iran
E-mail: bmehrazma@yahoo.ocm

Keywords: 8-oxoguanine, DNA damage, Molecular dynamics, GROMACS.

Introduction:

Ionizing radiation and cellular metabolism can cause oxidative DNA damage. The reccurrence of damaging, if not be repaired by DNA repair enzymes, may alter the genetic information and can lead to cancer or aging. In this respect, the most abundant oxidative damage, 8-oxo-7,8-dihydro-2'-deoxyguanosine (8-oxoguanine), has received a great attention. Guanine, due to its low oxidative potential, has a tendency to be oxidized in C8 position. The produced 8-oxoG has the ability to form both 8-oxoG:C base pair and 8-oxoG:A Hoogsteen mispair, which produces GC to TA transversion mutation. Here we used molecular dynamics, to study structural and dynamics differences between a native DNA and damaged DNA containing two 8-oxoG lesions in opposite strands.

Methods:

The available crystal structure (PDB ID:1N2W) was utilized to generate the correct 8-oxoG:C base pair[1]. The native DNA was constructed using HyperChem release 7. This sequence context had the advantage of being palindromic (CGCCAATTGGCG:CGCCAATTGGCG), so it served as a benchmark of a sufficient simulation time. To produce the force field for the modified base, we used the RESP charges from John H. Miller and coworkers work [2], and utilized the same procedure to specify the missing parameters. A 12 A˚ cutoff was applied to the nonbonded interactions. After solvation by TIP3P model and neutralization, the Steepest Descent minimization was carried out, followed by NVT equilibriation in 3 steps. Solvent was equilibrated while increasing the temperature from 50 to 310 K, in 5 steps, with time intervals of 50 ps. Next DNA was equilibrated in 150 ps. Then the whole system was subjected to a 3 ns NVT equilibration without applying any constraints. At last a 8 ns MD production run with a time step of 1 fs was carried out. The coordinates were saved every 2 ps. The Berendsen thermostat was used to maintain the temperature at constant value of 310 K. All MD calculations were performed by GOMACS 4.5.3. Curves+ was applied to extract the average helicoidal parameters [3], including minor groove width, intra-base pair parameters and inter-base pair parameters.

Results and Discussion:

Root mean square deviations(RMSDs) from both native and damaged DNA are shown in figure 1, left. Obviously the healthy DNA is very stable during 8 ns simulation, however the damaged DNA is more labile. The root mean square displacements(RMSFs) for both duplexes were analyzed. The native DNA backbone showed stable RMSF, except in extremities. The RMSF for damaged DNA backbone indicated the same instability, due to PBC end effect, as well as some changes in damaged moieties.

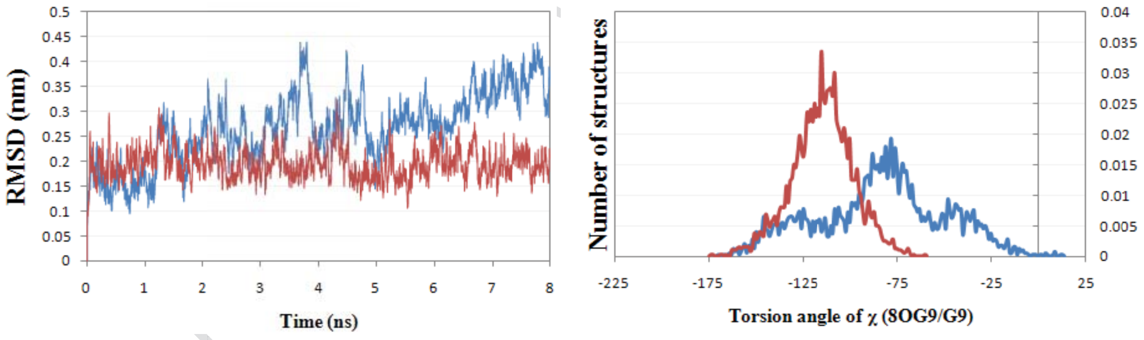

Figure 1. RMSD for all 12 base pairs, relative to the average structure (the left panel). Population distribution of the torsion angle of χ at 8-oxoG (blue) and G (red) at position 9, (the right panel), for native (red lines) and damaged DNA (blue lines).

The presence of the two 8-oxoGs on opposite strands, showed differences in magnitude of axis bending. The minor groove width for damaged DNA is slightly broader and shallower than healthy DNA. Changes in torsion angles at particular base levels were also observed. For instance torsion angle of χ at position 8-oxoG had a broader distribution, implying mobility of this angle at that position (figure1, right). We saw more Opening parameter value for base levels of A5-T20 and T8-A17, less Twist value for base levels of C4-A5 and T8-G9. with these changes, there was disturbance in Watson-Crick hydrogen bonding in certain base pairs. The radial distribution functions of water for all the electronegative atoms of the damaged bases and their flanking bases and the corresponding healthy DNA bases and all their complementary bases, were analyzed. The only deviations from native DNA in the major groove was observed for atom N7. Since it is protonated in the modified form, the first hydration shell for N7, is somewhat larger, with higher water occupancy.

Conclusions:

The existence of 8-oxoguanine in both strands in a palindromic DNA, shows some alterations in conformational quality of the dodecamer. Deviations in helical axis kink, sugar puckering and torsional angles, together propose more flexibility in damaged DNA. Changing in dynamics of the water molecules surrounding the N7 atom of the base is also observed. So, we suggest that these subtle differences could have an impact on damage recognition by the hOGG1 and FpG enzymes, before triggering the repair mechanism**.**

References:

[1]V.Thiviyanathan, A.Somasunderam, T.K. Hazra, S. Mitra, D.G. Gorenstein; ”Solution Structure of a DNA duplex containing 8-Hydroxy-2’-Deoxyguanosine” ; J .Mol. Biol; 433-442, 2003.

[2]J. H. Miller, C. P. Fan-Chiang, T. P. Straatsma, A. Kennedy; ”8-Oxoguanine Enhances Bending of DNA that Favors Binding to Glycosylases” ; JACS ; 6331-6336, 125, 2003.

[3]R. Lavery, M. Moakher, J. H. Maddocks, D. Petkeviciute, K. Zakrzewska; “Conformational analysis of nucleic acids revisited: Curves+” ; Nucleic acids research; 37,5917-5929,2009.

Determination of stable structure for Tryptophan cage using Molecular dynamics simulation

Seifollah Jalili[a], Farangis Mansoori[b]
a Department of Chemistry, K.N.Toosi University of Technolog
b Department of Chemistry, K.N.Toosi University of Technology
Email: amnmansoori@yahoo.com

Key words: Folding, Molecular dynamic, Tryptophan cage, Rmsd,

Introduction:

Understanding protein folding is critical in molecular biology. Molecular dynamic simulation (MD)performed from simple lattice models with no solvent to all atom models with implicit continum solvent and explicit solvent model are used to supplement experiments. In implicit solvent model folded structure kinetically may trap in high energy minimum [1-3]. We have suggested a way to avoid this problem. Here MD simulation has been used to study folding of Tryptophan cage (TC5B)a mini protein from its fully extended conformation. The measuring of main-chin root mean square deviation (rmsd) is criterion to determine the stable structure. The final structure has beenproduced with 1.6Årmsd related to NMR native structure.

Methods:

The simulations of peptide folding were performed in NPT ensemble with Amber ff99 force field. A continum solvent model,generalized born, was used and the shake algorithm was applied for hydrogen atoms in protein. Steepestdescentminimization was run and followed by conjugate gradient. Berendesen and longevin thermostat was used to control temperature.

Result and discussion:

At first there were many stric clashes. Minimization caused the system to clean up and fix up hydrogen position. The system was heated to 325k with Berendesen thermostat and then MD was run. Theproduced lowest energy structure had 3.25Årmsd. Hydrogen bond(hbond) analysis showed that some unusual intermolecular hbond kept folded structure in high energy minimum. Second MD was run with longevin thermostat. This thermostat works by simulating random collision as a molecule in solvent might feel instead of simply scaling the velocities as the Berendesen thermostat do. This method equilibrates the temperature effectively and may allow phase space to be explored quicker.That system was heated to around 375k and was run for several Nanoseconds and then was slowly cooled back to 325k. This avoided the problem with still being kinetically trapped at 325k. The lowest energy structure from this simulation had rmsd 1.6A and the final structure was stable. For this simulation clustering analysis with all the structure that resulted from trajectories was done. Theproduced clusters appeared significant pattern. Progression of first cluster to final cluster showed a Meta stable transition cluster. It suggested that this proteinhas two state folding processes.

Conclusion:

This study suggests a way for MD simulation of TC5B folding in implicit solvent to avoid folded structure being in high energy minimum. It has been showed that usingBerendesen thermostat and heating and cooling the system reduced the rmsd from 3.25Åto 1.6Å. So the stable structure has been produced. An intermediate state in clustering analysis showed this protein must have had two state folding processes.

References:

[1]L. Qiu, S. Pabit, A. Roberg and S. Hagen, J. Am. Chem. Soc. 2002, 124, 12952.
[2]C. Snow, B. Zarovic, V. J. Pande, J. Am. Chem. Soc. 2002, 124, 14548.
[3]C. Simmerling, B. Strockbine, A. Roitberg , J. Am. Chem. Soc. 2002, 124, 11258.

Elucidation of chemo- and regioselectivity in the alkylation of 6-methyl uracil using GIAO/^{13}C NMR

M. Bakavoli[a], H. Eshghi[a], A. Shiri[a], T. Afrough[a], J. Tajabadi [a*]
[a]Department of Chemistry, School of Sciences, Ferdowsi University, Mashhad, Iran
Email: jtaj2@yahoo.com

Keywords: chemo- and regioselectivity, 6-methyl uracil, GIAO/^{13}C NMR, DFT

Introduction:

Uracil is an interesting heterocyclic compound with few reactive centers which makes its alkylation reactions interesting from the viewpoint of chemo- and regioselectivity. The aim of this paper is to demonstrate the application of GIAO/^{13}C NMR chemical shifts for confirming the expected chemo- and regioselectivity of the alkylation of 6-methyl uracil.

Methods:

All the structures (Fig 1) were fully optimized with the GAUSSIAN G09 program at the B3LYP/6-31+G(d,p) theoretical level in the gas phase and Harmonic vibrational frequencies were evaluated at the same level in order to confirm the nature of the stationary points found.

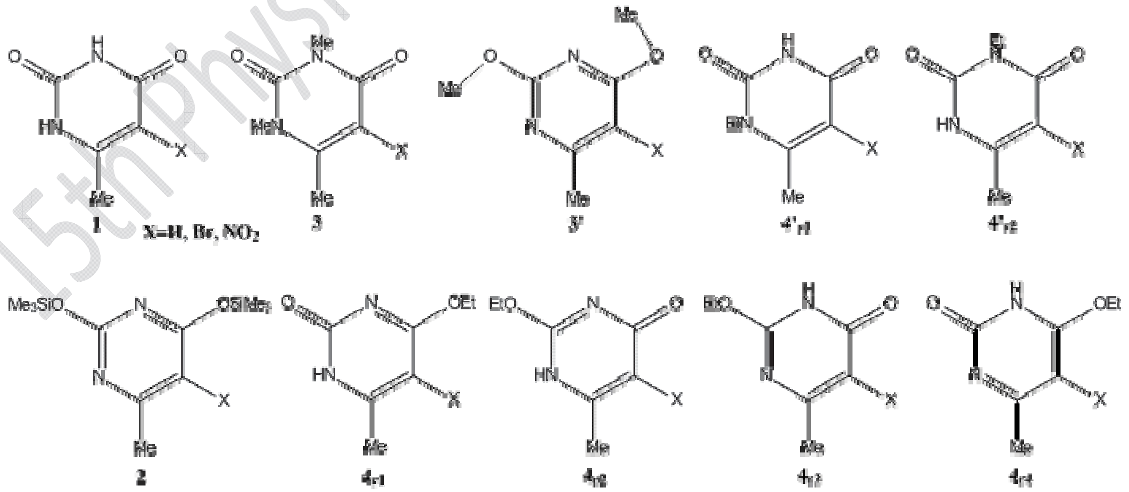

Fig 1: Structures of studied compounds

After the optimization, ^{13}C isotropic shielding were calculated with GIAO method [1] at the mPW1PW91/6-31+G(d,p) level, utilizing the PCM continuum method with UFF radii (acetone for X=NO_2 and chloroform for other compounds). The chemical shift relative to TMS for each nucleus in the molecule of interest (δ_i) is determined from the computed shielding constants computed for the same nucleus type in the reference compound (σ_{ref}), the computed shielding constants for each nucleus in the molecule of interest (σ_i), and the known experimental chemical shift for the reference compound (δ_{ref}) (see Eq. 1) [2]:

$$\delta_i = \sigma_{ref} - \sigma_i + \delta_{ref} \qquad (1)$$

Calculated chemical shifts are determined either using TMS as a single computational reference or using the second approach that was proposed recently [3], using methanol as the reference for sp^3-hybridized carbons and benzene for sp- and sp^2-hybridized carbons [the multi-standard (MSTD) approach]. Moreover, to evaluate the methods and the basis sets for prediction of calculated chemical shifts, this GIAO/^{13}C NMR procedure was employed for six major isomers at B3LYP/6-31+G(d,p) and mPW1PW91/6-311+G(2d,p) levels of theory. To reduce systematic errors, we use empirical scaling in this work, derived from linear regression analysis. Empirically scaled calculated chemical shifts are computed according to Eq. 2:

$$\delta_{scaled} = (\delta_{calc} - b) / m \qquad (2)$$

Where m and b are the slope and intercept resulting from a regression calculation on a plot of δ_{calc} against δ_{exp}.

Results and discussion:

According to calculated and experimental ^{13}C chemical shifts of carbons attached to N or O atoms, the chemo selectivity of studied reactions can be rationalized as follows:

1) In reaction of (1) with HMDS, O- silylation is preferred over N- silylation.
2) In reaction (2) with methyl iodide, N- methylation is preferred.
3) In reaction (2) with ethyl iodide, O- ethylation is preferred.

To study the regioselectivity, the difference between calculated and experimental ^{13}C NMR chemical shifts for all regioisomers of each compound shows that 4_{r1} is the preferred regioisomer.

Our study shows that the mPW1PW91 is a better hybrid functional than B3LYP with same basis set and surprisingly, a larger basis set 6-311+G(2d,p) has a grater mean absolute deviation (MAD) relative to standard basis set 6-31+G(d,p) (especially unscaled values).

Conclusions:

GIAO/^{13}C NMR chemical shifts with the mPW1PW91/6-31+G(d,p) level provides a powerful tool in the study of chemo- and regioselectivity problems in organic chemistry.

Reference:

[1] R. Ditchfield, *Mol. Phys.,* 1974, *27,* 789

[2] M. W. Lodewyk, M. R. Siebert, D. J. Tantillo, Chem. Rev. 2012, 112, 1839–1862

[3] Ariel M. Sarotti and Silvina C. Pellegrinet *J. Org. Chem.*, 2009, *74* (19), pp 7254–7260

Modeling the Molar Diamagnetic Susceptibility of Diverse Aliphatic Organic Compounds via Molecular Descriptors

Saadi Saaidpour*
Department of Chemistry, Sanandaj Branch, Islamic Azad University, Sanandaj, Iran
Email: saadisaaidpour@gmail.com*

Introduction:

Quantitative structure–property/activity relationships (QSPR/QSAR) are tools of modeling property/activity as defined by mathematical functions of molecular structure. The QSPR can be used to predict physicochemical properties of organic compounds by using theoretical descriptors. The diamagnetic susceptibility (χ) of compounds is an important physicochemical property. If a substance has no permanent magnetic dipole, but has one induced in it by an external field, this induced magnetic field will oppose the applied field. This effect is known as diamagnetism and is a universal property that is shown by most inorganic compounds. It is most perceptible when all electrons are paired, that is, when they have no permanent spin moment. For a diamagnetic substance χ is negative, small, independent of the magnetic field intensity, and independent of temperature [1].

Materials and Methods:

All diamagnetic susceptibilities data of the present investigation were obtained from the CRC Handbook of Physics and Chemistry 2010 [2]. Molar diamagnetic susceptibility range was from (-220.80×10^{-6}) to (-17.40×10^{-6}) $cm^3.mol^{-1}$. The molecular structures of all compounds were drawn into the HyperChem 7.5 program and pre-optimized using MM+ molecular mechanics method. The molecular descriptors were calculated by using the Molecular Modeling Pro plus (MMP+) software. After the calculation of molecular descriptors, a stepwise regression was used to develop the linear QSPR model using calculated descriptors. The selected descriptors are three valence molecular connectivity indices of orders 0, 1 and 3 (${}^0\chi^v$, ${}^1\chi^v$, ${}^3\chi^v$) (topological descriptors) [3] and molecular weight, MW (constitutional descriptors) [6]. The general purpose of multiple regressions is to quantify the relationship between predictor variables and a dependent variable. A multi-linear model can be represented as: $y = b_0 + b_1x_1 + b_2x_2 + b_3x_3 + \ldots + b_kx_k$ **(1)**

Leave one out cross validation (LOO-CV) is one of the QSPR model internal validation. The predictability of the QSPR model is determined using the LOO-CV method. The QSPR model developed using only training set chemicals is then applied to the external validation set chemicals to verify, more reliably, the predictive ability of the model. Another method for validation of the model is Y-scrambling. A crucial problem of a QSPR model is the applicability domain (AD). The chemical domain of applicability is a theoretical region in the space defined by the modeled response and the descriptors of the model, for which a given QSPR should make reliable predictions.

Results and Discussion:

A small number of molecular descriptors ($^{0}\chi^{v}$, $^{1}\chi^{v}$, $^{3}\chi^{v}$ and MW) proposed were used to establish a QSPR model. The best equation obtained for the molar diamagnetic susceptibility of the organic compounds is:

$$\chi_m = 5.5072 + 1.0917[^{0}\chi^{v}] + 8.7633[^{1}\chi^{v}] + 6.0228[^{3}\chi^{v}] + 0.1934[MW] \quad (2)$$

$$n = 150, R^2 = 0.9922, R^2_{adj} = 0.9919\,, Q^2_{LOO} = 0.9915\,, s = 1.0382, F = 4597.994$$

Molecular topological descriptors included the three valence molecular connectivity indices of orders 0, 1 and 3 ($^{0}\chi^{v}$, $^{1}\chi^{v}$, $^{3}\chi^{v}$). Molecular connectivity indices are topological indices that encode two-dimensional structural information into numerical values or indexes. The molecular structure is expressed topologically by a hydrogen-suppressed graph. The carbons (and hetero atoms) are represented as vertices, and bonds connecting atoms are represented as edges. The results indicate that the valence connectivity indices increase as χ_m increases. With increasing the number of atoms and the number of valence electron of the atom in compounds the molecular weight (MW) increases. Another molecular descriptor is molecular weight in the MRA model. According to equation 2, MW is directly proportional with χ_m.

Conclusion:

The selected molecular descriptors have a clear mechanistic meaning: they are related to both the molecular size of the chemical and its electronic features relevant to molar diamagnetic susceptibility. Application of the developed model to a testing set of 50 compounds demonstrates that the new model is reliable with good predictive accuracy and simple formulation.

References:

[1] A.T.Atkins, *Physical Chemistry*, 3rd edn. Oxford University Press, Oxford (1986).
[2] D.R. Lide, *CRC Handbook of Chemistry and Physics*, 90th Edition, CRC Press, Taylor and Francis, Boca Raton, FL (2010).
[3] R. Todeschini and V. Consonni, *Handbook of Molecular Descriptors*, Wiley-VCH: Weinheim, Germany (2000).

Molecular structure and resonance interactions effects on NMR tensors and NQR frequencies of hallucinogenic analogues

N. Ahmadinejad[a*], A.A. Salari[a], A. Tahan[b]
[a] Department of chemistry, Shahre Rey branch, Islamic Azad University, Tehran ,Iran
[b]Semnan branch, Islamic Azad University, Semnan, Iran.
Email:nedaahmadinejad8810@yahoo.com

Key words: Harmine, Harmaline, NQR parameters, NMR tensors, NBO interpretation.

Introduction:

β-Caroline alkaloids such as harmine [$C_{13}H_{12}N_2O$] and harmaline [$C_{13}H_{14}N_2O$] (see Fig.1) are natural products which are available in a wide range of medicinal plants [1]. They possess different biological natures such as hypotensive, hallucinogenic or antimicrobial activities [2]. Researchers demonstrated that harmine and other β-Carbolines interfere the action of reactive oxygen species, protecting the nervous system and that this behavior is due to their antioxidative properties [3]. Many researches were performed by spectrophotometric techniques for analysis and separation of β-Carboline alkaloids [4-6]. Unfortunately, the affective ab initio studies on the interested structures have not performed yet. In this study, with the objective of understanding further the structural facts of hallucinogenic new compounds, we modeled two harmine and harmaline structures using DFT methods. The basic interest of the present study is to investigate the effects of partial structural differences and resonance interactions on the NMR chemical shielding and EFG tensors at the site of nitrogen nuclei and finally NBO interpretation of structural factors.

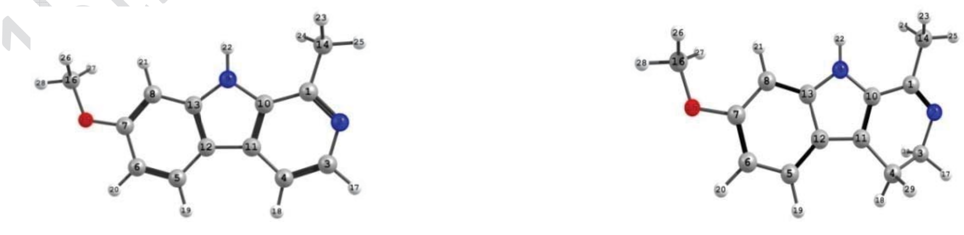

a) Harmine b) Harmaline

FIG.1.Optimized structures of a) Harmine and b) Harmaline.

Computational details:

Geometry optimizations were performed at the B3LYP/6-311++G** level on two analogues of harmine and harmaline. NBO analysis, the Electric-field gradient (EFG) and GIAO nuclear magnetic shielding calculations was then performed at the same level on the optimized structures [7-9]. All calculations were performed by using the Gaussian program [10].

Result and Discussion:

The obtained results showed that NMR shielding tensors of nitrogen atoms in both structures are strongly affected by chemical environment. Hence, nitrogen atoms which have similar chemical positions, they have almost similar chemical sheilding, e.g. N_2 and N_9 atoms in both structures. furthermore, intra-molecular interactions such as resonance interactions play the important role in determining the NMR tensors of the considered compounds. So that, N_9 atom has more value of chemical shielding (σ_{iso}) than N_2 atom in two structures. NBO analysis also showed that the lone pair electrons of N_9 have a lower occupancy and higher resonance energy than the lone pair electrons of N_2, i.e. the resonance interactions produced the strong chemical shielding in this position. The comparison of NQR parameters of N_2 and N_9 nuclei is represented that N_2 nucleus has more χ and q_{zz} value than N_9 former in two structures. In addition, these parameters are different in two analogues and their values in the harmine structure are more than it is in harmaline structure. These results are in reasonable agreement with the NMR and NBO data.

Conclusion:

This study provides a sensible picture from the structural differences for both harmine and harmaline analogues. The results represented that the chemical environment and resonance interactions for development of aromaticity nature are effected NMR chemical shielding tensors and NQR parameters on nitrogen nuclei in both considered structures. However, it can be concluded that by increasing lone pair electrons contribution of nitrogen atoms in ring resonance interactions and aromaticity development, the values of NMR chemical shielding around them increase while χ and q_{zz}values of these nuclei decrease.

References:

[1] T.G. Bidder, et al., Life Sci. 25 (1979) 157.

[2] P.W. Coddling, Can. J. Chem. 61 (1983) 529.

[3] Y.B. Gouan, E.D. Louis, W. Zheng, J. Toxicol. Environ. Health Part A 64 (2001) 645.

[4] T.R. Bosin, K.F. Faull, J. Chromatogr. 428 (1988) 229.

[5] J. Adachi et al., J. Chromatogr. 538 (1991) 331.

[6]L. Martı´n et al, J. Pharm. Biomed. Anal, 32 (2003) 991.

[7] E. D. Glendening, A.E. Reed, J.E. Carpenter, F. Reinhold, NBO Version 3.1.

[8]R. Cammi, J. Chem. Phys. 109, 3185 (1998).

[9] M. Tokman, D. Sundholm, P. Pyykkö, J. Olsen, Chem. Phys. Lett. 265 (1997)60.

[10] M.J. Frisch et al., Gaussian 03, Revision D.01, Gaussian Inc., Wallingford CT,2004.

Theoretical Study of acetylene Adsorption Energy on Nano Metal Crystal

Zahra Pournurouz*
Department of Chemistry, Islamic Azad University North Tehran Branch-Iran
E-mail:n.pornuroz@gmail.com

Key words: Adsorption, acetylene, Nano- Metal Crystal, Adsorption Energy

Introduction:

Intermediate metals play a major role in catalytic processes and facilitate chemical reactions by absorbing substances on their surface. Diversity in the adsorption phenomena,high expenses and need to the repeatability of the process explain the reason of using calculative chemical approaches with less expenses,repeatability and high precision.Most metals have a close array in solid state; Cu,Ag and Au are from the cubic type with filled Centered faces (FCC).Diameter of metal particles Cu,Ag,Au is 0.256,0.289 and0.288 nm respectively[1]. Considering 4 atoms per each unit cell for copper,silver and gold nanoparticles, the adsorption in these metals has been assessed and their thermodynamic functions and absorption power[2] have been discussed. Based on what has been mentioned in the reference[3], chemical absorption decreases along with the series of intermediate elements. At the beginning of the elements series, chemical absorption bonds are so strong that cannot be broken easily, and at the end of the series they are so weak that cannot be shaped adequately for the proper speed of the covered surface. Therefore the optimum state can be observed at the middle of the elements series. In this page, we determinated effects of changing nano metal crystal in order to compare them in columns on the binding energy of acetylene adsorption .by acetylene adsorption modeling gas molecule adsorption on Cu ,Ag and Au metals.

Computational Methods:

Frequency calculations in B3LYP level of density function theory (DFT) with the base series of metal LANL2Z and Acetylene 6-31G were conducted by Gaussian 98 software. In order to analyze the Acetylene absorption on Nano surface of metal crystals, two states have been taken into account: I) Close (Metal- C_2H_2) which stands for absorbed Acetylene on crystal surface of metal in tangent state. II) Remote (Metal- C_2H_2) which stands for the system with Acetylene in a distance 0.5 Ȧ farther than tangent state.

Results And Discussion:

The calculated of $\Delta G_{(ads)}$(C_2H_2+metal) were obtained -400.058,-210.763 and -90.381 kJ/mol for Cu,Ag and Au. The adsorption energy is always regarded as a measure of the strength of adsorbate–substrate adsorption. The adsorption energies Eads are defined as: Eads = Esub + Eads −Eads/sub, where Eads/sub is the total energy of adsorbate–substrate system in the equilibrium state, Esub and Eads are the total energy of fixed substrate and free adsorbate alone, respectively.

Based on this definition, negative values indicate heat in process [2]. The calculated of $\Delta E_{(ads)}$(C_2H_2+metal) were obtained -137.632,-210.763 and -74.136 kJ/mol for Cu,Ag and Au. The result exhibit that entropy of close forms for copper,silver and gold Nano-crystals in tangent condition is less effective than remote forms due to the decrease in electron distribution of system. Indicate the difference between calculated dipole moment in forms of close and remote for Acetylene molecules respectively which shows asymmetry of molecular load distribution. [5]

Conclusion:

Based on these results, the adsorption process of C_2H_2 on these metal Nano crystals is autonomous (negative values of Gibbs energy) and heat producing (negative values of E_{ads}). Magnitude of E_{ads} values indicates a stronger absorption between C_2H_2 on surfaces of Nano metal crystals reduces from Cu to Au Which indicates a decrease in adsorption force in a group from top to the bottom due to the increase in atomic diameter,Based on what has been mentioned in the reference[3]This entropy decline in close mode is due to the decrease of freedom levels at the time of surficial absorption, since in this mode the movement of molecules declines from 3 to 2 dimensions.

Reference:

[1]Charles P. Paul. translated by NimaTaghavinia.,an introduction on Nano-technology, Sanati Sharif University,Iran.18(2008)

[2]Zhang,R. Wang,B and et all .,Applied Surface Science., 257,1175–1180(2010)

[3]Gomes, J.R.B.; Ramalho, J.P, Surface Science. ,604, 428–434(2010)

[4] Computational study of molecules adsorbed on metal surfaces,[ASC27-UH-C]

[5]Ferna´ndez, E.M., Eglitis, R.I., Borstel, G., Balba´s, L.C., Computational Materials Science. 39,587–592 (2007)

Theoretical Study (DFT) Of Gas Adsorption On Nano Metal Crystal

Zahra Pournurouz*
Department of Chemistry, Islamic Azad University, North Tehran Branch-Iran
E-mail:n.pornuroz@gmail.com

Key words: Adsorption, Hydrogen, Nano- Metal Crystal, Adsorption Energy

Introduction:

Intermediate metals play a major role in catalytic processes and facilitate chemical reactions by absorbing substances on their surface. Diversity in the adsorption phenomena,high expenses and need to the repeatability of the process explain the reason of using calculative chemical approaches with less expenses,repeatability and high precision.Most metals have a close array in solid state;Ni,Cu are from the cubic type with filled Centered faces (FCC) and Zinc form close-packed hexagonal.Diameter of metal particles Ni,Cu,Zn is 0.249 ,0.256 and0.266nm respectively[1].Considering 4 atoms per each unit cell for nickel , copper and zinc nanoparticles, the adsorption in these metals has been assessed and their thermodynamic functions and absorption power[2] have been discussed. Based on what has been mentioned in the reference[3], chemical absorption decreases along with the series of intermediate elements. At the beginning of the elements series, chemical absorption bonds are so strong that cannot be broken easily, and at the end of the series they are so weak that cannot be shaped adequately for the proper speed of the covered surface. Therefore the optimum state can be observed at the middle of the elements series. In this page, we determinated effects of changing nano metal crystal on the binding energy of hydrogen adsorption.by hydrogen adsorption modeling gas molecule adsorption on Ni ,Cu and Zn metals.

Computational Methods:

Frequency calculations in B3LYP level of density function theory (DFT) with the base series of metal LANL2Z and Hydrogen 6-31G were conducted by Gaussian 98 software. In order to analyze the Hydrogen absorption on Nano surface of metal crystals, two states have been taken into account: I) Close (Metal- H_2) which stands for absorbed Hydrogen on crystal surface of metal in tangent state. II) Remote (Metal- H_2) which stands for the system with Hydrogen in a distance 0.5 Ȧ farther than tangent state.

Results And Discussion:

The calculated of $\Delta G_{(ads)}(H_2+metal)$ were obtained -97.599,-73.783 and +132.789 kJ/mol for Ni, Cu and Zn. The adsorption energy is always regarded as a measure of the strength of adsorbate–substrate adsorption. The adsorption energies Eads are defined as: Eads = Esub + Eads −Eads/sub, where Eads/sub is the total energy of adsorbate–substrate system in the equilibrium state, Esub and Eads are the total energy of fixed substrate and free adsorbate alone, respectively.

Based on this definition, negative values indicate heat in process [2]. The calculated of $\Delta E_{(ads)}(H_2+metal)$ were obtained -5.476,-4.581 and +3.988 kJ/mol for Ni, Cu and Zn. The result exhibit that entropy of close forms for nickel , copper and zinc Nano-crystals in tangent condition is less effective than remote forms due to the decrease in electron distribution of system. Indicate the difference between calculated dipole moment in forms of close and remote for Hydrogen molecules respectively which shows asymmetry of molecular load distribution. [5]

Conclusion:

Based on these results, the adsorption process of H_2 on these metal Nano crystals is autonomous (negative values of Gibbs energy) and heat producing (negative values of E_{ads}). Magnitude of E_{ads} values indicates a stronger absorption between H_2 on surfaces of Nano metal crystals reduces from Ni to Zn Which indicates a decrease in absorption force in a row from the left to the right as we don’t Ovservation adsorption on surface nano metal zinc ,Based on what has been mentioned in the reference[3], This entropy decline in close mode is due to the decrease of freedom levels at the time of surficial absorption, since in this mode the movement of molecules declines from 3 to 2 dimensions.

Reference:

[1]Charles P. Paul. translated by NimaTaghavinia.,an introduction on Nano-technology, Sanati Sharif University,Iran.18(2008)

[2]Zhang,R. Wang,B and et all .,Applied Surface Science., 257,1175–1180(2010)

[3]Gomes, J.R.B.; Ramalho, J.P, Surface Science. ,604, 428–434(2010)

[4]Computational study of molecules adsorbed on metal surfaces,[ASC27-UH-C]

[5]Ferna´ndez, E.M., Eglitis, R.I., Borstel, G., Balba´s, L.C., Computational Materials Science. 39,587–592 (2007)

Configurational behaviors of 1,2-dihalosilaethene. A hybrid density functional theory study and natural bond orbital interpretation

Parinaz Omidi,[1] Seiedeh Negar Mousavi[2], Hooriye Yahyayi[3] and Davood Nori-Shargh[2]
[1]Chemistry Department, Science and Research Branch, Islamic Azad University, Arak, Iran
[2]Chemistry Department, Science Faculty, Arak Branch, Islamic Azad University, Arak, Iran
[3] Chemistry Department, Zanjan Branch, Islamic Azad University, Zanjan, Iran

Keywords: Generalized anomeric effect, ab initio, NBO, 1,2-dihalosilaethene

Introduction:

The maximization of an interaction between the best donor lone pair and the best acceptor bond plays an important role on the preferred geometry of many molecules.[1-3] The most dominant configuration-controlling factor in carbohydrate compounds is known as the *anomeric effect* (*AE*).[4] Although the importance of the hyperconjugative interactions in some acyclic compounds has investigated, there is no published experimental information about the stereoelctronic interactions on the configurational properties of 1,2-difluoro- (**1**), 1,2-dichloro- (**2**), 1,2-dibromo (**3**) and 1,2-diiodosilaethene (**4**).

Computational details:

Hybrid DFT calculations were carried out using the B3LYP/Def2-TZVPP level of theory with the GAUSSIAN 03 package of programs.[5] The main purpose of the present work was to study the impacts of the stereoelectronic interaction effects, dipole-dipole interactions on the configurational preferences (i.e. *Z* and *E* configurations) in compounds **1-4**. An NBO analysis was then performed for the *Z* and *E* configurations of compounds **1-4** by the NBO 5.G program contained in the PC-GAMESS interface.[6]

Results and Discussion:

Hybrid-density functional theory (B3LYP/Def2-TZVPP) based method and NBO interpretation were used to study the configurational behaviors of 1,2-difluoro- (**1**), 1,2-

dichloro- (**2**), 1,2-dibromo (**3**) and 1,2-diiodosilaethene (**4**). The results obtained showed that the *Z* configuration of compound **1** is more stable than its corresponding *E* configuration. Interestingly, the stability of the *Z* configuration, compared to its corresponding *E* configuration, decreases from compound **1** to compound **4**. The Gibbs free energy difference values (at 298.15 K and 1 atm) between the *E* and *Z* configurations (i.e. $\Delta G_{E\text{-}Z}$) of compounds **1-4** are 1.91, 0.38, -0.04 and -0.51 kcal mol^{-1}, respectively, as calculated at the B3LYP/Def2-TZVPP level of theory. Based on the results obtained, the *E* configuration of compound **4** is more stable than its corresponding *Z* configuration. The NBO analysis of donor-acceptor ($LP\rightarrow\sigma^*$) interactions showed that the *generalized anomeric effects* (*GAE*) decrease from compound **1** to compound **4**. Therefore, the *GAE* justifies the increase of the *E* configuration stability, compared to its corresponding *Z* configuration, from compound **1** to compound **4**. The correlations between the *GAE*, bond orders, pairwise steric exchange energies (*PSEE*), $\Delta G_{E\text{-}Z}$, dipole-dipole interactions, structural parameters and configurational behaviors of compounds **1-4** have been investigated.

Conclusion:

The results obtained showed that the *GAE* decrease from compound **1** to compound **4**. Therefore, the rationalization of the configurational preferences solely in terms of the *GAE* succeeds to account quantitatively for the configurational properties of compounds **1-4**.

Refrences:

[1]J.-M. Lehn, G. Wipff; H-B. Burgi, *Helv. Chim. Acta* **1974**, *57*, 493.
[2]D. Nori-Shargh, H. Yahyaei, J .E. Boggs, *J. Mol. Graph. Model.* **2010**, *28*, 807.
[3]D. Nori-Shargh, J.E Boggs, *J. Phys. Org. Chem*. 2010, doi:10.1002/poc.1728.
[4]E. Juaristi, G. Cuevas, A. Vela, *J. Am. Chem. Soc*. 1994, *116*, 5796 -5804.
[5]M.J. Frisch, et al, Gaussian 03, Revision B.03, Gaussian, Inc., Wallingford CT, 2004.
[6]E.D. Glendening, J.K. Badenhoop, A.E. Reed, J.E. Carpenter, J.A. Bohmann, C.M. Morales, F. Weinhold, Theoretical Chemistry Institute, University of Wisconsin, Madison, WI, 2004. NBO Version 5.G.

Synthesis, characterization and theoretical study of some new phosphohydrazides

F. Molaei, K. Gholivand
Department of Chemistry, Faculty of Sciences, Tarbiat Modares University, Tehran, Iran
Email: foroogh_molaei@yahoo.com

Keywords: Phosphoramide, Hydrazide, DFT calculation, NBO analysis.

Introduction:

Phosphoramides are an efficient class of compounds with applications as urease and acetylcholinesterase inhibitors and stereoselective catalysts [1]. Due to the high oxophilic nature of phosphoryl group, these compounds are also efficient complexant molecules for lanthanides [2]. Hydrazide and hydrazone functional groups have shown significant role as pharmaceutical agents, possessing antimicrobial, antitubercular and antitumor activities [3]. Putting together the important functional groups in one molecule may cause new biological properties. Continuing our study on phosphoramide chemistry, here we report the synthesis and spectral characterization of 5 new phosphohydrazides based on tert-butyl carbazate with the general formula $R_2P(O)[NHNHC(O)O\text{-}tBu]$, R= -OPh (1), -OH (2) and $RP(O)[NHNHC(O)O\text{-}tBu]_2$, R= -Ph (3), -OPh (4), -NHPh (5). In order to study the structural and electronic parameters of the compounds in the gas phase, DFT quantum chemical calculations have been also performed.

Methods:

Compounds 1-5 were prepared by the reaction of tert-butyl carbazate with the corresponding phosphoryl chloride derivative as intermediate in the presence of triethylamine (for scavenging HCl) in dry tetrahydrofurane or acetonitrile at 0 ^oC. After stirring for 5-8 h, the precipitate was filtered, washed with water and dried. The compounds were fully optimized in a vacuum at the B3LYP/ 6-311+G** level. The stretching frequencies, NBO charges and charge densities of the optimized molecules were also calculated at the B3LYP/6-311+G** level. All quantum chemical calculations have been carried out using the Gaussian 03 package.

Results and discussion:

In the IR spectra, the P=O stretching frequency changes from 1164 to 1192 cm^{-1}, while the values of 1237 and 1303 cm^{-1} were calculated for the phosphoryl vibration in all of the optimized molecules. The $^{31}P\{^1H\}$NMR spectra illustrate a single resonance in the title compounds and the phosphorus chemical shifts vary from -3.10 to 18.80 ppm. ^1H NMR spectra show that the coupling constants $^2J_{PNH}$ between phosphorus atom and the α proton of the hydrazide group are extended from 27.8 (in 3) to 38.9 Hz (in 1). NBO analysis revealed that the positive charges on phosphorus atom are in the range of 2.450 (in 1) to 2.128 (in 3). Moreover, the energies of electronic delocalizations of oxygen and nitrogen lone pairs over σ* bonds around phosphorus atom are widely studied.

Conclusion:

Compared with carbacylamidophosphates containing CO-NH-PO moiety, phosphohydrazide derivatives which have N-N-P or N-N-P-N-N group, show much higher values for germinal $^2J_{PNH}$. This may be attributed to the different electronic delocalizations in these molecules. The electronic properties of the substituents on phosphorus atom are also influential factors on the magnitude of the coupling constant.

References:

[1] J.C. Bollinger, J. Levy-serpier, J. Debord, B. Penicaut, J. Enzym. Inhib. Med. Chem. 3 (1990) 211.
[2] K. Gholivand, H.R. Mahzouni, M.D. Esrafili, Theor. Chem. Acc. 127 (2010) 539.
[3] C. Ventura and F. Martins, J. Med. Chem. 51 (2008) 612.

Quantum chemistry studies on reactivity of the levo-dopa drug linked to to c_{60}

Roya Ahmadi[a*], Marjan Firoozeh[b] ,Laleh Allahkaram[c]
a Azad university Shahre -rey branch, Tehran, Iran
b Azad university Shahre -rey branch, Tehran, Iran
Email: Roya_ahmadi_chem@yahoo.com, Marjan.firuzeh@gmail.com,
Laleh_allahkaram@yahoo.com

Key words: Fullerene, HartreE_ Fock , hydrophobic, Levo-dopa

Introduction:

Many particular features have made derivatives fullerenes the object of numerous investigations over the last decade [1]. Among them, the chemical, photo physical and electrochemical properties play a major role, especially in view of possible applications, ranging from medicine to material science, to artificial photosynthesis. Low solubility of the fullerenes in fluids limits application of these materials as medicinal effective material. But hydrophobic size, three-dimensionality and electron properties cause its use as medicine. Levodopa is a medication used to treat Parkinson's disease. Parkinson's disease is associated with low levels of a chemical called dopamine in the brain. Levodopa is turned into dopamine in the body and therefore increases levels of this chemical. Levodopa is used to treat the stiffness, tremors, spasms, and poor muscle control of Parkinson's disease [2]. Mechanical quantum calculations in theory level of HF/6-31G* were performed on structure of Levo-dopa and nano fullerene-levo-dopa and some different properties such a chemical shielding isotropy (σ_{iso}) and chemical shifts in this work were studied.

Materials and methods:

then NICS calculations have done in 6-31G* basis set in HF methods and in gas phase. The gauge-included atomic orbital (GIAO) approach was used in the chemical shielding tensor calculations and chemical shielding isotropy (σ_{iso}) and chemical shift (δ) were obtained by $\sigma_{iso} = (\sigma_{11} + \sigma_{22} + \sigma_{33})/3$ and $\delta = \sigma_{11} - \sigma_{iso}$ In this report, at the first levo-dopa drug located on fullerene and its derivatives with c_{60} were optimized.

Apparatus:

In this report was used of computer for calculating the values of chemical shielding isotropy and chemical shift. Total calculations were done with use of Pentium 3, with processor intel®, core i4, with memory of 4 gigabytes and inside of operating system of windows xp. All calculations were done in Hartree-Fock and in the 6-31G * basis set using Gaussian 98 software and in gas phase.the figure of Levo-dopa (R) and its nano carrier with c_{60}(R-C_{60}) carrier of F, is shown in figure 1.

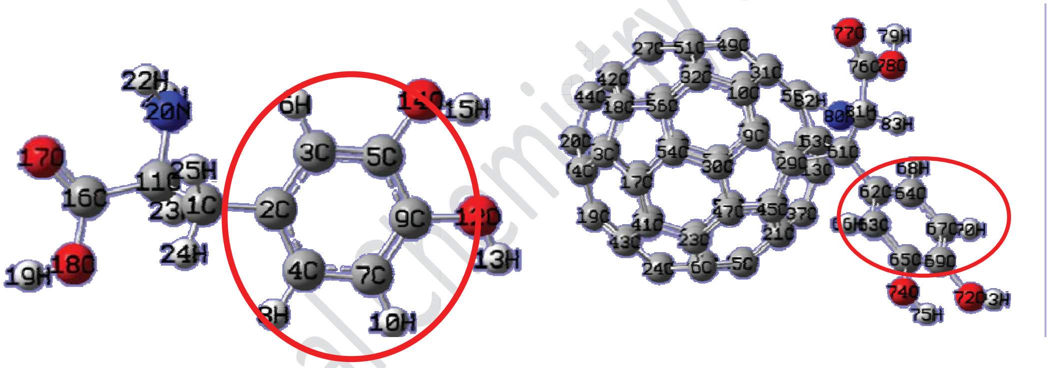

Figure.1 Levo-dopa and Levo-dopa-c_{60}

Result and discussion:

	R-C_{60}			R		
	H_{66}	H_{68}	H_{70}	H_6	H_8	H_{10}
σ_{iso}	24.6168	25.3174	26.5701	25.2617	26.3944	26.8601
Δ	7.9808	7.2802	6.0275	7.3359	6.2032	5.7375

Table.1.values of σ_{iso} and δ in (R-C_{60}), and (R)

compound	gap energy	chemical hardness	Dipole moment	chemical potential
R	0.14380	0.224515	4.2838	-0.080715
R-C_{60}	0.26548	0.13274	5.5242	-0.14669

Table.2.values of gap energy, chemical hardness, Dipole moment, chemical potential in (R), and (R-C_{60})

The results showed that the values of gap energy and chemical hardness were decreased in nano carrier, whereas dipole moment and chemical potential had higher value. in addition, considering NICS(0) parameter inside ring, the comparison between drug and nano carrier showed that the value of this parameter in Nano carrier is more than the one in drug ,also the hydrogens inside benzene ring more have been deshielded.

Conclusion:

The result showed by connecting of fullerene to drug, reactivity will be more in the other hand, the value of dipole moment indicated that solubility of drug will increase in polar solvent in body, such as aqua. Hydrogen deshielding in benzene ring of fullerene Nano carrier of drug, and decreasing of chemical shielding isotropy can be indicated the capacity of these hydrogens in participating in electrophil substitution reactions.

Reference:

[1] H. Hirsch, M. Brettreich , Fullerenes: Chemistry and Reactions, Wiley-VCH, Weinheim, 2005.

[2] Barnett-Cowan M, Dyde RT, Fox SH, Moro E, Hutchison WD, Harris LR (2010) "Multisensory determinants of orientation perception in Parkinson's disease"

Molecular Dynamics Simulations Study of Two Single Mutations of Coil 2B of Human Lamin A/C

D. Mohammad-Aghaie*, Z. Jafari
Department of Chemistry, Shiraz University of Technology, Shiraz, 71555-313, Iran
Corresponding author's email: d_aghaie@sutech.ac.ir

Key words: Lamins, Mutation, Molecular Dynamics Simulation

Introduction:

Lamins are the major constituents of a filamentous network of proteins, underling the inner nuclear membrane, termed nuclear lamina. They are grouped as A- and B-type lamins, on the basis of their biochemical properties and behavior, during mitosis. [1] Three types of lamins with significant sequence identity are known in human: lamin A/C, B1 and B2. Lamins A and C, encoded by the *LMNA* gene, form the core scaffold of the nuclear lamina. Dilated cardiomyopathy (DCM) is a condition whereby the normal muscular function of the myocardium is altered by specific or multiple aetiologies. Most of the DCM-related mutations, fall in the Lamin A/C gene in particular in the Coil 2B domain of the encoded protein. [2] In this study we have applied molecular dynamics simulations method to investigate the effect of two single mutations (R335W and E347K) on the structural properties of lamin's Coil 2B domain. In this respect some structural parameters, involving root mean square deviations (RMSD), solvent accessible surface areas (SASA) and gyration radiuses (R_g) were computed and compared.

Method:

We have performed molecular dynamics (MD) simulations on the structure of Coil 2B of human lamin (PDB ID: 3V5B) and its two mutants (PDB IDs: 3V4Q and 3V4W, respectively corresponding to the R335W and E347K mutations) at 310 *K*. The initial structures, taken from protein data bank, were submitted to Gromacs pdb2gmx command, in order to obtain

Gromacs formatted structures and suitable topology files, necessary for running simulations. The OPLS force filed was chosen for protein simulation, while the water was simulated using SPCE model. We arranged three separate simulations, one for wild type human lamin and the other two, for its mutants. Each protein was dissolved in water and the systems were neutralized by adding appropriate number of ions. The steepest descent algorithm was employ -ed to run energy minimization, continued by two short position restrained MD simulations in NVT and NPT ensembles, each for 100 ps. Finally, three 5 ns simulations were performed on the energy minimized and equilibrated systems, at 310*K*. The Berendsen thermostat/barostat with coupling constants of 0.1 and 2 ps, were employed to run NPT simulations. Gromacs simulation package 4.5.5 [3], was utilized for all of the calculations and analysis of the results.

Results and discussion:

In order to study structural changes, due to single point mutations in Coil 2B of human lamin, 5 ns simulations were performed on the wild lamin and its two mutants. RMSD, SASA and R_g were calculated and compared for three studied structures. The Coil 2B of human lamin has 74 aminoacids, with residue numbers: 313-386. In R335W mutation, the Arginine (positively charged) has been replaced with Tryptophan (non-polar), and in E347K mutation, Glutamic acid (negatively charged) has been substituted by Lysine (positively charged). The evolution of protein structures during simulations, were examined by calculating RMSD's of the trajectories, with respect to energy-minimized structures. RMSD plot for 3V4W structure showed increasing higher values with respect to the ones for 3V5B and 3V4Q, indicating more structural changes in this mutant during simulation process. Gyration radius of a protein is a measure of its compactness. R_g plots of 3V5B and 3V4Q showed almost steady values, while in case of 3V4W, we observed considerable decrease in R_g value. This again confirms the continuous structural changes of this mutant over simulation time, towards more compactness. We calculated total SASA for the studied proteins and observed higher values for 3V4Q structure. In R335W mutation, Tryptophan shows higher hydrophobic SASA value in comparison to Arginine. This is due to the non-polar nature of this aminoacid. In the other mutation, E347K, Lysine shows greater hydrophobic SASA in comparison to Glutamic acid.

Although in both mutations the new aminoacid has greater hydrophobicity, but this difference is more obvious in case of R335W mutation, leading to higher total SASA for 3V4Q structure comparing to 3V5B and 3V4W. The results show that E347K mutation leads to more compact structure with less solvent accessible surface area in comparison to the other mutation R335W. Higher RMSD and lower R_g values, along with lower SASA indicate the more evident structural changes in 3V4W mutant.

References:

[1] Gruenbaum, Y., Margalit, A., Goldman, *et* al., *Nat. Rev. Mol.Cell Bio*. 6, 21-31, 2005.

[2] Bollati, M., Barbiroli, A., Favalli, V., Arbustini, E., Charron, P., Bolognesi, M., *Biochem. Biophys. Res. Commun.* 418, 217-221, 2012.

Study of the glassy temperature of dicationic ionic liquid by molecular dynamic simulation

A. Soltanabadi*, S. Yeganegi, D. Farmanzadeh
Department of Physical Chemistry, Faculty of Chemistry, University of Mazandaran, Babolsar, Iran
Email: a_soltanabadi@yahoo.com

Keywords: Geminal dicationic ionic liquid, Molecular dynamic Simulation, Density, Radial distribution function, Diffusion coefficient, temperature

Introduction:

Room temperature ionic liquids (ILs) are a class of organic salts with melting points near the room temperature [1]. Geminal dicationic ionic liquids (ILs), a new category of IL family, have been developed recently and found to possess unique properties compared to conventional monocationic ILs [2-3]. This paper reports the molecular dynamic simulation of (DILs) $C_3(mim)_2X_2$, X= Br^- BF_4^-, ntf_2^- and PF_6^- ILs at the 300K and 1 atm. Also molecular simulation of $C_3(mim)_2(ntf_2)_2$ carried out in different temperature (300K-450K). Densities, detailed microscopic structures, mean-square displacements (MSD) and self-diffusivities for different temperature calculated and discussed.

Computational details:

Molecular dynamic simulations have been carried out using DL-POLY ver. 2.20 code. The simulated fluids consist of 120–180 ionic complexes. Lopes et al [4] force field was adopted for the simulations.

Results and discussion:

The simulated densities of ($C_3(mim)_2X_2$, X= Br^- BF_4^-, ntf_2^- and PF_6^-) DILs were calculated by NPT simulations at 450 K and 1 atm and for $C_3(mim)_2(ntf_2)_2$ carried out at different temperature (298-450) where results are shown in Fig 1. For $C_3(mim)_2(ntf_2)_2$ at the temperature 330K, there is a crack in density which can be due to a glassy temperature. We investigated the liquid structure by calculating various radial distribution functions (RDFs). The RDFs of anion-cation, anion-anion cation-cation and anion-geometric center of imidazolium rings of cation are calculated. The simulated RDFs for the anions around geometric center of imidazolium rings in Fig. 2 shows that anions are tend to accumulate around the imidazolium rings. The self-diffusion has been calculated for time ranges of 3-10 ns at different temperature and discussed.

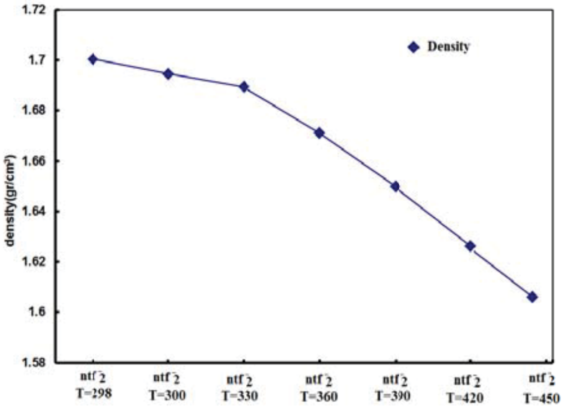

Fig.1.density $C_3(mim)_2(ntf_2)_2$ at different temperature

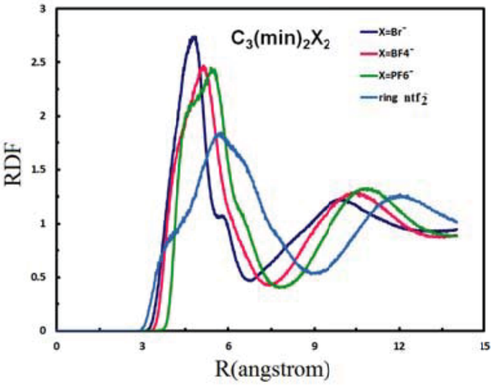

Fig. 2. RDF for center of imidazolium ring and different anions

Conclusion:

The densities, microscopic structure, mean square displacement, self-diffusion coefficients are calculated. The results show that for $C_3(mim)_2(ntf_2)_2$ there is a glassy temperature at 330K. The simulated RDFs show that the anions are well organized around imidazolium ring. The calculated values of diffusion coefficients show that the order of the calculated anion self diffusions are as follows $Br^- < BF_4^- < PF_6^- < ntf_2^-$.

References:

[1] P. Wasserscheid etal.; “Ionic Liquids-New “Solutions” for Transition Metal Catalysis”; Chem. Int. Ed; 39, 3772-3773, 2000.

[2] X. Han etal.; “Using Geminal Dicationic Ionic Liquids as Solvents for High-Temperature Organic Reactions”; Org. Lett.; 7, 4205-4208, 2005.

[3] Jui. Cheng etal.; “Synthesis and characterization of dicationic ionic liquid s that contain both hydrophilic and hydrophobic anions”; Tetrahedron, 66, 6150-6155, 2010.

[4] J. Lopes et al.; “Modeling Ionic Liquids Using a Systematic All-Atom Force Field”; J. Phys. Chem. B. 108, 2038-2047, 2004.

Theoretical study of geminal dicationic ionic liquids 1,3- bis[3-methylimidazolium-1-yl]butane halides

A. Soltanabadi*, D. Farmanzadeh, S. Yeganegi
Department of chemistry, Faculty of chemistry, University of Mazandaran, Iran
Email: a_soltanabadi@yahoo.com

Keywords: Geminal dicationic ionic liquid, electronic structure, DFT

Introduction:

Geminal dicationic ionic liquids DILs have higher melting point, wider liquid range, and better thermal stability compared to conventional monocationic ILs[1-3]. we calculated the 1,3-bis[3-methylimidazolium-1-yl]butane ($[C_4(mim)_2{}^{2+}]$ dication (Fig. 1) and 1,3- bis[3-methylimidazolium-1-yl]butane halides ($[C_4(mim)_2X_2]$, X=halides= F^{-}, Cl^{-}, Br^{-} and I^{-}) dicationic ionic liquid structures, stable configurations, ionic interactions and hydrogen bond and compared with each other.

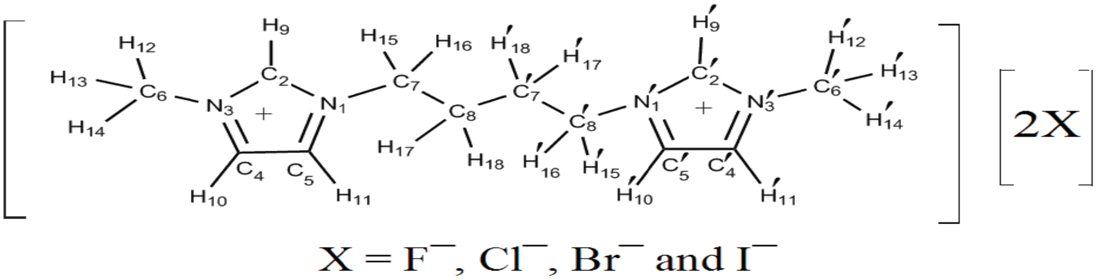

Fig. 1. Geminal dicationic ionic liquids.

Computational details:

Geometry optimization and calculation of the electronic properties of the geminal dicationic ionic liquids have been carried out at DFT/B3LYP level of theory with the 6-311++G** basis set. The atomic charges calculated by natural bond orbital (NBO). G03 program was used in all computations.

Results and discussion:

The optimized structure for $C_4(mim)_2^{2+}$ shows that two imidazolium rings tend to have the maximum distance from each other. Optimized structure of $C_4(mim)_2F_2$ show that F^- anions prefer to locate almost in the plane of imidazolium ring and there are two hydrogen-bond interaction. However, in the other ILs, ($C_4(mim)_2X_2$,X=Cl, Br and I) results in the bending of the rings towards each other and making a U-shaped structure, which causes the anions to be closer to the atoms of the two rings and there are eight hydrogen-bond interaction.

Conclusion:

The results show that there are significant difference in geometrical structure between $C_4(mim)_2F_2$ and corresponding [$C_4(mim)_2X_2$], (X=halides= Cl^-, Br^- and I^-) Also there are two Hydrogen bond for $C_4(mim)_2F_2$ structure and eight Hydrogen bond for ($C_4(mim)_2X_2$,X=Cl, Br and I) structure. In summary, the obtained results show that molecular geometry and electronic properties for $C_4(mim)_2F_2$ is completely different from other DILs and the energy gap of any DILs with desired cation can by modified with selecting appropriate anion.

Reference:

[1] C.M. Jin etal.; “Polyethylene glycol functionalized dicationic ionic liquids with alkyl or polyfluoroalkyl substituents as high temperature lubricants”; J.Mater. Chem; 16, 1529-1535, 2006.

[2] S. Mohamad etal.; “Conventional Study on Novel Dicationic Ionic Liquid Inclusion with β-Cyclodextrin”; Int. J.Mol. Sci; 12, 6329-6345, 2011.

[3] X. Han etal.; “Using Geminal Dicationic Ionic Liquids as Solvents for High-Temperature Organic Reactions’; Org. Lett; 7, 4205-4208, 2005.

Monte Carlo Simulation of Nanostructured Adamantane Self-assembly

B. Shirforoush Sattari [a*], A. Rastkar Ebrahimzadeh[a], J. J. Sardroodi[a] , Masoumeh Ighaei [a]
[a] Molecular Simulations Lab., Department of Chemistry, Faculty of Science, Azarbaijan Shahid Madani University, Tabriz, Iran; (Email: ne_sattary@yahoo.com)

Key words: Self-assembly, Diamondoids, Adamantane, Monte Carlo, Nanothechnology, RDF.

Introduction:

Self-assembly has been used to form highly ordered structures with features at the supra-molecular (1–100 nm) scale, and has been a focal point for decreasing the functional size of electronic, mechanical, and other devices. Diamondoids such as adamantane have recently been the subject of substantial interest for self-assembly, chemical patterning, and fundamental diamondoid chemistry research. Adamantane as a building block has attracted interest for the tunable properties it impart to SAMs, including geometric, localized electrical potentials, and optoelectronic effects. Adamantane is a molecular analog for diamond. Diamond is a material that has long inspired interest for both practical and aesthetic reasons. The T_d symmetric cage forms the core of the cubic diamond unit cell, and can be considered the smallest possible hydrogen-passivated diamond nanoparticle, or diamondoid. It is important and necessary to study self-assembly of these molecules in order to obtain reference data, such as temperature, pressure, structure factor, and bonding properties for application in nanotechnology such as building molecular electronic devices. To the best of our knowledge self-assembly of nanostructured adamantane by Monte Carlo simulation method has not been reported yet.

Simulation methods:

Monte Carlo simulations were performed in the isothermal–isobaric ensemble by using the MCCCS Towhee simulation package [1]. To simulate the self-assembly, three different temperatures (150 K, 300 K, 450 K) were chosen according to experimental data for adamantane [2] which were related to it's different phases at the pressure 1 atm. All of the models used in this work employ a Lennard–Jones (LJ) potential. For the LJ system, a cubic simulation cell with 125 particles and periodic boundary conditions was used in isothermal-isobaric Monte Carlo NPT-MC simulations. Lennard–Jones interactions were cut- off at one-half the box length and standard tail corrections were applied [3]. The Ewald summation technique [3] was used to calculate electrostatic energies. The Monte Carlo moves consisted of volume changes, configurational bias (CB) regrowths [4] , translation of the center-of-mass, and rotation about the center-of-mass. Acceptance ratios for volume and particle moves were kept at approximately 50% . Amber96 [5] is the force field that was utilized in this study.

Results and discussion:

The main feature of adamantane is that at low temperatures we can observe ordered crystal structures . From the RDF graph of adamantane at different temperatures. we can observe gas (figure1.a), liquid (figure1.b) and solid (figure1.c) characteristics. In the RDF figures of adamantane, sharper peaks can be observed as the temperature decreases.

Conclusion:

We have performed a Monte Carlo study of the self-assembly process of adamantane due to temperature variations. From the MC simulation study of the adamantane, we may conclude the following: (1) The nature of self-assembly in these molecules is a structure-dependent phenomenon. (2) Final self-assembly structures depend on the different bonding types present in the molecular and intramolecular interactions of these various molecules.

Initial

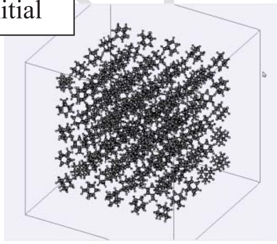

a

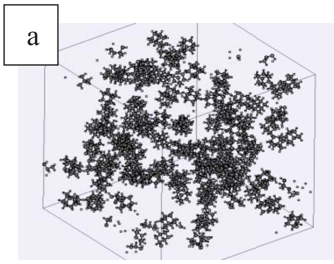

b

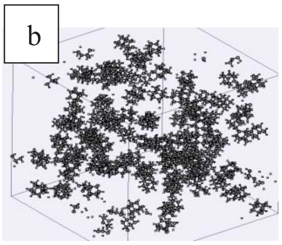

c

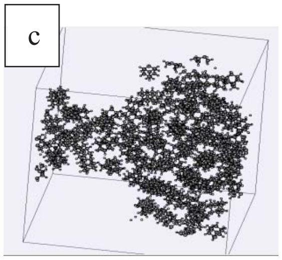

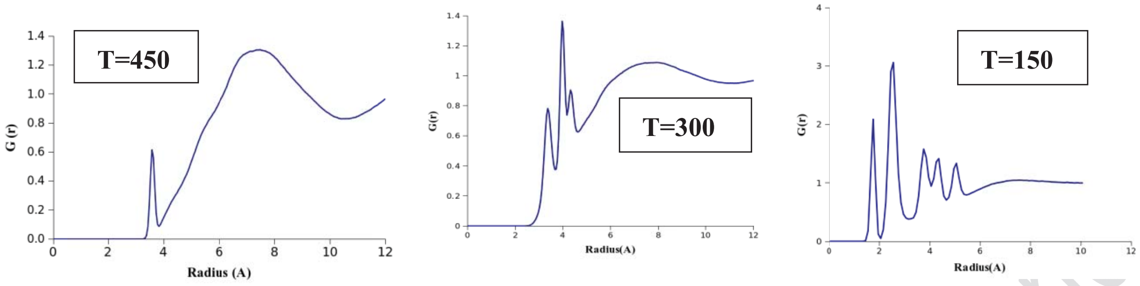

Figure1. Snapshot from MC simulation and RDF of Adamantane at 100K(c) , 300K(b) , 450K(a)

References :

[1] http://towhee.sourceforge.net.

[2] J. Reiser, E. McGregor, J. Jones, R. Enick and G. Holder , "Adamantane and Diamantane; Phase Diagrams, Solubilities, and Rates of Dissolution"; Fluid Phase Equilibria.; 117, 160-167, 1996.

[3] M.P. Allen, D.J. Tildesley; "Computer Simulation of Liquids", Clarendon, Oxford, 1987.

[4] J.I. Siepmann; D. Frenkel; "Configurational bias Monte Carlo: A new sampling schem for flexibal chains"; Mol. Phys. Chem; 75, 59–70, 1992.

[5] W. D. Cornell, P. Cieplak, C. I. Bayly, I. R. Gould, K. M. Merz Jr., D. M. Ferguson, D. C. Spellmeyer, T. Fox, J. W. Caldwell, P. A. Kollman; "A Second Generation Force Field for the Simulation of Proteins, Nucleic Acids, and Organic Molecules"; J. Am. Chem. Soc.; 117, 5179-5197, 1995.

Quantitative correlations between the vibrational frequencies and electron delocalizations in 2-D-1,3-dioxane, -dithiane and –diselenane. A hybrid-density functional theory study and natural bond orbital interpretation

Samireh Rasoolabadi[a] Seiedeh Negar Mousavi[b], Davood Nori-Shargh[c]
[a]Department of Chemistry, University of Tehran, Tehran, Iran
[b]Department of Chemistry, Arak Branch, Islamic Azad University, Arak, Iran
E-mail:s.rssoolabadi@yahoo.com

Keywords: 2-D-1,3-dioxane, vibrational frequency, electron delocalization, molecular modeling

Introduction:

The knowledge about conformational properties of heterocyclic compounds is of very general interest since saturated heterocyclic compounds comprise a large segment of organic and inorganic chemistry and are quite widespread in nature, e.g., in alkaloids, carbohydrates, and plant growth regulators, among
other compounds.

Since the preferred geometry of many molecules can be viewed as the result of the maximization of an interaction between the best donor lone pair and the best acceptor bond ,the stereoelectronic interactions are expected to play an
important role in the conformational properties of heterocyclic compounds The most dominant conformation-controllingfactor in carbohydrate compounds is known as the anomeric effect (AE).

Materials and methods:

The correlations between the C_2-D stretching vibrational frequencies and the stabilization energies associated with $LP_{ax}X\rightarrow\sigma^*_{C2\text{-}D}$ and $LP_{eq}X\rightarrow\sigma^*_{C2\text{-}D}$ (X=O, S, Se) electron delocalizations in 2-D-1,3-dioxane (**1**), -dithiane (**2**) and –diselenane (**3**) have been investigated by means of hybrid-density functional theory (hybrid-DFT: B3LYP/6-311+G**) based method and natural bond orbital (NBO) interpretation.

Result and discussion:

Based on the optimized ground state geometries using the B3LYP/6-311+G** level of theory, the NBO analysis of donor-acceptor ($LP\rightarrow\sigma^*$) interactions revealed that the $LP_{ax}X\rightarrow\sigma^*_{C2\text{-}D}$ and $LP_{eq}X\rightarrow\sigma^*_{C2\text{-}D}$ electron delocalizations decrease from compound **1** to compound **3**. The results obtained showed that by the decrease of the stabilization energy associated with $LP_{ax}X\rightarrow\sigma^*_{C2\text{-}D}$ and $LP_{eq}X\rightarrow\sigma^*_{C2\text{-}D}$ electron delocalizations, the $LP_{ax}X$ and $LP_{eq}X$ non-bonding orbital occupancies increase from the axial and equatorial conformations of compound **1** to compound **3** but the $\sigma^*_{C2\text{-}D}$ anti-bonding orbital occupancies decrease. These facts reasonably explain the increase of the C_2-D bond energies and stretching vibrational frequencies from compound **1** to compound **3**. Importantly, the F_{ij} off-diagonal element values of $LP_{ax}X\rightarrow\sigma^*_{C2\text{-}D}$ and $LP_{eq}X\rightarrow\sigma^*_{C2\text{-}D}$ electron delocalizations decrease from the axial and equatorial conformations of compound **1** to compound **3** which could be justified by the increase of the X atom radius from compound **1** to compound **3**. The correlations between the $LP_{ax}X\rightarrow\sigma^*_{C2\text{-}D}$ and $LP_{eq}X\rightarrow\sigma^*_{C2\text{-}D}$ electron delocalizations, bond orders, structural parameters and C_2-D stretching vibrational frequencies of compounds **1-3** have been investigated.

Refrence

[1] J.AM.Chem.Soc.,1986,108,p:2109
[2] J.Chem.Soc,Chem.commun.,1987,595
[3] Acta Chem.Scand,1973,27,2676

Conformational behaviors of 2-halo-1,2,4,5-tetrahydrobenzo[*d*]oxepines. A hybrid-density functional theory study and natural bond orbital interpretations

Sahar Saadatfard*, Seiedeh Negar Mousavi, Davood Nori-Shargh
[a]Department of Chemistry, University of Tehran, Tehran, Iran
[b]Department of Chemistry, Arak Branch, Islamic Azad University, Arak, Iran
E-mail:sasaadat80@yahoo.com

Keywords: anomeric effects, stereoelectronic interactions, molecular modeling, ab initio, 2-halo-1,2,4,5-tetrahydrobenzo[d]oxepines

Introduction:

Conformational equilibria in alicyclic molecules has been studied in the past several years. Theoretical treatments of cycloalkanes have also provided values in reasonable agreement with experimental . Contrary to the abundance of information in the cyclohexane area, there has been a paucity of data concerned with conformational properties in heterocyclic systems.

The knowledge about conformational properties of heterocyclic compounds should be of very general interest since saturated heterocyclic compounds comprise a large segment of organic and inorganic chemistry and are quite widespread in nature, e.g. in alkaloids, carbohydrates, and plant growth regulators, among other compounds.

It is well known that the stereoelectronic interactions could play an important role on the conformational properties of heterocyclic compounds. There is a stereoelectronic preference for conformations in which the best donor lone pair is antiperiplanar to the best acceptor bond**.**

Materials and methods:

Hybrid-density functional theory (hybrid-DFT: B3LYP/6-311+G**) based method and natural bond orbital (NBO) interpretation have been used to examine the impacts of the hyperconjugative, electrostatic and steric effects on the conformational behaviors of 2-fluoro-

1,2,4,5-tetrahydrobenzo[d]oxepine (1), 2-chloro-1,2,4,5-tetrahydrobenzo[d]oxepine (2) and 2-bromo-1,2,4,5-tetrahydrobenzo[d]oxepine (3).

Result and discussion:

B3LYP/6-311+G** results showed that the axial conformations of compounds 1-3 are more stable than their corresponding equatorial conformations and the axial conformation stability, compared to its corresponding equatorial conformation, increases from compounds 1→3. Based on the results obtained from the NBO analysis, there are significant anomeric effects associated with the electron delocalization for compounds 1-3. The endo-anomeric effect associated with $LP_1O_3 \rightarrow \sigma^*_{C2-X}$ and $LP_2O_3 \rightarrow \sigma^*_{C2-X}$ electron delocalizations increases from the axial conformation of compound 1 to compound 2 but decreases from compound 2 to compound 3. The exo-anomeric effect decreases from compounds 1→3. The anomeric effect [i.e. Σ(endo-anomeric effect+exo-anomeric effect)$_{eq}$-Σ(endo-anomeric effect+exo-anomeric effect)$_{ax}$] increases from compounds 1→3. Dipole moments of the equatorial conformations of compounds 1-3 are greater than those of their corresponding axial conformations and dipole moment difference between the axial and equatorial conformations [$\Delta(\mu_{eq} - \mu_{ax})$] decreases from compounds 1→3. Therefore, the anomeric effect associated with the electron delocalizations explain the conformational preferences in compounds 1-3 but the electrostatic model associated with the dipole-dipole interactions fails to account the conformational preferences in compounds 1-3. The correlations between the anomeric effect, electrostatic model, ΔG_{eq-ax}, bond orders, dipole-dipole interactions, structural parameters and conformational behaviors of compounds 1-3 have been investigated**.**

Refrences:

[1] Can,J.chem.,1992,70,p:2650

Stereoelectronic interaction effects on the conformational properties of *cis*-5-tert-butyl-2-phosphinoyl-1,3-dioxane, -dithiane and –diselenane.

Zahra Khoram[a*], Seiedeh Negar Mousavi,[b] Davood Nori-Shargh[c]
Department of Chemistry, Arak Branch, Islamic Azad University, Arak, Iran
E mail: khoramzahra@gmail.com

Keywords: *cis*-5-tert-butyl-2-phosphinoyl-1,3-dioxane, anomeric effects, stereoelectronic interactions, molecular modeling

Introduction:

Conformational equilibria in alicyclic molecules has been studiedin the past several years. Theoretical treatments of cycloalkanes have also provided values in reasonable agreement with experimental. The knowledge about conformational properties of heterocycli compounds should be of very general interest since saturated heterocyclic compounds comprise a large segment of organic and inorganic chemistry and are quite widespread in nature, e.g. in alkaloids, carbohydrates, and plant growth regulators, among other compounds.

It is well known that the stereoelectronic interactions could play an important role on the conformational properties of heterocyclic compounds There is a stereoelectronic preference for conformations in which the best donor lone pair is antiperiplanar to the best acceptor bond. Praly and Lemieux have stressed that the anomeric effects (AE) must be considered as the difference between the sum of the endo- and exo-anomeric effects (e.g. endo-AE and exo-AE) in the equatorial conformer and the same sum for the axial conformer. Also, they have suggested that there is no any endo-AE in the equatorial conformer, therefore, it is exclusively stabilized by exo-AE interactions Anomeric effect exo-AEeq _ ◌ًexo-AEax endo-AEax

Materials and methods:

The impacts of the hyperconjugative, electrostatic and steric effects on the conformational behaviors of *cis*-5-tert-butyl-2-phosphinoyl-1,3-dioxane (**1**), -dithiane (**2**) and –diselenane (**3**) have been investigated by means of hybrid-density functional theory (hybrid-DFT: B3LYP/6-311+G**) based method and natural bond orbital (NBO) interpretation. B3LYP/6-311+G** results showed that the axial conformations of compounds **1-3** are more stable than their corresponding equatorial conformations.

Result and discussion:

Effectively, the axial conformation stability, compared to its corresponding equatorial conformation, increases from compound **1** to compound **3**. The NBO results showed the *anomeric effect* associated with the electron delocalization decreases from compound **1** to compound **3**. Therefore, the *anomeric effect* fails to account for the increase of the axial conformation stability, compared to its corresponding equatorial conformation, from compound **1** to compound **3**. On the other hand, dipole moments of the equatorial conformations increase from the equatorial conformation of compound **1** to compound **3** while the corresponding values for the axial conformations decrease. Dipole moment difference between the axial and equatorial conformations [$\Delta(\mu_{eq} - \mu_{ax})$] increases from compound **1** to compound **3**. Therefore, the rationalization of the conformation preference solely in terms of the *electrostatic model* associated with the dipole-dipole interactions succeeds in accounting qualitatively for the increase of the axial conformation stability in compounds **1-3**. The correlations between the *anomeric effect*, *electrostatic model*, $\Delta G_{eq\text{-}ax}$, bond orders, dipole-dipole interactions, structural parameters and conformational behaviors of compounds **1-3** have been investigated.

References:

[1]J.org.chem,1989,54, p:5191

Study of Single and multi-walled Carbon Nanotubes as filter of vanadium by computational chemistry method

Zahra Feyli[a*], Soheil Sobhanardakani[b], Reza Sahraee[c], Abbas Farmany[a], M.Erfan Zand[d]
aYoung Researchers Club, Hamedan Branch, Islamic Azad University, Hamedan, Iran
a Department of the Environment, Hamedan Branch, Islamic Azad University, Hamedan, Iran
c Department of the Chemistry, Ilam University, Ilam, Iran
d Department of Chemistry, Payame Noor University, Shiraz, Iran
z.feyli@iauh.ac.ir

Keywords: Carbon Nanotubes, filter, vanadium, DFT

Introduction:

The carbon-based nanostructures [1], especially single [2] and multiwalled carbon nanotubes (MWCNTs) [3], have been extensively studied for their role as solid substrates, mainly due to the accessibility of enormous surface area that can be readily functionalized [4]. Thus how treated surfaces can be used to adsorbed heavy transition metals, which may be presence in water, waste and etc. The main question of this study is the investigation of capability of CNTs as filters for adsorption of vanadium ions in industrial wastewaters.

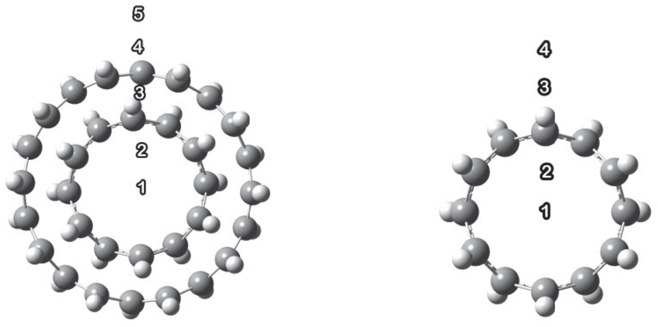

Figure 1. Adsorption sites for single and multi-wall CNTs used in this study.

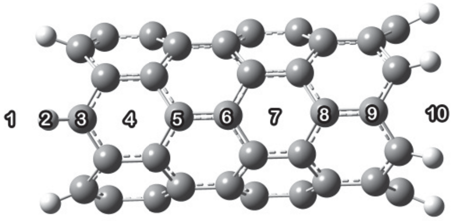

Figure 2. Longitudinal adsorption sites for single and multi-wall CNTs used in this study.

Methods:

Ab initio calculations were carried out, using the density functional theory (DFT) and the hybrid B3LYP functional with 6-31 G* basis set without any symmetry restrictions in the singlet ground state, in order to optimize both nanotubes and complex of nanotube with vanadium ions. Calculated vibrational frequencies without imaginary frequencies ensure the stable structures.

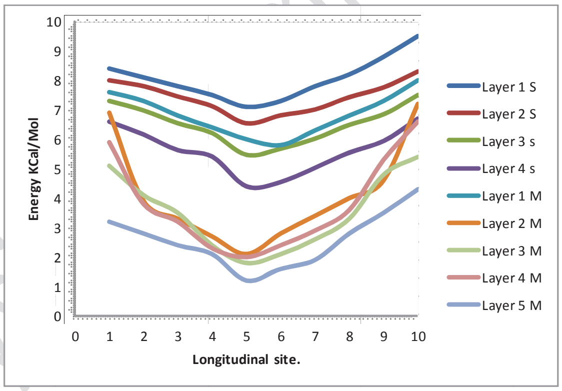

Figure 2. Binding energy of CNT/Vanadium ions at different sites and layers

Results and Discusions :

Binding energies were calculated via the difference in energy of CNT/V complexes from those of isolated fragments (see Figure 1). The calculations was performed in both gas phase an solution conditions. The results show that vanadium interacts more strongly with carbon atoms at site 4 and 5 of single and multi-wall CNTs, respectively. The distance of maximum interaction in these, cases correspond to the value of 2 Å.

Conclusions:

From these and more detailed considerations, it can be concluded that single wall CNTs could be used as a better adsorbent for vanadium ions, which are present in industrial wastewaters. The studies on longitudinal adsorption sites indicate that the interaction of vanadium ions with edge atoms of CNTs is stronger.

Reference:

[1] R. Ströbel, et al., Journal of Power Sources 84 (2) (1999) 221.
[2] A. Ansón, et al., Carbon 42 (7) (2004) 1243–1248.
[3] G.Q. Ning, et al., Materials Science & Processing 78 (7) (2004) 955.
[4] M. Endo, et al., Philosophical Transactions of the Royal Society A 362 (2004) 2223.

Study of Singleand multi-walled Carbon Nanotubes as filter of vanadium by computational chemistry method

Zahra Feyli[a*], Soheil Sobhanardakani[b], Reza Sahraee[c], Abbas Farmany[a],
aYoung Researchers Club, Hamedan Branch, Islamic Azad University, Hamedan, Iran
z.feyli@iauh.ac.ir
aDepartment of the Environment, Hamedan Branch, Islamic Azad University, Hamedan, Iran
bDepartment of the Chemistry, Ilam University, Ilam, Iran

Keywords: Carbon Nanotubes, filter, vanadium, DFT

Introduction:

The carbon-based nanostructures[1], especially single [2] and multiwalled carbon nanotubes (MWCNTs) [3], have been extensively studied for their roleas solid substrates, mainly due to the accessibility of enormous surfacearea that can be readily functionalized [4]. Thus how treatedsurfaces can be used to adsorbed heavy transition metals, which may be presence in water, waste and etc. The main question of this study is the investigation of capability of CNTs as filters for adsorption of vanadium ions in industrial wastewaters.

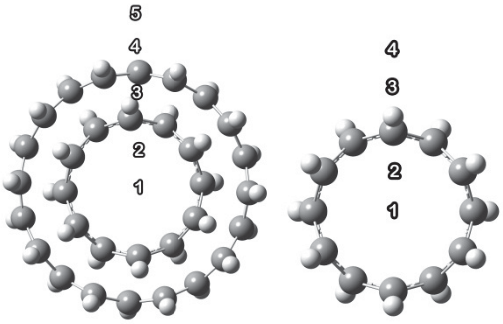

Figure 1. Adsorption sites for single and multi-wall CNTs used in this study.

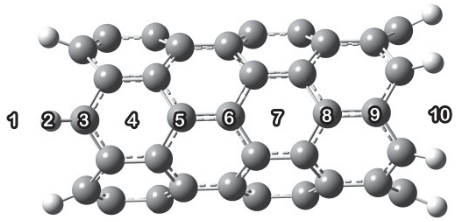

Figure 2. Longitudinaladsorption sites for single and multi-wall CNTs used in this study.

Methods:

Ab initio calculations were carried out, using the density functional theory (DFT) and the hybrid B3LYP functional with 6-31 G* basis set without any symmetry restrictions in the singlet ground state, in order to optimize both nanotubes and complex of nanotube with vanadium ions. Calculated vibrational frequencies without imaginary frequencies ensure the stable structures.

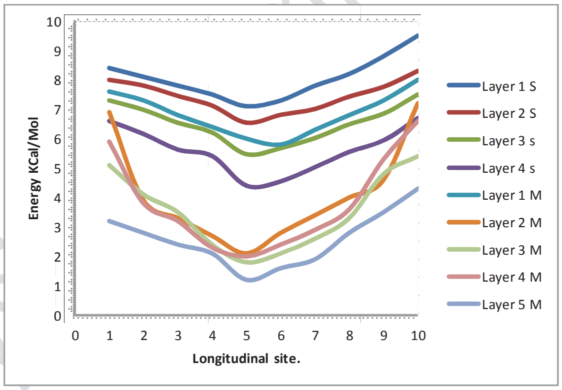

Figure 2. Binding energy of CNT/Vanadium ions at different sites and layers

Results and Discusions:

Binding energies were calculated via the difference in energy of CNT/V complexes from those of isolated fragments (see Figure 1).The calculations was performed in both gas phase an solution conditions. The results show that vanadium interacts more strongly with carbon atoms at site 4 and 5 of single and multi-wall CNTs, respectively. The distance of maximum interaction in these, cases correspond to the value of 2 Å.

Conclusions:

From these and more detailed considerations, it can be concluded that single wall CNTs could be used as a better adsorbent for vanadium ions, which are present in industrial wastewaters. The studies on longitudinal adsorption sites indicate that the interaction of vanadium ions with edge atoms of CNTs is stronger.

Reference:

[1] R. Ströbel, et al., Journal of Power Sources 84 (2) (1999) 221.
[2] A. Ansón, et al., Carbon 42 (7) (2004) 1243–1248.
[3] G.Q. Ning, et al., Materials Science & Processing 78 (7) (2004) 955.
[4] M. Endo, et al., Philosophical Transactions of the Royal Society A 362 (2004) 2223.

Study of the solvent polarity impacts on the stability of Erythromycin ethyl succinate by means of hybrid density functional theory based method

Elahe Shahabifar,[1] Seiedeh Negar Mousavi[2], Hooriye Yahyayi[3] and Davood Nori-Shargh[2]
[1]Chemistry Department, Science and Research Branch, Islamic Azad University, Arak, Iran
[2]Chemistry Department, Science Faculty, Arak Branch, Islamic Azad University, Arak, Iran
[3]Chemistry Department, Zanjan Branch, Islamic Azad University, Zanjan, Iran
Email: e_shahabifar@yahoo.com

Keywords: Erythromycin ethyl succinate, DFT, solvent effect

Introduction:

Erythromycin is a broad-spectrum antibiotic with activity against gram-positive and gram-negative bacteria, and other infectious agents, including *Chlamydia trachomatis*, mycoplasmas (*Mycoplasma pneumoniae* and *Ureaplasma urealyticum*), and spirochetes *(Treponema pallidum* and *Borrelia* species). Erythromycin has good activity against *Streptococcus pneumoniae*, *S. pyogenes* (group A beta-hemolytic streptococci), and *Staphylococcus aureus*. Resistant strains of both streptococci have been encountered, especially in populations recently exposed to erythromycin.[1] The incidence of resistance to group A streptococci has ranged from 1 to 18% in small studies to up to 60% in a population that had been widely treated with erythromycin for respiratory infections.[1-3] Most strains of *S. aureus* are currently sensitive to erythromycin. However, the incidence of resistance is increasing. Resistance may develop to erythromycin alone, or may be the result of cross-resistance to other macrolides.[1] In this work, we have investigated the impacts of the solvent polarity on the stability of Erythromycin ethyl succinate by means of the B3LYP/3-21G* level of theory with the GAUSSIAN 03 package of programs.[4]

Computational details:

Hybrid DFT calculations were carried out using the B3LYP/3-21G* level of theory with the GAUSSIAN 03 package of programs.[4] The main purpose of the present work was to study the impacts of the solvent polarity on the stability of Erythromycin ethyl succinate.

Results and Discussion:

Hybrid-density functional theory (B3LYP/3-21G*) based method was used to study the impacts of the solvent polarity on the stability of Erythromycin ethyl succinate. The results obtained showed that the stability of Erythromycin ethyl succinate increases by the increase of the solvent polarity. Based on the results obtained, Erythromycin ethyl succinate stability has the greater corresponding value in water and methanol. The correlations between the solvent polarity, and Erythromycin ethyl succinate stability have been investigated in water, acetone, methanol, ethanol and dichloromethane as solvents.

Conclusion:

The results obtained showed that the results obtained showed that the stability of Erythromycin ethyl succinate increases by the increase of the solvent polarity.

Refrences:

[1]R.M. Robins-Browne, M.K.R. Mackenjee, M.N. Bodasing, H.M. Coovadia, Am. J. Dis. Child., **1983**; 137: 282-5.

[2]H. Seppälä, A. Nissinen, H. Järvinen, et al. *Engl. J. Med*., **1992**; 326(5): 292-297.

[3]R. Kelley, G. Langley, L., *Clin. Pediatr.,* **1993**: 744-745.

[4]M.J. Frisch, et al, Gaussian 03, Revision B.03, Gaussian, Inc., Wallingford CT, 2004.

Molecular Dynamics Simulation of Some Organic Compounds Solubilization into the Nanometric Core of CTAB micelle

S. Soleimanzadegan[a,*], H. Farsi[a,b], F. Ebrahimi[b,c]
[a] Department of Chemistry, University of Birjand, P.O. Box: 97175-615, Birjand, Iran
[b] Solar Energy Research Department, University of Birjand, Birjand, Iran
[c] Physics Department, University of Birjand, P.O. Box: 97175-615, Birjand, Iran
Email: sara_soleimanzadegan@yahoo.com

Keywords: Nanometric core, CTAB, Micelle, Molecular Dynamics.

Introduction:

Today, normal micelles widely are used in green chemistry to dissolve insoluble organic compounds in water and to do organic reactions in aqueous media. In order to elucidate the nature of micellar effects on the properties of solubilized molecules, to understand the reaction mechanism in micellar systems and to design the micellar systems, it is essential to know the solubilization sites of molecules inside the micelle's nanometric core[1]. The objective of this work is determination of the location of some solubilized ring compounds into cetyltrimethylammonium bromide (CTAB) micelle and their affects on shape and size of micelle by Molecular Dynamic (MD) Simulations.

Computational methods:

The simulations and their analysis were performed with Gromacs 4.5.4 molecular dynamics package [2] and MARTINI coarse-grained force field [3]. The CTAB micelle was built using 80 CTA^+ ions. In the first simulation, the micelle was solvated by 4294 water molecules in a cubic box (corresponding to a 0.22 M CTAB solution), which is well above the CMC. Eighty bromide ions were added to neutralize the system. In the other systems we added 40 additive molecules respectively: aniline, pyrrole, thiophene and cyclohexane in each system. The systems were subjected to energy minimization and an equilibration run of 60 ns in a NPT ensemble. Equations of motion were integrated with the leapfrog algorithm with a time step of 0.03 ps. The production simulation was run for 1.2μs in NPT ensemble.

Results and discussion:

The density profiles of different systems have been plotted in Figure 1.

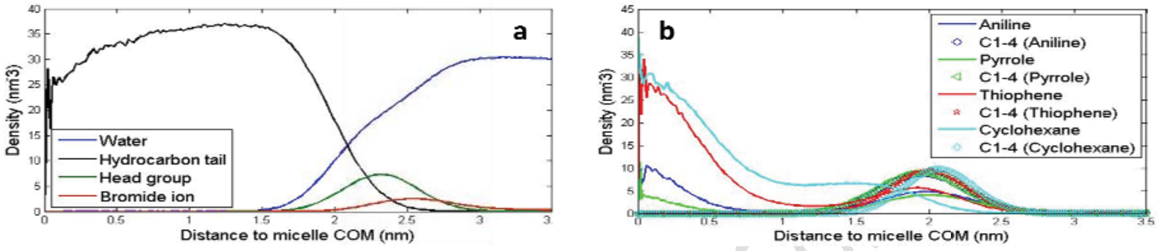

Figure 1: a) different parts in the system of CTAB micelle and b) different additives inside the micelle.

The parameters for size and shape of the micelle without and with additives are shown in Table 1.

Table 1: The size and shape parameters of micelles.

	Radius of gyration	Radius of micelle	Moments of inertia	Accentricity
Systems	R_g(nm)	R_s(nm)	I_{max}/I_{min}	η
CTAB	1.812	2.337	1.283	0.130
CTAB+aniline	1.858	2.397	1.334	0.151
CTAB+pyrrole	1.845	2.380	1.333	0.151
CTAB+tiophene	1.889	2.436	1.269	0.125
CTAB+cyclohexane	1.954	2.520	1.225	0.105

Conclusion:

The radius of CTAB spherical micelle without additives is 2.337 nm. The solubilization of organic compounds inside the nanometric core enlarges the normal micelle and the solubilized molecules are distributed on the base of their own polarity in the several regions of micelle.

References:

[1] M. J. Rosen, “surfactants and interfacial phenomena”; (2004), John Wiley & Sons, Inc., Hoboken, New Jersey.

[2] B. Hess, C. Kutzner, D. van der Spoel, E. Lindahl, J. Chem. Theory Comp. **4** (2008) 435.

[3] S. J. Marrink, H. J. Risselada, S. Yefimov, D. P. Tieleman, A. H. D. Vries, J. Phys. Chem. B, **111** (2007) 7812.

Investigation and compare of antioxidant properties of some of phenolic compound by density functional theory

M. M. Heravi[a]*, Kh. Hoseini[a], M. Bozorgmehr[a],T. Ardalan[b]
[a] Department of Chemistry , Mashhad Branch , Islamic Azad university , Mashhad , Iran
[b] Department of Chemistry , Mashhad Branch , Islamic Azad university , Mashhad , Iran, young researcher club
Email: kh.hoseini94@yahoo.com

Key word: Antioxidant, DFT, Phenol, BDE, Thymol.

Introduction:

Antioxidants are of great interest because of their involvement in important biological and industrial processes. In general, compounds with antioxidant activity have been found to possess anticancer, anti-cardiovascular, anti-inflammation and many other activities.

The liquid-phase autoxidation (peroxidation) of oils and lipids is an important process in chemical and biological systems. The underlying chemical reactions are described by a free-radical chain mechanism, where the oxygen-derived peroxyl radicals of hydrocarbon substrates ($ROO^{\cdot}$) are the key participants. The destructive peroxidation processes can effectively be inhibited by antioxidants (InH), which trap peroxyl free radicals in a fast reaction:

$ROO^{\circ} + InH \rightarrow ROOH + In^{\circ}$

The oxidation chain is subsequently terminated by reactions of In° with ROO° or In° .Among many classes of inhibitors, phenols are probably the most important chain-breaking antioxidants in biochemical systems. The high reactivity of phenolic antioxidants is frequently explained by low energies of the O-H bond, related to thermodynamic stabilization of the aromatic radical In°. The effectiveness of their inhibiting action in oxidative processes is determined by a number of factors relating to the structure, medium, and conditions. One of the most important is the bond dissociation energy (BDE) of the phenolic hydroxyl bond.

Methods:

The molecular structures and energies of the reaction stationary points are calculated with the well-studied and efficient DFT B3LYP technique using the GAUSSIAN-03 program. The accurate O□H bond dissociation enthalpies for Thymol, and 2-methoxy-4-vinil phenol have been calculated by using the B3LYP procedure with 6-311G and 6-311G** and 6-311++G** basis sets. The accurate O□H bond dissociation enthalpies for a series of meta and para substituted Thymol (X=H, CH3, F) have been calculated by useing the B3LYP procedure with 6-311++G** basis set.

Results and discussion:

Bond dissociation enthalpy, BDE, is defined as BDE = H(R◌̊) + H(H◌̊) –H(R–H)

Where H(R◌̊) is the total enthalpy of the radical, H(H◌̊) is the total enthalpy of the abstracted hydrogen atom, and H(R–H) is the total enthalpy of the molecule.The calculated BDE for Thymol and 2-methoxy-4-vinil phenol is 86.72kcal/mol and 79.78kcal/mol, respectively.

Conclusion:

The B3LYP/6-311++G** method can be used for the calculation of accurate O–H bond dissociation enthalpy. Strong electron withdrawing groups, both at the para and meta positions, increase the O–H bond strength from that in the unsubstituted Thymol molecule. The electron donating group at the para position reduces the O–H bond strength of Thymol, whereas the same at the meta position dose not have any strong effect on the BDE (O–H).The F should be considered as borderline groups, because they behave as electron donating group at the para position and electron donating group at the meta position of Thymol.

Reference:

[1] M.Reis and etal, A theoretical study of phenolic compounds with antioxidant properties, European journal of the Medicinal Chemistry 42 (2007) 440-446.

[2] N.M.Khlestov and A.N.Shendrik, Quantum-Chemical DFT calculations of the energies of the O–H bond of phenols, Theoretical and Experimental Chemistry 46 (2010) 279-283.

[3] Lenka Rottmannova and etal, Applicability of DFTB+ method for the calculations of O–H bond dissociation enthalpis of phenols, Acta Chemica Slovaca (2010) 12-19.

DFT study of antioxidant properties and the reactivity of OH groups on saffron petals

M. M. Heravi[a]*, Y.Sabahi[a], M. Bozorgmehr, P.Ardalan[b]
[a] Department of Chemistry , Mashhad Branch , Islamic Azad university , Mashhad , Iran
[b] Department of Chemistry , Mashhad Branch , Islamic Azad university , Mashhad , Iran, young researcher club
Email:yaldasabahi@ymail.com

Key words: DFT, Antioxidant, Kaempferol, BDE.

Introduction:

Reactive oxygen and nitrogen radical species ($OH^{\cdot}$, $ROO^{\cdot}$, $NO^{\cdot}$, …) present in our body are produced by γ, X-ray and UV radiations. They can potentially damage almost all types of biologically important molecules like lipids, amino acids, carbohydrates and nucleic acids. Against antioxidants are a group of substances that, when present at low concentrations in relation to oxidisable substrates that have to be repaired and reduced, significantly inhibit or postpone oxidative processes, while often being oxidized themselves.

Among the natural the phenolic antioxidants, the flavonoid family is the most important class. It has been reported the scavenging activity of phenolic antioxidant is related to the bond dissociation enthalphy (BDE) of the O-H groups present in the structure.

Saffron petals are a rich source of kaempferol flavonoid.

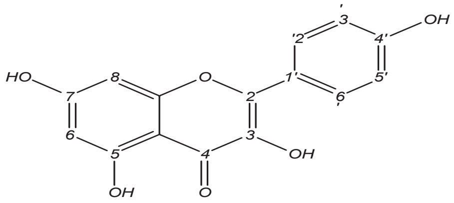

Molecular structure of kaempferol

Computational methods:

All calculations were performed using the Gaussian 03 program package. The B3LYP exchange correlation potential was used for optimizing energies in conjugation with the 6-

31G, 6-311G, 6-311G(d,p) basis sets. Geometry optimization of kaempferol and its 3-OH, 5-OH, 7-OH and 4'-OH radical species performed. BDE was calculated as the difference in total enthalpy between the kaempferol radical and the kaempferol according to the following reaction: R-OH $\longrightarrow RO^{\cdot} + H^{\cdot}$

Result and discussion:

The DFT calcluted BDE values with B3LYP/6-311G(d,p) four radical forms give the following BDE sequence for the present OH groups: C5-OH:106.16296 Kcal/mol, C7-OH: 93.789664 Kcal/mol, C4'-OH: 88.812898 Kcal/mol and C3-OH: 77.753023 Kcal/mol.Lowest BDE value belongs to C3-OH, thus the most stable radical in the gas phase is 3-OH species. BDE values decrease for C4'-OH with electron-donating groups (NH_2, CH_3,OH) in orto position of B ring.

Conclusion:

In this work the antioxidant properties of kaempferol in saffron were investigated. The most stable radical in the gas phase is the 3-OH species. The 5-OH, 7-OH, 4'-OH radicals lie at higher energy. Electron-donating substituents decrease of OH BDE, whereas electron-withdrawing groups cause it increase.

Reference:

[1] Z.Dhaouadi and etal; DFT study of the reaction of quercetin with OH radical; Journal of Molecular Structure:THEOCHEM 904,35-42; 2009.

[2] Z.S.Markovic and etal; Structural and electronic features of baicalein and its radicals; Monatsh Chem; 142:145-152; 2011.

[3] N.T.Manojlovic and etal; DFT study on the reactivity of OH groups in emodin; Monatsh Chem; 140: 1311-1318; 2009.

[4] R.Guzman and etal: A density functional study of antioxidant properties on anthocyanidins; Journal of Molecular Structure 935,110-114; 2009.

Computational investigation of plausible species in linkage isomerization of nitro- and nitrito-pentaamminecobalt(III) complexes

N. Hasani, A. Eslami*, S. Yeganegi
Faculty of chemistry, University of Mazandaran, P.O. Box47416-95447,Babolsar, Iran
Email: Eslami@umz.ac.ir
Hasaninahid@ymail.com

Keywords: DFT, Linkage Isomer, Nitro, Nitrito, Thermodynamic, Kinetic

Introduction

Linkage isomerism is observed in coordination compounds when an ambidentate ligand (e.g.,NO_2^-) binds the metal center through the one or the other of its two terminal donor atoms, giving rise to two different complexes. A well-known classic example in this sense refers to the nitro/nitrito isomerism in complexes of pentaamminecobalt(III). The kinetic and the thermodynamic of the spontaneous isomerization of corresponding complexes have been studied both in solution and solid state [1-3]. This reaction was proved to be intramolecular by different experimental techniques. The nature of transition state and deeper understanding of reaction mechanism using experimental data are still unanswered. Hence, in this study a quantum mechanical approach was employed to elucidate the electronic structure of nitro- and nitritopentaammine cobalt(III) complexes (as shown in Fig.1) and its transition state. Also, the thermodynamic and kinetic data of the isomerization was evaluated using the computational methods.

Fig. 1. The optimized structures of nitrito (right side) and nitro (left side) linkage isomers.

Computational details:

Density functional calculations have been carried out by Gaussian 2009 package using B3LYP (Becke–Lee–Yang–Parr) model. All the molecular structures have been fully optimized in gas phase using the quasi-relativistic effective core potential (ECP’s) for cobalt. It should be noted that the DNP basis set includes a double-zeta quality basis set that added a p-type and d-type polarization function to hydrogen and heavier atoms, respectively; and it is equivalent to 6-31G+ (P,d) Gaussian basis sets.

Results and discussion:

The results related to the collected structural data from our theoretical study showed that the agreement between the computed and experimental data is not good. This discrepancy might be ascribed to the crystal environment such as the electrostatic part of H-bond interactions and/or crystal packing effects.Also,to determine the activation energy of linkage isomerization reaction, an optimized TS structure identified by the quadratic synchronous transit (QST) methods which this structure can be ascribed as a heptacoordinate rearrangement, with the NO_2 moiety in a η^2 coordination. Thermodynamic parameters obtained in gas phase specified that the nitro isomer more stable than the nitrito complex which these results are in agreement with the experimental evidences.

Conclusion:

In the present work, we report a comprehensive study on the thermodynamic and kinetic of the linkage isomerization of nitro- and nitritopentaammine Co(III) using DFT method. Our results suggest that the nitro isomer is slightly favored in the gas phase with respect to nitrito one. Also we showed the nature of transition state of nitrito/nitro interconversion in the gas phase.

Reference:

[1] A.Eslami; *Themochim. Acta*; 409, **2004** 189-193.

[2] H. Ciofini, C. Adamo; *J. Phys. Chem. A.*; 105 **2001** 1086- 1092

[3]A.Eslami,N.Hasani;*J. Therm. Anal. Calorim.*,**2012** In Press, doi:10.1007/s10973-012-2470-8.

HOMO-LUMO calculation of Novel ruthenium multicarboxylic acidfor dye sensitized solar cell application

Ahmad Sousaraei, HashemShahroosvand*, MahammadShadman
[a]Chemistry Department, University of Zanjan, Zanjan, Iran

Keywords: Dye, HOMO-LUMO, Solar cell, Ruthenium

Introduction:

The dye-sensitized nanocrystalline solar cell (DSC) offers special opportunities in the realm of renewable energy sources primarily stemming from its use of low-cost materials and its lack of stringent conditions required for device manufacturing [1].The LUMO of the dye must be sufficiently high in energy to promote efficient charge injection into the TiO2 film and the HOMO should be sufficiently low in energy for efficient regeneration of the oxidized dye by the hole transport material (HTM) [2].

Materials and methods:

As a typical procedure, four new complexes of ruthenium nitrosyl tri nitrate with btec acid and Bphen were synthesized by changes in pH and reactions conditions [3].The simulations have been performed with the Gaussian 09 program

Result and discussion:

To gain further insight into the electron density distribution within the frontier and other close lying orbitals, we performed quantum chemical calculations on the Ruthenium 1,2,4,5-benzentetracarboxylic bahtophenanthroline (RMCC) using density functional theory (DFT) at the B3LYP/LANL2DZ level. In the ground state, the electron density of RMCC for the highest occupied molecular orbital (HOMO) and HOMO-1 is shared by the nitrogen moiety and ruthenium core. For RMCC (4) there is a c electronic coupling between the phenyl ring of btec and the p-system of Bphen, lifting the LUMO level higher than that of the other RMCCs. The predicted effect is an increase of the HOMO-LUMO gap of RMCCcompared with other RMCCs dye, which is in good agreement with the experimental observations. These energy levels are able to inject energetic electrons into the conduction band of TiO_2 and accept electrons from iodide ions, respectively. This indicates that mismatching of the energy levels of LUMO and HOMO does not determine the low IPCE performance of the RMCC/TiO_2 solar cell.

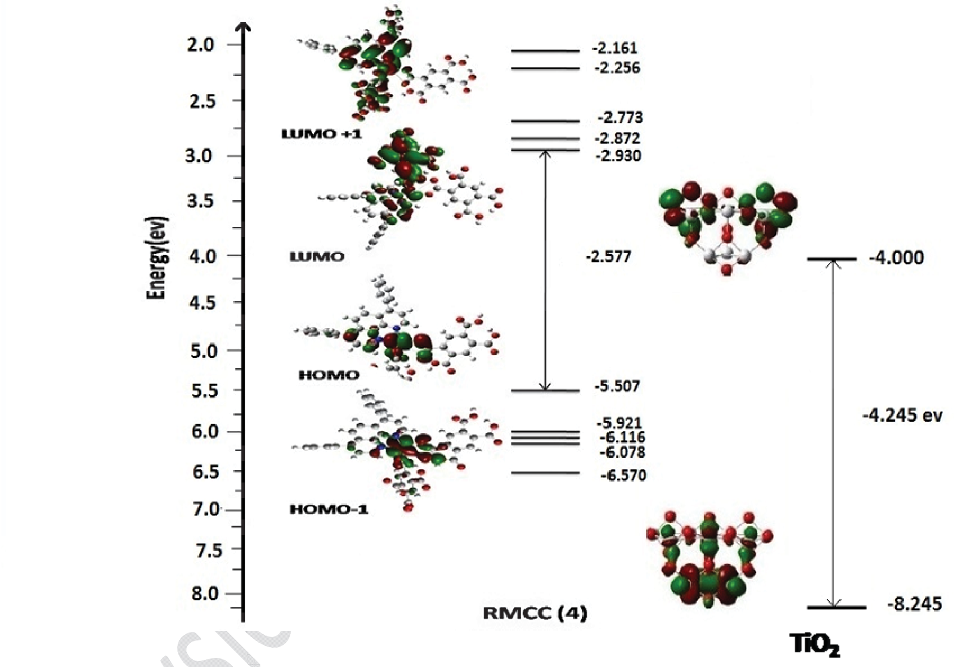

Conclusion:

HOMO-LUMO calculations of a new amphiphilicruthenium(II) dye with 1,2,4,5-benzentetracarboxylic acid (H_4btec), Bphenanthroline (BPhen) have been indicated the suitable band gap for dye-sensitized solar cells applications.

References:

[1] B. O'Regan and M. Gratzel, "A low-cost, high-efficiency solar cell based on dye-sensitized colloidal TiO_2 films," Nature, 353 (1991)737–740.

[2] N. Robertson, Optimizing Dyes for Dye-Sensitized Solar Cells, Angew. Chem. Int. Ed. 45 (2006)2345-2338.

[3] H.Shahroosvand, FahimehNasouti, Ahmad Sousaraei, submitted to Dye&Pigment(2012).

Theoretical studies on tautomerism of (N-N) 6-Hydroxide 5-Flourocytosine

B.Chahkandi*a ,A.Mahboobifara
aDepartment of Chemistry, Shhahrood Branch, Islamic Azad University, Shahrood ,Iran
(Email: B.chahkandi@Gmail.Com)

Molecule5-Flourocytosine is one of the derivatives of pyrimidine that its aspiration is dangerous[1]. the investigated molecule 6-Hydroxide 5-Flourocytosine that its tautomer in the gas phase and the calculate with the use of density function theory with method of DFT which is one of the functions in the B3LYP in level B3LYP/6-311++G(d,p)[2]. Under the figure we see molecule 6-Hydroxide 5-Flourocytosine.

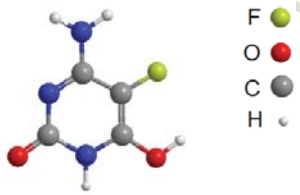

Figure1. 6-Hydroxide 5-Flourocytosine

we investigated it , it has 10 tautomerism and 5 toautomers has the possibility of the shift of (N-N).

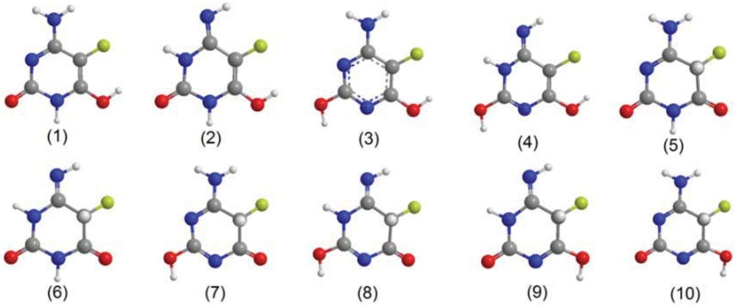

Figure2. The image of 10 tautomer which have the shift of (N-N).

drawing the molecules with the software Gauss view and calculated with the Gaussian 03software has been done[3].the intended temperature is 298.15 oK. at first we, optimized the structures and then we do the frequency accounting on them.

انرژی (هارتری/ذره)	نام مولکول
-569.5636	1
-569.5597	2
-569.5687	3
-569.5465	4
-569.5757	5
-569.5768	6
-569.5538	7
-569.5492	8
-569.5495	9
-569.5452	10

Table1. Of the investigated energy molecule tautomers6-Hydroxide 5-Flourocytosine in the gas phase according to the Hartree.

in this research the amount of keq, ΔG, ΔH, ΔEhave been extracted.

Table2. The investigated thermodynamic and synthetic functions.

	۱→۲(T۱)	۳→۴(T۲)	۵→۶(T۳)	۷→۸(T۴)	۹→۱۰(T۵)
ΔE	3.2053	14.1584	-0.2679	2.9461	2.2609
ΔH	2.8294	13.9583	-0.4279	2.8827	2.4366
ΔG	3.9024	14.245	-0.175	2.9078	2.2527
Keq	1.۳۷۷۹*۱۰-۳	3.٦٠٨٠*۱۰-۱۱	1.۳٤۳٦	7.۳۸٤۹*۱۰-۳	2.۲۳*۱۰-۲

After the calculation we understand that the tautomer ٥ is stability and tautomer 10 is unstablemolecules.we understand that tautomerism T3 has rather Keq withthe number amount(Keq =1.۳٤۳٦) .

Keywords: Tautomer, DFT, Energy, stability

Reference:

[1] J.D. Watson, F.H.C. Crick, Nature 171 (1953) 964–967.

[2] A. K. Rappe, ClJ. Casewit, K. S. Colwell and W. A. Goddard, J. phys. Chem., 94 (**1990**) 8897.

[3] M.J. Frisch and et.al, Gaussian 2003, Gaussian, Inc,. Pittsburgh PA, (**2003**).

Nicotine Adsorption Capacities of Single-Walled Carbon Nanotubes: a Steered Molecular Dynamics Study

Sara Fazeli[1], Muhammad Shadman[1,]*, Morteza Vahedpour[1]
[1]Department of Chemistry, Faculty of Science, University of Zanjan, P.O.Box 313, Zanjan, Iran.
(*Corresponding author E-mail address: Shadman@znu.ac.ir)

Key words: Nicotine, Carbon Nanotube, Molecular Dynamic, Physisorption.

Introduction:

Nicotine is an alkaloid present in several plants such as eggplant, tomato and green pepper, but its major source is tobacco, used for cigarette manufacture [1]. Normally, one cigarette contains 0.7mg of nicotine.In proper nomenclature, nicotine is 3-(1-Methyl-2-pyrrolidinyl)pyridine. Figure 1 shows the chemical structure of nicotine molecule.Nicotine's structure was deduced by Pinner.The negative effects of nicotine on public human health include heart disease, cancer and respiratory disorders and even it was implied that nicotine might be geotaxis. Therefore, the smoking pollution is one of the major problems in the world [2-3]. In the past years, great efforts have been made in the development of adsorption of nicotine by proteins and nano-structures in order to remove it. It is an effective and convenient way to add some additives such as active carbon, zeolite, in the filter tips. Carbon nanotubes (CNT), a fascinating new material, are attracting more and more attention since their discovery. The studies of carbon nanotubes used as absorbents have also been reported experimentally [4]. In this research, we try to illustrate the dynamic behavior of nicotine adsorption outside of single-walled carbon nanotubes (SWCNTs) using a powerful method of molecular dynamics (MD).

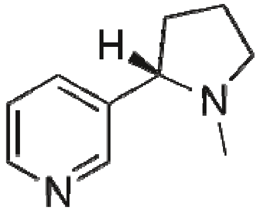

Figure 1. The chemical structure of nicotine molecule

The model used and the MD simulations performed:

In this work, we used MD simulations to investigate nicotine adsorption in (5,5), (10,10), (15,15), (22,22) and (29,29) SWCNTs while the nanotube length of them is fixed at 10 nm. The amount of nicotine molecules around of each SWCNT is calculated considering density of nicotine and nanotube diameter that is found in Ref. [5]. Also, we simulated the nicotine adsorption capacities of the planar carbon surface in order to compare the nicotine adsorptivity of SWCNT. All MD simulations and analyses were performed using the NAMD and VMD softwares respectively [6].

Results and discussion:

For each complex system, a total 25 ns MD simulation was performed that the first 5 ns is related to equilibrium step and in the next 20 ns, the production has done to achieve the thermodynamics data in order to molecular analyses. The During the MD simulation, the nicotine may depart from their original position. The results show that, the SWCNTs as the adsorbent material have the highest adsorptivity capability of nicotine molecules. Also from the MD runs, it can be noted that the interaction between nicotine and SWCNT walls leading to phase transitions and capillary condensation. The interior surface of open-ended SWCNT also exhibit a stronger binding energy for adsorbing molecules compared to the planar carbon surface. Also, our work is not completed and it will be continued.

Conclusion:

Our results indicate how the dynamics of the nicotine molecules are an important consideration for understanding of nicotine and SWCNT interactions. Physical incorporation of atoms or molecules of nicotine outside SWCNT occurs through charge transfer effects due to the suitable inner diameter of SWCNT. Therefore, it can be the predicted the SWCNT can be become promising material for the application in cigarette industry.

Reference:

[1] P. Dome, et al., *Neuroscience and Biobehavioral Reviews*, 34 (**2010**) 295-342.

[2] V. Rakic, et al., *water research*, 44 (**2010**) 2047-2057.

[3] E. G. Perez et al., *Bioorganic & Medicinal Chemistry Letters*, 19 (**2009**) 251-254.

[4] Z. Chen, *Applied Surface Science*, 252 (**2006**) 2933-2937.

[5] D. M. Ackerman, et al., *Molecular Simulation*, 29 (**2003**) 677-684.

[6] J. C. Phillips et al., *Journal of Computational Chemistry*, 26 (**2005**) 1781-1802.

Why bis (1,2,4,5-benzentetracarboxylic) nitrato ruthenium (II) is not suitable case for dye sensitized soalr cell application?

Alireza Faghih, Hashem Shahroosvand*, Mahammad Shadman
[a]Chemistry Department, University of Zanjan, Zanjan, Iran

Keywords: Dye, Band gap, Solar cell, Ruthenium, Nitrato.

Introduction:

The conversion of sunlight to electricity using dye-sensitized solar cells (DSCs) represents one of the most promising methods for future large scale power production from renewable energy sources.Briefly DSCs contain five components: (1) a conductive mechanical support, (2) a wideband gap semiconductor film,(3) a sensitizer,(4) electrolyte or hole conductor,and (5) a counter electrode.The sensitizer is a key component harvesting the solar radiation and converting it to electric current by electron injection into the wide band gap semiconductor.As the most successful sensitizers to date, ruthenium complexes used in conjunction with an ionic liquid electrolyte to overcome leakage problems of volatile electrolytes have exhibited remarkable efficiency and stability.[1]

Materials and methods:

As a typical procedure, two new complexes of ruthenium nitrosyl tri nitrate with btec acid were synthesized by changes in pH and reactions conditions [2]. The simulations have been performed with the Gaussian 09 program.

Results and discussion:

To gain further insight into the electron density distribution within the frontier and other close lying orbitals, we performed quantum chemical calculations on the Ruthenium 1,2,4,5-benzentetracarboxylic(btec) using density functional theory (DFT) at the B3LYP/LANL2DZ level. In the ground state, the electron density of Ru complex for the highest occupied molecular orbital (HOMO) and HOMO-1 is shared by the ring of btec. For Ru complex there is a electronic coupling between the phenyl ring of btec and the Ru metal core, decrease the LUMO level lower than that of the other Ru complexes. These energy levels are not able to inject energetic electrons into the conduction band of TiO_2 . This indicates that mismatching of the energy levels of LUMO and HOMO does determine the low efiiicency performance of the synthesised Ru complexs/TiO_2 solar cell.

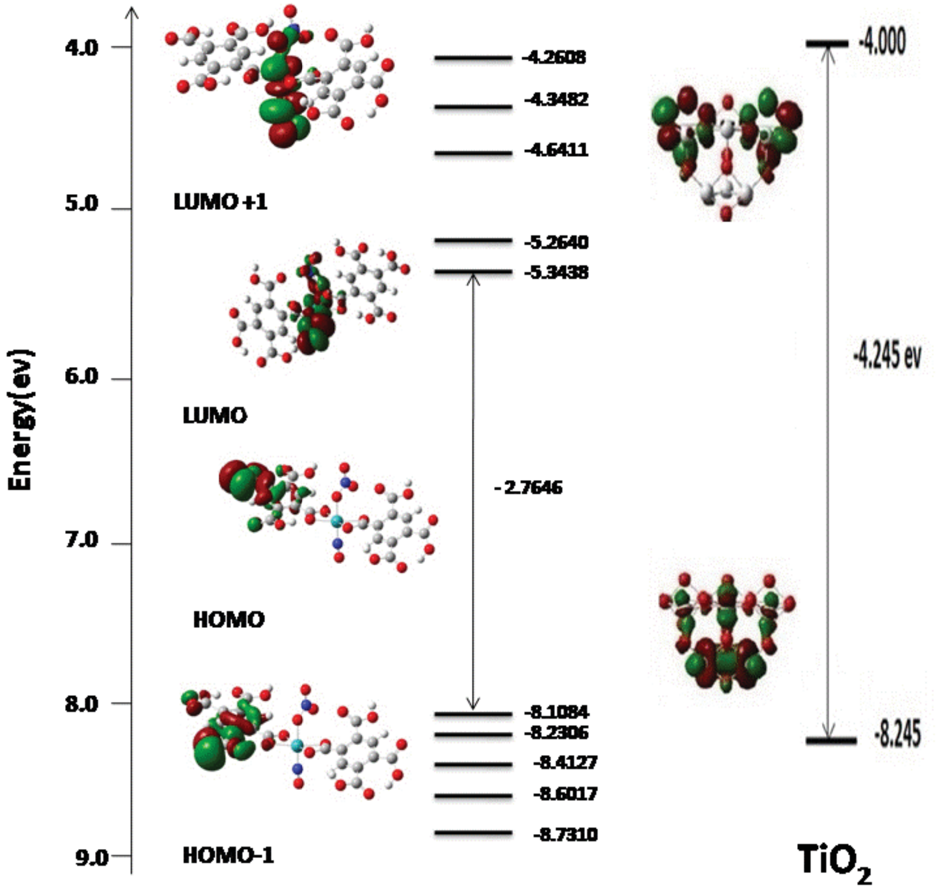

Conclusion:

Summery, we calculate HOMO-LUMO of novel bis 1,2,4,5-benzentetracarboxylic Ruthenium with nitrato as anchoring group. The mismatching of the energy levels of LUMO and HOMO does determine the low efiiicency performance of the synthesised Ru complexs/TiO_2 solar cell.

References:

[1] J-H. Yum, R. Humphry-Baker, Sh. M. Zakeeruddin, M. K. Nazeeruddin, M. Gratzel, , nano today, 5 (2010), 91-98.

[2] H.Shahroosvand, Fahimeh Nasouti, New Material for Electrochemical System, accepted manuscript (2012).

MP2 Study the Kinetics and Hardness Profile of SN2 Reaction in Haloalkanes of Cl^- and Br^-:the Effects of CH_3 Group Substitutions

S. Mandegar[1], and H.R. Shamlouei[2]*

[1] Islamic Azad University, Omidieh Branch, Omidieh, Iran

[2] science Department, Lorestan University, Khorramabad, I.R. Iran

Introduction:

The haloalkanes (also known as Halogenoalkanes) are a group of chemical compounds, consisting of alkanes, such as methane or ethane, with one or more halogens linked, such as chlorine or fluorine, making them a type of organic halide. The important types of haloalkanes are CFCs. CFCs are chlorofluorocarbons which are the compounds containing carbon with chlorine and fluorine atoms attached. They were used as refrigerants, propellants for aerosols, for generating foamed plastics like expanded polystyrene or polyurethane foam, and as solvents for dry cleaning and for general degreasing purposes. Unfortunately, CFCs are largely responsible for destroying the ozone layer. In the high atmosphere, the carbon chlorine bonds break to give chlorine free radicals. It is these radicals which destroy ozone.Studying the chemistry of haloalkanes can be useful for understanding the reaction which take place in atmosphere [1,2]. The importance of haloalkanes are so high that very researchers work to underestand their chemistry [3,4,5]. In this research the kinetic of nucleophilic substitution reaction in which the F^- attacks to CH_3Cl and CH_3Br and therefore takes out the Cl^- and Br^- to make new haloalkanes was studied. The effect of CH3 substitution on the kinetics of reaction then is investigated by replacing one of the hydrogen atoms with CH_3 groups.

Methods:

The kinetics of nucleophilic substitution reaction in which Cl^- and Br^- are replaced by F^- was studied by MP2 method, 6-311++g** basis set and Gaussia03W package. The kinetic study was done for a series of reactions. The studied reactions are described by Eq.s 1 to 4.

$$CH_3F + Cl^- \rightarrow CH_3Cl + F^- \qquad \text{Eq.1} \qquad CH_3CH_2F + Cl^- \rightarrow CH_3Cl + F^- \qquad \text{Eq.2}$$

$$CH_3F + Br^- \rightarrow CH_3Br + F^- \qquad \text{Eq.3} \qquad CH_3CH_2F + Br^- \rightarrow CH_3Br + F^- \qquad \text{Eq.4}$$

The CH_3 substitution instead of one of methyl group hydrogen is the difference between reactions illustrated in Eq. 1 and 3 as well as difference between Eq.2 and 4. The energy surface were calculated for each reaction, the transition state (TS) and activation energy of them were calculated, and then the results were analyzed. Then the chemical hardness profile versus reaction coordinate of these reactions was calculated.

Results :

As the first part of the research, the energy surfaces of the reactions were calculated by the method and basis set mentioned previously. In Fig.1 to 4 the energy surfaces for the reaction described in Eq. 1 to 4 are shown.

Fig.1 the energy surface for the reaction illustrated in Eq.1 and 2

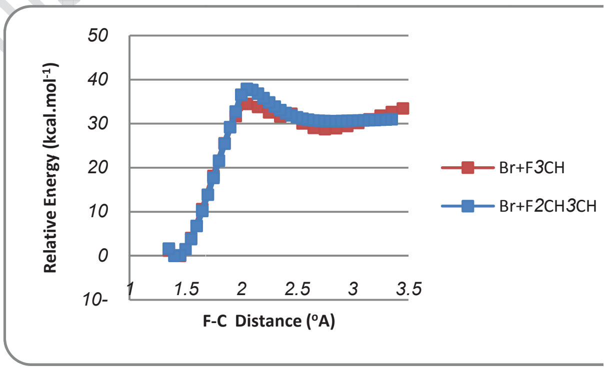

Fig.2 the energy surface for the reaction illustrated in Eq.3 and 4

After calculation the energy surface, the structures of transition state for the studied reactions were initially estimated by energy surface calculations and then were optimized by method and basis sets mentioned previously. Then the activation energies for each reaction were calculated. In table1 the list of calculated activation energies is presented.

Table1. The list of calculated activation energies for each reactant

Reaction	Activation Energy(kcal.mol^{-1})	Reaction	Activation Energy(kcal.mol^{-1})
Cl^-+CH_3F	638.36	Br^-+CH_3F	2712.02
$Cl^-+CH_3CH_2F$	559.19	$Br^-+CH_3CH_2F$	2751.23

The results of calculated activation energies show that presence of CH_3 group in alkyl halide molecules will increase the amount of activation energy. This consequence can be explained by the fact that the SN2 reactions are more difficult for substituted carbons than nonsubstituted ones. To ensuring the structure of TS, the IR spectrum of transition state was calculated and then the negative vibrational mode were looked for. Existence of one negative vibrational mode confirms the structure of TS. Every calculated IR frequencies for these transition state shows that these transition states are really exist. Other results show that presence of additional CH_3 group in TS structure makes it more unstable and the IR frequency for its vibration will be more negative.

As the final segment the chemical hardness for each reaction was calculated and the differences between the reactant and the TS in them were computed. The amount of calculated hardness difference trend has the same behavior as seen in activation energy.

Conclusion :

The haloalkanes especially CFCs are very important in industrial process. In this research the kinetics of nucleophilic substitution (SN2) reaction were studied. For this reason the energy surface for the reactions of Cl^- and Br^- with CH_3F and CH_3CH_2F and the activation energies of them were calculated. As the result of this research the activation energy for substituted haloalkanes are greater than non substituted ones. The IR frequency of transition state was done to ensure the correctness of TS structure. All of first frequency number of IR spectrum are negative and approved the works. The chemical hardness profile and the hardness difference of them were calculated. as the consequence the same behavior as seen previously for the activation energy was seen.

Reference:

[1] John Stanley Hannah, " Chlorofluorocarbons:a scientific, environmental, and regulatory assessment ", (1987), George Washington University

[2] W. E. Mooz, Kathleen A. Wolf, Frank A. Camm, "Potential constraints on cumulative global production of chlorofluorocarbons " (1986), United States. Environmental Protection Agency, Rand Corporation

[3] Vladimir L. Orkin and Victor G. Khamaganov, "Rate constants for reactions of OH radicals with some Br-containing haloalkanes" Journal of Atmospheric Chemistry, Vol.16, (1993), P:169

[4] V. L. Orkin and E. E. Kasimovskaya, "Ultraviolet absorption spectra of some Br-containing haloalkanes "*Journal of Atmospheric Chemistry* Vol.21, (1995) P:1

[5] Jonathan S. Nimitz, Stephanie R. Skaggs, "Estimating tropospheric lifetimes and ozone-depletion potentials of one- and two-carbon hydrofluorocarbons and hydrochlorofluorocarbons " *Environ. Sci. Technol*., Vol.26 (1992), p:739

Steered Molecular Dynamics Simulation of Adriamycin Drug Uptake by N-isopropylacrylamideCopolymers

MortezaAlihosseyni[1], Muhammad Shadman[1,*], Morteza Vahedpour[1]
[1]Department of Chemistry, Faculty of Science, University of Zanjan, P.O.Box 313, Zanjan, Iran.
(*Corresponding author E-mail address: Shadman@znu.ac.ir)

Keywords: Molecular model, Drug copolymers, Force field, Adriamycin, Thermoresponsive polymers

Introduction:

Thermoresponsive polymers, which are usually formed by amphiphilic copolymers, have attracted growing interestdue to their tremendous potential applications in medicine especially as vehicles for drug delivery. Poly(N-isopropylacrylamide) (P-NIPAM) is a typical thermosensitivepolymeric material, which exhibits a reversiblethermoresponsive phase transition in an aqueous solution andaround the lower critical solution temperature (LCST) (it is32°C for pure P-NIPAM) [1–2]. Based on the LCST behavior, several P-NIPAM-containing block copolymers have been used as a noveldrug carrier in the field of drug target. When P-NIPAM forms the hydrophilic shell of the micelle, the drug is released and exhibits its bioactivity for a time period upon local heating. The simplicity of the micelle formed by self-assembly of amphiphilic block copolymers and the drug encapsulations by physical mixing are extremely attractive features of polymeric micelles. Adriamycin (Doxorubicin, ADR) is an active medicine against many cancers. It is most commonly used in the treatment of neoplastic diseases, but the unmodified ADR rapidly releases from the liposome upon intravenous injection while too many doses could cause side effects [3]. Therefore, it is necessary to develop the safe and efficient drug carriers that can deliver ADR exclusively without provoking adverse reactions in disease therapy. Several P-NIPAM-containing polymeric micelles have been adopted to reduce adverse drug reactions.In this work, applying molecular dynamics (MD) and considering two molecules: poly(N-isopropylacrylamide)-block-poly(ethylene glycol) and (N-isopropylacrylamide-coacrylic acid), we can study the structure and chemical properties of stability, diffusion and binding energy between molecules. The MD is widely used in drug design to study the three-dimensional properties and interaction energies of molecules, and can be used in simulation studies, etc. Thus, predictive computational models can be used to accelerate the selection process of lead compounds to deliver drugs from large polymer libraries prior to synthesis and biological characterization [4].

The simulation details:

The steered molecular dynamics (SMD) simulation with GROMACS force field was performed while the drug is in the vicinity of the polymer molecule in the presence of water molecules, and the interaction energy is calculated between of them. This energy is evaluated with respect to van der Waals and hydrogen bond forces. Thus, the radial distribution function (RDF) of drug is intended. The length of simulation in NPT and NVT ensembles in equilibrium and production steps are 500 ps and 3 ns respectively at 300 K and 1 atm.The drug-loaded copolymer molecules were modeled by placing Adriamycin drug adjacent to each polymeric molecule separately.All SMD simulations and analyses were performed using the NAMD and VMD softwares respectively [5].

Results and discussion:

The results have shown that The P-NIPAM chains played a key role in stabilization of the carrier, because the P-NIPAM chains exhibit hydrophilicity below the LCST. The release of the drug-loaded in the polymeric micelles upon heating above the LCST is due to the P-NIPAM structural deformation. Therefore, the release amount of ADR could be controlled by the temperature of the aqueous solution. Also, our work is not completed and it will be continued.

Conclusion :

The SMD simulations were applied to investigate the drug delivery polymeric system.The results exhibit an improved dissolution and biodegradability in the drug-loaded in the polymeric micelles. These properties indicate that the N-isopropylacrylamide-coacrylic acid copolymer is an excellent carrier for controlling drug delivery and release.

Reference:

[1] M. Heskins, J. Guillet, *J. Macromol. Sci., Part A: Pure Appl. Chem.* 2 (**1968**) 1441-1455.
[2] Y. Hirokawa, T. Tanaka, *J. Chem. Phys.* (**1984**) 6379-6380.
[3] P.Qiao, Q.Niu, Z. Wang, D. Cao, *Chem. Eng. J.* 159 (**2010**) 257-263.
[4] M. Subashini,et al., *J. Mol. Model*. 17 (**2011**) 1141-1147.
[5]J. C. Phillips et al., *Journal of Computational Chemistry*, 26 (**2005**) 1781-1802.

Interaction of CO with BNnanocluster surface(Corrected)

Sima Mehdi Shishvan,JavadBeheshtian*
Department of Chemistry, ShahidRajaee Teacher Training University, P.O. Box 16875-163, Tehran, Iran
j.beheshtian@Gmail.com

Keywords: Boron Nitridenanocluster,Density functional theory, Adsorption, CO.

Introduction:

Boron nitride (BN) nanomaterials are expected to have vast variety applications as electronic devices, high heat- resistance semiconductors, and insulator lubricants because of providing convenient stability at high temperatures with high electronic insulation in air and also hydrogen storagematerials [1].Boron Nitride(BN) is a compound of Boron and Nitride with a chemical formula BN.As a toxic gas, carbonmonoxide still remains as one of the major gaseous pollutants, when the concentration of CO increases, it is dangerous for human body. Several theoretical researches for CO adsorption on various surfaces have been reported[2].We performed DFT calculations to study the adsorption of CO on the B16N16 andB24N24fullerene-like nanocluster.

Computational methods:

All calculations were performed using DFT within M062Xmethod and has been widely used in the nanostructure studies.6-311G** all electron basis sets were used for the optimization, frontier molecular orbital (FMO) analyses, and energy calculations.The adsorption energy of CO molecule on the pure B_nN_n cluster was obtained using the following equation,

E_{ads}=E (B_nN_n/CO) – E (B_nN_n) – E (CO),where E (B_nN_n/CO) is the total energy of B_nN_n/CO complex and E (B_nN_n) or E (CO) is referred to the energy of an isolated $B_nN_n$or COmolecule, respectively.All calculations were implemented in GAUSSIAN 09 package of programs.

Results:

We carried out full structural optimization of the $B_{16}N_{16}$ and $B_{24}N_{24}$ nanoclusters with and without CO gas molecule to examine the energetic, structural, and electronic properties. To find the most favorable adsorption configurations, the adsorbate under consideration is initially placed at different positions above the cluster surface with different orientations. A1, A1 and B1, B2 structures are related to $B_{16}N_{16}$ and $B_{24}N_{24}$ respectively,which shown in Fig.1.Detailed information are listed in Table1 and Table2. In these structures the higher energy is related to A1 and lower energy is related to B2.

The highest occupied molecular orbital (HOMO) and the lowest unoccupied molecular orbital (LUMO) is also desired structures were drawn which For $B_{16}N_{16}$ and $B_{24}N_{24}$shown in Fig2.

Table.1 The adsorption energy (E_{ads}) of CO on the $B_{16}N_{16}$ and$B_{24}N_{24}$nanoclusters, and the change of $B_{16}N_{16}$ and $B_{24}N_{24}$ HOMO–LUMO gap(ΔE_g) upon the adsorption process.

Configuration	E_{ads}(kJ/mol)	ΔE_{gap}(ev)
A1	-10.70	9.14
A2	-8.71	9.13
B1	-8.76	8.75
B2	-6.78	8.76

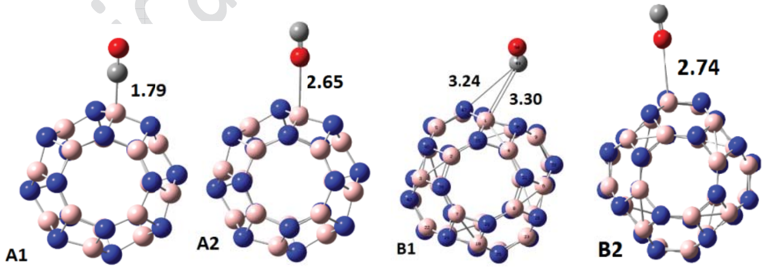

Fig.1 Optimized structures of stable CO/$B_{16}N_{16}$ and $B_{24}N_{24}$ complexes. Distances are in A °

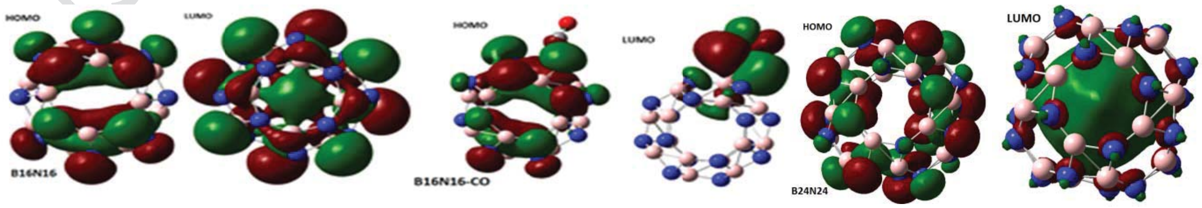

Fig.2 HOMO and LUMO of stable $B_{16}N_{16}$ and B_{16} N_{16}-CO nano-cages and B24N24.

Table2. HOMO–LUMO gap (ΔE_g) for B16N16 and B24N24

Configuration	ΔE_{gap}(ev)
B16N16	9.11
B24N24	8.76

With respect to data, it can be inferred that $B_{16}N_{16}$ and $B_{24}N_{24}$nano-cages function as a gas sensor device against CO molecule.in respect to ΔE_{gap}(ev) A1,A2,B1.B2 and B16N16 , B24N24 all of theminsulators.

Reference:

[1] Nima KarachiAsadollahBoshraSiamakJadidi, " DFT based insights into reactivity descriptors of encapsulated B24N24 nanocages" (2011).

[2] J. Beheshtian, Z. Bagheri, M. Kamfiroozi, A. Ahmadi, " A theoretical study of CO adsorption on aluminum nitride nanotubes" Struct Chem.

[3] K. Azizi, S. MajidHashemianzadeh, Sh. Bahramifar,"Density functional theory study of carbon monoxide adsorption on the inside and outside of the armchair single-walled carbon nanotubes", Current Applied Physics 11 (2011) 776-782.

[4] M.N.Huda and A.K.Ray, "Novel silicon-carbon fullerene cage " Eur. Phys. J. D 31. 63-68(2004).

[5]JavadBeheshtian,Ali AhmadiPeyghan,ZarghamBagheri,MohammadKamfiroozi "Interaction of small molecules (NO, H2,N2, and CH4) with BN nanocluster surface"(2012).

Interaction of CO with BN nanocluster surface

Sima Mehdi Shishvan, Javad Beheshtian*
Department of Chemistry, Shahid Rajaee Teacher Training University, P.O. Box 16875-163, Tehran, Iran
j.beheshtian@Gmail.com

Keywords: Borone Nitride nanocluster, Density functional theory, Adsorption, CO.

Introduction:

Boron nitride (BN) nanomaterials are expected to have vast variety applications as electronic devices, high heat- resistance semiconductors, and insulator lubricants because of providing convenient stability at high temperatures with high electronic insulation in air and also hydrogen storage materials [1]. Borone Nitride (BN) is a compound of Borone and Nitride with a chemical formula BN. As a toxic gas, carbonmonoxide still remains as one of the major gaseous pollutants, When the concentration of CO increases, it is dangerous for human body. Several theoretical researches for CO adsorption on various surfaces have been reported[2].We performed DFT calculations to study the adsorption of CO on the B16N16 and B24N24 fullerene-like nanocluster.

Computational methods:

All calculations were performed using DFT within M062X method and has been widely used in the nanostructure studies.6-311G** all electron basis sets were used for the optimization, frontier molecular orbital (FMO) analyses, and energy calculations. The adsorption energy of CO molecule on the pure BnNn cluster was obtained using the following equation,

Eads=E (BnNn/CO) – E (BnNn) – E (CO), where E (BnNn/CO) is the total energy of BnNn/CO complex and E (BnNn) or E (CO) is referred to the energy of an isolated BnNn or CO molecule, respectively. All calculations were implemented in GAUSSIAN 09 package of programs.

Results:

We carried out full structural optimization of the B16N16 and B24N24 nanoclusters with and without CO gas molecule to examine the energetic, structural, and electronic properties. To find the most favorable adsorption configurations, the adsorbate under consideration is initially placed at different positions above the cluster surface with different orientations. A1, A1 and B1, B2 structures are related to B16N16 and B24N24 respectively, which shown in Fig.1. Detailed information are listed in Table1 and Table2. In these structures the higher energy is related to A2 and lower energy is related to A1.

The highest occupied molecular orbital (HOMO) and the lowest unoccupied molecular orbital (LUMO) is also desired structures were drawn which For B16N16 and B24N24 shown in Fig2.

Table.1 The adsorption energy (Eads) of CO on the B16N16 and B24N24 nanoclusters, and the change of B16N16 and B24N24 HOMO–LUMO gap (ΔEg) upon the adsorption process.

Configuration	Eads(kJ/mol)	ΔEgap(ev)
A1	-104.17	4.66
A2	737.12	9.10
B1	-102.77	6.43
B2	-103.14	6.42

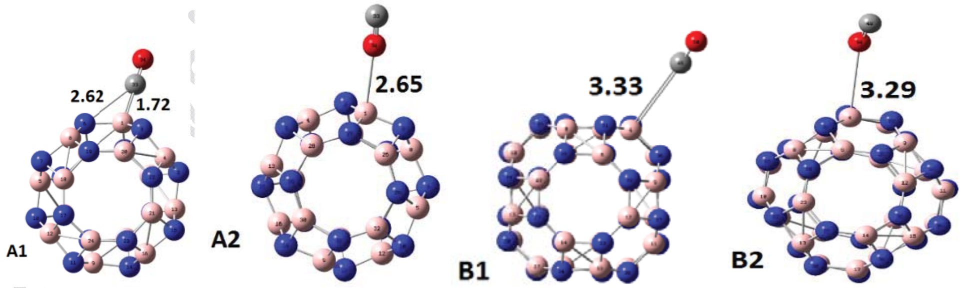

Fig.1 Optimized structures of stable CO/ B16 N16 and B24N24 complexes. Distances are in A °

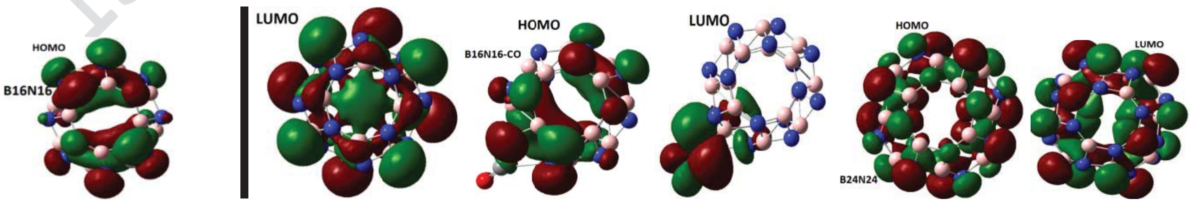

Fig.2 HOMO and LUMO of stable B16N16 and B16 N16 -CO nano-cages and B24N24.

Table2. HOMO–LUMO gap (ΔEg) for B16N16 and B24N24

Configuration	ΔEgap(ev)
B16N16	5.73
B24N24	6.43

With respect to data, it can be inferred that B16N16 and B24N24 nano-cages function as a gas sensor device against CO molecule.in respect to ΔEgap(ev) A1,A2,B1.B2 and B16N16 , B24N24 all of them insulators.

Reference:

[1] Nima Karachi • Asadollah Boshra • Siamak Jadidi, " DFT based insights into reactivity descriptors of encapsulated B24N24 nanocages" (2011).

[2] J. Beheshtian, Z. Bagheri, M. Kamfiroozi, A. Ahmadi, " A theoretical study of CO adsorption on aluminum nitride nanotubes" Struct Chem,

[3] K. Azizi, S. Majid Hashemianzadeh, Sh. Bahramifar, "Density functional theory study of carbon monoxide adsorption on the inside and outside of the armchair single-walled carbon nanotubes", Current Applied Physics 11(2011) 776-782.

[4] M.N.Huda and A.K.Ray, "Novel silicon-carbon fullerene cage " Eur. Phys. J. D 31. 63-68(2004)

[5] Javad Beheshtian, Ali Ahmadi Peyghan, Zargham Bagheri, Mohammad Kamfiroozi "Interaction of small molecules (NO, H2,N2, and CH4) with BN nanocluster surface"(2012)

Theoretical molecular structure and vibrational frequencies of $TlX_3(C_2H_6OS)_2$ (X = Cl, Br, I) complexes

B. Sohrabi*, F. Manteghi*, E. Maddahi*
*Department of chemistry, Iran University of Science and Technology, P.O. Box 16765-163, Tehran, Iran
Email: f_manteghi@iust.ac.ir

Key words: Thallium halide, Frequency, B3LYP, 6-311G(p,d), Lanl2dz.

Introduction:

The halide complexes of thallium (III) in aqueous solution are the most stable metal halide complexes, and they have been intensively studied. Thallium complexes have been used for various applications in diverse fields such as photoelectric cells, insoluble anodes, corrosion inhibitors and fungicides. The detailed structural, equilibrium and dynamics studies have been performed for the thallium (III) halide complexes in aqueous solution [1]. The synthesis of thallium (III) chloride and bromide and iodide was performed in solution by chlorination, bromination and iodination, respectively, of the suspensions of the corresponding thallium (I) halides in acetonitrile. Crystalline compounds $TlX_3(CH_3CN)_2$ (X = Cl, Br, I) were prepared from the acetonitrile solutions. Thallium (III) halide in dimethylsulfoxide solution were obtained by dissolving the corresponding solid compounds $TlX_3(CH_3CN)_2$ (Cl, Br, I) in DMSO. [2]

Methods:

In this work, for the calculations, the title complexes first were optimized by B3LYP with 6-311G(p,d) and Lanl2dz basis sets in the gas phase, 6-311G(p,d) basis set used for light atoms like(H,O,C,S) and Lanl2dz basis set used for heavy atoms like(Tl,X). After the optimization in order to confirm the convergence to minima on the potential surface and to evaluate the zero-point vibrational energies, harmonic vibrational frequencies and corresponding IR intensities of the title complexes were determined using analytic second derivatives with the B3LYP/6-311G (d, p), Lanl2dz method. [3]

Apparatus:

All the calculations were performed using Gaussian 09 program on a personal computer and Gauss View program was used for visualization of the structures.

Results and discussion:

Some of the calculated bond lengths of (1), (2) and (3) are given in Table 1. The selected parameters are very important for these structures and especially, Tl-X bond is the only difference between three structures. Both experimental and calculated (Tl-O) and (Tl-X) distances of (3) are longer than those of (2) and similarly of (2) are longer than those of (1). These compounds consist of 24 atoms, so they have 66 vibrational modes according to 3N-6, and belong to the point group C1 with only identity (E) symmetry element or operation. It is difficult to determine the vibrational assignments of these complexes due to their low symmetry. According to the calculations, 28 normal vibrational modes of both conformations are below 400 cm^{-1} and others are above 400 cm^{-1}. [2]

Table 1. Some selected bond lengths of TlX3(DMSO)2 (X =Cl, Br, I) complexes.

Compound/number	r(Tl-O) Å		r(Tl-X) Å	
	Exp.[11]	B3LYP	Exp.[11]	B3LYP
$TlCl_3(DMSO)_2$/1	2.346 2.394	2.371 2.372	2.3818 2.3975 2.4079	2.526 2.534 2.614
$TlBr_3(DMSO)_2$/2	2.383 2.435	2.415 2.412	2.5069 2.5201 2.5288	2.709 2.692 2.739
$TlI_3(DMSO)_2$/3	2.469 2.468	2.454 2.454	2.717 2.692 2.717	2.936 2.849 2.936

Conclusion:

The theoretical applications of B3LYP method with 6-311G(p,d) and Lanl2dz effective core basis set for $TlX_3(C_2H_6OS)_2$ (X = Cl, Br, I) complexes have been completed with good results. The results obtained in this study also indicate that B3LYP/6-311G(p,d), Lanl2dz method is reliable and it makes easier the understanding of vibrational spectrum and structural parameters of the title complexes.

Reference:

[1] Cemal Parlak, Özgür Alver, Metin Bilge, Hasan Bircan Theoretical molecular structure and vibrational frequencies of TlX_3 $(C_2H_6OS)_2$ (X = Cland Br) complexes

[2] Asadi, H. R., Maliarik, M., Ilyukhin, A., Murashova ,E., Thallium(III) Chloride in Organic Solvents:Synthesis, Solutions and Solvates. The Crystal Structures of Trichlorobis (dimethylsulfoxide)thallium(III)and ribromobis(dimethylsulfoxide)thallium(III), Inorg. Chim. Acta, 362, 2293-2298, 2009.

[3] Frisch, A., Nielsen, A.B., Holder, A.J., Gaussview Users Manual, Gaussian Inc. 2000.

Spectrophotometric determination of acidity constants of Thorin in water, Water-Triton X-100, water-Brij-35 and water-CTAB micellar media solutions by chemometrics method

Ali Niazi[a,*], Meysam Karamivand[b]

[a]Department of Chemistry, Faculty of Sciences, Islamic Azad University Arak Branch, Arak, Iran [b]Department of Chemistry, Islamic Azad University Arak Branch, Arak, Iran

[*] E-mail: a-niazi@iau-arak.ac.ir & ali.niazi@gmail.com

The acidity constants of Thorin in water,water-Triton X-100, water-Brij-35 and water-CTAB micellar media solutions at 25 °C and an ionic strength of 0.1 M KNO3 have been determined spectrophotometrically. To evaluate the pH-absorbance data, a resolution method based on the combination of soft- and hard-modeling is applied. The acidity constants of all related equilibria are estimated using the whole spectral fitting of the collected data to an established factor analysis model. DATAN program applied for determination of acidity constants[1-2-3]. Results show that the pK_a values of Thorin are influenced as the percentages of a neutral and an cationic surfactant such as Triton X-100, Brij-35 and CTAB, respectively, added to the solution of this reagent. Effect of surfactant on acidity constants and pure spectrum of each component are also discussed.

Keywords: Thorin, acidity constants, Triton X-100, Brij-35, CTAB, Spectrophotometric

References

[1] A. Niazi, A. Yazdanipour, J.B. Ghasemi, A. Amini, S. Bozorgzad, M. Kubista. Chem. Eng.Comm, 195 (2008) 1257.

[2] A. Niazi, A. Yazdanipour, M. Ramezani, Chin. Chem. Lett, 18 (2007) 989.

[3] A. Niazi, M.Ghalie, A. Yazdanipour, J. Ghasemi, Spectrochim. Acta Part A, 64 (2006) 660.

Classical and statistical Thermodynamics

Investigation on Metalosalen Complexes Binding to ct-DNA using UV/Vis spectroscopy

N. Sohrabi[a*], G. Ghasemi[b], N. Rasouli[a], M. Jahangiri Lahkani[a]
a Department of Chemistry, Payame noor university, Tehran, I. R. IRAN
b Department of Chemistry, Rasht Branch, Islamic Azad University, Rasht, Iran
Email:sohrabnas@pnu.ac.ir

Key words: Salen, Schiff Base Ligand, Ct-DNA, Ct-DNA Thermal Deneration

Introduction:

Schiff base was first reported by Hugo Schiff in 1864 [1]. Schiff bases can be prepared by condensing carbonyl compounds and amines in different conditions and in different solvents with the elimination of water molecules. Schiff bases have been playing an important part in the development of coordination chemistry. Schiff base metal complexes have been studied extensively because of their attractive chemical and physical properties and their wide range of applications in numerous scientific areas. These types of complexes have been vigorously explored in recent years and such studies have been the subject of many papers and reviews. Many of them are centered on the catalytic activity of Schiff base complexes in a large number of homogeneous and heterogeneous reactions. It is difficult to cover in this chapter the literature on Schiff base metal complexes, which embraces very wide and diversified subjects comprising vast areas of organometallic compounds and various aspects of bioinorganic chemistry.

Salen type complexes are a fundamental class of compounds in coordination chemistry, known since 1933[2]. They have been extensively studied and more than 2500 have been synthesized [3]. The argument of this study is the synthesis and characterization of metal complexes and the study of their interaction with native deoxyribonucleic acid (DNA). It is in fact known that DNA is a major target of anticancer drugs and that the most common clinically used metallo-based anticancer-drugs are today platinum compounds able to covalently bind to the DNA macromolecule [4].

Materials and methods:

In this study, physicochemical properties of salen type complexes N,N′-bis(Salicylidene)1,2-ethylenediamine nickel, N,N′-bis(Salicylidene)1,2-ethylenediamine copper, Cu(II)Salen(O) and Ni(II)Salen(O) were investigated by UV/Vis spectroscopy method and the denaturation of ct-DNA solution presence and absence of salen type complexes studied between 24-86 ^{o}C. The melting points were calculated using Igor software.

Apparatus:

Spectrophotometer model Perkin - Elmer (lambda 25) that is equipped thermal bath was used. This device is connected to a computer. Digital pH meter with an accuracy of one hundredth Metrohm model and adjustable temperature.

Result and discussion:

Interaction of small molecules with double helix is known to increase the melting point temperature at which the double helix denatures into single stranded DNA . the melting temperature can be determined by monitoring the absorbance of the DNA at 260nm as a function of temperature. Thermal denaturation profile of CT-DNA solution in the absence and presence of increasing amount of four Schiff base complexes, were obtained by plotting the absorbance for each solution by mole ratio of any Schiff base to CT-DNA as 0, 0.013, 0.026, 0.052 and0.104 as a function of temperature. It is known that when the temperature in the solution increases, the double stranded DNA gradually dissociate into single strand; T_m is therefore defined as a temperature where half of total base pairs is unpaired. The DNA melting temperature T_m is strictly related to the stability of the double helix, and the interaction of chemical with DNA may alter T_m, by stabilizing or destabilizing the final complex. The presence of the positive charge on the intercalate should further increase the attractive interaction with the negatively charged phosphate groups and help the intercalative mechanism[5]. The melting temperature carried out for CT-DNA in the absence of any added complex revealed at T_m of 74.5±0.5°C under our experimental condition, the melting temperature of CT-DNA $1.268*10^{-5}$ M increase about 1 to 8°C at mole ratio of Schiff base to CT-DNA as 0 , 0.013, 0.026, 0.052 and0.104 .These results are indicative of strong metal complex=DNA interaction, that stbilizesthe native DNA conformation.

Conclusion:

The increasing of melting temperature (Tm) of CT-DNA upon addition of Schiff base complexes represents the stable interaction between CT-DNA and Schiff base complexes.

Reference:

[1] H. Schiff. Annalen, 1864, 131, 118.
[2] P. Pfeiffer, E. Breith, E. Lübbe and T. Tsumaki, *Liebigs Ann.*, 1933, 503, 84.
[3] C. T. Dalton, K. M. Ryan, V. M. Wall, C. Bousquet and D. G. Gilheany, *Top. Catal.*, 1998, 5,75.
[4] V. Brabec and J. Kasparkova, *Drug Resistance Updates*, 2005, 131, 146.
[5] (a) Mandal, S. S., Vinaykumar, N., Varshney, U., and Bhattacharya, S. (1996) J. Inorg. Biochem. 63, 265. (b) Bhattacharya, S., and Mandal, S. S. (1997) Biochem. Bioph

Viscometery and UV/Vis Spectral Investigation on Interaction of Bis 5-Phenyl Azo Salicyl aldehyde Ethylene di imin Cobalt (II) With Calf Thymus Deoxy Ribonucleic Acid .

N.Sohrabi* , N.Rassoli , M.Kamkar.d
Department of Chemistry P.N.U of Iran 19395-3697
E.MAIL : sohrabnas@pnu.ac.ir

Keyword: Salen , DNA , UV/Vis Spectroscopy , Viscosity , Thermal Denaturation

Introduction:

Schiff-base ligands have been reported to show a variety of biological action by virtue of the azomethine linkage, which is responsible for various anti-bacterial, anti-fungal, anti-cancer, anti-viral, herb cal, clinical and analytical activities and this activity tends to increase in metal(II) Schiff-base complex [1] . The chemistry of Schiff-base ligands and their metal complex has expanded enormously and encompasses a vast area of organometallic compounds and various aspect of bioinorganic chemistry [2]. The chemistry of metal complexes containing Schiff base ligands derived from condensation of aldehydes and amines is of enduring significance, since they have common features with metalloprophyrines with respect to their electronic structure and catalytic activities that mimic enzymatic oxidation [3].

Arturo Silvestre et all , reported on the interaction of calf thymus DNA with Fe(III) Salen, that results obtained have been interpreted in terms of an electrostatic binding of $[Fe(salen)]^+$ cation and the phosphate group of DNA [3]. Design and synthesis of small synthetic systems that recognize specific sites of DNA is an important area of much current research these could be at least in part due to the formation of none covalently associated complexes by several such molecules with nucleic acids.

In this study the interaction of CoBBASE with CT-DNA was analyzed by using UV/Vis spectroscopic method in various conditions as concentration and temperature, and then binding constants, binding mode, and the binding thermodynamic parameters was determined. The results obtained by UV/Vis spectroscopy with changing in temperature, DNA thermal denaturation and viscositymetery.

Materials and Methods:

In this study we use CoBBASE that is a red solid with Mw = 532.24g/mol and CT-DNA that obtained from Sigma Aldrich and NaCl , HCl, H_2SO_4, EDTA. Absorbance spectra were recorded using a lambada 25 double beam spectrophotometer. The absorbance measurements were performed by keeping the concentration of the CT-DNA constant while varying the CoBBASE added to the cell. The absorbance at 403 nm was recorded after each addition of CoBBASE and repeat this way in various temperatures such as, 30, 35, 40, 45 and 50°C. The intrinsic binding constant K_b was determined for interaction between CoBBASE and CT-DNA.

Also we studied the effects of addition of various concentration of metal complex with concentration of $9.4*10^{-5}$mM to CT-DNA. And then the viscosities of solution contain CT-DNA and CoBBASE complex were studied by Ostwald viscometer.

Denaturation and changing in melting temperatures for DNA in the absence and in the presence of various CoBBASE complexes were measured by following the changes in the UV/Vis absorption spectra at 260 nm as a function of temperature. The absorption intensities at 260 nm were plotted against individual temperatures in the presence of each concentration of CoBBASE complex, and the midpoints of the inflection regions in the temperature vs A_{260} curves were taken as the corresponding T_m values.

Results and discussion:

The UV/Vis spectra of CoBBASE at 25°C between 200-700 nm showed two peaks at 275 and 403 nm , that peak on 403nm assigned to transfer charge in complex.

To study about thermal stability of CoBBASE , we repeat UV-vis spectroscopy in various concentration with increasing temperature in 30,35,40,45 and 50°C .

The UV-vis spectra of interaction between CoBBASE and CT-DNA were recorded in various temperatures. UV-vis spectra shows that by increasing concentration of CoBBASE vs CT-DNA absorbance increase and it has the same treat for all temperatures 25, 30,35,40,45 and 50°C.

Intercalating agents are expected to destack the base pairs causing elongation of the double helix resulting in an increase in the viscosity of CT-DNA. On the other hand viscosity of CT-DNA in the presence of $Co2^+$ BBASE, which bind to CT-DNA by non-intercalative mode has been found to decrease in the presence of small amount of complex and subsequently increase as the CoBBASE concentration increases.in the presence of CoBBASE complex viscosity of CT-DNA has been found to dependence on complex concentration[4].

The viscometers data shows that there are two phase of binding between the Co (II) complex and CT-DNA. In principle, decrease in viscisity could be explained by the effects like change in conformation flexibility or salvation of the CT-DNA molecules. by increasing in CoBBASE concentration, viscosity of CT-DNA show increase, it would indicate that the binding of CoBBASE complex with CT-DNA could be surface binding or by forming bridged adduct.

Interaction of small molecules with double helix is known to increase the melting point temperature at which the double helix denatures into single stranded DNA . the melting temperature can be determined by monitoring the absorbance of the DNA at 260nm as a function of temperature.

Thermal denaturation profile of CT-DNA solution in the absence and presence of increasing amount of CoBBASE, were obtained by plotting the absorbance for each solution by mole ratio of CoBBASE to CT-DNA as 0, 0.013, 0.026, 0.052 and0.104 as a function of temperature.

It is known that when the temperature in the solution increases, the double stranded DNA gradually dissociate into single strand; T_m is therefore defined as a temperature where half of total base pairs is unpaired. The DNA melting temperature T_m is strictly related to the stability of the double helix, and the interaction of chemical with DNA may alter T_m, by stabilizing or destabilizing the final complex. The presence of the positive charge on the intercalate should further increase the attractive interaction with the negatively charged phosphate groups and help the intercalative mechanism[5].

The melting temperature carried out for CT-DNA in the absence of any added complex revealed at T_m of 74.5±0.5°C under our experimental condition, the melting temperature of CT-DNA $1.268*10^{-5}$ M increase about 1 to 8°C at mole ratio of CoBBASE to CT-DNA as 0 , 0.013, 0.026, 0.052 and0.104 .These results are indicative of strong metal complex=DNA interaction, that stbilizesthe native DNA conformation.

Conclusion:

The binding of CoBBASE complex to CT-DNA, while the wavelength of maximum absorption ,λ_{max} does not show considerable changes the amount of absorption increases, represents the outside-binding and hydrophobic interaction modes. The increasing of viscosity of CT-DNA upon addition of CoBBASE represents the stable interaction by non-intercalative mode between CT-DNA and CoBBASE.

The CT-DNA-binding process is endothermic for CoBBASE and has the large positive entropy value. These can be represent the predominate role of electrostatic interactions and outside binding mode. The increasing of melting temperature (Tm) of CT-DNA upon addition of CoBBASE represents the stable interaction between CT-DNA and CoBBASE.

References :

[1] (a) Sigman, D. S., Bruice, T. W., Mazumder, A., and Sutton,C. L. (1993) Acc. Chem. Res. 26, 98. (b) Barton, J. K., and Pyle, A. M. (1990) Prog. Inorg. Chem. *38*, 413. (c) Burkhoff,A. M., and Tullius, T. D. (1988) *Nature 331*, 455. (d) Riordan, C. G., and Wei, P. J. (1992) *J.* Am. Chem. Soc. 116, 2189.

[2] (a) Tan, J. D., Hudson, S. E., Brown, S. J., Olmted, M. M.,and Mascharak, P. K. (1992) J. Am. Chem. Soc. 114, 3841. (b) Nagai, K., Carter, B. J., Xu, J., and Hecht, S. M. (1991) J. Am. Chem. Soc. 113, 5099. (c) Nicolau, K. C., Maligres, P.,Shin, J., de Leon, E., and Rideout, D. (1992) J. Am. Chem.Soc. 114, 7825.

[3] Sato, K., Chikira, M., Fujii, Y., and Komatsu, A. (1994) J. Chem. Soc., Chem. Commun., 625.

[4] (a) Gravert, D. J., and Griffin, J. H. (1993) J. Org. Chem.58, 820. (b) Gravert, D. J., and Griffin, J. H. (1996) Inorg.Chem. 35, 4837.

[5] (a) Mandal, S. S., Vinaykumar, N., Varshney, U., and Bhattacharya, S. (1996) J. Inorg. Biochem. 63, 265. (b) Bhattacharya, S., and Mandal, S. S. (1997) Biochem. Biophys.

Viscosity Behavior of Glass-forming Liquids and Fluidity Equation

M. H. Ghatee* and M. Zare

Department of chemistry, Shiraz University, Shiraz, Iran, 71454

(E-mail: ghatee@susc.ac.ir)

Keywords: Glass-formers, Correlation, Dynamic crossover, Fluidity equation.

Introduction

A glass forming liquid is known to not forming crystals upon cooling and undergoes a liquid–glass transition. When the temperature of a liquid decreases its viscosity increases and below the melting point (T_m), in the case of a supercooled liquid, near to the glass transition temperature (T_g), the viscosity continues increasing until the liquid solidifies. Some information about the nature of the glass transition can be attained by surveying the manner in which the viscosity approaches to a limiting value in the solid state. Recently, we have developed a new equation for the temperature dependent viscosity of ionic liquids [1]. In this investigation, we examined the applicability of this equation for the conventional glass-forming liquids including α-phenyl-o-cresol, salol and tri-α-naphthylbenzene. Also dynamic crossover phenomenon as a common behavior for glassy liquids is investigated.

Results and discussion

According to the temperature dependence of viscosity, liquids are classified as strong or fragile [2]. When the viscosity of a liquid follows Arrhenius equation, it is considered as a strong liquid, but a fragile liquid has quite non-Arrhenius behavior. There is some evidence for existing two different regimes in the temperature dependent viscosity of a glass forming liquids. As the temperature of a fragile liquid decreases, its temperature dependence of viscosity smoothly crosses over to a strong regime. The temperature in which this transition takes place is called fragile-to-strong, FS, crossover temperature T_x, where $T_g < T_x < T_m$. Fig. 1 shows the Arrhenius plot (log □ vs. $1/T$) of glassy liquids, where □ is the viscosity. Both strong and fragile behaviors and thus FS crossover are observed. At low temperatures the viscosity conforms to an Arrhenius behavior, but a non-Arrhenius behavior is observed for $T > T_x$. We have shown that the following simple linear equation can be used for $T > T_x$ [1]:

$$\left(\frac{1}{\eta}\right)^{\phi} = a + bT \qquad (1)$$

where *a* and *b* are constants characteristics of the liquid. □ is the fluidity exponent and in general depends on the liquid. Recently [3], we found that the ($-a/b$) is an estimation of T_x. For $T > T_x$ the dynamic viscosity values were fitted using the Eq. (1). The parameters of the Eq. (1), the correlation coefficient squared (R^2) and the values of T_x=($-a/b$) are listed in Table 1. Also, the values of T_x which obtained directly from the Fig. 1 are listed in the Table 1. A good agreement is observed among the resulted T_x values by two alternative methods. As is expected, T_x takes place in the interval from T_g to T_m.

Table 1. Fitting parameters of Eq. (1), R^2, T_x, T_g and T_m.

Liquids	*a*	*B*	□	R^2	$(-a/b)^a$	T_x^b	T_g	T_m
α-phenyl-o-cresol	-8.23	0.0326	0.392	0.996	252	247	220	323
salol	-8.46	0.0336	0.332	0.999	252	257	220	318
tri-α-naphthylbenzene	-7.26	0.0182	0.331	0.997	399	397	340	442

[a] T_x from the Eq. (1), [b] T_x from the Fig. 1

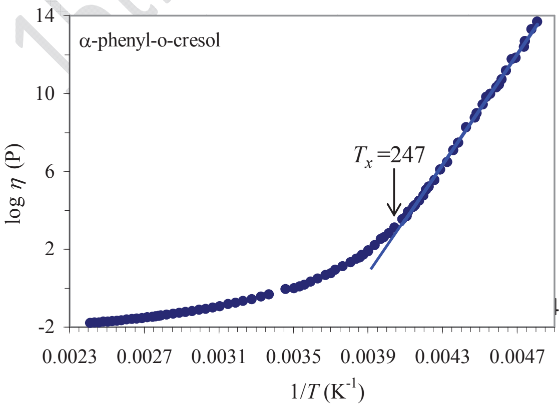

Fig. 1. The dynamic crossover phenomenon in the viscosity behavior for three common glass-forming liquids. (●) experimental viscosity; the blue solid lines represent Arrhenius law.

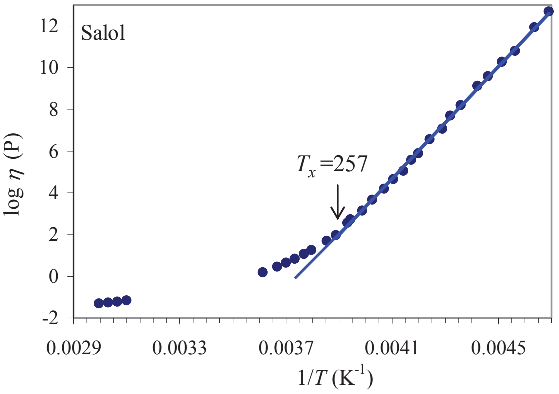

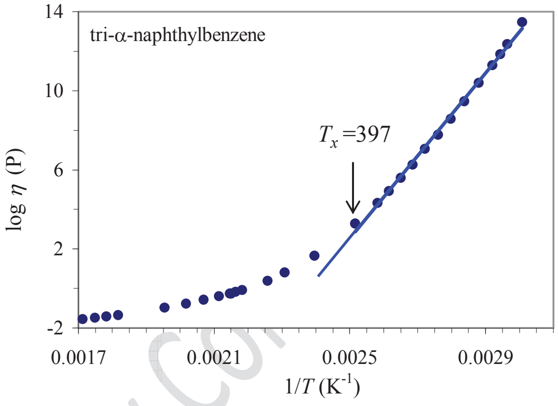

References:

[1] M.H. Ghatee et al.; Fluid Phase Equilib.; 291, 188–194, 2010.

[2] C.A. Angell; J. Non-Cryst. Solids; 13, 131–133, 1991.

[3] M.H. Ghatee and M. Zare; Fluid Phase Equilib.; 311, 76–82, 2011.

Protonation Constants of 5'-IMP in Different Aqueous Solutions of Methanol

F. Kiani [a*], F.Gharib [b], A. A. Rostami [c], S. Sharifi [d], A. Bahadori [d]
[a]Chemistry Department, Faculty of Sciences, Islamic Azad University, Ayatollah Amoli Branch, Amol, Iran
[b]Chemistry Department, Shahid Beheshti University, G. C., Tehran, Evin, Iran
[c]Physical Chemistry Department, Faculty of Chemistry, University of Mazandaran, Mazandaran, Iran
[d]Chemistry Department, Faculty of Sciences, Islamic Azad University, Arak Branch, Arak, Iran
Email: farhoush_kiani@yahoo.com

Keywords: Dissociation Constants, Inosine 5'-monophosphate, Methanol, spectroscopic study

Introduction:

Inosine 5'-monophosphate (IMP) is a nucleotide (Scheme 1). The acid-base behavior of nucleotides, nucleosides, and polynucleotides is essential to deduce the speciation and the possible conformational changes with pH or the amount of organic solvent in solution. But in determination of acidity constans of these molecules we are faced with several drawbacks, such as low solubility in aqueous solutions and the low values of acidity constants. Therefore, we forced to choose mixed solvents [1]. Two solvents mixed together produce a solvent with quite different properties, both, physically (dielectric, density and viscosity) and chemically (acid-base and donor-acceptor properties). By mixing solvents of different polarity in proper ratio, dielectric constant of the medium can be varied and, at the same time, the strength of dissolved acids and bases. It should also be emphasized that solvent mixtures can be more convenient than individual solvents owing to enhanced solubilising efficiency, increased sharpness of color change of indicators during titration and more manageable shape of acid-base titration curves [2]. However, chemists have usually attempted to understand solvent effects in terms of polarity, defined as the overall solution capabilities that depend on all possible (specific and nonspecific) intermolecular interactions between solute and solvent molecules [1]. In this study the protonation constants of Inosin 5'-monophosphate (IMP) have been determined in different aqueous methanol mixtures to examine the dependence of acid-base equilibria on solvent composition.

Materials and Methods:

Sodium salt of Inosin 5'-monophosphate and methanol were of analytical reagent grade (Merck). These chemicals were used without further purification. Sodium perchlorate (Merck) was dried under vacuum at room temperature. NaOH solution was prepared from a titrisol solution (Merck). Perchloric acid (Merck) was used as supplied. All dilute solutions were prepared from double-distilled water with conductance equal to (1.3 ± 0.1) μS. All measurements were performed at 25 °C. The protonation constants were evaluated from the measurements of absorbance versus emf by titration of 25 mL Sodium salt of Inosin monophosphate (1.0 to 3.0) $\times 10^{-3}$ mol dm^{-3} with 0.1 mol dm^{-3} sodium hydroxide solution and a constant ionic strength of 0.1 mol dm^{-3} $NaClO_4$ and mole fraction of organic solvent 0 to 60 % methanol (v/v). The recorded emf values were then converted to p_cH (-log[H^+]) using a method described in the literature [1].

Apparatus:

The electromotive force was measured using a Metrohm model 781 pH ion-meter. A combined glass-pH electrode (model 6.0258.000) was modified by replacing its aqueous KCl solution with 0.01 mol dm^{-3} NaCl + 0.09 mol dm^{-3} $NaClO_4$ saturated with AgCl. All titrations were carried out in an 80 mL thermostatted double-walled glass vessel. Spectrophotometric measurements were performed on a UV-vis Shimadzu 2100 spectrophotometer and using thermostatted matched 10 mm quartz cells. The absorbance and the emf (–log[H^+]) of the solution were measured simultaneously.

Results and Discussion:

The protonation constants of IMP have been determined based on the relation A = f(pH) [3]. The measured absorbance and p_cH from the spectrophotometric titration were conducted using the computer

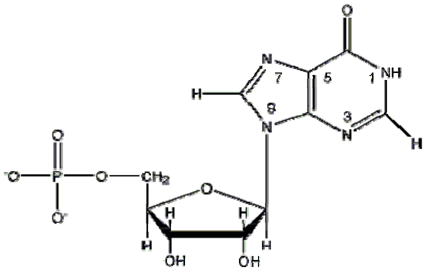

Scheme 1. Chemical Structures of Inosine 5′-monophosphate (IMP)

program which employs a least-squares method. the results obtained for the various protonation constants in different aqueous solutions of methanol , eq 1, are shown in Figure 2.

$$H_nL^{n-1} + H^+ \rightleftarrows H_{1+n}L^{n+} \qquad K_{1+n} = [H_{1+n}L^{n+}] / [H_nL^{n-1}][H^+] \qquad (1)$$

where HL represents inosine 5'-monophosphate and n may be 0, 1 or 2 for the different protonation equilibria of the base. With little differences, the protonation constant values obtained in this work are in agreement with those reported before. The differences are possibly due to the different experimental method and the different background electrolyte used. The IMP^{2-} shown in Scheme 1 may bind with two protons at the phosphate group and one at the purine moiety, (N-7). It was proposed that $H_3(IMP)^+$ releases its first proton from $P(O)(OH)_2$, the second one from H^+ (N-7) and the third one again from the phosphate group. A forth proton is released in the alkaline pH range from the neutral H (N-1) site [4].

Conclusion:

Aqueous organic solvent, mainly methanol and ethanol mixtures have been widely used due to the sparingly or insolubility of many compounds in pure water as solvent. The protonation constants of Inosine 5'-monophosphate (K_1 to K_2) were determined in binary mixtures water-methanol using a combination of potentiometric and spectrophotometric methods. Effect of solvent composition on pure spectrum of each component are also investigated. There is linear relationship between acidity constants and the mole fraction of methanol in the solvent mixtures. As precent of methanol increases in solvent mixtures the protonation constants also increased.

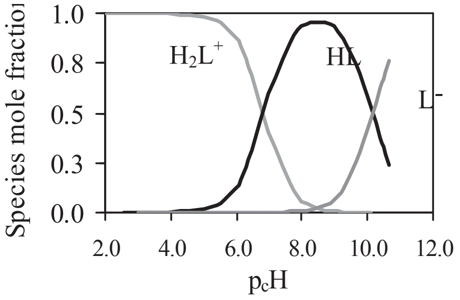

Figure 1. Distribution diagrams of the different species of IMP in water

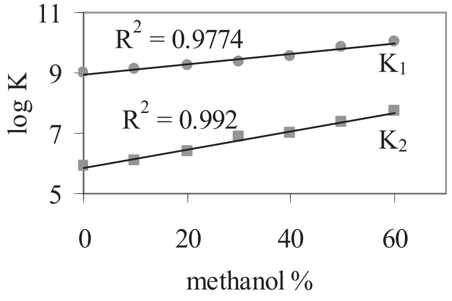

Figure 2. Plots of the experimental values of log K_1 and log K_2 of IMP versus % methanol (v/v)

Referencces:

[1]. Shamel, A. et al.; "Protonation Constants of Adenine and Adenosine in Different Aqueous Solutions of Methanol and Ethanol."; J. Chem. Eng. Data; 55, 5176–5181, 2010.

[2]. Niazi, A. et al.; "Spectrophotometric determination of acidity constants of Alizarine Reds in water, water-Brij-35 and water-SDS micellar media solutions"; Spectrochim. Acta, Part A ; 64, 660-664; 2006.

[3]. Beck, M. T. and et al.; "Chemistry of complex equilibria"; Ellis Harwood; New York; 1990.

[4]. Gharib, F. et al.; "Interaction of dimethyltin(IV) dichloride with 5'-IMP and 5'–UMP"; Appl. Organometal. Chem.; 22, 215–220, 2008.

Density calculation using an extended LJ potential-based equation of state for quantum light molecules at supercritical region

Majid Moosavi
Dept. of Chemistry, Faculty of Sciences, University of Isfahan, Isfahan 81746-73441, Iran
Email: m.mousavi@sci.ui.ac.ir

Keywords: Equation of state, ELJ potential, Quantum light molecules, Molar density.

Introduction:

Fluid densities are needed in many engineering problems such as process calculations, simulations, equipment and pipeline design, and liquid metering calculations. Fluid densities are usually calculated using correlations or equations of state. A large number of publications deal with the development or improvement of equations of state. These equations must be simple, accurate, and also predictive so that they can be used when experimental data are not available.

Theory:

A general equation of state has been suggested on the basis of an effective near-neighbor pair potential of an extended Lennard-Jones (ELJ) (12,6,3). This regularity is valid for all types of solids and fluids, even for those do not work with the LIR EoS [1] and also equation proposed by Ghatee and Bahadori [2]. The ELJ (12,6,3) potential function is given by [3]:

$$U = \frac{N}{2} z \left(\frac{C_{12}(T)}{\bar{r}^{12}} + \frac{C_6(T)}{\bar{r}^6} + \frac{C_3(T)}{\bar{r}^3} \right) \tag{1}$$

where $\bar{r}$ is a mean near-neighbor distance and z is the average number of nearest neighbors, and the $C_i(T)$'s are temperature dependent parameters. On the basis of the ELJ (12,6,3), the general equation of state has been obtained as follows [3] (ELJ-based EoS):

$$(Z-1)V_m^2 = e(T) + \frac{f(T)}{\rho} + g(T)\rho^2 \tag{2}$$

where *e(T)*, *f(T)*, and *g(T)* are temperature dependent parameters. The molar density of these systems at any temperature and pressure can be calculated via the following equation:

$$g(T)\rho^5 + e(T)\rho^3 + f(T)\rho^2 + \rho - \frac{P}{RT} = 0 \qquad (3)$$

Results and discussion:

In this work, the extended Lennerd-Jones potential-based equation of state (ELJ-based EoS) has been extended to predict the density of quantum light molecules up to extremely high temperature, high pressure (HTHP) conditions at supercritical region. There are no upper and lower density limitations for this EoS. Having the temperature dependence of the parameters of the new EoS, the parameters can be determined at any temperature for each of quantum light molecules, including hydrogen (H_2), para-hydrgen (p-H_2), Deuterium (D_2), helium (He), and neon (Ne). A comparison with literature tabulated values has been made. The results show that the ELJ-based EoS can be used to reproduce and predict the density of quantum light molecules within experimental errors. The average absolute deviations are better than 0.13 %.

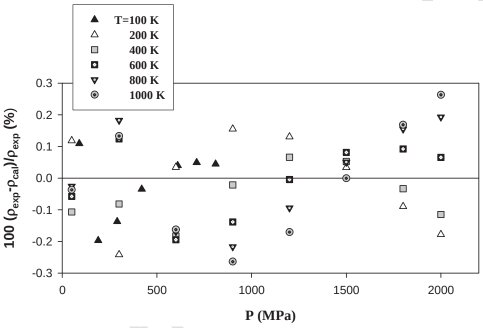

Fig. 1. Percent deviations between the experimental and calculated density data for H_2.

Table 1. The statistical parameters between experimental and calculated densities for quantum light molecules.

Fluid	Bias (%)	AAD (%)	RMSD (%)	NP
H_2	-0.0130	0.1257	0.1629	281
P-H_2	-0.0057	0.0799	0.1006	84
D_2	-0.0062	0.1103	0.1379	187
He	0.0949	0.0995	0.2280	120
Ne	0.0009	0.0558	0.683	135
Overal	0.0142	0.0942	0.2625	807

Conclusion:

The extended Lennerd-Jones potential-based equation of state (ELJ-based EoS) was developed to predict the density of quantum light systems up to the extremely high temperature, high pressure

(HTHP) conditions and found that it can be applied for these compounds successfully. Our results are in good agreement with the experimental and the previous literature data up to high temperatures and pressures. In general, the ELJ-based EoS can provide a simple procedure for prediction of thermodynamic properties of different classes of hydrocarbons.

References:

[1] G.A. Parsafar, E.A. Mason, J. Phys. Chem. 97, 9048–9053, 1993.

[2] M.H. Ghatee, M. Bahadori, J. Phys. Chem. B 105, 11256–11263, 2001.

[3] G.A. Parsafar, H.V. Spohr, G.N. Patey, J. Phys. Chem. B 113, 11977–11987, 2009.

Study Of Ni(II)-G lycinamide Complex Formation By Spectrophotometric Method In Various Temperatures And pH=4.0 , I=0.5

N.Tajdini[a]*
Nilofar_tajdini@yahoo.com
[a]Department of Chemistry, Islamic Azad University, Vramin Pishva, Iran

Keywords: Glycinamide, SQUAD, Optical absorption, Formation constants

Introduction:

The metal coordination in metal amino acid complexes has received much attention [1-2].

Methods:

All experiments were carried out in double distillated water at pH=4.0 potassium hydrogen phthalate ,hydrochloric acid buffer and 0.5M $NaClO_4$ .In typical experiment, 2ml of $Ni(NO_3)_2$ solution 0.03M in 0.5M $NaClO_4$ (ionic strength) was titrated by glycinamide 0.24M solution.UV-Vis spectra of combinations were recorded in range of 200-800nm in 10 minutes after adding 50µl glycinamide solution.

Results and discussion:

◌́◌́◌́◌́◌́◌́◌́◌́The figure 1 show typical titration spectras of $Ni(NO_3)_2$ upon increasing addition of glycinamide at 25.0^oC. The observed spectral changes were used for determining the combining constants due to by using SQUAD program which was developed to empower the evaluation of the best combining constants due to absorbance measurements by using a non-linear least-square method. The input data consist of (a) the absorbance values(b) the total glycinamide and $Ni(NO_3)_2$ concentrations. The Gauss-Newton non-linear least-squares algorithmis is used for making minimum total residual squares,calculating of eq.no.1.

$$U = \sum_{i=1}^{I} \sum_{k=1}^{NW} \left(A_{i,k}^{cal} - A_{i,k}^{obs} \right)^2 \tag{1}$$

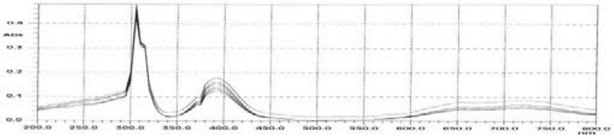

Figure1.The titration absorption spectra of $Ni(NO_3)_2$ (0.03M) by Ga (0.24M) in $NaClO_4$ 0.5M at 298K

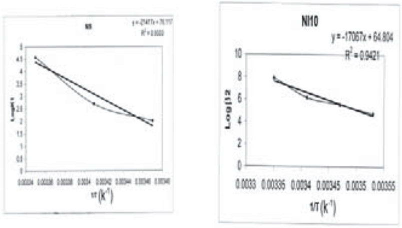

Fig. 2,3. The vant't Hoff plots of Ga to $Ni(NO_3)_2$

Table 1. Thermodynamic parameters and binding constants for binding of $Ni(NO_3)_2$ to Glycinamide

T (K)	log β (M^{-1})	ΔG^0_T (kJ mol^{-1})	ΔH^0_T (kJ mol^{-1})	ΔS^0_T (J mol^{-1} K^{-1})
283	4.74±0.84	-25.7	326.8	1245.6
288	5.53±0.71	-30.5	326.8	1240.6
293	6.17±0.47	-34.6	326.8	1233.4
298	7.94±0.00	-45.3	326.8	1248.7
303	8.50	-49.3	326.8	1241.3

Conclusion:

in respect to our results,the stoichiometry of glycinamide-$Ni(NO_3)_2$ combining are as 1:1 and 2:1.

References:

[1] Y. Prashanthi, K. Kiranmai, N.J.P. Sabhashini, Shivaraj, Spectrochim. Acta A.,70,30 (2008).

[2] A.A. Shoukry, M.M. Shoukry, Spectrochim. Acta A.,70,686 (2008).

Modelling the Vapor-Liquid Equilibria Using Modified van der Waals Family Equations of State

Mohammad Mehdi Papari[1,*], Sayed Mostafa Hosseini[2], Jalil Moghadasi[2]
[1]Department of Chemistry, Shiraz University of Technology, Shiraz, 71555-313, IRAN
[2]Department of Chemistry, Shiraz University, Shiraz, 71454, IRAN
Email: Papari@sutech.ac.ir

Keywords: Equation of state; Fugacity coefficient; VLE, Mixing rule

Introduction:

The knowledge of vapor-liquid equilibria (VLE) properties of fluids and fluid mixtures is important for separation processes and production operations including refinery and petroleum reservoir industries. Under these circumstances the development of PVT EOSs and PVT correlations for modeling of the VLE properties can be highly useful.

Recently Papari et al. [1] modified van der Waals (vdW) family EOSs to improve their ability to represent the volumetric properties of compressed liquids of various fluids.

In this work we employ the revised method developed previously by Chen et al. [2] and the modified vdW family EOS to model the vapour-liquid equilibrium of non-polar and polar fluids. The modified van der Waals type EOS includes the Scott [3] and Carnahan-Starling (CS) [4] repulsion terms.

The method:

The revision method used in this work includes two parts: 1) modification of van der Waals co-volume of pure fluids and 2) revision of fugacity expression for the saturated liquid. A temperature-dependent revision factor was introduced to the liquid fugacity coefficient expression derived from traditional isothermal integration, and the vapor pressure of pure liquids was then successfully reproduced.

The revised fugacity coefficient for liquid phase is then formulated as:

$$\phi^{L} = \alpha(T_r)\,\phi^{L}_{EOS} \qquad (1)$$

The subscript EOS stands for properties determined from equations of state employed in this work.

Results and discussion:

We applied our method to model the VLE and PVT behaviour of 23 pure substances and 7 binary mixtures. Typically, the saturated density-temperature curves for argon and CO_2 and have been shown in Figures 1 and 2, respectively. The solid lines represent the saturated densities obtained from vdW-CS EOS together with our method and the dashes lines are those calculated from the vdW-CS EOS. The markers are those taken from the literature [5]. As it is obvious, our method can successfully model the PVT behaviour fluids including monatomic or polyatomic molecules in both liquid and vapour states. The same behaviour has been observed for vapour pressure of all studied fluids.

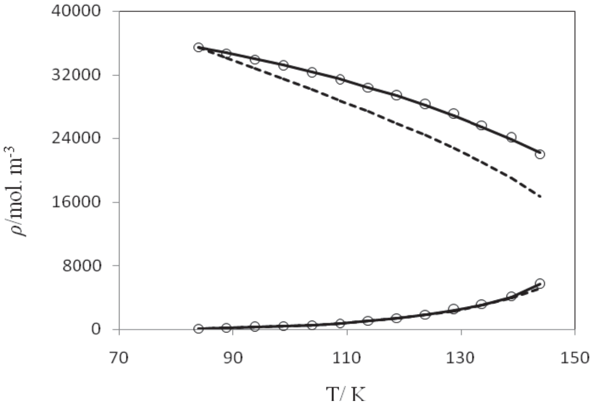

Figure 1 Saturated density-temperature curve for argon.

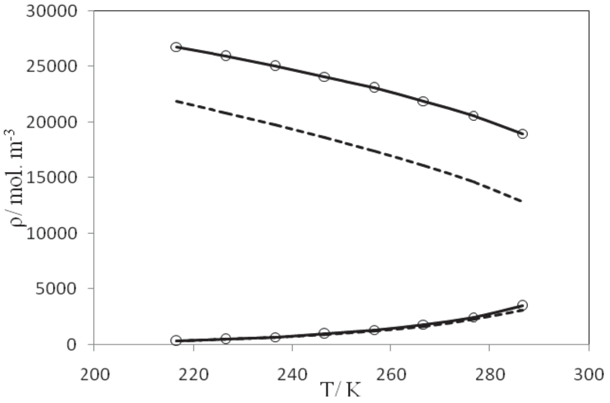

Figure 2 The same as Fig. 1 for CO_2 .

References:

[1] M.M. Papari, J. Moghadasi, S. M. Hosseini, F. akbari, J. Mol. Liq. 158 (2011) 57–60.

[2] G.-J. Chen et al., Chem. Eng. Sci. 55 (2000) 4913-4923

[3] R.L. Scott, in: H. Eyring, D. Henderson, W. Jost (Eds.), Physical Chemistry: an Advanced Treatise, Academic Press, New York, (1971).

[4]. N. F. Carnahan and K. E. Starling, J. Chem. Phys., **51** (1969) 635-636.

[5] NIST chemistry webbook.

Excess Molar Enthalpies of isobutanol (1) + 1-alkanols (C_1–C_3) (2) at 298.15 K and Correlated with NRTL model

H. Iloukhani[a], K. Khanlarzadeh*[a]

a Department of Physical Chemistry, Faculty of Chemistry, Bu-Ali Sina University, Hamedan , Iran

Email: kh.khanlarzadeh@basu.ac.ir

Key words: Excess molar enthalpy, Isobutanol, Methanol, Ethanol, 1-Propanol, NRTL model

Introduction:

The thermophysical properties are important to quantify the deviation from ideality of the thermodynamic functions of mixtures, which result essentially from molecular interactions [1]. 1-alkanols are of great interest nonideal compounds due to they can form complex structure [2]. In this project excess molar enthalpies, for binary mixtures of isobutanol + methanol, ethanol and 1-propanol at 298.15 K were measured experimentally by a solute calorimeter. The experimental results were correlated with a polynomial Redlich–Kister equation [3] for binary mixtures to estimate the coefficients. The excess molar enthalpies are negative over the entire range of composition for all mixtures. These indicate that isobutanol interacts more strongly with 1-alkanols (C_1–C_3). The experimental results were explained according to the NRTL model [4].

Materials and methods:

Isobutanol, methanol, ethanol and 1-propanol ($w > 0.99$) where w is mass fraction, were purchased from Merck and used without further purifications. Densities and refractive indices were measured and their values were in good agreement with values found in the literature. Mixtures were prepared by weighing the liquids in ground stoppered weighing bottles, taking due precaution to minimize the evaporation losses.

Apparatus:

A Parr 1455 solution calorimeter was used to measure the excess molar enthalpies. The measurements were carried out in an isolated room at 298.15 K and ambient pressure. The All the weighings were performed on an electronic balance (AB 204-N Mettler) accurate to 0.1 mg.

Excess molar enthalpies of (water + methanol) at 298.15 K and ambient pressure were also measured to check the reliability of the apparatus used in this study.. The accuracy of the calorimeter was therefore considered reliable.

Result and discussion:

The experimental excess molar enthalpies, H_m^E, values were determined from the following equation

$$H_m^E/J \cdot mol^{-1} = -\left(C_P + \frac{C_V}{n}\right)\Delta T$$

Heat capacity of the calorimeter was determined by following of Operating Instruction Manual. For the intermediary mixture compositions, it is not possible to determine H_m^E, directly from pure reagents due to limited volume of the cell and vessel. Hence, a mixture is used in Dewar vessel whose H_m^E, can be previously determined, and the value of H_m^E, is calculated by

$$H_m^E/J \cdot mol^{-1} = -\left(C_P + \frac{C_V}{n}\right)\Delta T + \frac{n_0}{n} H_{m_0}^E$$

Conclusion:

The excess molar enthalpies H_m^E, are reported for {methanol, ethanol and 1-propanol} in isobutanol at 298.15 K and ambient pressure over whole range of mole fractions. The sign of H_m^E for all systems are negative and the magnitude of H_m^E values decreases with increasing of chain length. These indicate that isobutanol interacts more strongly with 1-alkanols (C_1–C_3).

Reference:

[1] K. Khanlarzadeh, H. Iloukhani, J. Chem. Thermodyn.; 43, 1583– 1590, 2011.

[2] M.Costas and etal; J. Chem. Soc., Faraday Trans. I,; 81, 635-670, 1985.

[3] O. Redlich and etal; Ind. Eng. Chem.; 40, 345–348, 1948.

[4] H. Renon and etal; J. AIChE; 14, 135–144, 1968.

Heat of mixing of binary mixtures consist of butylacetate (1) + 1-alkanols (C_1–C_3) (2) at 298.15 K and ambient pressure

K. Khanlarzadeh*[a], H. Iloukhani[a]

a Department of Physical Chemistry, Faculty of Chemistry, Bu-Ali Sina University, Hamedan , Iran

Email: kh.khanlarzadeh@basu.ac.ir

Key words: Heat of mixing, Butylacetate, Methanol, Ethanol, 1-Propanol, Wilson model.

Introduction:

Heat of mixing data is extensively used to test and improves theories of mixtures and provides thermodynamic data for the development and design of chemical engineering processes. In this paper heat of mixing, for binary systems of butylacetate + methanol, ethanol and 1-propanol at 298.15 K and atmospheric pressure were measured experimentally. The experimental results were correlated with a polynomial with Redlich–Kister equation [1] for binary mixtures to estimate the coefficients. The binary excess molar enthalpies for all systems under investigation are found to be positive over the entire range of compositions. The experimental results were explained according to the Wilson model [2].

Materials and methods:

Butylacetate and 1-alkanols ($w > 0.99$) were purchased from Merck and used without further purifications. Densities and refractive indices were measured and their values were in good agreement with values found in the literature [1]. Compounds were stored in brown glass bottles and fractionally distilled immediately before use. All the weighings were performed on an electronic balance (AB 204-N Mettler) accurate to 0.1 mg.

Apparatus:

A Parr 1455 solution calorimeter was used to measure the excess molar enthalpies. The measurements were carried out in an isolated room at 298.15 K and ambient pressure. The excess molar enthalpies of (water + methanol) at 298.15 K and ambient pressure were also measured to check the reliability of the apparatus used in this study. The accuracy of the calorimeter was therefore considered reliable. More details of apparatus are described in the literature [3].

Result and discussion:

The experimental heat of mixing, H_m^E, values were determined from the following equation

$$H_m^E/J \cdot mol^{-1} = -\left(C_P + \frac{C_V}{n}\right)\Delta T$$

Molar heat capacity of the mixture was calculated according to Venkatesulu etal [4] and heat capacity of the calorimeter was determined by following of Operating Instruction Manual. For the intermediary mixture compositions, a mixture is used in Dewar vessel whose H_m^E, can be previously determined, and the value of H_m^E, is calculated by

$$H_m^E/J \cdot mol^{-1} = -\left(C_P + \frac{C_V}{n}\right)\Delta T + \frac{n_0}{n} H_{m_0}^E$$

The excess molar enthalpies are positive over the entire range of composition for all mixtures. These indicate that butyl acetate interacts more weekly with 1-alkanols (C_1–C_3).

Conclusion:

Heat of mixing determination is considered to be of prime interest, as this property is essential in characterizing the mixing process of the mixture. The sign, magnitude and symmetry of this property are due to molecular interactions operating among the constituents of mixtures. The interactions between like and unlike molecules in liquid mixture are reflected by excess molar enthalpy data of liquid mixtures.

Reference:

[1] J.A. Riddick and etal; Organic Solvents; 4th ed.; John Wiley& Sons: New York, 1986.

[2] G.M.Wilson; Vapor-Liquid Equilib. XI.; J. Am. Chem. Soc. 86, 127–130, 1964.

[3] H.A. Zarei and etal; Thermochimica Acta; 427, 201–205, 2005.

[4] D.Venkatesulu and etal; Thermochim. Acta; 242, 33–39, 1994.

A systematic study on the salting effect of some kosmotropic salts on some aliphatic alcohols: study of the phase separation ability using cloud point titration method

Ebrahim Nemati-Kande [a]*, Hemayat Shekaari [b]

[a] Department of Chemistry, College of Sciences, University of Tehran, Tehran, Iran

[b] Department of Physical Chemistry, University of Tabriz, Tabriz, Iran,

Email: Nemati.ebrahim@gmail.com

Keywords: Salting effect, Free Energy of Hydration, Cloud point, Kosmtropicity.

Introduction:

When a kosmotropic salt was added to an aqueous solution of an aliphatic alcohol, the system becomes an immiscible aqueous biphasic system (ABS), above a critical concentration of electrolyte. On the other word, the hydrated ions of the electrolyte enforce the alcohol to exclude from the rest of the solution as an independent phase. Thus the alcohol molecules were "slated-out", and separated to form an ABS [1]. Ananthapadmanabhan and Goddard [2] was studied the salting effect of some salts on polymers. However there is no report on the systematic study of the slating effect of different kosmotropic salts on different alcohols in the literature. In this respect, we measured the binodal curves of some aliphatic alcohols + some kosmotropic salts to study the salting effect of these systems.

Materials and methods:

The aliphatic alcohols are ethanol (99.5 %), 1-propanol (99.5 %), 2-propanol (99.7 %), 2-methyl-2-propanol (99.5 %) and 2-buthanol (99.5 %), and the salts are trisodium citrate, disodium hydrogen citrate, diammonium hydrogen citrate, disodium tartrate, disodium carbonate, disodium sulfite, disodium tiosulfate, and dipotassium oxalate all with the analytical purity. All chemicals used in this work were purchased from reliable suppliers and used without further purification. The cloud point titration method was performed to collect the binodal curve data. In this method, an appropriate amount of aqueous solution of slat solution or alcohol was placed in a thermostatted double-wall glass vessel, and the solution was titrated with the alcohol solution or vice versa, until the solution turned turbid; which indicated the formation of two liquid phases.

Result and discussion:

The binodal curves of diammonium hydrogen citrate + alcohol + water and alcohols + salts + water systems at T= 298.15 K were shown in Figures 1. a and 1. b, respectively, as examples.

Figure 1. Binodal curves of diammonium hydrogen citrate (*ca*) + alcohol (*m*) + water (Figure 1. a) and alcohols (*m*) + salts (*ca*) + water (Figure 1. b) systems at T = 298.15 K.

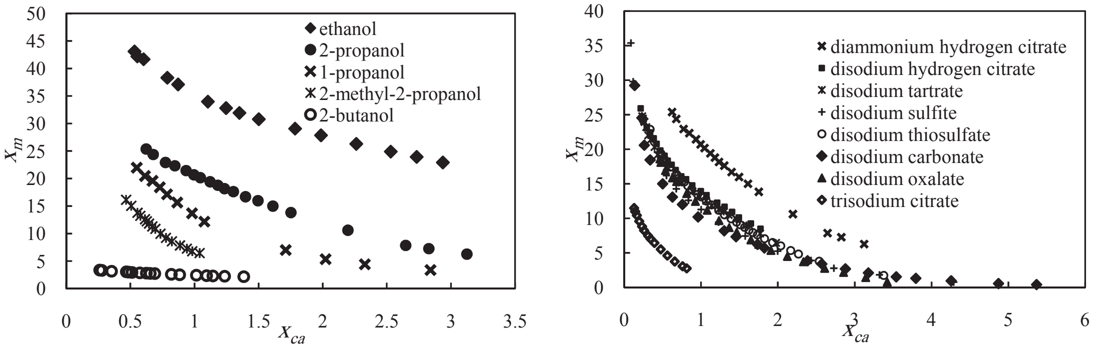

Based on the measured binodal curves it can be concluded that phase separation ability of different alcohols and ions are as follows:

Alcohols: 2-buthanol > 2-methyl-2-propanol > 1-propanol > 2-propanol > ethanol

Anion: citrate > carbonate > sulfite ≈ oxalate> tartrate ≈ thiosulfate > hydrogen citrate

Cations: $Na^+ > K^+ > NH_4^+$

Conclusions:

The phase formation ability of different alcohols can be attributed to the factors that can be affecting the magnitude of the intermolecular interactions, such as boiling point and dielectric constant of the alcohol. Also, it was found that, the more the free energy of hydration of the ion the more the salting-out ability of the ion [3].

References:

[1] Walter, H.; D. E. Brooks, D. Fisher, Partitioning in Aqueous Two Phase Systems, Academic Press, New York, 1985.

[2] K. Anantapadmanhaban, E. Goddard, Langmuir. 3 (1987) 25-31.

[3] F. j. Marcus, J. Chem. Soc. Farady Trans. 87 (1991) 2995-2999.

Experimental and theoretical investigation of ATPSs composed of some aliphatic alcohols + disodium tartrate + water at *T* = 298.15 K

Ebrahim Nemati-Kande [a]*, Hemayat Shekaari [b], Ali Rafi Dargahi [a]

[a] Department of Chemistry, College of Sciences, University of Tehran, Tehran, Iran

[b] Department of Physical Chemistry, University of Tabriz, Tabriz, Iran,

Email: Nemati.ebrahim@gmail.com

Keywords: Liquid–liquid equilibrium, Wilson, Alcohol, Disodium tartrate, ATPS.

Introduction:

Study of the mixed solvent systems in the presence of an added electrolyte is an attractive field to study. When the concentration of the added salt exceeds a critical criterion, the one phase mixed solvent system becomes an immiscible biphasic system, so that, the concentration of the one of the solvents is more than the other, in each of the phases. [1] In recent years several research groups have focused on the measurement and thermodynamic investigation of the aqueous two phase systems (ATPSs) composed of an aqueous solution of a short chain aliphatic alcohol in the presence of an electrolyte. Disodium tartrate is a biodegradable and nontoxic salt and therefore, can be used as a proper and green substitute for traditional inorganic salts.

This paper is continuation of our studies on different ATPSs, in which the tie-line compositions and binodal curves of 1-propanol, 2-propanol, 2-methyl-2-propanol or 2-butanol + disodium tartrate + water ATPSs were determined experimentally. Also, the generalized Wilson model [2] was successfully used for the correlation of the tie-line data and binary interaction parameters were also reported.

Materials and methods:

All chemicals used in this work were purchased from reliable suppliers. Binodal curves of the studied ATPSs were collected using cloud point titration method. For the determination of the tie-lines, feed samples (about 20 cm^3) were prepared by mixing appropriate amounts of alcohol, salt and water in the vessel. Then the mixture was allowed to settle for 8 h. After separation of the two phases, the concentrations of the salt in the top and bottom phases were determined by flame photometry. The concentration of alcohols in both phases was determined by refractive index measurements performed at 298.15 K using a refractometer (Atago, model DR-A1, Japan).

Result and discussion:

The experimental tie-line data for the studied systems were correlated using generalized Wilson model. The generalized Wilson model for the excess Gibbs energy, G^E, is built up from two contributions: a segment based local composition Wilson contribution to account the short-range interaction contribution, $G^{E,SR}$, and a Pitzer–Debye–Hückel (PDH) contribution to account the long-range interaction contribution , $G^{E,LR}$,

$$G^E = G^{E,SR} + G^{E,LR} \tag{1}$$

The experimental tie-line compositions were correlated using generalized Wilson model and the result of the correlation were reported in Table 1 for the ATPSs composed of 1-propanol and 2-propanol alcohols, as examples.

Table 1. Values of restricted parameters of e-Wilson model for the studied alcohol (*m*) + disodium tartrate (*ca*) + water (*w*) systems at *T* = 298.15 K.

system	$H_{wca}{}^a$	$H_{caw}{}^a$	H_{wm}	H_{mw}	H_{cam}	H_{mca}	$10^2 Dev$
1-propanol+*ca*+*w*	5.5457	0.4393	0.4997	1.442	4.1303	-3.6921	2.63
2-propanol+*ca*+*w*	5.5457	0.4393	1.3389	0.5808	-0.8151	3.1303	2.10

Conclusion:

The liquid-liquid equilibrium of the ATPSs composed of some aliphatic alcohols + disodium tartrate + water systems were studied experimentally and theoretically. Based on the obtained deviations (*Dev*), reported in Table 1, it can be concluded the performance of the generalized Wilson model in the correlation of the tie-line compositions is very good.

Reference:

[1] P. A. Albertsson, *Partitioning of Cell Particles and Macromolecules*, 3rd ed.; Wiley-Interscience: New York, 1986.

[2] E. Nemati-Kande, H. Shekaari; S. A. Jafari, Fluid Phase Equilibr. 2012, 321, 64–72.

Phase Behavior for the Aqueous Two-Phase Systems Containing Tetrabutylammonium bromide and Kosmotropic Salts

Rahmat Sadeghi*, Hossein Hooshyar
Department of Chemistry, University of Kurdistan, Sanandaj, Iran
*Email:rsadeghi@uok.ac.ir

Key words: Aqueous two-phase, Tetraalkylammonium ions, liquid-liquid equilibrium, kosmotropic salts

Introduction:

Aqueous two-phase systems (ATPS) are biphasic systems composed mainly by water. This kind of systems have been successfully applied for the separation of different kinds of solutes, such as metal ions [1], proteins, DNA and RNA [2], cells or viruses.

In recent years, considerable interest has arisen concerning the behavior of tetraalkylammonium salts in aqueous solution, particularly with regard to their anomalous thermodynamic behavior, hydration, and apparent structure-promoting influence in water. So far, many thermodynamic and spectroscopic studies have indicated the concept of "structure maker" appropriate for a tetrabutylammonium bromide (TBAB) ion. Lee et al. [3] determined the liquid-liquid equilibrium (LLE) behavior of TBAB, benzene, and water mixture. However, data for the phase diagram of the TBAB + salt + water systems have not been reported at present. In this work, we reported LLE data for the TBAB+ kosmotropic salts (Na_3PO_4, Na_2CO_3, Na_2SO_4, NaH_2PO_4, Na_2HPO_4 and Na_3-citrate) ATPSs.

Experimental Section:

Materials. TBAB, Na_3PO_4**.** $12H_2O$, Na_2CO_3, NaH_2PO_4.$2H_2O$, Na_2SO_4, Na_2HPO_4 and Na_3-citrate were analytical grade reagents and purchased from Merck.

Procedure. The experiments were carried out using a glass vessel with a working volume of 50 cm^3 to determine the phase equilibrium (binodal curve). The glass vessel was provided with an external jacket in which water was circulated at constant temperature using a thermostat. The binodal curves were determined by the cloud point method. A salt solution of known concentration was titrated with the TBAB solution or vice versa, until the solution turned turbid. The composition of the mixture was determined by mass using an analytical balance with a precision of 1.0×10^{-7} kg). Determination of the tie-lines included a series of ATPSs formed by mixing appropriate amounts of TBAB, salt, and water in the vessel which was placed in a thermostatted bath. The feed samples were prepared by mixing appropriate amounts of TBAB, salt, and water in the vessel. The mixture was placed inside an equilibrium cell, where it was agitated in order to allow an intimate contact between the phases, and the thermodynamic equilibrium was finally achieved byletting the mixture at rest for 24 h. After separation of the two phases, the concentrations of sodium citrate in the top and bottom phases were determined by titration with hydrochloric acid. The concentration of TBAB in both phases was determined by refractive index measurements performed at 298.15 K using a refractometer (QUARTZ RS-232, Ceti, Belgium) with a precision of ±0.0001. The relation between the refractive index, n_D, and the mass fractions of polymer, w_1, and salt, w_2 is given by: $nD = a_0 + a_1w_1 + a_2w_2$. The values of coefficients a_0, a_1 and a_2 for the applied system were obtained as 1.3315, 0.1513, and 0.1545.

Results and Discussion:

LLE data and phase diagrams of new aqueous two-phase systems, composed of TBAB + $Na_3PO_4.12H_2O$, Na_2CO_3, $NaH_2PO_4.2H_2O$, Na_2SO_4, Na_2HPO_4 and Na_3-citrate, were determined at T = (298.15, 308.15, and 318.15) K. The effect of temperature and anion on the bimodal has been studied. It was found that an increase in temperature caused the expansion of the two-phase region. This is because the effects of a decrease in temperature on the structure of water is qualitatively similar to that of a kosmotropic (structure-making) ion and therefore can promote the phase-forming ability in the investigated system as a favorable factor for salting-out of IL. The salts share a common cation but contain different anions, it is easy to see that the salting-out ability of the anions follows the ordering PO_4^{3-}>HPO_4^{-2} (low salt concentration)>Cit^{3-}>HPO_4^{2-} (high salt concentration)>$CO_3^{2-} \approx SO_4^{2-}$>$H_2PO_4^{-}$.

Conclusions:

LLE data for the aqueous TBAB+ kosmotropic salts have been determined at T = (298.15, 308.15, and 318.15) K. The effect of temperature on the phase diagram has been studied and shown that the two-phase area is expanded with a decrease in temperature. The ability of the kosmotropic salts studied for phase separation follows the order: PO_4^{3-}>HPO_4^{-2} (low salt concentration)>Cit^{3-}>HPO_4^{2-} (high salt concentration)>CO_3^{2-} ≈ SO_4^{2-}>$H_2PO_4^{-}$ which can be explained by Gibbs free energy of hydration of anions.

References:

[1] Y. Akama, A. Sali, Talanta 57 (2002) 681–686.
[2] F. Luechau, T.C. Ling, A. Lyddiatt, Sep. Purif. Technol. 68 (2009) 114–118.
[3] L. Lee and H. Huang, Fluid Phase Equilibria 205 (2003) 133–147.

Calculation of liquid densities for binary mixtures of n-butane and isobutane using by ISM equation of state

Maryam Mojahed Taghi[a*] and Zahra Sharafi[a,]

[a]Islamic Azad University, Marvdasht branch, Chemistry Department, Marvdasht, Iran

Email: mojahedm@gmail.com

Keywords: Liquid densities, Equation of state , Boiling point, Heat of vaporization

Introduction:

In this study, we apply an equation of state based on statistical-mechanical perturbation theory to liquid mixtures. Three temperature-dependent quantities are needed to use the equation of state (EOS): the second virial coefficient, $B(T)$, effective van der Waals covolume, $b(T)$, and a scaling factor, $\alpha(T)$. Based on the theory, all the three temperature-dependent parameters depend only on the repulsive branch of the potential function, and therefore, by our procedure, can be found from ΔH_{vap} and ρ_{nb}. It has considerable predictive power.

Method:

In this section, we summarized the results of derivation of the statistical mechanical equation of state, which was derived by Ihm et al. [1], from statiscal-mechanical perturbation theory. This equation of state is:

$$\frac{P}{\rho kT} = 1 + \rho \sum_{ij} x_i x_j (B_{ij} - \alpha_{ij} F_{ij}) + \rho \sum_{ij} x_i x_j G_{ij} \alpha_{ij} \tag{1}$$

where x_i and x_j are mole fractions, and the summations run over all components of mixture. The quantities α_{ij} and B_{ij} are related to the pair potential $u_{ij}(r)$. G_{ij} and F_{ij} are defined [2] as follow

$$F_{ij} = \frac{1}{1-\xi_3} - \left(\frac{d_i d_j}{d_{ij}}\right) \frac{\frac{1}{6}\pi\rho \sum_k x_k d_k^{\,2} (4\delta_k + 1)}{(1-\xi_3)(1 + \frac{2}{3}\pi\rho \sum_k x_k d_k^{\,3} \delta_k)} \tag{2}$$

$$G_{ij} = \frac{1}{1-\xi_3} + \left(\frac{d_i d_j}{d_{ij}}\right) \frac{\frac{1}{6}\pi\rho \sum_k x_k d_k^{\,2} (4\lambda_k - 1)}{(1-\xi_3)(1 - \frac{2}{3}\pi\rho \sum_k x_k d_k^{\,3} \lambda_k)} \tag{3}$$

Where : $\xi_3 = \frac{1}{6}\pi\rho\sum_k x_k d_k{}^3$ with $\delta_k = 0.22\lambda_k$. (4)

The equation for calculating d_k is : $b_k = \frac{2}{3}\pi d_k{}^3$ (5)

The simplest combining rules for predicting unlike-molecule interactions from like-molecule interactions are an arithmetic mean for $\rho_{nb}{}^{-1/3}$ and a geometric mean for ΔH_{vap} .

$$(\rho_{nb})_{ij}{}^{-1/3} = (1/2)[(\rho_{nb})_i{}^{-1/3} + (\rho_{nb})_j{}^{-1/3}] \qquad (6)$$

$$(\Delta H_{vap})_{i\,j} = [(\Delta H_{vap})_i\,(\Delta H_{vap})_j]^{1/2} \qquad (7)$$

Once $(\rho_{nb})_{ij}$ and $(\Delta H_{vap})_{ij}$ are known, the values of α_{ij}, b_{ij} and $(B_2)_{ij}$ follow according to Ref [3].

Result and Discussions:

This work proves that the ISM equation of state can be applied to predict the *PVT* behavior for fluid mixtures. The most important advantage of this EOS than other equations is simplicity and also needs less input information for fluids. In practical, knowledge of only two constants, heat of vaporization and liquid density at the normal boiling point that are almost available for fluids is sufficient to determine the *PVT* surface of the fluids.

Conclusion:

The results in **Table I** show that agreement between our calculated data and experimental data is very good.

Table I. Comparisons between Calculated and Experimental Values [4] of Compressed Liquid Densities for Mixtures of (x_1 n-butane + x_2 isobutane)

X_1	T(K)	P(kPa)	ρ_{exp}(kg. m^{-3})	NP^a	AAD%^{b}
0.25	240	481.6-6977.0	621.79-628.56	14	0.62
	280	491.4-6984.1	578.14-588.18	14	0.72
	320	1010.3-7034.9	529.04-544.07	13	3.74
0.50	260	503.9-6987.3	605.31-613.20	14	0.2
	300	312.0-7003.6	559.40-571.85	15	1.7
	340	998.6-7084.7	506.59-525.72	13	4.9
0.75	280	494.5-7039.4	588.49-597.80	14	0.4
	300	576.66-7005.5	565.16-505.7	14	1.47
	340	1008.5-7019.3	513.55-531033	13	4.5

[a] NP: number of data points

[b] $AAD\% = 1/N \sum_{i=1}^{N} 100 \left| \frac{\rho_{i,\exp} - \rho_{i,cal}}{\rho_{i,\exp}} \right|$

References:

[1] Ihm G., Song Y., Mason E.A., J. Chem. phys. **94** (1991) 3839.

[2] Ihm G., Song Y., Mason E.A., Mol. Phys. **75** (1992) 897.

[3] Sharafi Z., Boushehri A., Int. J. Thermophysics. **26(3)** (2005) 785.

[4] Kayukawa Y., Hasumoto M., Kano Y., Watanabe K., J. Chem. Eng. Data **50**(2005) 565-578

Solvent effects on protonation of trimetoprim in different aqueous solutions of methanol

Nayyer Mohammadian Tarigi[a], Ali Shamel*[a], Azar Vahedi[a]
[a]Department of chemistry,Islamic Azad university Ardabil branch, Ardabil, Iran.
E-mail: nmohamadiant@yahoo.com

Key words: Thrimetoprim, Solvent effect, Potentiometer, Protonation constant.

Introduction:

For decades, a great amount of experiments have allowed the proposition of some empirical polarity scales, most of them derived from experiments where single solute models are used to probe (spectrophotometrically, thermodynamically, kinetically, etc.) the interaction with olvents of different polarities. A collection of excellent reviews is available regarding the olvent effect and polarity issues. Solvent effects on transition metal complexes have been reviewed, and more attention has been paid to binary solvent mixtures in this field.[1-2-3] olutesolvent interactions are much more complex in mixed solvent systems than in pure solvent due to the possibility of preferential solvation by any of the solvents present in the mixtures. Moreover, the solvent-solvent interactions produced in solvent mixtures can affect the solute-solvent interactions, and therefore they can also effect preferential solvations.[4-5]

Materials and methods:

Trimetoprim (Fluka, analytical reagent grade) was recrystallized from hot water, washed with ethanol, and dried over P2O5. Equivalent weights were checked by titration against a standard alkali solution. Methanol was obtained from Merck as an analytical reagent grade material and was used without further purification. All dilute solutions were prepared from double-distilled water with a specific conductance equal to (1.3 (0.1) μS ·cm-1.

Apparatus:

A Jenway pH-meter, model 3520(precision of 0.001 units of pH), was used for pH measurements. The hydrogen ion concentration was determined with a combination electrode (Jeneay). A thermostat having accuracy of ±0.1 ºC maintained the temperature of the potentiometric cell. [Model: EX.1200-30-6 STH, this oven is made in Iran]. The sampler model Boaco and the sampler model R88OE enjoyed accuracy of 10-100 and 100-1000 micro, respectively.

Result and discussion:

In this study, the effect of solvent on protonation constant of trimetoprim ($C_{14}H_{18}N_4O_3$ with 290.32 molecular mass and 98% purity) was determined in mixed of water and ethanol with various percents of ethanol such as %, 10%, 20%, 30%, 40%, and 50% in (25±1)°C . During titration process, potential changes were measured and recorded after adding specific amounts of titration solution. Then, based on these empirical results, the required computations were conducted in Excel Microsoft and the most suitable model was chosen through minimizing error function.

Conclusion:

According to these parameters, the effect of solvent on the porotonation constant was investigated and the amount of pK in various percents of water and ethanol was determined. The Results show that pk would be increased if percent of ethanol was raised that can be related to the parameters named Kamlet-Taft.

References:

[1] Reichardt, C. *SolVents and SolVent Effects in Organic Chemistry*, 3rd
ed.; Wiley-VCH: Weinheim, 2004.

[2] Hush, N. S.; Reimers, J. R. Solvent Effects on the Electronic Spectra of Transition Metal Complexes. *Chem. Re*V. **2000**, *100*, 775–786.

[3] Isutsu, K. *Electrochemistry in nonaqueous Solutions*; Wiley-VCH: Weinheim, 2002.

[4] Marcus, Y. Use of Chemical Probes for the Characterization of Solvent Mixtures, Completely Nonaqueous Mixtures. *J. Chem. Soc., Perkins Trans.* **1994**, *2*, 1015–1021.

[5] Gharib, F. Aghaei, H Shamel, A. Taghvamanesh, A. and shafiee, G., Ionic Strength Dependence of Formation Constants and Complexation of Glutamine with Dioxovanadium (v).

Astudy of solvent effect on protonation constant of pyridine carbaldehyde in Different Aqueous Solutions of Methanol

Nayyer Mohammadian Tarighi[a], Ali Shamel*[a], Farrokh Gharib[b], Ali Parastar[a]
[a]Department of chemistry,Islamic Azad university Ardabil branch, Ardabil, Iran.
[b]Chemistry Department, Shahid Beheshti University, G. C., Tehran, Evin, Iran
E-mail: nmohamadiant@yahoo.com

Key words: Solvent effect, Pyridine carbaldehyde, Protonation constand, Potentiometer.

Introduction:

Leor (2001) studied the effect of solvent, structure, and temperature on ionization balance constant in Phenols and Pyridiniom ions of mixture of water and 1-4 Dioxan (0-70%) with weight loss of dioxin in 10-50 temperature changes and observed that the effect of structure and temperature demonstrates the possibility of using Hamtz equation and the model of Marshal Quist in all temperatures and this equation allows the investigation and analysis of the three effects in order to develop pk [1]. W.Y.Ma et al. (200) computed the effect of different solvents using theoretical approach and obtained the 4 kinds of balances in gaseous phase and they studied the effect of solvent polarity on the recent balances and specified that solvent polarity has a considerable effect on entire energy reduction [2]. The study on the solvent effect on the reaction constant of tert-butyl radical addition to 2-substituted allyl cholorides (Yuh- wern wu, 2005) which lead to determine ρ Hamit parameter of S_H2' free radical reaction in different solvents so that it indicated some degrees of reaction capability with electron effect of substitutions [3].

Materials and methods:

Pyridine carbaldehyde C_6H_5NO was obtained from Fluka as analytical reagent grade material and used without further purification. Methanol was from Merck (reagent grade) and was used as received. Sodium chloride was from Merck and was dried under vacuum at room temperature for at least 72 h before use. The NaOH solution was prepared from titrisol solution (Merck), and its concentration was determined by several titrations with standard HCl. All dilute solutions were prepared from double-distilled water with a specific conductance equal to (1.3 (0.1) μS ·cm-1.

Apparatus:

A Jenway pH-meter, model 3520(precision of 0.001 units of pH), was used for pH measurements. The hydrogen ion concentration was determined with a combination electrode (Jeneay). A thermostat having accuracy of ±0.1 ºC maintained the temperature of the potentiometric cell. [Model: EX.1200-30-6 STH, this oven is made in Iran]. The sampler model Boaco and the sampler model R88OE enjoyed accuracy of 10-100 and 100-1000 micro, respectively.

Result and discussion:

In this study, a base solution with specified density and determined ionic power was prepared and another acid solution with specified density of given substance was prepared, too. Base solution and acid solution were alkali metered. Constant k of nornset and conditioned potential were obtained and finally was computed in excel through minimizing error function of parameters.

The effect of solvent on the porotonation constantions of pyridine carbaldehyde (C_6H_5NO and mw=107.11) was investigated different mixtures of water and methanol were as (0%, 10%, 20%, 30%, 40%, 50%) and all of the experiments were carried out at (25±1) ℃ .

During titration changes in potential against volume increament were recorded. Then calculation were done by excel software using minimizing the error Function. After that the mast suitable model was chosen.

Conclusion:

Other calculation were done in excel and based on these calculations were done in excel and based on these calculation, influence of solvent on the Protonation constant was investigated. Pyridine carbaldehyde was in the form of HL^+ and it bas K_1 protonation constant. The result shows that amount of K_1 decrease by increasing of Methanol. Also, the influential effecr of solvent was assessed on the basis of equation. Parameters a, b, s also was determined. The results shows that the effect of s is higher in comparision cuith other parameters.

References:

[1] J.Lior, Effects solvent, structure and temperature on the ionization equilibrium constant of phenols and pyridinium ions in mixtures of water and 1,4-Dioane, J. Sol Chem, 30,7(2001) 641-655.

[2] W.Y.Ma,Y.F.Zhu,J.H.Zhou,Y.Z.Fang; Solvent effect on the structures and isomerization of germylenoid GeH2LiF, J.Mol Struct; 817,(2007),77-81.

[3] Y. w. wu; H. T. Hung; Zhau-Jie Huang-Ming Huang and Iyh-Ferng Yang, The solvent effect on the reaction constant of tert-butyl radical addition to 2-substituted allyl cholorides, Tetrahedron, 61(2005) 4461-4466.

Study of complexation of dioxouranium(VI) ion with Isoleucine

S. Seifi Arpatapeh [a*], F. Kamaly[b] , A. Shamel [b], and F. Gharib [c]
[a] *Department of Chemistry, Islamic Azad University, Young Researchers club, Ardabil Branch, Iran*
[b] *Department of Chemistry, Islamic Azad University, Ardabil Branch, Iran*
[c] *Department of Chemistry, Shahid Beheshti University, Tehran, Evin, Iran*
(E-mail: so_seifi@yahoo.com)

Abstract

The formation of complex species of dioxouranium(VI) ion with isoleucine were studied in aqueous solution in the pH range of 1.0-3.6 at 25°C and constant ionic strength 0.1 mol dm^{-3} $NaClO_4$ using a combination of potentiometric and spectrophotometric techniques. Results showed evidence for formation of the following species: UO_2HL^{2+} and $UO_2(HL)_2^{2+}$.

Keywords: Dioxouranium(VI), Isoleucine, Spectrophotometry, Stability constant

Introduction:

Uranium is a trace constituent in rock phosphate, which is extensively used as a source of phosphorous for fertilizers and livestock feed supplements. Calcium phosphate, for example, a source of calcium used as an animal feeding supplement, can present concentrations of uranium as high as 200 ppm. Thus, the investigation of the pathway, uranium (from feeding) → animal → human, is particularly important, as far as the radiological protection of the general population in concerned. Interaction between amino acids, peptides, and proteins with transition metal ions plays an important role in biochemistry and biology. Great attention has been paid to elucidating and interpreting the thermodynamic and structural characteristics of these biological ligands complexes.

Experimental:

The present work deals with the study of dioxouranium(VI), UO_2^+, complexes by isoleucine. The method of determination of the stability constant based on the relation $A = f([H^+])$ [1-2]. Using a combination of spectrophotometric and potentiometric methods, absorbance and pH were measured for a solution containing UO_2^+ with a large excess of each ligand. Treatments of the spectrophotometric data in the range 250-285 nm (in the interval of 5 nm) obtained during the titrations as a function of the H^+ concentration was conducted with the computer program (Microsoft Excel Solver). The program allows calculation of stability constants for different stoichiometric models.

Results and Discussion:

The complex $M_xH_yL_z^{(nx+y-z)+}$ formed, is characterized by its stoichiometry (x:y:z), where M and L represent the metal ion and each ligand, respectively. To determine the stability constant of the complexation or protonation of the ligands, equation (1) is defined by β_{xyz} [1].

$$xM^{+n} + yH^+ + zL^- \leftrightarrows M_xH_yL_z^{(nx+y-z)+} \qquad (1)$$

$$\beta_{xyz} = [M_xH_yL_z^{(nx+y-z)+}] / ([M^{+n}]^x[H^+]^y[L^-]^z) \qquad (2)$$

The method of determining ε_M was previously described [1] and its values at different wavelengths are used in this work. Using a suitable computer program (Microsoft Excel Solver), the data were fitted for estimating the formation constant of equation (2). We used the Gauss - Newton nonlinear least - squares method in computer program to refine the absorbance by minimizing the error squares sum from the following equation.

$$U = \sum(a_i - b_i)^2 \qquad i = 1,2,3,\ldots$$

where a_i is a quasi-experimental and b_i is a calculated one.

The protonation constant of the ligands have been used for computation of the stability constants, β_{xyz}, of the metal-ligand. In aqueous solution the ligands exist in its anionic form (L^-), zwitterionic species (HL), and cationic form (H_2L^+). In acidic pH, in this case, the predominant species for complexation is HL. The spectrophotometric titration data were analyzed as before [2]. For finding the proposed species, the spectrophotometric titration data were analyzed by offering the following species to the computer program: UO_2L, UO_2HL^+, UO_2HL_2, $UO_2H_3L_2^{+2}$,

$UO_2H_3L_3^+$, $UO_2H_4L_4^+$. As expected, all the proposed species were systematically rejected by the computer program except UO_2HL^+ and $UO_2(HL)_2^+$. The model finally chosen, formed by UO_2HL^+ and $UO_2(HL)_2^+$, resulted in a satisfactory numerical and graphical fitting.

References:

[1] F. Gharib, Phys. Chem. Liq. 45 (2007) 105.
[2] F. Gharib, M. Sayadian, A. Shamel, M. M. Moghaddam, J. Mol. Liq. 138 (2008) 9.

Investigation of Thermodynamic Properties of the Ternary Electrolyte System Based on Pitzer Model at T=298.15

M. A. Bagherinia[1,*], G. R. Vaghar[1], M. Pournaghdi[1], A. Azarinezhadian[1]

[1]Department of Chemistry, Faculty of Science, Lahijan Branch, Islamic Azad University, Lahijan, Iran.

(*Corresponding author *E-mail address*: mabagherinia@yahoo.com)

Keywords: Thermodynamic properties, $CoCl_2$, $Co(NO_3)_2$, Pitzer model, Potentiometric method.

Introduction:

In this work, the results relating to the thermodynamic properties for the ternary solutions of $[CoCl_2 + Co(NO_3)_2]_{(aq)}$ using the potentiometric method and based on Pitzer ion interaction model are reported at 298.15 K. The Pitzer model is one of the most famous and useful models in electrolyt solutions [1-2]. This paper is a continuation of the research on ternary aqueous electrolyte solutions [3]. The potentiometric measurements reported in this work were carried out with a galvanic cell containing a solvent polymeric membrane Co^{2+}- ion selective electrode (Co^{2+}-ISE) and Ag-AgCl electrode and various series of this mixed salt electrolyte system, at ionic strengths of 0.001 to 6.000 $mol.kg^{-1}$. A series of concentrated mixed electrolyte solutions, characterized by their molal salt ratio (r = 1.00, 2.50, 5.00, 7.5, 10.00, 15.00) was used in a standard addition technique to modify the molality of the mixed electrolyte in the experimental cell.

Potentiometric measurements:

The cell arrangements in this work were as (A) Co–ISE | $CoCl_2$ (m_{A0}) | Ag-AgCl, (B) Co–ISE | $Co(NO_3)_2$ (m_{B0}) | Ag-AgCl, (C) Co–ISE | $CoCl_2$ (m_A), $Co(NO_3)_2$ (m_B) | Ag-AgCl and (D) Co–ISE | $Co(NO_3)_2$ (m_{B0}) | NO_3–ISE. The electromotive force (emf) of cell (A) was measured so as to calibrate the electrode pair composing the cell (A). Then the emf of cell (B) was measured to get the selectivity coefficient (K^{pot}) of the Ag-AgCl electrode for NO_3^- ions. The emf of cell (C) was measured for determination of activity coefficients of $CoCl_2$ in the mixed electrolyte solution. Finally, the emf of cell (D) was measured to find the parameters of Pitzer equation for single salt $Co(NO_3)_2$ electrolyte solution.

Calculation of thermodynamic properties:

The mixed ionic interaction parameters (${}^{S}\theta_{ClNO_3}$ and ψ_{COClNO_3}) were determined for the studied ternary system according to the Pitzer graphical method [4]. Then these parameters obtained were used to predict the thermodynamic properties of the system under investigation by the Pitzer model. The osmotic coefficients (ϕ) (fig. 1), the mean activity coefficients of $Co(NO_3)_2$ (fig. 2) and the excess Gibbs energy (fig. 3) were calculated for all of the series of solution.

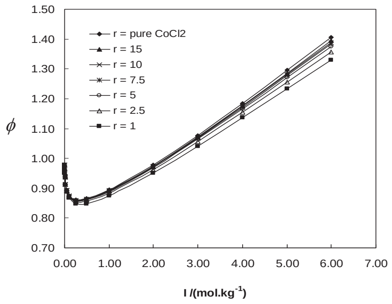

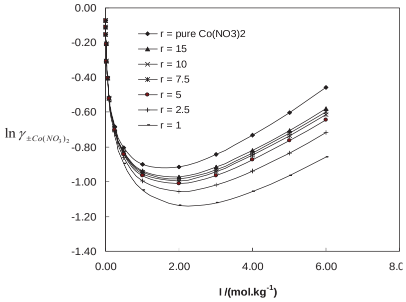

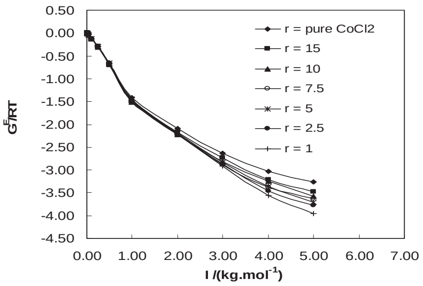

Fig. 1. . Variations of osmotic coefficient. Fig. 2. . Variations of activity coefficients of $Co(NO_3)_2$. Fig.3. Variations of excess Gibbs energy

Conclusions:

The thermodynamic properties of the system $[CoCl_2 + Co(NO_3)_2]_{(aq)}$ were studied by a potentiometric method using a solvent polymeric Co^{2+}-selective membrane electrode and an Ag-AgCl electrode 298.15 K. The results showed that the Pitzer model could be used to describe this aqueous system satisfactorily. The mixing Pitzer parameters (${}^{S}\theta_{ClNO_3}, \psi_{CoClNO_3}$) were determined for this system. The parameters were then used to calculate thermodynamic properties such as the osmotic coefficients (ϕ), the activity coefficients of $Co(NO_3)_{2(aq)}$ in the mixture ($\gamma_{\pm Co(NO_3)_2}$) and the excess Gibbs energy (G^E) which is one of the most important thermodynamic properties.

References:

[1] K.S. Pitzer, J. Phys. Chem. 77 (**1973**) 268–277.

[2] K.S. Pitzer, J.J. Kim, J. Am. Chem. Soc. 96 (**1974**) 5701–5707.

[3] M.A. Bagherinia, M. Giahi, M. Pournaghdy, G. R. Vaghar, J. Chem. Thermodyn., 44 (**2012**) 169–176.

[4] K.S. Pitzer, J. Solution Chem. 4 (**1975**) 249–265.

Solvent Effects on Protonation and Complexation of Histidine with Molybdenum(VI) in Different Aqueous Solutions of Methanol

Ipak Torkpoor *[1], Farrokh Gharib [2], Ali Shamel [1]

[1] Chemistry Department, Islamic Azad University, Ardabil Branch, Ardabil, Iran

[2] Chemistry Department, Shahid Beheshti University, G. C., Tehran, Evin, Iran

E-mail: iptorkpoor@yahoo.com

Key words: Protonation Complexation, Histidine, Molybdenum(VI), Methanol -water mixtures, Kamlet-Taft solvatochromic parameters, Solvent Effect

Introduction:

The formation constants of the species formed in the systems H^++ Mo(VI) + histidine and H^++ histidine have been determined in different aqueous solutions of methanol (0-40 % v/v) at 25 °C and constant ionic strength (0.1 mol dm^{-3} sodium perchlorate), using a combination of spectrophotometric and potentiometric techniques. The composition of the complexes was determined by the continuous variations method [1-2].

Experimental:

The present work deals with the study of molybdenum(VI) complexes by histidine. The method of determination of the stability constant based on the relation $A = f([H^+])$ [1-2]. Using a combination of spectrophotometric and potentiometric methods, absorbance and p_cH were measured for a solution containing Mo(IV) with a large excess of the ligand. Treatments of the spectrophotometric data in the range 250-290 nm (in the interval of 5 nm) obtained during the titrations as a function of the H^+ concentration was conducted with the computer program. The program allows calculation of stability constants for different stoichiometries models.

Results and Discussion:

It was shown that molybdenum(VI) forms a mononuclear 1:1 complex with the amino acid of the type MoO_3L^{2-} at pH 5.8. The protonation and formation constants in various media were analyzed in terms of Kamlet-Taft parameters. Single-parameter correlations of the formation constant, K_S, versus α (hydrogen-bond donor acidity), β (hydrogen-bond accepter basicity) and π^* (dipolarity/polarizability) are poor in all solutions, but multi-parameter correlations represents significant improvement with regard to the single-parameter models. Linear relationship is observed when the experimental $\log K_S$ is plotted versus the calculated ones while all the Kamlet-Taft parameters are considered. Finally, the results are discussed in terms of the effect of solvent on protonation and complexation.

References:

[1] F. Gharib; F. Sadeghi; *Appl. Organometal. Chem*., 21, 218-225,2007.
[2] F. Gharib; *Phys. Chem. Liqs*., 45, 105-112,2007.

Thermodynamic study of molecular interactions in binary systems

A. Pasandideh*[a]

[a] Department of Chemistry, Science and Research Branch, Islamic Azad University, Khouzestan, Iran

Email: pasandideh.a@gmail.com

Keywords: Methyl iso butyl ketone, 2-Alkanols, Excess molar volumes

Introduction:

Excess properties of mixtures provide information about the molecular interactions between the various components and can be used for the development of molecular models describing the thermodynamic behavior of mixtures [1–2].

The thermodynamic properties of mixtures are of great industrial interest**.** The property studied has proved to be meaningful from a thermodynamic point of view, as it provides direct information about the energetic effects arising between the molecules present in the mixture, so it can help to explain the rearranging of the bondings that occurs during the mixing process, which is essential when studying new theoretical approaches to the liquid state, either pure or mixture.

Materials and methods:

Methyl iso butyl ketone,2-propanol, 2-butanol, 2-pentanol, 2-hexanol and 2-heptanolwere purchased from Merck with purity higher than 99%,and used without further purifications. The density of the pure compounds and mixtures was measured by means of an Anton Parr DMA 4500 oscillating U-tube densimeter, provided with automatic viscosity correction.

Results and discussion:

The excess molar volumes V_m^E for the three binary systems were evaluated using the equation

$$V_m^E = \sum_{i=1}^{N} x_i M_i (\rho^{-1} - \rho_i^{-1}) \quad (1)$$

Where ρ is the density of the mixture, ρ_i is the density of pure component *i*, x_i is the mole fraction, M_i is the molar mass of component *i*, and *N* stands for the number of components in the mixture. V_m^E for the binary systems were fitted by the least-squares method to the Redlich–Kister[3] equation

$$V_{ij}^E = x_i x_j \sum_{k=0}^{n} A_k (x_i - x_j)^k \quad (2)$$

Experimental data and fitted equations for the three binary systems are depicted in Fig. 1.

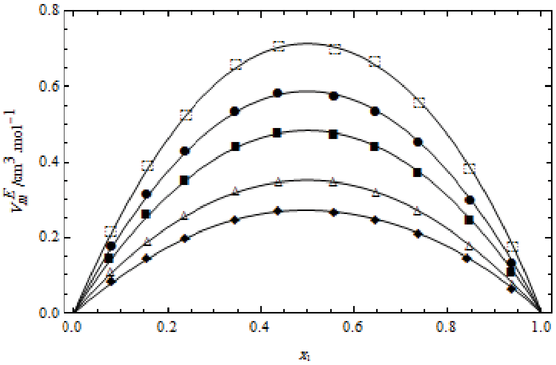

Fig. 1 Excess molar volumes V_m^E vs. mole fraction of Methyl iso butyl ketone with for binary mixtures of methyl iso butyl ketone with (♦) 2-propanol, (Δ) 2- butanol, (■) 2-pentanol, (●) 2-hexanol, (□) 2-heptanol at $T = 308.15$ K. The solid curves were calculated from coefficients of equation (2)

Excess molar volume of binary mixtures containing methyl iso butyl ketone with 2-propanol, 2-butanol, 2-pentanol, 2-hexanol and 2-heptanol are positive over the whole range of mole fractions. The positive V_m^E values for mixtures of methyl iso butyl ketone with 2-alkanols can be ascribed to dominance of disruption of H-bonds between alkanols over dipole-dipole interactions between 2-alkanols and methyl iso butyl ketone molecule.

Conclusions:

Excess molar volumes, of methyl iso butyl ketone and 2-alkanols were obtained from experimental results and fitted by Redlich–Kister type equation.Positive quantities show that dominant factors are physical interactions and negative values suggested that the main factor in the interactional forces is chemical interactions.

Reference:

[1]Iloukhani,H. Almasi,M; "Densities, viscosities, excess molar volumes, and refractive indices of acetonitrile and 2-alkanols:Experimental results and application of the Prigogine–Flory–Patterson theory; Thermo chem Acta. **495**,139**–**148(2009)

[2]]Almasi,M. Sarkoohaki,B; "Densities, Viscosities, of Binary Mixtures of Cyclohexanon and 2-Alkanols. J. Chem. Eng.Data **2012**, 57, 309–316.

[3] Redlich,O. Kister, A.T. ; " Algebraic representation of thermodynamic properties and the classification of solutions. Ind. Eng. Chem. **40**, 345–348 (1948)

Densities and derived thermodynamic properties study for the binary mixtures of (1-hexyl-3-methylimidazoliumtetrafluoroborate + Aminopropanol, or isobutanol) at different temperature with application of the PFP theory

F. Kermanpour, H. Zaheri Niakan*
Department of Chemistry, Faculty of Chemistry, Bu-Ali Sina University, Hamedan, Iran
Email:cht66@yahoo.com

Keywords: Ionic liquids, Excess molar properties, Redlich- Kister correlation, PFP theory

Introduction:

Study of ionic liquids (ILs) as solvents has received an increasing attention in the last years from fundamental and applied points of view [1]. ILs has been used for reducing or eliminating the hazards from volatile organic solvents, solvents in analysis, synthesis, catalytic reactions, and separation processes. ILs have been accepted as "green-chemicals" which excited both the academia and the chemical industries due to their unique properties, and are liquids wide temperature range including room temperature. To design any process involving ILs on an industrial scale, it is necessary to know some thermo physical properties such as viscosity and density [2,3]. In this work, the thermodynamic properties for the binary mixtures of 1-hexyl-3-methylimidazoliumtetrafluoroborate ([C_6mim][BF_4]) with Aminopropanol (AP) and isobutanol have been investigated. We have measured densities, ρ, for the binary mixture of $\{x_1[C_6mim][BF_4]+x_2\text{Aminopropanol}\}$ and $\{x_1[C_6mim][BF_4]+x_2\text{isobutanol}\}$ at atmospheric pressure in the temperature range of (293.15 to 338.15) K and in the entire composition range. The excess molar volumes, V_m^E, partial molar volume, $\bar{V}_{m,i}$, excess partial molar volume, $\bar{V}_{m,i}^E$, partial molar volume at infinite dilution, $\bar{V}_{m,i}^*$, apparent molar volume, $\bar{V}_{\varphi,i}$, the excess thermal expansion coefficients, α^E, isothermal coefficient of excess molar enthalpy $(\partial H_m^E/\partial p)_{T,x}$, were calculated from the experimental values of densities . These data were correlated with the Redlich- Kister equation.

Materials and methods:

All of chemical materials were purchased from Merck, Germany (purity for [C_6mim][BF_4] ≥ 0.98%, water (K.F.) ≤ 1.0%, and for AP ≥ 0.99%, water (K.F.) ≤ 0.3% for isobutanol≥ 0.99%) and were used without further purification. The purities of the components were verified by measuring the densities, viscosities, and refractive indices which were in good agreement with the literature values. the compounds were degassed just before use**.**

Apparatus:

The densities of the pure components and their binary mixture were measured with an Anton Paar digital vibrating U-tube densitometer (model DMA 4500) with a resolution of 5×10^{-5}g.cm^3. The densitometer was calibrated with bi-distilled, freshly degassed water, and with dry air from time to time at the whole temperature range, and at ambient pressure. The temperature in the cell was regulated to ±0.01K, with a thermostat. Temperature in the cell was measured by means of two integrated platinum thermostat. Measured density values are precise to 1×10^{-5}g.cm^3.

Results and discussion:

excess molar volumes for binary mixture of {x_1[C_6mim][BF_4] + x_2AP} shows S-shaped dependence on composition with positive values in the [C_6mim][BF_4] rich-region and negative values at the opposite extreme. with increasing temperature, it increases. We can observe that the excess molar volumes present a minimum at $x_1 = 0.05$, and maximum at $x_1 \approx 0.65$ to 0.75 for this system. V^E for {x_1[C_6mim][BF_4]+$x_2$isobutanol} are negative with a minimum at $x_1 = 0.35$. The strength of ion-dipole interaction between the ILs and the solvent is in agreement with the increasing order of the absolute values of V^E. The increase in the magnitude of the positive V^E values with increasing temperature can be attributed to the decreasing importance of hydrogen bonding with increasing temperature. If interactions between unlike molecules are stronger than those exist between like molecules, as a consequence negative V^E will be observed.

Conclusion:

the positive deviation of the V_m^E indicates that the interactions are weak. Other factors that affect the volume are molecular shape and size of components in the mixture. The Prigogine–Flory–

Patterson theory predicting the excess molar volumes with the agreement between the theoretical and the experimental. In the PFP theory, there is no explicit polar contribution and although the theory does not consider all the possible interactions existent in the mixtures under study.

References:

[1] G. Garcia-Miaja, J. Troncoso, L. Romani, J. Chem. Thermodynamics 41 (2009) 334-341.
[2] F. Kermanpour, H. Z. Niakan, J. Chem. Thermodynamics, 48 (2012) 129–139.
[3] T. Welton, Chem. Rev. 99 (1999) 2071-2084.

Thermodynamic properties study for the binary mixtures of 3-amino-1-propanol+ isobutanol, 2-propanol at temperature range of 293.15-338.15 K: Experimental results and application of the Prigogine–Flory–Patterson theory

F. Kermanpour, H. Zaheri Niakan*
Department of Chemistry, Faculty of Chemistry, Bu-Ali Sina University, Hamedan, Iran
Email:cht66@yahoo.com

Keywords: Binary mixture, Excess molar properties, Density and viscosity, PFP theory

Introduction:

In the present work, densities, ρ, and viscosities, η, for binary mixture of (x13-amino-1-propanol+x2isobutanol) and (x13-amino-1-propanol+x22-propanol) have been measured at atmospheric pressure and in the entire composition range. These quantities have been used to calculate excess molar volumes, V_m^E, viscosity deviations, $\Delta\eta$.. These excess and deviation quantities have then been fitted to the Redlich– Kister equation [1]. The obtained correlations were used to calculate the other thermodynamic functions such as thermal expansion coefficient, α, and its excess value, α^E, and isothermal coefficient of excess molar enthalpy $(\partial H_m^E/\partial P)_{T,x}$. Results of such calculations were used for interpreting intermolecular interactions that exist between molecules of the binary mixture, qualitatively. The Prigogine-Flory-Patterson (PFP) theory has been successful in prediction the volumetric properties of various kinds of binary mixtures [2,3]. In this theory, excess thermodynamic properties of a binary mixture are separated into three contributions: the interactional contribution which is proportional to the interaction parameter, χ_{12}; free volume contribution which arises from the difference between size of two components; and pressure contribution which depends on the internal pressure and reduced volume of the components. In this work, we have investigated the PFP theory as a method to predict the V_m^E of these binary mixtures. Results of these calculations were used for interpreting intermolecular interactions that exist between molecules of the binary mixture.

Materials and methods:

The alcohols purchased from Merck Company (with purities in mass fraction greater than 0.995 for isobutanol and 2-propanol, and 0.99 for 3-amino-1-propanol), and were used without further purification. The density and viscosity of the pure compounds were compared to literature data.

Apparatus:

The densities of the pure components and their binary mixture were measured with an Anton Paar DMA 4500 Oscillating U-tube densitometer, and the uncertainties were estimated to be within $\pm 1\times10^{-2}$ kg m^{-3}. The temperature in the cell was regulated to ±0.01K with a solid state thermostat. The apparatus was calibrated once a day with dry air and double- distilled freshly degassed water. Dynamic viscosities were measured with an Ubbelohde viscometer.

The mass of dry bottle was first determined. The less volatile component of the mixtures was introduced in the bottle, and the total mass was recorded. Subsequently, the other component was added, and the mass of bottle including two components was determined. Each mixture was immediately used, after it was mixed by shaking. All the weightings were performed on an electronic digital balance (AB 204-N Mettler) accurate to ±0.1 mg. The uncertainty in the mole fraction is estimated to be lower than $\pm 1\times10^{-4}$.

Results and discussion:

The excess molar volumes and viscosity deviations of both binary mixtures are negative within the entire composition range and become more negative with increasing temperature from (293.15 to 333.15) K. The increase in the magnitude of the V^E values with increasing temperature can be attributed to the decreasing importance of hydrogen bonding with increasing it.

Conclusion:

The densities of these binary mixtures were measured over the temperature range and over the entire composition range. Data of the excess molar volumes for these binary mixtures were calculated from the values of the experimental density. The calculated excess molar volumes using the PFP model are comparable with experimental values**.** Viscosities of the binary mixtures under study were measured and their deviations were calculated as a function of composition and temperature. The results of calculations show that viscosity deviations are negative over the composition range at all temperatures for both mixtures, and become less with increasing it.

References:

[1] O. Redlich, A.T. Kister, Ind. Eng. Chem 40 (1948) 345–348.
[2] F. Kermanpour, H. Z. Niakan, J. Chem. Thermodynamics, (2012) In press.
[3] P. J. Flory, R. A. Orwoll, and A. Vrij, J. Am. Chem. SOC. 86 (1964) 3507-3514.

Thermodynamics and excess properties of {trichloromethane + amines} at (293.15, 298.15, 303.15 and 308.15) K. Experimental results and application of the Flory theory.

[e], J.Rajabi [d] and H.Bagheri **M. Rakhshi** *[a] , M. Ghanbari[a], M. Rezaei-Sameti[b] , S. Nadali [c]
*[a]Department of Physical Chemistry, Faculty of Chemistry, University of Bu-Ali Sina, Hamadan 65174, Iran
*Corresponding author (Emil: **m.rakhshi.chem@gmail.com**)
[b]Departemnt of Chemistry, Faculty of Science , Malayer University, Malayer, Iran
[c]Islamic Azad University , Thehran South Branch, Tehran, Iran
[d]Islamic Azad University , azad university of gonbad , gonbad , Iran
[e]Islamic Azad University , Thehran Orient Branch, Tehran, Iran

Keywords*:* Thermal expansion coefficients; Excess thermal expansion coefficients; Isothermal Coefficient of pressure excess molar enthalpy; Flory theory.

Introduction:

Thermal expansion coefficients α , and their excess values α^E, and isothermal coefficient of pressure excess molar enthalpy $(\partial H_m^E/\partial P)_{T,x}$ ‘ of the binary and ternary mixtures formed by Trichloromethane + *n*-butyl amine , + *s*-butyl amine, and + diethyl amine were measured at (293.15,293.15, 303.15 and 308.15) K for the liquid region and at ambient pressure . The thermal expansion coefficients α , and their excess values α^E, and isothermal coefficient of pressure excess molar enthalpy $(\partial H_m^E/\partial P)_{T,x}$ ‘ calculated from experimental densities [1-3]. Negative values of α^E or positive value of $(\partial H_m^E/\partial P)_{T,x}$ for binary mixtures may be attributed to strong chemical or specific interactions between the components present in the mixtures or to structural contributions arising from the geometrical fitting of one component into the other due to differences in the molar volumes and free volume between unlike molecules**.**

Methods:

The excess thermal expansion coefficients and isothermal coefficient of pressure excess molar enthalpy were correlated as a function of the mole fraction by using the Redlich–Kister equation for binary ,respectively. in this work for predicted the experimental and other thermodynamic parameters we used the flory model [3].

Results and discussion :

In this work for predicted the experimental and other thermodynamic parameters we used the Flory model . The Flory model has been commonly employed to analyze the molar volume of the mixture and the excess molar volume parting from the equation of the state in function of the reduced variables:

$$\frac{\tilde{P}\tilde{V}}{\tilde{T}} = \left[\frac{\tilde{V}^{\frac{1}{3}}}{\tilde{V}^{\frac{1}{3}}-1}\right] - \left[\frac{1}{\tilde{V}\tilde{T}}\right] \qquad (1) \qquad , \qquad \tilde{V} = \frac{V}{V^*} = \left[\frac{1+(\frac{4}{3})\alpha T}{(1+\alpha T)}\right]^3 \qquad (2)$$

$$\tilde{T} = \frac{T}{T^*} = \left[\frac{\tilde{V}^{\frac{1}{3}}-1}{(\tilde{V}^{\frac{4}{3}})}\right] \qquad (3)$$

Conclusions:

The excess function $\left[\frac{\partial V_{\mathrm{m}}^{\mathrm{E}}}{\partial T}\right]$ was computed by analytical differentiation of (2) at (293.15 K to 308.15 K) and $V_{\mathrm{m}}^{\mathrm{E}}$ of this work we have also obtained isothermal coefficient of pressure excess molar enthalpy , $(\partial H_{\mathrm{m}}^{\mathrm{E}} / \partial P)_{\mathrm{T},x}$, and excess thermal expansions coefficient α^{E}. The comparison between experimental and theoretical values are graphically represented in Fig 1 (A_1 to A_3 and B_1 to B_3) . The obtained results show a good agreement between theory and experimental data.

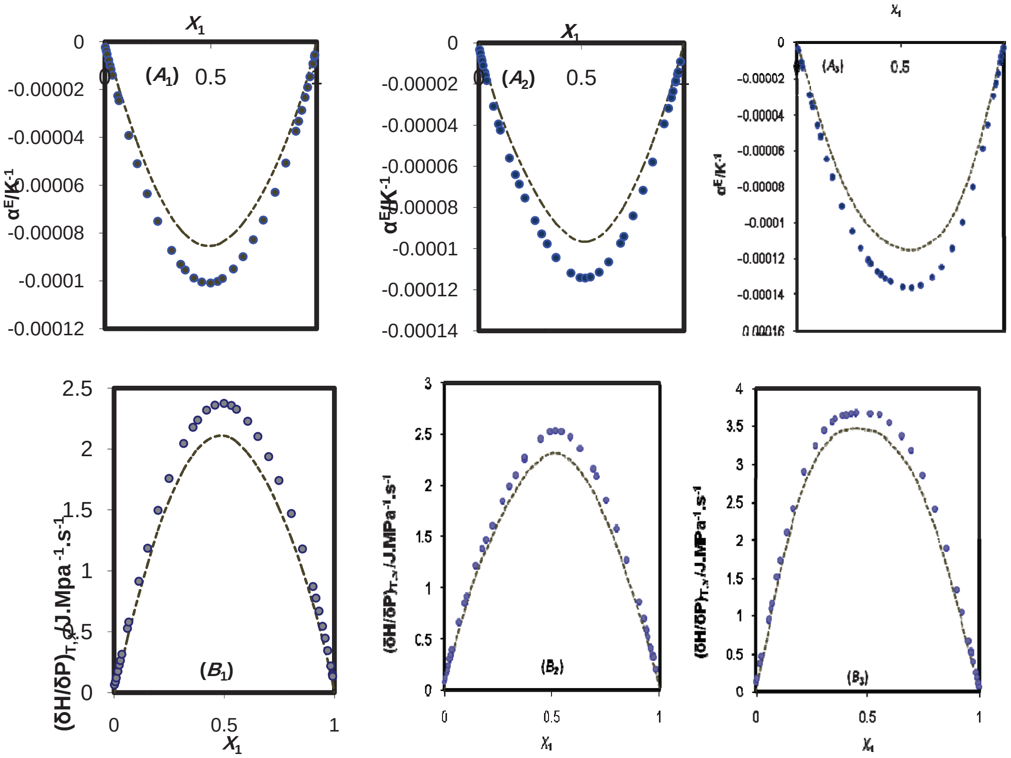

Fig. 1 . Plot of excess thermal expansion coefficients α^E, and isothermal coefficient of pressure excess molar enthalpy $(\partial H_m^E / \partial P)_{T,x}$, against mole fraction for {(A_1,B_1); trichloromethane+ *n*-butyl amine, (A_2, B_2); trichloromethane +*s*- butyl amine, (A_3 , B_3) ; trichloromethane + diethyl amine } 308.15 K. (●) Experimental; (……) calculated by using Flory theory.

Refrences:

[1] M.Rezaei-Sameti, M. Rakhshi, *Afr. J. Pure.Appl. Chem.* 5(7) , (2011) 158.

[2] M.Rezaei-Sameti, H.Iloukhani, M. Rakhshi, *Russ.J. Phy .Chem A.* 84 , (2010) 2023.

[3] S. Bagheri, M. Rakhshi, M.Rezaei-Sameti, *J. Iran. Chem . Res.* 3,(2010) 245.

Determination of macroscopic protonation constants of L-alanine in aqueous solutions of 1,4-dioxane

Mehry Seyed mojarad [a *] , Farrokh Gharib [b]
a. Department of Chemistry, Ardabil Branch, Islamic Azad University, Ardabil, Iran
(*Email: me.mojarad89@yahoo.com)
b. Department of Chemistry, Shahid Beheshti University, G. C., Tehran, Evin, Iran

Keywords: L-Alanine; Macroscopic protonation constants; 1,4-dioxane; Potentiometry.

Introduction:

The importance and vital role of α-amino acids and their peptides in living systems is well known. Nonetheless, there are research subjects in relation to amino acids and peptides that should be investigated [1]. The protonation constants of α-amino acids in organic solvent media are often different from those in water alone, as these media tend to be lipophilic rather than hydrophilic [2-3]. The ionization constant is an important physicochemical parameter of a substance, and knowledge of this parameter is of fundamental importance for a wide range of applications and research areas. Moreover, knowledge of this constant is needed to determine the distribution constants using the potentiometric method. There are several methods for the determination of dissociation constants, but potentiometry is still one of the most commonly used methods because of its accuracy and reproducibility [4].

Experimental:

The macroscopic protonation constants of L-alanine have been studied in different aqueous solutions of 1,4-dioxane (0-50 % by v/v) using a potentiometric method at 25 °C and constant ionic strength 0.1 mol dm^{-3} (NaCl). The electromotive force, *E*, was measured using a pH meter Precisa model 960. The combined glass-pH electrode (model 6.0258.000) was modified by replacing its aqueous KCl solution with 0.01 mol dm^{-3} NaCl + 0.09 mol dm^{-3} $NaClO_4$ saturated with AgCl. All titrations were carried out in a 80 mL thermostated double-walled glass vessel. To exclude carbon dioxide from the system, a stream of purified nitrogen was passed through a sodium hydroxide solution and then bubbled slowly through the reaction solution.

Results and discussion:

L-alanine macroscopic protonation constants are expressed as K_1 and K_2 according to the reactions:

H_2L^+ $H^+ + HL$ $K_2=[H_2L^+] / [H^+] [HL]$ (1)

HL $H^+ + L^-$ $K_1=[HL] / [H^+] [L^-]$ (2)

The macroscopic protonation constant values have been determined using the potentiometric technique under the same condition of temperature, ionic media, and mole fraction of 1,4-dioxane and calculated using the computer program (Microsoft Excel Solver) which employs a nonlinear least-squares method [5].

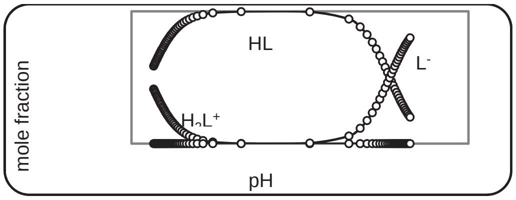

Fig. 1 Distribution diagram of the different species of l-alanine in water at 25±0.1°C and an ionic strength of 0.1 mol dm^{-3} (NaCl)

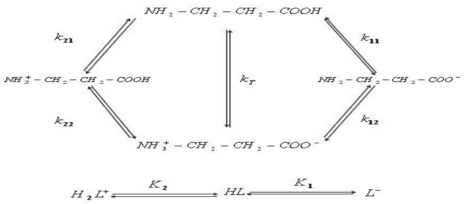

Scheme 1 Microscopic and macroscopic dissociation equilibria of l-alanine

Table 1 Macroscopic protonation constants of the carboxylic, K_2, and the amino, K_1, and the methyl ester, K_{21} groups of l-alanine at 25±0.1°C, different aqueous solutions of 1,4-dioxane, and an ionic strength of 0.1 mol dm^{-3} (NaCl)

dioxane %	logK$_2$	logK$_1$	log K$_{21}$ methyl ester
0	9.04	2.01	8.38
10	8.91	2.15	8.33
20	8.79	2.28	8.24
30	8.67	2.48	8.18
40	8.54	2.61	8.12
50	8.43	2.87	8.05

Conclusions

L-alanine is an ampholyte compound with one acidic and one basic functional group in its molecule. Depending on the pH of the aqueous solutions, this compound can exist as a protonated form H_2L^+, as a neutral form HL (as unionized HL^0 or as a zwitterion $HL^{\pm}$, which are indistinguishable by acid-base titration), or as an anionic form L^- (Scheme 1).

The two macroscopic protonation constants of l-alanine in water-1,4-dioxane mixed solvents have different behavior (Table 1). The protonation constant of the amino group of the amino acid, K_1, increased as the solvent became enriched in the organic component, but the protonation constant of the carboxylic acid group, K_2, decreased as the organic solvents increased in the mixture**.**

References:

[1]. M. Jabbari and F. Gharib, Acta Chim. Slov. **2010**, 57, 325-331.

[2]. R. P. Carty and C. H. W. Hirs, J. Biol. Chem. **1968**, 243, 5256-5265.

[3]. D. E. Schmidt and F. H. Westheimer, Biochemistry **1971**, 10, 1249-1253.

[4]. L. Zapala, Journal of Solution Chemistry **2011**.

[5]. Sigel, S. Interactions of metal ions with nucleotides and nucleic acids and their constituents. Chem. Soc. Rev. **1993**, 255-267.

Solvent Effect on Tautomeric and Microscopic Protonation Constants of Glycine in Different Aqueous Solutions of 1,4-Dioxane

Mehry Seyed Mojarad*[1], Ali Shamel[1], Farrokh Gharib[2]

[1] Chemistry Department, Islamic Azad University, Ardabil Branch, Ardabil, Iran

(* E-mail: me.mojarad89@yahoo.com)

[2] Chemistry Department, Shahid Beheshti University, Tehran, Evin, Iran

Keywords: Solvent effect; Kamlet-Taft; Glycine.

Introduction:

Depending on the pH values of the media, an amphiprotic compound (such as glycine) may exist in four different microforms. Although, the neutral form of an amino acid is more lipophilic and hence more effective in diffusing through the cellular membrane as compared with the charged forms, the macroscopic protonation constants can provide no information about the equilibrium that produces HL^o (with no charge) species. The tautomeric and the protonation microconstants can describe the amount of various microforms of an amino acid at different pH values. Aqueous-organic solvents, mainly 1,4-dioxane, mixtures have been widely used due to sparingly or insolubility of many compounds in pure water as solvent. Further, any physicochemical property of solution can be easily varied by changing the composition of water or the organic solvent in the mixtures. However, chemists have usually attempted to understand solvent effects in terms of polarity, defined as the overall solution capabilities that depend on all possible (specific and non-specific) intermolecular interactions between solute and solvent molecules. Many reports on solvent polarity scales have been published in the last few decades [1]. Previously, the solvent effect on the protonation equilibrium was believed to be guided chiefly by electrostatic interactions (Born model) [1]. However, recent studies have revealed that the change in macroscopic properties such as the dielectric constant of the solvent, cannot be the sole factor [1]. It is desirable to develop other empirical functions to take into account the complete picture of all intermolecular forces acting between solute and solvent molecules.

Experimental:

The electromotive force, *E*, was measured using a Precisa model 960pH ion-meter. The combined glass-pH electrode (model 6.0258.000) was modified by replacing its aqueous KCl solution with 0.1 mol dm^{-3}NaClmol dm^{-3}NaCl saturated with AgCl. The electrode was soaked for (15 to 20) minutes in a water-1,4-dioxane mixture before the potentiometric measurements. All titrations were carried out in a 80 mL thermostated double-walled glass vessel. To exclude carbon dioxide from the system, a stream of purified nitrogen was passed through a sodium hydroxide solution and then bubbled slowly through the reaction solution.All measurements were performed at 25 °C and constant ionic strength (0.1 mol dm^{-3} sodium chloride). The protonation constants were evaluated from measurements of the emf by titration of a 25 mL glycine or glycine methyl ester [$(5.0\text{-}8.0)\times10^{-3}$ mol dm^{-3}] solution with a 0.1 mol dm^{-3} sodium hydroxide solution both in the same ionic strength and mole fraction of organic solvent of 1,4-dioxane [(0 - 50) % by v/v].

Results and Discussion:

The protonation constants were obtained from systematic emf measurements of the following cell: GE/HCl-NaCl, H_2L^+ + HL + L^- in water-1,4-dioxane/NaCl/Ag-AgCl, where GE is the glass electrode and H_2L^+, HL and L^- are the different species of the amino acid involved in the protonation equilibria studied. The four microscopic protonation constants of glycine could be calculated from the macroscopic protonation constants of the amino acid if the value of only one microscopic constant (for example k_{21}) was available. The value of k_{21} was determined from measurement of glycine methyl ester with this assumption that the protonation constant of the compound is the same as that of k_{21} (the uncharged form) for the amino acid. This assumption is the best approximation available in the literature for this purpose [2]. So, the values of k_{11}, k_{12}, k_{22}, and k_T have been calculated as:

$$K_2 = k_{21} + k_{22} \tag{1}$$

$$1/K_1 = 1/k_{11} + 1/k_{12} \tag{2}$$

$$k_T = k_{21}/k_{22} = k_{12}/k_{11} \tag{3}$$

The two macroscopic protonation constants of glycine in water-1,4-dioxane mixed solvents have different behavior. The protonation constant of the amino group of the amino acid, K_1, decreased as the solvent became enriched in the organic component, but the protonation constant of the carboxylic acid group, K_2, increased as the organic solvents increased in the mixtures. It is very difficult to interpret the variation of the protonation constant values of glycine with respect to the percentage of the organic solvents in the mixtures using the dielectric constant of the solutions as a single parameter.In general, the standard free energy of protonation equilibria consists of two terms: an electrostatic term, which can be estimated by the Born equation and a non-electrostatic term, which includes specific solute-solvent interactions. When the electrostatic effects predominate, then in accordance with the Born equation, a plot of $\log_{10}K$ versus the reciprocal of the dielectric constant of the media, ε, should be linear. To obtain a quantitative method for evaluation of the solute-solvent interaction on protonation constants, we used the method introduced by Kamlet, Abboud and Taft (KAT). The KAT equation contains non-specific as well as specific solute-solvent interactions separately, and that the latter could be subdivided into solvent Lewis-acidity interactions (hydrogen-bond accepter, HBA solute, and hydrogen-bond donor, HBD solvent) and solvent Lewis-basicity interactions (HBD solute-HBA solvent). In general, all of these parameters constitute more comprehensive measures of solvent polarity than the dielectric constant or any other single physical characteristic alone, because they reflect more reliably the complete picture of all intermolecular forces acting between solute and solvent molecules. In general, this approach has been widely and successfully applied in the correlation analysis of all kinds of solvent-dependent processes. The multiparametric equation, Eq. 4, has been proposed, using the solvatochromic solvent parameters, α, β and π^* which have been introduced in previous reports. $\log K = A_0 + a\alpha + b\beta + p\pi^*$ (4)

Although the solvent polarity is identified as the main reason of the variation of $\log_{10}K$ values in water-organic solvent mixtures, but the results show any single-parameter correlations of $\log K_1$ and $\log K_2$ values individually with π^*, α, and β did not give good results in all cases. However, the correlation analysis of $\log K_1$ and $\log K_2$ values with dual-parameter equations indicate significant improvement with regard to the single- or multi-parameter models. The expressions of the KAT equation for each property are obtained and are given as dual-parameters (including β and π^*) using the Linest program and discussed using the KAT parameters.

References:

[1] Reichardt, C.: Solvents and solvent effects in organic chemistry, 3ndedn. VCH, New York (2004)

[2] Gharib, F., J. Chem. Eng. Data **55**, 1547-1553 (2010)

Binding and spectral investigation on interaction of $Cu(Pirox)_2(DMF)_2$ with ct-DNA : A Thermodynamic approach

N.Sohrabi*, S.Ghafari, M.Taei, H.Hadadzade
Assistant Professor, Department of Chemistry, Payame Noor University, PO BOX 19395-3697, Tehran-Iran
email: sohrabnas@pnu.ac.ir

Keywords: Cu(II) piroxicam complex, Calf thymus deoxyribonucleic acid (ct-DNA), Ethidium bromide (EB), UV/Vis spectroscopy.

Introduction:

Piroxicam (PX) (4-hydroxy-2-methyl-*N*-2-pridyl-2H-1,2-benzothiazine-3-carboxadiamide-1,1-dioxide) (Scheme1a) belongs to a class of non-steroidal pharmaceuticals with anti-inflammatory properties which are used to treat rheumatoid, arthritis and post operative inflammations[1]. Drugs belonging to the non-steroidal anti-inflammatory drug group (NSAID) are not only used as anti-inflammatory and analgesic agents, but also exhibit chemopreventive and chemosuppressive effects on various cancer cell lines. Cu(II) complexes of these NSAIDs show better anti-cancer effects than the bare drugs. The Cu(II)–NSAID complexes have also been implicated to have better anti cancer effect. It has been shown that the structure of the Cu(II)–piroxicam complex is a bis complex having octahedral geometry and the crystal of the complex from DMF has monoclinic crystal structure[2]. The probes for nucleic acids reported include organic dyes, such as ethidium bromide (EB),bisimidazole, metal complex and photosensitive agent. EB (Scheme1b) is a powerful mutagen widely used in biochemical research for visualizing nucleic acids[3].

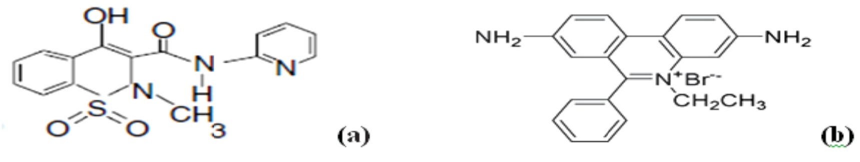

Scheme 1. Structures of piroxicam (a) and EB (b).

Materials and methods:

In this work we use of Cu(Pirox)$_2$(DMF)$_2$ and Tris-Hcl buffer (pH=7.0). Calf thymus DNA (ct-DNA) was purchased from Sigma Chemical. The UV/Vis spectrum was measured using a Perkin Elmer Lamba25 UV/Vis spectrophotometer equipped with thermal bath.

Results and discussion:

The binding of Cu(Pirox)$_2$(DMF)$_2$ to calf thymus DNA has been studied in view of thermodynamic using UV/Vis spectroscopy. The interaction of Cu(Pirox)$_2$(DMF)$_2$ with calf thymus DNA at various conditions such as ionic strength, concentration and temperature was also investigated using UV/Vis technique. In order to test if the complex bind to DNA via intercalation, EB was employed (Figure2). The thermodynamic parameters for binding of Cu(Pirox)$_2$(DMF)$_2$ with ct-DNA are determined using the following equation (Table1).

$$\frac{[DNA]}{(\varepsilon_a - \varepsilon_f)} = \frac{[DNA]}{(\varepsilon_b - \varepsilon_f)} + \frac{1}{K_b(\varepsilon_b - \varepsilon_f)} \qquad (1)$$

$$\partial \text{Ln } K_b / \partial(1/T) = -\Delta H_b° / R \qquad (2)$$

$$\Delta G_b° = -RT \text{ Ln } K_b \qquad (3)$$

$$\Delta S_b° = (\Delta H_b° - \Delta G_b°) / T \qquad (4)$$

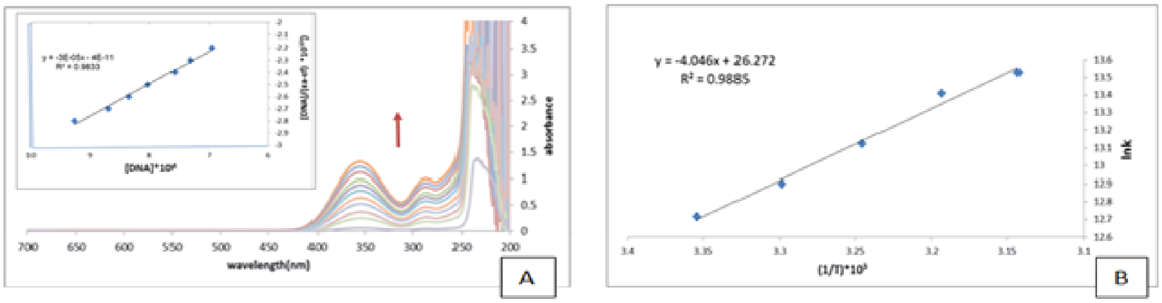

Figure1.Absorption spectra Cu(Pirox)$_2$(DMF)$_2$ in the presence of ct-DNA at increasing amounts [complex].Inset: plot of [DNA]/(εa_εf) vs [DNA] **(A)**. Van't Hoff plots of binding Cu(Pirox)$_2$(DMF)$_2$ with ct-DNA**(B).**

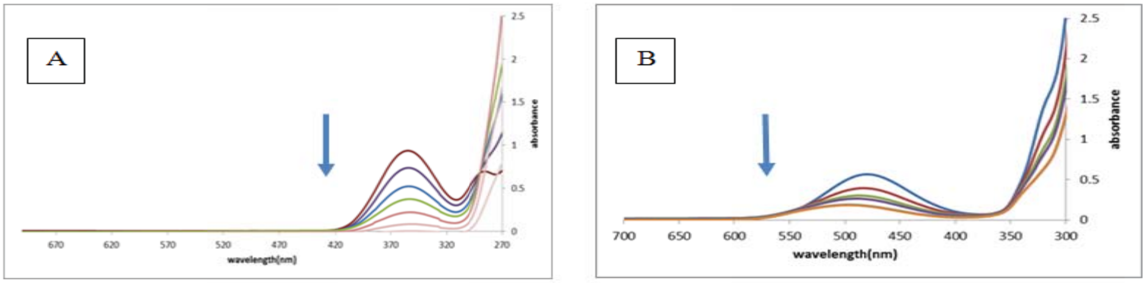

Figure2.The effect of DNA on the absorption spectrum of Cu(Pirox)$_2$(DMF)$_2$ **(A)** and EB**(B).**

Table1. Thermodynamic parameters for the interaction between Cu(Pirox)$_2$(DMF)$_2$ with ct-DNA

TEMP	Ln K	Δ H_b (cal/mol)	Δ G_b (cal/mol)	Δ S_b(cal/mol.°k)
298	12.7169±0.04	8040.2112±802.61	-7534.55±25.82	52.2380±2.61
303	12.8992±0.04	8040.2112±802.61	-7770.74±25.82	52.1556±2.61
308	13.1224±0.04	8040.2112±802.61	-8035.55±25.82	52.1686±2.61
313	13.4091±0.04	8040.2112±802.61	-8344.34±25.82	52.3217±2.61
318	13.5281±0.04	8040.2112±802.61	-8552.83±25.82	52.1548±2.61

Conclusion:

The results show that the complex is stable against temperature and ionic strength and can bind to ct-DNA by the electrostatic binding mode. It seems that the driving force is entropy and this interaction is an hydrophobic intraction upon the positive Entropy and enthalpy. That is also consistent with outside binding mode. Competitive binding with a standard intercalator like ethidium bromide (EB) indicate that the binding mode of Cu(Pirox)$_2$(DMF)$_2$ with DNA is not the classical intercalation binding.

References:

[1] Salma. Al-Kindy, Aisha Al-Wishahi, Fakhr Eldin O. Suliman," A sequential injection method for the determination of piroxicam in pharmaceutical formulations using europium sensitized fluorescence", *Talanta* **64** (2004) 1343–1350.

[2] Roy. S, Banerjee. R, Sarkar. M , " Direct binding of Cu(II)-complexes of oxicam NSAIDs with DNA backbone", *J. Inorg. Biochem* **100** (2006) 1320–1331.

[3] Shuyun Bi, Hanqi Zhang, Chunyu Qiao,Ying Sun, Chunming Liu," Studies of interaction of emodin and DNA in the presence of ethidium bromide by spectroscopic method",*Spectrochimica Acta Part A* **69** (2008) 123–129.

Investigation on ct-DNA thermal denaturation in interaction with $Cu(Pirox)_2(DMF)_2$

N.Sohrabi*, S.Ghafari, M.Taei, H.Hadadzade
Assistant Professor, Department of chemistry, Payam Noor University, PO BOX 19395-3697, Tehran-Iran
email: sohrabnas@pnu.ac.ir

Keywords: Cu(II) piroxicam complex , ct-DNA, Denaturation, Melting temperature (T_m).

Introduction:

Piroxicam (PX) (4-hydroxy-2-methyl-*N*-2-pridyl-2H-1,2-benzothiazine-3-carboxadiamide-1,1-dioxide) belongs to a class of non-steroidal pharmaceuticals with anti-inflammatory properties which are used to treat rheumatoid, arthritis and post operative inflammations[1]. Drugs belonging to the non-steroidal anti-inflammatory drug group (NSAID) are not only used as anti-inflammatory and analgesic agents, but also exhibit chemopreventive and chemosuppressive effects on various cancer cell lines. Cu(II) complexes of these NSAIDs show better anti-cancer effects than the bare drugs. The Cu(II)–NSAID complexes have also been implicated to have better anti cancer effect [2]. When the temperature is increased the double stranded DNA dissociates to single strands, generating hyperchromic effect. The melting temperature (Tm), a aluable parameter to study the metal complex-DNA interactions, is defined as the temperature where half of the total base pairs get unbound[3]. The melting temperature of DNA (T_m) in the presence of a binding molecule or metal can also be used to distinguish between intercalative and external binding modes. Usually, classical intercalation gives rise to higher ΔT_m values than either groove binding or outside stacking [4].

Materials and methods:

In this work we use of $Cu(Pirox)_2(DMF)_2$ and Tris-Hcl buffer (pH=7.0). Calf thymus DNA (ct-DNA) was purchased from Sigma Chemical. The UV/Vis spectrum was measured using a Perkin Elmer Lamba25 UV/Vis spectrophotometer equipped with thermal bath.

Result and discussion:

Melting temperatures were measured in Tris-Hcl buffer solutions pH 7.0 containing 300 µM DNA. The temperature was scanned from 25 to 85ºC. Denaturation curve of ct-DNA represent at various mol ratios of [Cu(Pirox)$_2$(DMF)$_2$] to DNA were investigated and then the melting temperature values (T_m) were estimated by Igor software (Table1). Then ΔH_m, T_m and other four parameters determined using the following equation and Sigma Plot software (Table2).

$$-\Delta\varepsilon_{260}(T)=\frac{(a_N+b_NT)+(a_D+b_DT)\exp[-\frac{\Delta H_m}{R}(\frac{1}{T}-\frac{1}{T_m})]}{1+\exp[-\frac{\Delta H_m}{R}(\frac{1}{T}-\frac{1}{T_m})]} \qquad (1)$$

ΔG_m determined using the following equation. Then thermodynamic stability curve of ct-DNA and the different molar ratio of Cu(Pirox)$_2$(DMF)$_2$ from the drawing changes ΔGm on T produced (Figure2).

$$\Delta G=\Delta H_m(1-\frac{T}{T_m})-\Delta C_p[(T_m-T)+T\ln\frac{T}{T_m}] \qquad (2)$$

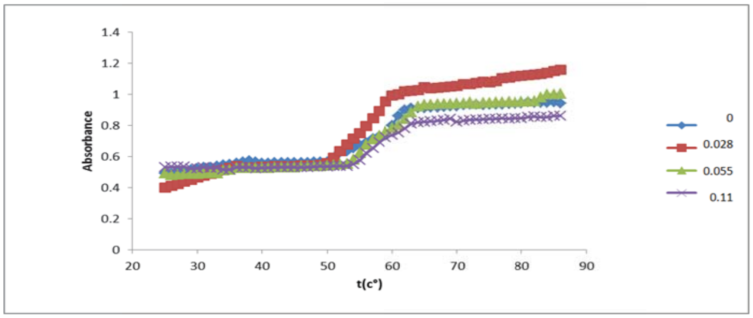

Figure1. Thermal denaturation graph of ct-DNA and Cu(Pirox)$_2$(DMF)$_2$ at different temperature (25-85°C).

Table 1. DNA melting temperature changes upon increasing the molar ratio of Cu(Pirox)$_2$(DMF)$_2$ to DNA were estimated by Igor software.

[Cu(Pirox)$_2$(DMF)$_2$] / [ct-DNA]	0	0.028	0.055	0.11
T_m (K)	333.171	330.301	330.179	330.118

Table2. Determination T_m and ΔH_m using equation **(1)** and Sigma Plot software.

[Cu(Pirox)$_2$(DMF)$_2$] / [ct-DNA]	0	0.028	0.055	0.11
T_m (K)	330.628	329.162	330.702	330.708
ΔH (kj/mol)	273745.76	382689.74	322336.59	451624.5

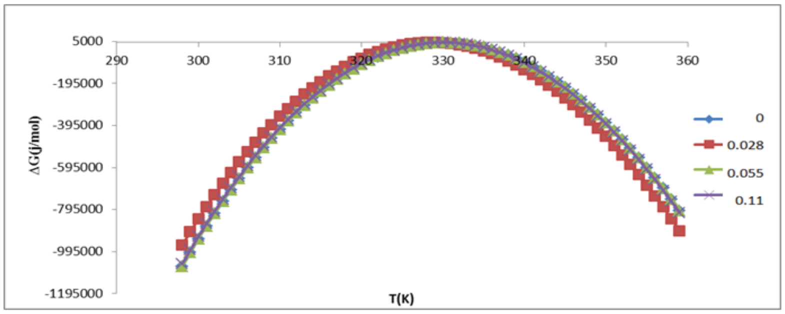

Figure2 . Thermodynamic stability curve of ct-DNA and the different molar ratio of Cu(Pirox)$_2$(DMF)$_2$

Conclusion:

Very small changes of T_m value confirmed outside binding mode. As observed, the curves all(Figure2) have the same structure and a peak that represents the most stable. The result show driving force is entropy and enaturation process was endothermic.

References:

[1] Salma M.Z. Al-Kindy, Aisha Al-Wishahi, Fakhr Eldin O. Suliman" A sequential injection method for the determination of piroxicam in pharmaceutical formulations using europium sensitized fluorescence", *Talanta* **64** (2004) 1343–1350.

[2] Sujata Roy, Rona Banerjee, Munna Sarkar" Direct binding of Cu(II)-complexes of oxicam NSAIDs with DNA backbone", *J. Inorg. Biochem.***100**(2006)1320–1331.

[3] Noor-ul H. Khan, Nirali Pandya, Nabin Ch. Maity, Manoj Kumar, Rajesh M. Patel, Rukhsana I. Kureshy, Sayed H.R. Abdi, Sandhya Mishra, Satyabrata Das , Hari C. Bajaj," Influence of chirality of V(V) Schiff base complexes on DNA, BSA binding and cleavage activity", *Eur. J. Med. Chem.***46** (2011) 5074-5085 .

[4] Burcu Turanlı-Yıldız, Tugba Sezgin, Z. Petek Cakar, , Canan Uslan, B. Sebnem Sesalan, Ahmet Gul, " The use of novel photobleachable phthalocyanines to image DNA"*, Synth. Met.***161** (2011) 1720– 1724.

Experimental and correlated tie-line data for aqueous mixtures of Formic acid with 2-ethyl-1-hexanol at T=298.2 K.

H. Ghanadzadeh Gilani[b]; S. Noury[a]; Sh. Asan[a,] *; M. Sangashekan[b].
[a]*Department of Chemistry,Faculty of Science, University of Urmia, Urmia, Iran*
[b]*Department of Chemical engineering, University of Guilan, Rasht, Iran*
* Corresponding author
E-mail address: shahinasan@yahoo.com (Sh. Asan)

Abstract:

Liquid–liquid phase equilibria (LLE) for the system of water/formic acid/2-ethyl-1-hexanol were investigated experimentally at temperature of 298.15 K.Atype 2 liquid–liquid phase diagram was obtained for this ternary system. These results were correlated simultaneously by the UNIQUAC model. The values of the interaction parameters between each pair of components in the system were obtained forthe UNIQUAC model using the experimental results. The root mean square deviation (RMSD) between the observed and calculated masspercents was 0.4885%. The mutual solubility of 2-ethyl-1-hexanol and water was also investigated by the addition of formic acid at temperature298.15 K.

Keywords: Liquid-liquid equilibrium; Tie-line data; Formic acid; 2-Ethyl-1-hexanol; UNIQUAC model; Separation factor; Distribution coefficient.

Introduction:

The separation of carboxylic acids from aqueous solutions resulting from fermentation processes or synthetic methods is industrially and scientifically important, the precise LLE data are needed and required in design of many chemical processes, separation operations, and fermentation industry [1]. formic acid is one of the most widely used carboxylic acids, which has many industrial applications. the extraction of this acid from aqueous mixtures using the liquid + liquid extraction technique is still an important problem. However, few important investigations have been carried out in recent years on the LLE measurements and the extraction of Formic acid from aqueous solutions by Guy Malmary [2], Zhenyu Li [3].

Methods:

The Formic acid and 2-ethyl-1-hexanol with stated mass fraction purities higher than 0.99% were purchased from Merck. The organic chemicals were dried over molecular sieves. Distilled and deionised water was used throughout all experiments. All materials were used as received without any further purification. The water content of the organic phase was measured by the Karl–Fisher method using Metrohm-870 KF Titrino plus Karl–Fisher titrator. The analysis for the two phases was done by direct titration of weighted sample against 0.1N sodium hydroxide with phenolphthalein as the indicator.

Results and discussion:

Since (2-ethyl-1-hexanol + water) and (2-ethyl-1-hexanol +formic acid) are two liquid pairs that are partially miscible and the only liquid pair (water + formic acid)is completely miscible, the ternary system behaves as a type 2 LLE [4]. The area of the two phase region depends on the solubility of water in the organic phase. It can be seen that the water solubility in 2-ethyl-1-hexanol is extremely low. In order to evaluate the extracting capability of 2-ethyl-1-hexanol for the separation of Formic acid from aqueous solutions, the separation factor (S) was calculated.The reliability of experimentally measured tie-line data can be determined by applying the Othmer-Tobias and Bachman correlation equation.

Conclusions:

The ternary system exhibited type-2 behaviour of LLE. The UNIQUAC model was used to correlate and analyse the experimental LLE data. The optimum UNIQUAC interaction parameters between Water, Formic acid, and 2-ethyl-1-hexanol were determined using the experimental liquid–liquid data. for the UNIQUAC model. In general, the LLE data of this ternary system can be correlated fairly well with this equilibrium model. The solubility of water in 2-ethyl-1-hexanol very low increases with amounts of Formic acid added to (water + 2-ethyl-1-hexanol) mixture. The RMSD% values in the correlation by UNIQUAC for the ternary system over the temperature range of 298.15 K were found to be 0.4885%.

References:

[1] H. GhanadzadehGilani, M. Golpour, S.S. Ashraf, F Phase Equilib.310 (2011) 192–197.

[2] G. Malmary, M. Faizal, J. Albet, J. Molinier, J. Chem. Eng. Data, 1997.

[3] Zh. Li, W. Qin, and Y. Dai, J. Chem. Eng. Data, 2003.

[4] M. B Gramajo De Doz, A. M Cases, J. ChemThermodyn. 50 (2008)1575-1579

(Liquid + liquid) equilibrium for ternary system of (water + phenol + cyclohexanone) at T=298.2 K

H. Ghanadzadeh [a], M. Sangashekan [a], SH. Asan [b,*], H. Heshmati [a].

[a] Department of Chemical Engineering, University of Guilan, Rasht, Iran

[b] *Department of Chemistry, Faculty of Science, University of Urmia, Urmia, Iran*

E-mail: shahinasan@yahoo.com

Key word: LLE, Ternary system, NRTL, UNIQUAC, phenol.

Abstract:

Experimental solubility curves and tie-line data for the (water + phenol + cyclohexanone) system was obtained at T = 298.2 K and atmospheric pressure. The tie-line data was determined by techniques karl-fischer and refractometry. This ternary system exhibits type-2 behavior of LLE. Distribution coefficients and separation factors were measured to evaluate the extracting ability of the solvent. The consistency of the experimental tie-line data was determined through the Othmer–Tobias and Bachman equations. The data were correlated with the NRTL (α = 0.25) and UNIQUAC models and the parameters estimated present root mean square deviations below 2%.

Introduction:

One of the important sections of the petrochemical industry is phenol production, especially for the production of resins [1]. Phenol is formed by oxidation of cumene in liquid phase, leading to cumene hydroperoxide (CHP); in following order: the CHP suffer a catalytic decomposition, producing phenol and acetone with water and α-methyl styrene as byproducts. So, a stream including phenol, water and small amounts of acetone and α-methyl styrene is produced at the end of the process [2]. The remotion of phenol from aqueous solutions is an environmental interest for a very toxic stream [3].

The distribution coefficients of phenol for systems (water + phenol + 1-decanol) and (water + phenol + tridecanol) have been published at T = 293.15 K [4]. The LLE data for the systems (water + phenol + tert-butanol) at 298.15 K and (water + phenol + 1-butanol), (water + phenol + 2-butanol) are reported at T = (298.15 and 313.15) K [5].

Methods:

The phenol and cyclohexanone with stated mass fraction purities higher than 0.99 were purchased from Chem-lab and Merck, respectively. The organic chemicals were dried over molecular sieves. Distilled and deionised water was used throughout all experiments. All materials were used as received without any further purification.

The water content of the organic phase was measured by the Karl–Fisher method using Metrohm-870 KF Titrino plus Karl–Fisher titrator. The refractive indices of both phases at equilibrium were measured and used for building standard curves.

Results and discussion:

Since the (phenol + solvent) mixture is the only liquid pair that is completely miscible and two liquid pairs (phenol + water) and (water + solvent) are partially miscible, these ternary systems behave as type-2 LLE [6].

In order to evaluate the extracting capability of cyclohexanone for the separation of phenol from aqueous solutions, the separation factor (S) was calculated.

The reliability of experimentally measured tie-line data can be determined by applying the Othmer-Tobias and Bachman correlation equation.

Conclusions:

The UNIQUAC and NRTL ($\alpha = 0.25$) models were used to correlate the experimental data and to calculate the phase compositions of the mixtures studied. The corresponding optimized binary interaction parameters were also calculated. Both the models give relatively good results for the system investigated. The separation factors and distribution coefficients for the organic solvent used in this work were calculated. The high separation factors for the cyclohexanone confirm the ability of these solvents for extraction of phenol from aqueous.

References:

[1] S. Matar, L.F. Hatch.; Chemistry of Petrochemical Process, second ed.; Gulf Professional Publishing; Hannover, 2001.

[2] J.G. Speight.; Chemical and Process Handbook; McGraw-Hill; New York, 2002.

[3] V. Dohnal, D. Fenclová.; J. Chem. Eng; Data 40 (1995) 478–483.

[4] K. Scott, A. Adhamy, I.F. McConvey.; J. Chem. Eng; Data 37 (1992) 391–393.

[5] L.H. Oliveira, M. Aznar.; (Liquid + liquid) equilibrium of {water + phenol + (1-butanol, or 2-butanol, or tert-butanol)} systems; J. Chem. Eng; 42 (2010) 1379–1385

[6] R.E. Treybal.; Liquid Extraction; McGraw-Hill; New York, 1963.

Solvent Effects on Protonation Constants of nicotinek acid in Different Aqueous Solutions of 1- etanol

Mina Ahmadzadeh, [1] Mahin Jane Dege sara, [1] Ali, Shamel, [1] Farrokh Gharib, [2]
[1] Chemistry Department, Islamic Azad University, Ardabil Branch, Ardabil, Iran
[2] Chemistry Department, Shahid Beheshti University, G. C., Tehran, Evin, Iran
Email: mina_ahmadi86@yahoo.com

Key words: Protonation constants, Nicotinek acid, etanol -water mixtures, Kamlet-Taft Solvatochromic parameters, Solvent Effect

Introduction:

The protonation constants of nicotinek acid have been determined in 10–80% (v/v) etanol-water mixtures at 25 °C and constant ionic strength (0.1 mol L^{-1} sodium perchlorate) by potentiometric technique and calculated using a suitable computer program which employs a nonlinear least- squares method. The effect of solvent composition on the protonation constants in the mixed solvents were correlated with the Kamlet-Taft solvatochromic parameters (α, β and π*). It was shown that $\log K_1$ and $\log K_2$ values of nicotinek acid increases with increasing etanol content up to 50% and then tend to decrease. Further, more an over-view of the effect of preferential solvation and solvent structure of electrolytes in etanol-water mixtures on the values of the protonation constants in these media were also discussed.nicotinek acid (an anti-bacterial compound) is determined in different aqueous solutions of 1- etanol.

Materials and methods:

Potentiometry titration is a well known reference method for pK_a determination, and it can be easily used in organic or hydro-organic solvents. To evaluate the protonation constants, first the calibration of the potentiometer and the electrodes should be performed by Gran’s method. The measured emf values in the potentiometric titration of the compound in the different aqueous solutions of 1- etanol are conducted with a suitable computer program for data treatments using a fitting method. All measurements were performed at 25 °C and constant ionic strength of 0.1 mol dm^{-3} sodium chloride.

In all cases, the procedure was repeated at least three times and the average values and the corresponding deviations from the average are reported in this work.

Apparatus:

A Jenway pH-meter, model 3520 (precision of 0.001 units of pH), was used for pH measurements.The hydrogen ion concentration was determined with a combination electrode (Jenway). A thermostat having accuracy of ± 0.1°C maintained the temperature of the potentiometric cell. [Model: EX.1200-30-6 STH, this oven is made in Iran].

Result and discussion:

The protonation constant values of nicotinek acid have been determined According to the obtained results, increasing the amount of the organic solvent reduces the dielectric constant in the aqueous-1-etanol mixtures and so, in accordance with the Born equation the protonated species of the nicotinek acid are expected to be more stable in media with lower dielectric constants. When electrostatic effects predominate, a plot of log K versus the reciprocal of the dielectric constant of the media should be linear. Previously, we have reported [1-2] that the dielectric constant alone cannot serve as a quantitative measurement of the solvent polarity. This property is often inadequate, since the dielectric constant description considers a solvent to be an unstructured continuum, not composed of individual solvent molecules with their own solvent-solvent interactions, and does not take into account specific solute-solvent interactions. In this work, we have used the method was introduced by Kamlet, Aboud, and Taft (KAT). The KAT equation contains separate terms for non-specific as well as specific solute-solvent interactions. Finally, the dependence of acid-base equilibria on solvent composition will be discussed from the determined coefficients of KAT parameters.

Conclusion:

In this work, the protonation constants of some nicotinek acid have been determined in etanol - water mixture of varying compositions (10–80% etanol by volume). It is very difficult to interpret the logK variations of the nicotinek acid studied by only macroscopic parameters of the etanol-water mixtures. It is known that one of the most important factors determining the equilibrium constants is the reaction medium, so, the solvent effect on protonation constants could be explained on the basis of dielectric constant of the medium, solvent structure, preferential solvation, and microscopic parameters (as Kamlet-Taft solvatochromic parameters). A Jenway pH-meter, model 3520 (precision of 0.001units of)was used for pH measurements. The hydrogen ion concentration was determined with a combination nelectrode (Jenway). A thermostat having accuracy of ± 0.1A Jenway pH-meter, model 3520 (precision of 0.001)

Reference:

[1] A, Shamel.; F, Jaberi.; F, Gharib. J. Chem. Eng. Data; 55, 5176-5181,2010.

[2] M, Jabbari.; F, Gharib. J. Sol. Chem; 40, 561-574,2011.

[3]. F. Gharib; F. Sadeghi; Appl.Organomet. Chem. 21, 218–225,2007.

Solvent Effects on Protonation Constants of trimetoprim in Different Aqueous Solutions of 1-propanol

Mina Ahmadzadeh, [1] Ali, Shamel, [1] Farrokh Gharib, [2]
[1] Chemistry Department, Islamic Azad University, Ardabil Branch, Ardabil, Iran
[2] Chemistry Department, Shahid Beheshti University, G. C., Tehran, Evin, Iran
Email: mina_ahmadi86@yahoo.com

Key words: Protonation constants, trimetoprim, propanol-water mixtures, Kamlet-Taft solvatochromic parameters, Solvent Effect

Introduction:

The role and timing of physic chemical profiling in drug research has significantly changed during the last decade. Determination of fundamentally important physic chemical properties such as dissociation, solubility and lipophilicity has been shifted to the early stage of drug discovery in order to facilitate the screening of drug like candidates.

The pK_a value is a key parameter to predict the dissociation state of a molecule with respect to pH. Knowledge of this parameter is essential in estimation of ADME properties since absorption and distribution are highly affected by the dissociation of the compound. However, many drugs are sparingly soluble in water and any experimental pK_a determination requires the use of an organic or hydro-organic solvent. Mixtures of water and organic solvent, mainly methanol, ethanol, or 1-propanol, are usually employed. In the present work, the protonation constants of trimethoprim (an anti-bacterial compound) is determined in different aqueous solutions of 1-propanol.

Materials and methods:

Potentiometry titration is a well known reference method for pK_a determination, and it can be easily used in organic or hydro-organic solvents. To evaluate the protonation constants, first the calibration of the potentiometer and the electrodes should be performed by Gran's method. The measured emf values in the potentiometric titration of the compound in the different aqueous solutions of 1-propanol are conducted with a suitable computer program for data treatments using a fitting method. All measurements were performed at 25 °C and constant ionic strength of 0.1 mol dm^{-3} sodium chloride.

In all cases, the procedure was repeated at least three times and the average values and the corresponding deviations from the average are reported in this work.

Apparatus:

A Jenway pH-meter, model 3520 (precision of 0.001 units of pH), was used for pH measurements.The hydrogen ion concentration was determined with a combination electrode (Jenway). A thermostat having accuracy of ± 0.1°C maintained the temperature of the potentiometric cell. [Model: EX.1200-30-6 STH, this oven is made in Iran].

Result and discussion:

The protonation constant values of trimetoprim have been determined According to the obtained results, increasing the amount of the organic solvent reduces the dielectric constant in the aqueous-1-propanol mixtures and so, in accordance with the Born equation the protonated species of the tri-methoprim are expected to be more stable in media with lower dielectric constants. When electrostatic effects predominate, a plot of log *K* versus the reciprocal of the dielectric constant of the media should be linear. Previously, we have reported [1-2] that the dielectric constant alone cannot serve as a quantitative measurement of the solvent polarity. This property is often inadequate, since the dielectric constant description considers a solvent to be an unstructured continuum, not composed of individual solvent molecules with their own solvent-solvent interactions, and does not take into account specific solute-solvent interactions. In this work, we have used the method was introduced by Kamlet, Aboud, and Taft (KAT). The KAT equation contains separate terms for non-specific as well as specific solute-solvent interactions. Finally, the dependence of acid-base equilibria on solvent composition will be discussed from the determined coefficients of KAT parameters.

Conclusion:

In this work, the protonation constants of some trimetoprim have been determined in propanol - water mixture of varying compositions (10–80% propanol by volume). It is very difficult to interpret the logK variations of the trimetoprim studied by only macroscopic parameters of the propanol-water mixtures. It is known that one of the most important factors determining the equilibrium constants is the reaction medium, so, the solvent effect on protonation constants could be explained on the basis of dielectric constant of the medium, solvent structure, preferential solvation, and microscopic parameters (as Kamlet-Taft solvatochromic parameters). A Jenway pH-meter, model 3520 (precision of 0.001units of)was used for pH measurements.The hydrogen ion concentration was determined with a combination nelectrode (Jenway). A thermostat having accuracy of ± 0.1A Jenway pH-meter, model 3520 (precision of 0.001).

Reference:

[1] A, Shamel.; F, Jaberi.; F, Gharib. J. Chem. Eng. Data; 55, 5176-5181,2010.

[2] M, Jabbari.; F, Gharib. J. Sol. Chem; 40, 561-574,2011.

[3]. F. Gharib; F. Sadeghi; Appl.Organomet. Chem. 21, 218–225,2007.

Thermodynamic Stability of mouse Ribonucleotide Reductase R2 Protein

Ali Rashidnia* , Ali Akbar Saboury and Reza Rofougaran
Institute of Biochemistry and Biophysics, University of Tehran, Tehran, Iran
Rashidnia@ibb.ut.ac.ir

Keywords: Ribonucleotide Reductase (RNR), Stability, Circular dichroism

Introduction :

Ribonucleotide Reductase (RNR) catalyzes the synthesis of the four deoxyribonucleotides needed for DNA synthesis and repair in cell. The RNR protein consists of two non-identical subunits, the R1 and R2 proteins. The latter protein contains an iron-tyrosyl free radical center essential for enzyme activity. This enzyme has been targeted for cancer treatment. Therefore, structural studies on this enzyme has important role for designing of new antimetabolites. Under physiological conditions, this protein has a high α-helical content. It is important to know how structure of RNR folds into their biologically active states and how these active states are stabilized.[1,2].

Materials and method:

the mouse R2 was purified protein by DEAE chromatography. R2 samples (0.18 mg/ml) and dodecyl trimethyl ammonium bromide (DTAB) were dissolved in 10mM potassium phosphate and 70 mM KCl buffer solutions of various pHs (pH 3, 7 and 10) at temperature of 25°C . The buffer conditions for the thermal denaturation experiments were the same as those used for DTAB unfolding (10 mM potassium phosphate, 70 mM KCl, pH 7) and the protein concentrations of 0.19 and 0.5 mg/ml were used. Circular dichroism (CD) spectra were obtained withan Aviv circular dichroism spectrometer . For equilibrium studies, the readings at 222 nm were compiled.

Result and discussion:

The Circular dichroism spectra were recorded in the temperature interval 8–90°C, at 222 nm and plots of standard- Gibbs free energy (ΔG°)of unfolding versus the temperature in protein concentrations of 0.19 and 0.5 mg/ml were obtained. The results only conform to the simple $N_2 \leftrightarrow 2N \leftrightarrow 2U$ model of unfolding The values of the thermodynamic parameters were obtained as: $T_m = 330.15$ K, $\Delta H_1 = 654.5$ kJ mol^{-1}, $\Delta H_2 = 115.5$ kJ mol^{-1}, $\Delta Cp_1 = 92.3$ kJ T^{-1} mol^{-1}, $\Delta Cp_2 = 3.6$ kJ T^{-1} mol^{-1} and $T_m = 338.15$ K, $\Delta H_1 = 254.9$ kJ mol^{-1}, $\Delta H_2 = 99.9$ kJ mol^{-1}, $\Delta Cp_1 = 18.21$ kJ T^{-1} mol^{-1}, $\Delta Cp_2 = 3.57$ kJ T^{-1} mol^{-1} for reactions 1 and 2 in protein concentrations of 0.19 and 0.5 mg/ml ,respectively. The interaction of DTAB with R2 in various pHs of (3,7,10) at temperature 25°C has been studies by CD. The values of 39.9 kJ mol^{-1}, 46.1 kJ mol^{-1} and 47.8 kJ mol^{-1}, were obtained for $\Delta G°_D(H_2O)$, in various pHs of (3,7 and 10) respectively.

Conclusion:

Hopefully, the analyses of the stability of RNR by denaturants and their effects on the secondary structure of the proteins would be used for rational new drug design.

Reference:

[1] K.R. Strand, Y.S. Yang, K.K. Andersson , E.I. Solomon, Circular dichroism and magnetic circular dichroism studies of the biferrous form of the R2 subunit of Ribonucleotide Reductase from mouse. Comparison to the R2 from E. coli and other binuclear ferrous enzymes, Biochemistry 42 (2003) 12223–12234.

[2] Georgieva. E. R, Ana Narvaez .J, Hedin .N, Gräslund.A , Secondary structure conversions of Mycobacterium tuberculosis Ribonucleotide Reductase protein R2 under varying pH and temperature conditions, Biophysical Chemistry 137 (2008) 43–48.

Study of dielectric behaviour of binary mixtures of cyclohexanol with cyclohexanone at 298.2 K

A. Ghanadzadeh[a], S. Shekarsaraee*[b]

a. Department of Chemistry, Faculty of science, Guilan University, Rasht, Iran
b. Department of Chemistry, Faculty of science, Tarbiat modares university, Tehran, Iran
(E-mail: setareh_shekarsaraee@yahoo.com)

Keywords: Dielectric constant; Dipole moment; Kirkwood factor; Binary mixtures.

Introduction:

Measurement of the dielectric constant (relative permittivity) is a useful technique for characterizing molecular structure, solute-solute and solvent-solute interactions, and molecular ordering in solutions.

The value of the dielectric constant is strongly related to molecular structure and intermolecular interactions [1-3].Relative permittivity measurements were made on binary mixtures of (cyclohexanol + cyclohexanone) for various concentrations at T = 298.2 K. The molecular dipole moments were determined using Guggenheim-Debye method in the temperature range of (298.2) K. The variations of effective dipole moment and correlation factor, g, with the mole fraction in these materials were investigated using Kirkwood-Frohlich equation.

Methods:

The densities of the solutions were measured at 298.2 K using DA-210 (Kyoto electronic) density meter. The refractive indices of the solutions were determined at a wavelength of 589 nm using an Abbe Refractometer (Model CETI). The density meter and the refractometer were initially calibrated before being used to perform measurements. The temperature was controlled by circulation of water through a jacket surrounding the sample and was measured to an accuracy of ± 0.1 K. The electrical capacitance of the dielectric cell was measured using a Wayne Kerr model 6425B Digibridge. Measurements of the capacitance required for calculating the static dielectric permittivity were performed at a frequency of 10 kHz.

Results and discussion:

Dielectric excess parameters, the Kirkwood correlation factor, dielectric parameters and refractive index have been reported for binary liquid mixtures of cyclohexanol and cyclohexanone at various concentrations. The parameters show systematic changes with concentration. The Kirkwood correlation factors indicate the existence of strong intermolecular interactions in these systems.The dipole moments of the binary mixtures of (cyclohexanol + cyclohexanone) were calculated using the Guggenheim-Debye equation [4]. The expression for the dipole moment is given by:

$$\mu^2 = \frac{27kT}{4\pi N_{A(\varepsilon_1+2)(n_1^2+2)}} \left(\frac{\Delta}{C}\right)_{C\to\infty}$$

Where ε_1 is the static permittivity and n_1 is the refractive index of pure non-polar solvent, k is the Boltzmann constant and N_A is Avogadro's number. The dielectric increment given by:

$\Delta=(\varepsilon_{12} - n_{12}^2) - (\varepsilon_1 - n_1^2)$ where the subscript 12 denotes a property of the solution. C is the molar concentration (mol / cm^3), and $(\Delta /C)_o$ is the limiting gradient of the plot of versus concentration. The permittivity and the refractive index values of these liquids were measured at 298.2 K. Dielectric permittivity increments of binary mixtures of (cyclohexanol+cyclohexanone)

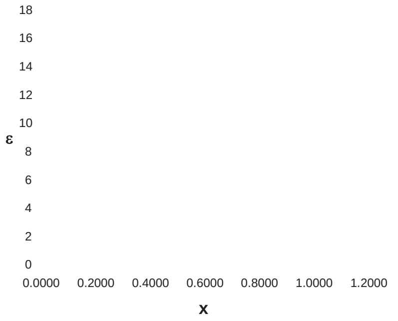

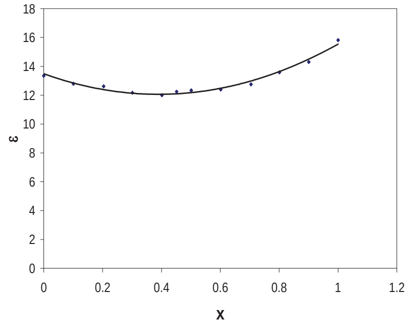

Fig.1. Dielectric permittivity of cyclohexanone as a function of mole fraction at 298.2 K

Fig.2. Dielectric permittivity of cyclohexanol as a function of mole fraction at 298.2 K

Conclusions:

At 298.2 K, values of the dipole moment and Kirkwood correlation factor for cyclohexanol with cyclohexanone were determined at various concentrations. These results yield a Kirkwood factor $g < 1$, and indicate a high degree of parallel dipole associations.

References:

[1] J. W. Smith, Electric Dipole Moment, Butterworth, London,1955.
[2] W. Dannhauser, A. F. Flueckinger, J. Phys. Chem. 68 (1964) 1814.
[3] G. M. Janini, A. H. Katrib, J. Chem. Educ. 60 (1983) 1087.

Refractive indices for aqueous solutions of ethylene glycol, D-mannitol, D-fructose, sucrose and maltose at T = 292.15 K and atmospheric pressure

Fardad Koohyar[a]*, Abbas Ali Rostami[b], and Mohama Javad Chaichi[b]
[a] Department of Chemistry, Babol Branch, Islamic Azad University, Babol, Iran
[b] chemistry Department, Mazandaran University, POBOX 453, Babolsar, Iran
Email: FardadKoohyar@yahoo.com

Keywords: Refractive index, Maltose, Aqueous solution, Molar concentration.

Introduction:

In optics the refractive index (n_D) of a substance (optical medium) is a number that describes how light, or any other radiation, propagates through that medium. The refractive index is a basic optical property of materials and its accurate value is often needed in many branches of physics, biology and chemistry [1,2]. Knowledge of the refractive index of aqueous solutions of salts and biological agents is of crucial importance in applications of evanescent wave techniques in biochemistry [3]. Chemical modifications may be detected by measurements of refractive index. Among the many possible applications is the control of adulteration of liquids.

Experimental Section:

Material. Ethylene glycol, D-mannitol, D-fructose, sucrose and maltose were purchased from Merck Company (Germany). They are used without further purification.

Apparatus and Procedure. Refractive indexes for the sodium D-line were measured with an Abbe reftactometer (CARL ZEISS, Model A, Germany).A minimum of three independent readings were taken for each composition.The uncertainties of the refractive index are ± 1 × 10^{-4}.

Table 1. Refractive indices (n_D) as functions of molar concentration (c) also K_n (obtained from equation 1) for aqueous solutions of D-Fructose at atmospheric pressure and T = 292.15 K

c (mol/L)	n_D	K_n	c (mol/L)	n_D	K_n	c (mol/L)	n_D	K_n
0.0954	1.3355	0.0252	0.9226	1.3565	0.0254	3.5128	1.4205	0.0249
0.2085	1.3384	0.0254	1.1244	1.3616	0.0253	4.0116	1.4326	0.0248
0.3275	1.3415	0.0256	1.6315	1.3744	0.0253	4.5255	1.4450	0.0247
0.5156	1.3462	0.0254	2.3645	1.3925	0.0251	4.9425	1.4547	0.0246
0.7133	1.3513	0.0255	2.9547	1.4070	0.0250	5.2137	1.4612	0.0246

Results and Discussion:

The experimental values of refractive index for aqueous solution of D-fructose at $T = 292.15$ K and different molar concentration are listed in Table 1.

It is clear that for this solution the refractive index values increases with the molar concentration increasing. Also the variation of refractive index against molar concentration is liner (Figure 1).

As seen in Figure 1 by plotting of the curve of refractive index versus molar concentration (c) for aqueous solution of D-fructose at $T = 292.15$ K the following equation obtained ($R^2 = 0.9999$):

$$n_D = 0.0246\,c + 1.3337 \qquad (1)$$

For different aqueous solutions we can write this equation (n_D vs c) and then obtain K_n. for each aqueous solution the coefficient K_n indicate the strength of this solution on decreasing of light velocity when the light move through of this solution. The value of K_n can be dependent on molecular weight, molecular structure and number of free electrons of solute molecule [4]. For example, the values of K_n increases as the weight of solute molecules increase.

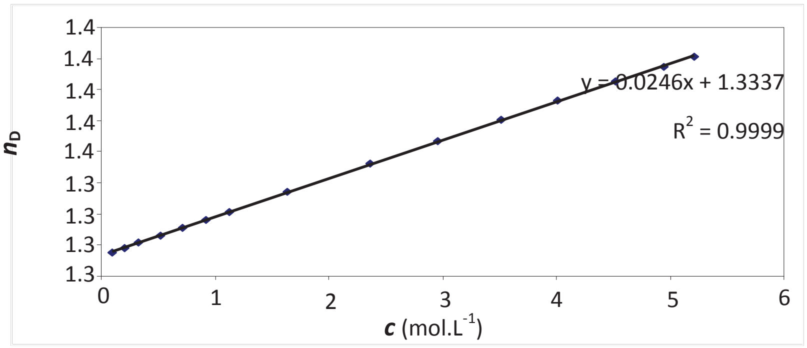

Figure 1. Refractive index (n_D) versus molar concentration (c) for aqueous solution of D-fructose at $T = 292.15$ K

Conclusion:

The experimental refractive index for aqueous solution of ethylene glycol, D-mannitol, D-fructose, sucrose and maltose were measured at $T = 292.15$ K and atmospheric pressure. We can obtain the experimental equation for fitting of refractive index.

References:

[1] R. Batista Santiago Neto and etal.; "Determination of absolute values of refractive index of liquids using an interferometric method" ; Revista de Fısica Aplicada e Instrumentacao; 17, 74-79, 2004.

[2] W.M. bin Mat Yunus etal.; "Refractive index of solutions at high concentrations" ; Applied Optics; 27, 3341-3343, 1988.

[3] G. Zocchi.; "Mechanical measurement of the unfolding of a protein" ; Europhysics Letter; 35, 633-638, 1996.

[4] F. Koohyar and etal.; "Refractive indices, viscosities, and densities for L-cysteine hydrochloride monohydrate + D-sorbitol + water, and glycerol + D-sorbitol + water in the temperature range between T = 303.15 K and T = 323.15 K" ; Journal of Solution Chemistry; 40, 1361–1370, 2011.

Study on the thermodynamic properties of binary systems of water + sodium thiocyanate, sodium bicarbonate, sodium acetate and sodium citrate at *T* = 292.15 K and atmospheric pressure

Fardad Koohyar[a*], Abbas Ali Rostami[b], Mohama Javad Chaichi[b], and Seyed Hamed Rahmanpour[c]

[a] Department of Chemistry, Babol Branch, Islamic Azad University, Babol, Iran
[b] chemistry Department, Mazandaran University, POBOX 453, Babolsar, Iran
[c] Faculty of Chemistry, Iran University Science & Technology, Iran
Email: FardadKoohyar@yahoo.com

Keywords: Viscosity, Density, Sodium thiocyanate, Binary system, Refractive index.

Introduction:

Studies on the thermodynamic properties (refractive index: n_D, viscosity: η, and density: ρ) of binary systems are being increasing usual as tools for the investigation of the nature of interaction between molecules in liquid mixtures [1]. Also the thermodynamic properties of aqueous solutions have the important applications in industrial fields such as food, Drug and oil [2,3].

Experimental Section:

Material. Sodium thiocyanate, sodium bicarbonate, sodium acetate and sodium citrate were purchased from Merck Company (Germany). They are used without further purification.

Apparatus and Procedure. Refractive indexes, densities and kinematic viscosities (υ) were measured using an Abbe refractometer (CARL ZEISS, Model A, Germany), a digital vibrating glass tube densimeter (DA-500E, China.) and three Ubbelhode viscometer with automatic measuring unit (SCHOTT, AVS 400, 1.Germany), respectively. The viscosity (η) obtain from kinematic viscosities ($\eta = \upsilon \times \rho$). The uncertainty of density is $\pm 1 \times 10^{-4}$ (g.cm^{-3}). Also the uncertainty of the refractive index and viscosity are $\pm 1 \times 10^{-4}$ and ±0.003 (mPa.s), respectively.

Table 1. Refractive indices, Densities, and Viscosities as functions of mole fractions of sodium thiocyanate, x_1, for aqueous solutions of sodium thiocyanate at atmospheric pressure and $T = 292.15$ K

x_1	ρ (g.cm^{-3})	n	η (mPa.s)	x_1	ρ (g.cm^{-3})	n	η (mPa.s)
0.0055	1.0102	1.3383	1.0339	0.0453	1.0916	1.3734	1.2235
0.0095	1.0189	1.3423	1.0512	0.0567	1.1129	1.3826	1.3139
0.0143	1.0291	1.3465	1.0701	0.0718	1.1397	1.3941	1.4764
0.0187	1.0385	1.3506	1.0868	0.0925	1.1741	1.4089	1.7943
0.0226	1.0466	1.354	1.1021	0.1347	1.2365	1.4356	2.7608
0.0282	1.0582	1.359	1.1252	0.1832	1.2981	1.4618	4.7006
0.0365	1.0747	1.3661	1.1703	0.2185	1.3382	1.4783	7.4532

Results and Discussion:

It can be seen in Table 1 that for aqueous solution of sodium thiocyanate the values of density, refractive index and viscosity (Figure 1) increases as the mole fractions of solute increase (at 292.15 K).

Most studies on viscosity are confined to the description of dilute solutions of solutes via determination of the *A*- and *B*-coefficients in the Jones-Dole equation [4]:

$$\frac{\eta}{\eta_\circ} = 1 + Ac^{1/2} + Bc \qquad (1)$$

Where η and $\eta_\circ$ are the viscosities of solution and solvent responsively.

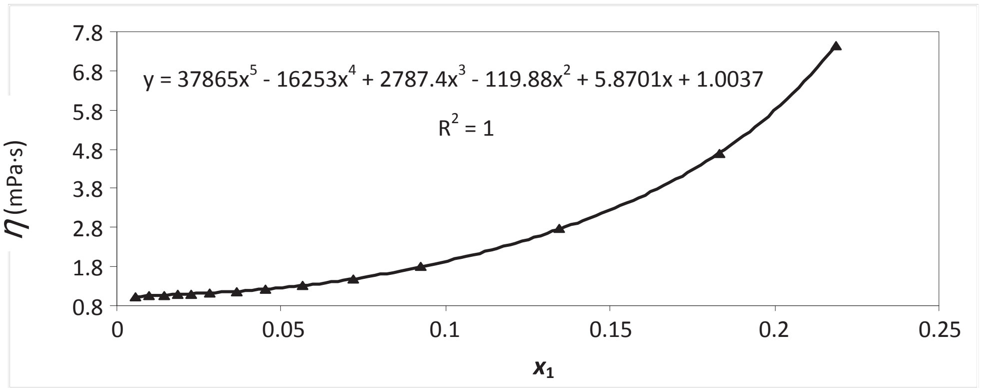

Figure 1. Variation of viscosities, η, against mole fraction of sodium thiocyanate, x_1, for binary system of water (1) + sodium thiocyanate (2) at $T = 292.15$ K

Conclusion:

Experimental viscosities, densities, and refractive indices for binary system of water + sodium thiocyanate, sodium bicarbonate, sodium acetate and sodium citrate were obtained over the wide range of composition and *T* = 292.15 K. some of the experimental equations was applied for fitting of the thermodynamic properties data.

Reference:

[1] F. Koohyar and etal.; "Study on the change of refractive index on mixing, excess molar volume, and viscosity deviation for aqueous solution of methanol, ethanol, ethylene glycol, 1-propanol and 1,2,3-propantriol at T = 292.15 K and atmospheric pressure" ; Research Journal of Applied Sciences, Engineering & Technology; Article in Press.

[2] Y.F. Hu.; "The thermodynamics of nonelectrolyte systems at constant activities of any number of components" ; Journal of Physical Chemistry. B.; 107, 13168-13177, 2003.

[3] S.D. Deosarkar and etal.; "Density, viscosity, surface tension, and refractive indices of ternary liquid mixtures" ; Journal of Chemical, Biological and Physical Sciences; 2, 654-660, 2012.

[4] P. Bohuon and etal.; "Process in ternary liquids: experimental study of mass transport under natural and forced convection" ; Journal of Food Engineering; 37, 451-469, 1998.

HSA-FCCP interaction: Aggregation behavior of HSA-FCCP complex

M. Mahmoodian-Moghaddam [a*], M. Pirouzi [a], M. R. Saberi [b], J.Chamani [a]
a Department of Biology, Faculty of Sciences, Mashhad Branch, Islamic Azad University, Mashhad, Iran
b Medical Chemistry Department, School of Pharmacy, Mashhad University of Medical Sciences, Mashhad, Iran
Email: mahmudian.maryam@gmail.com

Key words: HSA, FCCP, Zeta-potential, RLS.

Introduction

Protein is a vital chemical substance in our life and the predominant target of many drugs in the human body. Thus, investigate upon protein-drug interaction is very useful for determining the therapeutic effectiveness of drugs on bio targets. Human serum albumin (HSA) is the most important protein of the blood plasma that acts as a carrier for various drugs such as anti-cancer drugs [1]. It has been proved that macromolecule such as albumin notably accumulates in tumor tissues so HSA is a potential drug carrier of anti-cancer agents such as FCCP [2]. FCCP is a potent uncoupling agent that uncouples mitochondrial oxidation from phosphorylation, thus it can improve from energy production by mitochondria in cancer cells and cusses cell death [3]. In this work we study on the interaction between HSA and FCCP and aggregation behavior of HSA in response to the existence of FCCP by resonance light scattering (RLS) and Zeta-potential measurements.

Material and methods:

All reagents were purchased from Sigma-Aldrich Chemical Corporation (St. Louis, USA) and used without further purification. The concentration of HSA and FCCP were 1.5×10^{-3} and 10^{-10} mM, respectively. Stock solution of HSA and FCCP were always prepared freshly in the phosphate buffer solution with concentration of 50 mM at pH 7.4.

Apparatus:

The resonance light scattering spectroscopy was applied with an F-2500 spectrofluorometer (Hitachi, Japan) by simultaneously scanning the excitation and emission with $\Delta\lambda = 0$ nm. The zeta potential measurements were administered on a Zeta Sizer Non series-ZS (Malvern Instrument, UK) and a Dispersion Technology Software (DTS) at 298 K using drug.

Result and discussion:

The RLS measurement of HSA-FCCP system indicate that when the FCCP concentration reached to 1.49×10^{-12} mM the RLS intensity initiated to increasing because the complex is formed and also FCCP aggregated on the HSA. The zeta-potential measurement of HSA-FCCP system demonstrates there is an initial increase of the zeta-potential with increasing FCCP amounts to 1.42×10^{-12} mM, that correspond to initial point of aggregate. The positive value of the zeta-potential also proves the existence of electrostatic interactions between HSA and FCCP molecules. At higher concentration of FCCP there is a reversal in the sign of the zeta-potential which becomes negative that suggests interaction will continue via hydrophobic binding.

Conclusion:

The observed increase in RLS intensity proves that interaction between HSA and FCCP can occur then HSA can serve as carrier for deliver FCCP to bio target. The obtained result from RLS and Zeta-potential measurements express that the concentration of FCCP that is less than approximately 1.4×10^{-12} probably is appropriate to cancer therapy.

Reference:

[1] G. Zhang and etal ; “Study of the interaction between icarrin and human serum albumin by fluorescence spectroscopy” ; J. Mol. Struct; 881, 132-138, 2008.

[2] L. Trynda-Lemiesz. ; “Paclitaxel-HSA interaction. Binding sites on HSA molecule” ; Bioorg. Med. Chem ; 12, 3269-3275, 2004.

[3] B. Maro and etal ; “In vivo and in vitro effects of the mitochondrial uncoupler FCCP on microtubules” ; EMBO J. 1, 1347-1352, 1982.

Excess molar volume of Binary mixtures of2- Butanol , Cyclohexanon,Methylcyclohexane

D. moltaji[a*] , m. Almasi[a], zb. Nojini[b]

a Department of.chemistry Science and Research Branch, Islamic Azad University, Khouzestan,Iran

b- factulty 0f science shahid chamran university of ahvaz
Email : moltaji_davood@yahoo.com
m.almasi@khouzestan.srbiau.ac.ir

Key words: Excess molar volume ,Methyl Cyclohexane , Cyclohexanon , 2- Butanol

Introduction:

Most chemical and biochemical phenomena take place in solution. Solution is a homogeneous mixure of two or more substances. Since the relative values of ingredients of a solution can change limitedly, it is a system of the combination of variable percentages. Thermodynamic characteristics of solutions are obtained by measuring density, viscosity, etc. The importance of these characteristics can be mentioned as follows:

1. They are useful for the justification of physical andchemical processes in biological and engineering sciences ,agriculture ,pharmacy and many other sciences.
2. These properties can be used for better understanding of interactions between molecules and molecular structure.1

Materials and methods:

The substances used in this study were 2-Butanol,Cylohexanon and Methyl Cyclohexane. All used substances were Merck and Aldrich with a purity higher than 99.5%. The purity of these materials was verified by comparing their density and viscosity with the values obtained from other articles.

Apparatus:

The density of the pure compounds and mixtures was measured by means of an Anton Parr DMA 4500 oscillating U-tube densimeter, provided with automatic viscosity correction. The uncertainty of density measurement was ±1 × 10^{-5} g.cm^{-3}.

Result and discussion:

The excess molar volumes V_m^E for the binary systems were evaluated using the equation

$$V_m^E = \sum_{i=1}^{N} x_i M_i (\rho^{-1} - \rho_i^{-1}) \quad 1$$

where ρ is the density of the mixture, ρ_i is the density of pure component *i*, x_i is the mole

the mixture. V_m^E for the binary systems were fitted by the least-squares method to the Redlich–Kister [3] equation $V_{ij}^E = x_i x_j \sum_{k=0}^{n} A_k (x_i - x_j)^k \quad 2$

Experimental data and fitted equations for the three binary systems are depicted in Fig. 1.

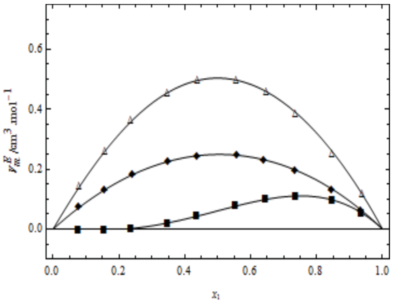

Fig. 1 Excess molar volumes at 298.15 K for the binary systems: Methyl Cyclohexane + Cyclohexanon ( ).

2- Butanol +Cyclohexanon ( ) and 2- Butanol +Methyl Cyclohexane (Δ)

Full line calculated with Redlich–Kister equation.

Excess molar volume was calculated for 2-Butanol+Cyclohexanon,2-Butanol+Methyl Cyclohexane and Methyl Cyclohexane+Cyclohexanon systems at a temperature range from 298 K. Excess molar volume was reported positive for each systems , and it increased with temperature . It seems that, as a result of mixing the solutions, an attraction state arises between them, and then they transform into monomer. The monomer state can occupy a large space, which , in turn, leads to increase in volume.

Conclusion:

Densities and excess molar volumes V_m^E of binary and ternary mixtures of 2-Butanol-Methyl cyclohexan and Cyclohexanon were measured at 298K. The measured data and calculated values of all systems are in good agreement.

References

[1]: Levine, I. 1976." Physical chemistry ", McGraw Hill.

[2] Almasi, M.; Iloukhani, H. Densities, Viscosities, and Refractive Indices of Binary Mixtures . Mixtures of Acetophenone and 2-Alkanols. J. Chem. Eng.Data **2010**, 55, 1416–1420

[3] Redlich, O., Kister, A.T.: Algebraic representation of thermodynamic properties and the classification of solutions and. Ind. Eng. Chem. **40**, 345–348 (1948)

Thermodynamic study of molecular interactions in binary systems

D. moltaji[a*] , m. Almasi[a], zb. Nojini[b]

a Department of.chemistry Science and Research Branch, Islamic Azad University, Khouzestan,Iran

b- factulty 0f science shahid chamran university of ahvaz

Email : moltaji_davood@yahoo.com.com

m.almasi@khouzestan.srbiau.ac.ir

key words: Thermal coefficient -2-butanol –cyclohexanon- Methyl Cyclohexane

Introduction:

Excess properties of mixtures provide information about the molecular interactions between the various components and can be used for the development of molecular models describing the thermodynamic behavior of mixtures [1– 2].

The thermodynamic properties of mixtures are of great industrial interest**.** The property studied has proved to be meaningful from a thermodynamic point of view, as it provides direct information about the energetic effects arising between the molecules present in the mixture, so it can help to explain the rearranging of the bondings that occurs during the mixing process, which is essential when studying new theoretical approaches to the liquid state, either pure or mixt ure.

Materials and methods:

The substances used in this study were 2-Butanol,Cylohexanon. All used substances were Merck and Aldrich with a purity higher than 99.5%. The purity of these materials was verified by comparing their density and viscosity with the values obtained from other articles.

Apparatus:

The density of the pure compounds and mixtures was measured by means of an Anton Parr DMA 4500 oscillating U-tube densimeter, provided with automatic viscosity correction. The uncertainty of density measurement was $\pm 1 \times 10^{-5}$ $g.cm^{-3}$.

Result and discussion:

Thermal coefficient of expansion for pure components is calculated by the following equation:

$$\alpha = -\rho^{-1}\left(\frac{\partial \rho}{\partial T}\right)_p \qquad (1)$$

Thermal dependence of density of pure components is indicated by the following equation:

$$\rho(T) = \sum_{i=0}^{4} A_i T^i \qquad (2)$$

In before – mentioned equation T is dead temperature.

Main expression denotes the relationship between molar volume of a mixture and its excess molar volume as follows : $V = \sum_{i=1}^{2} x_i V_i + V_m^E$ (3)

Where v_1 and x_1 are molar volume of component i. In case of mixtures, by differentializing equation2 we can obtain the following expression:

$$\left(\frac{\partial V}{\partial T}\right) = \left[\frac{\partial\left[\sum_{i=1}^{2} x_i V_i\right]_{p,x}}{\partial T}\right]_{p,T} + \left[\frac{\partial V_m^E}{\partial T}\right]_{p,x_i} \qquad (4)$$

Thus, thermal coefficient of expansion for mixtures is calculated by the following equation : (2)

$$\alpha = \frac{1}{V}\left[\left(\frac{\partial V_m^E}{\partial T}\right)_{p,x} + \sum_{i=1}^{2} \alpha_i x_i V_i\right] \qquad (5)$$

Where α and α_1 are thermal coefficient of expansion of mixture and pure component respectively .Figure 1. excess thermal coefficient of expansion α^E for two – component mixture 2- Butanol + Cyclohexanon at temperatures 298( ),◆303( ),■308( ) □and 313( ). ●

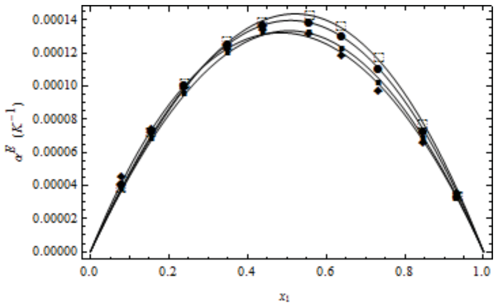

The values of thermal coefficient of expansion were obtained for 2- Butanol +Cyclohexanon. The values of this quantity were positive and regularly increased as the temperature grew up. The positive values of excess thermal coefficient of expansion that the expansion of solution is greater than liquids in their pure form.

Conclusion:

The values of thermal coefficient of expansion were obtained for 2- Butanol +Cyclohexanon .The measured data and calculated values of this systems are in good agreement.

References:

[1] Iloukhani, H., Almasi, M.: Densities, viscosities, excess molar volumes, and refractive indices of acetonitrile and 2-alkanols: Experimental results and application of the Prigogine–Flory–Patterson theory. Thermochim Acta. **495**, 139**–**148(2009)

[2] Almasi, M.; Iloukhani, H. Densities, Viscosities, and Refractive Indices of Binary Mixtures of Acetophenone and 2-Alkanols. J. Chem. Eng.Data **2010**, 55, 1416–1420.

Thermal Stability of Hen egg white lysozyme (HEWL) with Ni(II)salen

N. Sohrabi[a*], N. Rasouli [a], M. Raissi[a], S.Faraji[b]
a Department of Chemistry, Payame Noor University, 19395-3697, Tehran, Iran.
b Department of Physics Faculty of Science Shaheakord University , Shaheakord, Iran.
e-mail:nasrinsohrabi@yahoo.com*

Keyword: Lysozyme , Ni(II)Salen, Thermal stability ,Denaturation and Schiff base.

Introduction:

Schiff bases drived from Salicylaldehyde and diamines as N,N'-bis (Salicylaldehyd) ethylene diamine are one of the most synthetic ligand system with important in asymmetric catalysis[1]. In the area of bioinorganic chemistry interest in Schiff-base complex has containing sites in metallo-proteins and metallo enzymes [2]. Lysozyme is a global protein, cosists of 129 amino acids with a molecular weight of about 14.3KD. Its structure is stabilized by four disulfide bridges and the interior of the protein is almost hydrophobic while the surface is mostly polar[3,4].

So,In the present work thermal denaturation of lysozyme has been studied and the melting point of lysozyme in the presences and absences of Ni(II)Salen [Salen :N,N′-bis(Salicydene)1,2-diamino ethane] to analysis denaturation data we use Sigma plot and Igor softwores.

Materials and Methods:

Lysozyme (HEWL)Was obtained from cenajen and Ni(II)Salen synthesized in laboratory [5] and other chemical materials were obtained from merck company. All solutions was prepared freshly.

Apparatus:

The absorbance monitoring was performed on a Perkin-Elmer UV/Vis Lambada 2 equipped with thermostat cell compartment and lambada 2 software. The spectrophotometer was equipped with a cell thermostst bath .

Results and Discussion:

The UV/Vis titration experimants were made by addition of Ni(II)salen solution in to a 1.4ml curette containing the HEWL solution of appropriate concenteration. The titration of experiments were performed at various temperature with precision of ±1˚C.

The melting curves of both free HEWL and HEWL-Ni(II)sale complex in phosphate buffer were obtainal by measuring the lysozyme absorbance at 281 nm as a function of temperature. Melting temperatures were measured in phosphate buffer pH 7.0 containing 9.7 μM lysozyme. The temperature was scabbed from 25 until 93˚C.

In order to identify the solution properties of Ni(II)salen, we employed UV/Vis spectroscopy. the optical absorption Spectrum of Ni(II)Salen shows two bands in 321 , 392 nm and a weak band at 443 nm, we choose 392nm.

Conclusion:

In this work interaction of lysozyme with Ni(II)Salen in 5 mM phosphate buffer, pH=7 were studied using differential UV/Vis spectroscopy method at different temperatures.The temperatures absorbance measurements at 281 nm. Change in absorbance of protein-Salen complex with temperature were used to determine the denaturation of melting temperature T_m ,thermodynamic parameters, ΔH_m ,ΔG_m and the heat capacity change ΔCp_m between the native and denatured states.Then increasing of T_m upon addition of Ni(II)salen concentration show increasing protein stability with complx formation..

References

[1]E.N.Jacobsen, Acc.Chem.Res.33, 421-425, 2000.

[2] A. A, Khandar , B.Shaabani, F.Belaj, A .Bakhtiari, Polyhedron, 25, 1893-1900, 2006.

[3] J. M.Ruso, A. G. Perez, Inter. J. Biol. Macro., 33 , 67-69, 2003.

[4] P.Pirzadeh, A. A. Moosavi-Movahedi, B.Hemmateenejad, F. Ahmad, M.Shamsipur, A.A.Saboury, Colloids and Surfaces B:Biointerfaces, 52 , 31-33, 2006.

[5] C.R. Jacob, S.P.Varkey,P.Ratnasamy, Appl.Catal. A:Gen. 182 ,91-96,1999.

Determination of thermodynamic and thermoacuatic parameter of binary mixtures {methyl acrylate + benzene, + toluene, + o-xylene, + *m*-xylene, and *p*-xylene} at different temperatures and application of the Flory theory

M. Rezaei Sameti[1], M. Rakhshi[2], H. Seyed Al-Hosseini[2], H. Iloukhani[2]
[1]Department of Physical Chemistry, Faculty of Sciences, Malayer University, Malayer, Iran
[2]Faculty of Chemistry, University of Bu Ali Sina, Hamadan, Iran
E-mail.mrsameti@malayeru.ac.ir

Keywords: Flory theory; Moelwyn-Hughes; Isobaric; Isochoric acoustical ; Isochoric temperature coefficient

Introduction:

The studies of thermodynamic and thermoacuatic properties of binary mixtures provide useful information about physical forces acting between the molecules of the same substance in pure liquids and the nature of interactions between the unlike molecules [1-3]. When two liquids are mixed together, the resulting changes in physical and thermodynamic properties can be considered as a sum of several contributions due to free volume change, change in energy, change in molecular orientations, steric hindrances etc[4-5].

Results and discussion:

Thermal expansion coefficients α , and their excess values α^E , and isothermal coefficient of pressure excess molar enthalpy $(\partial H_{\mathrm{m}}^{\mathrm{E}} / \partial P)_{\mathrm{T},x}$ of the binary mixtures formed by {methyl acrylate + benzene, + toluene, +*o*-xylene, + *m*-xylene, and +*p*-xylene} were measured at (293.15-318.15)K for the liquid region and at ambient pressure. The obtained results were then compared with the calculated values by using the Flory theory of liquid mixtures. The results show a good agreement between theory and experimental data. From these data available volume (V_{a}), isothermal ($K^{/}$), isobaric (K), and isochoric acoustical parameters ($K^{//}$), isochoric temperature coefficient of the internal pressure (X), and Moelwyn-Hughes parameter (C_1), have been calculated. The excess thermal expansion coefficients and isothermal coefficient of pressure excess molar enthalpy were correlated as a function of the mole fraction by using the Redlich–Kister equation for binary mixture, respectively. The thermo acoustical method has also been employed to obtain the available volume, V_a, using the relation(1-2),

$$V_a = V_T\left[\frac{1}{K^{/}+1}\right] = V_T\left[\frac{1}{K^{//}+K}\right] \qquad (1) \qquad\qquad K^{/} = K + K^{//} = \frac{1}{2}\left[3+\frac{S^{*}(1+\alpha T)+X}{\alpha T}\right] \qquad (2)$$

The Flory model has been commonly employed to analyze the molar volume of the mixture and the excess molar volume parting from the equation (3) of the state in function of the reduced variables:

$$\frac{\tilde{P}\,\tilde{v}}{\tilde{T}} = \left[\frac{\tilde{v}^{\frac{1}{3}}}{\tilde{v}^{\frac{1}{3}}-1}\right] - \left[\frac{1}{\tilde{v}\,\tilde{T}}\right] \qquad (3)$$

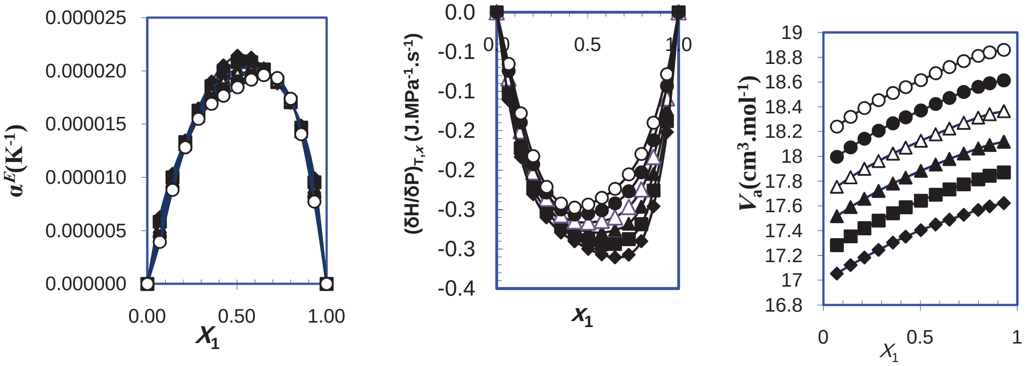

Fig. 1. Plot of V_a , α^E and $(\partial H^{\mathrm{E}}_{\mathrm{m}} / \partial P)_{\mathrm{T},x}$ against mole fraction for {(B$_1$);Ma + benzene , (B$_2$); Ma + toluene, (B$_3$) ; Ma + *o*-xylene, (B$_4$); Ma + *m*-xylene, (B$_5$); Ma + *p*-xylene, } at 293.15 K (♦), 298.15 K (■), 303.15 K (▲) ,308.15 K (Δ) ,313.15 K (●) ,318.15 K (o).

References:

[1]. M. Rezaei-Sameti, H. Iloukhani H, Rakhshi Russ. J. Phy. Chem., 84(2009) 2023-2032.

[2] M. Rezaei-Sameti, H. Iloukhani, M. Rakhshi, J. Mol. Liq., 149(2009) 96-100.

[3] M. Rezaei-Sameti ,H. Iloukhani, M. Rakhshi Phy. Chem. Liq., 48(2010) 608-617.

[4] C. Yang ,P. Ma ,Q. Zhou *J. Chem. Eng. Data*, *49* (2004),881–885

[5] AK. Nain, R. Sharma R, A. Ali J. Mol. Liq158(2011) 139-144

Complexation thermodynamics of dioxovanadium(V) by calix[4]arene in solution

Karim Zare and Solmaz Nasirvand Shaker
Chemistry Department, Science and Research Branch, Islamic Azad University, Tehran, Iran
Email: info@dr-karimzare.com

Key words: Calix[4]arene, Complexation, Dioxovanadium(V), Coordination.

Introduction:

Calix[n]arenes are one of the three major groups of organic macrocyclic host compounds in supramolecular chemistry [1]. They are composed of phenol units connected by ortho-methelene bridges and may complex to a variety of guests in solution as well in the solid state [2]. Several calix[n]arene–metal ion complexes have been reported, most of them require that the hydroxyl groups of the calixarene are derivatized to esters or ethers due to the poor solubility of the para-tert-butylcalix[n]arenes [3]. Calix[4]arenes are widely used as building units for construction of preorganized molecules for supramolecular and coordination chemistry applications. The coordination chemistry of the calix[4]arene-based ligands was recently reviewed. The calix[4]arene moiety can be substituted on the upper or lower rim with a large variety of substituents. The coordination properties of such ligands are tuned by appropriate choice of substituents, differing in hydrophilicity–hydrophobicity, the number and type of donor atoms present, etc. Another effect of substituents on the coordination ability is based on the change in geometry of calix[4]arene units due to the steric requirements of substituents [4].

Materials and methods:

Calix[4]arene - crown 6 ether.was obtained from Acros Organics Fig 1., sodium monovanadate and were purchased from Merck (p.a.) and used without further purification. All dilute solutions were prepared from double distilled water with a specific conductance equal to 1.2±0.1 μScm^{-1}.

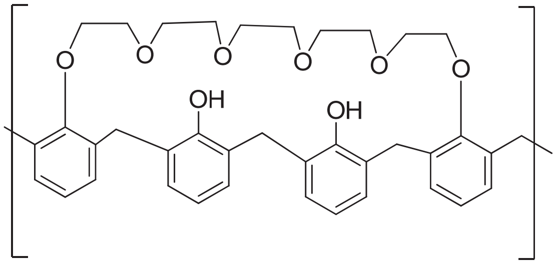

Fig 1. Structure of ligand calix[4]arene- crown 6 ether.

Apparatus:

A Jenway research pH-meter (model 827) was used for the pH measurements. The hydrogen ion concentration was measured with a Jenway combination electrode. The pH-meter was calibrated with Metrohm pH 4.0 and 7.0 buffers leading to pH estimate error of ±0.001 pH units. Spectrophotometric measurements were performed using a UV–Vis cary 300 scanning spectrophotometer with a Pentium4 computer using 10 mm quartz cells.

Result and discussion:

In this work, stability constant of vanadium(V) cation and Calix[4]arene were determined in metanol solution at 25 °C using spectrophotometric technique. The calixarene in this study was consistsed of four benzene rings which are arranged conically, so that hydroxyl groups form a coordination sphere where metal cation can be bound.

Conclusion:

A new dioxovanadium/calix[4]arene compound, has been synthesized under different conditions. We have prepared a new polymer including bis-bipyridyl-calixarene chelating agent ether at complex metal ions with tetrahedral coordination geometry. We concluded that, the molar ratio of ligand to metal was 1:1. The more electric charge effects on metal dioxovanadium is the electrostatic force is stronger so the formed complex is stronger. The stability constants of obtained complexes depend on two groups of upper rim and lower rim as well as size of rings. Amounts of equilibrium constants in L_1 ligand indicate that phenyl rings of calix with π electrons are agent of complexing. Its demonstrated chelating properties are currently explored in separation studies involving various metal ions of economical or environmental interest.

Reference:

[1] C. D. Gutsche, Monographs in Supramolecular Chemistry, Calixarenes, The Royal Society of Chemistry, London, 1989.

[2] J. Vicens, V. Bohmer, Calixarenes. A Versatile Class of Macrocyclic Compounds, Kluwer Academic, Dordrecht, 1991.

[3] R. Perrin, R. Lamartinc, M. Perrin, The Potential Industrial Applications of Calixarenes. Pure Appl. Chem; 65, 1549, 1993.

[4] C. D. Gutsche, Calixarenes Revisited, Royal Society of Chemistry, Cambridge, UK, 1997.

A DFT study of ^{17}O NMR parameters of Benzyl ethers Components

M. Rezaei Sameti , A. Kazemi , V. Mousa Zadeh
Department of physical Chemistry, Faculty of science, Malayer University, Malayer, 65157, Iran
E-mail address: mrsameti@malayeru.ac.ir

Key word: DFT, ^{17}O , NMR, Benzyl ethers

Introduction:

Nuclear Magnetic Resonance (NMR) is a useful technique for studying the structure of chemical and biological systems, from small molecules to complicated structures such as nucleic acids and proteins. Chemical shifts and spin–spin coupling serve to recognize the molecular conformation, composition and environment of the moiety. However, the investigation and understanding of the relationships between molecular structure and measured NMR parameters can sometimes be quite difficult, and need the support of theoretical calculations [1].Theoretical methods for the prediction of the nuclear magnetic resonance (NMR) parameters of molecules have become a useful quantum chemical tool. A number of papers have recently appeared in the literature concerning the calculation of NMR chemical shift (CS.) by quantum-chemistry methods [2-5].

Computational methods:

The entire calculations were performed at density functional (DFT) levels on a Pentium using Gaussian 03. The geometry of the title compounds in (Fig. 1) is fully optimized and ^{17}O NMR chemical shielding are calculated with GIAO and CSGT approach by applying B3LYP method at the 6–31G (d,p), 6-31++G(d,p) and 6-311++G(d, p) basis sets. The obtained shielding tensors were referenced against to an absolute shielding reference σ_{ref} =287.5 ppm

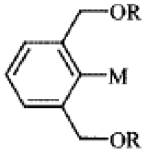

A_1 M=H, R=Me
A_2 M=H, R=Et
A_3 M=H ,R=i-Pr
A_4 M=H ,R=t-But
A_5 M=Br, R=t-But
A_6 M=Br, R=i-Pr
A_7 M=Br, R=Me
A_8 M=Br, R=Et
A_9 M=Li, R=Et
A_{10} M=Li, R=Me
A_{11} M=Br, R=i-pr

Fig. 1

Results discussions

The results show that in the compounds A_1 and A_2, A_4 and A_7 the GIAO method by 6-31++G (d,p), in compound A_3 and A_6 the CSGT method by 6-31++G(d,p) and 6-31G(d,p) respectively and in the compounds A_5 and A_{11} the GIAO method by 6-31G (d,p) are a good agreement with experimental. Fig.1 , Table 1

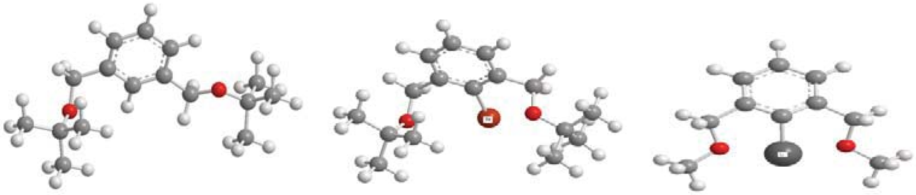

Fig. 1 Optimized of structures of Benzyl ethers derivatives

Table 1. Theoretical chemical shift and experimental chemical shift of Benzyl ethers ^{17}O NMR spectra (*ppm*), deviation error $\Delta\delta = \delta_{EXP} - \delta_{calc}$ with B3lyp/6-31++G(d,p).

Compounds	GIAO	CSGT	Exp. [a]	$\Delta\delta_{GIAO}$	$\Delta\delta_{CSGT}$
A1	-18.0	-2.7	-14.0	4.0	-11.3
A2	4.3	17.7	9.6	5.3	-8.1
A3	29.3	38.0	39.0	9.7	1.0
A4	35.4	39.5	49.0	13.6	9.5
A5	52.2	56.5	40.1	-12.1	-16.4
A6	34.3	44.2	33.0	-1.3	-11.2
A7	-21.3	-5.9	-20.0	1.3	-14.1
A8	2.5	16.2	-		
A9	14.1	20.3	-		
A10	52.0	-5.3	-		
A11	52.1	57.9	33.5	-18.6	-24.4

References

[1] A. Wong, K. J. Pike, R. Jenkins,G.J. Clarkson, T. Anupold, A. P. Howes, D.H. G. Crout, A. Samoson, R. Dupree,M.E. Smith,2006. J. Phys. Chem. A. 110: 1824-1835.

[2] C. Silly, J.Y. Legein, F. Calvayrac, 2004. Solid State Nuclear Magnetic Resonance 25: 241-251.

[3] C. Johnson1, E. A. Moore, M. Mortimer, Solid State Nuclear Magnetic Resonance,. 27, 155-164 (2005).

[4] D.A. Forsyth, A.B. Sebag,1997. J. Am. Chem. Soc 119: 9483-9494 .

[5] E. Virtanen, A. Valkonen, J. Tamminen, E. Kolehmainen ,2003. J. Mol. Structure 650 : 201-212 .

Thermodynamic study of heterogeneous interactions in the mixture of 1,2-Butanediol and 2-ethyl-1-hexanol through dielectric data at *T* = (298.2, 308.2 and 318.2) K

A. Ghanadzadeh Gilani*[a], H. Ghanadzadeh Gilani [b], M. Ansari [a]
a Department of Chemistry, Faculty of Science, University of Guilan, Rasht, Iran
b Department of Chemical Engineering, University of Guilan, Rasht, Iran
Email: masoumeh_chem@yahoo.com

Key words: Relative permittivity; Dipole moment; 1,2-Butanediol; Kirkwood factor; Excess free energy

Introduction:

Dielectric studies on binary mixtures are important for understanding the intermolecular interactions (dipole-dipole interaction and hydrogen bonding) in the mixture. The heterogeneous and homogeneous interactions in binary mixtures using dielectric measurements have been studied and reported by several investigators [1–3].1,2-butanediol (1,2BD) is one of four stable isomers of BD, which has many scientific and industrial applications. The presence of two hydroxyl groups in vicinal positions (at the positions 1 and 2) of this diol makes it suitable as a useful chemical intermediate in the manufacture of many chemical products. The separation of BDs from aqueous solutions using solvent extraction technique is industrially and scientifically important. It is recently reported that, 2-ethyl-1-hexanol (2EH) can be used as a good solvent for the extraction of BDs from aqueous solutions [4].

Materials and methods:

The chemicals 2-ethyl-1-hexanol (mass fraction purity > 99.5%) and cyclohexane (mass fraction purity > 99.9%) were obtained from Merck. 1,2-butandiol (mass fraction purity > 98%) was purchased from Fluka. appropriate amounts of the solute into 10 cm^3 volumetric flasks with an The high purity grade cyclohexane was used for the calibration of the dielectric cell.

Apparatus:

The refractive indices of the solutions were determined at a wavelength of 589 nm using an Abbe Refractometer (Model CETI). The densities of the pure compounds were measured at various temperatures using DA 210 (Kyoto electronic) density meter. The electrical capacitance of the dielectric cell was measured using a Wayne Kerr model 6425B Digibridge. A three-terminal dielectric cell was constructed for measurements on small volumes of solutions.

Result and discussion:

The heterogeneous interaction in the polar mixture may also be obtained from the modified Bruggeman equation.The heterogeneous interaction may be obtained by the excess permittivity (ε^E).The excess Helmholtz energy (ΔF^E) is almost equal to the Gibbs energy ΔG for a condensed phase and is a suitable parameter to evaluate the interaction (both the long-range and short-range) between the components. For the investigated temperature range, the deviation of ΔF^E for the system was found to be positive in both the solute-rich and solvent-rich regions. For this system, the excess free energy due to short-range interaction between dissimilar molecules (ΔF_{12}) are positive in the 1,2BD rich region, suggesting anti-parallel orientation of the dipoles.

T/K	x_2	$\Delta F_0^E(J/mol)$	$\Delta F_{rr}^E(J/mol)$	$\Delta F_{AB}^E(J/mol)$	$\Delta F^E(J/mol)$
298.2	0	0.00	0.00	0.00	0.00
	0.111	72.63	-5.30	-8.94	58.39
	0.199	114.88	8.65	-16.09	107.44
	0.291	139.70	31.58	-16.56	154.72
	0.345	148.22	47.12	-14.39	180.95
	0.399	151.02	62.27	-10.45	202.83
	0.448	145.50	73.57	-6.23	212.84
	0.501	141.02	85.40	-2.18	224.24
	0.563	125.36	93.06	2.19	220.61

Conclusion:

Values of static permittivity, Kirkwood correlation factors, Bruggeman parameter, excess permittivity, and excess Helmholtz energy for the binary liquid system of 1,2BD with 2EH studied at various concentrations have been reported. From the dielectric data, the heterogonous interactions for investigated mixture were calculated. For this system , the strength of the interaction between the unlike molecules reach a maximum when the composition is approximately 0.5 in 1,2BD.

Reference:

[1]M.K. Kroeger, *J. Mol. Liq.*, 36 (1987) 101-118.

[2]A. Ghanadzadeh, M.S. Beevers, *J. Mol. Liq.*, 100 (2002) 47-57.

[3]T. Thenappan, A. Prabakar Devaraj, *J. Mol. Liq.*, 123 (2006) 72-79.

[4]A. Ghanadzadeh, H. Ghanadzadeh , S. Abbasnejad , Kh. Bahrpaima, *Fluid Phase Equilib.* 291 (2010) 90–94.

Thermodynamic analysis of single and two-step oxidative dehydrogenation of propane with carbon dioxide

Farnaz Tahriri Zangeneh[a*], Saeed Sahebdelfar[b], Abbas Taeb[a]
[a] Department of Chemistry, Science and Research Branch, Islamic Azad University, Tehran Iran.
[b] Petrochemical Research and Technology Company, National Petrochemical Company, P.O. Box 1435884711, Tehran, Iran
Email: tahriri_zangeneh@yahoo.com

Key words: Oxidative dehydrogenation, Carbon dioxide, Propylene, Thermodynamics

Introduction:

Propane dehydrogenation (PDH) has received much attention to meet the ever-increasing propylene demand based on:

$$C_3H_8 \Leftrightarrow C_3H_6 + H_2 \qquad \Delta H^0_{298} = 124 \text{ kJ/mol} \qquad (1)$$

The reaction is highly endothermic and equilibrium limited. Consequently, the elimination of H_2 product by a mild oxidant such as CO_2 (via reverse water-gas-shift, reaction 2) over suitable (non-redox oxides, e.g. Ga_2O_3) catalysts can increase equilibrium conversions [1].

$$H_2 + CO_2 \Leftrightarrow CO + H_2O \qquad \Delta H^0_{298} = 40 \text{ kJ/mol} \qquad (2)$$

The reaction can also occur in single-step over redox oxide (e.g., Cr_2O_3 and V_2O_5) catalysts:

$$C_3H_8 + CO_2 \Leftrightarrow C_3H_6 + CO + H_2O \qquad \Delta H^0_{298} = 164 \text{ kJ/mol} \qquad (3)$$

The PDH in the presence of CO_2 is also of interest because it utilizes a greenhouse gas [2].

In this work, the chemical equilibria of single and two-step oxidative PDH with CO_2 are studied and the results are compared with those of simple conventional steam diluted PDH.

Materials and methods:

The equilibrium compositions were obtained by Gibbs free energy minimization of the gaseous system using Lagrange undermined multiplier method [3]. The resulting set of equation was solved by using Matlab software and the results were compared to reported data.

Result and discussion:

Figure 1 shows the equilibrium conversion of propane in the presence of steam and CO_2. Both steam and CO_2 increase the conversion due to lowering partial pressure of the hydrocarbons. CO_2 further increases the conversion, especially in two-step pathway, by consumption of H_2. Figure 2 shows that H_2/CO ratio of the product in two-step process decreases with CO_2 content of the feed and approaches to that of single-step (that is, zero) path, resulting the convergence of the two paths for CO_2-rich feeds as also confirmed by Fig. 1.

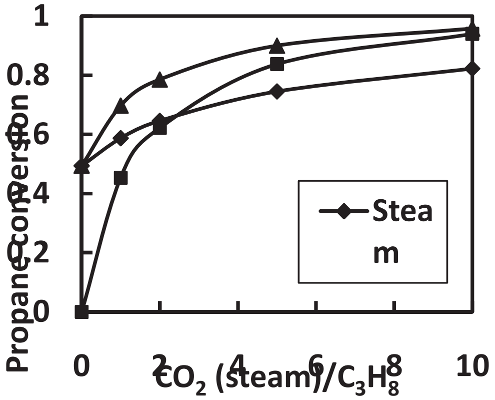

Figure 1. Effect of CO_2(or steam)/C_3H_8 on propane conversion at 873 K.

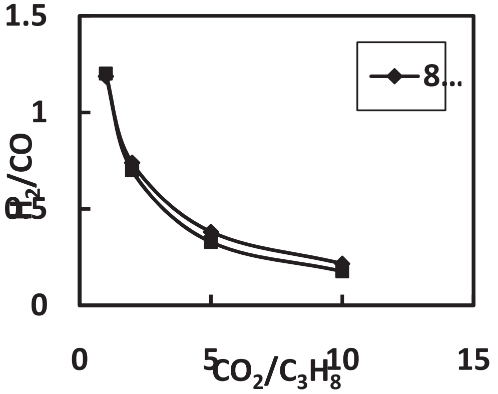

Figure 2. Effect of CO_2 (or steam)/C_3H_8 on two-step equilibrium H_2/CO molar ratio.

Table 1 shows the temperatures required for 50 and 60% propane conversions (typical commercial values) for different pathways. For 60% conversion, equimolar addition of CO_2 to the feed reduces the reaction temperature for no dilution and steam diluted by 54 and 29 K, respectively, illustrating the advantage of using CO_2 as a mild oxidant in PDH.

Table 1. Temperatures (K) required for 50 and 60% propane conversions (CO_2(steam)/C_3H_8=1, *P*=1 atm).

Conversion (%)	Temperatures (K)			
	No dilution	Steam	CO_2 (single-step)	CO_2 (two-step)
50	875	850	891	821
60	901	876	930	847

Conclusions:

Equilibrium calculations of CO_2 PDH give promising results. Using CO_2 as a mild oxidant, the reaction temperature could be reduced about 50 K for a given conversion; especially in two-step reaction pathway. In practice, however, the conversion levels are lower than equilibrium ones implying that further research is required to develop more efficient catalysts.

References:

[1] P. Michorczyk, J. Ogonowski, K. Zenczak, Activity of chromium oxide deposited on different silica supports in the dehydrogenation of propane with CO_2 – A comparative study, Journal of Molecular Catalysis A: Chemical; 349 (2011) 1-12.

[2] F. Tahriri Zangeneh, S. Sahebdelfar, M. Takht Ravanchi, Conversion of carbon dioxide to valuable petrochemicals: An approach to clean development mechanism, Journal of Natural Gas Chemistry; 20 (2011) 219-231.

[3] K. Faungnawaki, R. Kikuchi, K. Eguchi, Thermodynamic analysis of carbon formation boundary and reforming performance for steam reforming of dimethyl ether, Journal of Power Sources; 164, 73–79, 2007.

Thermodynamic study of poly(vinyl alcohol) solutions by viscometry

Abbas Mehrdad, Javad Jafari*

Department of Physical Chemistry, Faculty of Chemistry, University of Tabriz, Tabriz, Iran

Email: j.jafari89@ms.tabrizu.ac.ir

Key words: polymer solution, poly(vinyl alcohol), intrinsic viscosity, expansion factor

Introduction:

When high molecular weight nonionic polymer molecules dissolve in a fluid, they typically expand to form spherical coils. A polymer coil’s hydrodynamic volume depends upon the polymer molecular weight and its thermodynamic interaction with the solvent. Favorable polymer–solvent interactions also increase the hydrodynamic volume of the polymer coil. When the polymer–solvent interactions are unfavorable, the polymer coil volume is decreased. With unfavorable polymer–solvent interactions, polymer coils can completely collapse and become insoluble in the fluid. Polymer–solvent interactions depend upon the polymer molecular structure, chemical composition, solution concentration, solvent molecular structure, and the solution temperature [2,3].

Materials and methods:

The polyvinyl alcohol (PVA) used in this study was purchased from Merck Chemical Co. and had a reported nominal average molar mass of 72 kg·mol^{-1}. Distilled water was used for preparation of solutions. The polymer solutions were filtered before use and their viscosities were measured using a jacketed Ubbelohde viscometer with 0.4 mm capillary.

Results and discussion:

The viscosities of aqueous solutions of PVA were measured at various temperatures and concentrations of polymer. According to the Huggins equation, the intrinsic viscosity, [η], of the polymer is obtained by extrapolation of reduced viscosity to zero polymer concentration. The obtained intrinsic viscosities and Huggins constants, k_H, are listed in Table 1. Our data reveals that the Huggins constants for PVA in water are higher than the expected value (0.35). The obtained intrinsic viscosities of PVA are decreased by increasing temperature. Therefore, mixed water was changed to the weak solvents for PVA by increasing temperature. The values of expansion factor (α) which calculated using intrinsic viscosities are listed in Table 1. The values of expansion factor were decreased by increasing temperature. For evaluating of theta temperature and entropy of dilution parameter, the values of $(\alpha^5 - \alpha^3)$ plotted versus 1/T. From the intercept and slope of these plots the values of theta temperature and entropy of dilution parameter were calculated. The obtained theta temperature and entropy of dilution parameter are 420 K and -15, respectively. The obtained entropy of dilution parameter indicates that entropy of dilution parameter is negative that is, solvent molecules are ordered by PVA. The heat of dilution parameter, κ, were calculated and listed in Table 1. The obtained results indicate that heat of dilution parameter is negative that is, interactions of segment-solvent are favored toward segment-segment in PVA. By using entropy and heat of dilution parameters, the polymer-solvent interaction parameter, χ, and second osmotic virial coefficient,A_2, were calculated and listed in Table 1. The results of Table 1 indicate that polymer-solvent interaction parameters are increased by increasing temperature. Polymer-solvent interaction parameter and second osmotic virial coefficient are related to the thermodynamic quality of solvent in polymer solutions. A good solvent has a low value of polymer-solvent interaction parameter and positive value of the second osmotic virial coefficient, while a poor solvent has a high value of polymer-solvent interaction parameter and negative value of the second osmotic virial coefficient; therefore the results of Table 1 indicate that the quality water for PVA were decreased by increasing temperature.

Table 1. Some Thermodynamic and hydrodynamic parameters of PVA in water

T/K	$[\eta]/m^3 \cdot Kg^{-1}$	k_H	α	κ	χ	$10^3 A_2/m^3 \cdot mol \cdot Kg^{-2}$
293.15	0.08910	0.609	2.295	-0.6323	0.3143	2.81
298.15	0.08604	0.620	2.268	-0.6217	0.3249	2.69
303.15	0.08290	0.641	2.240	-0.6114	0.3351	2.57
308.15	0.08012	0.654	2.215	-0.6015	0.3450	2.45
313.15	0.07820	0.650	2.197	-0.5919	0.3547	2.32

Conclusion:

In this work, the polymer solution thermodynamic parameters were evaluated by temperature dependence of polymer chain expansion factor. The obtained thermodynamic parameters indicate that water becomes an increasingly weak solvent for poly(vinyl alcohol) with increasing temperature.

Reference:

[1] Y. Song, P.M Mathias, D. Tremblay,C. Chen, *Ind. Eng. Chem. Res.* 42 (2003) 2415-2422.
[2] L.T. Novak, C. Chen, Y. Song, *Ind. Eng. Chem. Res.* 43 (2004) 6231-6237.
[3] T.S. Rushing, R.D. Hester, *J. Appl. Polym. Sci.* 89 (2003) 2831-2835.

The effect of poly(ethylene glycol) on the volumetric and acoustic properties of sodium dodecyl sulfate in aqueous solutions

Rahmat Sadeghi*, Elham Bayat
Department of Chemistry, University of Kurdistan, Sanandaj, Iran
*E-mail: rsadeghi@uok.ac.ir

Keywords: Sodium dodecyl sulfate, Volumetric, Micellization, Thermodynamic

Introduction

In the past forty years the interaction between synthetic nonionic hydrophilic polymers and ionic surfactants dissolved in water has been extensively studied. The poly(ethylene glycol) (PEG)/sodium dodecyl sulfate (SDS)/water is a typically important system and has been investigated through many different techniques [1]. The (polymer + surfactant) mixtures have important properties for a wide range of industrial application fields as floatation processes, foaming control, detergency, and enhanced oil recovery. Comparison between thermodynamic properties of surfactants in water and aqueous polymer solutions is interesting and helpful for the better understanding of polymer-surfactant interaction [2,3]. These have convinced us in studying the micellization behavior and evaluation of associated parameters of anionic surfactant SDS in (water + PEG mixed solvent) system. In this work, we present our results on density and sound velocity measurements of solutions of SDS in water and in aqueous solutions of PEG2000, PEG6000 and PEG10000 over a range of temperatures at atmospheric pressure. The effects of polymer and temperature on the apparent molar volume and isentropic compressibility of SDS are studied. From these data, the variation of the critical micelle concentration (CMC) of SDS in pure water and in aqueous PEG solutions with temperature was obtained. Parameters of the micellization of the investigated surfactant in the absence and presence of PEG are also estimated.

Experimental Section

Materials. SDS (mass fraction purity > 0.98), PEG samples with nominal molar mass of 2000, 6000, 10000 were obtained from Merck and were used without further purification, and double distilled and deionized water was used.

Procedures. All the solutions were prepared by mass on a Sartorius CP225D balance precise to within ±0.00001 g. The density and sound velocity of the mixtures were measured at different temperatures with a digital vibrating-tube analyzer (Anton Paar DSA 5000, Austria).

Results and Discussion

In the present work, density and speed of sound measurements for SDS in pure water and in aqueous solutions of 0.1 %w/w of PEG2000, PEG6000 and PEG10000 at T = (288.15, 293.15, 298.15, 303.15 and 308.15) K were carried out in order to describe the effect of PEG on the thermodynamic properties of aqueous SDS solutions. From these data, the values of apparent molar volume, compressibility, and expansibility of the investigated solutions were obtained. Changes in the apparent molar volumes and isentropic compressibilities upon micellization were derived using a pseudophase-transition approach and the infinite dilution apparent molar properties of the monomer and micellar form of SDS in pure water and in the aqueous PEG solutions were determined. Critical micelle concentrations of SDS in the investigated solutions were estimated from the dependence of the determined thermodynamic data on concentration at different temperature and from which the variations of the CMC of SDS in water and in aqueous PEG solutions with temperature and PEG molar mass were obtained. Thermodynamic parameters of micellization of investigated surfactants in water and in aqueous solutions of PEG at different temperatures and PEG molar mass were estimated and it was found that at low temperature the micelle formation process is endothermic and therefore, this process must be entropically-driven. However, upon increasing the temperature, the enthalpic factor becomes more significant and, at temperatures higher than 303.15 K the micellization is enthalpy driven. The interactions between SDS and PEG were also discussed.

References

[1] Jonsson, B.; Lindman, B. Surfactants and polymers in Aqueous Solution; John Wiley & sons; New York, 1999.

[2] Ballerat-Busserolles, K.; Roux, A. H. *Langmuir*. **1997**, 13, 1946.

[3] Sadeghi, R.; Shahabi, S. *J. Chem. Thermodyn.* **2011**, 43, 1361.

Thermodynamic properties of surfactant Sodium 1-hexanesulfonate in water and in Aqueous Solutions of Poly(ethylene glycol) at Different Temperatures

Rahmat Sadeghi*, saivan solaimani
Department of Chemistry, University of Kurdistan, Sanandaj, Iran
*E-mail: rsadeghi@uok.ac.ir

Keywords: Sodium 1-hexanesulfonate, Micellization , Poly(ethylene glycol)

Introduction

It has been generally recognized that studies of thermodynamic and transport properties of surfactants are important to understand their behavior in solutions. One of the important properties of surfactants is the association of their amphiphilic molecules into micellar aggregates in aqueous solutions [1]. The micellization study of surfactants in solution is important because the performance of the surfactant in many interfacial processes depends on its concentration and orientation at the interface [2]. The surfactant concentration where the micelles start to form is known as the critical micelle concentration, abbreviated to CMC[1].The critical micelle concentration (CMC) is a key thermodynamic quantity of surfactant- water mixture.A great deal of research has been devoted to determining the CMC experimentally and through predictive techniques [3]. The CMC can be influenced by different factors such as chemical structure of surfactant (type of surfactant (ionic or non-ionic), alkyl chain length, head groups, valency of the counterion and different groups on alkyl chain), temperature, pressure and cosolute[1]. Polymer/surfactant mixtures are common in biological systems. Interaction of surfactants with water-soluble polymers has been extensively studied for their widespread applications in industry.Because of their characteristic physicochemical properties at different possible combinations the polymer and ionic surfactant mixed systems are interesting[4]..In this study The vapor-liquid equilibria properties of Sodium 1-hexanesulfonate (C5SO3Na) in pure water and in aqueous poly(ethylene glycol) (PEG) solutions were determined at 298.15k below and above the critical micelle concentration(CMC).

Experimental Section

Materials. Sodium 1-hexanesulfonate (C_6SO_3Na) purity > 99%), sodium chloride (purity > 99.5%), and poly(ethylene glycol) were obtained from Merck and were used without further purification. PEG had a nominal molecular weight of 6000. The manufacturer has characterized this polymer with charge/lot number S35317 203. Double distilled, deionized water was used.

Methods. In this study, the isopiestic method was used to obtain the osmotic coefficient of aqueous surfactant mixtures. The apparatus used for determination of water activity in the binary water + C6SO3Na solutions consisted of five-leg manifold attached to round-bottom flasks. Two flasks contained the standard pure NaCl solutions, two flasks contained the pure surfactant solutions and the central flask was used as a water reservoir. The temperature was controlled to within ± 0.05 K. After equilibrium had beenreached, the manifold assembly was removed from the bath, and each flask was weighed with an analytical balance with a precision of ±1 × 10-4 g. From the weight of each flask after equilibrium and the initial weight of salt and polymer, the the mass fraction of each solution was calculated.

Results and Discussion

The vapor-liquid equilibria properties of Sodium 1-hexanesulfonate (C6SO3Na) in pure water were determined at different Temperatures below and above the critical micelle concentration (CMC). Vapor-liquid equilibrium data such as water activity, vapor pressure, osmotic coefficientand activity coefficient were obtained through isopiestic method. The concentration dependence of all investigated thermodynamic properties exhibit a change in slope at the concentration in which micelles are formed. It was found that temperature has little effect on water activity in this system. It was found that the vapor pressure depression for a ternary aqueous C6SO3Na + PEG system is more than the sum of those for the corresponding binary solutions. the vapor pressure depression for binary aqueous surfactant solutions is very sensitive to the variation of temperature. vapor pressure depression of aqueous polymer solutions increase with increasing temperature.

References

[1] Sadeghi.R , Hosseini.R. *J. Iran. Chem. Soc.,* Vol. 7, No. 3,(**2010)**, pp. 621-629.

[2] T. N. Castro Dantas et al *Colloid Polym Sci* (**2009**) 287:81–87

[3] A.D.W. Carswell et al. *Colloids and Surfaces A: Physicochem*. Eng. Aspects 212 (**2003**) 147_ 153

[4] Sh. Saurabh, D. Joykrishna. Journal of Colloid and Interface Science 350 (2010) 220–228.

Thermodynamic study of molecular interactions in binary systems

A.gholaminia*,[a] , M.almasi[a] and *Z .nojini* [b]

[a] Department of Chemistry, Science and Research Branch, Islamic Azad University, Khouzestan, Iran
[b] Department of Chemistry, College of science, shahid chanran university, ahvaz 61357-43169,Iran
Email : **gholaminia89**@gmail.com
m.almasi@khouzestan.srbiau.ac.ir
zbnojini@gimiail.com

Keywords :Acetophenone ,methylisobuthylketon ,methylcyclohexane, viscosity

Introduction:

Excess properties of mixtures provide information about the molecular interactions between the various components and can be used for the development of molecular models describing the thermodynamic behavior of mixtures [1– 2].

The thermodynamic properties of mixtures are of great industrial interest**.** The property studied has proved to be meaningful from a thermodynamic point of view, as it provides direct information about the energetic effects arising rearranging of the bondings that occurs during the mixing process, which is essential when studying new theoretical approaches to the liquid state, either pure or mixture.

Material and Methods:

Acetophenone, methylisobuthylketon and methylcyxane, were purchased from Merck with purity higher than 99% , and used without further purifications. The mixtures were prepared by weighing known masses of pure liquids in airtight, narrow-mouth ground stoppered bottles taking due precautions to minimize evaporation losses. All of the mass measurements were performed on an electronic balance (Mettler AE 163, Switzerland) accurate to 0.01 mg. The uncertainty in the mole fraction was estimated to be $\pm 1.10^{-4}$

Apparatus:

The apparatus was calibrated once a day with dry air and bidistillated water. The temperature in the cell was regulated to ± 0.01 K with a solid state thermostat. Viscosities were measured with an Ubbleohde viscometer with an uncertainty of ± 1. 10^{-3} mPa.s.

Results and Discussion :

$\Delta\eta$ for the three binary systems were evaluated using the equation

$$\Delta\eta = \eta_{\mathrm{MIX}} - \mathrm{X}_1\eta_1 - \mathrm{X}_2\eta_2 \qquad (1)$$

where η_{MIX} is the viscosity of the mixture, η is the viscosity of pure component *i*, x_i is the mole fraction. $\Delta\eta$ for the binary systems were fitted by the least-squares method to the Redlich–Kister [3] equation

$$\Delta\eta = x_i x_j \sum_{k=0}^{n} A_k (x_i - x_j)^k \qquad (2)$$

Experimental data and fitted equations for the three binary systems are depicted in Fig. 1.

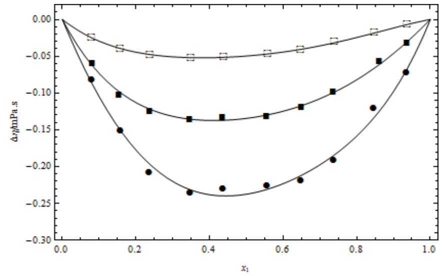

Fig. 1 viscosity deviation at 298.15 K for the binary systems: (■) methylisobuthylketon + acetophenone, (●) acetophenone +methylcyclohexane (□) methylisobthylketon +methylcyclohexane.Full line calculated with Redlich–Kister equation

$\Delta\eta$ for the three binary systems were negative. These effects arise due to dominance of chemical interaction such as dipole – dipole interaction between constituent molecules, known as strong specific interaction.

The sign of $\Delta\eta$ is in agreement with the conclusions by Fort and Moore [4], who proposed that this behavior is representative of systems where dispersion forces are predominant and do not take place the formation of heteromolecular complexes.

The negative values of $\Delta\eta$ may be attributed to (i) the existence of dispersion and dipolar forces between unlike molecules and (ii) the difference in size and shape of unlike molecules

Conclusions :

viscosities of binary and ternary mixtures of acetophenone (1) + methylcyclohexane (2) + methylisobuthylketon (3) were measured at 298.15 K.. The measured data and calculated values of all systems are in good agreement.

References:

[1] Iloukhani, H., Almasi, M.: Densities, viscosities, excess molar volumes, and refractive indices of acetonitrile and 2-alkanols: Experimental results and application of the Prigogine–Flory–Patterson theory. Thermochim Acta. **495**, 139–148(2009)

[2] Almasi, M.; Iloukhani, H. Densities, Viscosities, and Refractive Indices of Binary Mixtures of Acetophenone and 2-Alkanols. J. Chem. Eng.Data **2010**, 55, 1416–1420.

[3] Redlich, O., Kister, A.T.: Algebraic representation of thermodynamic properties and the classification of solutions. Ind. Eng. Chem. **40**, 345–348 (1948)

[4] R. Fort, W.R. Moore, Viscosities of binary liquid mixtures, Trans. Faraday Soc. 62 (1966) 1112–1119.

(Liquid + liquid) equilibria for ternary mixtures of (water + butyric acid + organic solvent) at T= 298.2 K

A. Ghanadzadeh Gilani*, M. Janbaz
Department of Chemistry, University of Guilan, 41335 Rasht, Iran
E-mail address:Janbaz_Mina@yahoo.com

Keywords: LLE ,Ternary system,NRTL,UNIQUAC

Introduction

Liquid–liquid equilibria (LLE) investigations for ternary aqueous Mixtures of carboxylic acids with organic solvents are important in the evaluation of industrial units for solvent extraction processes[1]. The accurate interpretation of phase equilibrium for the different ternary mixtures is a fundamental and important key to

Improving solvent extraction techniques. The carboxylic acid used in the current study was butyric acid (BA). It has many scientific and industrial applications.

Materials and methods

All chemicals used in this work (mass fraction purity > 0.99)were obtained from Merck. The aqueous and organic phases were weighed and analyzed to find the composition of the components in order to determine the LLE tie lines. For the complete determination of the LLE data, the following method was used. The concentrations of the acid (BA) in both phases were determined by potentiometer NaOH titration in the presence of phenolphthalein as an indicator. The water content of the organic phase was measured by the Karl–Fisher method .

Results and discussion

The LLE measurements were made at T= 298.2 K and under atmospheric pressure. Table 1 contains systems of (water + butyric acid+n-heptane), (water + butyric acid + toluene) and(water + butyric acid + methylcyclohexane). The experimental values of separation factor for each solvent are listed in table 1. This factor is found to be greater than 1 (S > 1) for the systems investigated, which means that extraction of BA by these solvents is possible.The separation factor is defined as the ratio of distribution coefficients of propionic acid (D2) to water (D1), S = D2/D1.

As seen from table 1 for these ternary systems, the separation factor changes in the order of the mixtures containing methylcyclohexane > n-heptane >toluene.

Table 1

solvent	S
Methylcyclohexane	1360.2
Toluene	770.9
n-Heptane	1336.9

Conclusions

The LLE values for the ternary systems were studied at T= 298.2 K and atmospheric pressure. Each ternary system exhibits type-1 behavior for the LLE.The UNIQUAC and NRTL solution models were used to correlate the experimental LLE results and to calculate the phase compositions of the mixtures studied. The corresponding optimized binary interaction parameters were also calculated. In general, the NRTL method gives better results than the UNIQUAC model for the three systems investigated.

References :

[1] A. Senol," Liquid–liquid equilibria for the system (water + carboxylic acid + chloroform): thermodynamic modeling", Fluid Phase Equilibria. 243,51–56,2006.

[2] H. Ghanadzadeh, A. Ghanadzadeh, Kh. Bahrpaima, S.L. Seyed Saadat,(Liquid + liquid) equilibria of (water + propionic acid + 2-ethyl-1-hexanol):experimental data and correlation, J. Chem. Thermodyn. 40 ,879–884,2008

[3] H. Ghanadzadeh, A. Ghanadzadeh Gilani, Kh. Bahrpaima, R. Sariri, J. Chem. Thermodyn 42 , 267–273.2010

[4] J. Zigova, E. Sturdik, Advances in biotechnological production of butyric acid, J. Ind. Microbiol. Biotechnol. 24 ,153–160.2000

[5] Ş.I. Kırbaşlar, S. Şahin, M. Bilgin, (Liquid + liquid) equilibria of (water + butyric acid + esters) ternary systems, J. Chem. Thermodyn. 39 , 1279–1285.2007

[6] Ş.I. Kırbaşlar, (Liquid + liquid) equilibria of the (water + butyric acid + dodecanol) ternary system, J. Chem. Thermodyn. 38 ,696–700.2006.

Viscosities of Binary Mixtures of *N, N*-Dimethylacetamide with homologe series of 2- Alkanols

G.hasanmirzaee*,[a] and M.almasi[a]

[a] Department of Chemistry, Science and Research Branch, Islamic Azad University, Khouzestan, Iran

Email: gelarehmirzaee@yahoo.com

m.almasi@khouzestan.srbiau.ac.ir

Keywords: N,N-dimethylacetamide(DMA), 2-alkanols,viscosity, viscosity deviation.

Introduction

This paper is part of our general work concerning the study of some physical and physicochemical properties of binary liquid mixtures in order to gain information about molecular interactions between the molecules in these systems [1-3]. It is wellknown that the knowledge of the dependence of dynamic viscosity on both temperature and composition

Of the system is needed for many engineering processes and the study of fluid phenomena [4].

In the present study the viscosities of binary mixtures of *N*,*N*- dimethylacetamide with 2-propanol, 2-butanol, 2-pentanol,2-hexanol and 2-heptanol, over the entire composition range were measured at 298.15 K and ambient pressure. From the experimental data, viscosity deviations $\Delta\eta$ calculated. The results have been fitted to the Redlich-Kister equation to determine the coefficients and estimate the standard error.

Materials and methods:

N, N-dimethylacetamide, 2-propanol, 2-butanol, 2-pentanol, 2-hexanol and 2-heptanol, were purchased from Merck with purity higher than 99%, and used without further purifications. Dynamic viscometer at 298.15 k The Were measured with anUbbelohde viscometer. Uncertainty of the viscosity measurements was estimated to be less $\pm 3 \times 10^{-3}$ mPa.s.

Results and Discussion:

The viscosity deviation $\Delta\eta$ in all of studied mixture systems were evaluated using the equation

$$\Delta\eta = \eta - x_1\eta_1 - x_2\eta_2$$

Where η is the viscosity of the mixture, η_1 and η_2 is the viscosity of pure component, x_1 and x_2 are the mole fractions, $\Delta\eta$ for the binary systems were fitted by the least-squares method to the Redlich–Kister equation [5] . $\eta_{ij} = x_i x_j\left(A_0 + \sum_{k=1}^{n} A_k(1-2x_i)^k\right)$

The variation of the Viscosity deviation with the mole fraction of *DMA* is shown in Figure 1

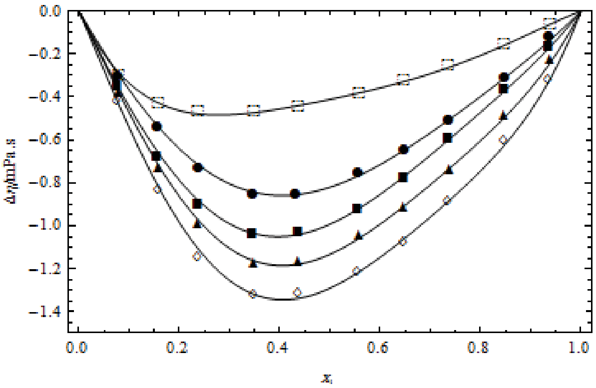

Fig.1 Viscosity deviations $\Delta\eta$ for binary mixtures of dimethyl acetamide with (⬚) 2-propanol, (●) 2-butanol, (■) 2-pentanol, (Δ) 2-hexanol, (♦) 2-heptanol at T = 298.15 K

Viscosity deviations of binary mixtures containing *N*,*N*- dimethylacetamide with 2-propanol, 2-butanol, 2-pentanol, 2-hexanol and 2-heptanol are negative over the whole range of mole fractions. In this case is stronger Interactions between similar molecules and broken of Hydrogen bonds between alkanols.

Conclusions:

Viscosities and viscosity deviations of binary mixtures of DMA + 2-alkanols were measured at 298.15 K .The results have been fitted to the Redlich-Kister equation .Viscosity deviations decrease furtheras the length of the alkyl chain of the primary alcohol increases.

Reference:

[1] Ritzoulis, G. Excess Properties of the Binary Liquid System Dimethyl sulfoxide + 2-Propanol and Propylene Carbonate + 2-Propanol. *Can. J. Chem.* **1989***, 67,* 1105-1108.

[2] Moumouzias, G.; Panopoulos, D.; Ritzoulis, G. Excess Properties of the Binary Liquid System Propylene Carbonate + Acetonitrile. *J. Chem. Eng. Data* **1991***, 36,* 20-23.

[3] Konti, A.; Moumouzias, G.; Ritzoulis,.*J. Chem. Eng. Data* **1997***, 42,* 614-618.

[4] W.E. Acree, Academic Press, New York, 1984.

[5] Redlich,O. Kister, A.T. ; " Algebraic representation of thermodynamic properties and the classification of solutions. Ind. Eng. Chem. **40**, 345–348 (1948).

Thermodynamic study of interactions between N, N-dimethylacetamide and homologe series of 2- Alkanols

G.hasanmirzaee*[,a] and M.almasi[a]

[a] Department of Chemistry, Science and Research Branch, Islamic Azad University, Khouzestan, Iran

Email: **gelarehmirzaee**@yahoo.com

m.almasi@khouzestan.srbiau.ac.ir

Keywords: n, n-dimethylacetamide, 2-Alkanols,Density, Excess molar volume**.**

Introduction

Multi component liquid mixtures have attracted the attention of researchers in the past decades .Physical properties are very important factors in chemical and engineering processes because of their influence upon the effectiveness of the operations. Mass and heat transfer processes and flow operations are evident examples of the importance of the knowledge for these properties [1,2].

In the present study the Densities of binary mixtures of *N*,*N*-dimethylacetamide with 2-Alkanos, over the entire composition range were measured at 298.15 K and ambient pressure. From the experimental data, excess molar volume V_m^E , calculated. The results have been fitted to the Redlich-Kister equation and the resulting coefficients have been calculated and estimate the standard error.

Materials and methods:

N,N-dimethylacetamide, 2-propanol, 2-butanol, 2-pentanol, 2-hexanol and 2-heptanol, were purchased from Merck with purity higher than 99% , The density of the pure compounds and mixtures was measured by means of an Anton Parr DMA 4500 oscillating U-tube densimeter, The uncertainty of the density measurements was estimated to be $\pm 1.10^{-5}$ g.cm^{-3}.

Results and Discussion

The excess molar volumes V_m^E for the three binary systems were evaluated using the equation

$$V_m^E = \sum_{i=1}^{N} x_i M_i (\rho^{-1} - \rho_i^{-1}) \tag{1}$$

where ρ is the density of the mixture, ρ_i is the density of pure component i, x_i is the mole fraction, M_i is the molar mass of component i, and N stands for the number of components in the mixture .The V_m^E values have been fitted using least squares to a Redlich-Kister type equation [3].

$$V_{ij}^E = x_i x_j \sum_{k=0}^{n} A_k (x_i - x_j)^k \tag{2}$$

Experimental data and fitted equations for the three binary systems are depicted in Fig. 1.

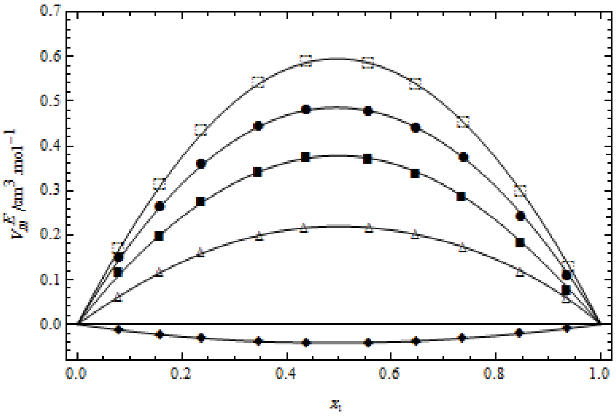

Fig. 1 Excess molar volumes V_m^E with mole fraction of dimethylacetamide wi-th (♦) 2-propanol, (Δ) 2- butanol, (■)2-pentanol, (●) 2-hexanol, (□) 2heptanol at T = 308.15 K. The solid curves were calculated from coefficients of equation (2)

excess molar volumes of binary mixtures of dimethylacetamide and 2-butanol ,2-pentanol,2-hexanol and 2- heptanol are positive over the whole range of mole fractions. The positive V_m^E values can be ascribed to broken of Hydrogen bonds between alkanols. In this case is stronger Interactions between similar molecules. and excess molar volumes of binary mixtures of dimethylacetamide and 2-propanol are negative over the whole range of mole fractions. Negative deviation of the V_m^E values can be ascribed to formation of hydrogen bonds betweend DMA and alcol molecules.In this case is stronger Interactions between dissimilar molecules.

Conclusions:

Densities and excess molar volumes V_m^E of binary mixtures of DMA + 2-Alkanols were measured at 298.15 K .The results have been fitted to the Redlich-Kister equation.Positive quantities show that dominant factors are physical interactions and negative values suggested that the main factor in the interactional forces is chemical interactions.

Reference:

[1] E. Alvarez, B. Sanjurjo, A. Cancela, J.M. Navaza, Eng. Res. Des. 78 (2000) 889.
[2] S. Kumar, K. Kusakabe, L.S. Fan, AIChE J. 39 (1993) 1399.
[3] Redlich,O. Kister, A.T. ; " Algebraic representation of thermodynamic properties and the classification of solutions. Ind. Eng. Chem. **40**, 345–348 (1948).

The study of osmotic coefficient and activity of 1-buthyl-3-methyl imidazolium chloride in lithium bromide aqueous solutions and their corresponding binary systems at 298.15 K.

M. T. Zafarani-Moattar, F. Frouzesh*

Physical Chemistry Department, University of Tabriz, Tabriz, Iran

Email: Farshid.chemistry@yahoo.com

Keywords: activity coefficient, osmotic coefficient, isopiestic method, [BmimCl], lithium bromide.

Introduction:

Osmotic and activity coefficient of mixed aqueous solutions, [BmimCl] in lithium bromide and their corresponding binary aqueous solutions have been measured by the isopiestic method at a 298.15 K. The osmotic coefficients for binary aqueous solutions were correlated by Pitzer–Archer model [1]. The activity coefficients of mixed electrolytes were calculated by Scatchard's neutral-electrolyte method [2].

Materials:

All the chemicals contained BmimCl and LiBr were obtained from Merck.

Apparatus:

For obtaining water activity and osmotic coefficient data of studied binary and ternary systems at T = 298.15 K, the isopiestic method was used. The details of this method have been introduced in ref [3].

Results and discussion:

We also used the following relation between the osmotic coefficient, ϕ, and the solvent activity a_w [4]:

$$\phi = \frac{-\ln a_w}{\nu \cdot m_s \cdot M_w}$$

The Pitzer – Archer model [1], is applied to correlate the osmotic coefficient results for the investigated binary solutions. Scatchard's model [2] is applied to correlate the osmotic coefficients of the studied mixed electrolyte solutions. The parameters of these models are reported in tables 1,2:

Table1. Parameters of Pitzer-Archer model at $T = 298.15$ K.

systems	$\beta^{(0)}$	$\beta^{(1)}$	$C^{(0)}$	$C^{(1)}$	$\sigma(\phi)$
BmimCl + H_2O	0.015	0.003036	0.002702	0.020	0.002
LiBr + H_2O	0.594	-0.835	0.001421	-0.358	0.005

Table2. Parameters of Scatchard's model at $T = 298.15$ K.

system	b_{01}	b_{02}	b_{03}	$\sigma(\phi)$	$\sigma(a)$
(BmimCl+LiBr+H_2O)	-0.169	0.029	0.005008	0.015	0.0009

Conclusion:

The accurate water activity and osmotic coefficient measurements have been carried out at T = 298.15 K on [BmimCl] in aqueous LiBr solutions. The experimental osmotic coefficient data for the aqueous binary IL or salt solutions and ternary system (BmimCl+LiBr+H_2O) were fitted satisfactorily to the Pitzer-Archer and Scatchard models respectively. The results show that, these models can bee satisfactorily used for studied systems in this research.

References:

[1] D.G. Archer, J. Phys. Chem. Ref. Data. 20 (1991) 509-555.

[2] K. S. Pitzer, G. Mayorga, J. Phys. Chem. 77 (1973) 2300–2308.

[3] M.T. Zafarani-Moattar, Sh. Sarmad, CALPHAD. 35 (2011) 331-341.

[4] R. A. Robinson, R. H. Stokes, Electrolyte Solutions, Butterworths, London, 1965.

Thermodynamic study of molecular interactions in binary systems

T.pourmansoor*,[a] and M.almasi[a]
[a] Department of Chemistry, Science and Research Branch, Islamic Azad University, Khouzestan, Iran
Email : **tpourmansoor**@yahoo.com
m.almasi@khouzestan.srbiau.ac.ir

Abstract :

Densities indices of mixing of methyl ethyl ketone with 2-propanpl ,2-butanol,2-pentanol,2-hexanol,2-heptanol, have been measured as a function of composition range at (T) 298.15 K and ambient pressure. Excess molar volumes Vm E was calculated and correlated by the Redlich-Kister type function to derive the coefficients and estimate the standard error. For binary systems methyl ethyl ketone + 2-Alkanols Vm E are positive .

Keywords :
Methyl ethyl ketone ,2-propanol, 2-butanol, 2-pentanol, 2-hexanol,2-heptanol,Excess molar volume

Introduction:

Excess properties of mixtures provide information about the molecular interactions between the various components and can be used for the development of molecular models describing the thermodynamic behavior of mixtures [1– 2].

The thermodynamic properties of mixtures are of great industrial interest**.** The property studied has proved to be meaningful from a thermodynamic point of view, as it provides direct information about the energetic effects arising between the molecules present in the mixture, so it can help to explain the rearranging of the bondings that occurs during the mixing process, which is essential when studying new theoretical approaches to the liquid state, either pure or mixture.

Material and Methods:

Methyl ethyl ketone, 2-propanol, 2-butanol, 2-pentanol, 2-hexanol, 2-heptanol, were purchased from Merck with purity higher than 99% , and used without further purifications. The mixtures were prepared by weighing known masses of pure liquids in airtight, narrow-mouth ground stoppered bottles taking due precautions to minimize evaporation losses. All of the mass measurements were performed on an electronic balance (Mettler AE 163, Switzerland) accurate to 0.01 mg. The uncertainty in the mole fraction was estimated to be $\pm 1.10^{-4}$

Apparatus:

The density of the pure compounds and mixtures was measured by means of an Anton Parr DMA 4500 oscillating U-tube densimeter, provided with automatic viscosity correction. The uncertainty of the density measurements was estimated to be $\pm 1.10^{-5}$ g.cm^{-3}. The apparatus was calibrated once a day with dry air and bidistillated water. The temperature in the cell was regulated to ± 0.01 K with a solid state thermostat. Viscosities were measured with an Ubbleohde viscometer with an uncertainty of $\pm 1.\ 10^{-3}$ mPa.s.

Results and Discussion:

The excess molar volumes V_m^E for the five binary systems were evaluated using the equation

$$V_m^E = \sum_{i=1}^{N} x_i M_i (\rho^{-1} - \rho_i^{-1}) \qquad (1)$$

where ρ is the density of the mixture, ρ_i is the density of pure component *i*, x_i is the mole fraction, M_i is the molar mass of component *i*, and *N* stands for the number of components in the mixture. V_m^E for the binary systems were fitted by the least-squares method to the Redlich–Kister [3] equation

$$V_{ij}^E = x_i x_j \sum_{k=0}^{n} A_k (x_i - x_j)^k \qquad (2)$$

Experimental data and fitted equations for the three binary systems are depicted in Fig. 1.

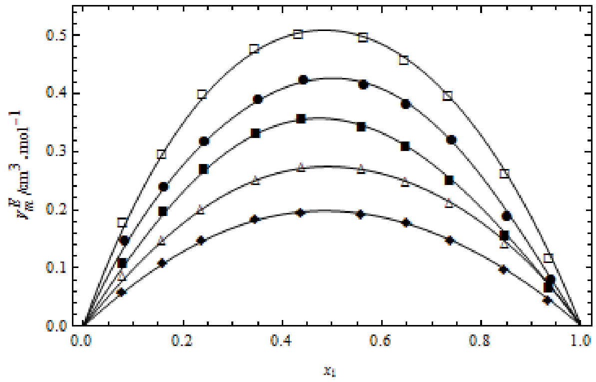

Fig. 1 Excess molar volumes at 298.15 K for the binary systems: (◆) methyl ethyl ketone +2-propanol, (△) methyl ethyl ketone+2-butanol, (■) methyl ethyl ketone+2-pentanol, (●) methyl ethyl ketone+2-hexanol, (□) methyl ethyl ketone+2-heptanol. Full line calculated with Redlich–Kister equation.

For the tow binary mixtures containing Methyl ethyl ketone + 2-Alkanols excess molar volumes are positive over the whole range of mole fractions. Positive values would indicate that molecular interactions between different molecules are weaker than interactions between molecules in the same pure liquid ,In the mixtures attractive interactions between unlike species decrease and repulsive interactions predominate, leading to positive excess molar volumes.

Conclusions :

Densities and excess molar volumes V_m^E of binary mixtures of Methyl ethyl ketone+ 2-Alkanols were measured at 298.15 K.. The measured data and calculated values of all systems are in good agreement.

References:

[1] Iloukhani, H., Almasi, M.: Densities, viscosities, excess molar volumes, and refractive indices of acetonitrile and 2-alkanols: Experimental results and application of the Prigogine–Flory–Patterson theory. Thermochim Acta. **495**, 139**–**148(2009)

[2] Almasi, M.; Iloukhani, H. Densities, Viscosities, and Refractive Indices of Binary Mixtures of Acetophenone and 2-Alkanols. J. Chem. Eng.Data **2010**, 55, 1416–1420.

[3] Redlich, O., Kister, A.T.: Algebraic representation of thermodynamic properties and the classification of solutions. Ind. Eng. Chem. **40**, 345–348 (1948)

A New Perturbed Hard sphere Chain Equation of State for Binary Mixtures of Refrigerants

Zahra Yazdanpanah Fard[a,*],Leila Maftoon Azad[b]
[a] Department of Chemistry, Marvdasht Branch, Islamic Azad University, Marvdasht, Iran
[b] Department of Chemistry, College of Sciences, Persian Gulf University, Bushehr, Iran
Email:z_yazdan_1982@yahoo.com

Key words: Perturbed hard sphere chain equation of state, refrigerants, binary mixtures

Introduction:

In this work we have developed our previous works [1,2], on the prediction of the equation of state for pure liquids, to incorporate refrigerant mixtures. The basic equation is a perturbed hard sphere chain (PHSC) equation of state proposed by Kim and Bae [3]. We showed that by using the boiling constants of fluids as scaling constants, one can obtain the temperature-dependent parameters of the equation of state [1,2]. Here we have checked the generalization of the equation to mixtures against the experimental PVT data for some binary mixtures of refrigerants.

Theory:

Generalization of the equation of the PHSC equation of state[1], to mixtures of any number of components is expressed as follows:

$$\frac{P}{\rho KT} = 1 + \rho \sum_{ij}^{m} x_i x_j r_i r_j b_{ij} g_{ij}\left(d_{ij}^{+}\right) - \sum_{i}^{m} x_i (r_i - 1)[g_{ii}(d_{ii}^{+}) - 1] - \frac{\rho}{KT} \sum_{ij}^{m} x_i x_j r_i r_j a_{ij} (q_{aij} + q_{bij}) \quad (1)$$

where P is the pressure, ρ is the number (molar) density, r_i and r_j are the number of segments for the i-th and j-th components, $g_{ij}\left(d_{ij}^{+}\right)$ the ij pair radial distribution function of hard spheres mixture at contact, and x_i and x_j are the number fraction of molecules of species i and j. q_{aij} and q_{bij} can be calculated as $q_{aij} = q_{a1} r_{ij} + q_{a2} r_{ij}^2 + q_{a3} r_{ij}^3$, $q_{bij} = q_{b1} r_{ij} + q_{b2} r_{ij}^2 + q_{b3} r_{ij}^3$. Parameters, b_{ij} and a_{ij}, in Eq. (1) are obtainable by choosing suitable combining rules. These parameters can also be expressed as universal functions of the reduced temperature. Our method of extension is similar to that proposed by Mehdipour and Ansari [4].

The boiling temperature T_{bij} and the boiling density, ρ_{bij} of the unlike components can be obtained by simple following combining rules.

Result and discussion:

The extended equation of state for mixtures has been employed to calculate the PVT properties of a number of refrigerant mixtures. The r values for pure substances are those previously obtained and reported in Ref. [2]. The results, summarized in Table 1, show that the agreement with experiment [5-8] is quite good.

Table 1. Comparison of the calculated density of mixtures with experiment

compound	T_b (K)	ρ_b (mol dm^{-3})	r_{ij}	ΔT (K)	ΔP(bar)	NP^b	AAD (%)
R22+R125	228.80	14.299	1.039	242.76-323.88	2.06-23.74	15	0.99
R22+R142b	247.65	13.891	1.037	242.07-328.53	0.99-14.48	15	3.48
R22+R124	246.28	13.184	1.033	242.61-332.42	1.01-16.41	15	0.10
R22+R152a	240.26	15.82	1.05	241.04-335.01	1.04-19.63	16	0.75
R124+R142b	262.50	11.33	1.034	241.28-350.72	0.38-13.8	16	1.66
R124+R152a	254.67	12.793	1.048	243.79-335.04	0.59-12.58	15	0.75
R32+R134a	233.85	17.550	1.03	320-350	21.31-24.64	16	1.05

^{b} Number of points

Conclusion:

A recently developed hard sphere chain equation of state is extended to predict the volumetric properties of liquid mixtures. For this extension, just combining rules are used. Therefore there is no adjustable parameters in addition to those optimized for pure components. Applying a strong law of corresponding states has aided to develop an equation of state with out referring to the intermolecular potential function or molecular sizes. Knowledge of the boiling parameters and parameter r for each component is sufficient to predict the whole PVT surface for any mixture. The average absolute deviation, compared to the experimental data is about 1% which is quite good.

Reference:

[1]L. Maftoon-Azad, and H. Mohamadi; Fluid Phase Equilib. , submitted.

[2] L.Maftoon-Azad, H. Mohamadi, and Z. Yazdanpanah, in preparation.

[3] I.H. Kim, Y.C. Bae ; Chem. Phys.; 260, 337–345, 2000.

[4] N. Mehdipour, T. Ansari ; Fluid Phase Equilibria; *305, 169–173*, 2011.

[5] M. Arnemann, and H.Kruse ; DKV-Tagungsbericht; 16(II), 427-440, 1989.

[6] C. Holcomb, J.Magee, J. Scott, S.Outcalt, and W.Haynes. Technote 1998.

[7]D.R.Defibaugh, and G.Morrison. ; J.Refrigeration, 18, 518-523,1995.

[8] U. Deiters and G.M.Schnneider. ;Ber.Bunsenges.Phys.Chem.;80,1316-1321, 1976.

Volumetric properties of binary systems of benzylamin with methanol , ethanol and 1-propanol at different temperatures

E. skandari*, H. Zarei
Department of Chemistry, Faculty of Chemistry, Bu-Ali Sina University, Hamedan, Iran
Email:skandariehsan@yahoo.com.

Keywords: Binary mixture, Excess molar properties, Density, Benzylamin, Alkanol

Introduction:

The excess properties of liquid mixture are important to understand and interpret the nature of interactions between the molecules of the mixtures. In recent years, there has been considerable upsurge in the theoretical and experimental investigation of the excess thermodynamic properties of binary liquid mixture.[1] Up to now, the binary mixtures containing alcohols and aromatics have been studied with considerable interest because these mixtures exhibit varying molecular interactions and are important from a practical point of view. Alcohols and aromatics are widely used in variety of industrial and consumer applications, such as perfumes, cosmetics, paint, varnish, drugs, fuel, explosives, fats, waxes, resin, plastics, rubber, detergents, DDT, Etc. [2]

We report densities, ρ , excess molar volumes, V_m^E , and partial excess molar volumes, V_i^E , their values at infinite dilution, $V_i^{E,0}$, thermal expansion coefficient, α, and its excess value, α^E, and isothermal coefficient of excess molar enthalpy $(\partial H_m^E/\partial P)_{T,}x$ for binary liquid mixtures of benzylamin with methanol, ethanol and 1-propanol at temperatures (293.15, 303.15, 313.15, 323.15, and 333.15) K and ambient pressure (81.5 kPa). These excess quantities were correlated with a temperature dependent Redlich–Kister equation.

Materials and methods:

Chemicals of high purity obtained from Merck. The stated purities of the solvents by the manufacturer were further ascertained by comparing their density with the corresponding literature values. They are in good agreement with literature values.

Apparatus:

The densities were measured with an Anton Paar digital vibrating u-tube densimeter (model DMA 4500) with a certified precision of $\pm 5\times10^{-5}$ g· cm^{-3}. The experimental procedures followed in the density determination, the detailed description of the equipment set up as well as solution preparation have been described previously [3].

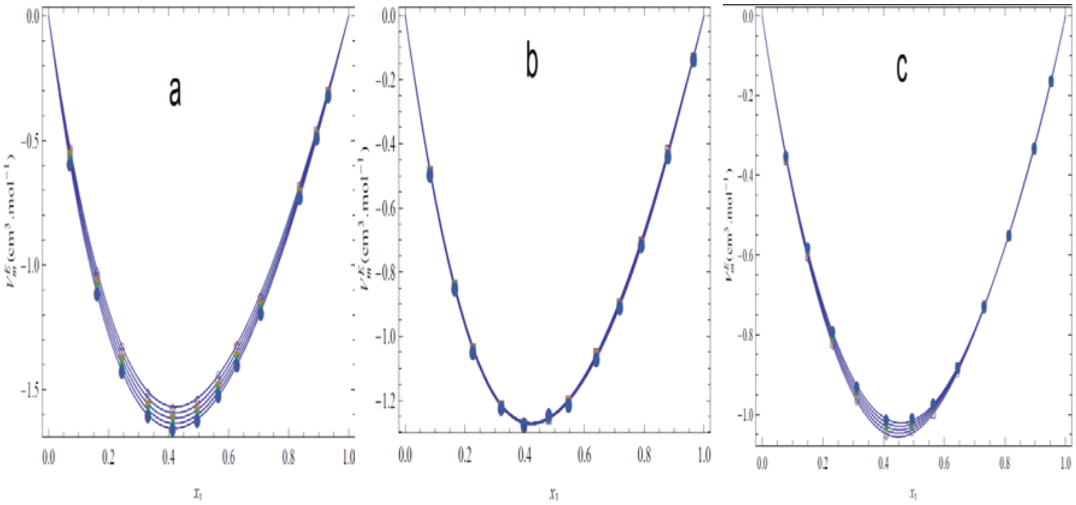

Figure 1. Experimental excess molar volumes for a)benzylamine (1)+ methanol (2) b) benzylamine (1)+ ethanol (2) c) benzylamine (1)+1- propanol (2) mixtures at different temperatures.o,293.15 K;□, 303.15K;▲, 313.15 K; ■, 323.15 K,●, 333.15 K. Solid curves represent the results calculated by the Redlich–Kister equation.

Results and discussion:

As shown in figure 1 the excess molar volumes for binary mixtures of benzylamine + methanol and benzylamine + ethanol are negative and become more negative with increasing temperatures and for benzylamine + 1-propanol is negative and become less negative with increasing temperatures. The values of excess molar volumes decrease with increasing chain length of alcohol.

Conclusion:

The hydrogen bond is a relatively strong, highly directional interaction. Orientation order of molecules changes with increasing temperature. The average number of hydrogen bonds per molecules decreases as the temperature is increased. The decreases of excess molar volume with increasing temperature, point out the decrease in average interaction between unlike molecules with increasing temperature. The decreases of V_m^E in benzylamine (1) + methanol (2) is larger than benzylamine (1) + ethanol (2) with increasing temperature. These observations indicate that hydrogen bonding between benzylamine (1) + methanol (2) is stronger than benzylamine (1) + ethanol (2).

References:

[1] J.M. Resa, S. Gonzalez, O.D. Zandaluce, J. Lanz, *J. Chem. Eng. Data* 24, 995 (2002).

[2] Slobodan P. Serbanovi c, Mirjana Lj. Kijev canin, Ivona R. Radovi c, Bojan D. Djordjevi c, Fluid Phase Equilibria 239 (2006) 69–82.

[3] H.A. Zarei, F. Jalili, J. Chem. Thermodyn. 39 (2007) 55–66.

Density calculation for liquid alkali metals over the whole liquid range

Shiva Sabzevari*, Majid Moosavi
Dept. of Chemistry, Faculty of Sciences, University of Isfahan, Isfahan 81746-73441, Iran
Email: sh.sabzevari@sci.ui.ac.ir ; m.mousavi@sci.ui.ac.ir

Keywords: Equation of state, Liquid alkali metal, Potential function, Density.

Introduction:

Alkali metals are widely used in modern science and technology, due to their unique combination of physicochemical properties, such as extremely high electrical and thermal conductivities, small densities and viscosities, etc. The measurement of thermophysical properties of liquid alkali metals especially at high temperatures is very difficult since most liquid metals are reactive at high temperatures. Thus, the prediction of these properties using accurate equations of state (EoSs) appears at present to be the only alternative to the experimental difficulties associated with their measurements. Ghatee and Bahadori [1] proposed a new EoS for cesium over the whole liquid range successfully. In this study, we have applied this EoS for all liquid alkali metals over the whole liquid range.

Theory:

Ghatee and Bahadori [1] proposed the following pair potential function for cesium which is called (6-3) potential function:

$$u(r) = A\varepsilon\left[\left(\frac{\sigma}{r}\right)^6 - \left(\frac{\sigma}{r}\right)^3\right] \tag{1}$$

Where A is a constant, ε is the potential well depth, and σ is the separation at which the potential is zero. The proposed EoS based on this potential energy is given as:

$$(Z-1)V^2 = C + B(1/\rho)$$

(2)

where C and B are temperature-dependent parameters of the isotherms and are derived as

$$C = C_2 + \left(\frac{C_1}{RT}\right), \qquad B = \frac{-B_1}{RT} \tag{3}$$

The molar density at any temperature and pressure can be calculated via the following equation:

$$C\rho^3 + B\rho^2 + \rho - \frac{P}{RT} = 0 \qquad (4)$$

Results and discussion:

Eq. (2) indicates that the isotherms of $(Z-1)V^2$ versus $(1/\rho)$ are linear for liquid alkali metals. Figs. 1 shows the isotherms of Eq. (2) (this work) and also the isotherms of the original LIR EoS in the range of 500-1800 K for liquid potassium. This figure shows that a softer potential in the form of Eq. (1) is more appropriate than the LJ (12-6) potential for liquid alkali metals over the whole range. Eq. (4) can be used to predict the density of alkali metals. The calculated densities show a great accordance with experimental data. The average absolute deviations are lower than 0.10 for all liquid alkali metals.

Table 1. Average percentual deviation (bias) and the average absolute deviation (AAD) between the calculated molar density values and experimental data [2-4] for different alkali metals at different temperature and pressure ranges.

LAM	ΔT(K)	ΔP(MPa)	bias	AAD	NP
Li	500-2000	10-100	0.0000	0.0005	94
Na	500-2000	10-100	-0.0001	0.0036	95
K	500-1800	10-100	-0.0032	0.0182	84
Rb	400-1600	10-100	-0.0165	0.0548	75
Cs	400-1950	10-100	-0.0374	0.0975	97
Total			-0.0115	0.0349	445

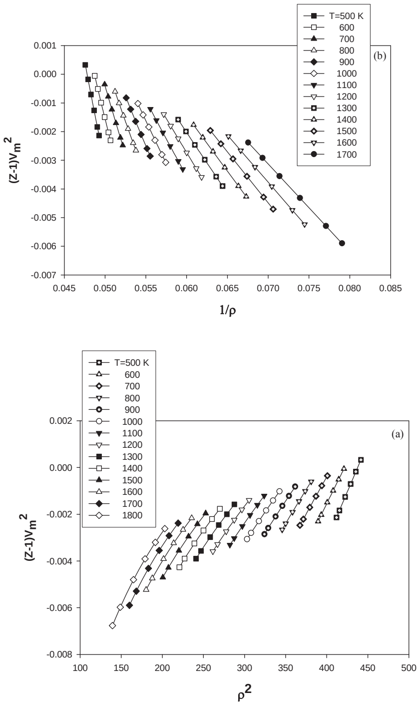

Fig. 1. Isotherms of liquid potassium based on (a) original LIR EoS [1] and (b) this work.

Conclusion:

The (6-3) Lennard-Jonse based equation of state was used to evaluate liquid alkali metal's density. The calculated densities are in agreement with experimental data, and also the isotherms have linear behavior over the whole range for all alkali metals.

References:

[1] M.H. Ghatee, M. Bahadori, J. Phys. Chem. B 105, 11256–11263, 2001.

[2] N.B. Vargaftik, et al., J. Eng. Phys. 35, 1361-1369, 1978.

[3] N.B. Vargaftik, et al., J. Eng. Phys. 35, 1415-1422, 1978.

[4] N.B. Vargaftik, et al., High Temp. High Press. 16, 233-238, 1984.

Thermodynamic properties of three binary systems consist of diethylketone, 2-butanol, ethylchloroacetate at temperatures (298.15, 308.15, 318.15) K

M. Habibi*, H. Iloukhani
Department of Physical Chemistry, Faculty of Chemistry, Bu-Ali Sina University, Hamedan, Iran
Email:mh_nefto@yahoo.com

Keywords: Diethylketone, 2-Butanol, Ethylchloroacetate, Excess molar volume, Viscosity deviation.

Introduction:

In this paper experimental densities, viscosities and derived thermodynamic properties of three binary mixtures consist of (diethylketone + 2-butanol), (diethylketone + ethylchloroacetat) and (2-butanol + ethylchloroacetate) at temperatures (298.15, 308.15, 318.15) K were presented.
Thermochemical properties are of great interest for the adequate design of industrial processes and for the oretical purposes. The interaction between solvents with polar groups and carbonyl group of ketone plays a crucial role in the structural effects, molecolar level and for practical applications.
When two or more solvent molecules are associated with one another to from a liquid mixture, it brings about a marked effect on the properties of the resulting system and differences in the intermolecular interactions of the solvents. This fact is well known as the transport phenomenon and thermophysical properties of mixed solvents.

Materials and methods:

diethylketone (w>.99), 2-butanol (w>.99), ethylchloroacetate (w>.99) where w is mass fractions. All matherials were purchased from Merck and were used without further purification.
Densities and viscosities of component were measured and their values were in good agreement with values found in the literature [1,2].

Apparatus:

The densities of the pure liquids and their mixtures were measured with an Anton Paar digital vibrating U-tube densitometer (model DMA 4500) with a resolution of 1×10^{-5}g.cm^{3}. The viscosities were measured with an ubbelohde viscometer with an uncertainty of 2×10^{-4}mpa.s.

The mixtures were prepared by weighing known masses of pure liquids in air tight, narrow-mouthed ground stoppered bottles taking due precautions to minimize evaporation losses.

All the mass measurements were performed on an electronic balance (Mettler AE 163,switzerland).

Results and discussion:

Excess molar volumes of diethylketone + ethylchloroacetat is negative but for the other binary systems containing diethylketone + 2-butanol and 2-butanol + ethylchloroacetate are positive over the whole range of mole fractions. Positive values would indicate that molecular interactions between different molecules are weaker than interactions between molecules in the same pure liquid and that repulsive forces dominate the behavior of the solutions. For diethylketone + 2-butanol and 2-butanol + ethylchloroacetate, attractive interactions between unlike species decrease because of breaking H-bondig and repulsive interactions predominate, leading to positive excess molar volumes.

The negative V_m^E values arise due to dominance chemical interaction between constituent molecules, such as heteromolecular association through the formation of H-bond, known as strong specific interaction. The viscosity deviations of three binary mixtures are negative.

Conclusion:

Densities and excess molar volumes V_m^E and Viscosity deviation $\Delta\eta$ of binary mixtures were measured. The experimental V_m^E and Viscosity deviation $\Delta\eta$ of binary systems were fitted by Redlich–Kister polynomial equation [3] and also The Viscosity measurements were provided a test of various empirical equations to correlate viscosity data of binary mixtures in terms of pure component properties. The measured data and calculated values of all systems are in good accordance, and are theoretically and statistically satisfying. No data are available in the literature for the present systems for direct comparison with our results.

References:

[1] J.A. Riddick, W.B. Bunger, T.K. Sakano, Organic Solvents Physical Properties and Methods of purification, 4, Wiley, New York, 1986.

[2] I. Aralaguppi and etal; J.chem. Eng. 48, 628-631, Data2003

[3] o. Redlich, A.T. Kister, Ind. Eng. Chem. 40 (1948) 345-348.

Investigation of volumetric properties of binary mixtures of benzylamine with 2-propanol, 1-butanol and 2-butanol at different temperatures.

M.Orang*, H. Zarei,
Department of Chemistry, Faculty of Chemistry, Bu-Ali Sina University, Hamedan, Iran
Email: mahdiehorang@yahoo.com

Keywords: Benzylamine, Excess molar volume, Binary mixture, Redlich- Kister, alkanol

Introduction:

Hydrogen-bonded systems are very interesting because they play a vital role in chemical, physical, and biological processes. It is well-known that alcohols are highly associated through hydrogen bonds, and this association decreases with the increase in molar mass of alkanols.

The mixtures of amine with alcohol are interesting for a number of scientific reasons, mostly connected to the formulation and testing of models to predict the properties of associating fluids, since the binary systems are composed of associating liquids. Both the primary amines and alcohols serve as are proton donors and proton acceptors, it is expected that there will be a significant degree of H-bonding, leading to self association in pure state. The aim of present work is to provide new experimental data on densities of the binary mixtures of benzylamine with 2-propanol, 1-butanol and 2-butanol at different temperatures. The excess molar volumes, $V_{\mathrm{m}}^{\mathrm{E}}$, the excess thermal expansion coefficients, α^{E}, isothermal coefficient of excess molar enthalpy $(\partial H_m^E/\partial p)_{\mathrm{T,x}}$, were calculated from the experimental values of densities. These data were correlated with the Redlich- Kister equation.[1-3]

Materials and methods:

All of the chemical were high purity grade and were used without further purification. The purities declared by the manufacturer were ascertained by comparing their densities and refractive indices with the litrature values. They are in good agreement with the literature values. The pure components were degassed just before use.

Apparatus:

The densities of the pure components and their binary mixture were measured by means of an Anton Paar digital vibrating U-tube densitometer (model DMA 4500), provided with automatic viscosity correction. The densitometer was calibrated with bi-distilled, freshly degassed water, and dry air. The temperature in the cell was regulated to ±0.01K, with a solid-state thermostat(Peltier). Temperature in the cell was measured by means of two integrated platinum thermometers. The mixture were prepared just before use by mass using a digital balance (model: Mettler AB 204-N) with an uncertainty of $\pm 1\times 10^{-4}$g.

Results and discussion:

The experimental values of density were used to calculate the excess molar volume, V_m^E, of the mixtures. Fig.1 shows that excess molar volume for all binary mixtures are negative over the entire range of composition and different temperatures. The absolute values of excess molar volume for all systems decrease with increasing temperature from (293.15 to 333.15) K. The negative values of excess molar volumes indicate strong cross association between benzyamine and alkanols.

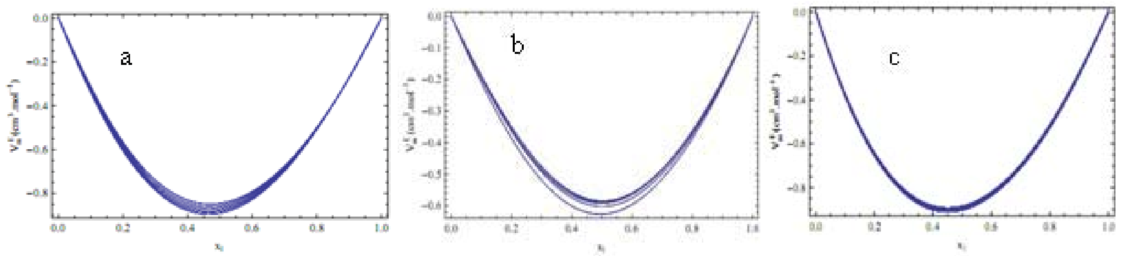

Fig.1. Excess molar volumes of binary mixture of benzylamine + , a) 1-Butanol, b) 2-Butanol, 3) 2-Propanol, lines from Redlich- Kister correlation.

Conclusion:

In this study, an attempt has been made to measure density at (293.15, 303.15, 313.15, 323.15, and 333.15) K, over the entire composition range of Bezylamine with 2-propanol, 1-butanol and 2-butanol. The excess molar volume, excess thermal expansion coefficients and isothermal coefficient of excess molar enthalpy were calculated and correlated by the Redlich–Kister type polynomial equation. Negative values of V_m^E, shows the presence of strong interactions.

References:

[1] G.P.Dubey, K.Kumar, J. Chem. Thermodynamics, 50 (2012) 7–14.

[2] G.P.Dubey, K.Kumar, Thermochimica Acta, 524 (2011) 7– 17.

[3] D.M. Jain, V.Shah, S.Rabadiya, S.Oswal, Journal of Molecular Liquids 144 (2009) 65–70.

Salt Effect on the Liquid-Liquid Equilibrium of (Water + Phosphoric acid + Dichloromethane or 1, 2-Dicholoroethane) Systems at T=298.15 K

M. Ebrahimi*[a], Kh. Bahrpaima[b], Z. Sharafi[a]

[a] Department of Chemistry, Marvdasht Branch, Islamic Azad University, Marvdasht, Iran

Email: m.ebrahimi2002@yahoo.com

[b] Department of Chemistry, Firoozabad Branch, Islamic Azad University, Firoozabad, Iran

Key words: LLE data, Phosphoric acid, Extraction processes, Salting effect, NRTL model.

Introduction:

The recovery of acids from dilute solutions is important and many solvents have been used to improve such recovery [1-2]. Liquid–liquid equilibrium (LLE) investigations for ternary mixtures are important in the evaluation of industrial units for solvents extraction processes. The presence of dissolved salt changes the phase equilibrium behavior of a mixture significantly. This phenomenon is often referred to as the salting in or salting-out effect. In present work, the effect of 10% NaCl and 10% $CaCl_2$ on LLE data for the ternary systems of (water + phosphoric acid (PA) + dichloromethane (DM) or 1, 2-dicholoroethane (DE)) were studied at 298.15 K and 1 atm.

Materials:

The chemicals 1, 2-dicholoroethane (0.99), dichloromethane (0.99), and phosphoric acid (0.99) were obtained from merck and were used without further purification. Distilled water was prepared in our laboratory and used throughout all experiments.

Methods and Apparatus:

The equilibrium between liquid phases was studied in a transparent water thermostat at T= (298.15) K. A 250 cm^3 glass cell connected to a thermostat was made to measure the LLE data. The equilibrium data were determined by preparing the ternary mixtures of known compositions. The prepared mixtures were introduced into the extraction cell and were stirred for 4 h, and then left to settle for 4 h or phase separation. After being allowed to reach equilibrium, samples were carefully taken from each phase the necessary rest time, the mixture split into clear and transparent liquid phases with a well defined interface. The samples of both phases were collected and the tie line values were obtained by titration of the samples with a known concentration NaOH aqueous solution.

Result and discussion:

The experimental tie-line data and binodal data for the ternary systems of [water + phosphoric acid + solvent (dichloromethane or 1, 2-Dicholoroethane)] with 10% NaCl and 10% $CaCl_2$ were determined at 298.15 K. The NRTL model was satisfactorily used to correlate the experimental LLE results. The corresponding optimized binary interaction parameters were also calculated. The distribution coefficients for phosphoric acid and the separation factors of the solvents were determined (Table 1).

Table 1. Separation Factors (*S*) at 298.15 K.

Solvent	**S**
DE + 10% NaCl	1.89
DE + 10% $CaCl_2$	1.98
DM + 10% NaCl	1.72
DM + 10% $CaCl_2$	1.24

Conclusion:

The LLE data for the ternary systems of (water + phosphoric acid + dichloromethane or 1, 2-dicholoroethane) with 10% NaCl and 10% $CaCl_2$ were studied at 298.15 K. In this work, NaCl and $CaCl_2$ significantly affect the solubility of PA in the organic solvents used in the experiments. The results also showed that the separation factors of the solvents in extracting PA, increase in presence of 10% $CaCl_2$ in 1, 2-dichloromethane solutions.

References:

[1] H.Ghanadzadeh ; A.Ghanadzadeh ; Kh.Bahrpaima ; ″Liquid phase equilibria of (water +

phosphoric acid + 1-butanol or butyl acetate) ternary systems at T = 308.2 K″ ; J. Chem. Thermodynamics ; 40,1666-1670,2008.

[2] N.Bourayou ; A.-H. Meniai ; ″Effect of calcium chloride on the liquid-liquid equilibria of the water-acetone system″ ; Desalination ; 206,198-204,2007.

Measurements and Modelling of Quaternary (Liquid + Liquid) Equilibria for Mixtures of (Water + Phosphoric acid + Dichloromethane + 1, 2-Dicholoroethane)

S. Doshman ziari*[a], Kh. Bahrpaima[b], Z. Sharafi[a]
[a] Department of Chemistry, Marvdasht Branch, Islamic Azad University, Marvdasht, Iran
Email: s.doshmanziari2002@yahoo.com
[b] Department of Chemistry, Firoozabad Branch, Islamic Azad University, Firoozabad, Iran

Key words: Quaternary mixtures, Phosphoric acid, Activity coefficient, NRTL.

Introduction:

Extraction of phosphoric acid from aqueous solutions is an important operation in chemical and petrochemical processes. Design of apparatus and determining the optimum operating conditions for extraction systems require the knowledge of multi-component liquid + liquid equilibrium (LLE) data [1-2]. In particular, LLE investigations for quaternary mixtures are important in the evaluation of industrial units for solvent extraction processes.

In this work, (liquid + liquid) equilibrium data (binodal and tie line data) for the quaternary mixtures of {water + phosphoric acid + dichloromethane (DM) + 1, 2-dichloroethane (DE) } at different ratio were obtained at 298.15 K and ambient pressure.

Materials:

All chemicals used in this work (mass fraction purity > 99%) were obtained from merck. Deionized and redistilled water was used throughout all experiments.

Methods and Apparatus:

A 250 ml glass cell was made to measure the LLE data. The equilibrium data were determined by preparing the quaternary mixtures of known composition compositions. The prepared mixtures with known compositions were located inside the cell and were vigorously agitated with a magnetic stirrer for 4 h. The mixtures were then settled for 4 h to completely separate in two-liquid phases and to get the equilibrium. The samples of both phases were collected and the tie line values were obtained by titration of the samples with a known concentration NaOH aqueous solution.

Result and discussion:

The experimental tie-line and binodal data for the quaternary systems of [water + phosphoric acid + dichloromethane +1, 2-dicholoroethane] at different ratio were determined at 298.15 K. The NRTL model was used to correlate the experimental data to obtain the binary interaction parameters of these components. The separation factor and distribution coefficient of the used mixed solvents were compared (Table 1). The results indicated that the extraction of phosphoric acid from aqueous mixtures with (25% dichloromethane +75% 1, 2-dicholoroethane) mixtures is preferred.

Table 1. Separation factors (*S*) at 298.15 K

Solvent	S
25% DE + 75% DM	1.68
50% DE + 50% DM	1.97
75% DE + 25% DM	2.55

Conclusion:

LLE data of the quaternary mixtures {water + phosphoric acid + dichloromethane + 1, 2-dicholoroethane} at different ratio were presented at 298.15 K. we conclude that for the extraction of phosphoric acid from aqueous mixtures, the mixed-solvents (25% dichloromethane + 75% 1, 2-dichloroethane) has a higher separation factor than the other ratio at the temperature studied.

References:

[1] A.Merzougui ; A.Hasseine ; A.Kabouche ; M.Korichi ; ″LLE for the extraction of alcohol from aqueous solutions with diethyl ether and dichloromethane at 293.15 K, parameter estimation using a hybrid genetic based approach″ ; Fluid Phase Equilibria ; 309,161-167, 2011.

[2] M.Mohsen-Nia ; H.Modarress ; F.S.Mohammad Doulabi ; ″Quaternary liquid–liquid

equilibria for systems of {(water + methanol or ethanol) + m-xylene + n-dodecane}″ ; Fluid Phase Equilibria ; 239,1-7,2006.

Modification of TM EOS and application to PPO-PS blend using glass transition data

F. Yosefi[a], M. Gomar[a]

[a]Department of Chemistry, Yasouj University, Yasouj, Iran

(Email: maryam_gomar63@yahoo.com)

Keywords: Equation of state, Density, Glass transition, Blend

Introduction:

Blending of polymers is a technique to obtain properties in thermoplastic materials not readily achieved in a single polymer. Virtually all technologically important properties can be improved in this way, some of the more important ones being flow properties, mechanical properties (especially impact strength), thermal stability, and price. Polymer blends can form single –phase or multiphase solids and melts. For polymeric substances, equations of state are also an important subject for scientists and polymer engineers because such equations are able to predict the behavior of polymers in a wide range of temperature and pressure particularly when experimental data are scare. In this study, the volumetric properties of poly (2,6-dimethyl phenylene oxide)+polystyrene (PPO/PS) blend are predicted by Tao-Mason equation of state (TM EOS) using glass transition data in different temperature, pressure and mole fractions.

Methods:

In 1994, Tao and Mason [1] calculated a perturbation correction term related to the effect of attractive forces and combined it with Ihm-Song-Mason equation of state (ISM EOS). The final form of the original TM EOS is expressed as follows:

$$\frac{P}{\rho KT} = 1 + (B_2 - \alpha)\rho + \frac{\alpha\rho}{1 - \rho b\lambda} + A_1(\alpha - B_{2)} b\rho^2 \frac{(e^{\frac{kTf}{T}} - A_2)}{1 + 1.8(\rho b)^4} \quad \dots\dots\dots\dots\dots\dots\dots\dots\dots\dots\dots\dots\dots\dots\dots \quad (1)$$

where P is the pressure, kT has its usual meaning, B_2 is the second virial coefficient, □□is the scaling factor, b is the effective van der Waals co-volume, and □ is the number density. We decided to investigate about a new corresponding states correlation in order that TM EOS could be applied to polymer blends. In this respect, the following correlation equation for B_2 using new scaling parameters, such as the molar density ρ_g, the glass transition point has been developed. The resulting correlation for the second virial coefficient reads as follows:

$$\rho_g B_2 = 1.033 - 3.0069\left(\frac{T_g}{T}\right) - 10.588\left(\frac{T_g}{T}\right)^2 + 13.096\left(\frac{T_g}{T}\right)^3 - 9.8968\left(\frac{T_g}{T}\right)^4 \dots\dots\dots\dots\dots\dots \quad (2)$$

Results and discussion:

As mentioned earlier, in order to develop a statistical mechanically-based equation of state for polymer blends, we performed some modifications on the Tao-Mason EOS. At first, a correlation equation for the second virial coefficient was developed using the temperature and the liquid state density at the glass transition point. In addition, we found that the adjustable parameter λ turns out to be temperature and pressure dependent. Using high density PVT data, the parameter λ was correlated by the following simple polynomial equation: $\lambda = a + bT + cP$. We performed the calculation of molar volume of PPO/PS using the TM EOS. The outcome of the computed results has been gathered sequentially in Figures 1-3. It is evident from these figures, that the agreement between the calculated specific volumes and the literature values [2] is quite satisfactory. In general, the obtained mean of the deviations for PPO/PS was found to be of the order of 0.89.

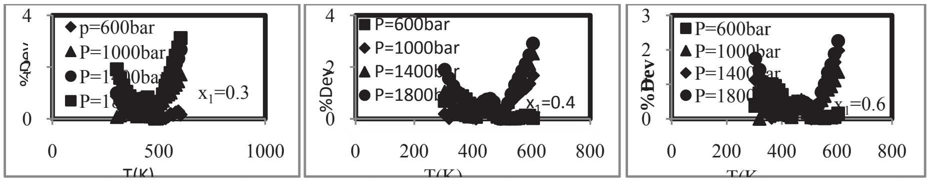

Fig1. Deviation plot for the predicted densities of PPO+PS at different temperatures, pressures and mole fractions with experiment[2]

Conclusions:

We have demonstrated that the present correlation along the modified TM EOS is capable of predicting specific volumes of the polymer blends over a broad temperature and pressure ranges.

References:

[1] Tao, F.M.; Mason, E. A. Statistical-Mechanical Equation of State for Nanpolar Fluids: Prediction of Phase Boundaries. *J. Chem. Phys.* **1994**, *100*, 9075.

[2] P. Zoller, D.J. Walsh, Standard Pressure-Volume-Temperature Data for Polymers, Technomic Pub. Co. Lancaster, PA, **1995**.

Volumetric properties of PEG-PPG blend by equation of state using surface tension

F. Yosefi[a], M. Gomar[a]
[a]Department of Chemistry, Yasouj University, Yasouj, Iran
(Email: maryam_gomar63@yahoo.com)

Keywords:, Polymer blend, Density, PVT Properties, Surface tension, Equation of state

Introduction:

For polymeric substances, equations of state are also an important subject for scientists and polymer engineers because such equations are able to predict the behavior of polymers in a wide range of temperature and pressure particularly when experimental data are scare. In this project, we applied the Tao-Mason equation of state (TM EOS) to prediction of liquid density of poly(propylene glycol) (PPG) + poly(ethylene glycol) (PEG) blends at compressed state with temperature range from 298.15 to 338.15 K and pressures up to 400 bar.

Methods:

The final form of the original TM EOS [1] is expressed as follows:

$$\frac{P}{\rho KT} = 1 + (B_2 - \alpha)\rho + \frac{\alpha\rho}{1-\rho b\lambda} + A_1(\alpha - B_2)b\rho^2 \frac{(e^{kTf/T} - A_2)}{1+1.8(\rho b)^4} \qquad (1)$$

where P is the pressure, kT has its usual meaning, B_2 is the second virial coefficient, α is the scaling factor, b is the effective Van der Waals co-volume, and ρ is the number density.

$$B_2\rho_f = 0.0804 - 2.1288{T^*}^{-1} + 8.5598{T^*}^{-2} + 7.4294{T^*}^{-3} - 3.3494{T^*}^{-4} \qquad (2)$$

$$\alpha\rho_f = a_1[exp(-c_1T^*)] + a_2\left\{1 - exp\left(-\frac{c_2}{{T^*}^{\frac{1}{4}}}\right)\right\} \qquad (3)$$

$$b\rho_f = a_1(1 - c_1T^*)[exp(-c_1T^*)] + a_2\left[1 - \left(1 + \frac{0.25c_2}{T^{*\frac{1}{4}}}\right) exp\left(-\frac{a_2}{T^{*1/4}}\right)\right] \qquad (4)$$

Results and discussion:

We have taken the surface tension and the freezing point data for prediction of volumetric properties of PPG+PEG polymer blends. Once these parameters are known, the temperature-dependent parameters of the equation of state, B_2, α and b, can be calculated using Eqs. (2)–(4). Using high density PVT data, the parameter λ was correlated by the following simple polynomial equation: $\lambda = a + bT + cP$. We performed the calculation of molar volume of PPG+PEG using the TM EOS. The outcome of the computed results for two mole fractions has been gathered sequentially in figures 1-2. It is obvious from these figures, that the agreement between the calculated specific volumes and the literature values [2] is quite satisfactory. In general, the obtained mean of the deviations for PPG+PEG for all range of temperatures, pressures and mole fractions were found to be of the order of 1.48.

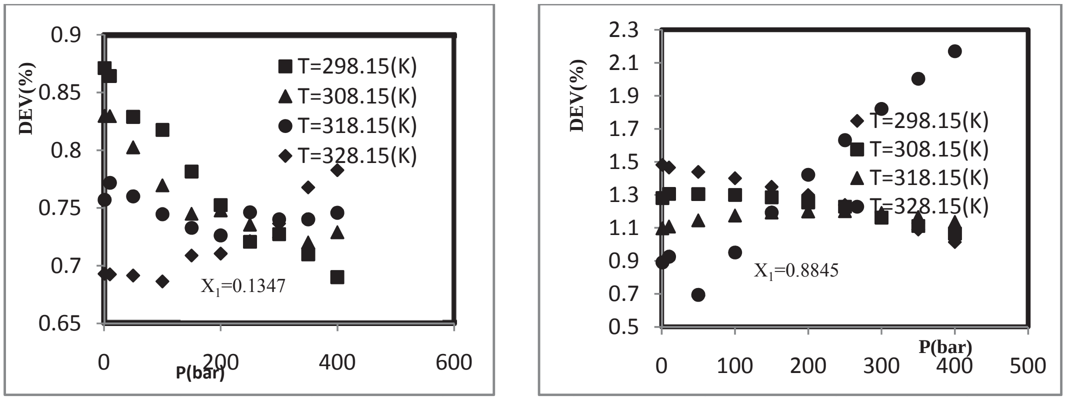

Fig1. Deviation plot for the predicted densities of PPG+PEG at different temperatures, pressures and mole fractions with experiment [2].

Conclusions:

Our procedure successfully predicts a statistical mechanical equation of state for density of PPG+PEG blends over a wide range of temperatures and pressures.

References:

[1] Tao, F.M.; Mason, E. A. Statistical-Mechanical Equation of State for Nanpolar Fluids Prediction of Phase Boundaries. *J. Chem. Phys.* 1994, *100*, 9075.

[2] Colin AC, Rubio RG, Compostizo A. Equation of state of a blend of water-soluble polymer: poly (propylene glycol) + poly (ethylene glycol). Polymer 2000, 41, 7407–14.

Aggregation Behavior Modulation of Ionic Liquid 1-Dodecyl-3-methylimidazolium Bromide by Sodium Salts in Aqueous Solutions

Rahmat Sadeghi[a]*, Roonak Golabiazar

[a]*Department of Chemistry, University of Kurdistan, Sanandaj, Iran*

*E-mail: rsadeghi@uok.ac.ir

Keyword: Ionic liquid, Micelle, Salt effect

Introduction:

Ionic liquids (ILs) are organic salts that are liquids at temperatures below 373.15 K. They have received considerable attention as alternatives to the traditional organic solvents. Because of their interesting physical and chemical properties, such as negligible vapor pressure, unique permittivity, high thermal stability, good solvents for both organic and inorganic substances, high electrical conductivity, and wide electrochemical window, ILs have been widely used as reaction media, separation solvents, and novel electrolytes [1,2]. In recent years, ILs based on 1-alkyl-3-methylimidazolium cation $[C_nmim]^+$ have received much attention and have been the most studied. An interesting aspect of such ILs is that the $[C_nmim]^+$ cations possess inherent amphiphilic character when their alkyl group is a longer hydrocarbon chain. It has been shown that, 1-dodecyl-3-methylimidazolium bromide $[C_{12}mim]Br$ behaves like a classical surfactant and forms aggregates in water with the critical micelle concentration (cmc) about 9.8 mM and then self-assembles to form lyotropic mesophases at higher concentrations [3]. Literature survey reveals that aggregation behavior of ILs can also be tuned by the addition of some inorganic salts, but the related investigation is very limited. Therefore, a systematical study on the effect of the salt nature on the aggregation behavior of ILs is necessary from the viewpoint of fundamental and applied aspects.

In this work, the aggregation behavior of 1-dodecyl-3-methy-limidazolium bromide $[C_{12}mim]Br$ has been investigated in aqueous salt additive solutions. The aim is to reveal the nature of salt additives to influence aggregation behavior of the IL in water. For this purpose, 4 kinds of salts with a wide range of physicochemical properties have been selected, including $NaNO_3$, Na_2SO_4,

Na_2CO_3, Na_3Cit. At the same time, conductivity, vapor pressure osmometry (VPO), and volumetric techniques at 288.15 to 313.15 K are used to study the effect of the nature and size of salt on the critical micelle concentration (CMC), the degree of cationic binding at the aggregates surface (β), thermodynamic parameters of micellization (ΔG_m°, ΔH_m°, ΔS_m°), of the ionic liquid in aqueous solutions.

Experimental Section:

The density and sound velocity of the mixtures were measured at different temperatures with a digital vibrating-tube analyzer (Anton Paar DSA 5000, Austria) with proportional temperature control that kept the samples at working temperature within (10^{-3} K). Conductometric measurements were taken in a digital conductivity meter (Metrohm model 712) with a sensitivity of 0.1% and a dipping-type conductivity cell with platinized electrodes

at a frequency of 1 MHz. The cell constant was calibrated with aqueous KCl solutions.

The vapor pressure osmometry was performed with the help of an Osmomat K-7000 (Knauer Inc.). The measuring chamber of the osmometer contains a reservoir of solvent, paper wicks to provide a saturated solvent atmosphere, and two thermistors that are placed in an airtight cell which measure resistance changes caused by changes in temperature.

Results and Discussion:

As a representative example, Figure 1 shows the variation in experimental conductivity of $[C_{12}mim]Br$ with IL concentrations in aqueous $NaNO_3$ solution. The concentration corresponding to the intersection of the two straight lines is defined as the critical aggregation concentration of the IL, which can be calculated by solving the two linear equations used for describing the two straight lines. Similar situations have been found for the ionic liquid in the presence of other salts at different temperatuers. As it is expected, a pronounced effect of the anions was observed on CMC of $[C_{12}mim]Br$. These values increase in the sequence: $NO_3^- < Cit^{3-} < SO_4^{2-} < CO_3^{2-}$. In other words, ability of the anions to promote aggregation of the IL was found to increase in the order: $CO_3^{2-} > SO_4^{2-} > Cit^{3-} > NO_3^-$. It is known that the formation of ionic liquid aggregates in aqueous solution results from a balance of two opposing interactions: (1) electrostatic repulsion between the cationic groups which disfavors aggregation and (2) attractive hydrophobic interaction involving the alkyl chains which favors aggregation. The former interaction can be reduced by adsorption of the IL anions onto the surface of the aggregates thereby lowering the CMC values and enhancing the aggregation of the IL. The latter interaction can also be reduced by increasing the attractive interactions of alky chains with solvents. From the plots of conductivity against concentration of the IL, the degree of counterion dissociation, α, can be obtained from the ratio of the slopes above and below the cmc, while the degree of counterion binding to micelle, β, is(1−α). It can be seen that the values decrease in the following order: $Cit^{3-} > NO_3^- > SO_4^{2-} > CO_3^{2-}$ at 298.15K.

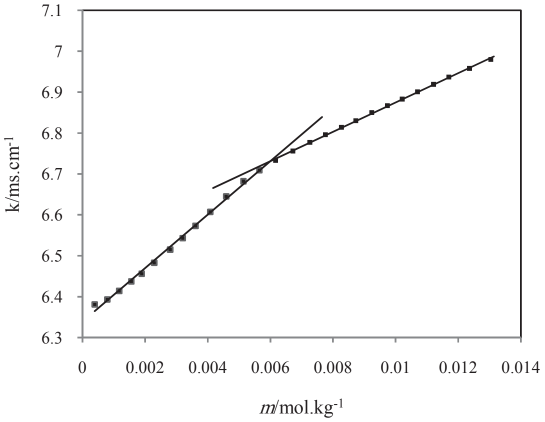

Figure1: Concentration dependence of the conductivities for aqueous solutions of [C_{12}mim]Br in the presence of 0.035 mol/kg $NaNO_3$at 298.15 K.

References:

[1] Welton, T. *Chem. Rev* . **1999**, 99, 2071.

[2] Wasserscheid, P.; Keim, W. *Chem., Int. Ed*. **2000**, 39, 3772.

[3] Wang, J.; Wang, H. *J. Phys. Chem. B* **2010**, 114, 1380.

Salt Effect on the Aggregation and Thermodynamic Properties of Ionic Liquid 1-Dodecyl-3-methylimidazolium Bromide in Aqueous Solutions

Rahmat Sadeghi[*], Roonak Golabiazar
[a]Department of Chemistry, University of Kurdistan, Sanandaj, Iran
[*]E-mail: rsadeghi@uok.ac.ir

Keyword: Ionic liquid, Aggregation, Salt effect

Introduction

Ionic liquids (ILs) have received considerable attention as greener replacements for traditional volatile organic solvents in a variety of fields such as chemical synthesis, catalytic chemistry, electrochemical device, separation, and biomass dissolution because of their unique physicochemical properties [1]. Recently, it has been reported that self-aggregation of imidazolium ILs occurs in solutions because of their inherent amphiphilic nature. Material preparation in ILs, chromatographic application of ILs, and environmental pollution control by ILs are often closely dependent on such aggregation behavior. Thus, the study of aggregation behavior of ILs in solutions is highly desired for the understanding of how IL participates in practical applications as a component [2]. In recent years, a number of research publications indicated aggregates formation of ILs in aqueous solutions. It was found that the aggregation behavior of ILs can be regulated and controlled by designing the alkyl chain length, cationic structure, and anionic type of the ILs. Literature survey reveals that aggregation behavior of ILs can also be tuned by the addition of some inorganic salts, but the related investigation is very limited [3]. Therefore, a systematical study on the effect of the salt nature on the aggregation behavior of ILs is necessary from the viewpoint of fundamental and applied aspects.

This work aims to study the regulated and controlled effect inorganic cations of the added salts on the aggregation behavior of 1-dodecyl-3-methylimidazolium bromide ($[C_{12}mim]Br$) in aqueous solutions. For these purposes, 5 chloride salts (NaCl, KCl, NH_4Cl, $(CH_3)_4NCl$, $MgCl_2$) were selected, and conductivity at 298.15 to 313.15 K, osmotic coefficient at 308.15 K, volumetric at 288.15 to 313.15 K are combined to study the salt effect on the aggregation of $[C_{12}mim]Br$. The results have been discussed from the influence of the nature and size of salt on the critical micelle concentration (CMC), the degree of cationic binding at the aggregates surface (β), thermodynamic parameters of micellization (ΔG_m°, ΔH_m°, ΔS_m°), of the ionic liquid in aqueous solutions.

Experimental Section:

The density and sound velocity of the mixtures were measured at different temperatures with a digital vibrating-tube analyzer (Anton Paar DSA 5000, Austria) with proportional temperature control that kept the samples at working temperature within (10^{-3} K). Conductometric measurements were taken in a digital conductivity meter (Metrohm model 712) with a sensitivity of 0.1% and a dipping-type conductivity cell with platinized electrodes
at a frequency of 1 MHz. The cell constant was calibrated with aqueous KCl solutions.
The vapor pressure osmometry was performed with the help of an Osmomat K-7000 (Knauer Inc.). The measuring chamber of the osmometer contains a reservoir of solvent, paper wicks to provide a saturated solvent atmosphere, and two thermistors that are placed in an airtight cell which measure resistance changes caused by changes in temperature.

Results and Discussion:

Typical experimental conductivities (κ), solvent activity (a_w), isentropic compressibility (k_s) and sound velocity (u) at 308.15 K for aqueous solutions of [C_{12}mim]Br in the presence of 0.035 mol/kg NaCl are shown in Figure 1 as a function of IL concentrations in the range of interest. The concentration corresponding to the inflection observed in the curve is considered to be the critical micelle concentration (CMC) of [C_{12}mim]Br in aqueous 0.035 mol/kg NaCl solution, and the CMC value can be calculated by solving the two linear equations below and above the inflection. Similar situations have been found for the ionic liquid in the presence of other salts at different temperatuers. As it is expected, a pronounced effect of the cations was observed on CMC of [C_{12}mim]Br. These values increase in the sequence: $Mg^{2+} < (CH_3)_4N^+ < NH_4^+ < K^+ <$ Na^+. In other words, ability of the cations to promote aggregation of the IL was found to increase in the order: $Mg^{2+} > (CH_3)_4N^+ > NH_4^+ > K^+ > Na^+$. This cation effect correlates well with the Hofmeister series, which provides an adequate qualitative description for the salt effect in several physical behaviors. It is known that the position of an cation in the Hofmeister series can be correlated with its charge and hydration radius. An increased hydration radius of the cation is usually accompanied by an increased polarizability.

From the plots of conductivity against concentration of the IL, the degree of counterion dissociation, α, can be obtained from the ratio of the slopes above and below the cmc, while the degree of counterion binding to micelle, β, is(1−α). It can be seen that the values decrease in the following order: $K^+ > Na^+ > (CH_3)_4N^+ > NH_4^+ > Mg^{2+}$ at 298.15K.

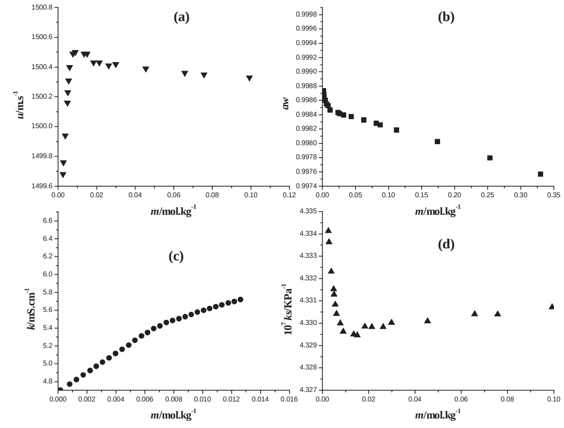

Figure1: Plots of (a) sound velocity, (b) solvent activity, (c) conductivities, (d) isentropic compressibility for aqueous solutions of $[C_{12}mim]Br$ in the presence of 0.035 mol/kg NaCl at 308.15 K.

References:

[1] Welton, T. *Chem. Rev* . **1999**, 99, 2071.

[2] Han, X.; Armstrong, D.W. *Acc. Chem. Res*. **2007**, 40, 1079.

[3] Wang, J.; Wang, H. *J. Phys. Chem. B* **2010**, 114, 1380.

Equation of State for Alkaline Earth Metals: Prediction from Surface Tension

F. Yousefi[a], M. Kaveh[a]

[a]Department of Chemistry, Yasouj University, Yasouj, Iran
(Email: kavehm1364@gmail.com)

Keywords: Alkaline Earth Metals, Density, Equation of state, Freezing point

Introduction:

The knowledge of thermodynamic properties of liquid metals is of considerable interest in industry. Liquid metals have a number of interesting characteristic, which make them applicable in high- temperature operations as heat transfer agent and reactor coolant. The most important characteristics of them are high boiling points, extended liquid range, high thermal conductivities, low vapor pressure, and high heat of vaporization. The present work is concerned with modifying the original Tao-Mason EOS [1] to calculate the temperature-dependent parameters of the equation of state for molten alkaline earth metals (Mg through Ba). It is shown that this procedure leads to an analytical equation of state which can predict the saturated liquid density of these metals from the melting point up to several hundred Kelvin above the boiling point within 0.654%. In the next section, we shall introduce the EOS in question.

Methods:

The final form of the TM EOS for pure substances is given by

$$\frac{P}{\rho KT} = 1 +$$

We decided to modify the original TM EOS in order that this EOS could be applied to alkaline earth metals. In this respect, we employed correlations for B_2, α and b proposed by Ghatee and Boushehri [2]. The scaling parameters for these correlations are surface tension and density, γ_f and ρ_f, both at freezing point, which are available for alkaline earth metals.

Results and discussion:

The goal of the present study has been centered in the modification of the Tao-Mason EOS and after that in the analysis of the capability of the modified TM EOS in predicting volumetric properties of alkaline earth metals. We performed the calculation of density of alkaline earth metals using modified TM EOS. The outcome of the computed result for Mg and Ca has been collected sequentially in Table1. It is evident from this Table, that the agreement between the calculated densities and the literature values [3] is quite acceptable. In general, the obtained mean of the deviations for all alkaline earth metals was found to be of the order of 0.048%.

Table 1. The calculated results for the saturated liquid density of Magnesium and ca Calcium compared with the experimental data [3].

T [K]	P [bar]	ρ_{cal}	ρ_{Exp}	Dev%
Mg				
23	3.586×10^{-3}	65.4413	66.77	1.99
1000	1.483×10^{-2}	64.5398	65.26	1.104
1100	6.288×10^{-2}	63.4720	64.25	1.211
1200	0.207	62.4171	62.52	0.165
1300	0.5616	61.3327	61.03	0.496
1400	1.309	60.2190	59.91	0.516
1500	2.705	59.0946	59.31	0.363
1600	5.070	57.9805	59.54	2.619
1700	8.774	56.8933	57.12	0.397
1800	14.21	55.8424	55.41	0.78
1900	21.77	54.8312	54.39	0.811
2000	31.82	53.8593	54.09	0.427

T [K]	P [bar]	ρ_{cal}	ρ_{Exp}	Dev%
Ca				
1114	2.056×10^{-3}	34.4498	34.82	1.063
1200	6.876×10^{-3}	33.9538	33.95	0.011
1300	2.307×10^{-2}	33.3816	33.42	0.115
1400	6.470×10^{-2}	32.8058	32.81	0.013
1500	0.1572	32.2278	32.88	1.984
1600	0.3401	31.6509	31.73	0.249
1700	0.6688	31.0765	31.08	0.011
1800	1.215	30.5036	30.49	0.045
1900	2.066	29.9288	29.93	0.004
2000	3.321	29.3479	29.35	0.007

Conclusions:

We have demonstrated that the present correlation along the modified TM EOS is capable of predicting density of the alkaline earth metals from the melting point up to several hundred degrees above their boiling points.

References:

[1] Tao, F. M., Mason, E. A., “Statistical-Mechanical Equation of State for Nonpolar Fluids: Prediction of Phase Boundaries”, *J. Chem. Phys., 100*, 9075–9084(1994).

[2] Ghatee, M. H., and A. Boushehri,; "Equation of state for Compressed Liquids from Surface Tension," *Int. J. Thermophys*. **17**, 945-957 (1996).

[3] Bystrov, P. I., Kagan, D. N., Krechetova, G. A and Shpilrain, E. E. Zhidrometallicheskie Teplonositeli Dlya Teplovgh Trubi Energeticheskih (Liquid Metal Heat-Carriers for Heat Pipe Facilities) (Nauka Press, Moscow, 1988).

Equation of State and Volumetric Properties of Compressed Liquid Based on Surface Tension

F. Yousefi[a], M. Kaveh[a]

[a]Department of Chemistry, Yasouj University, Yasouj, Iran

(Email: kavehm1364@gmail.com)

Keywords: Equation of state, Density, Surface Tension, Compressed liquids

Introduction:

The mechanical behavior of compressed liquids is needed for the design and analysis of many processes at high pressures. Many equations of state, dating back to the work of PG. Tait over 100 years ago, have been proposed for the correlation and prediction of the p-v-T properties of compressed liquids.The purpose of this work is to improve the Tao-Mason equation of state (TM EOS) to prediction of density of compressed liquid with even less input information.

Methods:

In 1994, Tao and Mason calculated a perturbation correction term for the effect of attractive forces and combined with ISM equations of state to present an improved equation of state (TM EOS).The general frame of the Tao-Mason EOS is [1]:

$$\frac{P}{\rho KT} = 1 + (B_2 - \alpha)\rho + \frac{\alpha\rho}{1 - \lambda b\rho} + A_1(\alpha - B_2)b\rho^2 \frac{(e^{\frac{kT_c}{T}} - A_2)}{1 + 1.8(b\rho)^4} \qquad (1)$$

Where

$$\alpha\rho_f = a_1[exp(-c_1 T^*)] + a_2\left\{1 - exp\left(-\frac{c_2}{T^{*\frac{1}{4}}}\right)\right\} \qquad (2)$$

$$b\rho_f = a_1(1 - c_1 T^*)[exp(-c_1 T^*)] + a_2\left[1 - \left(1 + \frac{0.25c_2}{T^{*\frac{1}{4}}}\right) exp\left(-\frac{a_2}{T^{*1/4}}\right)\right] \qquad (3)$$

$$B_2\rho_f = 0.0804 - 2.1288T^{*-1} + 8.5598T^{*-2} + 7.4294T^{*-3} - 3.3494T^{*-4} \qquad (4)$$

Results and discussion:

We have taken the surface tension and the freezing point data for prediction of volumetric properties of compressed liquid such as Xe, C_8H_{18}, C_6H_5-CH_3 and C_6H_6. Once these parameters are known, the temperature dependent parameters of the equation of state, B_2, α and b, can be calculated using Eqs.(2)–(4). Also using high density PVT data, the parameter λ was correlated by the following simple polynomial equation: $\lambda = a + bT + cP$. We performed the calculation of molar volume of compressed liquids using the TM EOS. The result has been gathered consecutively in figures 1-4. It is obvious from these figures, that the agreement between the calculated specific volumes and the literature values [2] is quite satisfactory. In general, the obtained mean of the deviations for compressed liquid was found to be of the order of 0.27%.

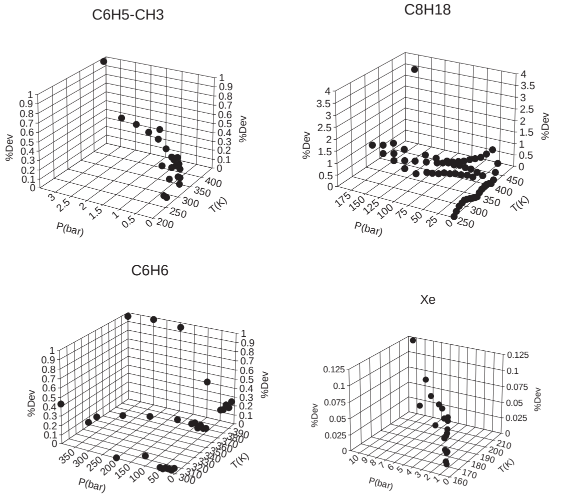
C6H5-CH3

C8H18

C6H6

Xe

Fig1. Deviation plot for the predicted densities of PPO+PS at different temperatures, pressures and mole fractions with experiment[2]

Conclusions:

We have demonstrated that the present correlation along the modified TM EOS is capable of predicting specific volumes of the polymer blends over a broad temperature and pressure ranges.

References:

[1] Tao, F.M.; Mason, E. A. Statistical-Mechanical Equation of State for Nanpolar Fluids Prediction of Phase Boundaries. *J. Chem. Phys.* 1994, *100*, 9075.

[2] Ghatee, M. H., and A. Boushehri,; "Equation of state for Compressed Liquids from Surface Tension," *Int. J. Thermophys*. **17**, 945-957 (1996).

Volumetric and Acoustic Studies of the Ionic Liquid 1-Butyl-3-Methylimidazolium Hydrogen Sulfate in Polyethylene Glycol Aqueous Solutions

Rahmat Sadeghi*, Tahere Moradian
Department of Chemistry, University of Kurdistan, Sanandaj, Iran
*E-mail: rsadeghi@uok.ac.ir

Keywords: Ionic liquid, Volumetric, Acoustic, poly ethylene glycol

Introduction

An aqueous solution of a water soluble polymer, such as poly ethylene glycol (PEG), when mixed with an aqueous solution of another water soluble polymer such as dextran or an organic or inorganic salt, separate into two phases. Liquid-liquid extraction utilizing these aqueous two-phase systems (ATPSs) has been used to separate and purify biological products from the complex mixtures in which they are produced [1,2]. Similar to the simple electrolytes, hydrophilic ILs based aqueous two-phase systems are formed when a hydrophilic IL and a certain salt or a certain water soluble polymer are combined with each other in aqueous solution. Although IL-salt aqueous two-phase systems have been studied extensively in recent years, however the information about the IL-polymer aqueous two-phase systems is very scarce in the literature [3]. In this work, we present our results on density and sound velocity measurements of ionic liquid 1-butyl-3-methylimidazolium hydrogen sulfate ([C_4mim][HSO_4]) in water and in aqueous solutions of poly(propylene glycol) 400 (PPG400), poly(ethylene glycol) 400 (PEG400) and 2000 (PEG2000) over a range of temperatures at atmospheric pressure that have not been previously published. The effects of polymer and temperature on the apparent molar volume and isentropic compressibility of [C_4mim][HSO_4] are studied.

Experimental Section

Materials. The polymers and IL were obtained from Merck and were used without further purification, and double distilled and deionized water was used.

Procedures. All the solutions were prepared by mass on a Sartorius CP225D balance precise to within ±0.00001 g. The density and sound velocity of the mixtures were measured at different temperatures with a digital vibrating tube analyzer (Anton Paar DSA 5000,Austria).

Results and Discussion

In the present work, in an attempt to obtain further evidence about the salting-out effect produced by the addition of ionic liquids to aqueous solutions of water soluble polymers this work is, thus, mainly focused on the study of the volumetric and acoustic properties of solutions of the model ionic liquid [C_4mim][HSO_4] in pure water and in aqueous solutions of PPG400, PEG400 and PEG2000 at different temperatures. For this purpose, density and speed of sound measurements for [C_4mim][HSO_4] in pure water and in aqueous solutions of 3.0 %w/w of PPG400, PEG400 and PEG2000 at T = (288.15, 293.15, 298.15, 303.15 and 308.15) K were carried out in order to study the variation in apparent molar volume, isentropic compressibility, and expansibility of the investigated solutions with IL concentration, temperature and polymer molar mass. The polymer-IL interactions were discussed on the bases of the obtained results and the results show that PPG400 has a salting-out effect on the aqueous solutions of [C_4mim][HSO_4], however PEG400 and PEG2000 have salting-in effects.

References

[1] H. Walter, D. E. books, D. Fisher, Partitioning in Aqueous Two-phase Systems, Academic Press, New York, **1985**.

[2] B.Y. Zaslavsky, Aqueous Two-Phase Partitioning, Physical chemistry and Bioanalytical Application, Marcel Dekker, New York, **1995**.

[3] R. Sadeghi, N. Ebrahimi, A. Mahdavi, *J. Chem. Thermodyn*. **2012**, 47, 48.

The effect of polymer molar mass for the aqueous two-phase systems Containing Polyethylen glycol and Di-sodium hydrogen citrate

Mohammed Taghi Zafarani-Moattar*, Parisa Jafari
*Physical Chemistry Department, Faculty of Chemistry, University of Tabriz, Tabriz, Iran, E-mail address: zafarani47@yahoo.com
Physical Chemistry Department, Faculty of Chemistry, University of Tabriz, Tabriz, Iran, E-mail address: Parisajafary14@yahoo.com

Keywords: Liquid–liquid equilibrium; di-sodium hydrogen citrate, Setschenow equation.

Introduction:

Aqueous two-phase systems (ATPS) formed by mixtures of two polymers, or one polymer and one inorganic salt, are important for separation and purification of biological materials such as enzymes and proteins[1, 2]. In the present work, we report LLE data for aqueous mixtures of PEG_{4000} or PEG600 $+Na_2C_6H_6O_7$ + H_2O at T= 298.15 K.

Methods:

A glass vessel with volume 50 cm^3, was used to carry out the phase equilibrium determinations. A salt solution of known concentration was titrated with the polymer solution or vice versa, until the solution turned turbid. For the determination of the tie lines, feed samples were prepared by mixing appropriate amounts of polymer, salt and water in the vessel. Then the mixture had been stirred was allowed to settle for 48h in designed temperature. After separation of two phases, the concentration of salt in the top and bottom phases was determined by flame photometry.

Results and Discussion:

For the studied system, the experimental binodal data were fitted by the least-squares regression method to the following empirical non-linear expression developed by Forotan[3],

$$wscal_i := a + b.(wp_i)^{0.5} + c.wp_i \tag{1}$$

Where w_p and w_s are the weight percent of the polymer PEG and salt $Na_2C_6H_6O_7$ respectively. Also *a*, *b* and *c* are the fitting parameters are collected in Table1.

Table1. Parameters and standard deviation for the

Table2. Values of parameters of Steschenow type,

T/K	K_s	k_p	Dev
298.15	3.2334	-0.7141	0.16

T/K	*a*	*b*	*c*	sd
298.15	31.7838	-5.9378	0.2361	0.03
308.15	37.9648	-7.1755	0.3016	0.05
318.15	35.8307	-6.8129	0.297	0.01

correlation of binodal data for suggestion systems.

(K_p, K_s) (kg.K.mol $^{-1}$), equation for {PEG4000 + $Na_2C_6H_6O_7$ + H2O}system at *T*= 298.15K

On the basis of obtained standard deviation, we conclude that the Eq.1 can be satisfactorily used to reproduce the binodal curves of the investigated system.

Figure1

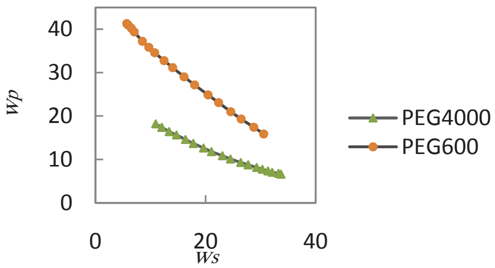

Figure2

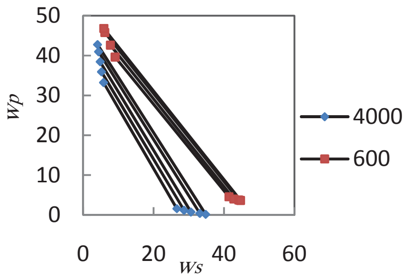

Fig1. Experimental and calculated binoda

Fig2. Plot of mass per cent polymer against mass percent salt

data from Eq. (1)for{PEG + $Na_2C_6H_6O_7$ salt to illustrate the effect of mass molecular on the slope and + H2O}system at *T*=298.15K.

length of tie-lines of the{PEG+$Na_2C_6H_6O_7$+H2O}system.

The Seteschenow type equation[4] with two parameters used for correlated the tie-line data in investigated system.On the basis of deviation reported in Table 2, it is interesting to note that the Seteschenow equation with only two parameters represents the experimental LLE data with good accuracy for the investigated system.

Conclusion:

For the system {PEG+ $Na_2C_6H_6O_7$ +H_2O}the binodal and tie-line data have been determined at *T*= 298.15K. It was found that tie lines data for these systems can be satisfactorily described by Setschenow equations.

Reference:

[1] S.C. Silvério, O. Rodriguez, J.A. Teixeria, E.A. Macedo, Fluid Phase Equilib. 296 (2010)173.
[2] B. Maestro, I. Velascob, I. Castillejo, M.A. Rodríguez, A. Cebolla, J.M. Sanz, J. Chromatogr. A 1208 (2008) 189.
[3] M. Forotan, N. Heidari, M. Mohammadlou, J. Chem. Eng. Data 53(2008) 242.
[4] M. J. Hey, D. P. Jackson, Hong Yan, Polymer. 46 (2005) 2567.

Phase Diagrams of Some Aliphatic Alcohols + Di-Sodium hydrogen Citrate + Water at *T* = 298.15 K.

Mohammed Taghi Zafarani-Moattar*, Parisa Jafari
*Physical Chemistry Department, Faculty of Chemistry, University of Tabriz, Tabriz, Iran, E-mail address: zafarani47@yahoo.com
Physical Chemistry Department, Faculty of Chemistry, University of Tabriz, Tabriz, Iran, E-mail address: Parisajafary14@yahoo.com

Keywords: Liquid–liquid equilibrium; di-sodium hydrogen citrate, Othmar-Tobias equation.

Introduction:

For large-scale processes, methods for recycling chemicals have been developed[1]. Greve and Kula have described the use of some two-phase systems composed of lower aliphatic alcohols + water + inorganic or organic salts for the extraction of salt from the primary bottom phase of protein extraction processes in polymer + salt systems.

Methods:

To carry out the solubility curve determination, a salt solution of known concentration was titrated with the alcohol solution or vice versa, until the solution turned turbid. For the determination of the tie lines, feed samples were prepared by mixing appropriate amounts of alcohol, salt and water in the vessel. Then the mixture had been stirred was allowed to settle for 48h in designed temperature. After separation of two phases, the concentration of alcohols in the top and bottom phases was determined by refractometer.

Results and discussion:

The obtained binodal data were fitted to the following empirical relationship developed by Merchuk[2]:

$$w_1 = a\exp(bw_2^{0.5} - cw_2^3) \qquad (1)$$

where w_1 and w_2 are the concentrations of alcohols and salt, respectively. The coefficients *a*, *b*, and *c* of Eq. (1) along with the corresponding standard deviation for the investigated system are given in Table 1.

Table 1. Values parameters of Eq. (1)

Alcohols	**a**	**b**	**$c.10^5$**	**sd**
1-propanol	224.10	-0.76	-5.33	0.03
2-propanol	73.72	-0.27	6.12	0.03

Table 2. values of parameters Eqs. (2)

Alcohols	***k***	***n***	***R^2***	***K_1***	***r***	***R^2***	**Dev**
1-propanol	0.27	1.70	0.99	2.01	0.58	0.98	0.52
2-propanol	0.56	0.74	0.99	2.08	1.50	0.98	1.10

On the basis of obtained standard deviation, we conclude that the Eq. (1) can be satisfactorily used to correlate the binodal data of the investigated system.

The correlation equations given by Othmer- Tobias (eq2a) and Bancraft (eq 2b)[3] have been used to correlate the tie-line compositions.

$$\left(\frac{1-w_1^t}{w_1^t}\right)=k\left(\frac{1-w_2^b}{w_2^b}\right)^n \quad \text{(2a),} \qquad \left(\frac{w_3^b}{w_2^b}\right)=k_1\left(\frac{w_3^t}{w_1^t}\right)^r \quad \text{(2b)}$$

Where k, n, k_1, and r represent fit parameters. Superscripts "t" and "b" stand for alcohol rich-phase and salt-rich phase, respectively. The values of parameters are given in Table 2. The solubility of an aliphatic alcohol in water and the mutual miscibility depends on the chain length and polarity values. Also higher polarity of 2-propanol as compared with 1-propanol is visible from the shift in the binodal as shown in Figure1.

Figure 1. Experimental and calculated tie-lines for the 2-propanol +salt +water + system at *T* = 298.15 K.

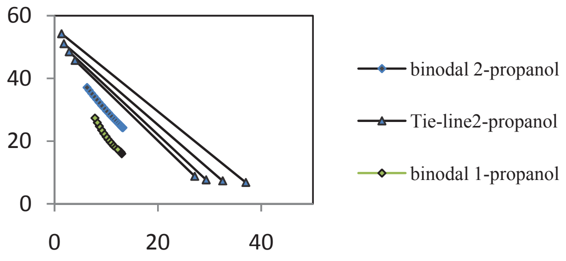

Conclusion:

For the system {Alcohol + $Na_2C_6H_6O_7$ + water} the binodal and tie-line data have been determined at T = 298.15K. It was found that tie-line data for these systems can be satisfactorily described by Othmar-Tobias equations.

Reference:

[1] A. Greve, M. R. Kula, J. Chem. Technol. Biotechnol. 50 (1991) 27.
[2] Merchuk, J. C. Andrews, B. A. Asenjo, J.A. *J. chromatogr. B.* (1998) 71.
[3] D. F. Othmer, P. E. Tobias, Ind. Eng. Chem. 34 (1942) 690.

Estimination of Ternary System (Water + Acetic acid + Cyclohexanol) under Ultrasonic Wave using GMDH-type Neural Network

Kh. Bahrpaima *[a], M. Bashiri [a]
[a] Department of Chemistry, Firoozabad Branch, Islamic Azad University, Firoozabad, Iran
E-mail: m.bashiri222@gmail.com

Key words: Ultrasonic wave; Phase equilibria; Ternary system; GMDH model.

Introduction:

In chemical industries, liquid extraction plays an important role as a separation process. The design and evaluation of industrial units for separation processes require reliable phase equilibrium data of the different mixtures involved in a given process. Especially, ternary liquid + liquid equilibrium (LLE) data are essential for a proper understanding of the solvent extraction [1, 2].

Ultrasonic refers to any study or application of sound waves that are higher frequency than the human audible range. Ultrasonic waves consist of frequencies greater than 20 KHz and exist in excess of 25 MHz. Effect of ultra sonic wave on LLE data of several ternary systems have been determined before and reported [3].

The new approach in this paper is using GMDH type-neural network in prediction of LLE data under ultrasonic wave (20 KHz) for the ternary system of (water + acetic acid + cyclohexanol). The predicted data by the proposed model was then compared with the experimental data.

Group Method of Data Handling (GMDH):

By the GMDH algorithm, a model is represented as a set of neurons in which different pairs of them in each layer are connected through a quadratic polynomial and, thus produce new neurons in the next layer. Such representation can be used in modeling to map inputs to outputs [4]. This model was used for prediction of experimental LLE data of (water + acetic acid + cyclohexanol) that has been determined before in our laboratory.

Result and discussion:

The experimental LLE data for (water + acetic acid + cyclohexanol) under ultrasonic at temperature of (298.2) K were predicted using GMDH model (Fig 1). The average RMSD value between the observed and calculated mass percent obtained.

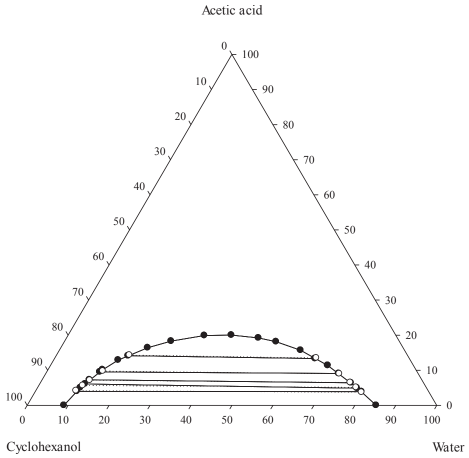

Fig 1. Phase diagram of (water + acetic acid + cyclohexanol).
(−) experimental data, (---) GMDH data

Conclusion:

LLE data of the ternary system (water + acetic acid + cyclohexanol) under ultrasonic wave were predicted using GMDH model at 298.15 K. The predicted data indicate good agreements with the experimental data.

References:

[1] G.R. Vakili-Nezhaad, M. Mohsen-Nia, V. Taghikhni, M. Behpoor, M. Aghahosseini, J. Chem. Thermodyn. 36 (2004) 314–348.

[2] D.S. Abrams, J.M. Prausnitz, AIChE J. 21 (1975) 116– 128.

[3] A. B. Hossieni, M.S. Thesis, Effect of ultrasonic wave on equilibria phase for the ternary system, (2011).

[4] M. Shaverdi, S. Fallahi, V. Bashiri; Applied Mathematical Sciences, 6 (2012) 319 – 332.

Measurement of Densities, Speed of sounds, and Water Activities for ternary system PEG4000+KNa(Tartrate)+H_2O at different temperatures

M.T. Zafarani-Moattar, F. Alizadeh-shilesar[a]

[a]Department of Chemistry, University of Tabriz, Tabriz ,Iran

(Email: fa.alizadeh.sh@gmail.com)

Keywords: density, water activity, speed of sound, isopiestic.

Introduction:

Thermodynamic properties of aqueous polymer-salt systems are necessary for a fundamental understanding of the phase-forming ability and also for the development of theoretical models for the prediction of the partitioning behavior of the two-phase system [1]. In this work, densities, speed of sound and water activities of equeous potassium sodium tartrate+ PEG4000 solutions have been measured and to calculate accurate limiting apparent volumes in concentration (0.03 mol. kg-1) of PEG. From the measurements of water activities by isopiestic methods, values of the vapor pressure of solutions were determined at T= 298.15 K. The experimental water activities have been correlated successfully with the Pitzer equation. The experimental density and speed of sound data were used to obtain apparent molar volume and apparent molar compressibility values at T= (298.15, 308.15, and 318.15) K, and these data were satisfactorily fitted to the Redlich-Mayer equations [2].

Methods:

The isopiestic apparatus used in this work was similar to the one used by Ochs et al [3].This apparatus consisted of a seven-leg manifold attached to round-bottom flasks. Two flasks contained the standard pure NaCl solutions; two flasks contained KNa(Tartrate) solutions; Two flasks contained the PEG solutions and the central flask was used as a water reservoir. After equilibrium, each flask was weighed by an analytical balance (Shimatzu, 321-34553, Shimatzu Co., Japan) with an uncertainty of $\pm 1\cdot 10^{-7}$kg. The water activity for the standard aqueous NaCl solutions at different concentrations and temperatures has been calculated from the correlation of Colin et al [4]. Densities and speed of sounds were measured with a vibrating-tube densimeter (Antoine Parr DSA-500, Austria). The apparatus was also tested with the density of a known molality of aqueous NaCl using the data given by Pitzer et al [5].

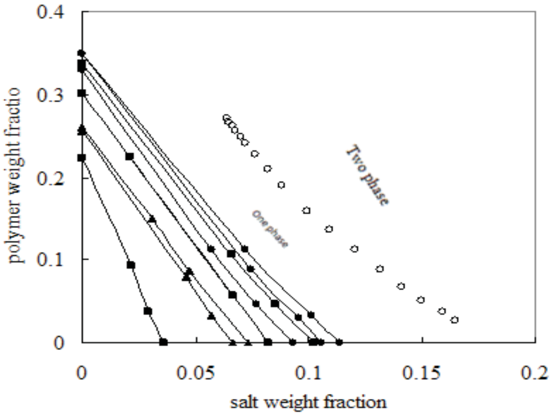

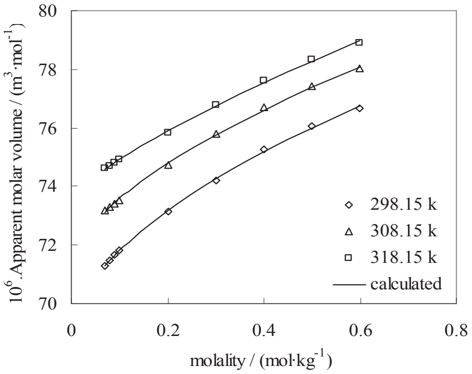

Results and Discussion:

Isopiestic Results. From the calculated osmotic coefficient data, ***Φ***, the activity of water in KNa(Tartrate)+PEG solution and the vapor pressure of this solution were calculated at isopiestic equilibrium molalities, with the help of the following relations:

$$(1)\quad \phi = \frac{\nu^* \phi^* m^*}{\nu m_1} \qquad\qquad (2)\quad \phi = -\frac{\ln a_s}{\nu m_1 M_2}$$

$$(3)\quad \ln a_s = \ln\left(\frac{p}{p^*}\right) + \frac{\left(B - V_s^*\right)\left(p - p^*\right)}{RT}$$

Molar volumes of liquid water were calculated using the density of water at different temperatures [6]. The vapor pressures of pure water were calculated using the equation of state of Saul and Wagner [7]. According to Figure 1, four points on each line has the same activity or chemical potential and these points are in balance with together, and line with the lowest activity located close to the bimodal curve.

Volumetric results. The molar volumes V_φ of solution were calculated from the densities of the solutions d using the following equation:

$$(4) \quad V_\phi = \frac{M_1}{d} - \frac{(d - d_0)}{m_1 d d_0}$$

Conclusions:

The accurate osmotic coefficient data measured at T = 298.15 K for aqueous KNa(Tartrate) + PEG solutions were fitted satisfactorily to the Pitzer model. The apparent molar volumes were calculated from the measured density and speed of sound data at T = (298.15, 308.15, and 318.15) K, and these data were also fitted to the corresponding Redlich-Mayer equations with good accuracy.

References:

[1] Berger, S. E. in Kirk-Othmer Encyclopedia of Chemical Technology, Vol. 13, 3rd ed.; Wiley-Interscience, New York, 1984, pp. 103-121.

[2] Redlich, O.; Mayer, D.M., 1964, The molal volumes of electrolytes, *Chem. Rev.*, 64: 221-227.

[3] Ochs, L. R. Kabiri-Badr, M. Cabezas,H. AIChE J. 36 (1990) 1908.

[4] Colin, E. Clarke, W. Glew, D. N. J. Phys. Chem. Ref. Data. 14 (1985) 489.

[5] Pitzer, K. S. Peiper, J. C. Busey, R. H. J. Phys. Chem. Ref. Data. 13 (1984) 1.

[6] Kell, G. S. J. Chem. Eng. Data. 20 (1975) 97.

[7] Saul, A. Wagner, W. J. Phys. Chem. Ref. Data. 16 (1987) 893.

Vapor–Liquid Equilibria, Density and Speed of Sound of Aqueous potassium sodium tartrate Solutions at different temperatures

M.T. Zafarani-Moattar, F. Alizadeh-shilesar[a]

[a]Department of Chemistry, University of Tabriz, Tabriz ,Iran

(Email: fa.alizadeh.sh@gmail.com)

Keywords: density, water activity, speed of sound, isopiestic.

Introduction:

In this work, densities, speed of sound and water activities of equeous potassium sodium tartrate solutions at different temperatures and atmospheric pressure have been measured and to calculate accurate limiting apparent volumes, enough data were determined in the dilute region (below 0.1 mol. kg-1). Sodium chloride were used as the isopietic standards for the calculation of activities. From the measurements of water activities by isopiestic methods, values of the vapor pressure of solutions were determined. The experimental water activities have been correlated successfully with the Pitzer equation. The experimental density and speed of sound data for potassium sodium tartrate were used to obtain apparent molar volume values at T= (298.15, 308.15, and 318.15) K, and these data were satisfactorily fitted to the Pitzer equation.

Methods:

The isopiestic apparatus used in this work was similar to the one used by Ochs et al [1].This apparatus consisted of a five-leg manifold attached to round-bottom flasks. Two flasks contained the standard pure NaCl solutions; two flasks contained potassium sodium tartrate solutions; and the central flask was used as a water reservoir. After equilibrium, each flask was weighed by an analytical balance (Shimatzu, 321-34553, Shimatzu Co., Japan) with an uncertainty of $\pm 1\cdot 10^{-7}$kg. The water activity for the standard aqueous NaCl solutions at different concentrations and temperatures has been calculated from the correlation of Colin et al [2]. Densities and speed of sounds were measured with a vibrating-tube densimeter (Antoine Parr DSA-500, Austria). The apparatus was also tested with the density of a known molality of aqueous NaCl using the data given by Pitzer et al [3].

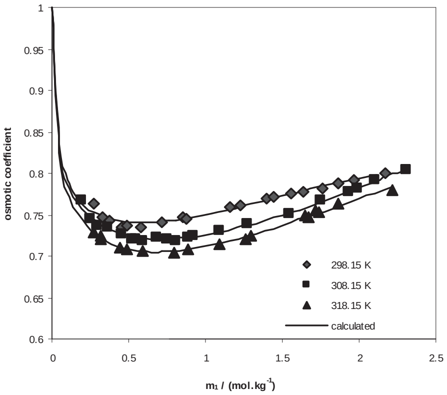

Figure 1. Experimental and calculated osmotic coefficient, plotted against molality of salt, *m*1, for the potassium sodium tartrate (1) + H2O (2) system studied with the Pitzer model.

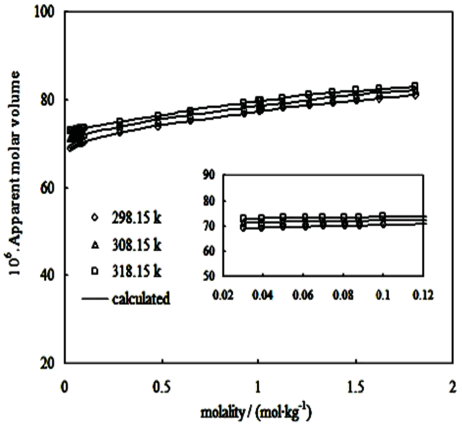

Figure 2. Experimental and calculated apparent molal volume, plotted against root of molality of salt, for the potassium sodium tartrate+H_2O (2) System studied with the Pitzer model.

Results and Discussion:

Isopiestic Results. From the calculated osmotic coefficient data, ***Φ***, the activity of water in potassium sodium tartrate solution and the vapor pressure of this solution were measured at isopiestic equilibrium molalities, with the help of the following relations:

$$(1)\quad \phi = \frac{\nu^* \phi^* m^*}{\nu m_1} \qquad\qquad (2)\quad \phi = -\frac{\ln a_s}{\nu m_1 M_2}$$

$$(3)\quad \ln a_s = \ln\left(\frac{p}{p^*}\right) + \frac{\left(B - V_s^*\right)\left(p - p^*\right)}{RT}$$

The second virial coefficients of water vapor at each working temperature were calculated using the equation provided by Rard and Platford [4]. Molar volumes of liquid water were calculated using the density of water at different temperatures [5]. The vapor pressures of pure water were calculated using the equation of state of Saul and Wagner [6].

Volumetric results. The molar volumes V_φ of solution were calculated from the densities of the solutions *d* using the following equation:

$$(4)\quad V_{\phi} = \frac{M_1}{d} - \frac{(d - d_0)}{m_1 d d_0}$$

Conclusions:

The accurate osmotic coefficient data calculated at T = (298.15, 308.15, and 318.15) K for aqueous potassium sodium tartrate solutions were fitted satisfactorily to the Pitzer model. The apparent molar volumes were calculated from the measured density and speed of sound data at T = (298.15, 308.15, and 318.15) K, and these data were also fitted to the corresponding Pitzer equation with good accuracy.

References:

[1] Ochs, L. R. Kabiri-Badr, M. Cabezas,H. AIChE J. 36 (1990) 1908.

[2] Colin, E. Clarke, W. Glew, D. N. J. Phys. Chem. Ref. Data. 14 (1985) 489.

[3] Pitzer, K. S. Peiper, J. C. Busey, R. H. J. Phys. Chem. Ref. Data. 13 (1984) 1.

[4] Rard, J. A. Platford, R. F. Pitzer, K. S. ActaVity coefficients in electrolyte solutions. (1991) 209.

[5] Kell, G. S. J. Chem. Eng. Data. 20 (1975) 97.

[6] Saul, A. Wagner, W. J. Phys. Chem. Ref. Data. 16 (1987) 893.

Prediction of Quarternary System (Water + Acetic acid + Cyclohexane + Cyclohexanone) using GMDH-type Neural Network

Kh. Bahrpaima *[a], Z. Motamedi [a]
[a] Department of Chemistry, Firoozabad Branch, Islamic Azad University, Firoozabad, Iran
E-mail: motamedi.p_zahra@yahoo.com

Key words: Liquid extraction; Phase equilibria; Quaternary system; GMDH model

Introduction:

Phase equilibrium data of quarternary systems are very important for simulation, design and optimize of separation operations. A large amount of investigation has been carried out in recent years on the liquid-liquid equilibrium (LLE) measurements of quarternary systems in order to provide further information about the phase behavior of such systems [1, 3].

Acetic acid is one of the simplest carboxylic acids. It is an important chemical reagent and industrial chemical, mainly used in the production of cellulose acetate mainly for photographic film and polyvinyl acetate for wood glue, as well as synthetic fibres and fabrics.

So the aim of this paper is the application of GMDH type-neural network for prediction of LLE data for the quaternary system (water + acetic acid + cyclohexane + cyclohexanone) at different ratio at 298.2 K.

Group Method of Data Handling (GMDH)

The group method of data handling (GMDH) is aimed at identifying the functional structure of a model hidden within the empirical data. The main idea of the GMDH is the use of feed-forward networks based on short-term polynomial transfer functions whose coefficients are obtained using regression combined with emulation of the self-organizing activity behind NN structural learning [4].

Result and discussion:

The experimental LLE data for (water + acetic acid + 25% cyclohexane + 75% cyclohexanone) (water + acetic acid + 50% cyclohexane + 50% cyclohexanone) and (water + acetic acid + 75% cyclohexane + 25% cyclohexanone) at temperature of (298.2) K were predicted using GMDH model. The average RMSD value between the observed and calculated mass percent obtained.

Conclusion:

Predicted LLE data of the quarternary systems {water + acetic acid + cyclohexane + cyclohexanone} using GMDH model at different ratio were presented at 298.15 K. It can be concluded that mixture of (50% cyclohexane + 50% cyclohexanone) with high separation factor may be adequate solvent to extract acetic acid from its dilute aqueous solutions.

References:

[1] H. Higashiuchi, Y. Sakuragi, Y. Arai; Fluid Phase Equilibr 110(1995) 197–204.

[2] H. Katayama, T. Hayakawa, T. Kobayashi; Fluid Phase Equilibr 44 (1998) 157–167.

[3] A. Arce, J. Martinez-Ageitos, O. Rodriguez, A. Soto; J. Chem. Thermodyn 33 (2001) 139–146.

[4] M. Shaverdi, S. Fallahi, V. Bashiri; Applied Mathemathical Sciences 6 (2012) 319_332.

Application of PHSC Equation of State to PEG and PPG Polymers

D. Mohammad-Aghaie*, F. Sabzi, H. Moslehi
Department of Chemistry, Shiraz University of Technology, Shiraz, 71555-313, Iran
Email: d_aghaie@sutech.ac.ir

Key words: Polymer, Polyethylene glycol (PEG), Polypropylene glycol (PPG), Perturbed Hard Sphere Chain (PHSC) Equation of State, Density

Introduction:

Macromolecular science has had a major impact on the way we live. It is difficult to find an aspect of our lives that is not affected by polymers. Polyethylene glycol (PEG) and Polypropylene glycol (PPG) have found wide range of applications in medicine, industry and agriculture. PVT (Pressure-Volume-Temperature) properties of polymers are important for both engineering and polymer physics. In addition to experimental measurements, equations of state provide powerful tools for prediction of thermodynamic properties and phase equilibrium calculations, over wide ranges of temperature and pressure.

The perturbed hard sphere chain (PHSC) equation of state, proposed by Song *et al*. [1] has employed to reproduce the thermophysical properties of a wide variety of normal fluids, including polymers. In the PHSC theory, molecules are assumed to be attracting chains of spheres (segments) that are connected by covalent bonds. Three terms appear in the total pressure equation: $P_{\text{hard-sphere}}$, $P_{\text{Chain connectivity}}$ and $P_{\text{vdW attraction}}$, respectively due to hard-sphere repulsion, covalent bonds between hard spheres and attractive van der Waals forces between non-bonded hard spheres. The PHSC equation of state for pure fluids has the following form:

$$\frac{P}{\rho k_B T} = 1 + r^2 b\rho g - (r-1)(g-1) - \frac{r^2 a\rho}{k_B T}$$

The segment based parameters, a, b and r, have clear physical interpretations. Both a and b are temperature dependent and the potential parameters, ϵ and σ appear in their equations [2].

Method:

The present work is devoted to the application of PHSC equation of state to calculate volumetric properties of PEG and PPG. In order to determine required potential parameters, ϵ and σ for the studied polymers, we fitted our calculated densities based on PHSC equation of state to the reported experimental densities in Ref. [3]. Using initial estimates for these parameters, they were varied until the best fit was obtained to the selected set of literature densities. Once these parameters were evaluated, the PHSC equation of state successfully predicted densities of PEG and PPG in different molecular weights.

Results and discussion:

PHSC equation of state was employed to calculate volumetric properties of four fractionation cuts of polyethylene glycol (PEG-200, PEG-300, PEG-400, PEG-600) and five fractionation cuts of polypropylene glycol (PPG-425, PPG-725, PPG-1000, PPG-2000 and PPG-4000) over wide ranges of temperature and pressure. In order to assess the validity of predicted densities, we compared them with the available literature data. Figures 1 and 2 respectively show the deviation plots of calculated densities for PPG425 and PEG200 from experimental values [3]. The acceptable agreement between these two sets of data, confirms the ability of PHSC equation of state in density prediction of pure polymers. Similar results were observed for other mentioned fractionation cuts of both studied polymers.

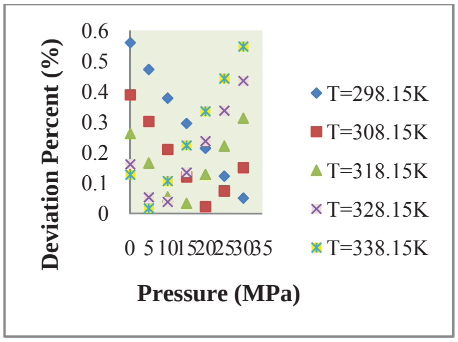

Figure 1. Deviation plot for calculated densities of PPG425 from experimental data [3]

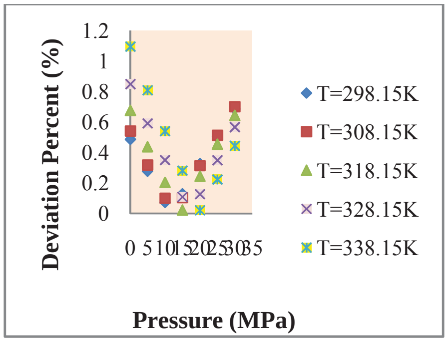

Figure 2. Deviation plot for calculated densities of PEG200 from experimental data [3]

References:

[1] Song,Y., Lambert, S. M., Prausnitz, J. M., *Ind. Eng. Chem. Res*. **33**, 1047-1057, 1994.

[2] Song, Y. Prausnitz, J. M., *Ind. Eng. Chem. Res*. **35**, 1225-1230, 1996.

[3] Chang, J. S., Lee, M. J., Lin, H. M., *J. Chem. Eng. Jpn*. **32** (5), 611-618, 1999.

Binding of alkali metal cations by calix[4]arene-crown-6 in methanol a thermodynamic study

Monireh Hajmalek*, Karim Zare, Mohammad Sajjad Khalili
Department of Chemistry, Islamic Azad University, Science and Reaserch Branch, Tehran, Iran
(E-mail : monirehajmalek@gmail.com)

Keywords: Calix[4]arene-Crown-6, Alkali cations, Stability constant, Complexation

Introduction:

Calixarenes represent a particularly significant class of the host molecules in supramolecular chemistry, which are generally made up of phenol units linked via methylene bridges[1]. Calixarenes are known to be good candidates in metallic cation recognition. Selectivity can be tuned by functionally modifying the preorganized platform defined by the phenolic moieties with a wide range of substituents. Of the many selective functionalisations possible, the introduction of polyether chains, first described by Ungaro and coworkers[2] in 1983, which are called calixcrowns. Calixcrowns has provided a new family of lipophilic basket bowl known for their considerable interest as selective ion transport agents, notably in the treatment of nuclear waste[3]. This ligands are capable to form complexes with cations of alkali and alkali-earth cations of metals. In this work we investigated the potential of calix[4]arenes-crown-6 ether derivatives in the ability of complexation with some alkali metal cations in methanol at 25^{o}C using UV-Vis spectrophotometric technique.

Experimental Section :

25,27-dihydroxycalix[4]arene-26,28-crown-6 was obtained from Acros Organics and used without further purification. Spectrophotometric measurements were performed using a UV–Vis Cary spectrophotometer with a Pentium 4 computer using 10 mm quartz cells. The system was thermostated at 25 °C by circulating water from an isothermal bath. For each experiment, a 2mL solution of the ligand, 2.0×10^{-4} mol dm^{-3}, was titrated with stepwise addition of metal cation solution 4.0×10^{-4} mol dm^{-3}. In the titration procedure after addition of a few drops of titrant, the absorbance was measured in the range 250–300 nm (in the interval of 1 nm) and the procedure extended up when the ratio of the metal ion to the ligand concentrations reaches to 2.

Results and Discussion:

Assuming that the absorbance of the ligand would change upon complexation with a metal cation, we performed spectrophotometric measurements. The complex MpLq formed is characterized by its stoichiometry, p and q, where M and L represent a metal ion and the ligand, respectively. To determine the formation constant of complexation, K_S, Eq. 1 is defined,

$$pM + qL \rightleftharpoons MpLq \qquad K_S = \frac{[M_pL_q]}{[M]^p\,[L]^q} \qquad (1)$$

Determination of the satability constant was calculated using a computer program (Microsoft Excel Solver) which employs a nonlinear least-squares method. This method has been described before[4]. Absorbance, A, was measured by successive addition of a metal ion solution to the ligand solution. The absorption bands of the ligand decrease upon addition of each metal ion solution in all cases.

Conclusions:

The results showed that the ligand is capable to complex with all the alkali cations by 1:1 metal to ligand ratios. Considering the formation constant values, the binding selectivity of the ligand towards alkali cations of the formed complexes are in the order $Cs^+ > K^+ > Na^+$.Ligand appears to be more efficient for chelating with Cs^+, as they have a crown net which perfectly matches the Cs^+ cation's size according to the rules of host –guest inclusion. The selectivity of the ligand towards Cs^+ can be explained by the preorganisation of the ligand and by the interaction of the softer cesium ion with the π-electron of two aromatic rings.

References:

[1] C.D. Gutsche, Monographs in Supramolecular Chemistry, Calixarenes, The Royal Society of Chemistry, London, 2nd Edition,2008.

[2] C. Alfieri, E. Dradi, A. Pochini, R. Ungaro and G. D. Andreetti, J. Chem. Soc. Chem. Commun. 1983, 1075.

[3] M.-J. Schwing-Weill and F. Arnaud-Neu, Gazz. Chim. Ital., 1997,127, 687 and references therein.

[4] F.Gharib, M. Hajmalek, R.A.Alamoti, A.Farajtabar, J. Mol. Liq. 2011,161-164,159.

Conductometric study of the new reactive dye with cetylpridinium chloride surfactant

H. Dezhampanah [a]*, A. Ghanadzadeh. S. E. Hadavi[b]

[a] Department of Chemistry, Faculty of Science, University of Guilan P.O. Box 1914, Rasht 0098,

[b] Department of Chemistry, Faculty of Science, University of Guilan

Iran. (***e-mail**: s_erfan_hadavi@yahoo.com)

Introduction:

Although, the interaction between dyes and surfactants has been studied in many papers, the studies in this area are still important and interesting for improving the dyeing process from theoretical, technological, ecological and economical points of view. The investigations into the behavior of different dyes in surfactant aqueous solutions can give useful information for understanding the thermodynamics and kinetics of the dyeing process and the finishing of textile material [1].

Reactive dyes are extensively used in dyeing processes in textile industry [2]. Dye molecules with phenyl groups can adopt a planar structure and readily tend to form intermolecular interaction that facilitates permanent aggregation under some experimental conditions.

In the present paper, we studied conductivity of mixtures of dye and surfactant over the range of concentrations at which these compounds are miscible. Mono-s-chloro triazinyl (MCT) was used as anionic reactive dye and Cetylpridinium chloride (CPC) was used as cationic surfactant. The method is used for calculation of equilibrium constant from which theoretical model was derived. The influence of temperature on ion pair formation is observed with this method.

Methods:

The conductance measurements of solutions were performed with Metrohm 712 digital conductometer using a dip type cell of cell constant 0.99 cm^{-1}. The specific conductivity of deionized water was measured before the each series of measurement at each temperature. Then the specific conductivity of an exact volume and known concentration of MCT solution (10^{-4}M) was measured. Binary mixtures of dye/surfactant were prepared by keeping the dye concentration constant but by increasing the surfactant concentration. Then the specific conductivity of each solution was measured. Measurements were made at 25.0, 30.0, 35.0, 40.0, and 45.0 ºC. The temperature of solutions was kept within the range of ± 0.1 ºC.

Results and discussion:

The results of experimental data show that, the measured conductances of the MCT – surfactant mixtures are lower than the sum of the specific conductivities of the individual MCT and of the individual surfactant molecule. The decrease in the measured values can be explained by the formation of a non-conducting or a less-conducting specie in the solution.

The equilibrium constants were calculated by using a theoretical model based on the deviation from linear behaviour. This model is based on the comparison between the measured conductivity of the dye–surfactant mixture and a theoretical straight line that represents the sum of the specific conductivities of the dye and the surfactant [2]. The calculated values of ΔG^o are given in Table 1 for the binding processes at various temperatures. As seen from Table 1, all ΔG^o values are negative for all temperatures. The negative ΔG^o values indicate that the binding process of MCT to the CPC occur spontaneously. Moreover, the ΔG^o values decrease with increasing of temperature for this process. This means that binding process is lowly spontaneous at higher temperatures. The negative ΔH^o value indicates that binding process is exothermic. Binding of MCT to the premicellar of CPC is accompanied by the positive ΔS^o value (Table 1). This means that the binding of MCT to the surfactant causes a decrease in the order of the process. In addition, it can be said from ΔS^o values that hydrophobic interactions play a major role in the interaction between the MCT and the CPC submicellar region.

Table 1: The values of; K ; ΔG^o ; ΔH^o and ΔS^o for MCT-CPC complex formation.

system	T (^{o}C)	K (M^{-2})	ΔG^{o} ($kJmol^{-1}$)	ΔH^{o} ($kJmol^{-1}$)	ΔS^{o} ($Jmol^{-1}K^{-1}$)
R2-CPC	25.0	3.78×10^{8}	-48.93	-6.75	141.54
	30.0	3.69×10^{8}	-49.70		141.73
	35.0	3.52×10^{8}	-50.39		141.67
	40.0	3.37×10^{8}	-51.10		141.66
	45.0	3.19×10^{8}	-51.77		141.57

References:

[1] M.Rashidi-Alavijeh, S. Javadiana, H. Gharibia, M. Moradia, A. R. Tehrani-Bagha, A. Asadzadeh Shahir, Colloids and Surfaces A: Physicochem. Eng. Aspects 380 (2011) 119–127.

[2]- H. Akbasx, C. Kartal, Dyes and Pigments. 72 (2007) 383-386.

Investigating the behavior of the Imidazolium based ionic liquids using the Yukawa potential model

M Shayan Nezhad*, M Bahadori,
Islamic Azad University Marvdasht Branch, Marvdasht, IranFax: +98 728 3311156
E-mail:shayan.m2010@gmail.com

Keywords: Ionic liquids, Yukawa potential model, Equation of state

A wide range of applications of ionic liquids, including green solvent for synthesis and separation and electrolyte, are expected due to their low melting point, low-flammability, negligible vapour pressure, high conductivity and electrochemical stability [1,2]. Structures and properties of ionic liquids are controlled by interactions between ions. The size, shape, and composition of the ions affect the thermodynamic properties of ionic liquids by influencing the crystal packing ability and lattice energy of the ionic liquid [3]. In general, the internal interactions of ionic liquids will decrease with an increase in the size and complexity of the anionic and cationic components. This is due to a greater charge delocalization and charge isolation.

The properties of polar liquids have been investigated using different theoretical and computing simulation techniques [4-6] Recently a procedure has been presented for studying the polar fluid properties using the Yukawa potential for representing the dispersion forces, and the dipolar-dipolar interactions[7]. In modeling the interaction of the molecules in a polar fluid, it is assumed that the constituent molecules are rigid spheres of equal size with a fix permanent point dipole moment that interacts via the Yukawa pair potential. Consequently, the total pair potential between two polar molecules interprets as follows

$$u(r_{12}) = u_0^Y(r_{12}) + u_{dd}(r_{12}) \qquad (1)$$

Where $u_Y(r_{12})$ is the Yukawa pair potential interaction and $u_{dd}(r_{12})$ is the dipolar-dipolar interaction between two permanent dipole moments of strength μ.

$$u_0^Y(r_1, r_2) = \begin{cases} \infty, & r_{12} < \sigma \\ -\dfrac{\varepsilon\sigma}{r_{12}} \exp\left[-z(r_{12} - \sigma)\right], & r_{12} \geq \sigma \end{cases}$$

(2)

$$u_{dd}(r_{12}) = \left[\frac{\mu_1 \cdot \mu_2}{r_{12}^3} - \frac{3}{r_{12}^5} (\mu_1 . r_{12})(\mu_2 . r_{12}) \right] \tag{3}$$

In this work the Yukawa potential model was used to derive an equation of state and investigate the interactions of the imidazolium based ionic liquids. To obtain the potential parameters, the potential function has been applied to derive the thermodynamic equation of pressure. Then, fitting the experimental *pVT* data [8] in the obtained isotherm yields the potential parameters. The obtaind parameters have a good agreement with the structural data.

References:

[1] Wasserscheid P., Van Hal R., Boesmann A. *Green Chem.* **2002**, 4, 400

[2] Mihkel K. Ionic Liquids in Chemical Analysis Edition: illustrated. CRC Press: **2008**.

[3] Wasserscheid P., Welton T *Ionic Liquids in Synthesis,* 2e. Wiley-VCH Verlag GmbH

[4]Gray C. G., Gubbins, K. E. *Theory of Molecular Fluids.* Oxford University Press: Oxford, **1984**; Vol. 1.

[5]Hansen I. R., McDonald I. R. *Theory of Simple Liquids*; Academic Press: London, **1986**.

[6]Allen M. P., Tildesley D. J. *Computer Simulation of Liquids*; Oxford University Press: Oxford, **1987**.

[7]Henderson D., Boda, D., Szalai I., Chan K. *J. Chem. Phys.* **1999**, *110*, 7348.

[8] http:www.ilthermo.com

Effect of pH on the phase separation in aqueous solutions containing poly (propylene glycol) and the kosmotropic salt sodium citrate at *T* = 298.15 K

S. Hamzehzadeh*[a] and M. T. Zafarani-Moattar[b]
[a] Chemistry and Chemical Engineering Research Center of Iran, Tehran, P.O. Box: 14335-186, Iran
[b]Physical Chemistry Department, Faculty of Chemistry, University of Tabriz, Tabriz, Iran
Email: hamzehzadeh@ccerci.ac.ir

Keywords: Phase diagram, Poly (propylene glycol), Kosmotropic salt, Salting-out effect.

Introduction:

Liquid-liquid extraction utilizing aqueous two-phase systems (ATPS's) has found its platform in several aspects of separation research both in industry and academia. When ATPS's are used for preparative purposes, e.g. for separation, isolation or purification of a product, the knowledge of the mechanism of the phase separation in the used system is important to increase the efficiency of the process or is of purely academic interest [1]. In this respect, this work is devoted to study the effect of the aqueous medium pH on the two-phase equilibrium behavior of the {poly (propylene glycol) (PPG P400) + sodium citrate} ATPS in order to obtain further information about the salting-out effects and the consequent phase separation in PPG-salt ATPS's. The effect of pH on the ATPS-promoting capability of citrate anions in the aqueous PPG solutions was explained based on the structural hydration Gibbs free energy (ΔG_{hyd}) of the citrate anions at different pH values. Furthermore, a local composition NRTL [2] model was examined to correlate the tie-line data of the investigated system at different pH values.

Materials and methods:

Polypropylene glycol P400 (PPG P400), was obtained from Fluka. Tri-sodium citrate (> 99 %) and citric acid (> 99.5 %) were supplied respectively by Fluka and Merck.

A phase diagram is constituted of a binodal curve and tie-lines. The determination of the binodal curves was carried out by a turbidimetric titration method [1]. For the determination of the tie-lines, feed samples of different known total compositions were prepared in the vessels. After separation of the two phases, the sodium (salt) content in the top and bottom phases was determined using a flame photometer. The concentration of polymer in each phase was also determined by refractive index measurements performed at 298.15 K.

Apparatus:

The pH of the concentrated salt stock solutions was controlled with a precision pH meter (Model: 692 pH / Ion Meter- Metrohm, Switzerland). A flame photometer (Model: PFP 7, Jenway, England) was used for the determination of the salt content in the top and bottom phases. The concentration of PPG in each phase was determined using a refractometer (Model: DR-A1, ATAGO Co., LTD., Japan).

Result and discussion:

The phase diagrams for the {PPG 400+ sodium citrate} ATPS were determined experimentally at $T = 298.15$ K and different medium pH values (3.00, 4.00, 5.00, 6.00, and 7.00). It was found that, the ATPS-promoting capability in the investigated system increases with increasing the aqueous medium pH. Using the structural thermodynamics of hydration, it was shown that the citrate ions with higher valence or more negative ΔG_{hyd} that exist in the lesser acidic medium pH are more efficient to promote the salting-out effect and the consequent phase separation, compared to those with minor valence or lesser negative ΔG_{hyd} found in the more acidic medium pH. Finally, the modified version of the segment-based local composition NRTL model [2] have been satisfactorily used to correlate the liquid–liquid equilibrium (LLE) data of the investigated system.

Conclusion:

In this work the influence of the aqueous medium pH on the salting-out effect caused by the addition of a kosmotropic (water-structuring) salt to an aqueous solution of PPG was assessed with reference to the phase behavior of {PPG 400 + sodium citrate} ATPS at different medium pH. The results were successfully interpreted using the corresponding composition phase diagrams and the kosmotropic nature of the citrate anions at different medium pH.

Reference:

[1] R. Hatti-Kaul; "Aqueous Two-Phase Systems: Methods and Protocols"; Methods in Biotechnology; vol. 11, Totowa, New Jersey: Humana Press, Inc.; 2005.

[2] R. Sadeghi; "A modified segment-based nonrandom two-liquid model for the calculation of vapor–liquid equilibrium of aqueous polymer–salt solutions"; Chem. Eng. Sci.; 61, 7786 – 7794, 2006.

Dielectric Behavior and Thermodynamic Investigation of Some Ternary Systems at Different Temperatures

A.Ghanadzadeh, M. Mosayebzadeh
Department of chemistry, faculty of science, Guilan University, Rasht, Iran
m_mosayebzadeh@ yahoo.com

Key words: Dielectric**,** Permittivity**,** ternary systems, Dipole moment

Introduction:

The static dielectric constant gives considerable information about the structural properties of polar compounds. The valuable information about the nature and strength of interactions in liquid solutions, over a range of mole fractions, can be obtained using dielectric studies. The molecular dipole moment of the material depends on its molecular interactions with its neighbours. By using dielectric permittivity, density and refractive index measurements, it is possible to obtain the dipole moment with the aim of giving valuable information about the geometrical structure of molecules, molecular association and dipole – dipole interactions [1].

In this study, we have investigated the tert-butyl alcohol in mixture of two non polar solvents at different temperatures.

Experimental:

All compounds for dielectric investigations were supplied by Merck and distillated before use. The electrical capacitance of the dielectric cell was measured using a Wayne Kerr model 6425B Digibridge. Measurements of the capacitance required for calculating the static dielectric permittivity were performed at a frequency of 10 kHz. A three-terminal dielectric cell was constructed for measurements on small volumes of solutions. The outer, inner and guard electrodes of the cell were made from stainless steel. The gap between the inner and the outer electrodes was about 1mm. The refractive indices of the solutions were determined at a wavelength of 589 nm using an Abbe Refractometer (Model CETI).

Theoretical consideration:

The Kirkwood model:

The dipole moments of the compounds were measured using the Guggenheim equation [2]:

$$\mu^2 = \frac{27kT\varepsilon_0}{N_A(\varepsilon_1+2)(n_1^2+2)}(\frac{\Delta}{C})_{C\to 0}$$

Where ε_0 is the permittivity in vacuum, ε_1 is the static permittivity and n_1 is the refractive index of the pure solvent. The dielectric incresments given by:

$$\Delta = (\varepsilon_{12} - n_{12}^2) - (\varepsilon_1 - n_1^2)$$

Where the subscript $_{12}$ indicates the solution, and $(\Delta/C)_{C\to 0}$ is the limiting gradient of the plot of Δ versus concentration. The Kirkwood correlation parameter, g, is a measure of the molecular association in polar liquids that for ternary systems, g is given by[3]:

Result and discussion:

It should be noted that the effect of temperature on measured dipole moment is very important. The dielectric permittivity of solution of these materials was observed to decrease as the Temperature increased as a consequence of: $\varepsilon \approx (\mu^2/kT)$

This effect is due to the existence of short rang dipole interaction, in this compounds.

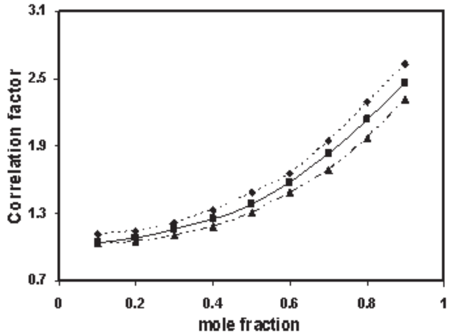

correlation factor versus mole fraction for ternary system of Tert-butyl alcohol in mixture of toluene+m-cyclohexane at 3 different temperatures

Conclusion

Results correspond to Kirkwood factor g>1, and indicate a high degree of parallel dipole association.

References

[1]. A.Ghanadzadeh.M.S.Beevers, J.Mol.Liq. 102 (2003) 365.

[2]. E.A.Guggenheim,Trans.Fraraday Soc.58 (1949) 714

[3]. S.Acharya, S.Mishra,B.Bhuyan, K.Garabadu, G.C.Mohanty. J.Mol.Liq 109 (2004)

Investigation of some physical properties of 1,2-Ethanediol+1,3-Propanediol binary mixtures

Mehrdad Moosavi, Setare Habibi*, Abbas A. Rostami
Faculty of Chemistry, University of Mazandaran, Babolsar, Iran
*Corresponding author e-mail address: Setarehhabibi@hotmail.com

Keyword: Glycol, Viscosity deviation, Excess molar volume, Binary mixtures

Introduction:

Study on the physical property plays a crucial role in understanding of intermolecular interaction and also with use of this physical data scientist can made divers molecular models or theories of solution to extend our knowledge about the molecular interaction between components. In this paper we investigated some thermodynamic and transport properties of 1,2-Ethanediol (Ethylene glycol) with 1,3-Propanediol because They are important industrial component. These glycols play significant role in industry such as antifreeze, plasticizer, humectant, solvent and extractor in automotive, tobacco, cosmetic, and petroleum industry [1]. Therefore, it is of great importance to determine some physical properties of glycols binary mixtures, because many industrial process requires accurate values of thermodynamic and transport properties of liquids [2,3] . In this work, density, viscosity, excess molar volume and viscosity deviation of 1,2-ethanediol + 1,3-propanediol was determined at temperatures of 298.15, 303.15, and 308.15 K.

Experimental

Materials. Ethanolamine and 1,3-Propanediol were supplied by Fluka. The purity of all materials was higher than 99 %.

Apparatus and procedure. The mass measurements were made on a single pan Mettler balance with an accuracy of ± 0.01 mg. Density (ρ) measurements of pure components and binary mixtures over the complete composition range were carried out using Anton Paar oscillating U tube densitometer (DA 500) with ± 10-4 g·cm-3 accuracy. The kinematic viscosity was measured with Ubbelohde viscometer with a Schott-Geräte automatic measuring unit model AVS 400 .

Results and discussion

Excess molar volume (V^E) and viscosity deviation (Δη) was calculated from density and viscosity measurement according to the following equation:

$$V^E = \sum_{i=1}^{n} x_i M_i \left(\frac{1}{\rho} - \frac{1}{\rho_i}\right) \qquad (1)$$

$$\Delta\eta = \eta - \sum_{i=1}^{n} x_i \eta_i \qquad (2)$$

Where, x, M, ρ and η are the mole fraction, molar mass, density, and dynamic viscosity, respectively. The subscript i shows the pure components. Figures 1 and 2 show that V^E and Δη are negative for all mixtures over the entire composition rang. The negative value of the excess molar volume indicates that the interactions between unlike diol are stronger than interactions of like components. For these systems interaction between hydroxyl functional group of components results in the formation of hydrogen bonding between like molecules and structural characteristics of component, might be responsible for negative V^E.

Figure1. plot of excess volume against EG mole fraction

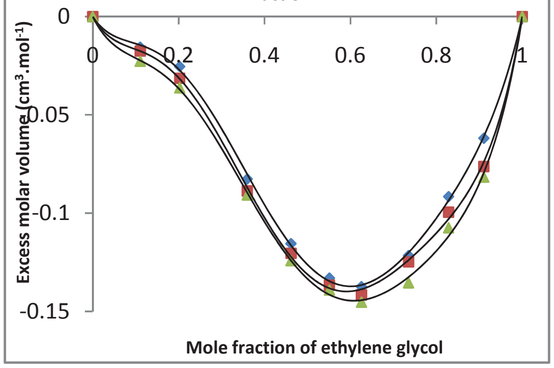

Figure2. plot of viscosity deviation against EG mole fraction

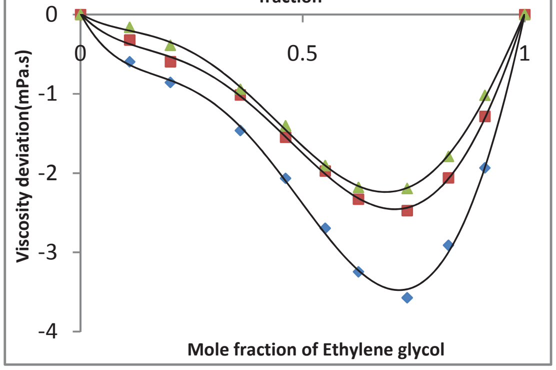

Conclusion:

Densities, viscosities, excess molar volume and viscosity deviation of (1,2-Ethanediol + 1,3-Propanediol) was determined over the whole concentration range. The calculated V^E and Δη values for all solutions were negative over the whole concentration range and temperatures.

References:

[1] G.O.Curme; C.O.Young; Ethylene glycol a contribution of chemistry to the automobile antifreeze; Ind. Eng. Chem; 17 (1925) 1117–1120.

[2] M.R.Kula; K.H. Kroner; H.Hustedt; Advance in biochemical Engineering, Springer-Verlag, Berlin; 1982.

[3] R.K.Shukla; A.Kumar; N.Awasthi; U.Srivastava; V.S.Gangwar; Density, viscosity and refractive index of binary liquid mixtures at 293.15, 298.15, 303.15, 308.15 and 313.15 K, Experimental Thermal and Fluid Science; 37 (2012) 1-11.

Density, Viscosity, Excess molar volume of Ethanol Amine with 1,3-Propanediol at Temperature of 298.15, 303.15, and 308.15 K

Setare Habibi*, Abbas A. Rostami and Abdollah Omrani
Faculty of Chemistry, University of Mazandaran, Babolsar, Iran
*Corresponding author e-mail address: Setarehhabibi@hotmail.com

Keyword: Ethanol amine, Density, Excess molar volume**,** Binary mixtures

Introduction:

In recent years, numerous studies have been done on some physical property of industrial solutions. Because, many industrial process requires accurate values of thermodynamic and transport properties of liquids [1] and these values are indispensable for many practical problem concerning heat transport, mass transport, fluid flow, and pipelines system [2]. Moreover, the physical properties not only provide information on the nature of intermolecular interactions taking place within the solution but also are essential for designing, testing, and extending of theoretical models of fluid mixtures [3]. Ethanolamine is used in aqueous solutions for scrubbing certain acidic gases. It is used as feedstock in the production of detergents, emulsifiers, polishes, pharmaceuticals, corrosion inhibitors, and chemical intermediates. In this work, we report Density, viscosity, Excess molar volume of (Etanolamine+1,3-Propanediol) over the entire composition range within the temperature range (298.15 , 303.15, 308.15) K.

Experimental

Materials. Ethanolamine and 1,3-Propanediol were supplied by Fluka. The purity of all materials was higher than 99 %.

Apparatus and procedure. The mass measurements were made on a single pan Mettler balance with an accuracy of ± 0.01 mg. Density (ρ) measurements of pure components and binary mixtures over the complete composition range were carried out using Anton Paar oscillating U tube densitometer (DA 500) with ± 10-4 g·cm-3 accuracy. The kinematic viscosity was measured with Ubbelohde viscometer with a Schott-Geräte automatic measuring unit model AVS 400 .

Results and discussion

The experimental values of densities and viscosities of Ethanolamine and 1,3-propanediol binary mixtures at temperatures of 298.15, 303.15, and 308.15 was determined. Figure 1 shows the variation of viscosity of Ethanolamine concentration at different temperatures. From the figure 1, it can be seen that the viscosity measurement are decrease with temperature and Ethanolamine concentration. In order to afford the extent of molecular-level interactions within (Etanolamine+1,3-Propanediol) we estimated excess molar volume (V^E) from experimental density data using the relationship: $V^E = \frac{X_1M_1+X_2M_2}{\rho} - \frac{X_1M_1}{\rho_1} - \frac{X_2M_2}{\rho_2}$

Here, x_1, x_2, and M_1, M_2 refer to the mole fractions and densities, respectively, of components1 and 2 in the mixture at a given temperature, and ρ is the density of the mixture. The variation of Ethanolamine and 1,3-propanediol binary mixtures with mole fraction of Ethanolamine are plotted in figure1. The negative V^E values are shows that the interactions between unlike molecules which are stronger than the interactions between like molecules as well as molecular accommodation of one component into free space of the others (packing effect).

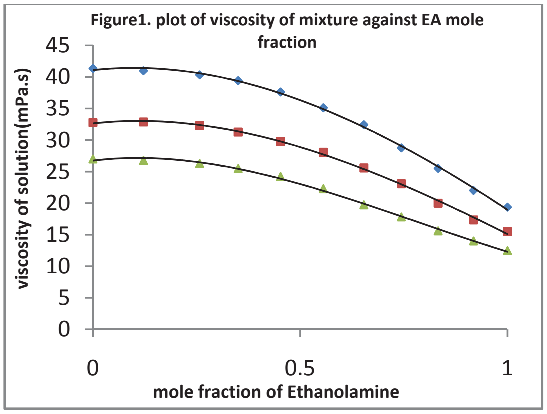

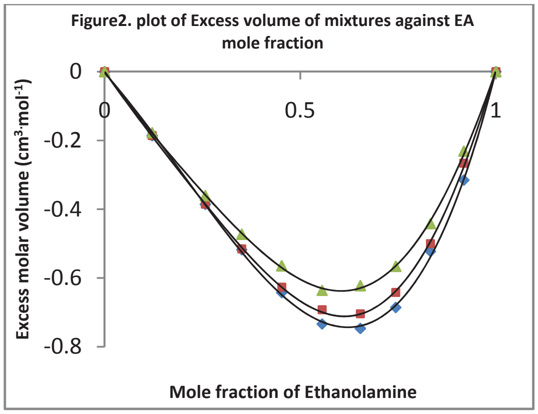

Conclusion:

Densities, viscosities, and excess molar volume of (Etanolamine+1,3-Propanediol) was determined over the whole concentration range. The calculated V^E values for all solutions were negative over the whole concentration range and temperatures.

References:

[1] M.R. Kula; K.H. Kroner; H. Hustedt; Advance in biochemical Engineering; Springer-Verlag, Berlin; 1982.

[2] R.K. Shukla; A. Kumar; N. Awasthi, U. Srivastava; V.S. Gangwar, Density, viscosity and refractive index of binary liquid mixtures at 293.15, 298.15, 303.15, 308.15 and 313.15 K, Experimental Thermal and Fluid Science; 37 (2012) 1-11**.**

[3] L. Wang; H. Xu; J. Zhao; C. Song; F. Wang; Density and viscosity of (3-picoline + water) binary mixtures from T = (293.15 to 343.15) K, J. Chem. Thermodyn. 37 (2005) 477-483.

Density and apparent molar volume of ionic liquids ([PnMIm]Br) and [HMIm]Br) in the aqueous D-glucose solutions at different temperatures

H. Shekaari*, Z. Ghasedi-Khajeh
Department of Physical Chemistry, University of Tabriz, Tabriz, Iran.
E-mail address: hemayatt@yahoo.com (H. Shekaari).

Keywords: Density, Ionic liquid, D-glucose, Apparent molar volume

Introduction:

The properties of aqueous Carbohydrate solutions are influenced due to existence the other solutes particularly the ions arising from dissolution of electrolytes.The wide usages of ionic liquids in carbohydrate chemistry made us to study their thermodynamic properties. These studies seem indispensable for better understanding of molecular interactions occurring in this type of ternary systems and developments in chemical reaction designing [1]. In the current work, the volumetric behaviours of D-glucose in several concentrations of aqueous ionic liquid ([PnMIm]Br and [HMIm]Br) solutions have been studied using density measurements at temperatures T = (288.15 to 318.15) K. The measured density values are used to calculate the standard partial molar volume (V_ϕ^0), partial molar expansivity (E_ϕ^0), hydration number (n_H) and volumetric interaction coefficients (V_{SIL} and V_{SILIL}) at different temperatures. These parameters have been discussed in terms of solute-solvent interactions and structure making/breaking abilities of D-glucose and ionic liquid.

Experimental:

2.1. Materials

D-glucose (>99.6%) were obtained from Merck and ([PnMIm]Br) and [HMIm]Br ionic liquids were prepared and purified by using the procedure described in the literature [2].

2.2. Apparatus and procedure

A vibrating-tube digital densimeter (DMA, 4500M, Anton Paar, Austria) was used to measure the densities of the solutions.

Results and discussion:

The apparent molar volumes (V_ϕ) of D-glucose in aqueous ionic liquid solutions were determined from the solution densities. The positive $\Delta_t V_\phi^0$ values obtained for D-glucose suggest that the hydrophilic–ionic interactions predominate over the hydrophobic–ionic interactions. According to McMillan-Mayer theory of solutions, volumetric interaction coefficients (V_{SIL} and V_{SILIL}) at different temperatures obtained. Positive V_{SIL} values mean that the D-glucose-IL interactions contribute a positive value to volume.In order to study the temperature dependence of the standard partial molar volume, the V_ϕ^0 values were fitted to the following equation:

$$V_\phi^0 = a_0 + a_1 T + a_2 T^2 \qquad (1)$$

Differentiation of Eq. (1) with respect to temperature at constant pressure was done to calculate partial molar isobaric expansions. The sign of second derivatives of the standard partial molar volume with respect to the temperature $(\partial^2 V_\phi^0 / \partial T^2)_p$ reflect the structure making and breaking ability of a solute in the solution. Small negative values of $(\partial^2 V_\phi^0 / \partial T^2)_p$ for D-glucose in aqueous ionic liquid solutions rather than water, indicate that this saccharide behaves as a structure breaker in water however, its structure-breaking tendency decreases in presence of ionic liquids. The obtained values of hydration number indicates that dehydration effect of ionic liquid on D-glucose increases as temperature increase [3].

Conclusions:

These experimental data have been used to obtain some thermodynamic characters including standard partial molar volumes (V_ϕ^0), partial molar expansivities (E_ϕ^0), hydration numbers (n_H) and interaction coefficients (V_{SIL} and V_{SILIL}) at different temperatures. All these parameters support the existence of strong solute-solvent interactions in the ternary solutions of present study.

References:

[1] M. Gericke, T. Liebert, T. Heinze, Macromol. Biosci. 9 (2009) 343-353.

[2] P. Nockemann, K. Binnemans, K. Driesen, Chem. Phys. Lett. 415 (2005) 131-136.

[3] N. Dey, B. K. Saikia, N. Haque, Canadian J. Chem. 58 (1980) 1512-1515.

Densities and Excess molar volumes for Binary Solutions of Water + Methanol and + Ethanol from (283.15 to 313.15) K

A.Shalmashi[a*], F.Amani[a]

[a] Chemical Technology Department, Iranian Research Organization for Science and Technology (IROST), Tehran, Iran

Email: shalmashi@irost.org

Key words: Density, Excess volume, Binary Solution, Methanol, Ethanol

Introduction:

Among the various thermodynamic properties, the excess volume, V^E, has been of much interest for the practical purpose of determining composition from the density measurement [1]. Density and excess molar volume are significant for the design of new processes and the study of molecular interactions in binary liquid systems [2]. The excess volumes are defined as:

V^E = Volume of the solution – (volume of pure A + volume of pure B).

In this paper Densities for binary solutions of two alcohol (Ethanol and Methanol) with water over the whole composition range have been measured at temperatures from (283.15 to 313.15) K in 10 K intervals and atmospheric pressure. From these data, the excess molar volumes (V^E) and their standard deviation δ (V^E) were calculated. This study is expected to give some information about the volume changes in these binary solutions that indicate the tendency of the water molecules with simple alcohols.

Materials and methods:

The chemical, absolute alcohols, methanol and propanol with high-purity grade reagents obtained from Merck (Darmstadt, Germany). Bidistilled water was used to prepare the sample mixtures.

Apparatus:

The densities of the pure components and binary mixtures were measured using a Gay-Lussac pycnometer supplied by a thermometer, which its volume was calibrated by using pure water.

The temperature of the solution in the pycnometer was kept constant in a bath with a thermostat. The temperature was controlled within ± 0.05 K of the desired temperature through thermometer of the pycnometer. Once the solution reached the desired temperature, it was weighted to within ± 0.0001 g with an analytical balance (Sartorius, 2842, GMBH, Germany). For each binary mixture, a set of 9 composition from (10 to 90) % w/w, was prepared and their densities were measured at the respective composition.

Results and Discussion:

The results indicated that V^E values are highly negative for binary solutions of methanol and ethanol with water over the entire mole fraction range and at all temperatures investigated for each binary system under study. The V^E profiles of two binary systems studied are characterized by an initial increase in negative values following maxima at about 60-70 % (w/w) and then a decrease.

Conclusion:

It is obvious that hydrogen bonds between the molecules of water and alcohols (methanol and ethanol) are primary responsible for the non-ideal behavior of these binary systems.

As results showed, the excess molar volumes for ethanol + water become less negative with increasing temperature and conversely the excess molar volumes for methanol+ water become more negative with increasing temperature[3]. For the methanol + water system, the temperature effect is hardly observable [4].

References:

[1] Manapragada V.; Excess Volumes of Binary Solutions of Methyl Formate, Ethyl Formate, Propyl Formate, and Benzyl Acetate with Bromo-, Chloro-, and Nitrobenzenes at (303.15, 308.15, and 313.15) K. J. Chem. Eng. Data 2008, 53, 265-270.

[2] Guangshun Chen ; Densities and Excess Molar Volumes for Sulfolane + Ethylbenzene, Sulfolane + 1- Methylnaphthalene, Water + N,N- Dimethylformamide, Water + Methanol, Water + N-Formylmorpholine, and Water + N-Methylpyrrolidone. J.Chem. Eng. Data 1995, 40, 1001-1004.

[3] Hossein A.; Temperature Dependence of the Volumetric Properties of Binary and Ternary Mixtures of Water (1) + Methanol (2) + Ethanol (3) at Ambient Pressure (81.5 kPa). J.Chem. Eng. Data 2007, 52, 2517-2526.

[4] Tong-Chun Bai ; Excess Molar Volumes for the Ternary Mixture N,N Dimethylformamide + Methanol + Water at the Temperature 298.15 K. J.Chem. Eng. Data 1999, 44, 491- 496.

Densities and Excess molar volumes for Binary Solution of Water + Propanol from (283.15 to 313.15) K

A.Shalmashi[a*], F.Amani[a]

[a] Chemical Technology Department, Iranian Research Organization for Science and Technology (IROST), Tehran, Iran

Email: shalmashi@irost.org

Key words: Density, Excess volume, Binary Solution, Propanol

Introduction:

The thermodynamic properties of real solutions may be expressed in terms of the excess functions, X^E, defined as the difference between the observed thermodynamic function of mixing and the function for an ideal solution. The excess volumes are defined as:

V^E = Volume of the solution – (volume of pure A + volume of pure B).

Among the various thermodynamic properties, the excess volume, V^E, has been of much interest for the practical purpose of determining composition from the density measurement. Density and excess molar volume are significant for the design of new processes and the study of molecular interactions in binary liquid systems. Excess volume could provide information on the possible interactions between components of a binary mixture, such as molecular associations and dipole-dipole and dipole-induced-dipole interactions. Furthermore excess volumes could indicate the deviation of a binary solution from the ideality.

In this paper we have reported densities for binary solution of propanol with water over the whole composition range at temperatures from (283.15 to 313.15) K in 10 K intervals and atmospheric pressure. From these data, the excess molar volumes (V^E) and their standard deviation δ (V^E) were calculated.

Materials and methods:

The chemical, absolute propanol with high-purity grade reagents obtained from Merck (Darmstadt, Germany). Bidistilled water was used to prepare the sample mixtures.

Apparatus:

The densities of the pure component and binary mixtures were measured using a Gay-Lussac pycnometer supplied by a thermometer, which was calibrated by using pure water. The temperature of the solution in the pycnometer was kept constant in a bath with a thermostat. The temperature was controlled within ± 0.05 K of the desired temperature through thermometer of the pycnometer. Once the solution reached the desired temperature, it was weighted to within ± 0.0001 g with an analytical balance (Sartorius, 2842, GMBH, Germany). For this binary mixture, a set of 9 composition from (10 to 90) % w/w, was prepared and their densities were measured at the respective composition.

Results and Discussion:

The results indicate that V^E values are negative for binary solution of propanol with water over the entire mole fraction range and at all temperatures investigated. The V^E profiles of this binary system studied are characterized by an initial increase in negative values following maxima at about 60-70 % (w/w) and then a decrease.

Conclusion:

As data in this study show, the excess volumes for propanol with water in each four investigated temperature were found to be highly negative across the mole compositions. It is obvious that hydrogen bonds between the molecules of water and propnol are primary responsible for the non-ideal behavior of this binary systems [1].

References:

[1] Ivona R.: Excess molar volume of the acetonitrile + alcohol systems at 298.15 K. Part I: Density measurements for acetonitril + methanol, + ethanol systems. J.Serb.Chem.Soc. **2002,** 67(8-9), 581-586.

Thermodynamic study of interactions between Dimethyl Carbonate and a homologous series of 2- Alkanols

N.Namaki shooshtari [a*]

a Department of Chemistry, Science and Research Branch, Islamic Azad University, Khouzestan, Iran

Email:navid29ab@yahoo.com

Key words: Excess molar volumes, Binary mixture, Dimethyl Carbonate, 2-Alkanols

Introduction:

The thermodynamic and excess molar properties of liquids and liquid mixtures have been used to understand the molecular interactions between the components of the mixture and also for engineering applications. The thermodynamic study of esters of carbonic acid holds considerable interest owing to their uses in industry for the synthesis of many chemicals, in pharmaceuticals, and in agricultural chemistry. Such chemicals are also used as extractive solvents [1-2].

Densities of binary mixtures of dimethyl carbonate with 2-Propanol, 2-Butanol , 2-Pentanol, 2-Hexanol and 2- Heptanol at temperatures: 298.15 K , 303.15 K , 308.15 and 313.15K were measured at the whole range of mole fraction. Excess molar volumes(V_m^E) were correlated by Redlich-Kister type equation as a function of temperature [3].

Materials and methods:

Dimethyl carbonate, 2-propanol, 2-butanol, 2-pentanol, 2-hexanol and 2-heptanol were purchased from Merck company with purity higher than 99%, then used without further purification. The density of the pure compounds and binary mixtures was measured by an Anton Parr densimeter. The uncertainty of the density measurement was estimated to 10^{-5} gr/cm^3.

Apparatus:

Densities of the pure liquids and binary mixtures at various temperatures were measured by means of an Anton Parr DMA 4500 oscillating U-tube densimeter, provided with automatic viscosity correction. and a digital balance made by Mettler Toledo company. temperature was regulated with laboratory bath made by Petrotest company.

Result and discussion:

The excess molar volumes V_m^E for binary systems were evaluated using this equation:

$$V_m^E = \sum_{i=1}^{N} x_i M_i (\rho^{-1} - \rho_i^{-1}) \tag{1}$$

where ρ is the density of the mixture, ρ_i is the density of pure component *i*, x_i is the mole fraction, M_i is the molar mass of component *i*, and *N* stands for the number of components in the mixture. V_m^E for the binary systems were fitted by the least-squares method to the Redlich–Kister equation: [3]

$$V_{ij}^E = x_i x_j \sum_{k=0}^{n} A_k (x_i - x_j)^k \tag{2}$$

Excess molar volume of all mixtures are positive and increase with increasing of chain length of 2- Alkanols and temperature rising.

Experimental data and fitted equations of binary systems are depicted in Fig. (1)

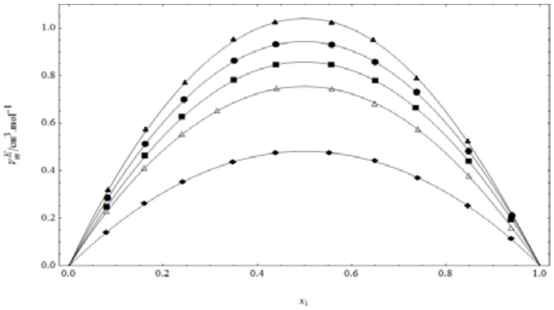

Fig. 1 Excess molar volumes V_m^E vs. mole fraction of Dimethyl carbonate with (♦) 2-propanol, (Δ) 2- butanol, (■) 2-pentanol, (●) 2-hexanol, (♣) 2-heptanol at $T = 298.15$ K. The solid curves were calculated from coefficients of equation (2)

Conclusion:

Positive quantities of excess molar volumes of Dimethyl carbonate and 2-alkanols mixtures show that dominant factors are physical interactions that become weaker with temperature rising.

Reference:

[1] Iloukhani, H., Almasi, M.; "Densities, viscosities, excess molar volumes, and refractive indices of acetonitrile and 2-alkanols "; J. Thermochim Acta. 495, 139–148(2009)

[2]] Almasi, M.; Sarkoohaki, B. "Densities, Viscosities, of Binary Mixtures of Cyclohexanon and 2-Alkanols";J. Chem. Eng.Data 2012, 57, 309–316.

[3] Redlich, O., Kister, A.T.;" Algebraic representation of thermodynamic properties and the classification of solutions". Ind. Eng. Chem. 40, 345–348 (1948).

Study of ionic liquid solvation interactions and thermodynamic properties using gas–liquid chromatography

K.Tabarheidar [a], H. Gharehmoshk Gharavi*[a], A. Sharifi, M. Mirzaei
[a] Department of separation methods, Chemistry and Chemical Engineering Research Center of Iran, Tehran, Iran
*email:h_gharavi85@yahoo.com

Key words: GC, Ionic liquid, Activity coefficient, Rohrschneider–McReynolds constant.

Introduction:

Ionic liquids (ILs) possess high-thermal stabilities, and negligible vapor pressure, and are highly tunable making them attractive solvent systems. GC employing IL stationary phases has proven to be a powerful tool for the determination of important thermodynamic properties involving mixtures of ILs and organic solvents [1]. The Rohrschneider–McReynolds system is the oldest accepted stationary phase classification systems [2,3].

In this work, two mixtures of ILs,50% $C_{12}(mpy)_2\text{-}(NTf_2)_2)$/50%($C_{12}(mim)_2(NTf_2)_2$) , and 50% ($C_{12}(mpy)_2\text{-}(NTf_2)_2$)/50% ($C_{12}(mim)_2\text{-}(BF_4)_2$) were chosen to determine multiple solvation interactions by Rohrschneider–McReynolds classification and to measure the ionic liquid thermodynamic parameters such as activity coefficients at infinite dilution ($\gamma^{\infty}{}_i$).

Materials and Methods:

Stationary phase (RTIL) on Chromosorb W-AW (60-80 mesh), was prepared. The value of $\gamma^{\infty}{}_i$ can be calculated from Equation 1 [4]:

$$\ln^{\infty}\gamma_i = \ln\left(\frac{nRT}{V^N P^{\text{Ş}}}\right) - P^{\text{Ş}}\frac{B^{11}\text{-}V^{\text{Ş}}}{RT} + \frac{2B^{12}\text{-}V_{\infty}}{RT}\,JP^{\circ}(1)$$

Equation 2 describes the Rohrschneider–McReynolds system in terms of the five probes and their corresponding phase constants; namely, benzene (X′), butanol (Y′), 2-pentanone (Z′), nitropropane (U′), and pyridine (S′) with the overall difference in the Kovats retention index (ΔI).

$$\Delta I = aX' + bY' + cZ' + dU' + eS' \qquad (2)$$

Results and discussion:

γ^{∞}_{i} values are listed in Table 1.$\gamma^{\infty}_{i}$for homological series of solutes increased with as the solute alkyl chain length increased. The smallest values of γ^{∞}_{i}, was observed for acetonitrile that is a polar compound. These polar compounds usually interact strongly with a polar IL.

Table 1.activity Coefficients at Infinite Dilution (γ^{∞}_{i}) for the Solutes at 313.15 K.

Solutes	$(C_{12}(mpy)_2\text{-}(NTf_2)_2)$ / $(C_{12}(mim)_2\text{--}(NTf_2)_2)$	$(C_{12}(mpy)_2\text{-}(NTf_2)_2)$ / $(C_{12}(mim)_2\text{--}(BF_4)_2)$
Benzene	2.67	3.48
Toluene	3.45	4.60
Ethyl benzene	4.71	-
Ethanol	4.02	3.83
Propanol	4.90	4.86
Acetonitrile	1.65	1.96
1,2-Dichloroethane	2.07	2.26
Cyclohexane	13.37	17.41
Heptane	17.27	30.40
Octane	33.91	44.83

Table 2 shows S_{12}^{∞}.The selectivity values indicate that these ILs can be used as efficient solvents in aromatic/aliphatic separations.

Table 2.the selectivity values at 313.15 K

IL_s	Octane/benzene	Cyclohexane/benzene	Toluene/benzene	Heptane/acetonitrile
$(C_{12}(mpy)_2\text{-}(NTf_2)_2)$ / $(C_{12}(mim)_{2.}\text{-}(NTf_2)_2)$	12.72	5.02	1.30	10.47
$(C_{12}(mpy)_2\text{-}(NTf_2)_2)$ / $(C_{12}(mim)_{2.}\text{-}(BF_4)_2)$	12.87	5	1.32	15.51

Table 3 gives the Rohrschneider–McReynolds constants. According to these, it can be deduced that these solvents are remarkably high polar.

Table 3.Rohrschneider-MacReynolds Constants of the Five First Test Solutes at 100 °C

column	X [a]	Y [a]	Z [a]	U [a]	S[a]	Av [a]	Ref
DB-5	27	66	71	93	63	64	3
OV-22	160	188	191	283	253	215	3
(C_{12}(mpy)$_2$-(NTf_2)$_2$) with (C_{12}(mim)$_{2-}$-(NTf_2)$_2$)	331	575	557	758	679	2901	this work
(C_{12}(mpy)$_2$-(NTf_2)$_2$) with (C_{12}(mim)$_{2-}$-(BF_4)$_2$)	394	886	607	887	777	3552	This work

Conclusions:

γ^{∞}_{i} for various solutes in the binary mixtures of ionic liquids inclusive of(C_{12}(mpy)$_2$-(NTf_2)$_2$)/(C_{12}(mim)$_{2-}$-(NTf_2)$_2$) and (C_{12}(mpy)$_2$-(NTf_2)$_2$)/(C_{12}(mim)$_{2-}$-(BF_4)$_2$), were measured, and a high selectivity at infinite dilution for aliphatic/aromatic separations, were observed in comparison to aromatic/aromatic separations for two mixtures of ionic liquids. The Rohrschneider–McReynolds constants evidenced the dual nature of IL stationary phases.

Reference:

[1] U.Doman´ska; M. Kro´likowska, J. Chem. Eng. Data. 2011, 56, 124–129.
[2]L. Rohrschneider,J. Chromatog. 1966, 22, 6–22.
[3]W. O. Mcreynolds, J. Chromatogr. Sci. 1970, 8, 685-691
[4] A.J.B. Cruickshank, M.L. Windsor, C.L. Young, Proc. R. Soc. 1966, 295, 259–270.

Solute-Solvent Interaction Effects on Protonation constants of Nicotinic Acid in Different Water-Methanol Mixtures

Shahin Madadi,[1] Ali Shamel,[1] Farrokh Gharib,[2]
[1] Chemistry Department, Islamic Azad University, Ardabil Branch, Ardabil, Iran
[2] Chemistry Department, Shahid Beheshti University, G.C.,Tehran, Evin, Iran
E-mail:Shahin_Madadi59@Yahoo.com

Key words: Protonation constants, Nicotinek acid, metanol -water mixtures, Kamlet-Taft Solvatochromic parameters, Solvent Effect

Introduction:

Nicotinic acid known as vitamin B_3 or niacin is one of the five vitamins associated with a pandemic deficiency disease in human diet. The deficiency of this compound in human diet causes serious central and peripheral nervous system. The biological function of this drug in human is believed to act through nicotinamide, which is contained in NAD and NADP coenzymes. Nicotinic acid penetrates into cells by means of active transport and passive diffusion, whose intensity is controlled by acid-base equilibria of the compound. Therefore, the acid-base equilibria of nicotinic acid should be known not only as a competing process in complexing reaction but also to explore its activity in cell-membrane transport.

In this work, the protonation constants of nicotinic acid is determined in different aqueous solutions of methanol to show how solvent and solvent mixtures with different dielectric constants affect the formation of the protonated species of this drug, using potentiometric method.

Experimental:

All measurements were performed at 25 °C and constant ionic strength (0.1 mol dm-3 sodium chloride). The electromotive force was measured using a Metrohm model 781 pH ion-meter. The combined glass-pH electrode (model 6.0258.000) was modified by replacing its aqueous KCl solution with 0.1 mol dm-3 NaCl saturated with AgCl. The electrode was soaked for (15 to 20) minutes in a water-alcohol mixture before the potentiometric measurements. All titrations were carried out in a 80 mL thermostated double-walled glass vessel. The protonation constants were evaluated from measurements of the emf by titration of a 25 mL nicotinic acid (2.0-5.0×10-3 mol dm-3) solution with a 0.1 mol dm-3 sodium hydroxide solution both in the same ionic strength and mole fraction of methanol (0 to 50 % by v/v). The measured emf from the potentiometric titration was conducted using the computer program (Microsoft Excel Solver and linest).

Apparatus:

A Jenway pH-meter, model 3520 (precision of 0.001 units of pH), was used for pH measurements.The hydrogen ion concentration was determined with a combination electrode (Jenway). A thermostat having accuracy of ± 0.1°C maintained the temperature of the potentiometric cell. [Model: EX.1200-30-6 STH, this oven is made in Iran].

Results and Discussion:

The protonation constants of nicotinic acid in water-methanol mixed solvents have different behaviors. log K_1 increases but log K_2 decreases with increasing the proportion of methanol in the mixtures. In general, the standard Gibbs energy of protonation equilibria consists of two terms: an electrostatic term, which can be estimated by the Born equation and a non-electrostatic term, which includes specific solute-solvent interaction. When the electrostatic effects predominate, then in accordance with the Born equation, the plot of log K versus reciprocal of dielectric constant of the media, ε, should be linear [1-2]. $\Delta\log K = (121.6n/r)(1/\varepsilon - 0.0128)$ where r is the common radius of the ions and n is the square summation of the charges involved in the protonation equilibria. Therefore, a change in polarity of the medium has a major role on log K_1 and log K_2 values. In this case the correlation between log K_1 with the reciprocal of the dielectric constant of the aqueous-alcohol mixtures is linear. However, the linearity of the correlation between log K_2 of nicotinic acid with the reciprocal of the dielectric constant of methanol-water mixtures is poor (with correlation coefficients between 0.93-0.97, respectively). This indicates that the protonation constants depend not only on electrostatic forces but also strongly depend on the solute-solvent interactions of the different species in the mixtures.

Therefore, it is necessary to elucidate the nature of solute-solvent interactions for a better understanding of solvent effects.

References:

[2].A, Farajtabar;F,Jaberi;F,Gharib. Spectrochim.Acta,PartA,83,213-220,2011.
[1].F, Gharib;A, Farajtabar;A.M,Farahani;F,Bahmani,J.Chem.Eng.Data,55,327-332,2010.

Solvent Effects on Protonation Constants of benzohydroxamic acid in Different Aqueous Solutions of 1- etanol

Shabnam jafari jahed, [1] leila fathe jenagard, [1] Ali Shamel, [1] Farrokh Gharib[2]
[1] Chemistry Department, Islamic Azad University, Ardabil Branch, Ardabil, Iran
[2] Chemistry Department, Shahid Beheshti University, G. C., Tehran, Evin, Iran
Email: shab_moones4@yahoo.com

Key words: Protonation constants, benzohydroxamic acid, etanol -water mixtures, Kamlet-Taft Solvatochromic parameters, Solvent Effect

Introduction:

The protonation constants of benzohydroxamic acid have been determined in 10–80% (v/v) etanol-water mixtures at 25 °C and constant ionic strength (0.1 mol L^{-1} sodium perchlorate) by potentiometric technique and calculated using a suitable computer program which employs a nonlinear least- squares method. The effect of solvent composition on the protonation constants in the mixed solvents were correlated with the Kamlet-Taft solvatochromic parameters (α, β and π*). It was shown that $\log K_1$ and $\log K_2$ values of benzohydroxamic acid increases with increasing etanol content up to 50% and then tend to decrease. Further, more an over-view of the effect of preferential solvation and solvent structure of electrolytes in etanol-water mixtures on the values of the protonation constants in these media were also discussed. benzohydroxamic acid is determined in different aqueous solutions of 1- etanol.

Materials and methods:

Potentiometry titration is a well known reference method for pK_a determination, and it can be easily used in organic or hydro-organic solvents. To evaluate the protonation constants, first the calibration of the potentiometer and the electrodes should be performed by Gran's method. The measured emf values in the potentiometric titration of the compound in the different aqueous solutions of 1- etanol are conducted with a suitable computer program for data treatments using a fitting method. All measurements were performed at 25 °C and constant ionic strength of 0.1 mol dm^{-3} sodium chloride.

In all cases, the procedure was repeated at least three times and the average values and the corresponding deviations from the average are reported in this work.

Apparatus:

A Jenway pH-meter, model 3520 (precision of 0.001 units of pH), was used for pH measurements.The hydrogen ion concentration was determined with a combination electrode (Jenway). A thermostat having accuracy of ± 0.1°C maintained the temperature of the potentiometric cell. [Model: EX.1200-30-6 STH, this oven is made in Iran].

Result and discussion:

The protonation constant values of benzohydroxamic acid have been determined According to the obtained results, increasing the amount of the organic solvent reduces the dielectric constant in the aqueous-1-etanol mixtures and so, in accordance with the Born equation the protonated species of the benzohydroxamic acid are expected to be more stable in media with lower dielectric constants. When electrostatic effects predominate, a plot of log K versus the reciprocal of the dielectric constant of the media should be linear.Previously, we have reported [1-2] that the dielectric constant alone cannot serve as a quantitative measurement of the solvent polarity. This property is often inadequate, since the dielectric constant description considers a solvent to be an unstructured continuum, not composed of individual solvent molecules with their own solvent-solvent interactions, and does not take into account specific solute-solvent interactions. In this work, we have used the method was introduced by Kamlet, Aboud, and Taft (KAT). The KAT equation contains separate terms for non-specific as well as specific solute-solvent interactions. Finally, the dependence of acid-base equilibria on solvent composition will be discussed from the determined coefficients of KAT parameters.

Conclusion:

In this work, the protonation constants of some benzohydroxamic acid have been determined in etanol -water mixture of varying compositions (10–80% etanol by volume). It is very difficult to interpret the logK variations of the benzohydroxamic acid studied by only macroscopic parameters of the etanol-water mixtures. It is known that one of the most important factors determining the equilibrium constants is the reaction medium, so, the solvent effect on protonation constants could be explained on the basis of dielectric constant of the medium, solvent structure, preferential solvation, and microscopic parameters (as Kamlet-Taft solvatochromic parameters). A Jenway pH-meter, model 3520 (precision of 0.001units of)was used for pH measurements. The hydrogen ion concentration was determined with a combination nelectrode (Jenway). A thermostat having accuracy of ± 0.1A Jenway pH-meter, model 3520 (precision of 0.001)

Reference:

[1] A, Shamel.; F, Jaberi.; F, Gharib. J. Chem. Eng. Data; 55, 5176-5181,2010.
[2] M, Jabbari.; F, Gharib. J. Sol. Chem; 40, 561-574,2011.
[3]. F. Gharib; F. Sadeghi; Appl.Organomet. Chem. 21, 218–225,2007.

Ionic Strength Dependence of Protonation Constants of Nicotinic Acid

shabnam Jafari jahed,[1] Ali Shamel,[1] Farrokh Gharib[2]

[1] Chemistry Department, Islamic Azad University, Ardabil Branch, Ardabil, Iran

[2] Chemistry Department, Shahid Beheshti University, G. C., Tehran, Evin, Iran

E-mail : shab_moones4@yahoo.com

Key words: Protonation constants, benzohydroxamic acid, etanol -water mixtures, Kamlet-Taft Solvatochromic parameters, Solvent Effect

Introduction:

The acidity or basicity of a compound in a given medium is influenced by both the electronic effects of the substituents and the solvent as well as the ionic strength effect of the medium. However, in a series of papers [1-2] on the ionic strength dependence of formation constants we reported some interesting features of the function log $\beta = f\ (I)$, where β and I refer to the formation or protonation constants and the ionic strength of the media, respectively. In particular, all the formation constants seem to follow the same trend as a function of ionic strength, if allowance is made for the different types of reaction stoichiometry and for the different charges of the reactants and the products. In determining a formation constant at a fixed ionic strength, in all cases, some uncertainties are always present. This fact is mainly due to the uncertainties in numerical values of stability constant.

The present work deals with the study of protonation constant of benzohydroxamic acid in different ionic strengths ranging from 0.1 to 0.7 mol dm^{-3} sodium chloride. The parameters which define this dependency were analyzed with the aim of obtaining further information with regard to their variation as a function of charges involved in the complex reaction. Moreover, a general equation was established for the dependence of formation constant on ionic strength. This equation gives the possibility of estimating a formation constant of a fixed ionic strength when its value is known at another ionic media in the range of $0.1 \leq I \leq 0.7$ mol dm^{-3} (NaCl) and therefore may give a significant contribution of solving many analytical and speciation problems.

Experimental:

All measurements were performed at 25 °C and different ionic strengths (0.1 - 0.7 mol dm^{-3} sodium chloride). The electromotive force was measured using a Metrohm model 781 pH ion-meter. All titrations were carried out in a 80 mL thermostated double-walled glass vessel. The protonation constants were evaluated from measurements of the emf by titration of a 25 mL benzohydroxamic acid (2.0-5.0×10^{-3} mol dm^{-3}) solution with a 0.1 mol dm^{-3} sodium hydroxide solution both in the same ionic strength. The measured emf from the potentiometric titration was conducted using the computer program (Microsoft Excel Solver and Linest).

Results and Discussion:

The dependence of the protonation constant on ionic strength can be described by a semi-empirical equation as: $\log K(I) = \log K(I^*) - f(I) + CI$where $f(I) = Z^*AI^{1/2}/(1 + BI^{1/2})$, $K(I)$ and $K(I^*)$ are the protonation constant of the actual and the reference ionic media, respectively. A is the parameter of Debye-Hückel equation, (A = 0.5115 at 25 °C), $Z^* = \sum(\text{charges})^2_{\text{reactants}} - \sum(\text{charges})^2_{\text{products}}$, C is an empirical parameter that its value is considered, and B is set equal to1.5 (a small error in fixing B is absorbed in the linear term C. Results of a series of investigations done by many researchers have showed that, when all the interactions occurring in the solution are considered, in the range 0 ≤ ionic strength ≤ 0.7, the empirical parameters are dependent on the stoichiometry of the formation reaction. If an approximate value of C is known, the protonation constant can be determined for the variation of ionic strength from I^* to I by the equation $\log K(I) = \log K(I^*) - f(I, I^*) + C(I - I^*)$ (1) where $f(I, I^*) = Z^*A[I^{1/2}/(1 + 1.5I^{1/2}) - I^{*1/2}/(1 + 1.5I^{*1/2})]$ I and I^* are the ionic strength of the solution by appropriate electrolyte. A preliminary analysis of the data showed that if a fixed value is assigned to C, the fit with eq 1 is not always good over the whole range of ionic strength from 0.1 to 0.7 mol dm^{-3}. This equation may be useful for small changes of ionic strength, but a better fit is obtained by adding a further term of the from $DI^{3/2}$ (D is another adjustable parameters). Therefore the data were fitted to the eq 2.$\log K(I) = \log K(I^*) - f(I, I^*) + C(I - I^*) + D(I^{3/2} - I^{*3/2})$ (2) The parameters for the dependence on ionic strength (C and D) were calculated by the fitting method and will be discussed.

References:

[1] F,Gharib;A, Shamel,Revs.Inorg.Chem.25,361-371,2005.

[2] M, Jabbari.;F,Gharib,J.Sol.Chem.40,561-574,2011.

Viscosity Prediction for Binary Mixtures by Using Different Models

Sh. Keshvari Aghmyooni[*a] , R. Tahery[b]

a Science Department, Islamic Azad University, Central Tehran Branch, Tehran, Iran

b Chemical Engineering Department, Islamic Azad University, Central Tehran Branch, Tehran, Iran

Email: keshvari.shima@yahoo.com

Keywords: Viscosity, Binary mixture, Un like pair interaction

Introduction:

The viscosity, particularly that of liquid mixtures, is required in most engineering calculation involved in the process, design in the petrochemical, petroleum, chemical and other chemical related industries.It is a thermo-physical property that is often embedded in equipment and process models.

There are a lot of equation to predict the viscosity of binary mixtures including McAllister, Tamura and Kurata and McLaughlin [1], but viscosity prediction by using these equations required more information. In this paper we present very simple models to predict viscosity of binary mixtures.

Theory and Method:

Several semi-empirical relations have been proposed to estimate the dynamic viscosity η of liquid- mixtures in terms of pure- component data. We are examining equations of Kendall and Monroe [2], Hind et al [3], and the Arrhenius equation [4].

The equation of Kendal and Monroe which has no adjustable parameter is expressed as [2]: $\eta = (x_1\eta_1^{1/3} + x_2\eta_2^{1/3})^{3}$ (1)

Hind et al, proposed the following equation [3]: $\eta = x_1^2\eta_1 + x_2^2\eta_2 + 2x_1x_2\eta_{12}$ (2)

η_{12} is attributed to unlike pair interaction it is approximately equal to $0.5(\eta_1 + \eta_2)$, Arrhenius, proposed the following equation [4]: $\eta_{mix} = \eta_1^{x_1}\eta_2^{x_2}$ (3)

η_{mix} is the mixture's viscosity, $\boldsymbol{\eta_1}, \eta_2, x_1, x_2$ respectivly are the viscosity and mole fraction of component 1 and 2.

Results and Discussion:

We used equations (1) to (3) for calculating viscosity of 53 binary mixtures. The average absolute deviation (%AAD) results of Arrhenius obtained %9.842 ,for Kendall & Monroe obtained %13.673, while the AAD% for Hind equation by using geometric mean and arithmetic mean is % 3.692 ,% 3.3.

Conclusions:

Hind et al equation gave more satisfactory results, because Hind et al equation has geometric mean and arithmetic mean of %3.696 and %3.35. Hence we can apply the Hind equation for prediction the viscosity of wide range of mixtures with good accuracy.

Reference:

[1] Oswal. S. L, Desai, H. S, Studies of viscosity and exess molar volume of mixtures, Fluid phase Equilib; 149, 359-376, 1998.

[2] Kendall .J, Monroe. K. P, Studies of viscosity and excess molar volume of binary mixtures, Fluid phase Equilib; 149, 359-376, 1998.

[3] Hind R. K. , McLaughlin. E , A.R. Ubbelohde, Studies of viscosity and excess molar volume of binary mixtures, Fluid phase Equilib; 149, 359-376, 1998.

[4] J. Iraving, Viscosity measurement and modeling of lipid-Supercritical carbon dioxide mixtures, J. Super. Fluids ; 11, 151-162, 1998.

n-octanol/water partition coefficient and solubility measurements of propranolol and atenolol at different temperatures

M. Mohsen-Nia[a*], A.H. Ebrahimabadi[b], B. Niknahad[a]

[a]Thermodynamic Research Laboratory, University of Kashan, Kashan, Iran

[b]Essentail Oils Research Center, University of Kashan, Kashan, Iran

E-mail: m.mohsennia@kashanu.ac.ir

Keywords: Propranolol, Atenolol, Partition coefficient, Solubility, Activity coefficient model

Introduction:

Propranolol is a non-selective beta blocker mainly used in the treatment of hypertension. Atenolol is a drug belonging to the group of drugs used primarily in cardiovascular diseases. The information obtained from the partitioning behavior of drugs in simple hydrophobic/hydrophilic systems such as *n*-octanol/water system can be used for prediction of the drug partitioning behavior in realistic biological membranes. The partition coefficient between n-octanol and water is defined as the ratio of the equilibrium concentrations of the test chemical in n-octanol saturated with water and water saturated with n-octanol and expressed as the logarithm of partition coefficient. The NRTL and UNIQUAC activity coefficient models were used for correlating of the equilibrium drugs concentrations in the n-octanol and water phases. The influence of temperature on the solubility is also discussed [1-2].

Materials and methods:

Propranolol and atenonol obtained from Tolid Daru Pharmaceutical Co., Iran. n-Octanol was supplied by Merck Co. Inc., Germany. n-Octanol and water were mutually saturated before performing the experiments. Stock aqueous solutions of propranolol or atenolol were prepared. Then n-octanol was added to specific volume of the aqueous solutions of propranolol and atenolol in glass flasks. The samples were maintained at a constant temperature with a temperature-controlled water bath. To determine the solubility of drugs, the calibration curves of drugs were established by using the standard solutions in the appropriate concentration range in n-octanol and Water. For each measurement, an excess mass of drug was added to a known mass of solvent, the analysis of the saturated solutions was carried out by UV spectrophotometer.

Apparatus:

The used UV spectrophotometer was Cintra6, GBC, Australia. The temperatures were controlled by Lauda ecoline re 206, thermostat water bath with an accuracy of ± 0.01 K.

Result and discussion:

The experimental equilibrium concentrations data at 298.15, 310.15 and 314.15K for the studied systems were determined by measuring the UV absorbance. The measured n-octanol/water partition coefficients at the different temperatures are 3.12±0.14 and 0.16±0.01 for propranolol and atenolol, respectively. The equilibrium concentrations data were correlated by the NRTL and UNIQUAC activity coefficient models. The variation of solubility with temperature was determined, solubility linearly increased with the increase in temperature.

Conclusion:

Propranolol is a liphophobic molecule and has a high partition coefficient. Atenolol has lipophilic and hydrophobic groups, so, there is not a significant difference between its solubility in n-octanol and water phases. Therefore the partition coefficient of atenolol is very lower than propranolol at the studied temperatures. The NRTL and the UNIQUAC models satisfactorily correlate the experimental equilibrium data however the NRTL model was more suitable for the studied system.

Reference:

[1] A. Brunet etal. ; " Effect of post-retrieval propranolol on psychophysiologic responding in post-traumatic stress disorder" ; Psychiatric Res.; 42, 503, 2007.

[2] M.Ch. Krugler etal. ; "Thermodynamic investigation of the water/n-octanol partition coefficient value of a 5-formyl-1, 2-dithiole-3-thione"; Thermochimica Acta; 424,143–147, 2004.

Investigation of some physical properties of Ethanol with diethylenetriamine (DETA) binary mixtures at T = (298.15, 303.15, and 308.15) K

A. A. Rostami*, M. Ramzani
Faculty of Chemistry, University ofMazandaran, Babolsar, Islamic Republic of Iran
Email: m.Ramezani 6363@Yahoo.com

Key words: Density, viscosity, Excess molar volume**,** Binary mixtures

Introduction:

The studies of thermodynamic and transport properties of binary liquid solutions contribute to the understanding of the intermolecular interactions existing among the different species in a solution and provide valuable information about changes with respect to composition and temperature. In this work, density, viscosity and excess molar volume of (ethanol + diethylenetriamine) was determined, because mixtures of alkanols with amines are interesting for a number of scientific reasons, mostly connected with the formulation of and testing of models to predict the properties of associating fluids, since the binary system under study is composed of an associating molecules of the alcohol and amines [1]. Ethanol is of interest in their own right and serve as simple examples of biologically and industrially important amphiphilic materials [2].

Materials and methods:

Diethylenetriamine were supplied by Fluka. The purity was higher than 97%. Ethanol were supplied by Merck, purity ≥ 99.9 % GC. densities and viscosities for ethanol + Diethylenetriamine were measured over the whole composition rane at 298.15, 303.15 and 308.15 K and at atmospheric pressure. From the experimental data, the excess molar volume,V^E, over the entire range of composition were calculated.

Apparatus:

The mass measurements were made on a single pan Mettler balance with an accuracy of ± 0.01 mg. Density (ρ) measurements of pure components and binary mixtures over the complete composition range were carried out using Anton Paar oscillating U tube densitometer (DA 500) with ± 10-4 g·cm-3 accuracy. The kinematic viscosity was measured with Ubbelohde viscometer with a Schott-Geräte automatic measuring unit model AVS 400.

Result and discussion:

The values of viscosity was measured and indicated in figure 1. This figure shows that viscosity decrease with increasing temperature and increase with increasing DETA mole fraction. This behavior is ascribed to a degree of self association among the DETA molecules are more than the degree of hetero association between DETA and ethanol molecules. Moreover, the excess molar volume, (V^E), was calculated from the experimental density measurement according to the following equation [3] and indicated in figure 2. : $V^E = \frac{X_1M_1+X_2M_2}{\rho} - \frac{X_1M_1}{\rho_1} - \frac{X_2M_2}{\rho_2}$

Where ρ is the density of the mixture and X_1, ρ_1, M_1, X_2, ρ_2, M_2, are the mole fraction, densities and molecular , weights of component 1 and 2, respectively. It is clear that the values of the excess molar volume are negative and are significant at each temperature throughout the entire composition range for DETA + ethanol mixture. moreover, the maximum absolute excess molar volume for a (DETA + ethanol) is observed in the ethanol-rich region of the solution. Strong interaction between solute and solvent molecules as well as packing effect, are two main point of V^E values.

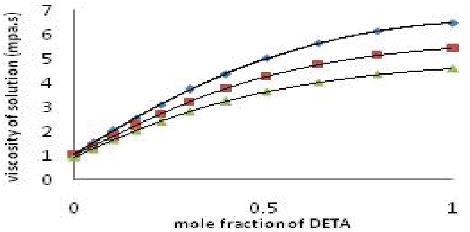

Fgure 1. plot viscosity of mixture against DETA mole fraction

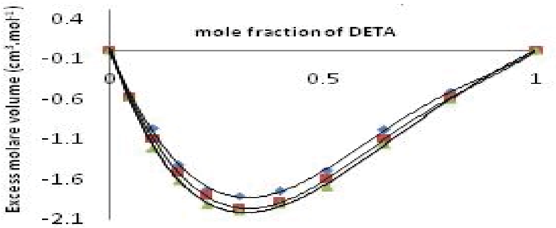

Figure2. plot of excess volume of mixtures against DETA mole fraction

Conclusion:

Densities and viscosities of diethylenetriamine with ethanol were determined over the whole concentration rang and temperature of 298.15, 303.15 and 308.15 K. these values decrease with increasing temperature. From the density value, excess molar volume was calculated that showed the negative results.

Reference:

[1] G.Dubey; M. Sharma, N. Dubey; Study of densities, viscosities, and speeds of sound of binary liquid mixtures of butan-1-ol with n-alkanes (C6, C8, and C10) at T = (298.15,303.15, and 308.15) K. J. Chem. Thermodynamics ; 40, 2008.

[2] A. Abida; A. K. Nain; S. Hyder; Molecular interactions in formamide + isomeric butanols; An ultrasonic and volumetric study; J. Solution Chem ; 32, 865-877,2003.

[3] A. Hartono;H. F .Svendsen; Density, Viscosity, and Excess Properties for aqueous Solution of diethylenetriamine(DETA); J. Chem.Thermodynamics ; 41,973-979,2009.

Solvent Effects on Protonation Constants of caffeic acid in Different Aqueous Solutions of 1- Metanol

S.Azimzadeh, [1] A. Shamel, [1] F. Gharib[2]
[1] Chemistry Department, Islamic Azad University, Ardabil Branch, Ardabil, Iran
[2] Chemistry Department, Shahid Beheshti University, G. C., Tehran, Evin, Iran
Email: S.azimzadeh82@yahoo.com

Key words: Protonation constants, Caffeic acid,metanol -Water mixtures, Kamlet-Taft Solvatochromic parameters, Solvent Effect

Introduction:

The protonation constants of caffeic acid have been determined in 10–80% (v/v) metanol-water mixtures at 25 °C and constant ionic strength (0.1 mol L^{-1} sodium perchlorate) by potentiometric technique and calculated using a suitable computer program which employs a nonlinear least- squares method. The effect of solvent composition on the protonation constants in the mixed solvents were correlated with the Kamlet-Taft solvatochromic parameters (α, β and π*). It was shown that $\log K_1$ $\log K_2$ values of caffeic acid increases with increasing metanol content up to 50% and then tend to decrease. Further, more an over-view of the effect of preferential solvation and solvent structure of electrolytes in metanol-water mixtures on the values of the protonation constants in these media were also discussed. caffeic acid is determined in different aqueous solutions of 1- metanol.

Materials and methods:

Potentiometry titration is a well known reference method for pK_a determination, and it can be easily used in organic or hydroorganic solvents. To evaluate the protonation constants, first the calibration of the potentiometer and the electrodes should be performed by Gran's method. The measured emf values in the potentiometric titration of the compound in the different aqueous solutions of 1- metanol are conducted with a suitable computer program for data treatments using a fitting method. All measurements were performed at 25 °C and constant ionic strength of 0.1 mol dm^{-3} sodium chloride.

in all cases, the procedure was repeated at least three times and the average values and the corresponding deviations from the average are reported in this work.

Apparatus:

A Jenway pH-meter, model 3520 (precision of 0.001 units of pH), was used for pH measurements.The hydrogen ion concentration was determined with a combination electrode (Jenway). A thermostat having accuracy of ± 0.1°C maintained the temperature of the potentiometric cell. [Model: EX.1200-30-6 STH, this oven is made in Iran].

Result and discussion:

The protonation constant values of caffeic acid have been determined According to the obtained results, increasing the amount of the organic solvent reduces the dielectric constant in the aqueous-1-metanol mixtures and so, in accordance with the Born equation the protonated species of the caffeic acid are expected to be more stable in media with lower dielectric constants. When electrostatic effects predominate, a plot of log K versus the reciprocal of the dielectric constant of the media should be linear.Previously, we have reported [1-2] that the dielectric constant alone cannot serve as a quantitative measurement of the solvent polarity. This property is often inadequate, since the dielectric constant description considers a solvent to be an unstructured continuum, not composed of individual solvent molecules with their own solvent-solvent interactions, and does not take into account specific solute-solvent interactions. In this work, we have used the method was introduced by Kamlet, aboud, and Taft (KAT). The KAT equation contains separate terms for non-specific as well as specific solute-solvent interactions. Finally, the dependence of acid-base equilibria on solvent composition will be discussed from the determined coefficients of KAT parameters.

Conclusion:

In this work, the protonation constants of some caffeic acid have been determined in metanol - water mixture of varying compositions (10–80% etanol by volume). It is very difficult to interpret the logK variations of the caffeic acid studied by only macroscopic parameters of the metanol-water mixtures. It is known that one of the most important factors determining the equilibrium constants is the reaction medium, so, the solvent effect on protonation constants could be explained on the basis of dielectric constant of the medium, solvent structure, preferential solvation, and microscopic parameters (as Kamlet-Taft solvatochromic parameters). A Jenway pH-meter, model 3520 (precision of 0.001units of)was used for pH measurements. The hydrogen ion concentration was determined with a combination nelectrode (Jenway). A thermostat having accuracy of ± 0.1A Jenway pH-meter, model 3520 (precision of 0.001)

Reference:

[1] A, Shamel.; F, Jaberi.; F, Gharib. J. Chem. Eng. Data; 55, 5176-5181,2010.
[2] M, Jabbari.; F, Gharib. J. Sol. Chem; 40, 561-574,2011.
[3]. F. Gharib; F. Sadeghi; Appl.Organomet. Chem. 21, 218–225,2007.

Convexity and Thermodynamic Stability

M. Bamdad
Department of Chemistry, Faculty of Sciences, Shahid Chamran University, Ahvaz, 61357-43169, Iran.
mbamdad@scu.ac.ir

Key words: entropy, internal energy, heat capacity, isothermal compressibility.

Introduction:

Thermodynamic stability term, frequently used when the comparison between systems, chemical reactions, and chemical products are studied. But it seems there is no mathematical criterion to be specified for concept of stability and the most stable system.

In this study an attempt made to express thermodynamic stability term clearly and accurately based on mathematical view using the previous literatures. Thus to provide a quantitative expression redefines and study the convexity.

Methods

The convexity of the internal energy is an important property directly related to the stability of thermodynamic system at equilibrium [1]. A convex set contains all the points of any line segment joining two points of the set.

In the figure, ADC the straight line is a convex set but ABC the curve is not. It is clearly observed that D lies between AC of course for a straight line. The systems located on this line would be thermodynamically stable [2]. For such systems it is proven that:

$$C_V = T\left(\frac{\partial S}{\partial T}\right)_V = -T\left(\frac{\partial^2 F}{\partial T^2}\right)_V \geq 0$$

$$\frac{1}{\kappa_T} = -V\left(\frac{\partial P}{\partial V}\right)_T = V\left(\frac{\partial^2 F}{\partial V^2}\right)_T \geq 0$$

where *F* is free Helmholtz energy and κ_T is isothermal compressibility [3].

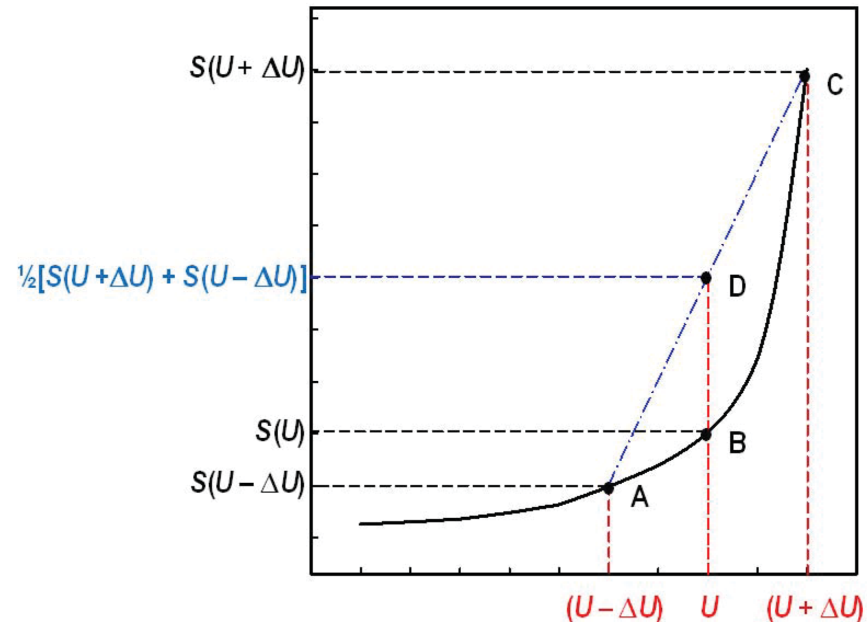

References

[1] Dorlas, T. C., Statistical Mechanics Fundamentals and Model Solutions, Institute of Physics Publishing, Bristol and Philadelphia, 1999.

[2] Callen, H. B., Thermodynamics and an Introduction to Thermostatistics, 2nd Edition, John Wiley and Sons, 1985.

[3] Galgani, L., and Scotti, A., *Physica*, **42**, 242-244, 1969**.**

Solvent effects on protonation constants of picolinic acid in different aqueous solutions of ethanol

Kh.Iranpour [a*] ,A. Shamel [a]
[a] Department of Chemistry, Islamic Azad University, Ardabil Branch, Ardabil, Iran
Email: kha.iranpour@yahoo.com

Key words: Protonation constant, Picolinic acid, Ethanol-water mixtures, Solvent effect

Introduction:

Knowledge of the physicochemical properties of the solvent, to understand the intermolecular interactions between solute-solvent and also solvent-solvent molecules, is required for proper bench work. These interactions generate new solvent properties that are absent in the pure solvent molecules which leading to phenomena such as preferential solvation that makes the nature of solute–solvents more complex. The pK_a value is a key parameter to predict the dissociation state of a molecule with respect to pH. Many compounds are sparingly soluble in water and any experimental pK_a determination requires the use of an organic or hydro-organic solvent. Mixtures of water and organic solvent, mainly methanol, ethanol, or 1-propanol, are usually employed. In the present work, the protonation constants of picolinic acid is determined in different aqueous solutions of ethanol. It has been proposed that the tryptophan metabolite picolinic acid (pyridine-2-carboxylic acid) has a physiological role in the absorption of zinc. Picolinic acid, in common with its organic derivative ethyl picolinate, is a bidentate chelating agent of divalent metals [1-6].

Materials and methods:

Potentiometry titration is a well known reference method for pK_a determination, and it can be easily used in organic or hydro-organic solvents. To evaluate the protonation constants, first the calibration of the potentiometer and the electrodes should be performed by Gran's method. The measured emf values in the potentiometric titration of the compound in the different aqueous solutions of ethanol are conducted with a suitable computer program for data treatments using a fitting method. All measurements were performed at 25 °C and constant ionic strength of 0.1 mol dm^{-3} sodium chloride.

Apparatus:

A Jenway pH-meter, model 3520 (precision of 0.001 units of pH), was used for pH measurements.The hydrogen ion concentration was determined with a combination electrode (Jenway). A thermostat having accuracy of ± 0.1°C maintained the temperature of the potentiometric cell. [Model: EX.1200-30-6 STH, this oven is made in Iran].

Result and discussion:

The protonation constant values of picolinic acid have been determined according to the obtained results, increasing the amount of the organic solvent reduces the dielectric constant in the aqueous ethanol mixtures and so, in accordance with the Born equation the protonated species of the picolinic acid are expected to be more stable in media with lower dielectric constants. In this work, we have used the method was introduced by Kamlet, Aboud, and Taft (KAT). The coefficients of KAT parameters, α, β and π* are different with each other and are almost in the order of α > π* >β. The multiple regression analysis of the data in different ranges of ethanol lead to the following preliminary conclusions: I) The protonation constants are strongly influenced by the specific solute-solvent interactions as indicated by the percentage contribution of α □and β parameters. II) Among the solvatochromic parameters of the solvent mixtures, the hydrogen bond accepter basicity parameter of the solvent is the most important, the hydrogen-bond donor acidity parameter and the polarity parameter play relatively small roles in variation of protonation constants of the picolinic acid.

Finally, the dependence of acid-base equilibria on solvent composition will be discussed from the determined coefficients of KAT parameters.

Conclusion:

In this work, the protonation constants of some picolinic acid have been determined in ethanol - water mixture of varying compositions (10–50% ethanol by volume). It is very difficult to interpret the logK variations of the picolinic acid studied by only macroscopic parameters of the ethanol-water mixtures. It is known that one of the most important factors determining the equilibrium constants is the reaction medium, so, the solvent effect on protonation constants could be explained on the basis of dielectric constant of the medium, solvent structure, preferential solvation, and microscopic parameters (as Kamlet-Taft solvatochromic parameters).

Reference:

[1] http://www.hbci.com/wenonah/hydro/picolia.htm.
[2] M. Jabbari.; F. Gharib. ; Acta Chim. Slov; 57, 325–331,2010.
[3] F. Gharib; F. Sadeghi; Appl.Organomet. Chem; 21, 218–225,2007.

Physical and electrochemical properties of metallic ionic liquids [Bu_3N Bn] [MCl_m] (MCl_m = $AlCl_4$, $FeCl_4$, $ZnCl_3$, $SnCl_5$, $CuCl_3$)

Y.Ghayeb[a], A.R.Hajipour [a], Z. Heidari Pebdani*[a]

[a] Department of chemistry, Isfahan University of Technology, Isfahan, Iran.

Email: zenabheydari.pebdani@yahoo.com

Key words: Ionic liquids, Density, Viscosity, Electrical conductivity

Introduction:

Room temperature ionic liquids (ILs) often show very useful properties such as high viscosity and density, high thermal stability, chemical stabilities and wide electrochemical windows. [1] ILs is in its infancy, it is necessary to characterize the pure ILs by their physicochemical properties including their transport properties as such information allows us to determine their use in industrial processes [2-3]. We have determined the densities and viscosities and of some metallic ILs. In this paper, we have considered the [Bu_3N Bn] cation and the metal chloride [MCl_m] anion, which were synthesized for the first time in our laboratory. The density, dynamic viscosity, refractive index, surface tension and electrical conductivities determined at the temperature range from 298.15 to 363.15 K with high accuracy.

Materials and methods:

Tributylamine was purchased from Sigma- Aldrich. Ethylenglicol, $AlCl_3$, $FeCl_3$, $ZnCl_2$, $SnCl_4$ and $CuCl_2$ were purchaced from Merck (>99%). The purity of the Ethylenglicol was verified by measuring the viscosity (η), densities (ρ), refractive index (n_D), surface tension (σ) and electrical conductivity, which were in good agreement with the literature values. The purity of the sample was further confirmed by, FT-IR and Mass spectroscopy.

Apparatus:

The dynamic viscosities (η) of these ILs were measured with a model LVDV-I PRIME digital Brookfield Co. Product. The surface tension of the ILs was measured with a KRUSS-K9 tensiometer by the ring method. Refractive indexes of the ILs were determined by using a refractometer supplied by SUR BERLIN. The apparatus was calibrated with ethanol.

Result and discussion:

The density, refractive index, electrical conductivity, dynamic viscosity, and surface tension data for the ILs were measured as a function of the temperature at atmospheric pressure at 298.15 *K*. This result confirms the good purity of the IL synthesized in our laboratory. In this case, viscosity decreases with increased temperature but, the density of ILs studied decrease nearly linearly with increasing temperature, but at a rate less than viscosity. The structures of all ILs synthesized in the present study were characterized using FT-IR*,* and elemental analysis (CHNS), and the results confirmed the desired structures.

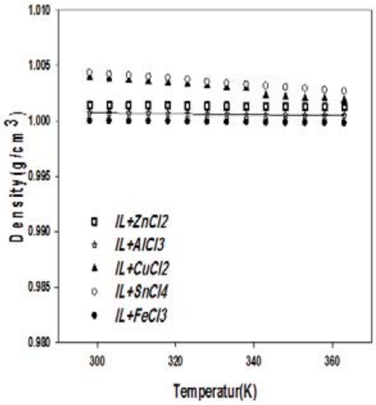

Fig: 1. Plot of the density (ρ)as a function of For four RTILs

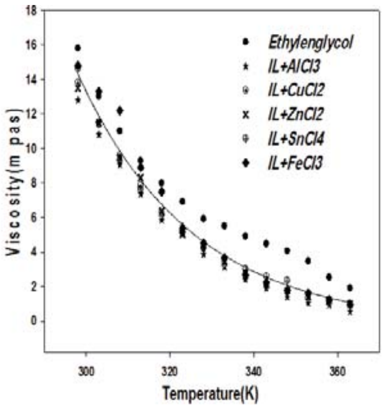

Fig: 2.Ttemperature dependence of dynamic viscosity (η) for four RTILs.

Conclusion:

The data of physical properties on ILs are essential for both theoretical research and industrial application. The establishment of the databases in this respect will definitely promote the research and development of ILs. Thus, in this work, we have carefully measured several important physical properties of ILs [Bu_3N Bn] - MCl_m (MCl_m = $AlCl_4$, $FeCl_4$, $ZnCl_3$, $SnCl_5$, CuCl3) over a wide range of temperature. Obviously, much more attention should be paid on the measurement of physicochemical properties of ILs.

Reference:

[1]. M. Kanakuboa, and etal, " Fluid Phase Equilibria 302 10–13; 2011.

[2]. A. B. Pereiro, and etal, " J. Chem. Eng. Data 52, 377-380; 2007.

[3]. M. Freemantle. "An Introduction to Ionic Liquids, Published by the Royal Society of Chemistry, www. Rsc. Org; 2010.

Thermophysical properties of acidic ionic liquids based on tributylamine at various temperatures

Y.Ghayeb[a], A.R.Hajipour[a], Z. Heidari Pebdani *[a]

[a] Department of chemistry, Isfahan University of Technology, Isfahan, Iran.

Email: zenabheydari.pebdani@yahoo.com

Key words: Ionic liquids, Physical properties, Temperature dependence.

Introduction:

Ionic liquids (ILs) are fascinating materials: salts with a melting point below 100°C, some even liquid at room temperature [1-3] due to their physical properties (low vapor pressure, high thermal and electro-chemical stability, high ion conductivity, and a good solvation ability)[2]. Our research on ILs focuses mostly on thermophysical properties of ILs. In spite of importance of properties of ILs in different applications, a small number of thermophysical data is available in the literature. The main aim of this project is to reporte these materials. ILs was synthesized for the first time in our laboratory. This is important on its own, but also from a technological point of view in order to advance a rational development of IL related applications. It is crucial to understand how physico-chemical properties depend on molecular level properties like structure, interactions, and dynamics.

Materials and methods:

Tributylamine, was purchased from Sigma- Aldrich. DMSO (>99% of purity), Sulfuric acid (98%) and nitric acid (78%) and phosphoric acid (99%) and Choleric acid (37%) were purchased from Merck. The purity of the DMSO was verified by measuring the viscosity (η), refractive index (n_D), surface tension (σ), Electrical conductivity, densities (ρ) and pH which were in good agreement with the literature values. The purity of the ILs was further confirmed by FT-IR and ^{1}H-NMR spectroscopy.

Apparatus:

The dynamic viscosities (η) of these ILs were measured with a model LVDV-I PRIME digital the Brookfield Co. Product. The surface tension of the ILs was measured with a KRUSS-K9 tensiometer by the ring method. Refractive indexes of the ILs were determined by using a refractometer supplied by SUR BERLIN. The apparatus was calibrated with Ethanol.

Results and discussion:

The density, refractive index, electrical conductivity, dynamic viscosity, and surface tension data for the ILs were measured as a function of the temperature at atmospheric. This result confirms the good purity of the IL synthesized in our laboratory. In this case, viscosity decreases with increased temperature (fig: 2). For each of the four dried RTILs, was determined as a function of T at temperatures of (293.15 to 343.15) K(fig: 1). The structures of all ILs synthesized in the present study were characterized using FT-IR, H^1-NMR, and elemental analysis (CHNS), and the results confirmed the desired structures.

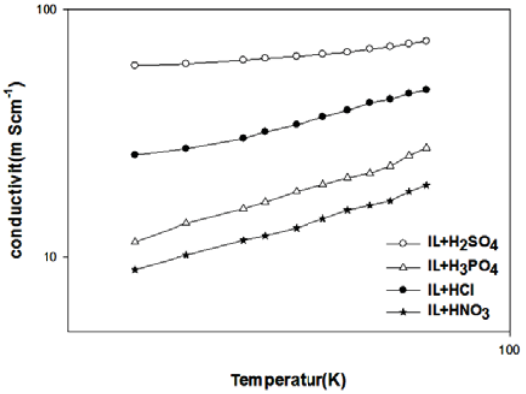

Fig: 1. Plot of the electrolytic conductivity as a function of for four RTILs

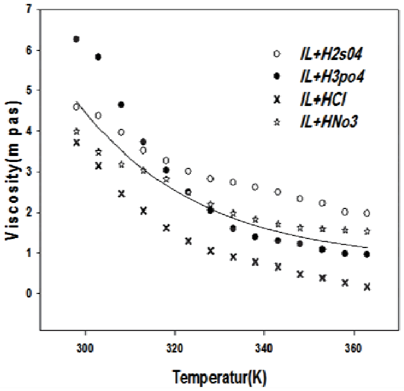

Fig: 2.Ttemperature dependence of dynamic viscosity (η) for four RTILs.

Conclusion:

The data of physical properties on ILs are essential for both theoretical research and industrial application. The establishment of the databases in this respect will definitely promote the research and development of ILs. Thus, in this work, we have carefully measured several important physical properties of ionic liquids tributyl ammonium chloride, tributyl ammonium nitrate, and tributyl ammonium hydrogen sulphate and tributyl ammuniom dihydrogene phosphate over a wide range of temperature. Obviously, much more attention should be paid on the measurement of physicochemical properties of ILs.

Reference:

[1]. J. Safarov and etal; "J. Chem. Thermodynamics; 43, 1315–1322, 2011

[2]. S. S. Moganty and etal; "Eng. Chem. Res.**,** 49, 5846–5853; 2010

[3]. M. Freemantle. "An Introduction to Ionic Liquids, Published by the Royal Society of Chemistry, www. rsc. org; 2010.

Calculation of spinodal density in subcritical region for liquid argon

S. A. Razavizadeh*[a], F. Alirezapoor[b]
[a] Department of Chemistry, Faculty of sciences, Payame Noor University (PNU), shiraz, Iran
[b] Department of Chemistry, Payame Noor University (PNU), Estahban, Iran
(Email: razavi_zadeh@yahoo.com)

Key words: Equation of state, Subcritical, Spinodal density, Argon.

Introduction

Equations of state are used for calculation of thermodynamic properties and phase behavior of fluids. One of the applications of equation state is calculation of spinodal density. The spinodal density is the locus of vanishing first derivative of isotherms, $\left(\frac{\partial p}{\partial \rho}\right)_T = 0$. In this work by using of proposed equation of state [1] which is expressed in terms of reduced variables, we calculated spinodal density in subcritical region for liquid argon. This equation is expressed in the following nondimensional form

$$p_{r=} \zeta \rho_r T_r - [1+\tau \rho_r^2 A][1-\upsilon \rho_r B] \tag{1}$$

where A and B are defined [1,2] :

$$A = \sum_{i=0}^{2} a_i x^i + \alpha_{na}|x|^{4+\delta} \quad , \quad B = \sum_{i=0}^{2} b_i x^i + \beta_{na}|x|^{4+\delta} \tag{2}$$

We will denote the reduced spinodal densities by z_{sl} where $z_{sl} = \rho_{sl/}\rho_c$ is the spinodal density of the liquid. It should be noted that $\lim_{T \to T_c} z_{sl} = 1$ since the spinodal curve shares the same tangent with the critical isotherm at the critical point.

Calculation method

In the subcritical region of density and temperature, the temperature dependence of parameters must be known. To find this dependency we assumed the following relation:

$$a_i^k(t) = a_i^k(0) + c_i^k |t|^{\varepsilon_i^k}$$

$$b_i^k(t) = b_i^k(0) + d_i^k |t|^{\varepsilon_i^k} \qquad (k = c,\ l,\ v),\ (i=0,\ 1,\ 2) \qquad (3)$$

Here, *c*, *l*, and *v* stand for critical, liquid, and vapor, respectively. Where $\varepsilon > 0$ and c_i^k and d_i^k are parameters. We find out that for fitting the equation, spinodal densities is essential for each temperature. Because of absence of experimental spinodal densities we calculated spinodal densities from generic van der Waals equation of state.

Then we applied $\left(\frac{\partial p}{\partial \rho}\right)_T = 0$ for equation (1) and we obtained the following equation

$$\frac{\zeta T_r\left(1+v z_k^2 \mathcal{B}_k^{(1)}\right)}{(1-v\mathcal{B}_k z_k)^2} - 2\tau \mathcal{A}_k z_k - \tau z_k^2 \mathcal{A}_k^{(1)} = 0 \qquad k=(sl) \qquad (4)$$

By replacing parameters of eqs 3 in eq 4 we have

$$\frac{\zeta T_r[(1+v(b_1(0)+d_1|t|^{\varepsilon})z_k{}^2]}{[1-v(1+d_{0k}|t|^{\varepsilon})z_k]^2} - \tau z_k[2(1+c_{0k}|t|^{\varepsilon}) + (a_1(0)+c_1|t|^{\varepsilon})z_k] = 0 \qquad (5)$$

According to eq 5 spinodal density (z_k) can be calculated for liquid argon.

Result and discussion

The comparison of calculated spinodal densities of original van der Waals and equation of state (5) is shown in Fig 1.

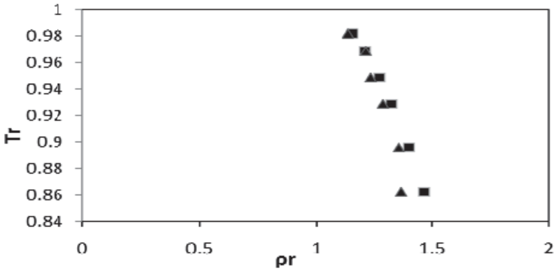

Fig 1. Calculated spinodal densities from original van der Waals (▲), and from equation 5 (■)

Results indicate that the calculated spinodal densities by the proposed equation of state over the whole subcritical temperatures especially in the neighborhood of the critical point are good agreement with the calculated spinodal densities of original van der Waals.

Conclusion

The temperature dependence of coefficients a_{0k}, $a_1^{(k)}$, b_{0k} and $b_1^{(k)}$ (k=sl, sv) determine the temperature dependence of the spinodal curve and vice versa. Using equation of state, spinodal density can be calculated. The obtained results show calculated spinodal density has more acceptable representation near critical point.

References

[1]. B. C. Eu; K. Rah; J. Phys. Chem. B.; 107, 4382-4391, 2003.

[2]. B. C. Eu; J. Chem. phys; 114, 10899, 2001.

Densities, speed of sound and isentropic compressibilities of three binary mixtures Benzyl alcohol with *tert*-butanol, 1,2-butandiol and 2-methyl-1-butanol

Mohammad Mehdi Alavianmehr*, Nahid Hemmati

Department of Chemistry, Shiraz University of Technology, Shiraz, 71555-313, Iran

Phone: 0917-716-7775, Fax: 98-711-735-4520, alavianmehr@sutech.ac.ir

Key words: Alcohols; Binary mixtures; Density; Speed of sound

Introduction:

Despite the extensive studies on thermodynamic properties of binary mixtures of alcohols [1-3], so far relatively less attention has been given to the mixtures containing an aromatic alcohol. Accurate information about the real behavior of these systems is very important for synthesis and design of chemical processes, so efforts have been made to overcome this lack of data. Benzyl alcohol was chosen for the present study because, except for its usage in perfumery, it is widely used in microscopy as the embedding material. Benzyl alcohol is also important as a solvent for gelatin, cellulose acetate, and shellac and in pharmaceutical applications as an antimicrobial agent.

Materials and methods:

Densities and speeds of sound for pure liquids and their binary mixtures were measured using an Anton Paar DSA 5000 vibrating u-tube densimeter and sound analyzer, with a certified precision of $\pm 1\cdot 10^{-6}$ g.cm^{-3} and ±0.1 m·s^{-1}, respectively. Before the measurements, all the components were partially degassed (20 min) using an ultrasound (MISONIX Ultrasonic Liquid Processors). Solutions were prepared by mass using an analytical balance (SartoriusTE124S) with a precision of $\pm 1\cdot 10^{-4}$ g and kept in sealed flasks. The experimental uncertainties in the density and speed of sound are estimated to be better than $\pm 5\times 10^{-6}$ g cm^{-3} and ±0.05 m s^{-1}, respectively.

Results and Discussion:

In the present study, the composition and temperature dependence of volume and compressibility changes upon mixing for binary mixtures Benzyl alcohol with *tert*-butanol, 1, 2-butandiol and 2-methyl-1-butanol were investigated using densimeter DSA 5000 (Anton Paar, Austria). Densities and speed of sound were measured over the entire range of composition and at six temperatures 25°C, 30°C, 35°C, 40°C, 45°C, and 50°C and ambient pressure. The excess properties were calculated using the experimental data points and fitted with the Redlick-Kister type equation. Further the effect of temperature on excess properties was also investigated. The experimental densities and speed of sound of pure liquids of this work agree well with those reported in literature. This agreement gives a verification of the results obtained by the densimeter. Further, the excess molar volumes, V_m^E, were calculated from the experimental densities for pure and mixtures. Typically, the below Figure shows the experimental excess molar volume as a function of the benzyl alcohol mole fraction (x_1) for [benzyl alcohol + *tert*-butanol] mixture at three temperatures.

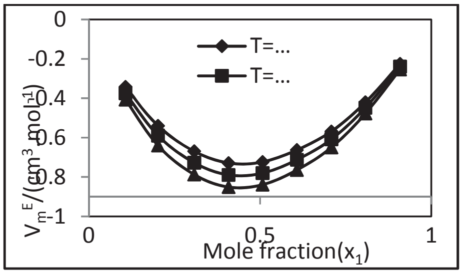

Conclusion:

As outlined earlier all systems under study showed non-ideal behavior. This non-ideality can be explained by two factors intermolecular forces in the mixture and enhanced rigidity. The main source of intermolecular interactions comes from hydrogen bonding between the components and also interaction between electrons of benzene ring and proton of alkanols.

References:

[1] H. A. Zarei, S. Asadi, H. Ilukhani; "Temperature dependence of the volumetric properties of binary mixtures of (1-propanol, 2-propanol and 1,2-propanediol) at ambient pressure (81.5 kPa)" ; J.Mol. Liq; 141, 25-30, 2008.

[2] E. Zorebski, B. Luboweiecka-Kostka; “Thermodynamic and transport properties of (1,2 ethanediol+1-nonanol) at temperatures from (298.15 to 313.15)K” ; J. Chem. Thermodym; 41, 197-204, 2009.

[3] E. Zorebski, M. Geppert-Rybczynska, B. Maciej; “Densities, Speeds of Sound, and Isentropic Compressibilities for Binary Mixtures of 2-Ethyl-1-hexanol with 1-Pentanol, 1-Heptanol, or 1-Nonanol at the Temperature 298.15 K” ; J. Chem. Eng. Data; 55, 1025-1029, 2010.

Thermodynamic denaturation of α-Lactalbumin presence of cetylpyridinium chloride and hexadecyl trimethyl ammonium bromide

R.gamoori [a]* , Dr Z.Saadati[b]

[a] Department of chemistry , Islamic Azad University , Omidiyeh Branch , Omidiyeh , Iran

[b] Department of chemistry , Islamic Azad University , Omidiyeh Branch , Omidiyeh , Iran

Abstract:

In this work , we determined the stability parameters of α-Lactalbumin in presence of cetylpyridinium chloride (CPC) and hexadecyl trimethyl ammonium bromide (HTAB) as cationic surfactants. The experiments took place over the temperature range of 298 K to 318 K. For each transition curve at any specific temperature , the conventional method of analysis , which assumes a linear concentration dependence of the pre- and post- transitionbase lines , gave the most realistic values for $\Delta G_D(H_2O)$.

Keywords : α-Lactalbumin , Surfactant , Denaturation , Protein stability

Introduction:

α-Lactalbumin is a small metallo protein that exists in mammalian milk. As a regulatory subunit of lactose synthase system[1] . Recently , the intraction of α-LA with all clasess of surfactants was studied by Daniel E.Otzen [2].

Here , we show that the sigmoidal transition curves were obtained for α-LA due to its intraction with CPC and HTAB . This enables us to evaluate the thermodynamic stability of α-LA at each temperature.

Methods:

The concentration of α-LA was determined experimentally by using the value of 29210 $M^{-1}.cm^{-1}$ for the molar absorption coefficient(ε) at 280 nm. For optical measurements ,all solution were prepared in 50mM phosphate buffer at pH=8.0. The device used a Lambda35 spectropolarimeter equipped with a temperature control peltier 6+6 .

Results and discussion:

The Gibbs free energy of denaturation ,ΔG_D, was calculated as a function of CPC and HTAB concentration by assuming a two-state mechanism[3,4] and using the following equation [5]:

$$\Delta G_D = -RT \ln K = -RT \ln(F_D/(1-F_D)) = -RT \ln [(Y_N - Y_{obs})/(Y_{obs} - Y_D)] \qquad (1)$$

The ΔG_D was plotted against [denaturant] and a linear least-squares analysis was used to fit the ΔG_D and [denaturant] data to the following relation [6]:

$$\Delta G_D = \Delta G_D(H_2O) - m[\text{denaturant}] \qquad (2)$$

For example , the CPC estimates shown in table1.

Table1:

Parameters characterizing the CPC denaturation for α-Lactalbumin at various temperatures.

T / K	m / (kj.mol^{-1}.M^{-1})	$\Delta G_D(H_2O)$/(kj.mol^{-1})
298	858 . 10^{-3}	10.29
308	928 . 10^{-3}	13.88
318	776 . 10^{-3}	10.40

Reference

[1] Eugene A.Permyakov,Lawrence J.Berliner. FEBS Letters 473(2000) 269-274

[2]Daniel E.Otzen , Pankaj Sehgal , Peter Westh.Journal of Colloid and Interface Science 239 (2009) 273-283

[3]W.Pfeil , P.L.Privalov , Biophys.Chem.4(1976)33-40

[4] P.L.Privalov , Adv. Protein Chem. 33(1979) 167-241

[5]C.N.Pace , Trends Biotechnol. 8 (1990)93-98.

[6]R.F.Greene, C.N.Pace, J.Biol.Chem.249(1974)5388-5393

Thermodynamic characterization of the betaine and sarcosin effect on Protein stability

S . Makvandi [a*] , Z . Saadati [a]

[a] Department of chemistry, Faculty of sciences, Islamic Azad University, Omidiyeh Branch Omidiyeh, Iran

Email: Makvandi_Sara@yahoo.com

Key words: Denaturation, Osmolytes, Betaine, Sarcosin, Protein stability.

Introduction:

Osmolytes are cosolvents that are used to protect organism from harsh environmental stresses. These molecules stabilize proteins, not interacting with them directly but altering the solvent properties of surrounding water and hence protein-solvent interactions [1].their effect seems to be general for all proteins. Those having enhancing effect on protein functions are called counteracting osmolytes and those having no inhibitory or enhancing effect are called compatible osmolytes [2]. There are various mechanisms that have been used to explain the observation on the effect of osmolytes on the protein denaturation equilibrium, native (N) state ↔ denatured (D) satte [3]. The most widely used mechanism is due to Timasheff. Small proteins tend to exhibit all-or-none transitions between their native and unfolded forms in equilibrium. This holds particularly for equilibrium conditions, while in kinetic measurements there may be folding intermediates, or temporary off-pathway misfolding events. Such all-or-none transitions are characterized by a shift in population, where fully native proteins are in equilibrium with fully denatured proteins. The stability of a protein is defined as the difference in Gibbs free energy between the denatured (D) and native (N) state: $\Delta G° = -\mathrm{RT}\ln K = -\mathrm{RT}\ln\frac{\mathrm{D}}{\mathrm{N}}$

Materials and methods:

Beta lactalbumin(Blg) and Betain and sarcosin wase purchased from sigma. each heat-induced transition curve was analysed for T_m (midpoint of denaturation) and ΔH_m (enthalpy change at T_m) using a non-liner least-squares analysis according to the relation,

$$y(T) = \frac{Y_N(T)+Y_D(T)\exp\left[-\frac{\Delta H_m}{R\left(\frac{1}{T}-\frac{1}{T_m}\right)}\right]}{1+exp\left[-\frac{\Delta H_m}{R\left(\frac{1}{T}-\frac{1}{T_m}\right)}\right]}$$

the analysis of the transition curve, it was assumed that a parabolic function describes the dependence of the optical properties of the native and denatured protein molecules. a plot of ΔH_m versus T_m gave the value of ΔC_p, the temperature-independent heat capacity change at constant pressure. Using values of T_m, ΔH_m and ΔC_p, the value of ΔG_D at any T, $\Delta G_D(T)$ was estimated with the help of the Gibbs-Helmholtz equation,

$$\Delta G_D(T) = \left(\frac{T_m - T}{T_m}\right) - \Delta c_p\left[(T_m - T) + T\ln\left(\frac{T}{T_m}\right)\right]$$

Apparatus:

Thermal denaturation studies were carried out in a Lambda 35 spectropolarimeter equipped with a peltier type temperature controller (PTP 6+6) with a heating rate of 1°c/min.

Result and discussion:

β-Lactoglobulin is the major whey protein of ruminant. In the research is done thermal denaturation of β-lactoglobulin in the absence and presence of varying concentrations of Betain and Sarcosin in the 298 nm and in the temperature range 20-90ºc. Was shown that the thermal stability of proteins in the presence of Betain and Sarcosin is increased and against of the thermal denaturation and accumulation in an artificial environment, the proteins are protected.

The results show that increase in concentration of osmolyte, increases $\Delta G°_D$. And whatever $\Delta G°_D$ is more positive, the thermodynamic stability of proteins in the presence of osmolyte , Increasing.

Conclusion:

We can use of osmolyte to improve the stability of protein in the field of protein manufacturing. Stabilizations achieved by additives are simpler and less expensive than stabilization resulting from protin engineering. A further advantage is that the stabilizing agent could be added to the protein solution just when desired, for instance during stronger or in the course of a thermal treatment.

Reference:

[1] S.N. Timasheff, The control of protein stability and association by weak intractions with water: how do solvents affect these processes?Annu. Rev. Biophys. Biomol.22(1993)67-97
[2] Q. Zou, B.J. Bennion, The molecular mechanism of stabilization of proteins by TMAO and its stability to counteract the effect of urea, J. Am. Chem. Soc.124(2002)1192-1202
[3] D.W. Bolen, Trimethylamine-N-oxide counteracts urea effect on rabbit muscle lactate dehydrogenase function: a test of the counteraction hypothesis, Biophys. 74(1998)2666-2673

Phase Equilibrium of Water + Formic Acid + 1-Heptanol ternary Liquid Systems at T=298.15 K.

H. Ghanadzadeh Gilani[b], Sh. Asan[a,*], A. Oladzadeh[b], M. Azadian[b].
[a]Department of Chemistry,Faculty of Science, University of Urmia, Urmia, Iran
[b]Department of Chemical engineering, University of Guilan, Rasht, Iran
E-mail address: shahryar.oladzadeh@gmail.com

Abtract:

Liquid–liquid equilibrium data of the solubility (binodal) curves and tie-line end compositions are presented for mixtures of [water (1) + formic acid (2) + 1-Heptanol (3)] at 298.15K and 101.3±0.7 kPa UNIQUAC model. The reliability of the model has been analyzed against the LLE data with respect to the distribution ratio and separation factor. The root mean square deviation (RMSD) between the observed and calculated mass percents was 0.4885%.

Keywords: Liquid-liquid equilibrium; Tie-line data; Formic acid; 1-Heptanol; UNIQUAC model; Separation factor; Distribution coefficient.

Introduction:

The efficient separation of organic acids from aqueous solutions is an important concept in the chemical fermentation industry where many solvents have been tested to improve such recovery [1–2]. In this work, 1-Hetanol, a protic and polar aliphatic compound of low vapor pressure is used as a solvent in the separation of carboxylic acids from water. Most heavy normal n-alkanol solvents used to extract a carboxylic acid show a distribution coefficient less than one [3]. Nevertheless, such studies, besides other purposes, are indispensable in calibration and verification of analytical models. Liquid–liquid equilibrium (LLE) data for extraction of a carboxylic acid from water through heavy n-alkanols is scarce in the literature [4]. In the course of the present study, the LLE of the ternary system (water/Formic acid/1-Heptanol) were investigated experimentally at T= 298.15 K, and the values for the interaction parameters were obtained for the UNIQUAC model. The values of the interaction parameter in the UNIQUAC model with temperature dependent were also investigated for this system. The effect of Formic acid addition on solubility of water in 1-Heptanol (organic phase) was also investigated at T= 298.15 K.

Method:

The Heptanol and Formic acid were obtained from Merck with mass fraction purities of 0.995 and 0.998, respectively. The purity of these materials was checked by gas chromatography and used without further purification. Distilled water was used throughout all experiments.

Results and discussion:

Since (formic acid + water) and (1-Heptanol +formic acid) are two liquid pairs that are completely miscible and the only liquid pair (water + 1-Heptanol) is partially miscible, the ternary system behaves as a type 1 LLE [5]. The area of the two phase region depends on the solubility of water in the organic phase. It can be seen that the water solubility in 1-Heptanol is extremely low. In order to evaluate the extracting capability of 1-Heptanol for the separation of Formic acid from aqueous solutions, the separation factor (S) was calculated.The reliability of experimentally measured tie-line data can be determined by applying the Othmer-Tobias and Bachman correlation equation.

Conclusions:

An experimental investigation of equilibrium behavior of the system composed of water/Formic acid/1-Heptanol was carried out at T=298.15 K. The UNIQUAC model was used to correlate the experimental LLE data. The optimum UNIQUAC interaction parameters between water, Formic acid, and 1-Heptanol were determined using the experimental liquid–liquid data. The RMSD value between the observed and calculated mass percents with a reasonable error was 2.58% for the UNIQUAC model. The solubility of water in 1-Heptanol increases with amounts of Formic acid added to water + 1-Heptanol mixture.

Refrences :

[1] H. GhanadzadehGilani, M. Golpour, S.S. Ashraf, Fluid Phase Equilib.310 (2011) 192–197.

[2] H. GhanadzadehGilani , M. Golpour, B. AbbasiSouraki, J. Chem. T. dyn. 49(2012)39-45

[3] H. GhanadzadehGilani , A. Ghanadzadeh Gilani , S. Shekarsaraee , H. Uslu J. Chem. T. dyn 53 (2012) 52–59.

[4] A. Senol, Fluid Phase Equilibria 243(2006)51–56.

[5] A. GhanadzadehGilani, N. Paktinat, M. Moghadam, J. C. Thermodyn. 43 (2011) 569–575.

(Liquid + liquid) equilibria in ternary aqueous mixture of Formic acid with 1-Hexanol at T = 298.2 K.

H. Ghanadzadeh Gilani[a]; A. Oladzadeh[a]; SH.Asan[b, *]; S. Nemati Matak[c].
[a]Department of Chemical engineering, University of Guilan, Rasht, Iran
[b]Department of Chemistry,Faculty of Science, University of Urmia, Urmia, Iran
[c]Department of Chemistry,Faculty of Science, Islamic Azad University of Rasht, Rasht, Iran
E-mail: shahryar.oladzadeh@gmail.com

Key word: LLE, Ternary system, UNIQUAC, Formic acid, 1-Hexanol.

Abstract:

Ternary equilibrium data for the mixtures of {water + Formric acid + 1-Hexanol} were determined at T = 298.2 K and atmospheric pressure. Solubility data were determined by the cloud-point titration method. In order to obtain the tie-line data, the concentration of each phase was determined by acidimetric titration, the Karl–Fischer technique. The experimental tie-line data were correlated using the UNIQUAC model. The reliability of the experimental data was determined through the Othmer–Tobias and bachman plot. Distribution coefficients and separation factors were evaluated over the immiscibility regions.

Introduction:

Precise (liquid + liquid) equilibrium (LLE) data of ternary mixtures are necessary for design and simulation of many chemical processes and separation operations [1–2]. In general, type of solvent and temperature are the most important factors which influence separation effectiveness, immiscibility region and LLE behavior of ternary systems. The pure FA is widely used in food and beverage industries, where high purity raw materials are necessary [3].More recently, the solubility and tie-line data for the ternary systems consisting of water, FA and organic solvents at various temperatures have been reported in our current publications [4]. In this research, 1-Hexanol was tested as organic solvent for recovery of FA from water. The focus of this study is placed on the phase behavior of LLE for ternary system of (Water + FA + 1-Hexanol).The values for the interaction parameters were obtained and the calculated compositions compared with the experimental ones. Distribution coefficients (D) and separation factors (S) were determined from the tie-line data to establish the possibility of the use of this solvent for the separation of FA from water.

Methods:

1-Hexanol with stated mass fraction purity higher than 0.99 was obtained from Merck. Deionized and redistilled water was used throughout all experiments. All materials were used as received without any further purification. The purity of the acid was checked through acidimetric titration with 1 N NaOH. The water content of the organic phase was measured by the Karl–Fisher method using Metrohm-870 KF Titrino plus Karl–Fisher titrator.

Results and discussion:

Since (Formic acid + Water) and (1-Hexanol +formic acid) are two liquid pairs that are completely miscible and the only liquid pair (water + 1-Hexanol) is partially miscible, the ternary system behaves as a type 1 LLE . The area of the two phase region depends on the solubility of water in the organic phase. It can be seen that the water solubility in 1-Hexanol is extremely low. In order to evaluate the extracting capability of 1-Hexanol for the separation of Formic acid from aqueous solutions, the separation factor (S) was calculated.

Conclusions:

Solubility and tie-line data for the (water + FA + 1-Hexanol) ternary system were obtained at T = 298.2 K. The UNIQUAC model was used to correlate the experimental data and to calculate the phase compositions of the mixtures studied. The corresponding optimized binary interaction parameters were also calculated. The model give relatively acceptable results for the investigated system. It is concluded that the solvent and temperature effects on the equilibrium data of the investigated systems are slight. The separation factors and distribution coefficients for the organic solvent used in this work were calculated.

References:

[1] H. GhanadzadehGilani , A. GhanadzadehGilani , S. Shekarsaraee , H. Uslu. J. C. Thermodyn 53 (2012) 52–59.

[2] A. Senol, Fluid Phase Equilib. 243 (2006) 51–56.

[3] B. Başlıoğlu, S. Cehreli, Fluid Phase Equilibria 312 (2011) 85– 92.

[4] M. Bilgin, I. Birman, Fluid Phase Equilibria 302 (2011) 249–253.

Liquid phase equilibria of (Water + Formic acid + 1-Octanol) ternary systems at T= 298.2K and atmospheric pressure.

H. Ghanadzadeh Gilani[a]; SH.Asan[b,*].M. Azadian[a].

[a]Department of Chemical engineering, University of Guilan, Rasht, Iran

[b]Department of Chemistry,Faculty of Science, University of Urmia, Urmia, Iran

E-mail: soroosh_net12@yahoo.com

Key word: LLE, Ternary system, UNIQUAC, Formic acid, 1-Octanol.

Abstract:

Liquid-liquid equilibrium (LLE) data including solubility curves and tie-line compositions were measured for mixtures of water (1) + formic acid (2) + 1-Octanol (3) at *T*=298.2 K and atmospheric pressure, *p* = 101.3± 0.7 kPa. The reliability of the experimental tie-line data was confirmed by using the Othmer-Tobias and Bachman correlations. The LLE data of the ternary systems were predicted by UNIQUAC method. Distribution coefficients and separation factors were evaluated for the immiscibility region.

Introduction:

It is widely used in the textile industry, tanning industry, rubber processing industry, and pharmaceutical industry.In the industrial synthesis of formic acid, for example, by the reaction of methanol and carbon monoxide and hydrolysis of the methyl formate formed, aqueous solutions containing (20 to 50) % acid are always obtained. When concentrated by distillation, these aqueous solutions give an azeotrope, so that the formic acid cannot be obtained directly in an anhydrous form. Distillation under pressure, extractive distillation, and azeotropic distillation are used to concentrate the solutions. These processes are of high-energy consumption. To reduce the cost of concentrating acid solutions, extraction can be applied as an alternative [1]. The extractions of formic acid equilibria have been studied by some researchers [2, 3]. This study is part of a research program on the recovery of carboxylic acids from dilute aqueous solutions using organic solvents. The objective of this work is to recover formic acid from dilute aqueous solutions by using environmentally friendly solvent with a high-boiling point. In this paper, LLE results were reported for the ternary system water + formic acid+ 1-Octanol at *T*= 298.2 K, for which no such data have previously been published.

Methods:

1-Octanol with stated mass fraction purity higher than 0.99 was obtained from Merck. Deionized and redistilled water was used throughout all experiments. All materials were used as received without any further purification. The purity of the acid was checked through acidimetric titration with 1 N NaOH. The water content of the organic phase was measured by the Karl–Fisher method using Metrohm-870 KF Titrino plus Karl–Fisher titrator.

Results and discussion:

Since (Formic acid + Water) and (1-Octanol +formic acid) are two liquid pairs that are completely miscible and the only liquid pair (water + 1-Octanol) is partially miscible, the ternary system behaves as a type 1 LLE. The area of the two phase region depends on the solubility of water in the organic phase. It can be seen that the water solubility in 1-Hexanol is extremely low. In order to evaluate the extracting capability of 1-Octanol for the separation of Formic acid from aqueous solutions, the separation factor (S) was calculated.

Conclusions:

Solubility and tie-line data for the (water + FA + 1-Octanol) ternary system were obtained at T = 298.2 K. The UNIQUAC model was used to correlate the experimental data and to calculate the phase compositions of the mixtures studied. The corresponding optimized binary interaction parameters were also calculated. It is concluded that the solvent and temperature effects on the equilibrium data of the investigated systems are slight. The solubility of water in alkohols decreases with an increase of carbon chain length. It is shown that formic acid is more soluble in the water phase than in the 1-Octanol phase. Separation factors, which are indications of ability of the solvent chosen to separate formic acid from water, were found between 5.53 and 15.24. The correlation results gave rmsd values of 1.5812 for the systems with 1-Octanol. These comparative data show that the correlation based on UNIQUAC model grants compatible results with experimental tie-line data.

References:

[1] H. Ghanadzadeh, A. Ghanadzadeh, Z. Aghajani, S. Abbasnejad, S. Shekarsaraee,. Chem. Thermodyn. 42 (2010)695-699

[2] H. Uslu, C. Bayat, S.Go¨kmen, Y.Yorulmaz, J. Chem. Eng. Data 2009, 54, 48–53.

[3] M. Bilgin, I. Birman, Fluid Phase Equilibria 302 (2011) 249–253

The Free Expansion of Hard Sphere Confined Fluid Using DDFT

F .Heidari*[a] , E. Keshavarzi[a]

[a]Department of Chemistry, Isfahan University of Technology ,Isfahan, Iran

Email: F.Heidari@ch.iut.ac.ir

Introduction:

Confined systems have attracted a great deal of attention during the past years because of their interesting and different behavior from the bulk. One of the theoretical approaches to study these systems is classical density functional theory (DFT) which is a remarkably successful theory for describing the behavior of the equilibrium structure of homogeneous and inhomogeneous fluids. Moreover, in the recent years the off equilibrium properties of such systems have represented a very active field of research. The extension of this framework to dynamical situations has motivated very recently a large number of studies that resulted in the formulation of dynamic density functional theory (DDFT) [1]. We are able to investigate a large variety of phenomena in various different fields using DDFT [2]. In this work, the relaxation of hard sphere confined fluid in a nanoslit pore has been studied using dynamical density functional theory.

Theory:

The Langevin equation for N Brownian particles of coordinate r interacting via an arbitrary pair potential $U(r^N)$ and experiencing an external field $V_{ext}(r)$ is [3]:

$$m\frac{d^2 r_i(t)}{dt^2}+\Gamma^{-1}\frac{dr_i(t)}{dt}=-\nabla_i U(r^N,t)+\eta_i(t) \tag{1}$$

where m is the mass of particles, $\eta(t)$ is a white noise term with the property $\langle\eta(t)\rangle=0$ and the constant Γ is mobility. When the constant Γ^{-1} is large, we may neglect the second derivative with respect to time in Eq. (1) and we obtain the stochastic equation of motion as,

$$\frac{dr_i(t)}{dt}=-\Gamma\nabla_i U(r^N,t)+\Gamma\eta_i(t) \tag{2}$$

According to Eq. (2), one can generate the equation for the probability distribution function $P(r^N,t)$ as:

$$\frac{\partial P(r^N,t)}{\partial t} = -\sum_{i=1}^{N} \nabla_i \left[v_i P(r^N,t) \right] \tag{3}$$

Where $v_i = \sum_{j=1}^{N} \Gamma_{ij} F_j$ and F_j is the force on *j*th particle. As the one body density is merely the integral of the probability distribution function, according to Eq. (3) and after some mathematical calculations we have:

$$\Gamma^{-1} \frac{\partial \rho(r,t)}{\partial t} = \nabla \left[\rho(r,t) \nabla \frac{\delta F[\rho(r,t)]}{\delta \rho(r,t)} \right] \tag{4}$$

Where $F[\rho(r,t)]$ is the Helmholtz free energy functional. For an equilibrium hard sphere fluid, Rosenfeld's fundamental measure theory provides a scheme for $F[\rho(r)]$ which may be used as an input to DDFT. Eq. (4) is the deterministic DDFT equation which has the form of continuity equation. Our system is a hard sphere fluid of diameter σ confined in a nanoslit pore with two attractive parallel and structureless walls. We have studied free expansion of fluid in absence of external potential using Eq. (4). In the initial configuration, at t=0, the temperature is fixed to $T = 1$, the attractive walls are set at fixed position separated by a porewidth, H=6 and bulk density is 0.3. In such condition system has strong oscillatory behavior. When the attractive external potential is switched off the oscillations of density profile become weaker and then disappear.

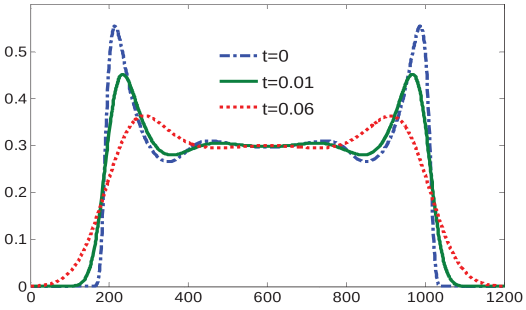

Conclusion:

The main reason of oscillatory behavior of this system lies in the influence of system walls. It will be disappear gradually when the external potential is switched off and its time evolution is predictable using DDFT.

References:

[1] U.B. Marconi and P. Tarazona, *J. Chem. Phys,* V.110, No. 16, P. 8032, 1998.

[2] W. Mickel, L. Joly, and T. Biben, *J. Chem. Phys*, V. 134, P. 094105, 2011.

[3] F. Penna and P. Tarazona, *J. Chem. Phys*, V. 124,P. 164903, 2006.

On the Calculation of Surface Thickness of Electrolyte Solutions Using Inversion Method

Mohsen Najafi[1] and Ali Maghari[2]

[1]Nuclear Science and Technology Research Institute, AEOI, Tehran, Iran
mmnajafi@aeoi.org.ir , msnnajafi@gmail.com
[2]Department of Physical Chemistry, School of Chemistry, College of Science,
University of Tehran, Tehran, Iran

Abstract:

In this paper, we investigate the vapor-liquid interfacial thickness of seven electrolyte solutions using the inversion procedure of experimental data of surface tension. In this method, the surface tension data has been performed to invert the vapor-liquid interfacial surface thickness by using the density functional and statistical associating fluid theories.

Introduction:

The boundary layer between two liquid and gas phases may be considered as a third phase with properties intermediate between those of a liquid and its vapor. From a microscopic point of view, there are unequal forces acting upon the molecules, i.e., the molecules near the surface are attracted sidewise and toward the bulk liquid, but experience less attraction in the direction of the bulk of gas. Inhomogeneity in the surface region causes to exist density gradient $d\rho(z)/dz \neq 0$ in the vertical direction, that is, $\rho(z)$ is changed with z. The density profile $\rho(z)$ in the direction perpendicular to the surface with thickness δ is usually approximated using the hyperbolic tangent function:

$$\rho(z) = \frac{1}{2}(\rho^{\mathrm{l}} + \rho^{\mathrm{v}}) - \frac{1}{2}(\rho^{\mathrm{l}} - \rho^{\mathrm{v}})\tanh\left[\frac{2(z - z_0)}{\delta}\right] \quad (1)$$

The vapor-liquid interfacial thickness δ plays an important role in the calculation of density profile. There are several ways to calculate the interfacial thickness. In this paper, the experimental data of surface tension is used to calculate the surface thickness of electrolyte solutions. This method that is called inversion method (IM) has been already used to determine surface thickness of pure fluids by writers.

Inversion Method:

The density functional theory is the most popular approach to the statistical mechanics of inhomogeneous fluids. In this theory, the surface tension γ can be expressed as follows

$$\gamma = \int_{-\infty}^{\infty} \left[p - p[\rho(z)] \right] \mathrm{d}z \qquad (2)$$

in which p is normal or vapor pressure and $p[\rho(z)]$ the tangential pressure, which is functional of density profile $\rho(z)$ and can be written as:

$$p[\rho(z)] = Z\rho(z)k_{\mathrm{B}}T \qquad (3)$$

where Z is the compressibility factor, k_{B} the Boltzmann constant and T the absolute temperature. In Eq. (3), the compressibility factor Z can be calculated by the EOS. The difference between vapor and tangential pressure i.e. $p - p[\rho(z)]$ is the surface excess pressure and it is important, because the integral of which forms the surface tension and the difference is dependent on density profile. Regarding to Eqs. (1-3), since the surface thickness δ plays an important role in the calculation of density profile, therefore the surface tension is a function of the interfacial thickness

$$\gamma = f(\delta) \qquad (4)$$

In the other word, having the surface thickness and using the above mentioned method, the surface tension of fluids can be calculated theoretically. Inversely, if it is considered the thickness as an adjustable parameter and the surface tension is given experimentally, the surface thickness of fluids can be calculated. Therefore, in this method, surface thickness is to be obtained from the experimental surface tension data. This is inversion method that is based on the idea that at a given temperature the density profile $\rho(z)$, appeared in Eq. (1), is determined by the surface thickness δ as

$$\rho^{(n)}(z,T) = \frac{1}{2}\left(\rho^{\mathrm{l}}(T) + \rho^{\mathrm{v}}(T)\right) - \frac{1}{2}\left(\rho^{\mathrm{l}}(T) - \rho^{\mathrm{v}}(T)\right)\tanh\left[\frac{2(z - z_0)}{\delta^{(n)}(T)}\right] \qquad (5)$$

where the superscript n refers to the iteration number. The inversion technique begins by employing an initial value of $\rho^{(1)}(z,T)$ from an initial guess of surface thickness $\delta^{(1)}(T)$. Then the series of data points $\left(\gamma^{(1)},T\right)$ generated by the application of the equation

$$\gamma^{(1)} = \int_{-\infty}^{\infty} dz \left[p - Zk_{\mathrm{B}}T\, \rho^{(1)}(z\,,\delta^{(1)}) \right] \qquad (6)$$

At each temperature, the deviation percent in the values of $\gamma^{(1)}(T)$ between this calculation and its experimental surface tension data is determined. The process is repeated until the deviation percent is smaller than 1%. Actually, the interfacial thickness δ is regressed with the minimization of the function

$$F = \left(\frac{\gamma_{cal} - \gamma_{\exp}}{\gamma_{\exp}} \right)^2 \tag{7}$$

By use of this method, the density profile, the surface excess pressure and the surface thickness are obtained simultaneously.

Safteos:

The SAFT EOS is based on extensions and simplifications of Wertheim's thermodynamic perturbation theory for associating fluids. In fact, the SAFT EOS has been initially proposed by Chapman et al. based on first-order theory of Wertheim and widely used in the past decade. Huang *et al* converted it into a very useful engineering equation. In SAFT a molecule is composed of *m* segments correspond to atoms, functional groups, or complete molecules . Each segment of the same kind has the same volume and interaction energy parameters. Molecules are represented as covalently bonded chains of segments that may contain sites capable of forming associative complexes. By use of the SAFT, the contribution to Helmholtz free energy of bonding between segments can be calculated from the background correlation function for segments. Several version of SAFT have been developed due to the different methods to calculate the free energy of monomers. Based on the SAFT EOS, the Helmholtz free energy for electrolyte solution is as follows:

$$F^{\text{electrolyte}} = F^{\text{id}} + F^{\text{hs}} + F^{\text{dis}} + F^{\text{chain}} + F^{\text{assoc}} + F^{\text{ion}} \tag{8}$$

Results:

In this paper, we calculated the surface thickness from the experimental data of surface tension (Inversion Method) of electrolyte solutions using SAFT EOS. In this relation, we considered four electrolyte solutions with the same cation Na^+ like NaI, NaBr, NaCl, NaF and three electrolyte solutions with the same anion NO_3^- like KNO_3, $NaNO_3$, $LiNO_3$. Experimental surface tension data has been taken from the following empirical relation that is valid in the range from 0 to 1 mol / kg and the temperature range from 288 to 307 K.

$$\gamma = \gamma^0 + \frac{d\gamma}{dm} m \tag{9}$$

In which *m* is molality and γ^0 is the surface tension at zero concentration. The results from the inversion method for calculating surface thickness of the solutions are shown in Figures 1 and 2. Figures show that increasing the radius of the ions reduces the thickness of the surface and this is independent on the ion charge. But it seems that the effect of increasing of the radii of anions in the surface thickness is more than cations and this shows that the influence of anions on the interfacial layer is more than cations.

As it is said before, the difference between vapor and tangential pressure is important, because the integral of which forms the surface tension and the difference is dependent on density profile. The values of surface excess pressure of the solutions is shown in Figure 3. This figure shows that the value has a maximum in the surface region.

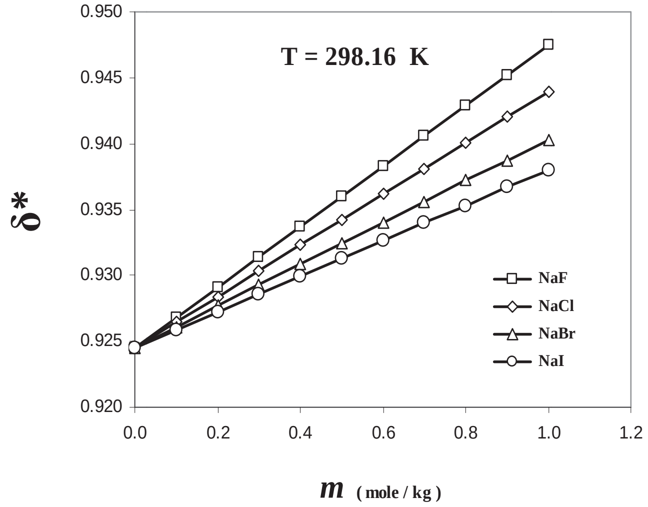

Figure 1: the surface thickness of electrolyte solutions with the same cation Na^+

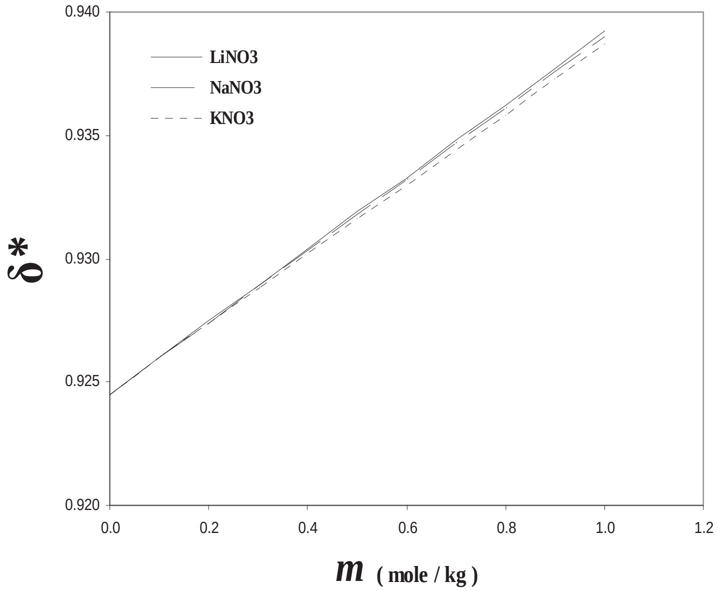

Figure 2: the surface thickness of electrolyte solutions with the same cation NO3$^-$

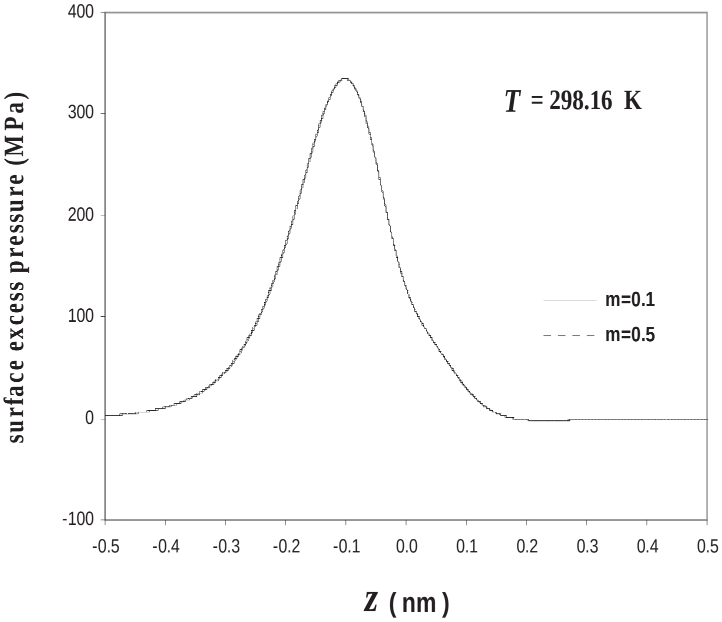

Figure 3: The surface excess pressure

References

[1] M. Najafi and A. Maghari, *J. Soution Chem*., **38**(2009)685

[2] S.H. Huang and M. Radosz, *Ind. Eng. Chem. Res.*, **29**(1990)2284

[3] C. Held, L.F.Cameretti and G. Sadowski, *Fluid Phase Equilibria*, **270**(2008)87

[4] N. Matubayasi, k. Tsunetomo, I. Sato, R. Akizuki, T. Morishita, A. Mutuzawa

and Y. Natsukari, *J. Colloid and Interface Sci*., **243**(2001)444

[5] N. Matubayasi, and R. Yashikawa , *J. Collaid and Interface. Sci.*, **315**(2007) 597

Application of the GMA equation of state to predict the metal-nonmetal transition

Majid Moosavi
Dept. of Chemistry, Faculty of Sciences, University of Isfahan, Isfahan81746-73441, Iran
Email: m.mousavi@sci.ui.ac.ir

Keywords: Metal-nonmetal transition (MNMT), GMA EoS,Liquid metals, Density.

Introduction:

The metal-non-metal transition occurs when the dense liquid is expanded to lower densities.The dense liquidis a metallic conductor in which the interparticle interactionsare dominated by the coulomb potential, whereas the interactionsin the non-metallic phase are weak van der Waals forces.Both types of interactions change with the thermodynamic state.Liquid metals such as mercury, rubidium, and cesium areelectrically conductive at normal conditions. They become nonmetallicwhen expanded to lower densities. The density of anelement may be regarded as the main criteria for its metallic or non-metalliccharacteristic.

The GMA(Goharshadi-Morsali-Abbaspour) EoS [1] which is based on the average potential energy is given by:

$$(2Z-1)V_m^3 = A(T) + B(T)\rho$$

(1)

where Z, V_m , and ρ are compressibility factor, molar volume, and density, respectively. With decreasing density, a gradual transition from metallic to non-metallic occurs in liquid metals such as Cs, Rb, Na, and Hg.In this work, the GMA EoS has been used to predict thistransition. As a result of this transition, some changes in the liquid structure happen and thereforea deviation from the linearity predicted by the GMA EoS is observed.In this approach only the experimental *p*-V-*T* data are required topredict such a transition. The predictions are in agreement with experimentalobservations.

Results and discussion:

Fig. 1 shows the linear regularityfor different isotherms of Cs in the range of 800 to 1950 K. For those isotherms in whichthe density at any state is greater than 9.03molL^{-1} (1.2 gcm^{-3}), the linearity holds very well.For those isotherms including the lower densities, thedeviation from the linearity is quite obvious.The deviation from the GMA EoS for 1600 K isotherm has been shown in Fig. 2 for which theexperimental data include both densities lower and higher than 9.03molL^{-1}.According to Fig. 1, when density decreases or temperature increases, some changes in the pair correlation function, *g*(*r*), (or in fact in density) of metals are observed. This result is in accord with the results obtained from the nearly free electron theory [2] and the neutron diffraction measurements [3,4].

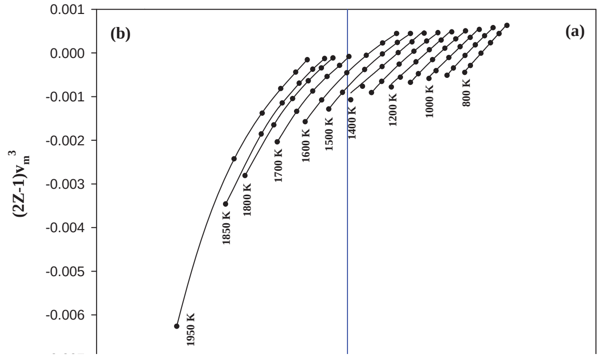

Fig. 1. The linearity of the GMA EoS for different isotherms in the range of 800 to 1950 K for Cs, (a) before the transition and (b) after the transition.

$(2Z\text{-}1)v_m^3$

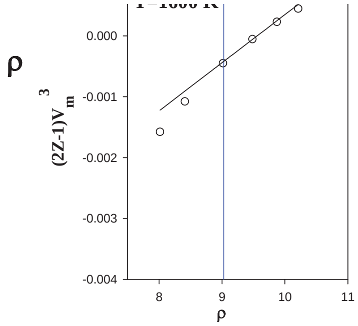

Fig. 2. The deviation from the GMA EoS for 1600 K isotherm.

Conclusion:

There are someapproximate methodstodistinguish the metallic and non-metallic states in liquid metals. TheGMA EoS along with thePVTdata can be used to predictthe MNMT in liquid metals as a simple and remarkable method. Such a predictionshows another application of this EOS.

References:

[1] E.K.Goharshadi, A.Morsali, M.Abbaspour, Fluid Phase Equilib.230, 170-175, 2005.

[2]W.C.Pilgrim, F.Hensel, J. Phys.: Condens. Matter 5, B183- B192, 1993.

[3] F.Hensel, G.F. Hohl, Rev. Press. Technol. 3, 163-168,1994.

[4]F.Hensel,H.Uchtmann, Annu. Rev. Phys. Chem. 40, 61-83, 1989.

Gaseous ion mobility of CO^+ ions in He and Ne

G. Afsahi[(*)1], A. H. Jalili [2], H. Behnejad [1]
[1]*Department of Physical Chemistry, Faculty of Chemistry, College of Science, University of Tehran,14174, Tehran,Iran*
[2]*Gas Science Department, Research Institute of Petroleum Industry, 14665-137, Tehran,Iran*
[(*)]gh_afsahi@ut.ac.ir

Keywords: Ion mobility, (n,6,4) potential, Pirani potential

Introduction: Analysis of charged particle transport in dilute gases under the influence of electric fields has theoretical and practical applications in science and technology [1-3]. Investigation of ions mobility in gases is an important issue in plasma chemistry, atmospheric physics, and numerical simulations of industrial plasma . There is now a large amount of data available for such analysis. Here, we compare ion mobilities calculated from the (n,6,4) and the Pirani's potentials with the experimental values for the two systems He-CO^+ and Ne-CO^+. The parameters of (n,6,4) potential model and Pirani's potential for He-CO^+ and Ne-CO^+ systems were obtained from experimental gaseous ion-mobility data. These potentials were then used to calculate the mobility of CO^+ ions in helium and neon gases at 300 K. Results show good agreement between the ion mobility data calculated via the (n,6,4) potential and experimental data. The Pirani's potential yields ion mobilities of a lower accuracy especially for He-CO^+.

Method of Calculation:

Under high electric field strength for producing charged particles in a neutral buffer gas, i.e. partially ionized plasma, where the ratio of the electric field strength, E, to the number density of the neutral gas, N, is high the ion energy is much greater than the thermal energy of the neutral molecules. In such circumstances the Enskog-Chapman's classical kinetic theory of dilute gases is no longer valid and instead the two-temperature theory of Viehland and Mason is useful to calculate the mobility of ions in neutral gases.

According to two-temperature theory, the mobility K and drift velocity v_d of an ion through a single-component neutral gas can be represented by

$$K = \frac{v_{\mathrm{d}}}{E} = \frac{3q}{8N}\left(\frac{\pi}{2\mu k_{\mathrm{B}} T_{\mathrm{eff}}}\right)^{1/2} \frac{1+\alpha}{\Omega^{(1,1)}(T_{\mathrm{eff}})} \qquad (1)$$

where q is the ion charge, k_{B} is Boltzmann's constant, $\mu = mM/(m+M)$ is the reduced mass with m and M being the ion and neutral masses respectively, and $\Omega^{(1,1)}(T_{\mathrm{eff}})$ is diffusion type collision integral, which is a function of effective temperature T_{eff} defined by

$$\tfrac{3}{2} k_{\mathrm{B}} T_{\mathrm{eff}} = \tfrac{3}{2} k_{\mathrm{B}} T + \tfrac{1}{2} M v_d^2 (1+\beta) \qquad (2)$$

The terms α and β include all of the higher approximations that occur in the kinetic theory and almost are smaller than 0.1 for most practical purposes. The gaseous ion mobility is connected to ion-neutral interaction potential through collision integral $\Omega^{(1,1)}(T_{\mathrm{eff}})$ [4].

Results:

At the first step, the parameters of the (n,6,4) ion-neutral interaction potential for the two systems He-CO$^+$ and Ne-CO$^+$ was estimated from the experimental ion mobility data using the procedure described by Viehland and Mason. The parameters of the Pirani's potential was evaluated by the method described by Laricchiuta et al. [5]. The average of percent absolute deviations (AAD%) of ion-mobilities calculated by these potentials from experimental data at 300 K are summarized in **Table 1. Fig. 1** compares the calculated mobilities of CO$^+$ ion in neutral buffers helium and neon. It can be seen that the (16,6,4) potential for He-CO$^+$ and (12,6,4) potential for Ne-CO$^+$ yield the best agreement with experimental results.

Table 1. Average and maximum (in parentheses) deviations of calculated ion mobilities from experimental data at 300 K.

System	**(8,6,4) potential [3]**	**(12,6,4) potential**	**(16,6,4) potential**	**Pirani's potential**
He–CO$^+$	4.53 (6.93)	4.52 (6.95)	3.24 (5.53)	7.47 (12.56)
Ne–CO$^+$	2.40 (6.82)	1.57 (2.61)	4.33 (6.70)	3.22 (9.49)

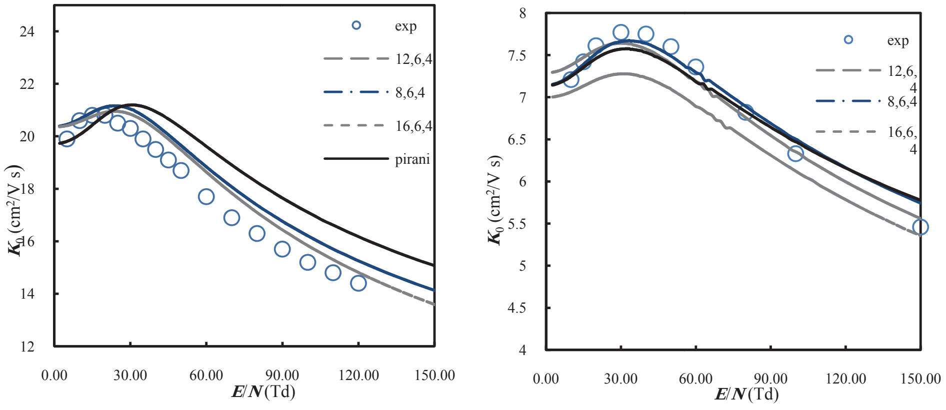

(a) (b)

Fig. 1: Experimental and calculated values of the standard ion-mobility, K, as a function of E/N for (a) He-CO^+ and (b) Ne-CO^+ at 300 K.

References:

[1] E.A. Mason and E.W. McDaniel, Transport Properties of Ions in Gases (Wiley, New York, 1988).

[2] A.H. Jalili, N. Seyed-Matin, L.A. Viehland and M. Shahsavan, *Chem. Phys.* 365, 94 (2009).

[3] A.H. Jalili, A. Abbaspour, H. Behnejad, and L. A. Viehland, *Mol. Phys.* 108, 35 (2010).

[4] L.A. Viehland, E.A. Mason, *Ann. Phys.* (N.Y.) 91, 499 (1975).

[5] A. Laricchiuta, G. Colonna, D. Bruno, R. Celiberto, C. Gorse, F. Pirani, M. Capitelli, *Chem. Phys. Lett.*, 445, 133 (2007).

Study of Structural Behavior of Hexylamine at the Interface of Water/Oil by Molecular Dynamics Simulation

Mohammad Hadi Ghatee, Fatemeh Borousan

(*Department of chemistry, Shiraz University, Shiraz, 71454 Iran*)

Tel: +98 711 6137353, Email: ghatee@susc.ac.ir

Key words: Density profile; Hexylamine; Molecular dynamics simulation; Orientation; water/oil interface

Introduction:

The characterization of the water/oil interface is an important subject of many investigations due to its relevance in various areas of chemistry, biology and technology. Field processing of crud oil features water/oil interface as a part of normal and enhanced oil recovery. Therefore, understanding the behavior of different components of the crud oil is vital to the quality of oil recovery. Hexylamine is one of the compounds constituting crude oil. It is colorless, free of suspended matter, partially miscible with water, and miscible with almost all common organic solvents. Synthetic oil is normally used to model and study the physical and thermodynamically property of the compounds constituting the crude oil. A synthetic oil consisting hexylamine in octane was used to model the behavior of the surfactant at oil/water interface. To achieve this, we used molecular dynamic simulation. Hence the macroscopic system is implemented by microscopic model. The structure of the surfactant, molecular orientation, the effects of concentration and temperature will be studied. [1-3]

Method:

Structural parameters required setting up the force field of octane, water, and hexylamine were determined by using GAUSSIAN 03 program. Molecular dynamics simulations were carried out using the DL-POLY package. Density profile, structural correlations, average orientation of hexylamine molecules at the interface of octane/water were simulated by a slab (consisting 256 octane,72 hexylamine) confined by 2668 water molecules on ether sides.

Result and discussion:

Simulated density profile of synthetic oil/water interface is shown in Figure 1 and 2. The force field validity can be verified by the simulated water density (1.03 g.cm^{-3} at 293 K). Hexylamine is found to form monomolecular layer at the octane/water interface. The profiles match this conclusion. According to the atoms profile, hexylamine extended at the interface such that amine group tends towards the water-side and alkyl group towards the oil-side of the interfacial region. The most probable structure for the hexylamine is to be linear conformation for the hexyl group.

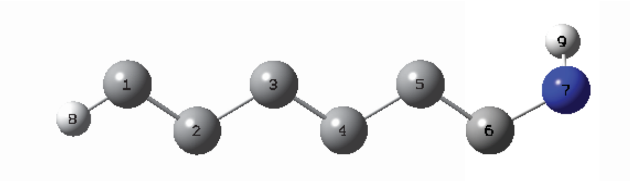

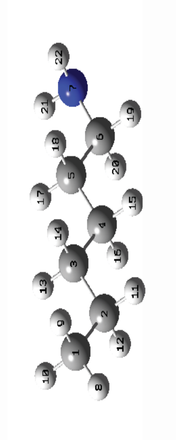

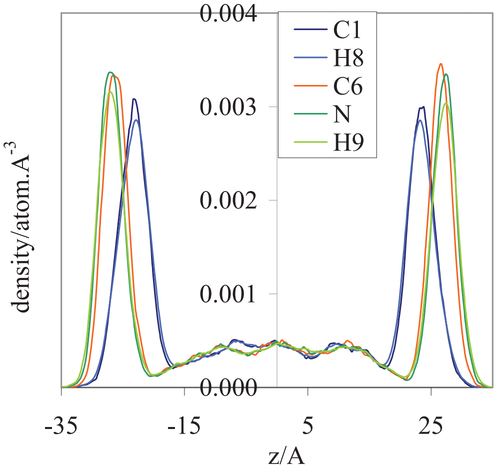

Figure 1

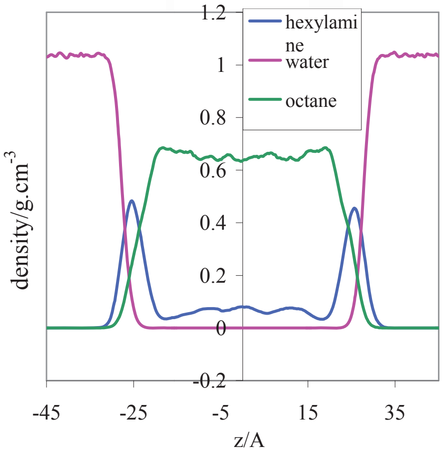

Figure 2

Conclusion:

Oil/water system has been simulated by classical molecular dynamics. Polar portion of crude oil hexylamine at the oil/water interface acts as a surfactant that can be captured by classical molecular dynamics. At equilibrium, hexylamine forms monolayer at the interface with characteristic orientation, leaving low and null concentration in oil and in water, respectively.

Reference:

[1] X. Hong Yan, Z. Zhen, S. Huan Quan, C. XuLong, L. ZhenQuan, S. Xin Wang, C. XiaoHong, L. XinHou, Science China Chemistry **2010** , 53, 945–949.

[2] M. Kunieda, K.Nakaoka, Y.Liang, C.R.Miranda, A.Ueda, S.Takahashi, H.Okabe, T.Matsuoka , JACS Articles **2010 ,**132, 18281–18286.

[3] D.M.Mitrinovic, Zh.Zhang, S.M.Williams, Zh.Huang, M.L.Schlossman, Journal of Physical Chemistry B **1999,** 103,1769-1783.

Many-body and quantum effects in some thermodynamic properties and infinite shear modulus of the HFD-like and Lennard-Jones fluids using the radial distribution function

M. Abbaspour*, A. Keyvanloo
Department of Chemistry, Hakim Sabzevari University, Sabzevar, Iran
(E-mail: abbaspour@sttu.ac.ir)

Keywords: Radial distribution function; Quantum correction; Many-body interaction

Introduction:

Using statistical mechanics methods, the thermodynamic properties such as pressure and internal energy can be obtained from the intermolecular potential and the RDF. The main difficulty arises in the calculation of those functions, and the problem has usually been solved by considering the RDF of the liquid phase for a LJ fluid [1].

In this work, many body and quantum effects have been considered in the calculations of pressure, internal energy, and the infinite-frequency shear modulus using the statistical mechanical formula with the two-body HFD-like and LJ potentials for neon and argon, respectively. The required RDFs have been used from three recently determined accurate expressions in the literature. MD simulations have been also applied to generate the expression for the RDF of HFD-like fluids in the extended ranges of temperatures and densities.

The quantum corrections for the neon system have been considered using the FH and WK approaches. The simple three-body potentials of Hauschild and Prausnitz [2], Wang and Sadus [3], and Guzman et al. [4] used with the two-body HFD-like potential of argon without requiring an expensive three-body calculation.

Results and discussion:

The statistical mechanical expressions have been used for calculation of the pressure, internal energy, and infinite frequency shear modulus of fluids argon and neon using the two-body and total (two-body plus three-body) HFD-like potentials and classical and quantum LJ potentials at different temperatures and densities using the three recently determined accurate expressions in the literature, respectively.

The obtained pressure results of fluid argon indicated that although the both three-body potentials of Wang and Sadus [3] and Hauschild and Prausnitz [2] have improved the pressure results to give better agreement with the experiment but the potential of Hauschild and Prausnitz has greater effect on the results. It is also shown that the three-body potential of Guzman et al. [4] has increased the pressure values and improved the results at lower temperatures.

The energy results of argon showed that although the three-body potentials of Wang and Sadus and Guzman et al. have small effects on the two-body energy but the three-body potential of Guzman et al. has improved the values at higher densities where the three-body effects dominant.

The pressure and energy results of fluid neon indicated that the both quantum potentials have increased the results. It is also shown that although the quantum FH potential has better effects on the pressure values but the quantum WK potential has greater effects on the energy results.

It is also shown that the three-body potentials decreased the infinite frequency shear modulus but the quantum potentials increased it.

Conclusions:

Many body and quantum potentials have been considered in the calculations of pressure, internal energy, and the infinite-frequency shear modulus using the statistical mechanical formula with the two-body HFD-like and LJ potentials for neon and argon, respectively. We concluded that the three-body potentials of Hauschild and Prausnitz [2] and Guzman et al. [4] have greater effects on the pressure and energy results, respectively. It is also concluded that the quantum FH potential has better effects on the pressure values but the quantum WK potential has greater effects on the energy results. It is also shown that the three-body potentials decreased the infinite frequency shear modulus but the quantum potentials increased it.

References:

[1] D.A. McQaarrie, Statistical Mechanics, Harper and Row, New York, 1975.

[2] T. Hauschild, J.M. Prausnitz, Mol. Simul. 11 (1993) 177.

[3] L. Wang, R.J. Sadus, J. Chem. Phys. 125 (2006) 144509.

[4] O. Guzman, F. del Rio, J.E. Ramos 109 (2011) 955.

Hydrogen bonding in nanoconfined water

H.Eslami, N.Heydari
Department of Chemistry, College of Science, Persian Gulf University, Boushehr, Iran
E-mail: heydarinh@gmail.com

Key words: Hydrogen bonding, Nanoconfined fluid, Molecular dynamics simulation

Introduction:

Water confined in nanometric geometries has a lot of application in different fields such as biology, engineering, geophysics, and atmospheric sciences. Water behavior in contact with surfaces is different from that of bulk. Therefore, the properties of bulk water cannot be extended to understand the molecular level properties of confined water such as hydrogen bonding, which affects the physical properties of water. The effect of confinement on the physical properties of water has been studied using both experimental and theoretical approaches. Although various experimental and theoretical researches exist in this field, not much is known about the connection of macroscopic properties to the molecular level properties, such as hydrogen bonding, in confined geometries. In this work we have simulated water confined between graphene surfaces at ambient pressures and over a wide range of temperatures, to investigate structure and dynamics of hydrogen bond network in water.

Method:

Various aspects of dynamics and structure of water molecules at interfaces could be interpreted in terms of the nature of the hydrogen bond network at the surface. Here we do molecular dynamics simulation to discover the microscopic pictures of hydrogen bond structure and dynamics in water, nanoconfined in hydrophobic pores. We have employed our recent simulation scheme in the NAPT ensemble to simulate a constant number of water molecules confined between graphene surfaces of constant surface area at constant temperature and constant parallel component of pressure. We have considered water OH as the hydrogen-bond donor and the water O as the hydrogen-bond acceptor. A geometric criterion, in which the distance between the hydrogen of the donor group, and the acceptor has to be less than 0.30 nm and the donor-hydrogen-acceptor angle has to be bigger than 130° has been chosen as the criteria for the hydrogen bond formation.

Simulations of SPC/E model of water, nanoconfined between graphene surfaces, in equilibrium with the bulk water, have been done. In this work the surface atoms are kept immobile and periodic boundary conditions were applied in the x and y directions. The temperature was kept constant at 300 K and the parallel component of pressure is fixed at 101.3 kPa. Simulations are done for 5 ns to achieve equilibrium and a large number of independent configurations were sampled over a 5 ns time span to be employed for extraction of target distributions.

Result and discussion:

The hydrogen bond dynamics is analyzed through investigating the following correlation function, introduced originally to study pure water.

$$C(t) = \frac{\langle h(0)h(t)\rangle}{\langle h(0)\rangle} \tag{1}$$

Where the population variable $h(t)$ is unity when a particular hydrogen-oxygen pair is hydrogen bonded at time t, and zero, otherwise. Shown in Figure 1 is the correlation function C(t) at three 1.0 nm thick slabs, parallel to the surfaces. An initially fast decay followed by a region of slow decay is seen in Figure 1. This function is shown to be coupled to the diffusion of water molecules. Therefore, while the initial fast decay shows the breaking of some hydrogen bonds, some of the water molecules diffuse back to form the new hydrogen bonds. The results in Figure 1 further indicate that The function C(t) decays slower close to the surfaces, compared to the bulk water. This is an indication of slower dynamics of the water in the confined region.

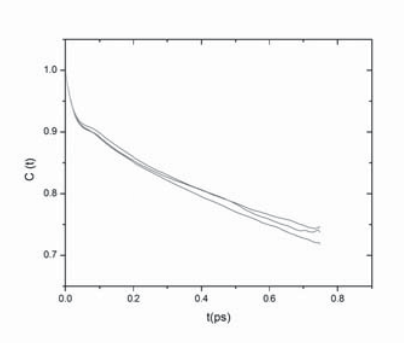

Figure 1. Correlation function C(t) at three 1.0 nm thick slabs parallel to the surfaces.

Size effect on zigzag spin coupling interaction in presence of magnetic field for 1-D Ising model of Nanosystem

Seyedeh Ameneh Paknejad[a], Farid Taherkhani[a]
[a]Department of Chemistry, Razi University, Kermanshah, Iran
Email: ameneh_paknezhad@yahoo.com

Keywords: Finite size free energy,Ising model,Nanosystems,Transfermatrix

Introduction:

Many physico-chemical systems can be represented by a lattice arrangement of molecules with including nearest-neighbor interactions approximately.The simplest version of this theory is the so-called "Ising model" . Ising model is able to explain many problems in physics and chemistry [1].1-D Ising model is much easier to be treated theoretically than 2- and 3-D ones[2-3].

[(Tp) Fe$(CN)_3$ Mn(5-MeOsalen). $2CH_3OH]_n$ [Tp^- = hydrotris(pyrazolyl)borate and 5-MeOsalen^{2-}= N ,N'-ethylenebis(5-methoxysalicylideneiminate)] is one of several compounds that provide the 1-D zigzag chain[4]. In this work we calculate partition function of Ising model with zigzag spin coupling interaction.

With the partition function of such model we can calculate its thermodynamic properties. To best of our knowledge,size effect on 1-DIsing model with zigzag spin coupling interaction in presence of magnetic field are explored . We investigate spin coupling interaction and magnetic field effect on finite size free energy of this model . Analytical expression for finite size free energy , and bulk free energy is derived for even , odd size of both ferromagnetic (FF) and ferromagnetic - antiferromagnetic (FA) zigzag spin coupling interaction . Deviation of free energy of finite size of spin array from its bulk limit is investigated for FF and FA spin chain as a function of ratio of magnetic field to spin coupling interaction "f" and ratio of zigzag spin coupling "n" (competition factor).

Method:

We use the transfer matrix method for investigation partition function of zigzag spin coupling interaction of 1-D Ising model in presence of magnetic field.

Result and discussion:

Deviation of free energy of both ferromagnetic zigzag spin coupling interaction (FF) finite size of spin array from bulk $\Delta A = \frac{A_{\text{finite}} - A_{\text{bulk}}}{A_{bulk}} \times 100$ is investigated as a function of f parameter for different size of spin arrays (N) . According to the Figures deviation of free energy of FF spin chain decreases as a function of f parameter. Increase of the size of spin chain deviation of free energy due to closeness of free energy of finite size to the bulk free energy decreases. Deviation of free energy decreases as a function of n parameter .There is a peak for finite size free energy

as a function of f parameter for both FF and FA spin chain . There is a peak for finite size free energy for FF spin chain as a function of n however for FA spin chain finite size free energy decreases as a function of n. As a result, increase of spin coupling interaction lead to decrease of finite size effect free energy.

Conclusion:

Size effect is considered on zigzag spin coupling interaction of 1-D Ising model in presence of magnetic field .

Bulk free energy and finite size free energy is investigated for zigzag spin coupling interaction of 1-D Ising model of Nanosystem in presence of magnetic field . Reduced bulk free energy for FA spin chain decreases versus f and competition factor n monotonically. Deviation of free energy decreases for both FA and FF spin chain with increase of absolute value of competition factor and f parameter.There is a peak for finite size free energy as a function of f parameter for both FA and FF spin chain. Finite size free energy vanishes for high absolute value of FA spin chain as a function of competition factor however peak of finite size free energy is remain for FF spin chain.

References:

[1] S. G. Brijsh. Rev.Mod.Phys(1967**)** pp.883-893

[2] H.J.W. Zandvliet.Europhys. Lett. 73 (2006), pp. 747–751.

[3] H.J.W. Zandvliet.Europhys. Lett. 74 (2006), pp. 1123–1124.

[4] S. Wang, M. Ferbinteanu, M. Yamashita. Inorg. Chem. 46 (2007),pp.610-612

Equations of State for Density Predictions Based on Melting Point Constants

M. Kiani [a,b], N. Azizi [a,*], R. Behjatmanesh-Ardakani [a], M. M. Alavian Mehr [b]

[a]Department of Chemistry, Payame Noor University, PO BOX 19395-3697 Tehran, Iran.
[b]Department of Chemistry, Shiraz University of Technology, Shiraz, 71555-313, Iran;
[*]E-mail:nasrinazizi20@yahoo.com

Keywords: Corresponding states principle; Equations of state; second virial coefficient; Volumetric Properties

Introduction:

The applicability of an equation of state to a given system is reliable if, in the first place, accurate input data are available. In practice, the input data may not be available for a given system, or it may not be possible to measure these data accurately for some systems. Hence, there is a need to extend the method by using alternative procedures. The purpose of this paper is to present a method for predicting densities of some different compounds from properties that are readily available at ordinary pressures and temperatures.

Method:

The equation of state obtained by Tao and Mason [1] has the following form:

$$\frac{P}{\rho kT} = 1 + (B-\alpha)\rho + \frac{\alpha\rho}{1-\lambda b\rho} + A_1(\alpha - B)b\rho^2\,\frac{(e^{kT_c/T} - A_2)}{1+1.8(b\rho)^4}$$

(1) where P is the pressure, kT has its usual meaning, B_2 is the second virial coefficient, α is the scaling factor, b is the effective Van der Waals co-volume, and ρ is the number density. Further, the parameters A_1, A_2, and κ are defined by:

$$A_1 = 0.143; \quad A_2 = 1.64 + 2.65\left[e^{(\kappa - 1.093)} - 1\right]; \tag{2}$$

$$\kappa = 1.093 + 0.26[(\omega + 0.002)^{1/2} + 4.50(\omega + 0.002)] \tag{3}$$

in which ω denotes the Pitzer acentric factor. Also, The ISM equation of state [2] has the following form:

$$\frac{P}{\rho kT} = 1 + \frac{(\alpha - B_2)\rho}{(1+\delta\, b\rho)} + \frac{\alpha\rho}{1-\lambda b\rho} \tag{4}$$

The constant λ is adjusted from a few high-density points, such as liquid densities. Both equations of state require usage of the second virial coefficient, $B_2(T)$, along with the parameters α and b. In this respect, the following correlation equation for B_2 using new scaling parameters, such as the enthalpy of fusion ΔH_{fus} and the molar density ρ_f, both at the melting point has been developed. Our resulting correlation for B_2 can be represented by the empirical expression:

$$B_2\rho_f = -0.56728757 - 2.7366315\left(\frac{\Delta H_{fusion}}{RT}\right)^2 - 0.15520679\left(\frac{\Delta H_{fusion}}{RT}\right)^4 \tag{5}$$

In practice, this requires Eq. (5) to be solved for the reduced Boyle's temperature and the reduced Boyle's volume, so that

$$\alpha\rho_f = a_1\left\{exp\left[-d_1\left(\frac{RT}{\Delta H_{fusion}}\right)\right]\right\} + a_2\left\{1 - exp\left[-d_2\left(\frac{\Delta H_{fusion}}{RT}\right)^{1/4}\right]\right\} \tag{6}$$

$$b\rho_f = a_1\left[1 - d_1\left(\frac{RT}{\Delta H_{fusion}}\right)\right] exp\left[-d_1\left(\frac{RT}{\Delta H_{fusion}}\right)\right] + a_2\left\{1 - \left[1 + 0.25d_2\left(\frac{\Delta H_{fusion}}{RT}\right)^{1/4}\right]\right\} ex\,p\left[-d_2\left(\frac{\Delta H_{fusion}}{RT}\right)^{1/4}\right] \tag{7}$$

where $a_1 = 0.762522$, $a_2 = 1.498476$, $d_1 = 0.368995$, and $d_2 = 2.759071$.

Results and Discussion:

We performed the calculation of density of molecular fluids using the TM and ISM EOS. As it is clear from Table 1, in most cases, the accuracy of the calculated densities using the present correlation is similar to those obtained from the Ghatee and Boushehri (GB) correlation [3].

Table 1. Percent deviation means of the calculated density properties with reference to literature data [4].

Fliud	NP	ΔT (K)	ΔP (bar)	AAD (%) density[a]	AAD (%) density[b]	AAD (%) density[c]	AAD (%) density[d]
Ar	298	95–700	0.5–1005	1.407	1.990	5.311	3.069
Xe	312	190–700	0.5–3200	2.207	1.919	1.646	3.523
N_2	326	119–600	0.5–1050	1.938	6.095	1.699	7.672
O_2	429	80–1000	0.5–820	1.746	0.790	2.055	1.260
CH_4	254	150–600	0.5–3500	1.722	3.145	1.825	3.434

C_2H_6	236	150–500	0.5–3000	3.046	2.845	4.791	2.840
C_3H_8	191	90–500	0.5–700	3.009	2.943	4.526	7.977
C_6H_6	167	330–370	0.47–780	1.976	0.874	3.715	1.388
C_7H_8	194	320–675	0.5–2700	4.139	3.579	4.379	3.859
C_8H_{18}	90	248.15–300	0.0054–1000	4.539	2.550	3.796	2.854

[a] Using the ISM equation of state through applying our correlation. [b] Using the ISM equation of state through applying GB correlation. [c] Using the TM equation of state through applying our correlation. [d] Using the TM equation of state through applying GB correlation.

Conclusions:

the conclusion that can be drawn is that the ISM as well as TM EOSs can properly represent the volumetric properties of several pure molecular fluids in a broad range of temperatures and pressures using the present correlation proposed for B_2. The good harmony between the proposed correlation with those given in literature reconfirm the reliability of the correlation.

Reference:

[1] Tao F.M.; Mason E.A.; “Statistical–mechanical equation of state for nonpolar fluids: prediction of phase boundaries”; J Chem Phys; 100, 9075-9084, 1994.

[2] Ihm G.; Song Y.; Mason E.A.; “A new strong principle of corresponding states for nanpolar fluids”; J Chem Phys; 94, 3839-3848, 1991.

[3] Ghatee M.H.; Boushehri A.; “Equation of state for compressed liquids from surface tension”; Int J Thermophys; 17, 945-957, 1996.

[4] NIST Standard Reference Database Number 69 http://webbook.nist.gov.

Calculation of internal energy of Argon fluid with hard-core square-well potential at different thermodynamic states

Hossein. Nikoofard, Zahra. Kalantar, Mokhtar. Ganjali
Faculty of chemistry, Shahrood University of Technology

Key words: Internal energy, Radial distribution function, Hard core, square-well potential, Argon fluid

Introduction:

The thermodynamic properties of a fluid can be obtained from the radial distribution function $g(r)$. Radial distribution function is the primary linkage between macroscopic thermodynamic properties and intermolecular interaction of fluid. For a long time, the square-well potential model has been the subject of extensive investigation using deferent statistical mechanical methods, either as simulation techniques or as a theoretical approach. The square-well SW fluid represents a good and simple model that includes the attractive and repulsive interactions which is able to reproduce the behavior of simple fluids, and also it is applicable for the complex fluids, and polar fluids [1, 2]. In this work, we applied SW potential for calculating internal energy of Argon fluid using an expression for $g(r)$ in an integral equation approach.

Result and discussion:

According to self-consistent Ornstein-Zernike (SCOZA), we defined following equation for the direct correlation function as:

$$c(r) = c_{HS}(r) + e^{-\beta\omega(r)} - 1 + G(r)$$

where $c_{HS}(r)$ is the hard-sphere direct correlation function given by the Verlet-Weis prescription, $\omega(r)$ is attractive tail of square-well potential, *G(r)* is a function that depends to thermodynamic states so that the core condition $g(r) = 0$ for $r < \sigma$ is satisfied that σ is diameter of particle [3]. We computed internal energy property of Argon along isotherm 152 K (near the critical temperature) at wide range of densities and compared with the experimental data in Table 1. Also, we compared our results for subcritical temperature T=148 K with experimental data in Table 2.

Table 1: Computational results are compared with experimental data [4] at super-critical temperature T=152 K

$\rho\ (mol/lit)$	$E_{experimental}\ (J/mol)$	$E_{computational}\ (J/mol)$
1.8582	1519.4	1501.94
2.4492	1401.8	1375.69
3.1268	1268.2	1230.69
25.458	-2073.1	-2187.34
29.692	-2690.7	-2705.66
32.931	-3132.9	-3024.06

Table 2: Computational results are compared with experimental data [4] at sub-critical temperature T=148 K

$\rho\ (mol/lit)$	$E_{experimental}\ (J/mol)$	$E_{computational}\ (J/mok)$
1.3817	1559.9	1547.87
2.5815	1315.6	1287
3.338	1163.1	1121.42
26.286	-2262.7	-2320.54
30.176	-2831.6	-2873.79
36.495	-3622.1	-3614.4

Conclusion:

It is found that our calculation results for internal energy property of Argon are in good agreement with experimental data in sub-critical and super-critical temperature. We used the quantity of width of potential well, $\lambda = 1.72$ for obtaining the best prediction of internal energy.

Reference:

[1] D. Henderson, O.H. Scalise, and W.R. Smith, J. Chem.Phys. 72, (1980), 2431

[2] L.V. Enrique, D. Miguel, and L.F. Rull, J. Chem. Phys.96, (1992), 2296

[3] D. Pini, A.Parola, L.Reatto, Mol Phys , vol. 100, no. 10,(2002), , pp. 1507-1516

[4] Richard B.Stewart and Richard T. Jacobsen, J.Phys.Chem.Ref.Data, Vol.18, No.2, (1989)

Prediction of compressibility factor of Argon fluid with hard-core square-well potential at different thermodynamic states

Hossein. Nikoofard, Zahra. Kalantar, Mokhtar. Ganjali
Faculty of chemistry, Shahrood University of Technology

Key words: compressibility factor, Radial distribution function, square-well potential, Argon fluid

Introduction:

The thermodynamic properties of a fluid can be obtained from the radial distribution function $g(r)$. The importance of $g(r)$ arises from the fact that, given the form of the potential of the intermolecular force, if the $g(r)$ is known as a function of r and the temperature *T*, the standard methods of statistical mechanics allow for the determination of all the equilibrium properties of the fluid. The usual approach to obtain $g(r)$ is through one of the integral equation theories [2]. Thermodynamic property of square-well (SW) fluids has been a subject of interest for many years because of their simplicity and their resemblance to real fluids with spherically symmetrical potentials, among other reasons. Therefore, at present there are available a considerable number of theories for this kind of fluid [1]. In this work, we applied SW potential for calculating compressibility factor of Argon fluid using an expression for $g(r)$ in an integral equation approach.

Result and discussion:

According to self-consistent Ornstein-Zernike (SCOZA), we defined following equation for the direct correlation function as:

$$c(r) = c_{HS}(r) + e^{-\beta\omega(r)} - 1 + G(r)$$

where $c_{HS}(r)$ is the hard-sphere direct correlation function given by the Verlet-Weis prescription, $\omega(r)$ is attractive tail of square-well potential, *G(r)* is a function that depends to thermodynamic states so that the core condition $g(r) = 0$ for $r < \sigma$ is satisfied that σ is diameter of particle [3]. We predicted compressibility factor of Argon along two isotherms

(T=280 K, T=230 K) and we compared our results with simulation and experimental data [4] at below figures:

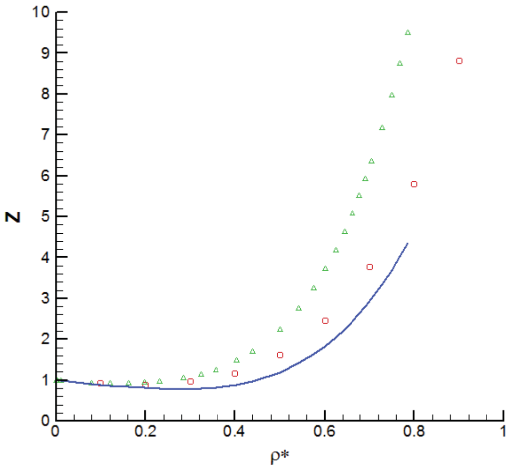

fig.1. Comparison of simulation (open circle) and experimental (delta) data with our results (solid line) at T=280 K

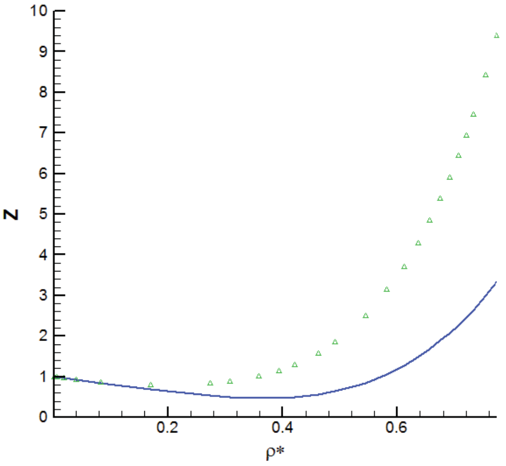

fig.2. Comparison of experimental (delta) data with our results (solid line) at T=230 K

Conclusion:

It is found that our calculation results for compressibility factor property of Argon are in good agreement with simulation and experimental data at low density. We used the quantity of width of potential well, $\lambda = 1.7$ for obtaining the compressibility factor at different thermodynamic states.

Reference:

[1] J.largo and J.R.Solana, J. Chem. Phys. 122, 084510 (2005)

[2] S.Bravo Yuste, M.Lopez de Haro, A.Santos, Phys Rev E Vol 53, No5 (1996), pp.4820-4826

[3] D. Pini, A.Parola, L.Reatto, Mol Phys , vol. 100, no. 10, (2002), pp. 1507-1516

[4] Richard B.Stewart and Richard T. Jacobsen, J.Phys.Chem.Ref.Data, Vol.18, No.2, (1989)

Isothermal compressibility prediction for pure compounds

P.Nematiyan[*a], R.Tahery[b]
a Science Department, Islamic Azad University, Central Tehran Branch, Tehran, Iran
b Chemical Engineering Department, Islamic Azad University, Central Tehran Branch, Tehran, Iran
Email: p_nematiyan@yahoo.com

Key words: Molecular diameter, Scaled Particle Theory, Isothermal Compressibility

Introduction:

The isothermal compressibility of liquids is useful thermodynamic quantities both for practical and theoretical purposes [1]. For example, κ_T is required for the calculation of the Debye-Htickel slope, A, in the Redlich-Rosenteld equation which is used for the determination of partial molar volumes V_{CA}^{0} of electrolytes in solution at infinite dilution from measurements of apparent molar volumes V_{CA} at finite concentrations.

Theory and Method:

There are a lot of methods to predict the isothermal compressibility of pure substance [2-3]. In this paper we used scaled particle theory (SPT) to predict the isothermal compressibility of pure substance.

In the recent years several theories have been developed for the treatment of fluids. For example the Percus-Yevick theory [4]. One of these theories, based on a hard sphere model of a fluid, is scaled particle theory (SPT). From this expression they derived an equation of state:

$$\frac{PV}{\mathrm{RT}} = \frac{1+y+y^2}{(1-y)^3} \qquad (1)$$

where p is the pressure, V is the molar volume, T is the temperature and $y = \pi a^3 N/6V$ is the packing fraction where, N is Avogadro's number and a is the hard sphere diameter of the pure component. The isothermal compressibility is defined by:

$$\kappa_T = -\frac{1}{V}\left(\frac{\partial V}{\partial P}\right)_T \qquad (2)$$

Combining Eqs. (1) and (2) the isothermal compressibility, κ_T, can be expressed as :

$$\kappa_T = \frac{\pi a^3}{6kT} \frac{(1-y)^4}{y(1+2y)^2} \qquad (3)$$

This relationship is dependent only on the liquid density and on the diameter of the molecular compounds. The hard sphere diameter can be calculated by surface tension, thermal expansion coefficients, gas solubility,…

Results and Discussion:

We used Eq.(3) to calculate the computation of isothermal compressibility of 62 pure substances in different temperatures (including alcohols, amines, halogenated hydrocarbons, saturated hydrocarbons, oxygen containing organic compounds and organic acids).

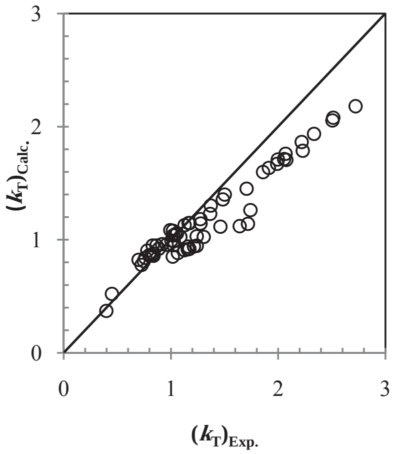

Fig. 1 Plot of $(k_T)_{Calc}$ versus $(k_T)_{Exp.}$ for studied pure substances.

Conclusions:

We calculated hard sphere diameter by using surface tension. By applying Eq. 3, κ_T was calculated for 62 pure substances. The calculated isothermal compressibility has been plotted versus experimental data. Good agreement has been seen for many cases.

Reference:

[1] K.C. Chao and R.L. Robinson, Equations of State in Engineering and Research; Adv, Chem. Ser., vol. 182, Am. Chem. Sot., Washington, 1979; R.H. Perry and D. Green, Perry's Chemical Engineers' Handbook, McGraw-Hill, New York, 6th ed., 1984.

[2]M.H. Ghatee, Kh. Shekoohi; “Relation between surface tension and isothermal compressibility: application of statistical mechanical equation of state”; Department of chemistry; 227, 1–7, 2005.

[3] R. K. Burkat and A.J. Richard; “Low-pressure studies of the isothermal compressibilities and specific volumes of organic liquids”; Department of Pharmaceutical Chemistry; 7, 271-277, 1975.

[4] J. K. Percus and G. J. Yevick; “ Statistical Approach to the Domain of Action of Collective Co-ordinates in the Many Body Problem” ; valter kidde laboratory of physics; 1057-1073,1957.

Comparison of bulk modulus as Benzene dense fluid using the perturbation theory and comparison with Peng-Robinson equation of state

V. Moeini [a] , M. Kamel [b*]
a Department of Chemistry, Payame Noor University, PO BOX 19395-3697 Tehran, Iran
b Department of Chemistry, Payame Noor University, PO BOX 19395-3697 Tehran, Iran
Email: kamel.maede@yahoo.com

Key words: Bulk modulus, Dense fluids, Perturbation theory, Peng-Robinson (PR) equation of state

Introduction:

The bulk modulus, is a scalar quantity relating an isotropic pressure to an average change in volume. It is the average of the three inverse linear compressibilities (change of length induced by pressure). Huang and O'Connell [1] checked the regularity for more than 250 fluids and used it as the basis of a correlation scheme for the volumetric properties of compressed liquids and liquid mixtures. Boushehri [2] presented a theoretical basis for this regularity interms of a statistical–mechanical equation of state [3]. Linearity of bulk modulus as a function of pressure: More than 100 years ago, a regularity has been discovered by Tait [4] in which isotherms of bulk modulus (reciprocal isothermal compressibility), $1/\beta = \rho(\partial p/\partial \rho)_T$, of a liquid as a function of pressure vary linearly.

Theory:

The regularity was originally suggested on the basis of a simple lattice-type model applied to a Lennard-Jones (12, 6) fluid [5] and calculated perturbation theory for bulk modulus of benzene .Perturbation theory (PT) is explicit in Helmholtz energy *A* with the two independent variables density ρ and *T*. At a given temperature, the pressure can be determined by Helmholtz energy

$$p(T,\rho) = -\left(\frac{\partial A}{\partial V}\right)_T \tag{1}$$

Using the general expression of the relation to the reduced Helmholtz energy $\phi = A/(RT)$ and its derivatives gives

$$\frac{p(\delta,\tau)}{\rho RT} = 1 + \delta\phi_\delta^r \tag{2}$$

Since the Helmholtz energy as a function of density and temperature is one of the four fundamental forms of an equation of state, all the thermodynamic properties of a pure substance can be obtained by combining derivatives of the reduced Helmholtz energy ϕ [6]. The purpose of this paper is to point out an expression for the bulk modulus of benzene dense fluid using perturbation theory. In this paper we present a simple method that keeps the first-order, second order and third order temperature dependence of parameters in perturbation theory versus inverse temperature. Then, the bulk modulus is calculated from perturbation theory. The Peng-Robinson (PR) EOS [7] may be used to compute the solubility parameter. This equation is given as :

$$p = \frac{RT}{V-b} - \frac{a(T)}{V(V+b)+b(V-b)} \tag{3}$$

In later stages, we attemped to calculate the bulk modulus by Peng-Robinson (PR) equation of state and taking its derivative with respect to volume as a testing the other equation of state.

$$\left(\frac{\partial p}{\partial V}\right)_T = -\frac{RT}{(V-b)^2} + \frac{(2V+2b)a(T)}{(V^2+2bV-b^2)^2} \tag{4}$$

Result and discussion:

The bulk modulus is computed for dense liquid and supercritical fluids using three different models. We have derived an expression for the bulk modulus of benzene dense fluid using the perturbation theory. To decrease adequately the deviation in the bulk modulus from the experimental data, it was necessary to extend the temperature series to second order and third order. Therefore, the present approach for obtaining the bulk modulus from *p–v–T* data contrasts with the experimental data by extension of the temperature series to second order $PT^{(2)}$, third order $PT^{(3)}$ and their derivatives. The bulk modulus predicts from this simple model are in good agreement with experimental data. The results show that the accuracy of this method is generally quite good.

References:

[1] Y. Huang, J.P.O'Connell; Fluid Phase Equilib; 37, 75-84, 1987

[2] A. Boushehri, Fu-M.Tao, and E.A.Mason; J.Phys.Chem; 97, 2711-2714, 1993

[3] G. Ihm, Y. Song, E.A. Mason; J. Chem, Phys. Chem; 99, 9248, 1995

[4] P. G. Tait; Physics and Chemistry of the Vayage of H.M.S. Challenger ; vol. 2, part IV, S.P. LXI, HMSO, London, 1888

[5] G. Parsafar and E. A. Mason, *J.Phys.Chem*. 97, 9048-9053, 1993

[6] V. Moeini; J.Phys.Chem.B; 110 3271, 2006

[7] D. Y. Peng, D.B.Robinson; Ind.Eng.Chem.Fund; 15, 59-64, 1976

Conformational distribution of ternary complex of Sm^{+3} with 5,7-dichloroquinoline-8-ol and 4-vinyl pyridine $[Sm\ (VP)_2\ (DCQ)_3]^{+3}$: A computational statistical mechanical approach

T. Hosseinnejad*
Department of Chemistry, Faculty of Science, Alzahra University, Vanak, Tehran, Iran
Email: tayebeh.hosseinnejad@alzahra.ac.ir

Key words: Conformational analysis, Sparkle model, Density functional theory, Partition function, Statistical mechanical approach.

Introduction:

During the recent years, there are many reports on the lanthanide ions imprinted polymer preparation [1] that describe a preconcentrative separation of lanthanide cations by co-polymerizing $[Ln\ (VP)_2\ (DCQ)_3]^{+3}$ ternary complexes, styrene and a cross linker. In this computational study, we confined our attention on the conformational population analysis of $[Sm\ (VP)_2\ (DCQ)_3]^{+3}$ complex to investigate the effect of internal degrees of freedom on the stability of conformers of this complex by density functional theory calculations.

Computational details:

All conformers of $[Sm\ (VP)_2\ (DCQ)_3]^{+3}$ complex were fully optimized at B3LYP/6-31G* level of theory. The 46 core and 4f electrons of samarium ion are replaced with the quasi-relativistic effective core potentials (RECPs) of Stuttgart group [2]. It is noteworthy that the initial conformations of $[Sm(VP)_2\ (DCQ)_3]^{+3}$ complex were deduced by carrying out a conformational search procedure based on sparkle/PM3 semi-empirical method [3]. All DFT calculations were performed using the GAMESS suite of programs [4] and MOPAC 2009 package [5] were utilized for semi-empirical investigations.

Result and discussion:

We have first designed a conformational search process to produce a reasonable set of the most stable conformers of $[Sm\ (VP)_2\ (DCQ)_3]^{+3}$ complex. For these conformers, the moments of inertia, vibrational frequencies and ground-state electronic energies were calculated in order to obtain the equilibrium constant, K_{IJ}, of the conformational conversion reaction between conformer I and J at various temperatures. In Table 1 we have reported the molecular partition functions ratios for electronic, vibrational and rotational contributions of the most stable conformer (expressed as C_1) and those corresponding to the other conformers at 298.15 K. The calculated relative electronic energies of all conformers, their electronic contribution of conformational distributions and total conformational distribution percents have been also presented in Table 1.

Table 1.

	$E_{elec,relative}$ (kcal.mol^{-1})	K_{elec}	K_{vib}	K_{rot}	K_{I1}	Electronic conformational distribution(%)	Conformational distribution(%)
C_1	0	1	1	1	1	59.41907	76.766
C_2	0.737	3.474	2.346	0.998	8.142	17.103	9.428
C_3	0.8456	4.167	2.429	0.983	9.953	14.258	7.712
C_4	1.121	6.638	2.135	0.972	13.784	8.950	5.568
C_5	3.350	285.876	0.598	0.994	170.092	0.207	0.451
C_6	4.149	1100.240	1.189	1.003	1313.455	0.054	0.058
C_7	5.347	8316.936	0.699	0.998	5810.796	0.007	0.013

Conclusion:

The analysis of conformational equilibrium constants for $[Sm(VP)_2(DCQ)_3]^{+3}$ complex indicates that not only the most stable conformer (C_1) should be favored with respect to all of other conformers from the electronic point of view, but also the electronic energy differences between conformer C_1 and all other conformers are so large that the rotational and vibrational contributions do not affect remarkably the order of conformational distributions. Survey of temperature effect on population distribution demonstrated that by raising temperature the less stable conformers were populated more and their conformational distribution percent values were increased.

References:

[1] S. Shirvani-Arani et al.; “Synthesis of nano-pore samarium (III)-imprinted polymer for preconcentrative separation of samarium ions fromother lanthanide ions via solid phase extraction”; Anal. Chim. Acta.; 623, 82-88, 2008.

[2] M. Dolg et al.;“A combination of quasirelativistic pseudopotential and ligand field calculations for lanthanoid compounds”; Theor. Chim. Acta. ; 85, 441-450, 1993.

[3] A. V. M. de Andrade et al.;“Sparkle model for the quantum chemical AM1 calculation of europium complexes”; Chem. Phys. Lett.; 227, 349-353, 1994.

[4] M. W. Schmidt et al.; “General atomic and molecular electronic structure system”; J. Comput. Chem.; 14, 1347-1363, 1993.

[5] MOPAC2009,J.J.P. Stewart, Stewart Computational Chemistry, Version 8.331M, web: HTTP://OpenMOPAC.net.

Evaluation of thermodynamic properties of polyethylene copolymer melts using GMA equation of state

A. Morsali [a], M. M. Heravi[a] and N. Khaki [a*]

[a] Department of Chemistry, Mashhad Branch, Islamic Azad University, Mashhad, Iran
(Email: niloofar_calendula@yahoo.com)

Keywords: GMA Equation of state, Polyethylene-propylene, Linear polyethylene, Polyethylene-1-butene

Introduction:

Concerning the scientific and industrial importance of polyethylene copolymer, endeavors have been made in this research to use a simple and accurate equation of state for prediction of thermodynamic properties of these compounds. Using GMA equation of state, different groups of polyethylene copolymer, including polyethylene-propylene, polyethylene-1-butene, linear polyethylene have been studied.

Theory:

The GMA equation of state [1-3] is based on the average potential energy and is given as:

$$(2Z-1)V_m^3 = A(T)+B(T)\rho \qquad (1)$$

where Z, V_m, and ρ are compressibility factor, molar volume, and molar density, respectively. The intercept and slope of this equation depend on temperature via the equations:

$$A(T) = A_0 - 2A_1/RT + 2A_2 \ln T/R \quad (2) \quad , B(T) = B_0 - 2B_1/RT + 2B_2 \ln T/R \quad (3)$$

where A_0–A_2 and B_0–B_2 are constants.

Results and discussion:

We have used the experimental PVT data for ethylene-propylene, ethylene-1-butene, linear polyethylene to plot $(2Z-1)V_m^3$ against ρ for each isotherm. As the tables 1 and 2 show the linearity holds very well for all isotherms. A more sensible test for the GMA equation of state is to calculate the differential thermodynamic properties, such as internal pressure (P_i), isothermal compressibility (κ) and thermal expansion coefficient (α) at different temperatures and pressures (Table 3).

Conclusion:

It has been concluded and ascertained that GMA Eos is capable of predicting the density of these compounds with a high degree of accuracy. A more sensitive test for any state equation is the prediction of differential thermodynamic properties. For such a test, GMA Eos predicted these properties with an acceptable degree of accuracy.

Table1: The minimum and maximum square of correlation coefficient (R^2) of Eq. (1)

fluid	*T(K)*	$P_{\min}-P_{\max}\,(\mathrm{atm})$	$\rho_{\min}-\rho_{\max}\,(\mathrm{mol\cdot L^{-1}})$	R^2 for GMA
polyethylene-1-butene	**313.7-493.5**	**0.99009-1980.198**	**0.006759-0.008568**	**0.9953**
polyethylene-propylene	**313.8-493.8**	**0.99009-1980.198**	**0.003919-0.004901**	**0.9948**
linear polyethylene	**313.8-493.6**	**0.99009-1980.198**	**0.003474-0.004746**	**0.9109**

Table2: The average of absolute percent deviations of the calculated densities.

fluid	$T_{\min}-T_{\max}\,(\mathrm{K})$	$P_{\min}-P_{\max}\,(\mathrm{atm})$	$\rho_{\min}-\rho_{\max}\,(mol\cdot L^{-1})$	$\left(100\times\left\|\rho_{\exp}-\rho_{\mathrm{cal}}\right\|/\rho_{\exp}\right)$
polyethylene-1-butene	**313.7-493.5**	**0.99009-1980.198**	**0.006759-0.008568**	0.91
polyethylene-propylene	**313.8-493.8**	**0.99009-1980.198**	**0.003919-0.004901**	0.52
linear polyethylene	**313.8-493.6**	**0.99009-1980.198**	**0.003474-0.004746**	1.83

Table 3: Calculated K_T ،α_P ،P_i for polyethylene-1-butene (some temperatures)

$P(atm)$	T(k)	ρ (mol/lit)	p_i (atm)	α_p (k^{-1})	k_T (atm^{-1})
0.990099	313.7	0.007933	5.55E+03	7.66E-04	7.29E-05
495.0495	333.5	0.007967	5.40E+03	6.17E-04	5.99E-05
198.0198	353.6	0.007595	4.13E+03	5.03E-04	7.79E-05
99.0099	373.8	0.007415	3.50E+03	3.77E-04	8.41E-05
990.099	393.9	0.00773	3.98E+03	3.35E-04	5.31E-05
1485.149	393.9	0.007891	4.38E+03	3.56E-04	4.52E-05
198.0198	414	0.007284	2.83E+03	2.05E-04	7.86E-05
495.0495	414	0.007439	3.12E+03	2.31E-04	6.57E-05
990.099	414	0.007652	3.57E+03	2.61E-04	5.23E-05

References:

[1] Goharshadi EK, Morsali A, Abbaspour M. Fluid Phase Equilibr.,230 (2005)170–5.

[2] Goharshadi EK, Berenji AR. J. Nucl. Mater., 348 (2006) 40–4.

[3] Goharshadi EK, Moosavi M. Thermo,chim. Acta, 447(2006) 64–8.

Prediction of the parameters of the average effective pair potential in liquid alkali metals using a new equation of state

Majid Moosavi[*], Shiva Sabzevari

Dept. of Chemistry, Faculty of Sciences, University of Isfahan, Isfahan 81746-73441, Iran

Email: m.mousavi@sci.ui.ac.ir

Keywords: Interaction parameters, Equation of state, AEPP, Metal-nonmetal transition.

Introduction:

It is possible to use an effective pair potential along with the pairwise-additive approximation for the potential to calculate the macroscopic properties of a dense system. Inversely, one can obtain the parameters of the average effective pair potential, namely σ, the separation at which the potential is zero, and ε, the depth of the potential well. In this work, we try to obtain the potential parameters of the liquid alkali metals from the parameters of a new proposed equation of state.

Theory:

The semi empirical (6-3) Lennard-Jonse potential function, which represents a softer repulsion and a greater attraction, is proper for different liquid alkali metals. The form of this potential is:

$$u(r) = A\varepsilon\left[\left(\sigma/r\right)^6 - \left(\sigma/r\right)^3\right] \qquad (1)$$

where A is a constant, ε is the potential well depth, and σ is the interatomic distance at which the potential function is zero. Using the Eq. (1) along with the well-known thermodynamic EoS for internal pressure, P_i, the GMA equation [1] can be modified as:

$$\left(2Z-1\right)V_m = C(T) + D(T)\rho \qquad (2)$$

The intercept and slope of this equation depend on temperature via the following equations:

$$C(T) = c_o - \frac{2c_1}{RT} + \frac{2c_2 \ln T}{R} \quad ; \quad D(T) = d_o - \frac{2d_1}{RT} + \frac{2d_2 \ln T}{R} \qquad (3)$$

The molecular parameters can be calculated using the numerical values of the c_1, c_2, d_1, and d_2:

$$r_m = -K\left(\frac{d_1 + d_2 T}{c_1 + c_2 T}\right)^{1/3} \quad , \quad \varepsilon = \left[\frac{-1}{N}\left(\frac{(c_1 + c_2 T)^2}{d_1 + d_2 T}\right)\right] \tag{4}$$

Results and discussion:

The values of r_m calculated from Eq. (4) and those obtained from X-ray diffraction measurements [2-4] for cesium, potassium, and sodium at their melting temperatures have been given in Table 1. As this table shows, the predicted values are quite close to the literature data. Fig. 1 shows the plots of r_m and *ε/k* versus temperature for cesium in the range of 350-2000 K, respectively. Structure change can be seen evidently in Fig. 1 on which up to 1350 K, r_m increases linearity with temperature and bends upward thereafter. According to the literature [2-4], there is a change in the cesium structure after 1350 K, the temperature on which the metal-nonmetal transition occurs. Fig. 1 also shows that the *ε/k* smoothly decreases with temperature. This result is also in agreement with the literature.

Table 1. The values of r_m calculated from Eq. (4) and those obtained from X-ray diffraction measurements [2-4] for cesium, potassium, and sodium at their melting temperatures.

Alkali metal	T_m/K	r_m/Å Eq. (4)	r_m/Å [2-4]
Cs	301.59	5.25	5.40
K	336.8	4.57	4.50
Na	370.87	3.70	3.72

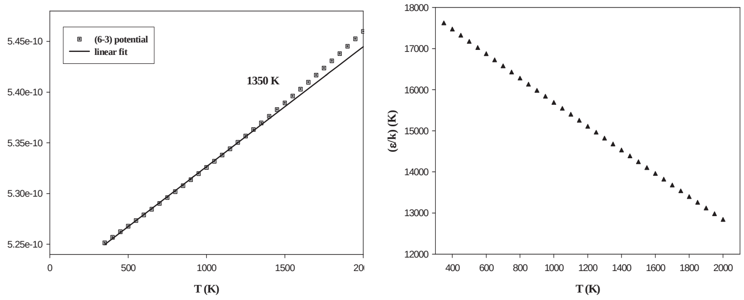

Fig. 1. Plot of r_m and *ε/k* versus temperature for liquid cesium in the range of 350-2000 K. The solid line is the linear fit to r_m values.

According to this method, the estimation of the molecular parameters is simpler and less costly than complicated experimental methods. Also, the used potential function is in fact an effective potential that includes both pair and many-body interactions in liquid alkali metals. The results show that the *ε/k* smoothly decreases with temperature while the parameter σ increases.

References:

[1] E.K. Goharshadi, A. Morsali, M. Abbaspour, Fluid Phase Equilib. 230, 170-175, 2005.

[2] R.C. Ling, J. Chem. Phys. 25, 609-613, 1956.

[3] W. Weickenmeier, U. Diemar, M. Wahl, M. Raab, W. Demtroder, W. Muller, J. Chem. Phys. 82, 5354-5363, 1985.

[4] M. Krauss, W. J. Stevenes, J. Chem. Phys. 25, 4236-4242, 1990.

Calculation of the critical point for the Ising model over two-layer triangular lattice using Cellular automata approach

Najmeh Sadr , Mehrdad Ghaemi
Department of chemistry, Kharazmi University, Tehran, Iran
Email : najmeh.sadr65@yahoo.com

Key Words: Cellular Automata ,critical point , Ising model

Introduction:

One of the most interesting phenomena in the physics of the solid state is ferromagnetism. Ferromagnetism and antiferromagnetism are based on variations of the exchange interaction, which is a consequence of the Pauli principle and the Coulomb interaction. [1]

The Ising model is a crude attempt to simulate the structure of a physical ferromagnetic substance[1,2].

The Cellular Automata (CA) are one of methods that could be used to describe the Ising model [1].

Two-Layer Ising Model:

Consider a two layer triangular lattice , with the periodic boundary condition ,each layer with r rows and p columns. The number of the sites in the lattice is $2\times r\times p=N$ .We consider the next nearest neighbor interactions as well, so the number of neighbor for each site is 7. In the two-layer Ising model , for any site we define a spin variable $\sigma^{1(2)}\ (i, j) = \pm 1$ in such a way that $i = 1,..., r$ and $j = 1,..., p$ where superscript 1(2) denotes the layer number.[1,3] We include the periodic boundary condition. tThe configuration energy (E) and the average magnetization of the lattice ($<m>$) and also the magnetic susceptibility (χ)and specific heat per spin (C) can be calculated for this model [3].

Method:

The Glauber method was used with checkerboard approach to update sites[1,4]. For this purpose the surface of two layers are checkered same as each others . For updating the lattice, we use following procedure : after updating the first layer , the second layer could be updated[3].

Calculation :

The critical point for the two-layer Ising model could be obtained from different approaches that we describe them as follow. When we start CA with the homogeneous initial state (namely, all of the sites have spin up or +1), before the critical point (K_c), the magnetization per spin (*m*) will decay rapidly to zero and fluctuate around that point. After the critical point, *m* will arrive to the nonzero point and fluctuate around it; and with increasing of *K*, the magnetization per site will increase. But at the critical point, *m* will decay very slowly to the zero point and the fluctuation of the system will reach to a maximum. For each *K*, the time that *m* reaches to the special point and start to fluctuate around it is called the relaxation time[3]. The obtained value for *K*c from these graphs is 0.212

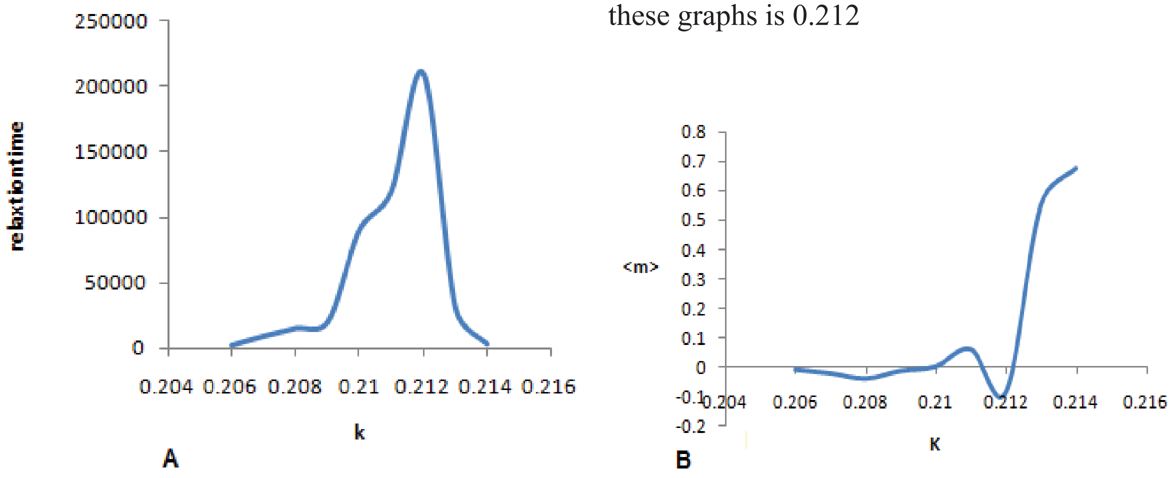

Fig. 1. A) Relaxation times versus. *K*. The maximum of the graph is *K*c **B)** <*m*> versus. coupling coefficients(*K*). The average for each K is calculated after its relaxation time. (The calculated data are the results for the lattice for which each layer has 60× 60 sites, starting from the homogeneous initial state with all spins up, time steps = 600000)

References :

[1]Ghaemi , M. Cellular Automata -Simplicity Behind Complexity Edited by Alejandro Salcido Published by InTech 2011.chap 21

[2] Huang, K.: Statistical mechanics. John Wiley and Sons, 2nd Edition, (1987)

[3] Asgari, Y.; Ghaemi M.; and Mahjani, M. G. Lecture Notes in Computer Science, 2004, 3305, 709-718

[4]Glauber, R.J.: J. Math. Phys. (1963) 4, 294

The critical point of the two-layer 3-state Potts model over square lattice (cellular automata approach)

Neda Khalili* ,Mehrdad Ghaemi
Department of Chemistry, Kharazmi University, Tehran, Iran
* Neda.Khalyly@gmail.com

Keywords: Potts Model; Ising Model; cellular automat; critical point

Introduction:

The Ising model is a crude attempt to simulate the structure of a physical ferromagnetic substance. This model plays a very special role in statistical mechanics and generates the simplest nontrivial example of a system undergoing phase transitions[1].

Since the exact solution of Ising models exists only for one- and two-dimensional models and there is not such solution for others, the simulation methods maybe used to obtain critical data and Cellular Automata(CA) is one of these simulation methods[2].

Potts model:

After the Ising model, the Potts model is perhaps the most prominent model of phase transitions in statistical mechanics [3].Consider a two-layer square lattice with the periodic boundary condition, each layer with p rows and r columns. Each layer has $r \times p$ sites and the number of the sites in the lattice is $2 \times r \times p = N$. We consider the next nearest neighbor interactions as well, so the number of neighbors for each site is 5. For any site, we define a spin variable $\sigma^{1(2)}(i, j) = 0, \pm 1$, so that $i = 1, \dots, r$ and $j = 1, \dots, p$[2].

Method:

We considered the isotropic, ferromagnetic and symmetric case in which $Kx = Ky = Kz \geq 0$.We have used a two-layer square lattice that each layer has (50×50) sites, and to reduce the finite size effects, the periodic boundary condition is used [2]. We let the system reaches to a stable state after some time step ($t=\tau$), and then to be updated up to the end of the automata . The time that m takes to reach a special value and start to fluctuate is known as the relaxation time (τ).

Conclusion:

We calculated the average value of magnetization per site <*m*>. By drawing the graph of <*m*> verses *K*, we could get the critical point(*K*c).The relaxation time increases before the critical point and reaches maximum at *K*c, but after the critical point, τ decreases. Hence, the critical point could be obtained Also from the graph of τ versus *K*.[2]

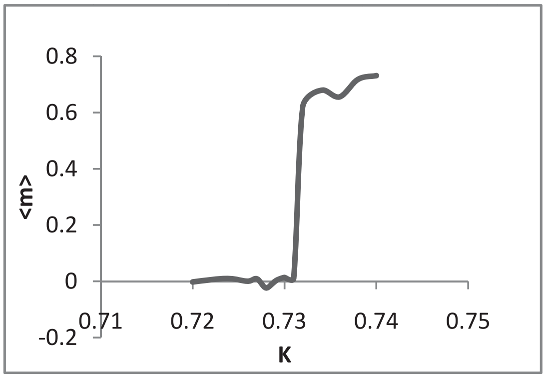

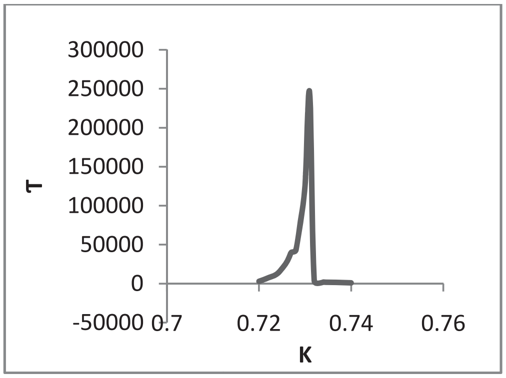

References :

[1] Ghaemi M,CELLULAR AUTOMATA-SIMPLICITY BEHIND COMPLEXITY ,edit by Alejandro Salcido, published by InTech, 2011.

[2] Asgari, Y.; Ghaemi M.; J. Theo. Comp. Chem. 2006, 2, 141-150

[3] Wu F. Y, Rev Mod Phys 54:235, 1982.

Generalized modified SAFT-BACK model for long chain hydrocarbons

A. Maghari and Z. Negaresh
Department of Physical Chemistry, University of Tehran, Tehran, Iran

keywords: modified SAFT-BACK, Equation of state, PVT properties, second order derivative properties, chain molecules

Introduction:

The thermodynamic properties of *n*-alkanes and their mixtures are important for practical interest, since they are involved in a number of refinery processes. More recently, a model based on Statistical Associating Fluid Theory (SAFT), called modified SAFT-BACK EOS, has been strongly tested to describe the phase equilibria as well as second thermodynamics derivative properties for C_1-C_{10} chain alkanes and their binary mixtures was developed by Maghari et al. [1-3]. This model EOS be able to describe the thermodynamic properties of chain fluids in whole of region, including near critical region.

In this work, we generalized the modified SAFT-BACK EOS for longer chain fluids and obtained both first and second derivative properties of C_{11} to C_{20} chain alkanes.

According to the modified SAFT-BACK EOS, the residual Helmholtz free energy for a fluid is written as a sum of the separate contribution to the energy

$$A^{\text{res}} \equiv A - A^{\text{ideal}} = A^{\text{seg}} + A^{\text{chain}} \tag{1}$$

$$A^{\text{seg}} = A^{\text{hcb}} + A^{\text{dis}} \tag{2}$$

in which the hcb and dispersion contributions to the segment Helmholtz free energies are as follows:

$$\frac{A^{\text{hcb}}}{Nk_{\text{B}}T} = m\left[\frac{\alpha^2}{(1-\eta)^2} - \frac{\alpha^2 - 3\alpha}{1-\eta} - (1-\alpha^2)\ln(1-\eta) - 3\alpha\right] \tag{3}$$

$$A^{\text{dis}} = m\sum_i \sum_j D_{ij}\left(\frac{u}{k_{\text{B}}T}\right)^i \left(\frac{\eta}{\tau}\right)^j \tag{4}$$

in which D_{ij} is a series of 36 universal constants fitted by Chen and Kreglewski [4] from the experimental data of argon. The chain formation contribution, appeared in Eq. (1) can be written as:

$$A^{\text{chain}} = A^{\text{chain,hcb}} + A^{\text{chain,dis}} \tag{5}$$

where the chain hcb and chain dispersion contributions are

$$\frac{A^{\text{chain,hcb}}}{Nk_{\text{B}}T} = \sum_i x_i(1-m_i)\ln g_{ii}^{\text{hcb}}(d_{ii}) \tag{6}$$

$$\frac{A^{\text{chain,dis}}}{Nk_{\text{B}}T} = \frac{\lambda A^{\text{chain,hcb}}}{A^{\text{hcb}}} A^{\text{dis}} \tag{7}$$

After the calculation of Helmholtz free energy from Eq. (1)-(7), the pressure, heat capacities and sound velocity can be obtained through the standard thermodynamic relations.

Results and discussion:

The EOS parameters ($u^0/k_{B,}$ m, $\upsilon^{00,}$ α) are adjusted using an objecting function averaged absolute PVT errors. Figure 1 shows the pressure versus density for C_{17} at several temperatures, which compared with available experimental data. Furthermore, the predictive ability of the model on the estimation of the second thermodynamic derivative properties for long chain fluids has been checked. In fact, the speed of sound is generally represented as a severe consistency test for EOS, since it involves the temperature and density partial derivatives of pressure. Figure 2 shows the speed of sound versus density for C_{17} at several temperatures. Excellent agreement between the experimental and the predicted values of the speed of sound are observed at higher temperature. The available correlated data, taken from NIST WebBook [5]

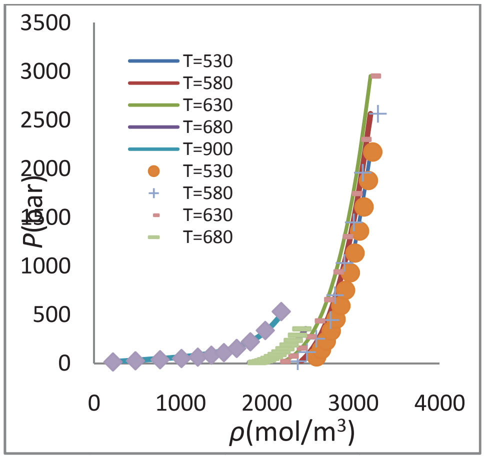

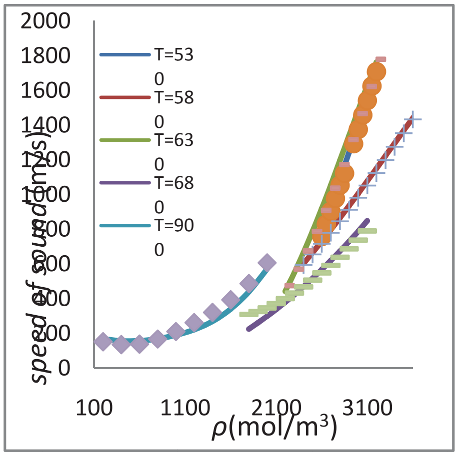

Fig1. The behavior of pressure for C_{17} **,** at five different temperatures and wide density.

Fig2. The behavior of sound velocity for C_{17} , at four different temperatures and wide density.

References

[1] A. Maghari, M. S. Sadeghi, *Fluid Phase Equilibria* **252** (2007) 152.

[2] A. Maghari, Z. Safaei, *J. Mol. Liquids* **142** (2008) 95.

[3] A. Maghari, M. Hamzehloo, *Fluid Phase Equilibria* **302** (2011) 195.

[4] S.S. Chen and A. Kreglewski, *Ber. Bunsen-Ges. Phys. Chem*. **81** (1977) 1048.

[5] NIST Chemistry Webbook, NIST Standard Reference Database Number 69, National Institute of Standards and Technology (http://webbook.nist.gov/chemistry).

Study of Surface tension, Density and Viscosity of Hexanoic acid by MD Simulation and Experimental Measurement

Mohammad Hadi Ghatee, Fatemeh Ghanavati
Department of chemistry, Shiraz University, Shiraz, 71454 Iran
Tel: +98 711 6137353, Email: ghatee@susc.ac.ir

Key words: Hexanoic acid; MD Simulation; Surface tension; Density; Viscosity.

Introduction:

n-Alkanoic acids have been probably the most frequently applied surface active agents in basic and applied research. In particular, volumetric, transport, and surface properties of carboxylic acids are important for theoretical and practical applications. In the case of carboxylic acids the information available in literature is limited. Hexanoic acid (caproic acid) is a yellowish transparent oily liquid with a pungent smell. Hexanoic acid is one of the oxidized form of compounds constituting crude oil. It is used in manufacturing of perfume, medicine, lubricating grease, rubber, and dyes.[1-3] To design chemical reactors and separation equipment efficiently, it is necessary to have data on fluid thermodynamic properties over a wide range of temperature. Molecular dynamics simulation has been popularly used recently to simulate properties of the liquid state of matter particularly the organic liquids. By the simulation, it is also possible to study the molecular structure of the liquid state at microscopic level, where particular interactions are responsible for the properties shown by the liquids. Both equilibrium and transport properties can be simulated. However the simulated thermodynamic properties are in general in a better agreement with experiment than the transport property such as viscosity.

Method:

Density functional theory (DFT) as implemented in GAUSSIAN 03 program was used to find the structural parameters required to set up the force field of the hexanoic acid. The simulations were performed using DL_POLY2.17 package. Surface tension, viscosity and density were both simulated and measured experimentally in our lab in the range 298 to 373K. Bulk and liquid/vapor structure were also studied by simulation.

Result and discussion:

The results of simulation for density are shown in Figure 1. The simulation was performed by using atom's charges based on CHELPG calculation. In the same figure the density we measured and of the literature are shown for comparison. The plots indicate that simulated density is underestimated with respect to both measurements, particularly at high temperatures. The density profile of the hexanoic acid/air interface shown in Figure 2 and 3 is very much similar to those of most polar liquids. The value of surface tension (σ) was calculated from the components of pressure tensor of the simulated box. Figure 4.

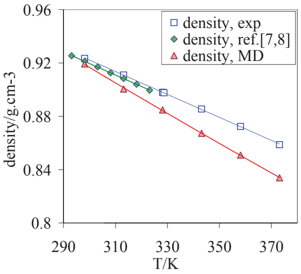

Figure 1.

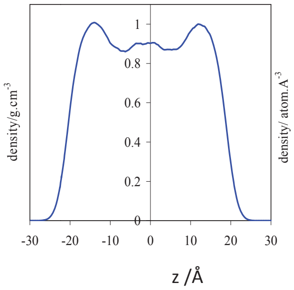

Figure 2. density profile at 298 K

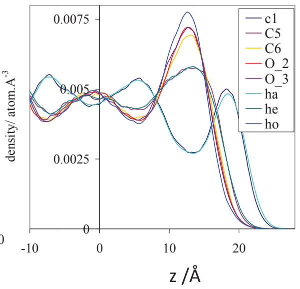

atoms density Figure 3.
profile at 298 K

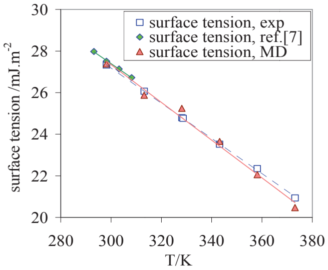

Figure 4.

Conclusion :

The simulated densities are very close to the experimental values at low *T*'s but show some deviations at high *T*'s (%*Dev*=2.89) with %*AAD*=1.75. In Figure 3, the atoms density profile at the interface indicates that the alkyl chain is extended towards the vapor side and the carboxylic group towards the liquid side of the interface. This can be expected structure of the liquid surface as the energetic of molecules at the interface imply. The simulated surface tension of hexanoic acid is plotted in Figure 4. The variation of surface tension with temperature is satisfactorily linear with linear correlation coefficient R^2=0.9876. The results are in good agreement with experimental measurements.

Reference:

[1] Levy, P. F. and *et al*; *Alkane Liquid Fuels Production from Biomass*; Wise, D. L., Ed.; CRC Liquid Fuels Developments: Boca Raton, FL, 1983; pp 159-188.

[2] Levy, P. F. and *et al*; Enzyme Microb.Technol; 3, 207–215.1981.

[3] Levy, P. F. and *et al*; Molyneaux, M. S. Liquid Fuels Production from Biomass; United States Department of Energy Report, DOE/ET/20050-T4; U.S. Department of Energy: Washington, DC, 1980.

[4] Pople, J.A.; Gaussian 03; Revision B.03; Gaussian; Inc; Pittsburgh PA; 2003.

[5] Smith, W.; T.R. Forester; http://www. dl.ac.uk/TCSC/Software/DL_POLY/main.html 1999.

[6] Suzuki, T. and *et al*; J. Chem. Inf. Comput. Sci; 41, 776-790, 2001.

[7] Cao, W. and *et al*; Ind. Eng. Chem. Res; 31, 2603-2619, 1992.

Molecular distribution in a binary solution with different radii on a nanoscale size

Mohsen Farshad*[a] , G.A.Parsafar[b]
[a]Department of Chemistry, Sharif University of Technology, Tehran, Iran
[b]Department of Chemistry, Sharif University of Technology, Tehran, Iran
Mohsen_farshad_l@yahoo.com

Confined systems have attracted a great deal of attention during the past years because of their theoretical and practical relevance. It is well-known that confinement effects can induce new types of phase transitionsincluding wetting, capillary condensation, and layering in fluids, whereas there are not any counterparts for them in the bulk[1-3].

In orderto investigate the entropy effect on the molecular distribution in a nanotube, we have considered the distribution of a binary hard spheres solution in this work. The investigation was carried out by using a simple model, in which the wall is considered to be a rigid-smooth surface and the species inside it are two types of hard spheres with different radii.

The entropy calculations have been done in two different extremedensities.In low densities of particles, we distribute the smaller particles at the head and the larger particles at the middle. In another experiment with the same low density particles, we set the smaller particles at the middle and larger particles at the head. We repeat the same experiment with the same arrangement of particles with high densities. In both densities, we considered that larger particles have more tendencies to be at the head instead of the middle in order to increase the entropy. The entropy was derived from Helmholtz equation (1).

$$dA = -SdT - pdV \qquad (1)$$

Whereas the pressure was derived from Carnahan Starling equation of state for hard sphere particles (2)[4].

$$\frac{pV}{nRT} = Z_{CS}^{HS} = \frac{1+\eta+\eta^2-\eta^3}{(1-\eta)^3} \qquad (2)$$

We compare the results of theoretical calculations and molecular dynamic simulations together that lead us to conclude that they both verify each other.

We also repeated the molecular dynamic simulation calculations with below set ups:

1- wall with Lennard-Jones potential and particles with Lennard-Jones potential.
2- Rigid wall and particles with Lennard-Jones potential.

In both experiments, we changed the Lennard-Jones parameters. In this workthere were a competition between entropy effect and energy effect to arrange the both type of particles in the confinednanotube. Finally we could found out theamount of energy and entropy effect on arrangements of particles in the nanotube.

Keywords: Entropy effect, hard sphere, radial distribution, dynamic molecular simulation

References:

[1] AmenehTaghizadeh and Ezat (Tahmineh) Keshavarzi, *J. Phys. Chem*. **B2011**, 115, 3551-3559.

[2] Gelb, L. D.; Gubbins, K. E.; Radhakrishnan, R.; Sliwinska-Bartkoviak, M. Rep. Prog. Phys. 1999, 62, 1573.

[3] G. Jackson, J. S. Rowlinson, F. Van Swol, *J. Phys. Chem.*, **1987**, *91* (19), pp 4907–4912.

[4]Carnahan NF, Starling KE, Equation of state for nonattracting rigid spheres. J ChemPhys 51:635–636, **(1969)**

Molecular distribution in a binary solution with different radii on a nanoscale size

Mohsen Farshad*[a] , G.A.Parsafar[b]
[a]Department of Chemistry, Sharif University of Technology, Tehran, Iran
Mohsen_farshad_l@yahoo.com

In orderto investigate the entropy effect on the molecular distribution in a nanotube, we have considered the distribution of a binary hard spheres solution in this work. The investigation was carried out by using a simple model, in which the wall is considered to be a rigid-smooth surface and the species inside it are two types of hard spheres with different radii.

The entropy calculations have been done in two different extremedensities.In low densities of particles, we distribute the smaller particles at the head and the larger particles at the middle. in another experiment with the same low density particles, we set the smaller particles at the middle and larger particles at the head. We repeat the same experiment with the same arrangement of particles with high densities. In both densities, we considered that larger particles have more tendencies to be at the head instead of middle in order to increase the entropy. The entropy was derived from Helmholtz equation.

$$dA = TdS - PdV$$

With deriving pressure from Carnahan Starling equation of state for hard sphere particles

$$\frac{PV}{nRT} = Z_{CS}^{HS} = 1 + \eta + \eta^2 - \eta^3/(1-\eta)^3$$

We compare the results of theoretical calculations and molecular dynamic simulations together and we concluded that they both verify each other.

We also repeated the molecular dynamic simulation calculations with below set ups:

1- wall with Lennard-Jones potential and particles with Lennard-Jones potential.
2- Rigid wall and particles with Lennard-Jones potential.

In both experiments, we changed the Lennard-Jones parameters.

Keywords : 1-Entropy effect 2-hard sphere 3-radial distribution 4-dynamic molecular simulation

References:

[1] AmenehTaghizadeh and Ezat (Tahmineh) Keshavarzi, *J. Phys. Chem*. **B2011**, 115, 3551-3559.

[2] G. Jackson, J. S. Rowlinson, F. Van Swol, *J. Phys. Chem.*, **1987**, *91* (19), pp 4907–4912.

[3]Carnahan NF, Starling KE, Equation of state for nonattracting rigid spheres. J ChemPhys 51:635–636, (1969)

Study of the Properties of Pure Oil and Oil/Water Interface by Molecular Dynamics Simulation

Mohammad Hadi Ghatee*, Zeinab Fotouhabadi
Department of chemistry, Shiraz University, Shiraz, 71454 Iran
Tel: +98 711 6137353, Email: ghatee@susc.ac.ir

Keywords: Oil/water interface, Accumulation, 4-Ethylpyridine, Surface tension, Molecular dynamics simulation

Introduction:

Most of the technological and biological processes occur at an interface [1]. Unlike the bulk materials, the interface system is a noncentrosymmetric environment. The surface compositions of liquids are different from the bulk due to unbalanced forces exerted on the molecules at the interface. Surface tension, among other properties, is the most important property that can be measured accurately, and represents the thermodynamic of the liquid surface. Surface entropy and surface energy can be determined very accurately from the measurement of temperature dependent surface tension. Accordingly density profile**,** surface thickness**,** and molecular orientation can be studied. Surface tension is the fundamental parameter of surface chemistry that characterizes the free energy per unit area required for formation of an interface between two phases at constant temperature, pressure, and chemical composition [2,3]. Parallel to the experimental advances, theoretical methods based on molecular dynamics (MD) computer simulation have contributed significantly to understanding the microscopic nature of liquid interfaces and molecular interactions at the level of atom or molecule [4].

In this work, using molecular dynamics simulation, we study the properties of pure oil, water, and oil/water system including material which their behavior is important as the properties of real system are concerned in processes such enhanced recovery (EOR) of crude oil.

Method:

The OPLS all-atom force field of Jorgensen and co-workers [6] was used to model the n-octane and 4-Ethylpyridine. The water were modeled by SPC/E (single point charge/extended). The simulations were performed using a subset of DL_POLY2.17 package

[5]. Density functional theory (DFT) as implemented in GAUSSIAN 03 program was used to find some structural parameters required to set up the force field of the systems.

Result and discussion:

The density profiles of the binary mixture of octane with 4-Ethylpyridine and the octane/water interface are shown in Figures 1 and 2, respectively. The density profile across the water and oil model system interface is illustrated in Figure 3. Radial distribution function (*g*(*r*)) of the octane/water/4ethyl-pyridine system is shown in Figure 4. The values of surface tension (σ) were calculated from the components of pressure tensor of the simulated boxes.

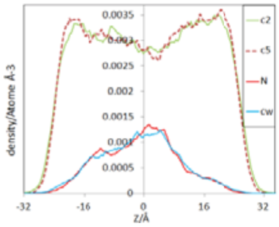

Figure 1

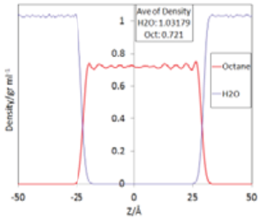

Figure 2

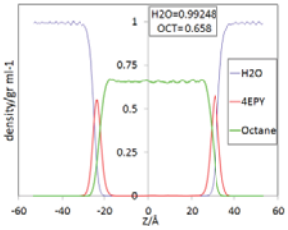

Figure 3

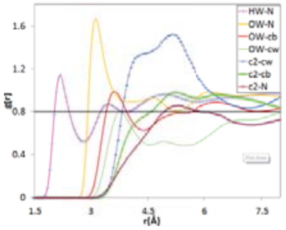

Figure 4

Conclusion:

In Figure 1, the atoms density profile indicates that 4-Ethylpyridine molecules tend to accumulate in the center of box and the ethyl chain is extended towards the octane phase and the nitrogen atoms pointing towards themselves. The results of some investigations has suggested that the association of the pyridine bases can occur as a result of N-π interactions between the nitrogen lone pair of one molecule and the aromatic ring π-electrons of another one [7]. The accumulation of 4-Ethylpyridine at the oil/water interface and the was observed at all temperature studied, as it is shown in Figure 3. These aromatics-rich layer formations may be a critical factor in determining the interfacial behaviors in EOR technology. When aromatic molecules (4-Ethylpyridine) accumulate at the interface, interfacial tension, decreases, similar to the case for adsorption of surfactants. The weak hydrogen bonding between the aromatic rings and the water protons, that it is seen in *RDF* of the ring nitrogen and the water proton in Figure 4, provides the mechanism for lowering the interfacial tension.

References:

[1] J. P. Nicolas, N. R. de Souza, J. Chem. Phys., 120,2464 (2004)

[2] M. H. Ghatee, A. R. Zolghadr, F. Moosavi, L. Pakdel, J. Chem. Phys. 134, 074707 (2011)

[3] J. L. Rivera, C. Mccabe, P. T. Cummings, Physical Review E 67, 011603 (2003)

[4] X. HongYan, et al. Sci China Chem 53, 945 (2010)

[5] DLPOLY 2.17 (Warrington, UK: Daresbury Laboratory,1999).

[6] W. L. Jorgensen, D. L. Maxwell, J. Tirado-Rives, J. Am. Chem. Soc. 118, 11236 (1996).

[7] E. Megiel, T. Kasprzycka-Guttman, A. Jagielska, L. Wroblewska, J. Mol. Struct. 569, 111 (2001).

Asymmetric critical behaviour of binary mixtures

A. Jamali*, H. Behnejad
Department of Physical Chemistry, School of Chemistry, University College ofScience, University of Tehran, Tehran 14155, Iran, asmajamali@khayam.ut.ac.ir

Key words: Coexistence curve, Binary mixtures, Mole fraction, Refractive index

Introduction:

The most important feature of critical behavior is universality class of 3D-Ising-like systems which indicates sufficiently close to the critical point, because of the large critical fluctuations, systems of different physical natures may exhibit similar critical behavior. Near the critical region of a binary solution, the different of the general density variable of two coexisting phases,$\Delta\rho_{cxc}$, can be described by universal power-law of the reduced temperature$\Delta\hat{T}$ near the critical point as:

$$\Delta\rho_{cxc} = \frac{\rho_2-\rho_1}{2\rho_c} = B_0\left|\Delta\hat{T}\right|^{\beta}, \qquad (1)$$

where$\Delta\hat{T} = (T - T_c)/T_c$,$T_c$ is the critical temperature,ρ is the general density variable, such as refractive index, mole fraction and volume fraction, the subscripts 1 and 2 represent upper and lower phases respectively,B_0 is the critical amplitude and β is the critical exponent. For 3D-Ising universality class its value is 0.326.This asymmetric criticality has been paid much attention in recent decade accompanied by the raise of the concept of the complete scaling proposed by Fisher and co-workers, which shows that the scaling fields should be considered as a linear combination of all physical fields [1]. Complete scaling turns out to cause a so-called Yang-Yang anomaly for the temperature dependence of the heat capacity in the two-phase region. Furthermore, the heat capacity plays an important role in describing the asymmetric criticality within the frame of the complete scaling theory. Recently Anisimovand et al. have extended the complete scaling to binary mixtures and tested the complete scaling by analysing experimental coexisting curve data for a series of binary liquid mixtures [2].

In this paper we investigate the critical behavior of some binary mixtures consisting Benzonitril, Nitrobenzen and normal-alkanesand we shall show how complete scaling can applied to liquid-liquid phase separation in binary mixtures.

Result and discussion:

The diameter of the coexistence curve ρ_d can be expressed as follows:

$$\rho_d = (\rho_1 + \rho_2)/2 = \rho_c + D_1\left|\Delta\hat{T}\right| + D_2\left|\Delta\hat{T}\right|^{1-\alpha} + D_3\left|\Delta\hat{T}\right|^{2\beta} + \cdots , \qquad (2)$$

where D_1, D_2 and D_3 are the system-dependent coefficients. It is almost impossible to simultaneously obtain the coefficients D_1, $D_2$and D_3 by fitting the experimental data of the coexistence curves to equation (2), hence by combining the coefficients for the weakly compressible liquid mixtures, Perez-Sanchez and co-workers proposed the diameter of the coexistence curve by [3]:

$$\Delta x_d = \frac{x_2+x_1}{2} - x_c \approx a_{eff}{B_0}^2\left|\Delta\hat{T}\right|^{2\beta} - b_{eff}\left(\left(\frac{\hat{A}_0^-}{1-\alpha}\right)\left|\Delta\hat{T}\right|^{1-\alpha} - \hat{B}_{cr}\left|\Delta\hat{T}\right|\right), \qquad (3)$$

where x is the mole fraction of the component with larger molecular volume (the mole fraction of normal-alkane in this work),a_{eff}, b_{eff} and B_0 are the system dependent amplitudes; $\hat{B}_{cr} = B_{cr}M/R$ is the dimensionless critical background of the heat capacity and $\hat{A}_0^- = A_0^- M/R$ is the dimensionless critical amplitude corresponding to the heat capacity in two-phase region, B_{cr} is the critical fluctuation-induced contribution to the background of the heat capacity, R is the gas constant, and M is molecular weight. In this work we have reached to experimental data for heat capacity of nitrobenzene-tetradecane[4] and we adopted $\hat{A}_0^- = 8.355$ and$\hat{B}_{cr} = 51.79$for this system and because of the absence of heat capacity data for the other nitrobenzene+n-alkane and Benzonitril+n-alkane mixtures these coefficients applied for the other systems. The results for 15 mixtures consisting Nitrobenzene, Benzonitril and normal-alkanes are given in Table 1. Furthermore, for refractive index an equation similar to equation (2) can be obtained and the corresponding coefficients,a_{eff},b_{eff} and $B_0$for the aforementioned mixtures can be obtained which are presented in Table 1. The obtained results(fit to the equation (2)) including the corresponding experimental data are given in Fig. (1) and Fig. (2).As these figures depict the coincidence is quite good.

Conclusion:

As mentioned we can fit experimental data of mole fraction and refractive index with equation (3). As the Table 1 shows,this equation can represent mole fraction and refractive index with reliable accuracy and also Figs (3)-(4) show that the contribution to the diameter from 2β term is more significant when mole fraction is order parameter, but when refractive index is selected as an order parameter both linear and 1-α terms are more significant instead, although it was thought in the past that the linear term by itself is more important for refractive index as the order parameter.

Table1. Critical parameters, amplitudes and asymmetry parameters for binary liquid mixtures of nitrobenzene and Benzonitril with n-alkanes; σ is the standard deviation of a fit of Eq.(3) to the experimental data.

Systems	x_c(alkanes)	T_c(K)								σ(Δx_d)	σ(Δn_d)
NB+C5	0.614	297.104	1.4272	1.15	0.095	0.004	-0.014	0.147	0.00441	0.0004	0.0002
NB+C6	0.573	293.1	1.4412	1.32	0.09	0.109	-0.018	-1.686	0.00708	0.001	0.00007
NB+C7	0.529	291.9	1.4504	1.47	0.084	0.046	0.008	-0.895	0.0052	0.001	0.00004
NB+C8	0.495	293.1	1.4653	1.59	0.079	0.111	-0.009	-1.415	0.00606	0.0004	0.0003
NB+C10	0.426	295.964	1.4652	1.84	0.073	0.148	0.014	0.065	0.00419	0.001	0.00003
NB+C11	0.394	298.0	1.4682	2.03	0.071	0.307	-0.039	1.096	0.00338	0.001	0.00002
NB+C12	0.37	300.4	1.4717	2.07	0.0697	0.309	0.065	0.143	0.00517	0.005	0.0002
NB+C13	0.346	303.0	1.4734	2.16	0.067	0.324	-0.016	-1.413	0.00461	0.001	0.00004
NB+C14	0.324	304.94	1.4752	2.23	0.066	0.339	-0.015	0.636	0.00333	0.001	0.00004
BN+C8	0.536	283.225	1.4478	1.45	0.065	0.070	0.003	1.34763	0.00333	0.001	0.00004
BN+C12	0.414	293.028	1.4607	1.88	0.056	0.119	0.051	-0.475	0.00394	0.002	0.00006
BN+C15	0.343	301.2	1.4656	2.17	0.052	0.135	0.126	1.43119	0.00308	0.002	0.00002
BN+C16	0.327	304.408	1.4663	2.23	0.051	0.153	0.095	1.28142	0.00342	0.002	0.00003
BN+C17	0.305	306.642	1.4673	2.31	0.0497	0.159	0.143	0.147	0.00353	0.002	0.00003
BN+C18	0.293	309.6	1.4669	2.39	0.049	0.164	0.137	-2.083	0.00417	0.002	0.00003

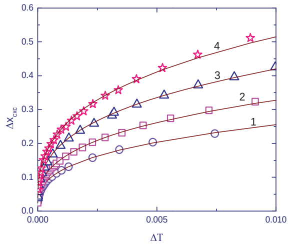

Fig.1. Mole fraction difference$\Delta x_{cxc} = \frac{|x_2 - x_1|}{2x_c}$ of the liquid-liquid coexistence curves for nitrobenzene+n-pentane(1), n-heptane (2), n-dodedecane (3), n-heptadecane (4). The solid curves represent Eq. (1)

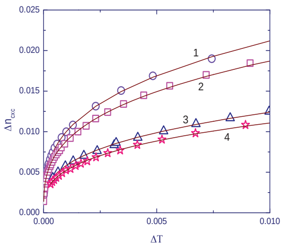

Fig.2. Mole fraction difference$\Delta n_{cxc} = \frac{|n_2 - n_1|}{2n_c}$ of the liquid-liquid coexistence curves for nitrobenzene+n-pentane(1), n-heptane (2), n-dodecane (3), n-heptadecane (4). The solid curves represent Eq. (1)

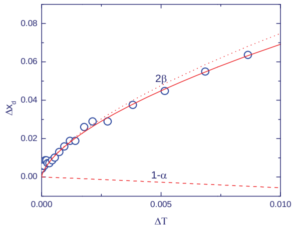

Fig.3. Diameter $\Delta x_d = \frac{x_2 + x_1}{2} - x_c$of the liquid-liquid coexistence curve for nitrobenzene+tridecane as a function of. The symbols indicate experimental data. The solid curves represent Eq. (3), the dotted curve represents the contribution from the 2β term, and dashed curve the contribution from the 1-α and linear terms.

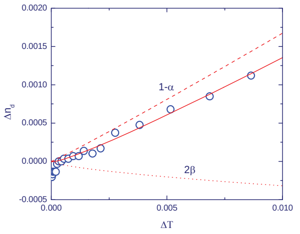

Fig.4. Diameter $\Delta n_d = \frac{n_2 + n_1}{2} - n_c$of theliquid-liquid coexistence curve for nitrobenzene+tridecane as a function of. The symbols indicate experimental data. The solid curves represent Eq. (3), the dotted curve represents the contribution from the 2β term, and dashed curve the contribution from the 1-α and linear terms

References:

[1] Y. C. Kim, M. E. Fisher, and G. Orkoulas, Physical Review **E 67**, 061506, 2003

[2] C. A. Cerdeiriña, M. A. Anisimov, and J. V. Sengers, Physical Review **E 77**, 031127, 2008

[3] G. Pérez-Sánchez, P. Losada-Pérez, C. A. Cerdeiriña, J. V. Sengers, and M. A. Anisimov, J. Chem. Phys. **132**, 154502, 2010

[4] P.L.Pérez, G. Gordyannis, C. A. Cerdeiriña, and C. Glorieux, J. Chem. Therm. **31**, 710, 2010.

Evaluation of Virial Coefficients at Wide Range of Temperature

M. Bamdad

Department of Chemistry, Faculty of Sciences, Shahid Chamran University, Ahvaz, 61357-43169, Iran.

mbamdad@scu.ac.ir

Key words: equation of state, virial coefficient, fluids, fundamental relations.

Introduction:

All gases behave like ideal gases at high temperatures and low pressures. As the pressure is increased, real gases shows more complicated behavior and their fundamental equations and hence other thermodynamical properties become analytically complicated [1]. The thermodynamic properties of gasses may readily be deduced from knowledge of the virial coefficients and their dependence on temperature:

$$U_{real} = U_{ideal} - nRT^2\left(\frac{1}{\overline{V}}\frac{dB}{dT} + \frac{1}{2\overline{V}}\frac{dC}{dT} + \cdots\right)$$

$$S_{real} = S_{ideal} - nR\left[\frac{1}{\overline{V}}\left(B + T\frac{dB}{dT}\right) + \frac{1}{2\overline{V}}\left(C + T\frac{dC}{dT}\right) + \cdots\right]$$

Methods:

Virial coefficients for simple models such as hard spheres potential are calculated and monitored. But the experimental data at wide range of temperature for virial coefficients of real fluid has not been reported [2]. Now, highly exact functional forms of multiparameter equation of state have been developed for non- and weakly polar as well as polar fluids [3]. These equations provide the possibility to calculate the virial coefficients with high accuracy, for different fluids at the wide range of temperature.

$$B(T) = \lim_{\rho\to 0}\left[\frac{\partial(P/\rho RT)}{\partial\rho}\right]_T$$

$$C(T) = \frac{1}{2}\lim_{\rho\to 0}\left[\frac{\partial^2(P/\rho RT)}{\partial\rho^2}\right]_T$$

Conclusion:

At the figure, the calculated virial coefficients are plotted versus temperature for two fluids, Argon at top and Methane at below.

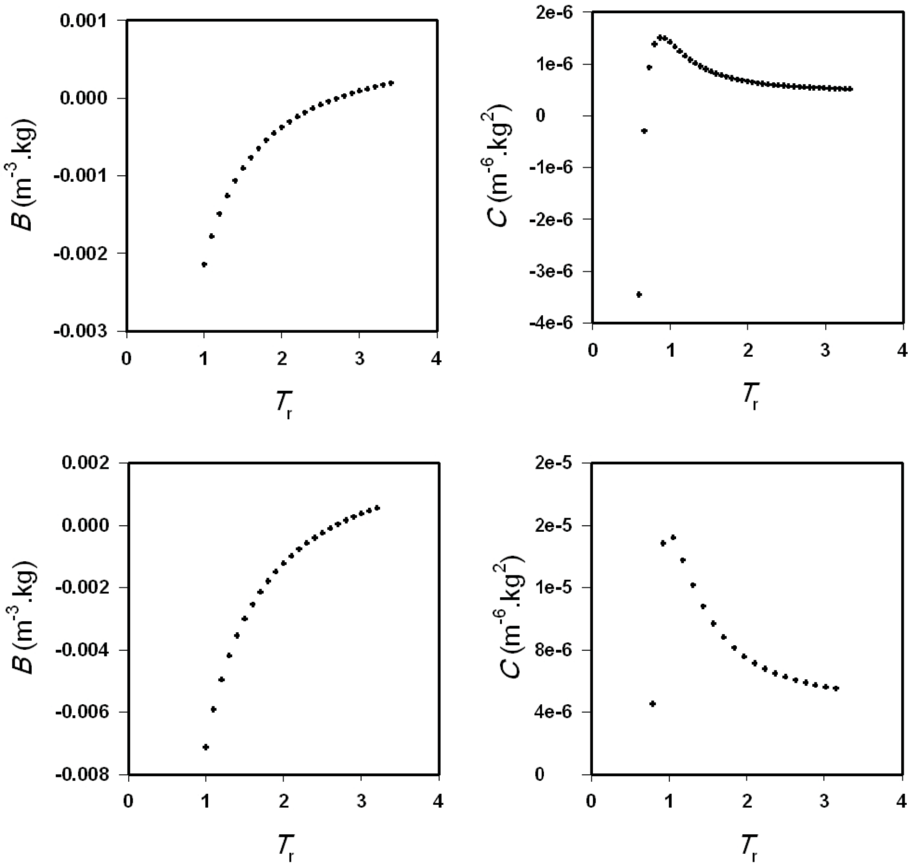

References:

[1] J. O. Hirschfelder, C. F. Curtiss and R. B. Bird, Molecular Theory of Gases and Liquids, JOHN WILEY & SONS, Inc., 1964.

[2] J. H. Dymond, and E. B. Smith, The Virial Coefficients of Pure Gases and Mixtures A Critical Compilation, CLARENDON PRESS OXFORD, 1980.

[3] R. Span, and W. Wagner, *Int. J. Thermophys.*, **24**, 1-39, 2003.

A Monte Carlo simulation of the adsorption of CO_2 and SO_2 gases in pure and functionalized single walled carbon nanotubes

Zahra Nickmand [a], Seyed Foad Aghamiri [a], Mohammad Reza Talaie Khozanie [a], Hassan Sabzyan [b]*

[a] Department of Chemical Engineering, University of Isfahan, Isfahan, Iran, I. R., 81746-73441
[b] Department of Chemistry, University of Isfahan, Isfahan, Iran, I. R., 81746-73441
Email: sabzyan@sci.ui.ac.ir

Keyword: Adsorption, Functionalized, GCMC, Molecular simulation, SWCNT

Introduction:

Different methods such as absorption, adsorption, cryogenics and membranes separation methods have been applied to capture and storage pollutant gases such as CO_2 and SO_2 [1,2]. Among these methods, adsorption has less energy consumption and can be used in a wide range of operating temperatures and pressures [3]. Results of a number of researches have shown that adsorption capacity and selectivity of nanotubes for adsorbing CO_2 are higher than those of other adsorbents [4,5]. Functionalization of the SWCNT is a method to improve the chemical and physical performances of the nanotubes.

In this work, grand canonical Monte Carlo (GCMC) simulation is used to model adsorption of CO_2 and SO_2 molecules by the pure and functionalized single walled carbon nanotubes (SWCNT and FSWCNT). Simulations are conducted for two cases: *i*) without and *ii*) with a 5.75 Å clearance between the outer surface of the CNT and the walls of the simulation box. The simulated isotherms for the adsorption of the pure gases on the FSWCNT can be used to choose the most suitable functional groups to increase the efficiency of adsorption for any adsorbate-adsorbent system.

Method and Computational Details:

GCMC method is employed to investigate the adsorption of the pure CO_2 and SO_2 gases in a SWCNT and its corresponding FSWCNT. All Monte Carlo simulation runs include 2×10^7 cycles. Each Monte Carlo cycle consists of three kinds of moves: translation, insertion and deletion of molecules, with probability of 20% for translation move and 40% for either of the insertion and deletion moves. The (**10,10**) armchair nanotube with a length of 5 nm, and a diameter of 1.35 nm considered for this simulation, is generated using the FORTRAN program coded by Sabzyan and Gholami [6].

Results and discussion:

Adsorption of pure CO_2 and SO_2 gases in SWCNT is modeled by GCMC simulation using two simulation boxes with different sizes. The cross section of the first simulation box is set to fit the nanotube such that molecules can be adsorbed just inside the nanotube, while the size of the second simulation box cross section is set larger than the nanotube diameter so that the adsorbate molecules can be adsorbed both inside and outside the nanotube, simultaneously. To explore the effects of functional groups on the adsorption phenomenon, two important factors: 1) the number of the functionalized carbon atoms and 2) the nature of the functional groups (entered in the simulation as potential parameters) are investigated.

Conclusion:

Obtained simulation results for SWCNT indicate that for the second simulation box, case (*ii*), by increasing the pressure pure CO_2 and SO_2 gases at first adsorb on the inside the CNT, but at higher pressures, adsorption outside the CNT becomes larger. Furthermore, for both gases the adsorbed amount for the second box is significantly larger than that in the first box, case (*i*). Also adsorption of pure molecules simulated inside FSWCNT show that the force field parameters and chemical (specific) interactions of the carbon atoms affected by functional group, has more important role than the number of affected carbon atoms.

References:

[1] W. Wang, X. Peng, D. Cao, Capture of trace sulfur gases from binary mixtures by single-walled carbon nanotube arrays: A molecular simulation study, Environ. Sci. Technol. 45 (2011) 4832–4838.

[2] T. Qiang, Zh. Zhigang, Zh. Wenpei, C. Zidong, SO_2 and NO selective adsorption properties of coal-based activated carbons, Fuel 84 (2005) 461–465.

[3] F. Su, Ch. Lu, W. Cnen, H. Bai, J. F. Hwang, Capture of CO_2 from flue gas via multiwalled carbon nanotubes, Sci. Total Environ. 407 (2009) 3017–3023.

[4] M. Cinke, J. Li, Ch. W. Bauschlicher Jr., A. Ricca, M. Meyyappan, CO_2 adsorption in single-walled carbon nanotubes, Chem. Phys. Lett. 376 (2003) 761–766.

[5] L. Huang, L. Zhang, Q. Shao, L. Lu, X. Lu, Sh. Jiang, W. Shen, Simulations of binary mixture adsorption of carbon dioxide and methane in carbon nanotubes: Temperature, pressure, and pore size effects, J. Phys. Chem. C 111 (2007) 11912-11920.

[6] H. Sabzyan, S. Gholami, Carbon nanotorus maker. 3rd International Congress on Nanoscience and Nanotechnology (ICNN 2010), 2010 Shiraz University, Shiraz, I. R. Iran.

Electrochemistry

Adsorption and corrosion inhibition of spearmint (*Mentha spicata* L.) leaves extract on mild steel

N. Soltani*

Department of Chemistry, Payame Noor University, PO Box 19395-3697 Tehran, IRAN.

* E-mail: nasrin_soltani2056@yahoo.com

Key words: Acid inhibition, Stainless steel; EIS; Polarization; Plant extract

Introduction:

Due to the general aggressive nature of acid solutions, inhibitors are commonly used to reduce the corrosive attack of acid solutions to the contacted metallic materials [1]. Unfortunately, many common corrosion inhibitors that are still in use today are health hazards. Therefore, there is still an increased attention directed towards the development of environmentally compatible, nonpolluting corrosion inhibitors. Okafor et al. [2] studied the inhibitive action of leaves, seeds and a combination of leaves and seeds extracts of *Phyllanthus amarus* on mild steel corrosion in HCl and H_2SO_4 solutions. Rocha and coworkers [3] reported the effect of aqueous extracts of mango, orange, passion fruit and cashew peels as corrosion inhibitors for carbon steel in 1 M hydrochloric acid. Presently, there is no reported work on inhibitive effects of spearmint *(Mentha spicata* L.) extract on acid corrosion of mild steels (MS) in hydrochloric acid solution. Therefore, we consider it necessary to study the effect of spearmint extract on the acid corrosion of MS in HCl solution. The investigation of corrosion parameters was performed by weight loss, electrochemical polarization measurements and electrochemical impedance spectroscopy. Quantum chemical calculations were performed to illustrate the process of adsorption of some specific components of the extract.

Materials and methods:

The aggressive solution of 2 M HCl was prepared by dilution of analytical grade HCl purchased from Merck. AR grade HCl (37%). The concentration range of spearmint extract employed was 1.0 to 4.0 g/L.

Apparatus:

Polarizations and Impedance measurements were carried out using the AUTOLAB model PGSTAT 35 instrument. Electrochemical experiments performed in a conventional three electrode electrochemical cell with the MS as a working electrode, a platinum counter electrode and saturated (3M) Ag/AgCl electrode as reference electrode.

Result and discussion:

Owing to the complex chemical composition of the spearmint *(Mentha spicata* L.) extract, it is quite difficult to assign the inhibitive effect to a particular constituent. However, we have performed some quantum chemical calculations to model the adsorption structures of the major chemical constituents of spearmint *(Mentha spicata* L.) extract (Fig. 1) and hence provide some insight into the nature of their interaction with the mild steel surface and their possible contributions to the overall inhibiting effect. Briefly, the main constituents of spearmint *(Mentha spicata* L.) leaves extracts, having number of hydroxil group (–OH), heteroatom oxygen and large number of aromatic rings. As the constituent molecules contain aromatic rings (л- electrons) and electron releasing groups attached to these aromatic rings, the availability of л-electrons to get bonded to the vacant d orbital of Fe is increased.

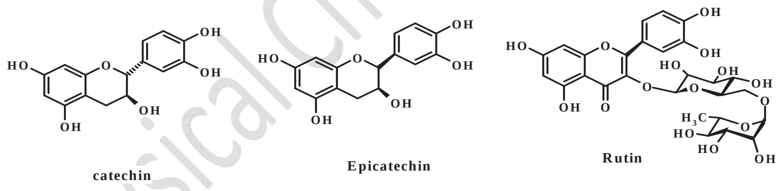

Fig. 1. Some chemical structures of spearmint *(Mentha spicata* L.) leaves extract

Conclusion:

The spearmint extract acts as a good inhibitor for corrosion of MS steel in 1 M HCl solution. The η (%) increases with increasing extract concentration. The inhibition action is performed via adsorption of the extract compounds on the steel surface. The adsorption process is spontaneous and follows Langmuir adsorption isotherm at all temperatures studied. The values of ΔG^{0}_{ads} were indicative of the physisorption. Activation energy decreases with addition of inhibitor. Quantum chemical calculations were performed to find out whether a clear link exists between the inhibitive effect of the extract and the electronic properties of its main constituents.

Reference:

[1] F. Eghbali, M.H. Moayed, A. Davoodi, N. Ebrahimi, Corros. Sci. 53 (2011) 513-522.

[2] P.C. Okafor, M.E. Ikpi, I.E. Uwaha, E.E. Ebenso, U.J. Ekpe, S.A. Umoren, Corros. Sci. 50 (2008) 2310–2317.

[3] J.C. da Rocha, J. A. da Cunha Ponciano Gomes, E. D′Elia, Corros. Sci. 52 (2010) 2341–2348.

Electrochemical determination of acetaminophen in the presence of ascorbic acid and propranolol using metalic Cu nanoparticles- Schiff base modified carbon paste electrode

N. Soltani*, N. Tavakkoli, A. H. Ataran, M. Maseratfar
Department of Chemistry, Payame Noor University, PO Box 19395-3697 Tehran, IRAN.
* E-mail: nasrin_soltani2056@yahoo.com

Key words: Modified electrode, metalic Cu nanoparticles, Acetaminophen, propranolol

Introduction:

Acetaminophen, or paracetamol (N-acetyl-p-aminophenol), is an antipyretic and minor analgesic drug that practically has no anti-inflammatory action. It is used for the relief of mild to moderate pain associated with headaches, backaches, arthritis and postoperative pains, reduction of fevers of bacterial or viral origin [1]. Therefore, the development of fast, sensitive and accurate methods for determining acetaminophen content are of clinical exigency. Construction of electrochemical sensors using modified electrodes continues to be an area of great interest and a relatively large amount of electrochemical research has been devoted to the development and application of these sensors for the analysis of biologically active compounds. The fabrication of electrodes modified with nanoparticles has been the focus of recent attention owing to enhancement of the response signal, increased sensitivity and better reproducibility [2, 3]. The present work a carbon paste electrode modified with metalic Cu nanoparticles and Schiff base was developed for the individual and simultaneous determination of acetaminophen (AC), ascorbic acid (AS) and propranolol (PR). The electrochemical behavior of these three molecules was investigated employing cyclic voltammetry (CV), differential pulse voltammetry (DPV) and chronocoulometry (CC).

Materials and methods:

All the chemicals reagents used in our experiments were of analytical grade and were used as received without further purification. Cu nanoparticles with diameters from 30 to 80 nm have been successfully synthesized via thermal decomposition of [Cu(O_4C_2)]-oleylamine complex according to literature [4].

Apparatus:

Voltammetric measurementswere carried out using an Autolab Potentiostat Galvanostat PGSTAT30 (Eco 10 Chemie, Utrecht, and The Netherlands). A conventional three electrode system was used for all electrochemical experiments, which consisted of a platinum wire as auxiliary electrode, an Ag/AgCl (3 mol L^{-1} KCl) as reference electrode, and a bare or modified CPE as working electrode. A Metrohm 781 pH meter, which was calibrated with standard pH buffer solutions, was used for pH measurements. XRD pattern was recorded by a Rigaku D-max C III, X-ray diffractometer using Ni-filtered Cu Kα radiation. Transmission electron microscopy (TEM) image was obtained on a Philips EM208 transmission electron microscope with an accelerating voltage of 200 kV.

Result and discussion:

The modified electrode exhibited electrocatalytic properties toward acetaminophen ascorbic acid and propranolol oxidation with a peak potential of 30.0, 25.0 and 35.0 mV lower than that at the bare carbon paste electrode, respectively. Also the enhanced peak current response is a clear evidence of the catalytic of the modified carbon paste electrode towards oxidation of acetaminophen, ascorbic acid and propranolol. The effect of pH and scan rate on the electrode process was investigated. Using differential pulse voltammetry the calibration curves of AC, AA and PR were obtained in the range of 3.5×10^{-7}-1×10^{-4} M, 2.3×10^{-4}-4.0×10^{-3} M and 4.8×10^{-7}-6.7×10^{-4} M respectively. The detection limit of AC was 2.6×10^{-8} M in the presence of 1 mM ascorbic acid and 0.01 mM PR. The proposed method was successfully applied in the determination of acetaminophen ascorbic acid and propranolol in several pharmaceutical formulations.

Conclusion:

The modified electrode not only improved the electrochemical catalytic oxidation of AC, AA and PR, but also resolved the overlapping anodic peaks. Moreover, the results obtained from the application of the proposed method for determining AC, AA and PR in real samples such as urine and pharmaceutical samples confirmed the good accuracy and precision of our proposed method.

Reference:

[1] H. Razmi, E. Habibi, Electrochimica Acta, 55 (2010) 8731–8737.
[2] S. Yuan, W. Chen, Sh. Hu, Materials Science and Engineering: C, 25 (2005), 479-485.
[3] M. Noroozifar, M. Khorasani-Motlagh, A. Taheri, Talanta, 80 (2010) 1657-1664.
[4] M. Salavati-Niasari, F. Davar, N. Mir, Polyhedron, 27 (2008) 3514–3518.

Using the Peukert's equation for predicting the discharging time of primary silver/zinc battery at any discharge rate

M. M. Loghavi*[a] and A. M. Ghasemi[a]

[a]Engineering Research Institute, Fars Engineering Research Center, Shiraz, Iran

Email: mohsen.loghavi@gmail.com

Keywords: Zinc/Silver Oxide, Battery, Peukert's Equation, Nano Silver(II) Oxide

Introduction:

With the beginning of the aerospace plans, it became obvious that the silver-zinc battery was the reasonable option for powering many of the critical systems and applications [1, 2]. In this work, zinc/silver oxide cells which use the mixture of nano and micro silver(II) oxide as cathode material were discharged at high-constant currents and then Peukert's equation was used for determining the peukert capacity to predict the discharge time at any discharge rate.

Methods:

In this research the cathode active material was mixture of nano silver (II) oxide, conventional (micro) silver(II) oxide and graphite powders. Both nano and conventional AgO were produced in our laboratory by chemical deposition method. By using these divalent silver oxide powders, four types of cathode electrodes were prepared with percent values showed in Table 1. The anode was gelled zinc metal powder. The grids for all electrodes were expanded form of silver-plated copper. Three-plate cells were used during this work. These contained two negative electrodes and one positive electrode. Both anode and cathode plates were 5.5 × 15.5 cm. cathode electrode wrapped in a teabag separator and inserted between the anode electrodes. The required quantity of 40 w/v% KOH solution was used as electrolyte. Chronopotentiometric data were recorded in our laboratory at room temperature while discharge currents were 20, 24 and 28 A and the cut-off voltage was 1.0 V.

Table 1. Percent values of silver (II) oxide powders used in cathode active material.

cell label	micro silver(II) oxide	nano silver(II) oxide	number of samples
A	100%	0%	3
B	80%	20%	3
C	60%	40%	3
D	40%	60%	3

For a one-ampere discharge rate, Peukert's Equation is usually quoted as being, $T = \frac{C}{I^n}$ where C is the capacity at a one-ampere discharge rate and I is the actual discharge current relative to 1 ampere [3]. T is the actual time to discharge the battery. The capacity at a one-ampere discharge rate is not usually given for practical cells. It is useful to reformulate the law to a known capacity and discharge rate: $T = \frac{C\left[\frac{C}{R}\right]^{n-1}}{I^n}$ (1)

Where, C is nominal battery capacity, R is hour rating, I is the nominal current at the given rate and n is Peukert's exponent. The numerator is actual peukert capacity, C_p. We also know that the Peukert Capacity C_{p1} and C_{p2} must be equal because this never changes for any one particular battery. Therefore we write: $C_{p1} = C_{p2}$ (2)

And therefore: $n = [log(R_2/R_1)]/[log(C_1/R_1) - log(C_2/R_2)]$ (3)

Results and Discussion:

The obtained results from Chronopotentiometric data and Peukert's equation are tabulated in Table 2. As can be seen in the middle box, Peukert constant and peukert capacity are calculated by using experimental data for different zinc/silver oxide cells. The Peukert value is directly related to the internal resistance of the battery. These values can be inserted into Eq. (1) to predict the discharging time at different discharge currents. For example, Right-side box illustrates the theoretical and the experimental discharging time of cells under 24 ampere current. We observe that Peukert constant is close to 1 at cell with 40% nano silver(II) oxide. It means with increasing discharge rate, capacity decreases insignificantly. The theoretical results of discharging time are in reasonably good agreement with the experimental results especially at cells A and C.

Table 2. Results of chronopotentiometric experiments and data of Peukert's equation.

Cell label	I (A)	R (hour)	$C_{experimental}$ (Ah)	n	C_p (Ah)	I (A)	$T_{theoretical}$ (hour)	$T_{experimental}$ (hour)
A	20 28	0.2115 0.1157	4.23 3.24	1.792	45.37	24	0.1526	0.1554
B	20 28	0.2030 0.1382	4.06 3.87	1.142	6.21	24	0.1648	0.1796
C	20 28	0.2095 0.1464	4.19 4.10	1.064	5.08	24	0.1727	0.1804
D	20 28	0.1695 0.1004	3.39 2.81	1.558	18.04	24	0.1276	0.1470

Conclusions:

Primary silver-zinc cells which use the mixture of nano and micro AgO as cathode active material were investigated during high-rate discharge. The Peukert capacity and the peukert constant were calculated. Peukert constant for cell C is close to one and the theoretical results showed a good agreement with the experimental results for discharging at 24 A.

References

[1] Smith, D. F.; Brown, C. *Journal of Power Sources*, 2001, 96, 121–127.

[2] Karpinski, A. P.; Makovetski, B.; Russell, S. J.; Serenyi, J. R. Williams, D. C. *Journal of Power Sources*, 1999, 80, 53–60.

[3] Linden, D.; Reddy, T. B.; *Handbook of Batteries*, McGraw Hill, 3d ed, 2001.

A Thermodynamic Study on the Binding of Human Serum Albumin with Beta Cyclodextrin

G. Rezaei Behbehani[a], , Sh. Rafiei[a,c*], A.A. Saboury[b]
[a]Chemistry department, Imam Khomeini International University, Qazvin, Iran
[b]Institute of Biochemistry and Biophysics, University of Tehran, Tehran, Iran
[c] Payam- Noor University, Tehran, Iran, shahnaz 22 rafiei@yahoo.com

Keywords: Human serum albumin, Cyclodextrins, Fluorescence, Isothermal titration calorimetry, Binding parameters.

Introduction:

The application of isothermal titration calorimetry method and fluorescence spectrum, UV-visible spectrum to determining the properties effect of BetaCyclodextrin (β-CD) on human serum albumin (HAS) is described in this paper. Our measurements provide useful information about the binding of β-CD to human serum albumin (HSA) that is important for potential clinical applications of this agent. Binding properties of β-CD is the subject of this paper. Variations of UV-Vis spectrum and fluorescence spectrum of HAS can help us to investigate the changes that are created in protein structure. It was shown that β-CD has quite a strong ability to quench the fluorescence launching from HSA by reacting with it and forming a certain kind of new compound.

The thermodynamics of the interaction between β-CD with HAS, host-guest Structure complex, in the presence of β-CD (35.242 mM) was investigated at pH 7 by isothermal titration calorimetry. A new solvation model was used to reproduce the enthalpies of HSA interaction β-CD within a broad range of complex concentration in the presence of β-CD (35.242 mM). The solvation parameters attained from the new model was attributed to the structural change and biological activity of HSA. From the binding parameters for the interaction of β-CD and HSA suggested that electrostatic interaction was the predominant intermolecular forces stabilizing the complex. On the other hand in presence of β-CD the binding parameters recovered from the new equation are not attributed to a structural change of HSA and its biological activity due to low concentration β-CD interaction and vice versa .

Materials and method:

Disodiumhydrogenphosphate (Na_2HPO_4 and β-cyclodextrin (β-CD) were purchased from Sigma Chemicals Co. HSA was obtained from Sigma-Aldrich (Taiwan, China) and . Protein concentrations were determined from absorbance measurements at 279 nm in 1 cm quartz cuvette. All other materials and reagents were of analytical grade, and solutions were made in 50 mM buffer phosphate using double-distilled water.

The isothermal titration calorimetric experiments were carried out on a VP-ITC ultra sensitive titration calorimeter (MicroCal, LLC, Northampton, MA). All ultraviolet-visible spectra were recorded in a UV-1100 spectrophotometer (Unico) double beam that was equipped by temperature regulation system. All fluorescence measurements were carried out on an 100-bio recording spectrophotometer (Perkin-Elmer corporate America).

Results and discussion:

We have shown previously that the heats of the macromolecules + ligands interactions can be reproduced by Eq. 1 in the aqueous solvent systems [1-4].

$$q = q_{\max} x'_B - \delta_A^{\theta}(x'_A L_A + x'_B L_B) - (\delta_B^{\theta} - \delta_A^{\theta})(x'_A L_A + x'_B L_B) x'_B \quad (1)$$

q is the heat of HSA + β-CD interaction at certain ligand concentrations and qmax represents the heat value upon saturation of all HSA. The parameters δ_A^{θ} and δ_B^{θ} exhibit the HSA stability in the low and high β-CD concentrations respectively. The positive values of δ_A^{θ} and δ_B^{θ} show that HSA is substantially stabilized by β-CD at 27 °C. x'_B, can be expressed as follows:

$$x'_B = \frac{p x_B}{x_A + p x_B} \quad (2)$$

x'_B is a fraction of bound ligand with the protein molecule and $x'_A = 1 - x'_B$ is the fraction of unbound ligand. Where x_B can be defined as follows:

$$x_B = \frac{[L]}{[L]_{\max}} \quad (3)$$

[L]is the concentration of ligand after every injection and [L]max is the maximum concentration of ligand upon saturation of all HSA. The heats of HSA+ β-CD interactions, q, were fitted to Eq. 1 over the whole β-CD compositions. In the fitting procedure, p was changed until the best agreement between the experimental and calculated data was approached. If the binding of ligand at one site increases the affinity for ligand at another site, the macromolecule exhibits positive cooperativity (p>1). Conversely, if the binding of ligand at one site lowers the affinity for ligand at another site, exhibits negative cooperativity (p<1). If the ligand binds at each site independently, the binding is non-cooperative (p=1).L_A and L_B are the relative unbound and bound ligand contributions to the heats of dilution in the absence of HSA. L_A and L_B can be calculated from heats of dilution of β-CD in water (q_{dilut}) as follows:

$$L_A = q_{dilut} + x_B\left(\frac{\partial q_{dilut}}{\partial x_B}\right), \qquad L_B = q_{dilut} + x_A\left(\frac{\partial q_{dilut}}{\partial x_B}\right) \tag{4}$$

δ_A^θ and δ_B^θ parameters have been also optimized to fit the data. The optimized δ_A^θ and δ_B^θ values are recovered from the coefficients of the second and third terms of Eq. 1. The small relative standard coefficient errors and the high r^2values (0.99999) support the method. The binding parameters for HSA+ β-CD interactions recovered from Eq. 1 were listed in Table 1. For a set of identical and independent binding sites, it is possible to use Eq. (5) for calculation of K_d and "g" in a very simple way as follows :

$$\frac{\Delta q}{q_{\max}} M_0 = \left(\frac{\Delta q}{q}\right) L_0 \frac{1}{g} - \frac{K_d}{g} \tag{5}$$

Where $\Delta q = q_{\max} - q$. q represents the heat value at a certain ligand and biomolecule concentration. M0 and L0 are total concentrations of HAS and ligand, respectively. qmax represents the heat value upon saturation of all HAS molecule. Kd is the dissociation equilibrium constant for the equilibrium:

$$M + L \Leftrightarrow ML \qquad K_d = \frac{[M][L]}{[ML]} \tag{6}$$

If q and qmax are calculated per mole of biomacromolecule then the molar enthalpy of binding for each binding site (ΔH) will be: $\Delta H = \frac{q_{\max}}{g}$.

Conclusion:

It has been confirmed that the extended coordination model, via equation 1 will satisfactorily reproduce the heats of HSA+ β-CD interaction. Prediction of number of binding sites on HAS molecule, structural changes, determining the binding enthalpies and associated binding constants for such a complicated system accurately, make this theory the most powerful one. The small value of δ_B^θ show that β-CD destabilizes the HAS structure in the high concentration of the β-C. The obtained results indicate that there is nine binding site with non-cooperativity for HSA+ β-CD interactions and the negative value of molar enthalpy (-4.248kJ mol-1 at 300 K) suggest that the binding process is only enthalpy driven, indicating that electrostatic interaction is more important in the sites of HAS.

This result presents by spectroscopic studies on the interaction with β-CD and HSA using fluorescence emission spectrum, UV-visible spectrum. From Fig. 2 it was shown that the fluorescence of HSA has been quenched for reacting with β-CD in the high concentration and forming a certain kind of new compound.

UV–Vis absorption measurement was proved to be a very convenient method to explore the structural change [6] and formation of a complex [3-2]. The typical absorption peaks of HSA centrate 279nm. From Fig. 2 we can see that the absorption peaks of the mixed solutions in [β-CD]=0.05 are more than the simple superposition of the characteristic absorption peaks corresponding to the β-CD and HAS and for [β-CD]=0.6 vice versa. This means that the HSA− β-CD supramolecular complex could form in aqueous buffer solution and β-CD destabilizes the HAS structure in the high concentration of the β-CD.

Acknowledgements:

Financial support from the Universities of Imam Khomeini (Qazvin) and Tehran and are gratefully acknowledged.

Table 1. Binding parameters for HSA+ β-CD interaction recovered from Eq. 1at pH=7. *p*=1 indicates that the binding is non-cooperative in one binding site. The positive value of $\delta^{\theta}{}_{A}$ show that β-CD stabilizes the HSA structure in low concentration. The binding process for HSA+ β-CD interaction is enthalpy driven, indicating that electrostatic interaction plays an important role in the interaction of HSA with β-CD.

p	1.00±0.01
g	8.90±0.03
$K_a / \mu M^{-1}$	697.32±12.08
$\Delta H / kJmol^{-1}$	-4.25±0.03
$\Delta G / kJmol^{-1}$	-16.33±0.03
$\Delta S / kJmol^{-1}K^{-1}$	0.040±0.001
δ_A^{θ}	3.56±0.07
δ_B^{θ}	0.023±0.02

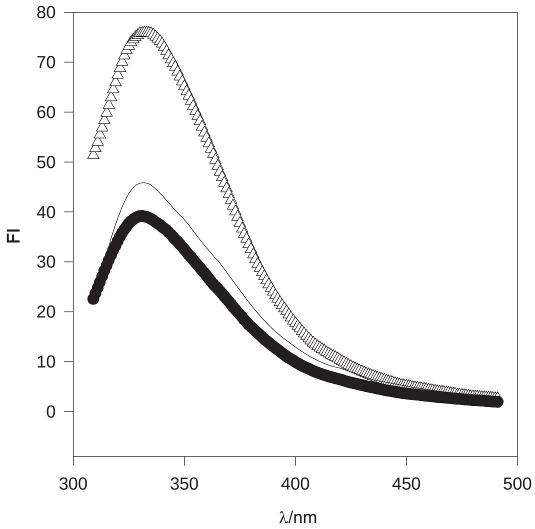

Figure 1. The fluorescence spectra of HAS(Δ) in presence of [β-CD]=0.05 (▲) and[β-CD]=0.6 (line) (T=300 K) [HAS] =117.80 μ M ; [β-CD]= 35.242mM .β-CD destabilizes the HAS structure in the high concentration of the β-CD. We can see that the fluorescence of

HSA has been quenched for reacting with high concentration β-CD

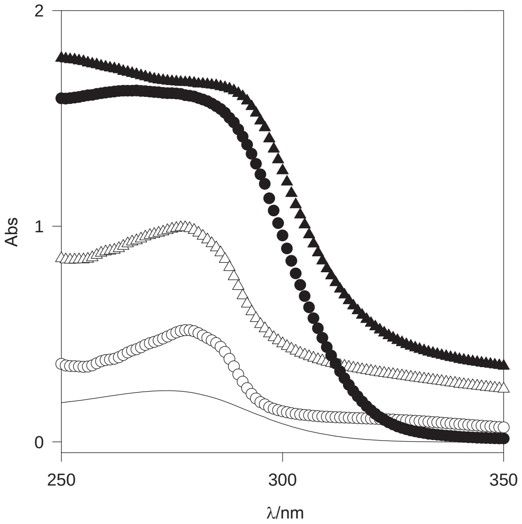

Figure 2. Comparison between absorption spectrum of HSA in different concentrations of β-CD in phosphate buffer (50 mM), pH=7 and 300°K. We can see the absorption peaks of the mixed solutions in [β-CD]=0.05 (Δ) are more than the simple superposition of the characteristic absorption peaks corresponding to the β-CD and HAS and for [β-CD]=0.6 (▲) vice versa.

References

[1] Cheng, F.Q.; Wang, Y. P.; Li, Z. P.; Dong, C.: Fluorescence study on the interaction of human serum albumin with bromsulphalein. Spectrochimica. Acta Part A: 65, 1144–1147 (2006)

[2] Rezaei Behbehani, G.: Application of a new method to reproduce the enthalpies of transfer of NaI from water to aqueous methanol, ethanol and iPrOH solvent systems at 289.15K. Bull. Korean Chem. Soc.2, 238-240 (2005)

[3] Rezaei Behbehani, G.: Application of the new solvation theory to reproduce the Enthalpies of transfer of LiBr, tetrabuthylammonium bromide and tetrapenthylamonium bromide from water to aqueous acetonitrile at 298 K. Acta Chim. Slov.52, 282-285 (2005)

[4] Paal, K.; Muller, J.; Hegedus, L.: High affinity binding of paclitaxel to human serum albumin. Eur. J. biochem.268, 2187-2191 (2001).

[5]Y. J. Hu, Y. Liu, J. Wang, X. Xiao, S. S. Qu, Study of the interaction between monoammoniumglycyrrhizinate and bovine serum albumin, J. Pharm. Biomed. Anal. 36(2004)915–919.

[6]F. L. Cui, J. Fan, J. P. Li , Z. D. Hu, Interactions between 1-benzoyl-4-p-chlorophenyl thiosemicarbazide and serum albumin: investigation by fluorescence spectroscopy, Bioorg.Med.Chem.12(2004)151–157.

Application of Multiwall Carbon Nanotubes and Rutin as a Mediator for Glutathione Analysis

M. Keyvanfard[a*], Z. Jalilian[b], H. Karimi-maleh[c], Kh. Alizad[a]
[a]Department of chemistry, Majlesi Branch, Islamic Azad University, Isfahan, Iran
[b]Department of chemistry, Shahreza Branch, Islamic Azad University, Isfahan, Iran
[c]Department of Chemistry, Science and Research Branch, Islamic Azad University, Mazandaran, Iran
E-mail: zeynab.jalilian@yahoo.com

Key words: Multiwall carbon nanotubes, Glutathione, Rutin, Modified electrode,

Abstract:

A new sensitive and selective electrochemical sensor was developed for electrocatalytic determination of glutathione (GSH) in pharmaceutical and biological samples. A voltammetric study of GSH has been carried out at the surface of carbon paste electrode modified with multiwall carbon nanotubes in the presence of rutin as a mediator. The electrochemical oxidation of GSH was investigated by cyclic voltammetry, chronoamperometry and square wave voltammetry (SWV) techniques. Under the optimized conditions, the peak current was linear to GSH concentration over the concentration range of 0.3 to 180 µmol L^{-1} using SWV. The detection limit was 0.09 µmol L^{-1}. The proposed method was successfully applied to the determination of GSH in the urine, tablet and hemolysed erythrocyte samples.

Introduction:

Drug analysis plays important roles in drug quality control, and has a great impact on public health [1-2]. Therefore, a simple, sensitive and accurate method for the determination of active ingredient is very important. Biological thiols, such as glutathione (GSH) occur widely in living tissues. GSH plays a vital role in human metabolism, including the detoxi¢cation of xenobiotics, cell homeostasis, radioprotection and antioxidant defense [3]. The objective of this research is to develop a novel, sensitive, selective and simple electrochemical method with good reproducibility and repeatability for the determination of GSH using unique properties of MWCNTs as a sensor and rutin as a mediator.

Materials and methods:

A 1.0 × 10−2 M GSH solution was prepared daily by dissolving 0.307 g GSH in water, and the resulting solution was diluted to 100 ml with water in a 100-ml volumetric flask. Spectrally pure graphite powder (particle size <50 µm) from Merck and multiwall carbon nanotubes (>90% MWCNTs basis, d × l = (110–70 nm) × (5–9 µm) from Fluka were used as the substrate for the preparation of the carbon paste electrode.

Apparatus:

All the voltammetric measurements were performed using an Autolab PGSTAT 302N, potentiostat/galvanostat (Utrecht, The Netherlands) connected to a three-electrode cell, Metrohm (Herisau, Switzerland) Model 663 VA stand, linked with a computer (Pentium IV, 1,200 MHz) and with Autolab software. A platinum wire was used as the auxiliary electrode. MWCNTPE and $Ag/AgCl/KCl_{sat}$ were used as the working and reference electrodes, respectively.

Result and discussion:

Result shows, at a surface of CPE, the layer of irregularly flakes of graphite powder were present and isolated with each other. After multiwall carbon nanotubes (MWCNTs) added to carbon paste matrix, it can be seen that MWCNTs were distributed on the surface of electrode with special three-dimensional structure, indicating that the MWCNTs were successfully modified on the MWCNTPE. Under the optimized conditions, The detection limit was 0.09 µmol L^{-1}. The proposed method was successfully applied to the determination of GSH in the real samples.

Conclusion:

A new voltammetric sensor developed for the determination of GSH is very rapid, reproducible, highly selective and sensitive, and can be used for real sample analysis. This mediator shows excellent catalytic effects on the oxidation of GSH. It has been found that, with cyclic voltammetry, the oxidation of glutathione occurred at a potential about 560 mV on the surface of the multi wall carbon nanotubes paste electrode in the present of rutin, while the oxidation GSH does not takes place at the surface of a carbon nanotubes paste electrode without rutin as a mediator up to +1.0 V.

Reference:

[1] Beitollahi H, Karimi-Maleh H, Khabazzadeh H, *Anal Chem* 2008, 80: 9848

[2] Ensafi A A, Karimi-Maleh H, *J Electroanal Chem* 2010, 640:75

[3] Sullivan D M, Wehr N B, Fergusson M M, Levine R L, Finkel T, *Biochemistry* 2000, 39: 11121.

Capacitive Transducer for Pitting Corrosion Monitoring of Carbon Steel

S.A. Nabavi-Amri*1, N. Karimpour-Khamene1, N. Mirbolooki-Moghaddam1
[1] Thermodynamic research lab, School of Chemistry, Damghan University, Damghan, Iran
Email: nabavi@du.ac.ir

Key words: localized pitting, corrosion monitoring, capacitive transducer, carbon steel.

Introduction:

Corrosion of pipelines and storage facilities is a significant problem for the oil and gas industry. The most destructive form of corrosion is localized pitting (LP) corrosion, in which the metal or alloy is perforated rapidly. A preliminary evaluation indicated that electrochemical noise analysis (ENA) could be an effective method to analyze LP corrosion. ENA is a nondestructive, in-situ method of monitoring natural corrosion processes [1]. To characterize the corrosion mechanism, Argonne used different signal processing algorithms to interpret the ENA data. Powerful signal processing technique that could be used to characterize the noise data in a frequency domain. The slope of the power spectral density (PSD) versus frequency of the transformed signal is believed to relate to the corrosion mechanism. Coupling the PSD analysis technique with ENA would be an important step in developing a practical tool for monitoring LP for industrial applications. Therefore, the low-frequency portion of the potential noise PSD could be used to characterize the pitting corrosion process. Inspecting a much lower frequency range of the potential noise PSD spectrum (e.g., beyond 10-3 Hz) may be necessary to differentiate dominating LP from uniformly distributed pitting [1-3].

Experimental method:

1. Materials:

The sample selected for study was carbon steel determined using Fisons ARL-3460 Quantometer and classified as GI1045 according to SAE-AISI number. For all the experiments, the carbon steel samples were polished with abrasive papers from 100 to 2000 grades, degreased with ethanol, cleaned with water.

2. Capacitive Transducer Measurements:

With corrections on the free-running (astable multi-vibrator) oscillator on the base of Integrated circuit 555 a capacitive transducer constructed.

3. Electrochemical (direct) Measurements:

A saturated calomel electrode (SCE) was used as reference. Cyclic polarization (CP) measurements were carried out with a 3000-B Niroo Potentiostat and Protek-608 equipped with interface to a Pentium 600 MHz computer

4. Electrochemical (indirect) Measurements:

During the capacitive transducer measurements, solution's electrical conductivity carried out with Metrohm 712 conductometer; and pH values determined using Behineh 200 pH-meter.

5. Optical Microanalysis:

The surface of the carbon steel electrode was observed and analyzed after each experiment by a WILD-M3Z Binocolar Leica optical microscope.

Experimental results and discussion :

We have reexamined and compared localized corrosion by using another conventional indirect methods such as Conductometric and pH metric, and direct methods such as Tafel polarization and Microscopic photography; and found that well correspond with operation of capacitive transducer to monitoring of LP corrosion. The corrosion of carbon steel in 3.5% NaCl seawater solutions, containing different amounts of ammonium heptamolybdate (AHM) or imidazole , respectively as corrosion inhibitor, in with/without aeration, were studied. The new method of corrosion monitoring using **Capacitive Transducer** can be considered a more conservative method of corrosion measurement with respect to than the other methods such as linear polarization and pH metric methods.

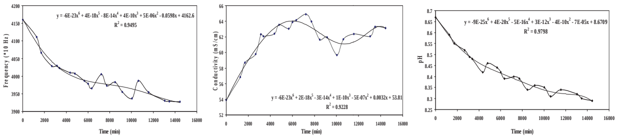

A B C

Fig 1. A) Frequency response of the transducer; B) Conductivity and C) pH variations vs time for corrosion of carbon steel in solution of NaCl 3.5 wt%, with aeration and with 0.05 mol/lit of imidazole as inhibitor.

Conclusion:

Our studies showed agreements between capacitive transducer response and the other direct and indirect methods such as pH metery, conductometery, micrographic studies, tafel polarization. It seems that some fluctuations in the all methods of our studies. It needs some more experiments that more realize the response for applicability aspects.

References:

[1] S. Masadeh, Journal of Minerals Characterization Engineering.4 (2005) 75-84.
[2] H.W. Song, V. Saraswathy, Int. J. Electrochem. Sci. 2 (2007) 1- 28.
[3] X. Jinag, Y.Z. Zheng, Corrosion Science 47 (2006) 447.

Thermodynamic investigation of acid green 25 and cationic alkyl ammonium bromid surfactants with different alkyl chain length

H. Dezhampanah [a*], R. Firouzi

[a] Department of Chemistry, Faculty of Science, University of Guilan P.O. Box 1914, Rasht 0098, Iran. (*e-mail: h.dpanah@guilan.ac.ir)

Keywords: Conductometry, Anionic dye, Cationic surfactant, Thermodynamics

Introduction:

The interactions between dye and surfactant molecules are important in various dyeing processes such as textile dyeing, photography and printing ink as well as in chemical researches such as biochemistry, analytical chemistry and photosensitization [1]. Various parameters (the charge and the alkyl tail length of the surfactants and the type and the position of the substituents in the aromatic ring of the dye molecules) can affect the interactions between surfactant and dye molecules.

The purpose of this study was to investigate the interactions of cationic surfactants; tetradecyltrimethylammonium bromide (TTAB), hexadecyltrimethylammonium bromide (CTAB) with anionic dye; Acid Green 25 (AG) by conductometric method. The influence of temperature and surfactant structure (the effect of alkyl chain length of surfactant) on ion pair formation is observed with this method.

Methods:

The conductance measurements of solutions were performed with Metrohm 712 digital conductometer using a dip type cell of cell constant 0.99 cm^{-1}. The specific conductivity of deionized water was measured before the each series of measurement at each temperature. Then the specific conductivity of an exact volume and known concentration of AG solution (10^{-4} M) was measured. Binary mixtures of dye/surfactant were prepared by keeping the dye concentration constant but by increasing the surfactant concentration. Then the specific conductivity of each solution was measured. Measurements were made at 25.0, 30.0, 35.0, 40.0, and 45.0 ºC. The temperature of solutions was kept within the range of ± 0.1 ºC.

Results and discussion:

The results of experimental data show that, the measured conductances of the AG – surfactant mixtures are lower than the sum of the specific conductivities of the individual AG and of the individual surfactant molecule. The decrease in the measured values can be explained by the formation of a non-conducting or a less-conducting specie in the solution.

The equilibrium constants were calculated by using a theoretical model based on the deviation from linear behaviour. This model is based on the comparison between the measured conductivity of the dye–surfactant mixture and a theoretical straight line that represents the sum of the specific conductivities of the dye and the surfactant [2]. The calculated values of ΔG^{o} are given in Table 1 for the binding processes at various temperatures. As seen from Table 1, all ΔG^{o} values are negative for all surfactants. The negative ΔG^{o} values indicate that the binding process of AG to the TTAB and CTAB occur spontaneously. Moreover, the ΔG^{o} values decrease with increasing of temperature for the all processes. This means that binding processes are lowly spontaneous at higher temperatures. The positive ΔH^{o} values indicate that binding processes are endothermic. Binding of AG to the premicellar of TTAB and CTAB are accompanied by the positive ΔS^{o} values (Table 1). This means that the binding of AG to the surfactant causes a decrease in the order of the process. In addition, it can be said from ΔS^{o} values that hydrophobic interactions play a major role in the interactions between the AG and the TTAB, CTAB submicellar regions.

Table 1: The values of; K ; ΔG^{o} ; ΔH^{o} and ΔS^{o} for AG-TTAB and CTAB complex formations

system	T (^{o}C)	K (M^{-2})	ΔG^{o} ($kJmol^{-1}$)	ΔH^{o} ($kJmol^{-1}$)	ΔS^{o} ($Jmol^{-1}K^{-1}$)
AG-TTAB	25.0	2.87×10^{6}	-36.84	5.28	142.35
	30.0	3.05×10^{6}	-37.61		142.55
	35.0	3.11×10^{6}	-38.29		142.43
	40.0	3.21×10^{6}	-38.99		142.39
	45.0	3.34×10^{6}	-39.71		142.39
AG-CTAB	25.0	3.98×10^{7}	-43.36	12.38	188.56
	30.0	4.32×10^{7}	-44.29		188.51
	35.0	4.77×10^{7}	-45.27		188.65
	40.0	5.11×10^{7}	-46.19		188.56
	45.0	5.51×10^{7}	-47.12		188.54

References:

[1] 1. J. Yang, J. Colloid Interface Sci. 274, 237, (2004).

[2] 14. S. Braˇcko, J. Špan, Dyes Pigments 45, 97, (2000).

The Study of Thermodynamic Constant ΔG_r , ΔS_r and ΔH_r ortho – Quinone and Azid ion by Cyclic Voltammetry method

Masoomeh Nilchi*, Hadi Shafie
Chemistry Department, Faculty of Science, Islamic Azad University, Arak Branch
Email: mitranilchi@yahoo.com

Abstract:

The standard electrode potential is a very important Parameter in biochemistry, analytical chemistry, etc [1]. In our previous work, we reported calculations of the standard electrode potential for a carbonyl compound. The electrochemical behavior of O-quinone (o – Q) and azid ion. The voltammetric data on the oxidation of 1 mM o - Quinone (o – Q) in the absence of azide ion, in aqueous solution containing 0.2 M phosphate buffer at pH 6.5 with a glass carbon electrod are shown in fig. 1 . These data describe a chemically reversible oxidation process, as follows from similarly sized peaks of the forward and reverse scans, with an oxidation peak potential (E^{ox}) of 0.159V and a reduction peak potential (E^{red}) of 0.09 V versus saturated calomel electrode. The conditional potential $E^{of} = (E^{ox} + E^{red})/2$ [2] were calculated as follows:

pH=6.5 , Eof= (0.159 + 0.09)/2=0.0.24
pH 6. 5 , E1 = 0.662 V (25 °C).
E2 = E1 + ESCE , E2 = 0.903 V (25 °C)

$\Delta G = -nFE$
$\Delta G = -174.251$ KJ/mol

$\Delta S = nF\left(\frac{\partial E}{\partial T}\right)_P$
$\Delta S = -0.347$ KJ/mol.K

$\Delta H = \Delta G + T\,\Delta S$
$\Delta H = -243.206$ KJ/mol

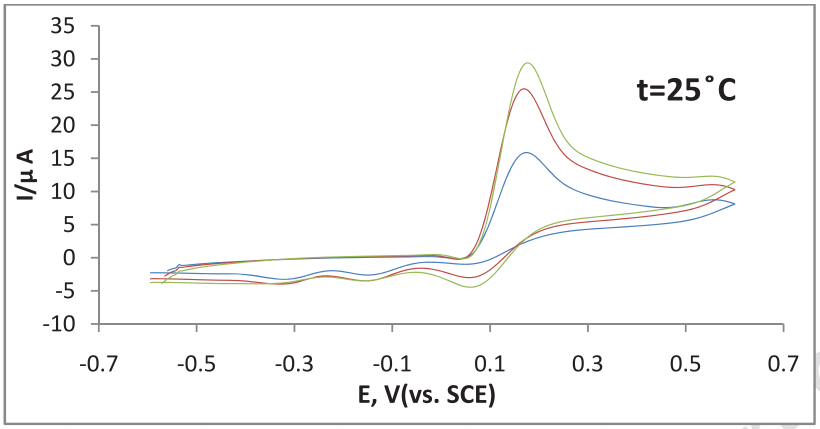

Fig. 1.

Keyword: Azid ion, Cyclic Voltammetry, o - Quinone, Thermodynamic Constant.

Introduction:

The cyclic voltammetry is very powerful in study the mechanism reaction, electrochemical. This is method with accounting for voltamograms between kind oxides in surface electrode, and kind reactants in the bulk solution mechanism reaction exactly are production. Thus so, rate constants of electron transfer and rate constants of reaction the former simulation and softwer ability deliberation. But times any group achievement use voltammogrames forms date thermodynamic diffusion not publication. Therefore this project investigation extraction thermodynamic constants electrochemical reaction payable. That in work very important parameter ISO-potential using. The ISO-potential with chang scanning rate invariable but change themperature is variable.The coefficient themperature $(\frac{\partial E}{\partial T})_P$quantities ΔS and ΔH electrochemical reaction to obtion. The electrochemical behavior of oxides o – Quinone (o – Q) in the absence of azide ion, in aqueous solution of pH=6.5 with a glass carbon electrode.

Reference:

[1] Y. Song, Y.Song, W. Xie, and D. Shi, Russ. J. Phys.Chem. 80, 1467 (2006).
[2] J. Wang, Analytical Electrochemistry, 2nd ed . (Wiley, New York, 2000).

Nano SBA15 mesoporous: A porous material for electrooxidation of metanol

E. Chiani[a*] , S.N.Azizi [a], Sh. Ghasemi[b]

a Department of chemistry, Faculty of sciences, mazandaran university, babolsar, Iran

b Department of nano chemistry, Faculty of sciences, mazandaran university, babolsar, Iran Email: elham_chiani@yahoo.com

Keywords: SBA-15 nanoparticles, modified electrode, methanol, electrocatalitic oxidation

Introduction:

Oxidation of methanol contains large overvoltage at most nonmodified electrode surfaces. The development of novel modified electrode for electro catalytic oxidation of methanol to decrease overvoltage is of interest. Some problems like relatively slow kinetics and continuous poisoning of the catalysts due to the presence of intermediates generated in the methanol oxidation reaction limit its performance [1] limit the performance of direct methanol fuel cells (DMFC). In this paper, we report a new zeolite-modified carbon paste electrode based on Nickel-SBA-15 nanozeolite for methanol electrooxidation. SBA-15 nanozeolite was synthesized using amorphous silica which extracted from sorghum with approximately 80% purity The synthesized SBA-15 nanozeolite particles are rodlike shape with average diameter of 82 nm and length in the range of 50-250 nm. Nickel-SBA-15 carbon paste electrode (Ni/SBACPE) was used to investigate the electrocatalytic oxidation of methanol in alkaline solution by cyclic voltammetry (CV) and chronoamperometry (CA).

Materials and methods:

Silicate solution was prepared by by Kalapathy et al. method [2]. Graphite powder, nickel chloride, methanol and Paraffin all purchased from Fluka. H_3PO_4 used in this work was also purchased from Merck. $EO_{20}PO_{70}EO_{20}$ (M_{av} = 5800) was purchased from Aldrich. In a typical synthesis, Copolymer p123 was dissolved in acidic solution . Alkaline sodium silicate solution was quickly added to this mixture added to the above solution and excess water was added to make up the solution to 80 ml. synthesized gel was in an oil . products were filtrated, washed with distilled water, and dried in an oven. Subsequently the sample was calcined. After the process, SBA-15 nanoparticles which was a white powder was obtained. Then SBA-15 nanoparticles immersed in 5 ml 0.1 M $NiCl_2$ solution to replace the Na^+ in the SBA-15 sample. Then, mesoporous silica was filtered and washed with deionized water and was dried in oven.

Apparatus:

The physical properties of synthesized mesoporous SBA-15 nanoparticles were characterized by XRD, EDX, SEM, TEM, FT-IR, BET/BJH and TGA.

Result and discussion:

mesoporous silica included Ni(II) was mixed with carbon paste to prepare Ni/SBACPE and then its electrocatalytic behavior was investigated with cyclic voltammetry and chronoamperometry. At the surface of Ni/SBACPE and in the presence of methanol,the anodic oxidation current is largely increased whereas the cathodic current is decreased. Catalytic rate constant is obtained from chronoamprograms which approved that the nickel included material siliceous (SBA-15) modified electrode. It can enhance the oxidation of methanol through a decrease in overpotential of methanol oxidation and overcome the low kinetic of reaction in alkaline solution.

Conclusion:

In this work, mesoporous SBA-15 nanoparticles was prepared from SSA with sol-gel method. Cyclic voltammetry of methanol on Ni/SBACPE showed that by using nano-sized zeolite, the oxidation current was increased with comparing to the carbon paste electrode (CPE). Also, the rate constant for the catalytic reaction (k) of methanol was obtained.

Reference:

[1] R. Lu; J. B. Zang; Y. H. Wang; Y. L. Zhao; Electrochimica Acta; 60, 329, 2012.

[2] U. Kalapathy; A. Proctor A; Journal Shultz Bioresource Technology; 73, 257, 2000.

Effect of organic additives in electroless Ni-P and Ni-P-Al_2O_3 composite coatings

H.Ashassi-Sorkhabi *, Z.Javadifar
Electrochemistry Researches Laboratory, Department of Physical Chemistry, Faculty of Chemistry, University of Tabriz, Tabriz, Iran
Email: habib.ashassi@gmail.com

Keywords; Electroless Ni-P; Corrosion resistance; organic additives; alumina

Introduction:

Ni-P electroless is one of the most important surface engineering technologies, which applied to industrial fields. Studies show that submicrometer and nanoparticles are able to modify the crystalline growth of the growing nickel films and create dispersion harding effects at low incorporation levels. The idea of codepositing various second phase particles in electroless nickel deposits and thereby taking advantage of their inherent uniformity, hardenability, wear resistance and corrosion resistance, has led to the development of electroless nickel composite coatings. In this study, the effect of some organic additives such as glucose and starch on morphology and hardness and also corrosion resistance of Ni-P coating matrix have been investigated and a comparisons between Ni-P and Ni-P-Al_2O_3 coatings has been done[1-3].

Materials and methods:

The used substrate was stainless steel with 1cm^2 surface area. All samples were prepared using 600-grad sic paper and then cleaned in saturated sodium hydroxide solution for 5 min. after the rinsing , specimens immersed in 30 vol% HCL solution for deoxidization for 1 min. then specimens were transferred immediately to the plating solution. The Ni-P electroless bath containing $NiSO_4$ 30 g/l , NaH_2PO_2 25g/l and suitable amounts of additive and stabilizer .In one bath were used glucose and in the other bath used starch .After preparing of bath and inserting of Al_2O_3 nanoparticles in bath was performed in 60 min. This deposition process was also carried out without the existence of particles. Characterization and corrosion properties of the synthesized deposits were performed by SEM, polarization and Electrochemical Impedance Spectroscopy (EIS) methods and also microhardness of coatings was measured [4].

Results and Discussion:

EIS measurements confirm the polarization results (Not shown here). The corrosion of Ni-P-glucose and Ni-P-starch and also these coating in present of Al_2O_3 nanoparticles has been investigated in 3.5% Nacl solution. The result are showed that EN, EN-glucose, EN-Al_2O_3-glucose almost showed the same corrosion resistance, but results have demonstrated that the presence of starch in coatings are improved the corrosion protection of the nanocomposite coating in 3.5% NaCl medium. The SEM analysis of coatings reveals that the coats obtained in the presence and absence of glucose and starch are not the same, in fact these organic additives are causing that coatings are being smoother and brightener than coatings in the absence of glucose and starch. Also the microhardness of EN-Al_2O_3 coating in the presence of starch is increasing.

Conclusions:

1. In Ni-P-Al_2O_3 composite coatings, by increasing the glucose, the deposit almost showed the same corrosion resistance with Ni-P-glucose and Ni-P coatings.
2. By additive glucose and starch, surface morphology was smoother than Ni-P coating.
3. corrosion resistance of Ni-P-Al_2O_3 composite coatings in the present of starch were increasing

References:

[1] J.N. Balaraju, T.S.N. Sankara, Narayanan and S.K. Seshadri , “Electroless Ni–P composite coatings” Journal of Applied Electrochemistry 33: 807–816, 2003.

[2] Hai-Ping Liu, Ning Li , Si-Fu Bi, De-Yu Li, Zhong-Li Zou, “Effect of organic additives on the corrosion resistance properties of electroless nickel deposits” Journal of Thin Solid Films,516 (2008) 1883-1889.

[3] J.N. Balaraju, Kalavati, k.s. Rajam, “Influence of particle size on the microstructure, hardness and corrosion resistance of electroless Ni-P-Al_2O_3 composite coatings” Journal of surface &Coatings Technology, 200 (2006) 3933-3941.

[4] I. Baskaran , T.S.N. Sankara Narayanan, A. Stephen “ Effect of accelerators and stablizers on the formation and characteristics and electroless Ni-P deposits Journal of Matrrials chemistry and physics”, 99 (2006) 117-126.

Inhibitive and adsorption behaviour of some N and O donor Schiff Bases on mild steel corrosion in hydrochloric acid solution

H.Ashassi-Sorkhabi[a], N.Jarrahian[a]*, Z.Frouzat[a]

*[a]Electrochemistry Researches Laboratory, Department of Physical Chemistry, Faculty of Chemistry, University of Tabriz, Tabriz, Iran

Email: n.jarahian89@ms.tabrizu.ac.ir

Key words: corrosion inhibitor, Schiff Base, Adsorption, Mild steel

Introduction:

Study of organic corrosion inhibitors is an attractive field of research due to its usefulness in various industries. Hydrochloric acid is generally used for the removal of undesirable rust in industrial processes. Inhibitors are usually used in these processes to control the corrosion of the metals.Most of the well-known acid inhibitors are organic compounds containing nitrogen, sulphur and oxygen [1–4]. These compounds can adsorb on the steel surface andblock the active sites decreasing the corrosion rate**.**Schiff bases have been reported as potential inhibitors on corrosion of different metals [6,7].In this research we studied the inhibition action of some N and O donor Schiff Bases on Mild Steel corrosion in 1 M HCl by polarization, electrochemical impedance spectroscopy (EIS) and weight loss measurements. The inhibitors were synthesized, characterized and used as new corrosion inhibitors for mild steel. The effect of various parameters such as temperature and inhibitor concentration on the protection efficiency has been studied. The adsorption of used compounds on the steel surface obeys Langmuir's isotherm [7].

Materials and methods:

Schiff base compounds as inhibitors were synthesized from equimolar amounts of 2-Aminophenol and the corresponding aldehyde through a condensation reaction in ethanol media [8].The acid solutions (1 M) were made from analytical grade 37% HCl (Merck) and double-distilled water. The concentration range of inhibitor employed was 2×10^{-4} to 1×10^{-2}M in 1M HCl. In this research we studied the inhibition action of some N and O donor

Schiff Bases on Mild Steel corrosion in 1 M HCl by polarization, electrochemical impedance spectroscopy (EIS) and weight loss measurements.

Apparatus:

Polarization and EIS experiments were carried out using anAUTOLAB Potentiostat-Galvanostat (PGSTAT30). A three-electrodecell configuration consisting of mild steel as working electrode(WE), a platinum electrode as counter (CE), and a saturated calomel electrode (RE) as a reference was used.

Result and discussion:

Polarization curves for mild steel electrodein 1MHCl, in the presence and absence of Schiff basesat various concentrations. Both cathodic and anodic reactionson mild steel electrode were inhibited in the presence of studiedcompounds. The Schiff bases affected cathodic reactionmore than anodic reaction. This result suggests that the additionof inhibitors retards the hydrogen evolution reaction[5].The capacitance of electricaldouble layer (C_{dl}) decreases in the presence of inhibitors. Decreasein the C_{dl}, which can result from a decrease in localdielectric constant and/or an increase in the thickness of theelectrical double layer, suggests that the inhibitor moleculesact by adsorption at the metal/solution interface[7].

Conclusion:

All examined Schiff base compounds act as good corrosioninhibitor in HCl media. Adsorption of Schiff bases on the steel surface is spontaneousand obeys the Langmuir's isotherm.Results obtained from all applied experimental methodsare in good agreement.

Reference:

[1] G. Schmitt, Br. Corros. J. 19 (1984) 165.
[2] V.S. Sastri, Corrosion Inhibitors – Principles and Applications, Wiley, Chichester, England, 1998.
[3] P. Ramesh, B. Babu, K. Thangavel, Anti-Corros. Methods Mater. 52 (2005) 219.
[4] A.S. Fouda, H.A. Mostafa, F.E. Heakal, G.Y. Elewady, Corros. Sci. 47 (2005) 1988.
[5] M. Lagrene, B. Mernari, M. Bouanis, M. Traisnel, F. Bentiss, Corros.Sci. 44 (2002) 573.

[6] H. Ashassi-Sorkhabi et al. / Electrochimica Acta 50 (2005) 3446–3452.

[7] H. Ashassi-Sorkhabi et al. / Applied Surface Science 239 (2005) 154–164.

[8] H. Hoss, H. Elias, Inorg. Chem. 23 (1993) 317.

Synthesis, electrochemical and theoretical studies of New Hydrazonics Schiff Bases as corrosion inhibitors

H.Ashassi-Sorkhabi[a],N.Jarrahian[a],Z.Frouzat[a]*

*[a]Electrochemistry Researches Laboratory, Department of Physical Chemistry, Faculty of Chemistry, University of Tabriz, Tabriz, Iran
Email: zahrafrozat@yahoo.com

Key words:corrosion,mild steel, quantum chemical, Schiff Base

Introduction:

The corrosion of steel is an enormous economic problem. Thus, efforts to develop more efficient and environmentally compliant methods to prevent corrosion have been ongoing [1, 2]. The use of inhibitor is one of the most practical methods to protect metals from corrosion, especially in aggressive media [3]. Among Schiff bases have been reported as potential inhibitors on different metals [4-6]. Acid solutions are generally used for the removal of rust and scale in industrial processes [7].Most of the well-known acid inhibitors are organic compounds containing nitrogen, sulphur and oxygen atoms [8,9]. Hydrazonics Schiff Bases were synthesized, characterized and used as new corrosion inhibitors of mild steel in the acidic media.Inhibitory effect of corrosion inhibitors has been studied by a series of techniques, such as potentiodynamic polarization, weight loss and quantum chemical calculation methods.We report the synthesis of Hydrazonics Schiff Bases and their inhibition action on the corrosion of mild steel in acid media and comparison of their protection powers.

Materials and methods:

Schiff base compounds as inhibitors were synthesized from equimolar amounts of 4-Pyridinecarboxylic acid hydrazide and the corresponding aldehyde through a condensation reaction in ethanol media.The acid solutions (1 M) were made from analytical grade 37% HCl (Merck) and double-distilled water. In this research we studied the inhibition action of some New Hydrazonics Schiff Bases on Mild Steel corrosion in 1 M HCl by polarization, electrochemical impedance spectroscopy (EIS) and weight loss measurements.

Apparatus:

Polarization and EIS experiments were carried out using anAUTOLAB Potentiostat-Galvanostat (PGSTAT30). A three-electrodecell configuration consisting of mild steel as working electrode(WE), a platinum electrode as counter (CE), and a saturated calomel electrode (RE) as a reference was used.

Result and discussion:

It has been found that all those Schiff base compounds are excellent inhibitors.results show that inhibition efficiency increases when the inhibitor concentration increases.all thermodynamic parameters such as associated activation energy and free Gibbs energy and heat of inhibitor adsorption on the steel surface have been determined.Obvious correlation was found between corrosion inhibition efficiency and quantum chemical parameters,using the linear and non-linear QSAR models.The obtained theoretical results have been compared with the experimental results.

Conclusion:

The results drawn from the different techniques are comparable and showed that with increasing inhibitor concentration, adsorption of inhibitor to metal surface and inhibition persent increase.in the case of these Hydrazonics Schiff Bases with increasing tempreture corrosion rate increase and inhibition effect decrease.the activation energy and the thermodynamic parameters for the corrosion process in the presence of the inhibitors were determind.by fitting the corrosion data it is found that the results agree with Langmuir and kinetic thermodynamic equation.

Reference:

[1] P. Lowmunkhong, D. Ungthararak, P. Sutthivaiyakit, Corros. Sci. 52 (2010) 30.

[2] B. Amo, G. Blustein, M. Perez, M. Garcia, M. Deya, M. Stupak, R. Romagnoli, Colloids Surf. A: Physicochem. Eng. Aspects 324 (2008) 58.

[3] Khaled M. Ismail. Acta (2007).

[4] A.A. Khadom, A.S. Yaro, A.A. H. Kadum, J. Taiwan Inst. Chem. Engine. 41 (2010) 122.

[5] M. Behpour, S.M. Ghoreishi, N. Soltani, Corros. Sci., 50 (2008)2172.

[6] M. Behpour, S.M. Ghoreishi, N. Soltani, M. Salavati-Niasari, Corros. Sci., 51 (2009) 1073

[7] F. Bentiss, M. Bouanis, B. Mernari, M. Traisnel, H. Vezin, M. Lagrende, Appl. Surf. Sci. 253 (2007)3696.

[8] H. Ashassi-Sorkhabi et al. / Applied Surface Science 239 (2005) 154–164.

[9] H. Ashassi-Sorkhabi et al. / Electrochimica Acta 50 (2005) 3446–3452.

Sonoelectropolymerization of Polypyrrole-SiC nanocomposite coatings on mild steel and corrosion protection

H. Ashassi-Sorkhabi*, R. Bagheri
Electrochemistry Researches Laboratory, Department of Physical Chemistry, Faculty of Chemistry, University of Tabriz, Tabriz, Iran
Email: habib.ashassi@gmail.com

Key words: Sonoelectrochemistry, Nano composite, Corrosion, Polypyrrole, EIS.

Introduction:

Using the ultrasound in electrochemical processes is called sonoelectrochemistry. In the last decade, the sonoelectrochemical synthesis of inorganic materials has experienced an important development motivated by the emerging interest in the nanostructures production [1]. In a sonoelectrochemical process, two clean energies (electrical and mechanical) are introduced into the reaction system to provide a high-energy microenvironment to perform a range of chemical reactions [2–4]. Sonoelectrochemistry, ultrasound with electrochemistry, is the rupture and formation of transient cavitations bubbles gives a large number of tiny regions of ultra high pressure and temperature which are known as hot spot. This may lead to a number of alterations in the electrochemical reaction kinetics and products formed. The rupture of bubble in the electrolyte/homogeneous medium produces forces, a general improvement of hydrodynamics and movement of species. Another attractive effect of ultrasound, cleavage of water molecules or organic additives helps in the forming intermediate reducing radicals. This behavior of sonoelectrochemistry finds of its way in arrested electroformation of nanocomposites, complex alloys [5]. Ultrasound was also shown to affect metal electrodeposition with benefit to the quality of the deposit, its adhesion and morphology, and also the diminution of brighteners and other additives, such as the toxic molecule thiourea, that needed in the silent systems [6]. The main objectives of this work are synthesis of PPy and PPy-SiC deposits through sonoelectrochemical route and its comparison their different properties. Characterization and corrosion properties of the synthesized deposits were performed by SEM, polarization and Electrochemical Impedance Spectroscopy (EIS) methods.

Materials and methods:

Electrochemical studies or experiments were done with AUTOLAB PGSTAT 30 potentiostate system and three electrode electrochemical cell. The working electrode was a mild steel; the counter electrode was a Pt plate and saturated calomel electrode (SCE) worked as reference electrode. For sonoelectrochemical experiment ultrasonic vibrator of frequency (25 kHz) was used (dr. hielscher ultrasonic processor Model UP 400S with titanium alloy horn (diameter: 3 mm)). Ultrasonic irradiation with galvanostatic method is used as a route to fabricate PPy-SiC nanocomposites and PPy coatings.

Results and Discussion:

The SEM analysis of coatings reveals that the coats obtained in the presence and absence of nanoparticles are not the same. The surface morphology changes in the presence of SiC nanoparticles, and nano particles inclusion in the deposits act as a physical barrier for diffusion of external corrosive chemicals due to nano-size of particles. Corrosion protection behavior of the PPy-SiC and PPy coatings in 3.5% NaCl solution was studied by open circuit potential sweep, electrochemical impedance spectroscopy (EIS) and polarization techniques. The results have demonstrated that the presence of SiC nanoparticles in the PPy coatings in addition of ultrasound irradiation are improved the corrosion protection of the coating in 3.5% NaCl medium.

Conclusions:

A new route has been followed for nanocomposite formation using sonoelectrochemical synthesis. Now the deposit obtained under sonication approaches towards a highly adherent, dense, and homogenous coat and the presence of nanoparticles increases the corrosion resistance of mild steel in salted water. The comparison of the corrosion performance of this nanocomposite coating and the nanoparticleless PPy coats showed that nanocomposite coating could provide a better protection against corrosion of mild steel, for longer periods.

Reference:

[1]Pankaj and etal.; "Theoretical and Experimental Sonochemistry Involving Inorganic Systems". 2010.

[2]C. Brett; "Piezoelectric transducer and Applications"; Sonoelectrochemistry; In: Antonio Arnau Vives (ed). Springer, 2008.

[3] BG. Pollet and etal.; "Sonoelectrochemistry-theory, principles and applications"; Recent Res Develop Electrochem; 4, 55–78, 2001.

[4] TJ. Mason and etal.; "Sonoelectrochemistry"; Ultrasonics; 28, 333–337, 1990.

[5] R. N. Chauhan; "sonoelectrochemical synthesis of ultra-fine copper deposits at ambient and sub-ambient temperatures" A Thesis Submitted in Partial Fulfillment; National Institute of Technology Rourkela; 2007.

[6] D. J. Walton; "Sonoelectrochemistry- application of ultrasound to electrochemical systems"; ARKIVOC; (iii), 198-218, 2002.

Study the effect of carbon active as an additve to the catalyst layer of gas diffusion electrode on the ORR kinetic.

Rasol Abdullah Mirzaie[a*], Rahil Yazdanshenas[a], Ahmad nozad goli kand[b]
[a] Fuel cell Research Laboratory, Dep. Of chemistry, Faculty of science, Shahid Rajaee University, Tehran, IRAN, E-mail address:Shahid_r1382@yahoo.com
[b] Institute of materials ,Atomic energy of organization of Iran

Key words: Gas diffusion electrode, PEM fuel cell, Carbon active addition, Surface area

Introduction:

One of the main problems of the commercialization of fuel cells is making electrodes .If the electrodes can be produced with desired properties, performance and reasonable price, making large – scale fuel cell would be possible[1]. One way that increases the performance of the electrodes can be increasing the surface area of catalyst layer that studied in this research by addition of different amounts of activated carbon. Sulfuric acid 2.5 M was used as electrolyte, Ag/AgCl electrode as reference electrode and Pt electrode as counter electrode [2]. Pt loading in all electrodes was 0.3 mg.cm^{-2}[3].

Preparation of gas diffusion electrodes:

To prepare the catalyst ink, Pt/C20% and 0.1, 0.2, 0.3,0.4,0.5, 1and 1.5 %wt of carbon active mixed and washed with PTFE, until the amount of PTFE reached 30%wt value. Then distilled water and isopropyl alcohol (Aldrich 99%) is added, and then 30 min Ultrasound used to create a highly dispersed mixture. After evaporating the solvents, an uniform paste obtained which uniformly spread over the carbon paper (0.64cm^2) and next sintered at 200^0 c for 1 h [4].

Electrochemical analyses:

A potentio state – galvano stat (zahner) was used to determine the electrochemical properties of the electrodes. Cyclic voltammetry (CV) measurements were conducted on the electrodes to investigate the effect of carbon active addition on the electrochemical active surface area (ECSA). Linear sweep voltammetry (LSV) was used to show the kinetically parameters.

Diffusion coefficient of oxygen can be measurable using Chornoamperometry (CHA) analysis. An impedance analyzer was used to reach the nyquest diagrams and extract the electronic resistance of electrodes .

Results and discussion

The effect of carbon active addition on the efficiency of the electrodes:

The results of LSV shows that the highest exchange current density is for the electrode with 1% wt carbon active, although in electrodes without carbon active better performance is observable. (Fig1)

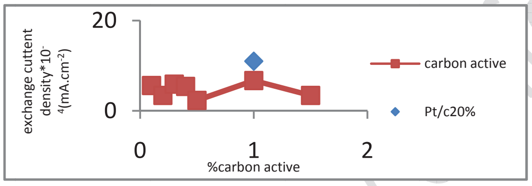

Fig1:exchang current density versus %carbon active

CV results:

From CV tests the electrochemical activated surface areas were calculated. (Fig2)

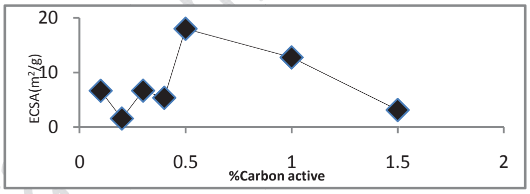

Fig2:electrochemical surface area versus

CHA results:

The diagrams and tables that reached from CHA tests showed that addition of any amount of carbon active in the catalyst layer lead to increasing the oxygen permeability.(Fig3)

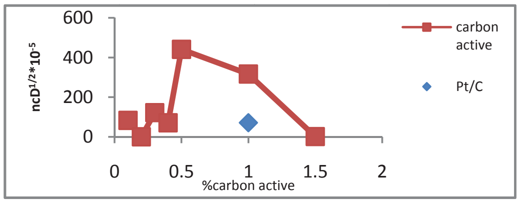

Fig3:oxygen permability versus %carbon

Impedance results:

As it can be inferred from previous results, the nyquest .

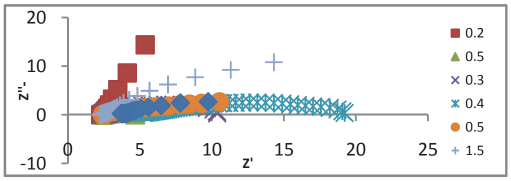

Fig4:nyquest digram for%carbon active

Conclusions:

The performances of gas diffusion electrodes have not been improved .An addition of carbon active in to the catalyst layer dose not enhanced the performance of electrodes although the surface area improved by addition of any amounts of graphite.

References:

[1]H.Ghribi, R.Mirzaie ,power sources 115(2003) 194-202

[2]J.H. Hirschenhofer, D.B. Stauffer, R.R. Engleman, M.G. Klett, FuelCell Handbook, Fourth ed., Parsons, Oxford, 1998

[3]J. Larminie, A. Dicks, Fuel Cell Systems Explained, Wiley, NewYork, 2000

[4]M. Uchida, Y. Aoyama, N. Eda, A. Ohta, J. Electrochem. Soc. 142 (1995) 463.

Caracterization of Nickel/Nano-Porous Carbon (Ni-NPC) Composite Structures as a new Material for Supercapacitors by Elelctrochemical Impedance Spectroscopy in Aqueous and nonaqueous Electrolyte

A.R.Madram[1] , F.Khashei*[2]
[1]Department of Applied Chemistry, Malek Ashtar University of Technology, Isfahan, Iran.
[2]Department of Chemistry, Payame Noor University, Isfahan, Iran.
Khafm@yahoo.com

Keywords: Nickel/Nano-Porous Carbon (Ni-NPC) Nanocomposite, Supercapacitor, Electrochemical Impedance Spectroscopy (EIS)

Introduction:

Electrochemical energy storage and conversion systems include batteries, fuel cells and electrochemical supercapacitors. Two type of electrochemical supercapacitors are currently under development, namely, the electric double-layer capacitor (EDLC) and redox-or pseudocapacitor (PsC). They have attracted much attention due to their high power and high capacitance. Energy storage arises mainly from the separation of electronic and ionic charges at the interface between electrode materials with a high specific area and the electrolytic solutions. In this research work, a new composite material (nickel/nano-porous carbon or Ni-NPC) was developed for supercapacitors. Ni-NPC was produced by electrolytic deposition. Electrochemical impedance spectroscopy is a method to measure complex impedance of electrochemical cells. EIS has been applied to study the conductivity of the electrodes. The measurements were performed at open circuit potential with a signal amplitude of 5mV. The spectra were acquired in a frequency range of 100 mHz-100 kHz in NaOH 1M and acetonitril electrolytes.

Materials and methods:

Pine wood powder was used as the starting material in the preparation of the porous carbon material. Wood powder was impregnated with $ZnCl_2$ by immersion into a aqueous solution of 1M HCl containing 20 g ZnCl2 under mechanical agitation at 25 °C for 10 h. The supernatant liquid was then separated by filtration and the remaining solid was oven-dried at 80 °C for 24 h. Ni-NPC was produced by electrolytic co-deposition of Ni ion and NPC particles on copper cylinder substrates. The surface morphology of composites were examined by SEM and EDX, and the electrochemical properties were tested by cyclic voltammetery (CV) and electrochemical impedance spectroscopy (EIS) in alkaline and organic electrolytes.

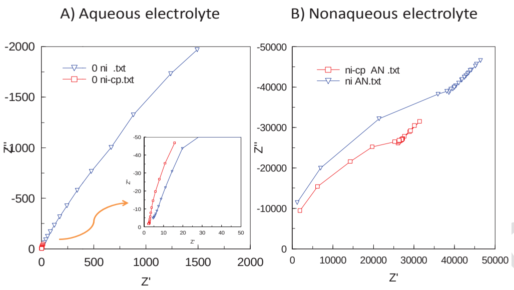

Apparatus:

Electrochemical characterization of the fabricated composite electrodes was studied using a potentiostat (PARS TAT 2273, Princeton Applied Research) controlled by a PowerSuite electrochemical software. A standard three electrode cell contained a working electrode, a platinum plate counter electrode and a Ag/AgCl reference electrode. The surface area of the working electrodes was 1 cm^2.

Result and discussion:

EIS was studied to further understand the Ni-NPC composite capacitive behavior associated with resistance of the electrode. The electrochemical impedance test was carried out in NaOH solution and acetonitril electrolyte with a frequency range of 100mHz-100kHz. Fig. A compares the Nyquist plots for the Ni and Ni-NPC electrodes. Ni-NPC electrode depressed semicircle in the high-frequency range corresponding to the charge transfer resistance, and a straight sloping line in the low-frequency range corresponding to the diffusive resistance can be observed for both samples. The high frequency value of the real part of complex impedance has been used for the estimation of the equivalent series resistance (ESR) of the electrodes. It is clear that the Ni-NPC has lower charge- transfer resistance and diffusive resistance compared with those of the Ni, confirming the superior capacitive behavior of the Ni-NPC electrode in aqueous electrolyte. It is observed that the semicircle diameter of Ni is longer than Ni-NPC, that results the resistance of acetonitril is larger than NaOH due to larger conductance of aqueous electrolyte.

Conclusion:

The improved capacitive behavior is in a good agreement with the impedance spectroscopy data. The equivalent series resistances of samples in non-aqueous was higher than those in aqueous electrolyte, due to larger conductance of aqueous electrolyte. This research confirmed that Ni-NPC electrode has better capacitive behavior than Ni electrode in aqueous and nonaqueous electrolytes.

Reference:

[1] R. Karimi Shervedani, A.R. Madram, J. Hydrogen Energy, 33, 2468-2476 (2008).
[2] A. SHOKROLAHI, Chinese Journal of Catalysis, 31: 1427–143 (2010).
[3] R. K. Shervedani, A.H. Alinoori and A.R. Madram, J. New Mat. Electrochem. Systems, 11, 259-265 (2008).

Study of the capacitance behavior of Ni and Ni-Cg electrodes in aqueous and non-aqueous electrolytes by electrochemical impedance spectroscopy

A.R.Madram[1] , F.Khashei*[2]
[1]Department of Applied Chemistry, Malek Ashtar University of Technology, Isfahan, Iran.
[2]Department of Chemistry, Payame Noor University, Isfahan, Iran.
Khafm@yahoo.com

Key words: Supercapacitor, Nickel/carbon graphite (Ni-Cg) composite, electrolyte, EIS

Introduction:

A new technology, the supercapacitor, has emerged with the potential to enable major advances in energy storage. Supercapacitors are governed by the same fundamental equations as conventional capacitors, but utilize higher surface area electrodes and thinner dielectrics to achieve greater capacitances. The nature of electrolytes plays a very important role in the electrochemical characteristics of supercapacitors. Generally, there are mainly two types of electrolytes used in supercapacitor technology: aqueous and non-aqueous electrolytes. The resistance of electrolytes can limit power density of supercapacitor cells ($P = \frac{V^2}{4R}$), while their operating voltage, restricted by the breakdown potential of the electrolyte, can limit the energy density ($E = \frac{1}{2}CV^2$).. In this research work, a new composite material (nickel/graphite carbon, Ni-Cg) was developed for supercapacitors. Ni-Cg was produced by electrolytic co-deposition of Ni ions and graphite on copper substrates. The surface morphology was examined by SEM and EDX, and the electrochemical properties were tested by cyclic voltammetry (CV) and electrochemical impedance spectroscopy (EIS) in aqueous and non-aqueous electrolytes.

Materials, methods and apparatus

1. Ni and Ni-Cg composite electrode (with 1cm^2 surface area) prepared by Electrodeposition method including electrolytic deposition (ELD).
2. Aqueous electrolyte (NaOH 1M) and non-aqueous electrolyte (Acetonitril)

3. A standard three-electrode cell containing Ni and Ni-Cg as the working electrodes, a plate of platinum as the counter electrode and Ag/AgCl saturated electrode as the reference electrode.
4. Potentiostat (PARSTAT 2273) controlled by a computer using a PowerSuite electrochemical software for CV and EIS studies.
5. Software of Zview (version: 2.3f) for Fitting of the impedance behavior performed on the basis of the equivalent-circuit models using.

Result and discussion:

Fig.A,B gave Nyquist plots of Ni and Ni-Cg electrodes in NaOH and acetonitril electrolytes in the frequency of 0.1– 100,000 Hz. These electrodes show a depressed semicircle in the high frequency region, which is indicative of a charge-transfer process. It is observed that the semicircule diameter of B is longer than A, that results the resistance of acetonitrilis larger than NaOH due to larger conductance of aqueous electrolyte. For the aqueous electrolyte, the imaginary part of the impedance spectra at low frequencies approached to a vertical line suggesting a capacitive behavior. Obviously, Nyquist plots at low frequency parts inclined. This phenomenon may be due to the fact that the electrolytes entered into micropores and caused the increase of electrolyte ions diffusion resistance. At intermediate frequencies, there is a straight line with a slope of approximately 45° for acetonitril, which is a common observation for carbon based supercapacitors.

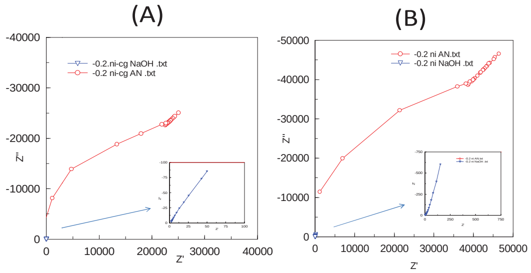

Conclusion:

The equivalent series resistances of samples in non-aqueous was higher than those in aqueous electrolyte, which can reduce the maximum power density. The low operating voltage of aqueous electrolyte will result in a low energy density compared with organic electrolytes.

Finally, the use of non-aqueous electrolytes has led to various new cell configurations with very high energy densities.

Reference:

[1] R. Karimi Shervedani, A.R. Madram, J. Hydrogen Energy 33, 2468-2476 (2008).

[2] R. K. Shervedani, A.H. Alinoori and A.R. Madram, J. New Mat. Electrochem. Systems, 11, 259-265 (2008).

[3] X. Li, Microporous and Mesoporous Materials 131, 303–309 (2010)

Fabrication of a Potentiometric Magnesium Ion Selective Electrode Based on Nano Conducting Polypyrrole Doped With Titan Yellow

R. Ansari[1], Z. Mosayebzadeh[2], A. Mohammad-khah[3]
[1,2,3] Chemistry Department, Faculty of science, University of Guilan, Rasht, Iran
E-mail: ransari@guilan.ac.ir

Key words: Solid state electrode, Magnesium ion, Potentiometry, Polypyrrole, Titan Yellow

Introduction:

Titan yellow is a compound with formula $Na_2C_{28}H_{19}S_4O_6$. It is a triazene dye used as a stain and fluorescent indicator in microscopy. It is also used as a reagent for the detection of magnesium (Figure 1).

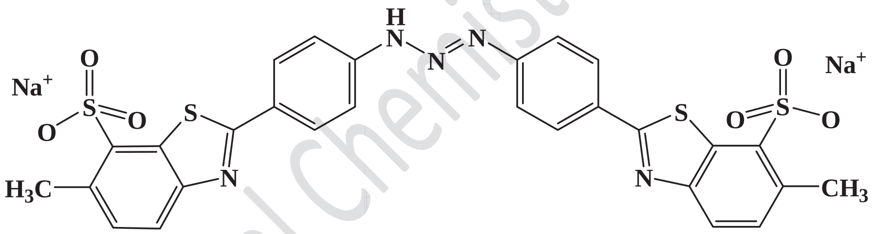

Figure 1. Structure of Titan Yellow

Polypyrrole is one of the important conductive polymers that are widely used in energy storage systems, biosensors and electronics [1, 2]. The electrochemical synthesis of polypyrrole has advantages of simple process, mass production and low cost.

Materials and methods:

Electropolymerization of pyrrole was carried out using cyclic voltammetry (CV) with scan rate of 10 (mv/s) and cyclic number of 20, in a solution 0.02M of pyrrole (monomer) and 0.01M of Titan Yellow as electrolyte solution. A pencil graphite microelectrode was used as working electrode.

Result and discussion:

The fabricated electrode (PGE/PPy/TY) showed high selectivity toward Mg^{2+} ions in the range of (1.0×10^{-5}-1.0×10^{-2} M) with a Nernstian slope of 28.22 ± 0.20 mV/decade. Over the whole concentration range the electrode reaches its equilibrium response time very short (less than 15s). The electrode revealed high reproducibility, repeatability and also good selectivity with respect to many cations including alkali, alkaline earth, and transition metal ions. The resulting values of the selectivity coefficients are summarized in Table 1. Scanning electron microscopy (SEM) pictures showed that the PPy polymer is electrodeposited onto pencil graphite electrode as nanostructure film which the average diameter of particles is 65 nm.

Table 1: Selectivity coefficients of PGE/PPy/TY electrode toward various interfering ions

Ion	K^{MPM}	Ion	K^{MPM}
Na^{+}	2.5×10^{-3}	Pb^{2+}	2.9×10^{-3}
K^{+}	3.8×10^{-3}	Mn^{2+}	3.2×10^{-3}
Cu^{2+}	3.1×10^{-3}	Zn^{2+}	1.6×10^{-3}
Ca^{2+}	4.5×10^{-4}	Co^{2+}	2.2×10^{-3}
Ni^{2+}	2.3×10^{-3}	Fe^{2+}	3.0×10^{-3}
Hg^{2+}	3.2×10^{-3}	Cd^{2+}	3.2×10^{-3}

Conclusion:

The advantages such as fast response time, low detection limit, simplicity of preparation, low cost, high shelf lifetime, high selectivity, sensitivity, accuracy and precision as well as good dynamic linear range, high repeatability and reproducibility make this electrode, potentially useful for measurement of free Mg (II) ions in real samples.

References:

[1]A. Mohammad-Khah, R. Ansari, A. F. Dellavar, Z. Moseybzadeh, “Nano structured potentiometric sensors based on polyaniline conducting polymer for analysis of Cr (VI)”, Bull. Korean Chem. Soc. 33(4) (2012), 1247.

[2]R. Ansari, A. Fallah Delavar, A. Mohammad-khah, “A solid state Cr(VI) ion-selective electrode based on polypyrrole”, Microchimi Acta. (2012) doi: 10.1007/s00604-012-0802-9.

Activity coefficients measurement of KCl +KNO_3 +Water +Proline system by Pitzer model at T=303.2 K

Bahram Ghalami-Choobar*, Fatemeh Sayyadi-Nodehi
Department of Chemistry, Faculty of Science, University of Guilan, P.O. Box 19141, Rasht, Iran
Email:fhsayyadi@yahoo.com

Keywords: Amino acid, Electrolytes, Pitzer equation, Thermodynamic properties.

Introduction:

Thermodynamic study of (salt+amino acid+water) system is useful to understand several biochemical processes such as protein hydration, denaturation and aggregation [1]. Additionally, the presence of electrolyte solutions has great effects on the structure and properties of proteins. So, a more profound understanding of the electrolyte effect on amino acid solutions is required [2]. In this work, the thermodynamic properties of the quaternary mixed electrolyte system (KCl+KNO_3+Proline+H_2O), using the potentiometric method, are reported.

Experimental and method:

All of the potentiometric measurements were made by using a digital multimeter whose resolution was 0.1 mV. The output of the multimeter was connected to a personal computer for data acquisition. The potentiometric measurements were performed on the galvanic cells without liquid junction of the type: K–ISE / KCl (m_1), KNO_3 (m_2), (100-w%) H_2O +w% Proline / Ag-AgCl, K–ISE / KNO_3 (m1), (100-w %) H_2O +w% Proline / NO_3–ISE over total ionic strengths from 0.001 to 3.000 mol. kg^{-1} for different series of salt molal ratios r (r = m_{KCl}/m_{KNO3} =0.1, 1, 2.5, 5.0, 10.0) and pure KCl in mixed solvent system containing 5% mass fraction of proline at T=303.2 K. The PVC based potassium ion selective electrode (K-ISE) and Ag–AgCl electrode used in this work were prepared in our laboratory and had a reasonably good Nernst response.

Results and discussion:

The emf measurements of galvanic cells were performed for determination of the experimental mean activity coefficients of KCl in the mixed electrolyte solutions in accordance to the Nernst equation (1),

$$E = E^0 + s\log(\gamma_{\pm KCl} I) \qquad (1)$$

Where E^0 and s indicate the cell constant potential and the Nernstian slope, respectively. The mixed ionic interaction parameters (θ_{ClNO3}, ψ_{KClNO3}) were evaluated for the studied ternary system, according to Pitzer graphical method by using the follow equation:

$$\ln\gamma_{\pm KCl} = \ln\gamma^0_{\pm KCl} + yI[(B^{\phi}_{KNO_3} - B^{\phi}_{KCl}) + I(C^{\phi}_{KNO_3} - C^{\phi}_{KCl})] + yI\left[\theta + \left(1 - \frac{y}{2}\right)I\psi\right] \qquad (2)$$

$$\ln\gamma^0_{\pm NaCl} = f^{\gamma} + B^{\gamma}_{KCl}I + \frac{3}{2}C^{\phi}_{KCl}I^2 \qquad (3)$$

$$B^{\phi}_{MX} = \beta^{(0)}_{MX} + \beta^{(1)}_{MX}\exp(-\alpha\sqrt{I}) \qquad (4)$$

Then, the parameters obtained with the Pitzer model were used to calculate the values of the mean activity coefficients of KCl, the osmotic coefficients, and the excess Gibbs free energies for the whole series of the studied mixed electrolyte system.

Table 1: Calculated values of some of thermodynamic properties for the investigated mixed electrolyte systems at 303.2 K.

$I(mol.kg^{-1})$	$\gamma_{\pm KCl}$	□	G^E/RT	$\gamma_{\pm KNO3}$
		r=10		
0.0013	0.9667	0.9892	0.0000	0.9665
0.0101	0.9209	0.9755	-0.0012	0.9196
0.0503	0.8651	0.9628	-0.0109	0.8592
0.0998	0.8402	0.9598	-0.0270	0.8286
0.2502	0.8112	0.9606	-0.0869	0.7778
0.5008	0.7965	0.9658	-0.2042	0.7098
0.7510	0.7962	0.9748	-0.3351	0.6364
1.0012	0.8064	0.9894	-0.4769	0.5573
1.2511	0.8272	1.0108	-0.6274	0.4764
1.5014	0.8593	1.0396	-0.7851	0.3971
1.7504	0.9039	1.0760	-0.9470	0.3233
2.0003	0.9632	1.1204	-1.1126	0.2566
2.4996	1.1366	1.2331	-1.4452	0.1501

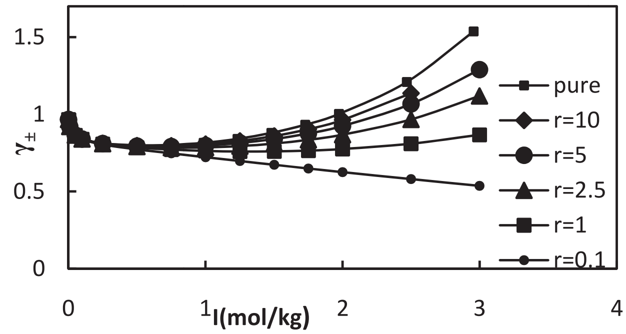

Figure 1: The plot of $\gamma_{\pm}$ vs. I at different molal ratio ($r = m_{KCl}/m_{KNO3}$) at 303.2 K.

Conclusion:

The mean activity coefficients of KCl in the KCl+KNO_3+proline+water system were determined by a potentiometric method using a solvent polymeric ion-selective membrane electrode and Ag–AgCl electrodes. We used the Pitzer ion-interaction model to get the thermodynamic properties.

References :

[1] B. Ghalami-Choobar ,S. Mirzaie, Journal of Molecular Liquids ;169, 124-129 , 2012.
[2] M. Kamali-Ardakani, H. Modarress, V. Taghikhani, M.K. Khoshkbarchi, The Journal of Chemical Thermodynamics ; 33 , 821–836, 2001 .

Kinetic study of the oxidation of epinephrine by digital simulation of cyclic voltammograms

M. Norouznia*[a] , L. Khalafi*[a], M. Rafiee[b]
[a] Department of Chemistry, Shahr-e-Qods Branch, Islamic Azad University, Tehran, Iran
[b] Department of Chemistry, Institute for Advanced Studies in Basic Sciences, Zanjan, Iran
l_Khalafi@yahoo.com

Keywords: kinetic study, epinephrine, digital simulation, cyclic voltammetry.

Introduction:

Epinephrine is one of the important catecholamine, plays a central role during physical or mental stress and also stimulates a series of actions of the sympathetic nervous system (SNS) known as the “flight or fight response” [1]. It prepares the body for action in perceived emergency situations, boosting the supply of oxygen and energy giving glucose to the brain and muscles [2]. The catechol group of epinephrine can be oxidized chemically or electrochemically to its *o*-benzoquinones as a good Michael acceptor that can be attacked by side chain amine group as nucleophile via an intramolecular addition reaction. Although the chemical or electrochemical oxidation path-way of catecholamines are well known, the kinetics of their cyclization reactions has been little investigated [3].

Materials and methods:

All experiments were performed with analytical reagent grade chemicals purchased from E. Merck. These chemicals were used without further purification. The stock solutions of epinephrine was prepared fresh daily by dissolving the compound in distilled water. The 0.15 M buffered solutions were prepared based on Kolthoff tables. The homogeneous rate constants were estimated by analyzing the cyclic voltammetric responses using the simulation CVSIM software.

Apparatus:

Cyclic voltammetry was performed using a Behpajoh Model BHP 2061-C potentiostat/ galvanostat. In the voltammetry experiments a glassy carbon disc (2 mm diameter) and a platinum wire were used as working and counter electrodes, respectively. The working electrode potentials were measured versus Ag/AgCl (KCl 3.0 M), all electrodes from AZAR electrode.

Result and discussion:

The results indicate the participation of the oxidation product of epinephrine in intramolecular cyclization reaction to form the corresponding H-indole derivatives. The oxidation potential of this product is less than epinephrine and it undergoes electron transfer at the electrode surface and its cyclic voltammograms show two independent redox couple. One of them is related to the redox reaction of epinephrine and the other, with less half-wave potential, is due to electron transfer of product. The anodic to cathodic peak current ratio and the ratio of reactant to product at various scan rates of cyclic voltammograms is good for the study of kinetic parameters of reaction. For more detailed the cyclization rate constants (k_{cyc}) were estimated by digital simulation of cyclic voltammograms based on proposed ECE mechanism. The results show that the cyclization reaction has considerable rate constants, and the reactivity, or observed rate constants, increases drastically from the pH values 4.0 to 8.0 which is related to deprotonation of ammonium group.

Conclusion:

The results of this work show that epinephrine is oxidized in water to its respective *o*-quinone the quinone is then attacked by the side chain amine group to form cyclized *o*-quinone derivative. The results shows that the anodic to cathodic peak current ratio, the reactivity, increases drastically from the pH values 4 to 6 and after that decrease slightly. The cyclic voltammograms were digitally simulated under ECE mechanism and the rate constant of reaction were obtained at various pH values considering the microscopic acidic dissociation constant of ammonium groups. There is a good agreement between the simulated voltammograms with those obtained experimentally.

References:

[1] D.L. Wong etal.;" Adrenergic Responses to Stress: Transcriptional and Post-transcriptional changes"; Acad. Sci.; 1148, 249-56, 2008

[2] M.G. Clark etal.;" Vascular and endocrine control of muscle metabolism"; Am. J. Physiol. Endocrinol. Metab.; 268,797-812, 1995.

[3]X. Liu etal.;" Spectroelectrochemical and Voltammetric Studies of L-DOPA" Electroanalysis; 15, 103-107, 2003.

Kinetic study of the oxidation of dopamine in the presence of aromatic amines

M. Khoshnam*[a] , L. Khalafi*[a], M. Rafiee[b]
[a] Department of Chemistry, Shahr-e-Qods Branch, Islamic Azad University, Tehran, Iran
[b] Department of Chemistry, Institute for Advanced Studies in Basic Sciences, Zanjan, Iran
l_Khalafi@yahoo.com

Keywords: cyclic voltammetry, digital simulation, dopamine, kinetic study.

Introduction:

Dopamine (4-(2-aminoethyl) benzene-1,2-diol (DA)) is a naturally occurring biogenic catecholamine formed by the decarboxylation of 3,4-dihydroxyphenylalanine and is a precursor to epinephrine and nor-epinephrine in a biosynthetic pathway [1]. It functions as a neurotransmitter in the central and peripheral nervous systems. Insufficient DA concentration due to the loss of DA-producing cells may lead to a disease called Parkinson's disease [2]. Dopamine can be oxidized chemically or electrochemically to its *o*-quinone derivative that are quite reactive and can undergoes Michael addition reactions by its side chain amine group or suitable nucleophiles which known as intra and intermolecular reactions respectively .

Materials and methods:

Dopamine, aniline, 4-methylaniline, 4-aminobenzoic acid, and 4-nitroaniline were reagent-grade materials; from E. Merck, respectively. These chemicals were used without further purification. The stock solutions of these compounds were prepared fresh daily by dissolving them in distilled water. Samples were prepared by taking the appropriate aliquots from the stock solutions followed by dilution with buffer solutions. The homogeneous rate constants were estimated by analyzing the cyclic voltammetric responses using the simulation CVSIM software.

Apparatus:

Cyclic voltammetry was performed using a Behpajoh Model BHP 2061-C potentiostat/galvanostat. In the voltammetry experiments a glassy carbon disc (2 mm diameter) and a platinum wire were used as working and counter electrodes, respectively.

The working electrode potentials were measured versus Ag/AgCl (KCl 3.0 M), all electrodes from AZAR electrode.

Result and discussion:

The reactions of electrochemically generated *o*-quinones, as Michael acceptors, from oxidation of dopamine in the presence of various aromatic amines with electron donating and withdrawing substituent as nucleophiles have been studied using cyclic voltammetry. The reaction mechanism is an ECE mechanism which has been supported by some diagnostic criteria of cyclic voltammetry at various scan rates. The competition between intramolecular and intermolecular Michael addition reaction were studied as a function of pH in the presence of various aniline derivatives (aniline, 4-methylaniline, 4-aminobenzoic acid, and 4-nitroaniline). The observed homogeneous rate constants (k_{obs}) for reactions were estimated by comparing the experimental voltammetric responses with the digitally simulated results. The effects of substituted group of aniline derivatives on interplay between inter and intramolecular reactions, their rate constants or reactivity and half-wave potential of final products were studied quantitatively.

Conclusion:

The results show that despite of presence of amine group on dopamine and possibility of intramolecular Michael addition, the nucleophilic addition of aromatic amines are the dominant reaction at mild acidic conditions. This is related to lower basicity of aniline derivative and their deprotonation at mild acidic conditions. The aniline derivatives with electron withdrawing character has less reactivity and rate constant, but they shows a good reactivity at more acidic conditions considering their less basicity. Also the scheme for the electrochemical oxidation of dopamine in the presence of aniline derivatives is proposed and tested by digital simulation. Based on an ECE mechanism, the observed homogeneous rate constants (k_{obs}) of Michael addition reaction have been estimated by comparison of the simulated results with experimental cyclic voltammograms at various pHs. The simulated cyclic voltammograms show good agreement with those obtained experimentally.

References:

[1]M.M.Karim etal; "Spectrofluorimetric estimation of norepinephrine using ethylenediamine condensation method"; J. Fluoresc.; 17, 427-436, 2007.

[2] S.Y. Yi etal;" Resolution of dopamine and ascorbic acid using nickel(II) complex polymer-modified electrodes"; J. Electro. Anal. Chem.; 602, 217-225, 2007.

Conductive Polymeric *meso*-tetra(p-carboxyphenyl)Porphyrin Film electrode for Trace Determination of Nickel

M. Jafarian*, M.A. Haghighatbin
Department of Chemistry, K.N. Toosi University of Technology
P.O. Box 15875-4416, Tehran, Iran
E-mail address: mjafarian@kntu.ac.ir (M. Jafarian)

Keywords: meso –tetra (p-carboxyphenyl) porphyrinato nickel(II), Modified electrode, Electropolymerization, Trace determination

Introduction:

Chemically modified electrodes for trace analysis have been a subject of researches for decades due to their advantage of selectivity coupled with the sensitivity enhancement of preconcentration. The preconcentration, which has a purely chemical rather than electrochemical mechanism, can be effected by covalent linkage [1], ion exchange [2] or complex formation reactions [3]. Therefore, selectivity is determined by the chemical reactivity of the electrode modifying agents rather than the redox potential of the analyte. Ni (II) is an essential metal that occurs at trace concentration levels in physiological and environmental systems. However, it's quite negative reduction potential, -1.2 V *vs* SCE [4], and propensity to form intermetallic compounds with other metallic species codeposited result in complex, matrix- dependent stripping patterns not suited for quantitation [5]. Therefore, development of electrodes with selective analyte collection properties is seems to be appropriate for trace level analysis of this metal.

Materials and methods:

Meso-tetra (4-carboxyphenyl) porphyrin (TCPP) and *meso*-tetra (4-carboxyphenyl) porphyrinato nickel (II) (NiTCPP) were synthesized and purified according to a procedure described previously [6].

Electrochemical studies were carried out in a conventional three-electrode cell powered by an electrochemical system comprising of EG&G model 273 potentiostat/galvanostat. Glassy carbon (GC) electrode (from Metrohm Ω) with the geometric area of 0.0314 Cm^2 was used as the substrate electrode.

Results and Discussion:

Stable polymer film electrodes were formed from *meso*-tetra(p-carboxyphenyl)Porphyrinato Nickel (II) using Cyclic Voltammetry(CV) (Fig.1). The nickel-porphyrin polymer films efficiently demetalated in acidic media at pH 1. Electrodes were placed in sample solution to preconcentrate Ni (II) and transferred to a blank electrolysis solution where the signal due to the Ni (II)/Ni (III) oxidation in the film was observed by Square Wave Voltammetry (SWV) (Fig.2). A detection limit of $3.2 \times 10^{-8} M$ was obtained for a 90 seconds exposure to the sample solution.

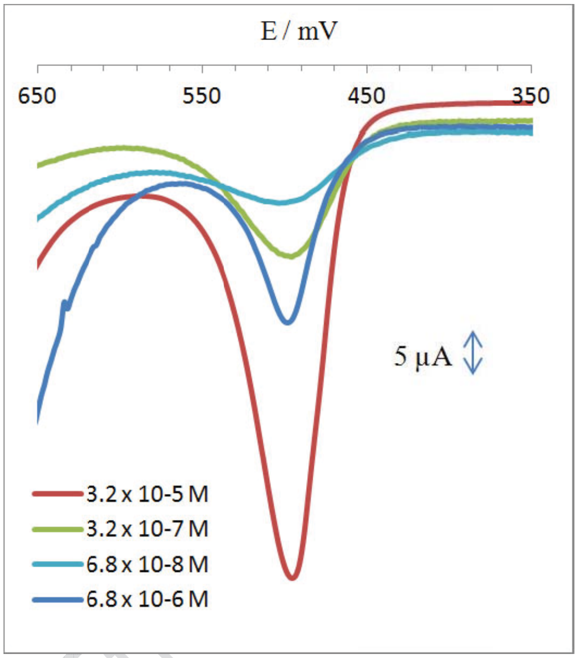

Figure 2

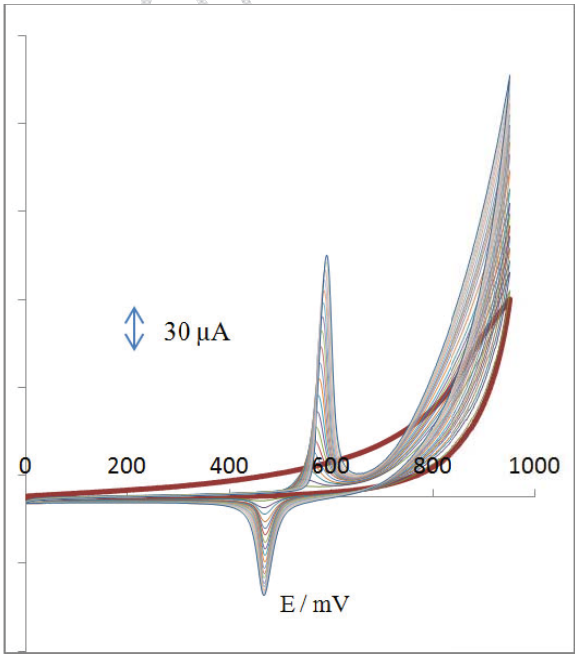

Figure 1

Conclusion:

Electrodes modified with electropolymerized porphyrin, which can be used as amperometric sensors, were easily and controllably formed and they were stable for long-time operations. The demetalated film could be regenerated with exposure to acid and reused for chemical preconcentration. In interference studies, a 10-fold excess of Co resulted in partial suppression of the Ni (II) signal, but no new signals were observed. Similar concentrations of cations of Zn, Cd, Pb, Cu and Fe did not appreciably influence the Ni (II) response.

References :

[1] Price, J. F.; Baldwin, R. P. Anal. Chem. 2003, 52, pp. 1940-1944.
[2] Cox, J. A,; Kuleska, P. J. Anal. Chim. Acta 2005, 154, pp. 71-78.
[3] Guadalupe, A. R.; Abruna, H. D. Anal. Chem. 2001, 57, pp. 142-149.
[4]Vydra, F.; Stulik, K.; Julakova, E. Electrochemical Stripping Analysis ; England, 1999 3rd Ed.
[5]Brainina, Kh 2. Stripping Voffammetry in Chemical Analysis: Wiley: New York, 2004.
[6] R.F. Pasternack, L. Francesconi, D. Raff, E. Spiro, Inorg. Chem. 1993,12, 2606–2611.

Kinetic study of electrochemical generation of diphenylamine derivatives of catechol

M. Shahbak*[a] , L. Khalafi*[a], M. Rafiee [b]

[a] Department of Chemistry, Shahr-e-Qods Branch, Islamic Azad University, Tehran, Iran
[b] Department of Chemistry, Institute for Advanced Studies in Basic Sciences, Zanjan, Iran
l_Khalafi@yahoo.com

Keywords: N-methylaniline, catechol, diphenylamine, voltammetry, digital simulation

Introduction:

Catechol is one of the common building blocks in organic synthesis and is produced in industrial scales as the precursor of pesticides, perfumes and pharmaceuticals. The most well-known characteristic of the catechols is that they can be easily oxidized mainly due to their antioxidant activity and low oxidation potentials [1]. The products of oxidation are the corresponding reactive and electron-deficient *o*-quinones. Considering their instability they can be produced only by in-situ methods and mild oxidation of catechols. One of the most successful in-situ generations of reactive *o*-quinones species is the electrochemical oxidation. [2] The Michal additions of aliphatic, aromatic, and benzylic amines to electrochemically generated *o*-quinone have been reported previously. The reaction products of aromatic amines with o-quinones have been reported to be diphenylamine derivatives or their related quinonic forms. Diphenylamine is a parent compound of many derivatives, which are used for the production of dyes, perfumery, pharmaceuticals, photography chemicals and further small-scale applications [3].

Materials and methods:

Catechol, 4-methylcatechol and N-methylaniline, reagent-grade, were prepared from Aldrich and used as received. All other chemicals were of proanalysis grade from E. Merck. These chemicals were used without further purification. The stock solution of catechols and N-methylaniline were prepared daily.

Apparatus:

Cyclic voltammetry and controlled-potential coulometry were performed using a Micro-Autolab model PGSTAT 10 potentiostat/ galvanostat. In the voltammetry experiments a glassy carbon disc (1.8mm diameter) and a platinum wire were used as working and counter electrodes, respectively. The working electrode potentials were measured versus an Ag/AgCl references electrode (all electrodes from AZAR electrode, Urmia, Iran). The homogeneous rate constants were estimated by analyzing the cyclic voltammetric responses using the CVSIM simulation software.

Result and discussion:

The reactions of electrochemically generated *o*-quinones from oxidation of catechol and 4-methylcatechol as Michael acceptors with N-methylaniline as nucleophile have been studied using cyclic voltammetry. Voltammetric responses show that oxidation of catechols followed by Michael addition of N-methylaniline. The reaction products are believed to be diphenylamine derivatives of catechols that undergo electron transfer at more negative potentials than the catechols. The observed homogeneous rate constants (k_{obs}) for Michael addition were estimated by digital simulation and show that the reactivity of 4-methyluinone is considerably less than o-quinone. The oxidation potentials of the desired products are drastically depend on the solution pH and their structures.

Conclusion:

The results of this work show that the reactivities of the quinones that derived from oxidation of catechol and 4-methylcatechol have been compared based on voltammetric studies and digital simulation. Their results show that the reactivity of 4-methylquinone is considerably less than *o*-quinone. This is related to the steric effect of methyl group and occupation of one positions of catechol with the methyl group that reduced the probability of reaction by half. Also the oxidation potentials of the desired products are drastically depend on the solution pH, same as catechols, and their structures. Presence of methyl group on diphenylamine structure forced it to the out of plane conformation that diminishes the possibility of resonance and electron donating possibility.

References:

[1] R.H. Bisby etal; " Effect of antioxidant potential in the oxygen radical absorption capacity (ORAC) assay" Food Chemistry; 108, 1002-1007, 2008.

[2] M. Rafiee ; "The Electron: The Simplest Chemical Reagent"; Synlett; 3, 503-504, 2007.

[3]O. Drzyzga, "Diphenylamine and derivatives in the environment: a review"; Chemosphere; 53, 809-818, 2003.

Application of Ozone-electrolysis method for treatment of Reactive Orange7 in aqueous media by using Ti/Sb-SnO_2 anode

Jalal Basiriparsa* , Zohreh Meratifashi
Department of applied chemistry, Bu-Ali sina university, Hamedan, Iran

Key words: Ozone-electrolysis, Treatment, Reactive Orange7, Ti/Sb-SnO_2 anode

Introduction

Textile wastewater is characterized by strong color, large amount of suspended solids, broadly fluctuating pH, high chemical oxygen demand (COD), bio toxicity and causes coloring of the receiving water environment. Although dyes constitute only a small portion of the total volume of wastes discharge in textile processing, but because of the chemical stability of these pollutants, they are not readily removed by traditional methods.

In recent years, a wide range of alternative technologies so called advanced oxidation processes (AOPs), are considered to be promising methods for the treatment of hazardous toxic organic pollutants in wastewaters. AOPs have emerged as potentially powerful methods that are capable of transforming the pollutants into harmless substances. Their oxidation mechanisms rely on the generation of very reactive free radicals, such as the hydroxyl radicals (OH°).

Common AOPs could be broadly classified in to ozone, ozone/UV, ozone/H_2O_2, ozone/UV/H_2O_2, photo catalysis, Fenton's process and ozone/electrolysis.

Some advantages of ozone-electrolysis are that: 1) Possibility of operation at room temperature and atmospheric pressure; 2) The process only requires electrical energy supply to be carried on and produce strong oxidants; 3) This process do not produce secondary pollutants.

Experimental (material and method):

An azo dye RO7, was selected as model solution, which was commercial dye and used without further purification. This azo dye was provided by alavan sabet company (Hamedan).

Other chemicals, purchased from Merck, were of analytical grade. All solutions were prepared by using deionized water.

Ozone gas produced from air by ozone generator (Onnic.ES215A). In all experiments, the samples of RO7 was taken periodically from the reactor and analyzed by the UV-visible spectrophotometer (JASCO. v- 630) via the decrease in absorbance at 480 (nm). COD measurements were also carried out to investigate the mineralization of the solution, according to a close reflux, colorimetric method using a HACH DR 2800 spectrophotometer.

Results and discussion:

Response surface methodology (RSM) was employed for experimental design, modeling and parameter optimization. Accordingly reduced quadratic model was developed to give the substrate color removal efficiency percentage, (CE%) as function of effective parameters such as: initial pollutant concentration, initial pH of the solution, electrolyte concentration and Current density.

Maximum color removal efficiency was achieved at the obtained conditions of: C_{dye}= 60 ppm, pH=4, C_{NaCl}=3.5 g/l, I=19 mA/cm^2 after 2.5 minute.

In optimum conditions, COD was investigated and COD reduced to 100% after 90 minute.

Maximum efficiency in the process was obtained in acidic conditions and high current density. because hypochlorous acid which is the most species in the solution has higher oxidation potential than hypochlorite ion. At low current density, the performance would be cost effective but need long treatment time, while at high current density it was of high efficiency but costly. The energy consumption decreased with the increase of salt concentration.

Conclusions:

Ozonation combined with electrolysis was used to remove color from dye solutions containing C.I Reactive Orange 7 by using Ti/Sb-Sno2 Coated on Ti as anode and a stainless steel as cathode. The effect of operation parameters on color removal efficiency was investigated and optimized by using RSM. The removal of efficiency of RO7 and COD of the aqueous solution in pH=4, initial dye concentration 60ppm, electrolyte concentration 3.5g/l, current density 19mA/cm^2 were 97.87 and 90 respectively.

Reference:

[1] N.Kishimoto and etal. Ozonation combined with electrolysis of 1,4-dioxane using a two-compartment electrolytic flow cell with solid electrolyte . water research 42, 379 – 385, 2008.

[2] K. Jiang-tao1 and etal. Effect of Sb dopant amount on the structure and electrocatalytic capability ofTi/Sb-SnO2 electrodes in the oxidation of 4-chlorophenol. Journal of environmental sciences 19,1380 –1386, 2007.

Thermodynamic study of the ternary (EMImCl+HCONH$_2$+H$_2$O) electrolyte system based on potentiometric method

Bahram Ghalami-Choobar*, Maryam Shekofteh-Gohari
Department of Chemistry, Faculty of Science, University of Guilan, Rasht, Iran
(Email: gohar2027@yahoo.com)

Key words: Activity coefficient, Potentiometric, Pitzer model, ionic liquid

Introduction:

Recently, ionic liquids due to some green characteristics are of crucial importance. The presence of ionic liquids (ILs) in different processes needs a deeper knowledge about the nonideality of these mixtures, essentially about their thermodynamic behavior [1].Up to now, the general methods such as the isopiestic vapor pressure , gas–liquid chromatography conductmetric and volumetric techniques have been used to measure the thermodynamic properties of mixtures containing ionic liquids [2] .In this work for the first time, the results relating to the thermodynamic properties of ([EMIM]Cl+HCONH$_2$+H$_2$O) system using the potentiometric method are reported. The potentiometric measurements were performed in various formamide-water mixed solvent systems containing 0,10,20,30 and,40 mass fractions of formamide over ionic strength ranging from 0.0025 to 2.2 mol.kg^{-1} at T=298.2K.

Experimental and Methods:

All of the potentiometric measurements were carried out using digital multimeter (Martini instruments Mi180) whose resolution was 0.1 mV. We used the PVC based EMIm ion selective electrode (EMIm-ISE) and Ag-AgCl electrode which were prepared in our laboratory. The mean activity coefficients for [EMIm]Cl in the mixed solvent (formamide-water) were determined from the emf measurements using the galvanic cell (A) in accoeding to equation (1)

Ag|AgCl|(EMIm)Cl(m), formamide (w%), water(1-w)%| EMIm-ISE (A)

$$E_A = E^\circ + s\log(I\gamma_\pm) \qquad (1)$$

Results and discussion:

The modeling of this ternary system was made based on the Pitzer ion-interaction model. According to the Pitzer model, the mean activity coefficient for [EMIMm]Cl in the ternary mixed solvent electrolyte ([EMIm]Cl +$HCONH_2$+ H_2O) system is written as:

$$ln\gamma_{\pm IL} = f^{\gamma} + B_{IL}^{\gamma} I + 1.5 C_{IL}^{\phi} I^2 \qquad (2)$$

$$f^{\gamma} = -A_{\phi}[\frac{\sqrt{I}}{1+b\sqrt{I}} + \left(\frac{2}{b}\right) ln\left(1 + b\sqrt{I}\right) \qquad (3)$$

$$B_{IL}^{\Upsilon} = 2\beta_{IL}^{(0)} + \frac{2\beta_{IL}^{(1)}}{\alpha^2 I}\left[1 - \left(1 + \alpha\sqrt{I} - \frac{\alpha^2 I}{2}\right) e^{-\alpha\sqrt{I}}\right] \qquad (4)$$

The Pitzer ion -interaction parameters together with E^0 and s were determined by combining Equations.1and 2 by an iteration minimization procedure employing the Microsoft Excel (solver) program (table 1). Figure 1 shows the mean activity coefficient of [EMIm]Cl versus the ionic strength..

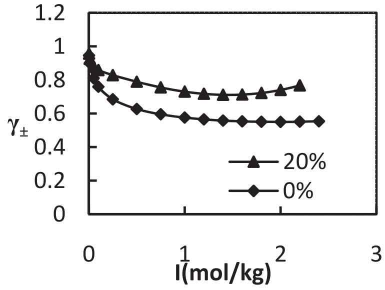

Figure1. The γ [EMIm]Cl versus I for 0 and 20 mass fraction of formamide .

Table1. the Pitzer parameters obtained

wt%	β⁽⁰	β^(1)	C^ø
	kg .mol⁻¹	kg .mol⁻¹	kg². mol⁻²
0	0.02892	0.15648	0.01705
20	-0.19289	1.20032	0.10004

Conclusions:

The mean activity coefficients of [EMIm]Cl in the [EMIm]Cl + formamide + water system were determined by a potentiometric method using a solvent polymeric ion-selective membrane electrode and Ag-AgCl electrodes at temperature 298.2 K. . It can be concluded that the Pitzer ion-interaction model satisfactory describes the system under investigated.

References:

[1] Gumez.E, Calvar.N,Dominguez.A,Macedo.E.A, J. Chem. Thermodynamics 43(2011) 908-913

[2] Ghalami-Choobar.B,Mirzaie.S, J. Molecular liquid 169(2012) 124-129.

Thermodynamic study of ternary [NaCl+Na_2HPO_4+H_2O] electrolyte system

Bahram Ghalami-Choobar*, Parya Mossayyebzadeh-Shalkoohi
Department of Chemistry, Faculty of Science, University of Guilan, Rasht, Iran
(Email: Parya.Mosayebzadeh@yahoo.com)

Key words: Activity coefficient, EMF, Pitzer model, Na_2HPO_4, NaCl

Introduction:

Recently, there has been an increasing amount of work concerning the investigation of the thermodynamic properties of mixed aqueous electrolyte solutions because of their importance in areas such as chemistry [1-2]. The solutions of sodium or potassium dihydrogen and hydrogen phosphates have been used extensively as standard buffer solutions for pH measurements. In the face of their importance, study of the thermodynamic properties on the most aqueous mixtures of these phosphate salts especially at higher molalities has not been performed [3]. In the present study, the results relating to the thermodynamic properties for the ternary mixture of (NaCl + Na_2HPO_4 +H_2O) over total ionic strengths from 0.0130 to 4.000 mol. kg^{-1} for different series of salt molal ratios r (r = m_{NaCl} /$m_{Na2HPO4}$=2.5, 5.0, 7.5, 10.0) and pure NaCl in aqeous system at T= 298.2K are reported.

Experimental and Methods:

All of the potentiometric measurements were made using a digital multimeter (Martini instruments Mi180) whose resolution was 0.1 mV. Potentiometric measurements were performed using the PVC based sodium ion selective electrode (Na-ISE) and Ag–AgCl electrode which were prepared in our laboratory. The Pitzer ion interaction model was used for the experimental data correlation and calculation of thermodynamic properties for mixed electrolyte solutions. According to the Pitzer model, the mean activity coefficient for NaCl in the ternary mixed electrolyte (NaCl+ Na_2HPO_4+ H_2O) system is written as:

$$\ln \gamma_{NaCl} = F + 2m_A\beta_A^0 + 2m_A\beta_A^1 \times \frac{1}{2I}\left[1-\left(1+2\sqrt{I}\right)\exp\left(-2\sqrt{I}\right)\right] + 2m_B\beta_A^0 + 2m_B\beta_A^1 \times \frac{1}{2I}\left[1-\left(1+2\sqrt{I}\right)\exp\left(-2\sqrt{I}\right)\right] + m_B\beta_B^0 + m_B\beta_B^1 \times \frac{1}{2I}\left[1-\left(1+2\sqrt{I}\right)\exp\left(-2\sqrt{I}\right)\right] + (1.5m_A^2 + 4m_Am_B + 2m_B^2)C_A^{\phi} + \frac{\sqrt{2}}{2}(m_Am_B + 2m_B^2)C_B^{\phi} + m_B\theta + (m_Am_B + m_B^2)\psi$$

Results and discussion:

The mean activity coefficients for NaCl in ternary mixed electrolyte ($NaCl + Na_2HPO_4 + H_2O$) system with different series of salt molal ratios r ($r = m_{NaCl} / m_{Na_2HPO_4} = 2.5, 5.0, 7.5, 10.0$) were determined from the emf measurments using the galvanic cell [Ag|AgCl|NaCl(m_1), Na_2HPO_4 (m_2), H_2O| Na-ISE]. The emf of this cell can be represented as the Nernst equation:

$$E = E^0 + s\log(\gamma_{\pm} I)$$

Figure 1 shows the mean activity coefficient of NaCl versus the ionic strength. It can be seen that the mean activity coefficient is reduced with increasing the molality fraction of NaCl in solution when the ionic strength of the electrolyte is fixed. The mixed ionic interaction parameters ($\boldsymbol{\theta}_{\mathbf{Cl}HPO4}$, $\boldsymbol{\psi}_{\mathbf{NaCl}HPO4}$) were evaluated for the studied ternary system, according to Pitzer graphical method(table 1).

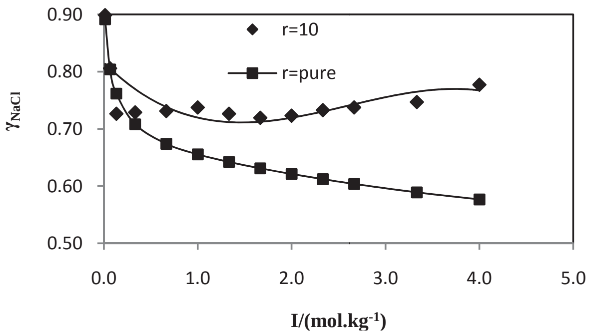

Fig 1. The γ_{NaCl} versus the ionic strength for r = 10 and pure

Table 1. Pitzer mixing parameters obtained

r	θ (kg.mol^{-1})	ψ(kg^2.mol^{-2})
10	0.2097	-0.0662

Conclusions:

The mixing Pitzer parameters θ_{ClHPO4}, $\psi_{NaClHPO4}$ were determined for this system. The Pitzer parameters obtained were used for the calculation of the other thermodynamic properties such as the osmotic coefficients, the activity coefficients of Na2HPO4 and the excess Gibbs free energy. It was seen that the Pitzer model can be used to analyze this system successfully.

References:

[1] B.Ghalami-Choobar, F. Sayyadi-Nodehi; Thermodynamic study of the quaternary electrolyte ($NaCl + NaNO_3 + HCONH_2 + H_2O$); J. Chemical Thermodynamics, 49, 104-113, 2012.

[2] B. Ghalami-Choobar; Thermodynamic study of the ternary mixed electrolyte (NaCl+NiCl2+H2O)system: J. Chemical Thermodynamics ,43, (2011), 901–907.

[3] D. Zˇ . Popovic´ , J. Miladinovic´ , M. D. Todorovic´ , M. M. Zrilic´,J. A. Rard; Isopiestic determination of the osmotic and activity coefficients of the {yKCl + (1 - y)K2HPO4}(aq) system at T = 298.15 , J. Chemical Thermodynamics, 43, (2011), 1877–1885.

Potentiometric investigation of pyridine-2,6-dicarboxylic acid and chelidamic acid - 2,9-Dimethyl-1,10-Phenanthroline complexes with some metal ions and comparing with solid state results

A. Shokrollahi*, M. Shahryari
Department of chemistry, Yasouj University, Yasouj,75918-74831,Iran
Email: ashokrollahi@mail.yu.ac.ir

Key words: Zinc, Cobalt, Pyridine-2,6-dicarboxylic acid, 2,9-Dimethyl-1,10-phenanthroline, Chelidamic acid.

Introduction:

The protonation constants of chelidamic acid(chel), Pyridine-2,6-dicarboxylic acid(pydc) and 2,9-Dimethyl-1,10-Phenanthroline(dmp), in all of the probability protonated forms, the equilibrium constants for the chel-dmp and pydc-dmp proton transfer system and the stoichiometry and stability constant of the complexation of this system with Co^{2+}, Zn^{2+} in aqueous solution were investigated by potentiometric *pH* titration method. The stoichiometry of the most complex species in solution were compared with corresponding crystalline metal ion complexes.

Materials and methods:

The concentrations of chel(L'), pydc(L) and dmp(Q) was 2.50 $\times 10^{-3}$ M, for the potentiometric pH titrations of them in the absence and presence of 1.25 9 10^{-3} M of metal ions in binary and Co-pydc-dmp ternary systems. In Zn-chel-dmp ternary system the concentration of dmp, chel and metal ion was 2.22×10^{-3} M, and 1.11×10^{-3} M respectively. A standard carbonate-free NaOH solution (0.095 M) was used in all titrations. Before an experimental point (pH) was measured, sufficient time was allowed for the establishment of equilibrium. Ligands' protonation constants and stability constants of proton-transfer systems and their complexes with the metal ion were evaluated using the BEST programand the corresponding distribution diagrams were depicted using Hyss2009 program as a new of older version. The value of autoprotolysis constant ($Kw = [H^+][OH^-]$) was calculated according to literature.

Apparatus:

A Model 794 Metrohm Basic Titrino was attached to an extension combined glass-calomel electrode mounted in an air-protected, sealed, thermostated jacketed cell maintained at 25.0 ± 0.1 °C by circulating water, from a constant-temperature bath Fisherbrand model FBH604, LAUDA, Germany, equipped with a stirrer and a 10.000-mL-capacity Metrohm piston burette. The *p*H meter-electrode system was calibrated to read -log $[H^+]$.

Result and discussion:

The determination of the equilibrium constants for the proton-transfer interactions between pydc or chel and dmp (1:1 molar ratio) in aqueous solution were reported previously by our researcher group[1,2]. The cumulative stability constants of the species $M_mL_lQ_qH_h$, (β_{mlqh}) as defined in our previous publications, [M = Zn^{2+}, Co^{2+}; L = pydc or chel; Q = dmp, H = proton, respectively, and m, l, q, and h are the respective stoichiometric coefficients] were calculated from the potentiometric pH titration curves using the BEST program in order to evaluate the most likely complex species in solution. These results and our previous reports revealed that, Zn^{2+} and Co^{2+} ions interacted relatively strong with chel alone and chel-dmp system while Co^{2+} and Ni^{2+} ions form relatively weak complexes with dmp alone and interaction of Zn^{2+} with it is considerable. The interaction of Ni^{2+} and Co^{2+} ions with pydc and pydc-dmp is conciderable.

Conclusion:

It is interesting to note that the stoichiometries of the some of the most abundant ternary complexes such as ZnL'Q, ZnL'QH,CoL_2 existing in solution, are very similar to those reported for the corresponding isolated complexes in the solid state.

Reference:

[1] J. Soleimannejad, H. Aghabozorg, M. Nasibipour, S. Najafi, F. Manteghi, A. Shokrollahi, E. Karami and M. Shamsipur, J. Iran. Chem. Soc., 9(2012) 415.

[2] H. Aghabozorg, E. Sadr-khanlou, A. Shokrollahi, M. Ghaedi and M. Shamsipur, J. Iran. Chem. Soc., 6(2009) 55.

Ni^{2+} and UO_2^{2+} ions ,Potentiometric study of complexation between Zn^{2+} with chel-aacr proton transfer and comparing with solid state results

B. Shokrollahi[*], M. Shahryari
Department of chemistry, Yasouj University, Yasouj,75918-74831, Iran
Email: ashokrollahi@mail.yu.ac.ir

Key words: Nickel(II), Zinc(II) and Uranium(VI), 9-Aminoacridine, Chelidamic acid.

Introduction:

The protonation constants of chelidamic acid(chel) and 9-Aminoacridine (aacr), in all of the probability protonated forms, the equilibrium constants for the chel-aacr proton transfer system and the stoichiometry and stability constant of the complexation of this system with UO_2^{2+}, $Zn^{2+}$and Ni^{2+} ions in 50% dioxane-50% water (V/V) solvent were investigated by potentiometric *pH* titration method. The stoichiometry of the most complex species in solution were compared with corresponding crystalline metal ion complexes.

Materials and methods:

For the potentiometric *p*H titrations of chel, aacr and chel-aacr in the absence and presence of 1.43×10^{-3}M metal ions The concentration of chel and aacr was set as 2.86×10^{-3} M for metal ion respectively. A standard carbonate-free NaOH solution (0.09566 M) was used in all titrations. The ionic strength was adjusted to 0.1 M with $NaClO_4$. Before measuring the experimental point (*p*H), for the establishment of the equilibrium sufficient time was undergone. Protonation constants of ligand and stability constants of proton transfer and their metal complexes were evaluated using the BEST program[1] and the corresponding distribution diagrams were depicted using Hyss2009 as a new version of older of this program [2]. The value of autoprotolysis constant for 50% dioxane-50% water (V/V) solvent ($K_w= [H^+][OH^-]$) was calculated according to literature [1].

Apparatus:

A Model 794 Metrohm Basic Titrino was attached to an extension combined glass-calomel electrode mounted in an air-protected, sealed, thermostated jacketed cell maintained at 25.0 ±

0.1 °C by circulating water, from a constant-temperature bath Fisherbrand model FBH604, LAUDA, Germany, equipped with a stirrer and a 10.000-mL-capacity Metrohm piston burette. The *p*H meter-electrode system was calibrated to read -log [H^+].

Result and discussion:

In order to evaluate the stoichiometry and stability of Zn^{2+}, Ni^{2+} and UO_2^{2+} complexes with hypydc-aacr association in a 50% dioxane-50% water (V/V) solvent, the equilibrium potentiometric *p*H titration profiles of hypydc, aacr and their 1:1 mixture were obtained in the absence and presence of Zn^{2+} Ni^{2+}, and UO_2^{2+} ions. The potentiometric titration curve of hypydc and hypydc-aacr was depressed considerably in the presence of UO_2^{2+}, Ni^{2+} and Zn^{2+} ions while obtained divergence for aacr-UO_2 is relative considerable and for aacr-Ni and aacr-Zn is week

The potentiometric *pH* titration curves of chel, aacr and their corresponding 1:1 mixture in the presence of Zn^{2+} Ni^{2+}, and UO_2^{2+} ions were fitted to the BEST program in order to evaluate cumulative stability constants of the likely complex species in solution.

Conclusion:

It is interesting to note that the stoichiometries of the some of the most abundant ternary complexes such as $ZnL_2Q_2H_4$, $NiL_2Q_2H_4$ and $UO_2L_2Q_2H_4$ existing in solution, are very similar to those reported for the corresponding isolated complexes in the solid state.

Reference:

[1]Martell, A. E.; Motekaitis, R. J. Determination and Use of Stability Constants, 2nd ed., VCH, New York, 1992.

[2] L. Alderighi, P. Gans, A. Ienco, D. Peters, A. Sabantini,A. Vacca, Coord. Chem. Rev. 184 (1999) 311.

Tetrazole derivatives as effective inhibitors for the corrosion of steel in 0.5 M H_2SO_4 solution

Ladan Edjlali*, Roghayeh Sadeghzadeh, Hossein Babazadeh, Parasto farsh foroush.
Department of Applied Chemistry, Faculty of Science, Islamic Azad University, Tabriz Branch, P.O.Box 1655, Tabriz, Iran
E-Mail:r.sadeghzadeh2010@yahoo.com, ladan_ejlali@yahoo.com

Key words: tetrazole, inhibitor, steel, corrosion, electrochemical polarization.

Corrosive solutions in the acidic tetrazole are more and more encountered in industry [1]. The importance of inhibitive protection in acidic solutions is increased by the fact that steels which are more susceptible to be attacked in aggressive media, are the commonly exposed metals in industrial environments. It is shown that the protective propertiesof tetrazole derivatives depend upon their ability to reduce corrosion rate and are enhanced at higher electron densities around the nitrogen atoms. Numerous works have been devoted to the corrosion inhibiting effect of aqueous soluble tetrazole on metallic materials [2].The effect of organic nitrogen compounds on the corrosion behaviour of metallic materials in aggressive solutions has been well documented [3–7]. Their choice is based on their low-cost and stability as corrosion inhibitors for metallic materials in acidic media. The most synthesised compounds are the nitrogen heterocyclic compounds, which are very known to be excellent complex or chelate formingsubstances witht metals of transition series. Their adsorption is generally explained by the formation of an adherent film on the metal surface [7-8]. The percentage inhibition efficiency was found to increase with increasing concentration of inhibitor to reach 96% at 10^{-3} M. This compound is efficient inhibitor.In the present work, we investigate the corrosion of steel in 0.5M H2SO4 by some newly synthesised tetrazole compounds. The effect of addition of tetrazole derivatives on the corrosion of steel in 0.5M H2SO4 solution is studied using weight loss measurements, electrochemical polarisation methods. This study permits to follow the evolution of the inhibitive effect of tetrazole derivatives on steel in 0.5M H2SO4. Polarisation measurements show that the tetrazole act as mixed inhibitors. The cathodic curvesindicate that the reduction of proton at the steel surface happens within a pure activating mechanism. We note a good agreement between gravimetric, electrochemical polarisationand methods.

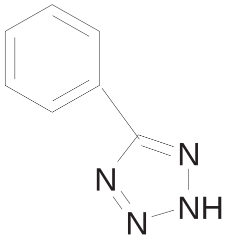

Fig.1. Molecular structure of tetrazolic derivative.

Reference:

[1] D. Bouzidi, S. Kertit, B. Hammouti, M. Brighli, J. Electrochem. Soc. India 46 (1997) 23.

[2] S. Kertit, B. Hammouti, M. Taleb, M. Brighli, Bull. Electrochem. 13 (1997) 241.

[3] S. Kertit, B. Hammouti, Appl. Surf. Sci. 93 (1996) 59.

[4] E. McCafferty, Corrosion Control by Coating, in: H. Leidheiser (Ed.), Science Press, Princeton, NJ, 1979, p. 279.

[5] S. Kertit, H. Es-Soufi, B. Hammouti, M. Benkaddour, J. Chim. Phys. 95 (1998) 2070.

[6] A. Chetouani, B. Hammouti, A. Aouniti, N. Benchat, T. Benhadda, Prog. Org. Coat. 45 (2002) 373.

[7]. K. Bekkouch, A. Aouniti, B. Hammouti, S. Kertit, J. Chim. Phys. 96 (1999) 838.

[8] Q. Liu, Z.Y. Zhu, W. Ke, C.I. Han, C.L. Zeng, Corros. Nace. 57 (2001) 730.

Electrochemical investingation of (4-bromo-3-(2,4dimethyl phenyl)isoxazol-5-yl)methanol on the corrosion of Steel in 1M HCl.

Ladan Edjlali*, Roghayeh Sadeghzadeh, Mostafa Hatefi, Afshin Razmi.
Department of Applied Chemistry, Faculty of Science, Islamic Azad University, Tabriz Branch, P.O.Box 1655, Tabriz, Iran
E-Mail:r.sadeghzadeh2010@yahoo.com, ladan_ejlali@yahoo.com

Key words: isoxazole, inhibitor, steel, corrosion, impedance spectroscopy (EIS)

Hydrochloric acid is often used as a pickling acid foriron and its alloys. The main goal is to remove undesirable corrosion products. To make secure from attack of acid, inhibitorsare frequently used. Organic nitrogen compoundson the corrosion behaviour of steel in acidic solutions are usually employed for their rapid action [1–6]. The existing data show that most of the organic inhibitors act by adsorption on the metal surface. The adsorption of inhibitors takes place through heteroatoms such as nitrogen, oxygen,phosphorus and sulphur, triple bonds or aromatic rings. Theinhibition efficiency should increase in the order O < N <S < P [9]. nitrogen-containing heterocyclic compoundsare considered to be effective corrosion inhibitors.The study was made by
using gravimetric, impedance spectroscopy (EIS) . The inhibition of steel in 1M HCl by new synthesised isoxazole compounds has been studied by weight loss, impedance spectroscopy (EIS) measurements. The results obtained reveal that these compounds are efficient inhibitors. The inhibition efficiency increases with the increase of inhibitor concentration and reached 98% at 10−3 M. The temperature effect on the corrosion behaviour of steel in1M HCl without and with the isoxazole at 10−3M was studied in the temperature range from 298 to 313 K. EIS measurements show that the increase of the transfer resistance with the inhibitor concentration. The aim of this work is to study the inhibiting effect of newly synthesized (4-bromophenl)isoxazol-5-yl)methanol on steel in 1M HCl. For this work, first we synthesized the above compound. 4bromophenyl (1) was transformed to 4-bromophenylbenzaldoxime (2) by using NH2OH in pyridine. The in situ generated nitriloxide from reaction between (2) and NaOCl, was reacted with propargylalcohol to produce (4-

bromophenyl)isoxazole-5-yl)methanol (3) in a cycloaddition procedure. The molecular structure of this compound is shown below. The effect of (4-bromo phenyl)isoxazol-5-yl)methanol(TMT) on the corrosion of steel in hydrochloric acid medium was studied using gravimetric, electrochemical impedance spectroscopy (EIS) measurements.

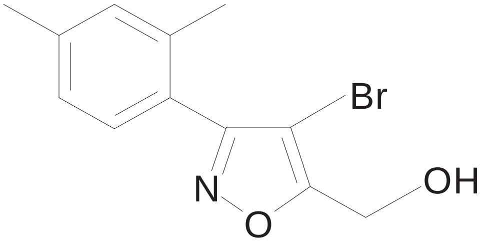

Fig1:(4-bromo-3-(2,4-di methyl phenyl) isoxazole-5-yl)methanol

Reference:

[1] Q. Liu, Z.Y. Zhu, W. Ke, C.I. Han, C.L. Zeng, Corros. Nace. 57 (2001) 730.

[2] D. Collins, R.E. Weyers, I.L. Al-Qadi, Corros. Nace. 49 (1993) 74.

[3] U.J. Ekpe, U.J. Ibok, B.I. Ita, O.E. Offiong, E.E. Ebenso, Mater. Chem. Phys. 40 (1995) 87.

[4] A. Chetouani, B. Hammouti, A. Aouniti, N. Benchat, T. Benhadda, Prog. Org. Coat. 45 (2002) 373.

[5] K. Bekkouch, A. Aouniti, B. Hammouti, S. Kertit, J. Chim. Phys. 96 (1999) 838.

[6] S. Kertit, K. Bekkouch, B. Hammouti, Rev. Métall. 97 (1998) 251.

[7] D. Bouzidi, S. Kertit, B. Hammouti, M. Brighli, J. Electrochem. Soc. India 46 (1997) 23.

[8] S. Kertit, B. Hammouti, M. Taleb, M. Brighli, Bull. Electrochem. 13 (1997) 241.

[9] S. Kertit, B. Hammouti, Appl. Surf. Sci. 93 (1996) 59.

Effect of hardness and softness of metals on the corrosion inhibitory of porphyrin compound

E. Kianpour*, M. Lashgari, S. Zakavi
Department of Chemistry, Institute for Advanced Studies in Basic Sciences, Zanjan, Iran
Email: Efat.kianpour@gmail.com

Key words: Metals corrosion; Tafel polarization; Neutral media; Porphyrin inhibitors; Reflective UV-Vis; Hard-soft acid-base theory.

Introduction:

Aluminum, iron and copper are engineering materials in widespread use. In the environments containing active ions like chloride, these ions accelerate the dissolution of the metal. Therefore, it is very important to protect these metals from corrosion. The use of corrosion inhibitors is one of the most practical methods for protection against corrosion. Because of some desirable properties, porphyrins seem to be attractive in the field of corrosion inhibitor. We reported the inhibitory action of meso-tetrakis(3-methoxy-4-sulphonatophenyl)porphyrin (H_2TAPS_4) on aluminum, iron and copper corrosion in 0.6 M NaCl solution [1-3].

Materials and methods:

H_2TAPS_4 was synthesized [4] and characterized by NMR (nuclear magnetic resonance) and UV–Vis (ultraviolet–visible) spectra. The metallic specimens used in the experiments were aluminum (99.999%), iron (99.98%) and copper (99.9%) rods. The test solutions were prepared from analytical grade sodium chloride and doubly distilled water. The concentration of corrosive solution was 0.6 M and that of inhibitor was 5×10^{-4} M. The electrochemical data of Tafel polarization curves was recorded by ZAHNER/ZENNIUM potentiostat/galvanostat instrument and processed by THALES software. The surface morphology was studied by a Philips Model XL30 scanning electron microscope. The UV-Vis spectra were also recorded by a Thermo Pharmacia Biotech Ultrospec 4000 spectrometer and Varian Cary 5 spectrometer respectively.

Results and discussion:

The electrochemical results (Table 1) indicated that the maximum performance is for copper, whereas the minimum is related to the aluminum metal. The reflective UV-Vis data (Table 2), moreover, revealed that the strongest metal/inhibitor interaction is due to copper and the greatest shift in the Soret band (red shift) is also witnessed for this metal inhibiting system. The electrochemical as well as spectroscopic findings were both approved by the SEM images and justified through the concepts of hard-soft acid-base (HSAB) theory.

Table 1: Potentio-dynamic results for Al, Fe and Cu corrosion in 0.6 M NaCl solution in the absence and presence of the synthetic inhibitor.

Sample	i_{corr} (nA/cm^2)	-E_{corr} (mV vs. Ag/AgCl, 3 M)	-E_{pitt} (mV vs. Ag/AgCl, 3 M)	η_{inhib}(%)
blank (Al)	937	1405	685	-
0.5 mM H_2TAPS_4 (Al)	358.1	1249	675	61.8
blank (Fe)	4204.1	748.6	807	-
0.5 mM H_2TAPS_4 (Fe)	1299.7	801.3	> 348	69.1
blank (Cu)	5597.1	218.1	135	-
0.5 mM H_2TAPS_4 (Cu)	472.1	102.1	45	91.6

Table2: Transmissive and reflective UV-Vis data for H_2TAPS_4 inhibitor.

sample	λ_s (nm)
Free H_2TAPS_4 (aq)	418(sharp)
H_2TAPS_4 adsorbed on Al	428(broad)
H_2TAPS_4 adsorbed on Fe	434(broad)
H_2TAPS_4 adsorbed on Cu	449(broad)

Conclusion :

H_2TAPS_4 is eco-friendly, recyclable, high stable and behaves as a mixed-type inhibitor. In the presence of this inhibitor, the risk of pitting is decreased remarkably for the copper and iron metals. The experimental observations were justified through HSAB theory.

References:

[1] S. ZOR, Turk. J. Chem, 26:403 (2002).

[2] I. D. Cunningham, T. N. Danks, J. N. Hay, I. Hamerton, S. Gunathilagan, and C. Janczak, J. Mol. Catal. A: Chem., 185:25 (2002).

[3] S. Zakavi and N. Gholami gharab, Polyhedron, 26:2425 (2007).

[4] E. B. Fleischer, J. M. Palmer, T. S. Srivastava, and A. Chatterjee, J. Am. Chem. Soc., 93:3162 (1971).

Electrochemical behaviour of methylene blue dye on the glassy carbon electrode (GC) in different concentrations

A.A. Rostami , F.Heydarpour
Faculty of Chemistry, University of Mazandaran, P.O.Bax 453, Babolsar, Iran.
Heydarpoor66@yahoo.com

Keywords : Electrochemical, CV, methylene blue, GC

Introduction:

Methylene blue (MB) is a synthetic phenothiazine dye with redox properties. It has many uses in a range of different fields, such as chemistry, biology, medicine and agriculture [1]. Also, due to its photodynamic and/or electrochemical properties, studies on its application in photogalvanic cells[2] and for chemically modified electrodes [3] have been developed. In this paper several electrochemical parameters along with the diffusion coefficient (a kinetic parameter) which obtained from the results of cyclic votammetric experiments of MB in different concentrations are reported.

Materials and methods:

The experiments are performed taking 25 mL of dye solution in the presence of 0.1 M H2SO4 in the appropriate media as a supporting electrolyte using glassy carbon electrode as a working,Pt-auxiliary electrode, all potentials are reported versus Ag/AgCl (saturated KCl) as a reference electrode at (25 ± 1) □C. Cyclic voltammograms of the dye solutions (0.05 ,0.01,0.001 M) are recorded in water, water-ethanol mixture, and Triton X-100 (0.001 M) at various scan rates up to 200 mV· s-1. GC electrode surface was cleaned by successively polishing it with a 0.05μM alumina slurry. Electrochemical measurements were performed in a one-compartment cell with a three-electrode configuration. CV study was conducted with a potentiostat/ galvanostat (EG&G model263).

Result and discussion:

The aggregation of the dyes in solution is an important phenomenon which must be taken into consideration during the interpretation of the cyclic voltammetric data. The studied dyes form dimers and higher aggregates in aqueous solutions at concentrations of more than 10^{-4} M.

It has been shown that for concentrations below 10^{-4} M the MB system fits the simple theory of CV in which the adsorption of the reactant is ignored. It was argued that, above 10^{-4} M concentrations, the adsorption of MB must be considered. Some different electrochemical parameters for MB at various concentrations of more than 10^{-4} M have been reported in Table 1

Figure 1 shows Cyclic voltammograms MB in different scan rate. Separation between the peak potentials (ΔEp) increases slowly with the increase in scan rate because the dye/leucodye couple deviates more and more from the reversibility. The effective diffusion coefficient values of the MB in water ,water-alcohol and water-Triton X-100 are (5.70, 3.70 and 1.80) 10^{-6}.D/cm^2.s^{-1} which shows the diffusion coefficient values in water-alcohol and micellar media are interestingly much smaller compared to pure water.

Table1. Electrochemical Data for CV of MB(0.001,0.01.0.05 M) in water Media in the presence of 0.1 M H2SO4 at scan rate of 100 mV/s.

concentrations (mol/lit)	E_{pa} (V)	E_{pc} (V)	$E_P\Delta$ (V)	i_{pa} (A/Cm^2)	i_{pc} (A/Cm^2)	i_{pa} / i_{pc}	$i_{pa} / V^{1/2}$	$i_{pc} / V^{1/2}$	0.058/ $E_P\Delta$
0.001	0.249	0.14	0.109	$1.32*10^{-5}$	$-1.37*10^{-5}$	0.963	$0.19*10^{-5}$	$0.193*10^{-5}$	0.532
0.01	0.23	0.18	0.05	$6.15*10^{-5}$	$-6.90*10^{-5}$	0.891	$0.87*10^{-5}$	$0.98*10^{-5}$	1.16
0.05	0.24	0.147	0.093	$1.75*10^{-4}$	$-2.09*10^{-4}$	0.837	$0.248*10^{-4}$	$0.295*10^{-4}$	0.62

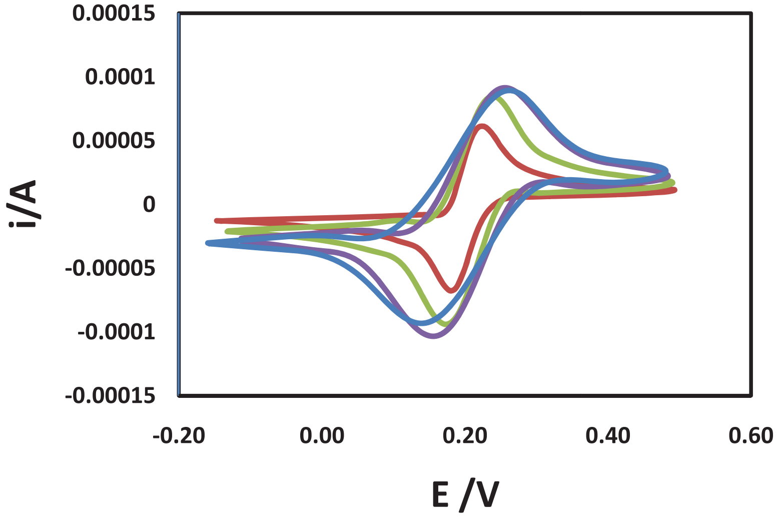

Figure1. Cyclic voltammograms of MB(0.01 M) in the presence of 0.1 M H2SO4with scan rates of (50, 100,150 , and 200) mV· s-1.

Conclusion:

The dimerization process is thus unfavorable in water-alcohol mixtures compared to that in neat water. the preliminary study shows the diffusion coefficient values in water-alcohol and micellar media are interestingly much smaller compared to neat water. It is interesting to note that a slight increase of solution viscosity results in the considerable decrease in the diffusion coefficient values for both 50 % volume fraction of water-ethanol and water-Triton X-100 mixtures.

Reference:

[1] http://www.methylene-blue.com/substance.php.
[2] D.H. Hay, S.A. Martin, S. Ray, N.N. Lichti, J. Phys. Chem. 85(1981) 1474.
[3] J. Bujdak, P. Komadel, J. Phys. Chem. B . 101 (1997)9065.

Poly(1-amino-9,10-anthraquinone) coating on stainless steel by electropolymerization

Mahsa. Meftah Niaki [a], Abdollah. Omrani [b*], Hossein. Nikoofard [a], Abbas Ali. Rostami [b]
a College of Chemistry, Shahrood University of Technology, Shahrood, Iran
b Faculty of Chemistry, Mazandaran University, Babolsar, Iran
Email: omrani@umz.ac.ir

Key Words: Corrosion, conductive polymers, resistant

Introduction:

The rate of corrosion of stainless steel can be reduced by a thin oxide layer (passive film) formed naturally on the metal surface [1]. In the last decade the conductive polymers have been studied by many authors for application to corrosion-resistant coating of metals. Conductive polymers coating has been assumed to be a possible treatment for the replacement of the chromate treatment on steel [2]. Conducting polymers do not only behave as barrier coating on common metals in corrosive media, but also prevent easy reach of corrosive ions on metal surface due to its own redox electroactivity for long exposure time in corrosive enviroments [3].

Materials and methods:

1-amino-9,10-anthraquinone (AAQ), Merck, was used without further purification. In all electrosynthesis experiments, 9 mM AAQ and 0.1 M $LiClO_4$ solutions were prepared by using triply distilled water. Investigation were carried out by analyzing the cyclic voltammetric responses using the software M 270.

Apparatus:

Cyclic voltametry (CV) experiments were performed using a Potentiostatic/Galvanostatic EG & G Model 263 A. The measurements were carried out in a single compartment three-electrode cell with stainless steel disc as working electrode (0.07 cm^2), platinum wire was used as counter electrode. An Ag/AgCl/ 3M KCL electrode system was employed as refrence electrode.

Result and discussion:

The coated steel surface was obtained under cyclic voltametric conditions with a potential sweep from -0.79 to 0.79 V. As can be seen Fig. 1, The corrosion potential (E_{corr}) of the PAAQ coated steel electrode is shifted in the negative direction (ΔE=0.084 V) compared to that of the anodic dissolution of steel in corrosive solutions. Both the cathodic and anodic currents decrease when steel is coated with PAAQ. The PAAQ coating restricts the anodic and cathodic reaction of steel in aggressive media.

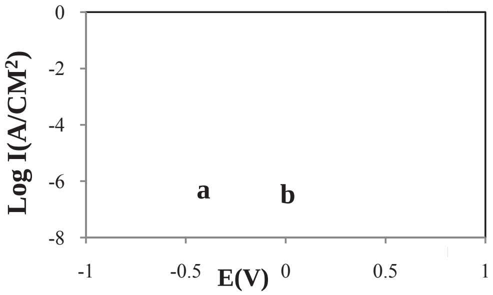

Fig. 1. Tafel curves for: (a) uncoated; (b) PAAQ coated steel electrodes which were obtained under cyclic voltametry conditions with a potential sweep between -0.79 and 0.79 vs. in 0.5 M HCl ($v = 2$ mV s^{-1})

Conclusion:

The results show that the coated PAAQ shift the electrode potential toward more positive potentials. The PAAQ as a conducting polymer coating exhibited effective protective behavior in highly corrosive media containing acidic chloride anions and decreased the corrosion rate of stainless steal.

Reference:

[1] C.O.A. Olsson, D. Landolt, ; ″Passive films on stainless steels-chemistry, structure and growth″ ; Electrochim. Acta 48 (2003) 1093_ 1104.

[2] J.O. Iroh, W. Su, ; " The effect of counter anions on corrosion resistance of steel covered by bi-layered polypyrrole film" **;** Electrochim. Acta 46 (2000) 15–24.

[3] D. Sazou, C. Georgolios, J. ; "Formation of conducting polyaniline coatings on iron surfaces by electropolymerization of aniline in aqueous solutions" ; Electroanal. Chem. 429 (1997) 81 –93.

Electroless nickel plating on AZ61 magnesium alloy

D.Seifzadeh[a] , Z.Rajabalizadeh[a]*
a Department of chemistry, Faculty of science, Mohaghegh Ardabili university, Ardabil, Iran Email:
z.rajabalizadeh@yahoo.com

Keywords: Electroless deposition, Nickel, Magnesium alloy, Corrosion resistance

Introduction:

Magnesium has low density, high strength to weight ratio and other good physical and mechanical characteristic, which makes it possible for structural applications in aerospace, electronics and automobile fields. Application of surface engineering technique is the most appropriate method to enhance the corrosion resistance of magnesium alloys. Among the various techniques that are available for this purpose, coating by electroless nickel is of special interest due to its good corrosion and wear resistance, deposit uniformity, electrical and thermal conductivity [1-3]. This study reports the work carried out on electroless nickel plating on AZ61 magnesium alloy. This coating has been characterized for its structure, morphology and corrosion characteristics.

Materials and methods:

After abrading, the AZ61 alloy substrate was cleaned in alkaline. Then the samples were immersed in etch solution (HNO_3 (50 ml/L) and CrO_3 (62 g/L)) for 30 s. Fluoride activation in HF (350 ml/L) for 10 min was the last step in pretreatment procedure. The plating bath was containing $NiSO_4.6H_2O$ (15 g/L), $NaC_2H_3O_2$ (13 g/L), $Na_2H_2PO_2.H_2O$ (14 g/L), HF (12 mL/L), NH_4HF_2 (8 g/L), Thiourea (1ppm), and NH_3 (pH adjusting to 6.4). All samples were plated at 82 ºC under ambient pressure. Scanning electron microscopy (SEM) and Energy dispersing X-Ray spectroscopy (EDS) were used for coatings characterization. Electrochemical impedance spectroscopy tests were performed using µAutolab3 instrument by applying 5 mV sinusoidal voltage in the frequency range of 1MHz to 100 mHz at rest potential.

Result and discussion:

SEM image showed that the morphology of the coating after 2h plating was uniform with spherical nodular structure (Fig.1). EDS analysis (not been shown) revealed that the coating contains phosphorous element with contents of 9.73 wt. %. The thickness of the coated samples was determined after 1, 3, 5, 7 h plating by cross-section morphology. The thickness was about 14, 24, 34, 35 µm, respectively. The Nyquist diagram of the AZ61 alloy after 3h plating has been shown in Fig.2. Comparison of the capacitive semicircle of the coated sample and bare sample revealed the high protective performance of Ni-P coating on AZ61 alloy.

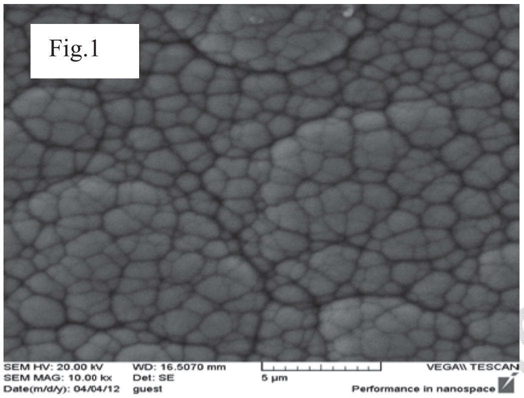
Fig.1

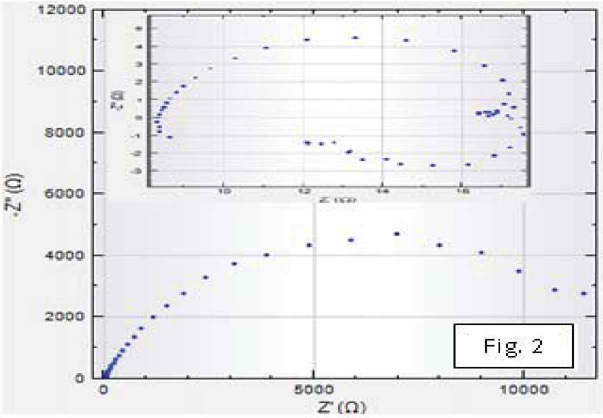
Fig. 2

Conclusion:

The results indicate that the Ni-P coating can provide good corrosion protection for AZ61 magnesium alloy. Deposition rate of the coatings has decreased versus time. Cross-section morphologies have shown that coatings have a good adhesion to the substrate.

References:

[1] J. S. Lian and et al; Electroless Ni–P deposition plus zinc phosphate coating on AZ91D magnesium alloy, Surf. Coat. Technol. 200 (2006) 5956-5062.

[2] R. Ambat and et al.; Electroless nickel plating on AZ91D magnesium alloy: effect of substrate microstructure and plating parameters, Surf. Coat. Technol. 179 (2004) 124-134.

[3] J. Li and et al.; The electroless nickel plating on magnesium alloy using $NiSO_4$. H_2O as the main salt, Surf. Coat. Technol. 200 (2006) 3010-3015.

Effect of two various temperatures on the electroless nickel plating on AZ61 magnesium alloy

D. Seifzadeh, Z. Rajabalizadeh

Department of chemistry, Faculty of science, Mohaghegh Ardabili University, Ardabil, Iran Email: z.rajabalizadeh@yahoo.com

Keywords: Electroless deposition, Nickel, Temperature effect, Thickness

Introduction:

The ultra light metal of magnesium alloys is widely applied to the fields of automobile, electronic products, aerospace, etc. Electroless nickel plating is an effective method to protect magnesium and its alloys from corrosion. Since the nickel-magnesium system is a classical example of cathodic coating on an anodic substrate, the coating porosity might influence the corrosion behavior and service life time of electroless nickel plated on magnesium [1, 2]. In this work, the effect of two different temperatures on the thickness of deposition, phosphorus content and morphology of the coating has been investigated.

Materials and methods:

After abrading, the AZ61 alloy substrate was cleaned in alkaline. Then the samples were immersed in etch solution (HNO_3 (50 ml/L) and CrO_3 (62 g/L)) for 30 s. Fluoride activation in HF (350 ml/L) for 10 min was the last step in pretreatment procedure. The plating bath was containing $NiSO_4.6H_2O$ (15 g/L), $NaC_2H_3O_2$ (13 g/L), $Na_2H_2PO_2.H_2O$ (14 g/L), HF (12 mL/L), NH_4HF_2 (8 g/L), Thiourea (1ppm), and NH_3 (pH adjusting to 6.4). Samples were plated at 65 and 82 ºC under ambient pressure. Scanning electron microscopy (SEM) and Energy dispersing X-Ray spectroscopy (EDS) were used for coatings characterization.

Result and discussion:

Fig. 1a and 1b show the cross-section microstructure of electroless Ni-P coating after 5h plating at 65 and 82 ºC, respectively. Apparently the coating thickness at 82 ºC (34 μm) is more than the thickness at 65 ºC (21μm). Therefore, as the temperature increases, the rate of deposition also increases. Apart from the deposition rate, temperature also affects the phosphorus content of the deposit and hence its properties. It is noticed from EDX analysis that there is a slight increase in P content as the temperature increase (8.13 wt. % at 65 ºC and 9.73 wt. % at 82 ºC). SEM micrographs (shown in Fig. 2 and 3) illustrate that the coatings possess a cauliflower type structure. The coated sample at 65 ºC has finer grain size as compared with the coated one at 82 ºC. As it can be seen from cross-section view, surface of coating at 65 ºC is so smooth. At 82 ºC due to high deposition rate, surface is composed of some coarser cauliflower nodules.

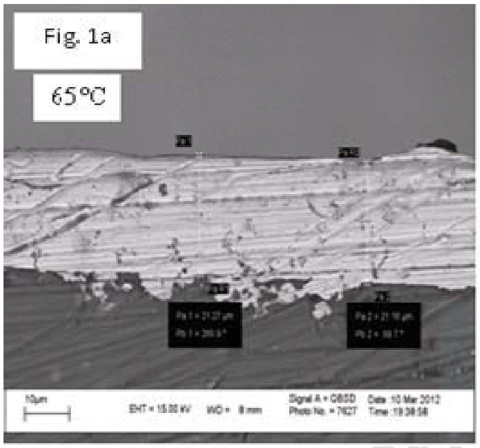

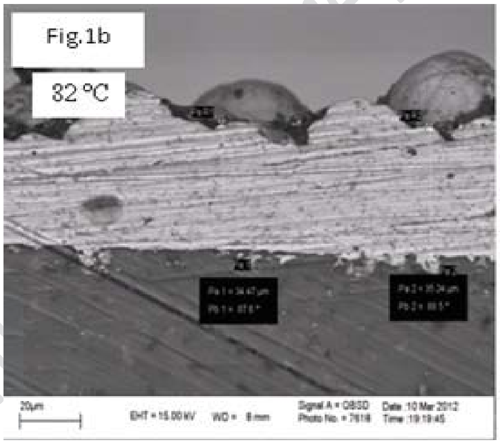

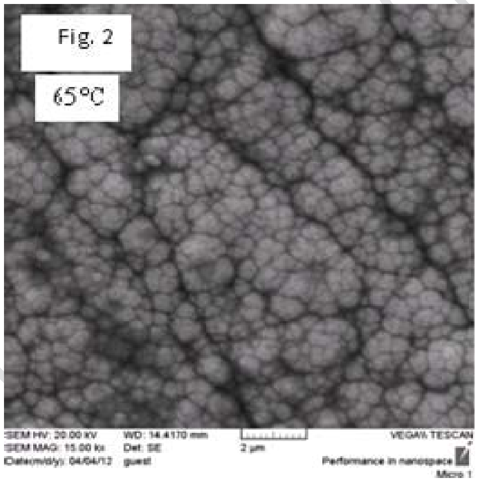

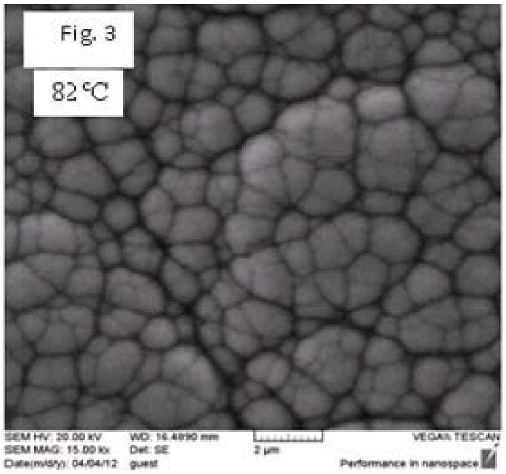

Conclusion:

Temperature is the most important parameter affecting the rate of deposition. Most of the oxidation and reduction reactions involved in the overall process required energy in the form of heat. Temperature also affects the P content and morphology of the coatings.

References:

[1] J. Li and et al. Studies of the porosity in electroless nickel deposits on magnesium alloy, Appl. Surf. Sci. 252 (2006) 2839-2846.
[2] Y. Song and et al. High corrosion resistance of electroless composite plating coatings on AZ91D magnesium alloys, Elecrtochim. Acta 53(2008) 2135-2143.

Electrochemical synthesis of nanocomposite of poly aniline / polyvinyl alcohol and study its corrosion

H. Sajadianfar [*], M. Sharifirad, S. Moradi, F. Amanifard
Department of Chemistry, Teacher research Bojnord, Iran
(Email: ce_sajadianfar@yahoo.com)

Introduction:

Several researchers have employed different post treatments after the synthesis of polymer films; however, there are no systematic studies on this aspect. On the other hand, when a polyaniline layer was deposited first and the electropolymerization was continued in a solution of poly aniline (PANI), a progressive transformation of the electrochemical behavior of the original polyaniline film has been observed. The polyaniline promotes the polymerization by providing electrocatalytic sites and nucleation centers. Thus, the conducting polyaniline surface is protected well and leads to better modification. Chemical polymerization of PANI also leads to newer polymers. Interestingly, both the newly formed polymers are found to have nanostructure. The preparation of nanostructured conducting materials has become an important branch of materials research. [1-5]

Experimental:

The poly aniline (PANI), and poly vinyl alcohol (PVA) were purchased from Merck, and cupric sulfate, nickel sulfate and silver nitrate from Alderich. The stock solutions of cupric sulfate, nickel sulfate and silver nitrate (10^{-1}, 10^{-1}, 2×10^{-1} mol dm^{-3}) were prepared in distilled water.Sodium Chloride (NaCl, 99%) was purchased from Merck (Darmstadt, Germany). Transmission electron microscopy (TEM) studies of the composite material were carried out at an accelerated voltage of 120 kV using a Philips CM200 TEM. Scanning electron microscopy (SEM) images are taken using a VEGA HV (high potential) 1500 V at various magnifications. The next portion of the solid was dried under vacuum and used for IR spectral analysis. The FTIR transmission spectrum of polypyrrole coating is recorded in horizontally attenuated total reflectance mode in the spectral range 3500–550 cm^{-1} using a Bruker spectrometer, Vector Series 22, Germany.

Result and discussion :

The effect of poly aniline (PANI)/ poly vinyl alcohol (PVA) on the corrosion reactions was determined by polarization measurements. The solutions were purged with hydrogen (99.999% Ar) for 45 min before use, and the H_2 atmosphere was maintained in the cell during all electrochemical experiments. Before each run, the clean Cu working electrode was quickly inserted into the solution and immediately cathodically polarized at -200 mV for 30 min to reduce any oxide on the copper surface. The scan started from the cathodic (-200 mV) to the anodic direction with the scan rate of 0.2 mV s^{-1}. Figure 1 shows examples of polarization curves for the copper electrode in 0.5 M NaCl solutions of pH 3.0. The cathodic corrosion reaction in chloride solutions should be the reduction of water.

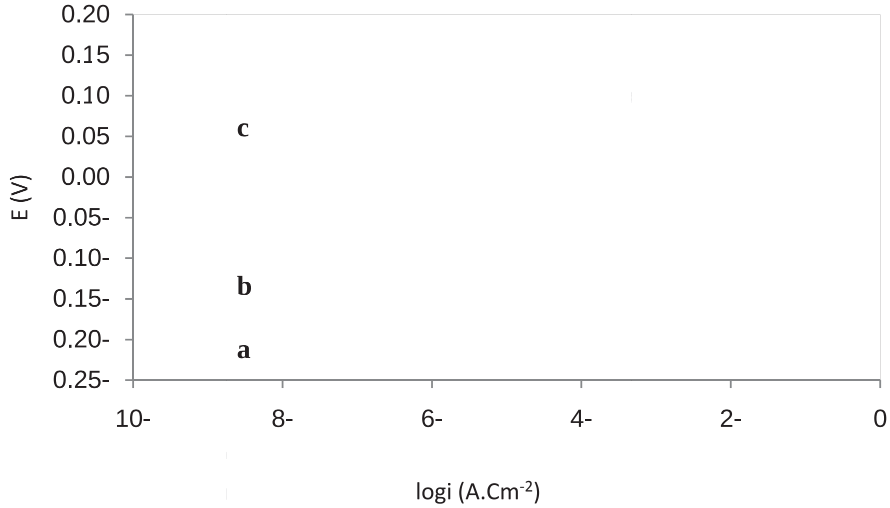

Figure 4. Potentiodynamic polarization curves recorded for polyDDS-metals/ DGEBA.TETA on copper electrode in 0.5 M NaCl solution: (a) poly aniline (PANI)/ poly vinyl alcohol (PVA).

Reference:

[1] D. Thromans, R.-H. Sun, J. Electrochem. Soc. 139 (1992) 1945.
[2] A.R. Katritzky, Comprehensive Heterocyclic Chemistry. The Structure, Reaction, Synthesis and Uses of Heterocyclic Compounds, vol. 5, Pergamon Press Ltd., London, 1984.
[3] M. Scendo, Corros. Sci. 49 (2007) 373.
[4] M. Elachouri, M.S. Hajji, M. Salem, S. Kertit, J. Aride, R. Coudert, E. Essassi, Corrosion 52 (1996) 103.
[5] B. Ramesh Babu, R. Holze, Brit. Corros. J. 35 (2000) 204.

Electropolymerization poly DDS / SiO2 nanoparticle and its corrosion

H. Sajadianfar [*], M. Sharifirad, S. Moradi, F. Amanifard
Department of Chemistry, Teacher research Bojnord, Iran
(Email: ce_sajadianfar@yahoo.com)

Introduction :

Electrically conductive adhesives based on Nano polymer–metal composite /Epoxy. Tri Etyhlene Tetramine (DGEBA.TETA) system containing poly (4-4-Diamino diphenyl sulfone), [polyDDS] and different metals (copper, nickel and silver) nanoparticles composite materials have been successfully developed and characterized. The blends were prepared by physical mixing of Nano polymer–metal composite within DGEBA.TETA matrix[1-6].

Experimental:

The mixing ratio of epoxy to hardener was kept constant at 10/2. The conductive filler (poly DDS-Cu, polyDDS-Ni, PolyDDS-Ag) content is described by different weight percent. The mixture was cast into a Teflon disc mold (2 cm diameter, 2.5 mm thick) and cured at 80°C for 5 h, followed by an additional curing at 120°C for 2 h. These process to be accomplished on the copper electrode for electrochemical analysis.

Electrochemical polarization is carried out using a Potentiostat/ Galvanostat, EG&G Model 263 A; USA with a PC and electrochemical set up that controlled with M 270 software. The working electrode was either a copper (99.99% purity) disk or rectangular sheet (area 1 cm^2). The electrodes are mechanically polished with abrasive paper (2400 grade) and rinsed with distilled water and finally dried under argon flow before each electrochemical experiment. After deposition, the working electrode with PolyDDS-Metals/Epoxy Composites are rinsed with double distilled water and then dried in the air.

Result and discussion :

A change in weight percent of polyDDS-metals also affects the average corrosion rate. The value of corrosion rate was calculated from the following equation:

$$K_s \text{ (mm/year)} = (m_1 - m_2/s\rho t) \times 8.76 \times 10^3 \qquad (13)$$

Where m_1 is the mass of the specimen before corrosion, m_2 is the mass of the specimen after corrosion, S is the total geometrical surface specimen area, t is the time of the corrosion test. With the calculated corrosion rate, the inhibition efficiency (IE_s) of inhibitors for the corrosion of copper was obtained by using the following equation:

$$IE_s\ (\%) = (k_{s,0}-k_s/k_{s,0})\times 100 \qquad (14)$$

Where $k_{s,0}$ and k_s are the corrosion rates of the copper specimens in solutions without and with inhibitors, respectively. Inhibition efficiencies of purine and adenine in the nitrate solutions obtained by the gravimetric method are presented in figure 1. The present study shows that the inhibition efficiency increases with an increase in the weight percent of polyDDS-metals. However, IE_s are higher for polyDDS-Ag. The data given to reveal that polyDDS-Ag acts as a good inhibitor in the spontaneous dissolution of copper in the investigated solutions. Probably such results can be accounted for by the different interaction of weight percent of polyDDS-metals with the copper surface. It was confirmed that the protective layer on the copper surface acts just as in deaerated (Figure 1) and nonde-aerated solutions in the presence of different weight percent of polyDDS-metals.

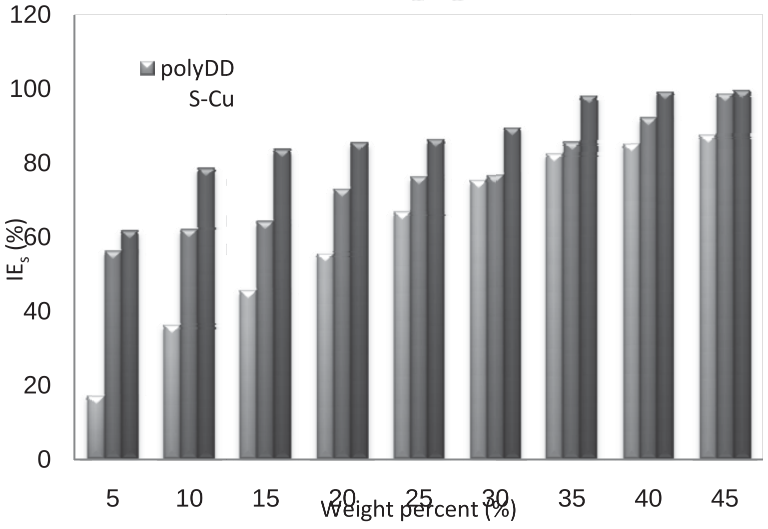

Figure1. Inhibition efficiency of copper determined by gravimetric method in 0.5 M NaCl solutions with different weight percent of (a) polyDDS-Cu.

Reference:

[1] B. Ramesh Babu, R. Holze, Brit. Corros. J. 35 (2000) 204.

[2] P.G. Fox, G. Lewis, P.J. Boden, Corros. Sci. 19 (1979) 457.

[3] V. Shinde, S.R. Sainkar, P.P. Patil, Corros. Sci. 47 (2005) 1352.

[4] Q.H. Cai, Y.K. Shan, B. Lu, X.H. Yuan, Corrosion 49 (1993) 486.

[5] I. Sekine, Y. Hirakawa, Corrosion 42 (1986) 272.

[6] G.N. Mu, T.P. Zhao, M. Liu, T. Gu, Corrosion 52 (1996) 853.

Electrocatalytic determination of penicillamine using multiwall carbon nanotubes paste electrode

M. Keyvanfard[a], N. Najjarian[b], K. Alizad[a] ,H. Karimi-maleh[c]
[a] Department of Chemistry, Majlesi Branch, Islamic Azad University, Isfahan, Iran
[b]Department of Chemistry, Shahreza Branch, Islamic Azad University, Isfahan, Iran
[c]Department of Chemistry, Science and Research Branch, Islamic Azad University, Mazandaran, Iran
E-mail: Keyvan45638@yahoo.com

Keywords:Penicillamine,Carbon Nanotubes Paste Electrode,Electrocatalysis,Chlorpromazine

Abstract:

In this work, we propose Chlorpromazine as a new mediator for the rapid, sensitive, and highly selective voltammetric determination of Penicillamine using multieall carbon nanotubes paste electrode. Using liner sweep voltammetry and under the optimum condition at pH 4.0, the electrocatalytic oxidation peak current of This modified electrode showed very efficient electrocatalytic activity for the anodic oxidation of PA shows a linear dependence on PA concentration in the PA concentration ranges of 0.5–500 µmol/L PA. The detection limits for PA was 0.2 µmol/L.

Introduction:

Penicillamine is a pharmaceutically important thiol compound frequently used as a medicinal agent against a number of diseases such as rheumatoid arthritis, cystinuria, liver disease or certain skin conditions, heavy metal poisoning and Wilson,s disease, a genetic disease that results in excessive copper deposits in the body tissues[1]. The pharmaceutical form is D-penicillamine, whereas it is toxic in its L-penicillamine form (because it inhibits the action of pyridoxine). Despite having no antibiotic effects, penicillamine is a metabolite of penicillin. The application of carbon nanotubes for fabrication of electrochemical sensors and biosensors is reviewed by many research groups. The electronic properties of these nanomaterials have been exploited as a mean of promoting the electron transfer reaction for a wide range of molecules and biological species [2-4].

Materials and methods:

Spectrally pure graphite powder (particle size <50 µm) from Merck and multiwall carbon nanotubes (>90% MWCNTs basis, d × l = (90–70 nm) × (5–9 µm) from Fluka were used as the substrate for the preparation of the carbon paste electrode. All solutions were freshly prepared with twice distilled water.

Apparatus:

For electrochemical investigation we used an Autolab PGSTAT 302N, potentiostat/ galvanostat (Utrecht, The Netherlands) connected to a three-electrode cell, Metrohm (Herisau, Switzerland) Model 663 VA stand, linked with a computer (Pentium IV, 1,200 MHz) and with Autolab software. The electrode prepared with carbon nanotubes was characterized by scanning electron microscopy (SEM) (Seron Tech. AIS 2100).

Result and discussion:

In conclusion, a multiwall carbon nanotubes paste electrode was used for the determination of PA in the presence of CHP as suitable mediator. The cyclic voltammetry and LSV investigations showed effective electrocatalytic activity of the modified electrode in lowering the anodic over-potential for the oxidation of PA. The peak current of linear sweep voltammograms (LSV) of PA increased linearly with their concentration in the ranges of 0.5–500 µmol/L PA. The detection limits for PA was 0.2 µmol/L. The RSD% for 1.0 and 10.0 µmol/L PA were 1.1% and 1.7%, respectively.

Reference:

[1] C. Smolarek, W.*Z.* Stremmel, Gastroenterol. 37 (1999) 293.
[2] A.A. Ensafi, H. Karimi-Maleh, Electroanalysis 22 (2010) 2558.
[3] A.A. Ensafi, H. Karimi-Maleh, J. Electroanal. Chem. 640 (2010) 75.
[4] H. Beitollahi H. Karimi-Maleh, Anal. Chem. 80 (2008) 9848.

Third generation glucose biosensor using covalently immobilized glucose oxidase onto poly(Aminothiophenol)/ carbon nanotubes electrode

S.Sharifyrad*[a], M.A.Kamyabi[b]
[a,b] Department of Chemistry, Zanjan University, PO Box 45195-313, Zanjan, Islamic Republic of Iran
Email:m.rad4294@gmail.com

The efforts to develop and improve glucose sensors have been made near five decades since Clark and Lyons reported the first enzyme electrode in 1962. For the first time, Updike and Hicks was immobilized glucose oxidase (GO_X) in a gel on an oxygen electrode and measured glucose concentration in biological fluids. One of the most challenging aspects in the development of highly sensitive glucose sensor is the selection of a suitable matrix for GO_X immobilization, with high mechanical strength, excellent conductivity and antifouling properties. Therefore, the development of high sensitive, low-cost, reliable glucose sensors having an excellent selectivity has been the subject of concern for decades, not only in medical science but also in the food industries [1-3].

In the present study, an electropolymerized film of 4-Aminothiophenol was prepared on the surface of a GC electrode modified with multi-walled carbon nanotubes, (CNTs) in 0.10 M HCl in methanol. Cyclic voltammetry was used for both the electrochemical synthesis of poly-(4-Aminothiophenol) on the surface of a multi-walled carbon nanotubes modified glassy carbon electrode (GCE), and characterisation of the polymers deposited on the GCE. The synergisitc effect of the high active surface area of both the conducting polymer and carbon nanotubes gave rise to a remarkable improvement in the electrocatalytic properties of the biosensor. The heterogeneous electron transfer rate constant was 3.7 s^{-1} in pH 7, indicating great facilitation of the electron transfer between GOx and poly(4-Aminothiophenol)/MWNTs adsorbed on the electrode surface. The modified GCE biosensor was exhibited two linear responses to glucose in the concentration range of 10-450 µM, with correlation coefficients of 0.98, good sensitivity (0.04 µA/µM), repeatability (RSD value of 1.6%) and long-term stability. This is a simple and easy approach for the fabrication of enzyme electrodes for the selective detection of glucose in a biological sample. The good performance of this glucose sensor could be attributed to the stability of poly(4-

Aminothiophenol)/MWCNT and this opens up new horizons in the field of functionalized MWCNT based glucose sensor related researches.

Keyword: Electropolymerization, Glucose biosensor, carbon nanotubes

Reference:

[1] Md. Mahbubur Rahman, A. J. Saleh Ahammad, Joon-Hyung Jin, Sang Jung Ahn and Jae-Joon Lee, *Sensors*, *10* (2010) 4855-4886.
[2] Sejin Park, Hankil Boo, Taek Dong Chunga, Analytica Chimica Acta 556 (2006) 46–57.
[3]Wang, J. Electrochemical Glucose Biosensors. Chem. Rev. 108 (2008) 814–825.

Electrocatalytic Oxidation of Dopamine, Ascorbic Acid and Uric Acid at Poly-4-Aminothiophenol on the Surface of Carbon Nanotubes/GC Electrodes

S.Sharifyrad*[a], M.A.Kamyabi[b]
[a,b] Department of Chemistry, Zanjan University, PO Box 45195-313, Zanjan, Islamic Republic of Iran
Email:m.rad4294@gmail.com

During recent years, great efforts have been devoted to the development of electrochemical sensors with electrosynthesized polymeric film electrodes. Modified electrodes prepared by electropolymerization have obvious advantages in the detection of analytes. For example, it can accelerate transmission of electrons on the surface of electrode, it has high selectivity and sensitivity due to the film homogeneity in electrochemical deposition, strong adherence to the electrode surface and large surface area [1-2]. Unlike conventional immobilization strategies for biosensors, electropolymerization has no limit in terms of the geometry and area of the electrode, and offers advantages with respect to thickness control, reproducibility and uniformity of the polymer film on the electrode surfaces with more complex geometries. In addition, electropolymerization permits simple electrode regeneration and can be easily extended to the production of microbiosensors. Many studies have indicated that polymer film modified electrodes show an enhanced response for the determination of various important biological and clinical species [3].

In this work, an electropolymerized film of 4-aminothiophenol was prepared on the surface of a GC electrode in 0.10 mol L^{-1} HCl in methanol by cyclic voltammetry (CV). The poly(4-aminothiophenol) on the surface of GCE showed excellent catalytic activity toward oxidation of some biological compounds and conspicuously enhanced the redox peak currents. The ternary mixture, which contains ascorbic acid (AA), dopamine (DA) and uric acid (UA), can be well separated from each other at the surface of this modified electrode. The separations of the oxidation peak potentials of AA-DA and DA-UA were over more than 184 and 147 mV, respectively. Using differential pulse voltammetry (DPV) technique, the calibration curves for AA, DA and UA were obtained over a wide range (0.5-55 mM for AA, 10-500 µM for DA and 0.5-7.0 mM UA at the poly(4-aminothiophenol) modified GCE) and with the sensitivity of 23.89 µA/mM, 0.20 µA/µM and 2.77 µA/mM for AA, DA and UA respectively. The theoretical limits of detection defined as 3s of the proposed method for AA, DA and UA were 0.27 mM, 3.73 µM and 0.29 mM, respectively. These results are somewhat similar (or worse) performances (in some cases) or superior ones (in most cases) than the previously reported modified electrodes in literatures [4-5].

Keyword: Electropolymerization, carbon nanotubes, Electrocatalytic

Reference:

[1] Volkov, A.; Tourillon, G.; Lacaze, P. C.; Dubois, J. E.; J. Electroanal. Chem., 115 (1980) 279.
[2] Chung, T. D.; Biosens. Bioelectron., 16 (2001) 1079.
[3] Trojanowicz, M.; Microchim. Acta, 143 (2003) 75.
[4] P.R. Roy, T. Okajima and T. Ohasaka. Bioelectrochemistry, 59 (2003) 1.
[5] P. Kalimuthu and S.A. John. Bioelectrochemistry, 77 (2009), 13.

Potentiometric investigation of glycine-2-aminopyrimidine proton-transfer system and its Cu^{2+}complexes

A. Shokrollahi*, N. Shokrollahi
Department of Chemistry, Yasouj University, *Yasouj, Iran*
E-mail: ashokrollahi@mail.yu.ac.ir

Keywords: glycine, 2-Aminopyrimidine, potentiometric studies, complexe

Introduction:

The interaction between amino acids with bases similar to metal ions [1] plays an important role in biochemistry and biology but has not been studied extensively. In near past the interactions between pyridine-2,6-dicarboxylic acid and 2-aminopyrimidines were considered [2], but the interaction of these bases with other amino acids such as glycine wasn't report.

In this work the protonation constants of glycine (gly)**,** 2-aminopyrimidine (2-apym) the equilibrium constants for the gly-2-apym proton transfer system and stoichiometry and stability of complexation of this system with Cu^{2+}ion in aqueous solutions. The stoichiometry of the most species in solution was compared to the corresponding crystalline cited complexes.

Materials and methods:

For the potentiometric *p*H titrations of glycine, 2-apym and glycine -2-apym in the absence and presence of 1.25×10^{-3} metal ion The concentration of gly and 2-apym was set as 2.5×10^{-3} M for metal ion respectively. A standard carbonate-free NaOH solution (0.09300 M) was used in all titrations. The ionic strength was adjusted to 0.1 M with $NaNO_3$.

Apparatus:

A Model 794 Metrohm Basic Titrino was attached to an extension combined glass-calomel electrode mounted in an air-protected, sealed, thermostated jacketed cell maintained at 25.0 ± 0.1 °C by circulating water, from a constant-temperature bath Fisherbrand model FBH604, LAUDA, Germany, equipped with a stirrer and a 10.000-mL-capacity Metrohm piston burette. The *p*H meter-electrode system was calibrated to read -log [H^+].

Result and discussion:

Primarily, the fully protonated forms of gly and 2-apym were titrated with a standard NaOH solution in order to obtain their protonation constants as the building blocks of the gly/2-apym adducts . The evaluation of the equilibrium constants for the interaction of GLY with 2-apym in different protonation forms was accomplished through comparison of the calculated and experimental *p*H profiles obtained with gly/2-apym present. In order to evaluate the stoichiometry and stability constant of Cu^{2+}complexes with gly-2-apym association in aqueous solution, the equilibrium potentiometric pH titration profiles of gly, 2-apym and their 1:1 mixture were obtained in the absence and presence of the Cu^{2+}ion.

Conclusion:

The protonation constants of gly and 2-apym the building blocks of the proton-transfer systems including gly/2-apym fragments and the corresponding stability constants of these systems were determined by potentiometric study. It is interesting to note that the stoichiometries of the some of the most abundant ternary complexes such as CuLQH existing in solution, are very similar to those reported for the corresponding isolated complexes in the solid state.

Reference:

[1] F.Kiani etal . ; "Complex Formation of Thorium (IV) Ion with Glycl-Glycine and Glycyl-Valine" ; Journal of Chemical and Engineering Data ; 54, 3247-3251, 2009.

[2] H.Eshtiagh Hosseini etal . ; " Structural aspects and solution behavior of etallosupramolecular compound of FeIII ion obtained by proton transfer" ; Journal of Coordination chemistry ; 64 , 3969-3979, 2011.

Spectrophotometric study of the complexation of two new synthetic Schiff base with some transition and heavy metal ions in acetonitril solvent

A. Shokrollahi*, T. Mehrpou, M. Montazerozohori
Department of Chemistry, Yasouj University, Yasouj, Iran
E-mail: ashokrollahi@mail.yu.ac.ir

Keywords:complexation,Schiff bases,Hypspec program, Hyss program,Spectrophotometric.

Introduction:

Thermodynamic studies of complexation reactions of Schiff bases with transition and heavy metal ions not only result is important information on the thermodynamics of complexation reaction, but also lead to a better understanding of the high selectivity of these ligands towards different metal ions. Therefore complexation reactions of metal ions with different ligands have been widely studied [1]. Bis (2-hydroxy -1-naphtaldehydene)-1,2-phenylendiamine(L^1) andBis (2-hydroxy -1-naphtaldehydene) -4-nitro -1,2-phenylendiamine (L^2), arenew synthesis Schiff base and there isnot any thermodynamic information about it and its complexation with metal ions. In this investigation the complexationbehaviour of the cited ligands with some metal ions such as Co^{2+}, Ni^{2+}, Cu^{2+}, UO_2^{2+}, Pb^{2+},Zn^{2+},Ce^{3+}, In^{3+} and Th^{4+} in acetonitril at 25 ºC and 0.05 M tetra ethylammonium perchlorate (TEAP) were studied by spectrophotometric method.

Materials and methods:

Analytical grade nitrate salts of metalions are purchased from Merckandused without any further purification.Lead perchlorate was purchased from Alfa Aesarcompany. The $L^1$and L^2ligandswere synthesized in our laboratory. Standard stock solutions of ligands (1.0×10^{-3}M) and the metal ions (1.0×10^{-3}M) were prepared by dissolving appropriate and exactly weighed (with an accuracy of ±0.0001g) amount of pure solid compounds in precalibrated 25.0 mL volumetric flasks and diluted to the mark with acetonitril. Working solutions were prepared by appropriate dilution of the stock solutions.

Apparatus:

Absorbance measurements were carried out with a Jasco model V-570 spetrophotometer (Jasco Co., Hachioji, Tokiyo, Japan).

Result and discussion:

The interaction of some Schiff bases with the metal ions was studied by adding various ratio of metal ions solution in acetonitrile. The complexation of these ligands was carried out spectrophotometrically in acetonitrile medium. In these experiments, ligand concentration was kept constant and metal ion concentration was increased of M/L ratio from 0-4 in excess. The increase in the concentration of the transition metal ions causes that one of the original peaks of the Schiff base ligands at about 300-400 nm gradually vanished and a new peak appeared at about 400-500 nm its intensity increases with the increase in the concentration of metal ions with very clear isosbestic points.The bands in 300-370 nm range in the spectrum of the ligand was assigned to $\pi \rightarrow \pi^*$ transition of the imine nitrogen atom in conjugation with the phenoxy group. Furthermore the spectrum data in 400–500nm range wasused for obtaining stoichiometry and stability constants of $L^1$and L^2complexes with metal ions using HypSpec program as a new version of PHab program [2]and the corresponding distribution diagram depicted by Hyss program [3].The observed types of formation complexes between $L^1$and $L^2$and the cited metal ions ML, ML_2 or/and M_2L.

Conclusion:

Based on the reported results the stability of complexes of two ligands with metal ions follows the$L^1 > L^2$.

Reference:

[1]A.Shokrollahi, M.Ghaedi, S.Alipour, A.H.Kianfar, Spectrophotometric Study of Complexation between a Series of Salophens and Some Transition Metal Ions in DMF Solvent, European Journal of Chemistry, 2, 324-330, 2011.

[2] P. Gans, A. Sabatini, A. Vacca, Talanta 43,1739–1753, 1996.

[3]L. Alderighi, P. Gans, A. Ienco, D. Peters, A. Sabatini, A. Vacca,Coord. Chem. Rev. 184, 311, 1999

Voltammetric determination of cysteamine using multiwall carbon nanotubes paste electrode in the presence of 3,4-dihydroxycinnaminc acid as a homogeneous mediator

M. Keyvanfard[1*], S. Sami[2], K. Alizad[1], Behzad Rezaei[3], H. Karimi-Maleh[1]
[1]Department of Chemsitry, Majlesi Branch, Islamic Azad University, Isfahan, Iran
[2]Department of Chemistry, Shahreza Branch, Islamic Azad University, Isfahan, Iran
[3]Department of Chemistry, Isfahan University of Technology, Isfahan, Iran
Email: keyvan45638@yahoo.com

Key words: Cysteamine, Multiwall carbon nanotubes, Electrocatalysis, 3,4-Dihydroxycinnaminc acid.

Introduction:

Cysteamine is an aminothiol compound used as a drug for the treatment of cystinosis [1]. A number of long term clinical trials have shown that cysteamine administration (as cysteamine hydrochloride) stabilises renal function, delays glomerular deterioration and improves linear growth [2]. Also, the cysteamine and its disulfide, cystamine, have been shown to be neuroprotective in a number of cell culture and animal models [3].

Numerous methods have been reported for the determination of CA in pharmaceutical and biological samples including chromatography, electrophoresis, gas chromatography with flame photometric detection, and electrochemical methods using modified electrodes. However, Long response time, expensive instruments, complicated procedure, and low detection capability are the shortcomings associated with most such methods reporte

Materials and methods:

Spectrally pure graphite powder (particle size <50 μm) from Merck and multiwall carbon nanotubes (>90% MWCNTs basis, d × l = (110–70 nm) × (5–9 μm) from Fluka were used as the substrate for the preparation of the carbon paste electrode.

Results and discussion:

Figure depicts the cyclic voltammetric responses from the electrochemical oxidation of 500 μM CA at the MWCNTPE in the presence of 500 μM 3,4-DHCA (curve c), CPE in the presence of 3,4-DHCA (curve b), MWCNTPE (curve d), and CPE (curve e). As shown, the anodic peak potential for CA oxidation at the MWCNTPE in the presence of 3,4-DHCA (curve c) and CPE in the presence of 3,4-DHCA (curve b) was about 0.217 mV, while at the MWCNTPE (curve d), the peak potential was about 620 mV. At the unmodified CPE and without mediator, the peak potential was about 670 mV of CA (curve e). From these results, it was concluded that the best electrocatalytic effect for CA oxidation was observed at the MWCNTPE in the presence of 3,4-DHCA (curve c). For example, results show that the peak potential of CA oxidation at the MWCNTPE in the presence of 3,4-DHCA (curve c) shifted by about 403 and 453 mV toward negative values when compared with that at the MWCNTPE and CPE without mediator (curve d and e), respectively.

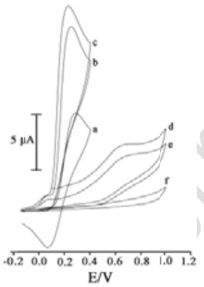

Figure: Cyclic voltammograms of 500 µM 3,4-DHCA at the surface of MWCNTPE in 0.04 M universal buffer (pH 4.0) at a scan rate of 10 mV s^{-1} in the absence and in the presence of 300 µM AC.

Conclusion:

The new voltammetric method for the determination of CA is very rapid, reproducible, selective and sensitive, and can be used for real sample analysis. The results show that the oxidation of CA is catalyzed at pH 7.0, whereas the peak potential of CA is shifted by 403 mV to a less positive potential at the surface of the MWCNTPE in the presence of mediator.

Reference:

[1] W.A.Gahl; "Early oral cysteamine therapy for nephropathic cystinosis"; European journal of pediatrics; 162,38-41,2003.

[2] J.G. Thoene; "Cystinosis"; Journal of inherited metabolic disease; 18,380-386,1995.

[3] P. Lochman, T. Adam, D. Fredecky, E. Hlidkova, Z. Stopover; "High-throughput capillary electrophoretic method for determination of total aminothiols in plasma and urine"; Electrophoresis 24,1200-1207,2003.

High selective and sensitive voltammetric sensor base on modified multiwall carbon nanotubes paste electrode and 3,4-Dihydroxycinamic acid for determination of ascorbic acid

M. Keyvanfard[a], R. Shakeri[b], K. Alizad[a] ,H. Karimi-maleh[c]
[a] Department of Chemistry, Majlesi Branch, Islamic Azad University, Isfahan, Iran
[b]Department of Chemistry, Shahreza Branch, Islamic Azad University, Isfahan, Iran
[c]Department of Chemistry, Science and Research Branch, Islamic Azad University, Mazandaran, Iran
E-mail: Keyvan45638@yahoo.com

Keywords: Ascorbic acid, 3,4-Dihydroxycinamic acid; Voltammetry; Carbon paste electrode; Multiwall carbon nanotubes

Introduction:

The interest in chemically modified electrodes (CMEs) has increased tremendously during the last decade owing to their potential applications and a large number of publications have been appeared [1].

Multiwall carbon nanotubes (MWCNTs) are now used extensively in the fabrication of novel nanostructure electrochemical sensors [2]. MWCNT-modified electrodes have many advantages over other forms of carbon electrodes due to high electrical and thermal conductivity, high chemical stability and high specific surface area which make them very promising candidates in a wide range of applications.

Materials and methods:

Vitamin C also is present in many other biological systems and multivitamin preparations, which are commonly used to supplement inadequate dietary intake. Nevertheless, it is widely used in foods as an antioxidant for the stabilization of color and aroma with subsequent extension of the storage time of the products [3].

The mediated oxidation of AA at the modified electrode was investigated by cyclic voltammetry (CV), chronoamperommetry.

Apparatus:

A carbon-paste electrode modified with multiwall carbon nanotubes (MWCNTs) was used for the sensitive and selective voltammetric determination of ascorbic acid (AA) in the presence of 3,4-dihydroxycinamic acid (3,4-DHCA) as mediator. Also, the values of catalytic rate constant (k), and diffusion coefficient (D) for AA were calculated.

Conclusion:

A new votammetric sensor developed for the determination of AA is very rapid, reproducible, highly selective and sensitive, and can be used for real sample analysis. This mediator shows excellent catalytic effects on the oxidation of AA. The results show that the oxidation of AA is catalyzed at pH 6.0, whereas the peak potential of AA is shifted by 140 mV to a less positive potential at the surface of the MWCNTPE in the presence of mediator.

Reference:

[1] Z. Gao, K.S. Siow, A. Ng, Y. Zhang, Anal. Chim. Acta 343 (1997) 49-57.
[2] J.B. Raoof , R. Ojani, F. Chekin, J. Electroanal. Chem. 633 (2009) 187–192.
[3] D.W. Martin, Jr., in: D.W. Martin, Jr., P.A. Mayes, V.W. Rodwell (Eds.), Harpers Review of Biochemistry, 19th ed., Lange, Los Altos, CA, 1983, p. 112.

Potentiometric study of complexation between Co^{2+} and pydc/2-apym proton transfer and comprising with solid state results

A. Shokrollahi[a*], Z. Fatemi[a], N. Shokrollahi[a], Z. Malekhosseini[a,b]
[a]Department of Chemistry, Yasouj University, Yasouj, Iran
[b]Young Researchers Clubs, Yasouj Branch, Islamic Azad University, Yasouj Iran
E-mail : ashokrollahi@mail.yu.ac.ir

Keywords: Pyridine-2,6-dicarboxylic acid, 2-Aminopyrimidine,, Solution studies, potentiometric

Introduction:

The different aspects of proton transfer systems have been studied by chemists in the recent years [1]. An interesting report in this area was investigation of the mechanism of proton transfer from intra-molecularly hydrogen-bonded acids and differences between nitrogen-to-oxygen and nitrogen-to-nitrogen proton transfer. Some examples of proton transfer polymerization have been also reported.

We have previously reported the protonation constants of Pyridine-2,6-dicarboxylic acid(pydc), 2-Aminopyrimidine(2-apym) species and the equilibrium constants for the proton transfer formation between them in several protonated forms in aqueous solution [2].In this work the stoiciometry and stability of complexation of this system with Co^{2+}ion in aqueous solutions. The stoichiometry of the most species in solution was compared to the corresponding crystalline cited complexes.

Materials and methods:

For the potentiometric *p*H titrations of pydc, 2-apym and pydc-2-apym in the absence and presence of 1.25×10^{-3} metal ion The concentration of pydc and 2-apym was set as 2.5×10^{-3} M for metal ion respectively. A standard carbonate-free NaOH solution (0.0951 M) was used in all titrations. The ionic strength was adjusted to 0.1 M with $NaNO_3$.

Apparatus:

A Model 794 Metrohm Basic Titrino was attached to an extension combined glass-calomel electrode mounted in an air-protected, sealed, thermostated jacketed cell maintained at 25.0 ±

0.1 °C by circulating water, from a constant-temperature bath Fisherbrand model FBH604, LAUDA, Germany, equipped with a stirrer and a 10.000-mL-capacity Metrohm piston burette. The *p*H meter-electrode system was calibrated to read -log $[H^+]$.

Result and discussion:

In order to evaluate the stoichiometry and stability constant of Co^{2+}complexes with pydc-2-apym association in aqueous solution, the equilibrium potentiometric *pH* titration profiles of pydc, 2-apym and their 1:1 mixture were obtained in the absence and presence of the Co^{2+}ion.. It was found that 2-apym forms relatively weak complexes with Co^{2+} ionsand considerable complexes with pydcacoording our previous report .The potentiometric *pH* titration curves of pydc, 2-apym and their corresponding 1:1 mixture in the presence of Co^{2+} ion were fitted to the BEST program in order to evaluate cumulative stability constants of the likely complex species in solution.

Conclusion:

It is interesting to note that the stoichiometries of the some of the most abundant ternary complexes such as CoLQH existing in solution are very similar to those reported for the corresponding isolated complexes in the solid state.

Reference:

[1] F.He et al ; “ Evidence for an intermolecular proton-transfer reaction induced by collision in gas-phase noncovalently bound complexes ” ;Journal of American Chemical Socity ; 121 , 4726-4727, 1999.

[2] H. Eshtiagh Hosseini and etal "Structural aspects and solution behavior of etallosupramolecular compound of FeIII ion obtained by proton transfer" ; Journal of Coordination chemistry ; 64 , 3969-3979, 2011.

Potentiometric studies of four new mixed inorganic-organic hybrid materials-based preyssler and wells-dawson heteropolyoxometallates some amino acids

A. Shokrollahi[a*] , Z. Fatemi[a], Z. Malekhosseini[a,b], M. Mirzaei[c],
[a] Department of Chemistry, Yasouj University, Yasouj, Iran
[b]Young Researchers Clubs, Yasouj Branch, Islamic Azad University, Yasouj Iran
[c] Department of Chemistry, Faculty of Sciences, Fedowsi University of Mashhad, Mashhad, Iran
E-mail : ashokrollahi@mail.yu.ac.ir

Keywords: Amino acids, Wells-Dawson, Inorganic-organic hybrid, Potentiometric study

Introduction:

There exists growing interest in metal oxide clusters, or polyoxometallates (POM) reflecting their diverse properties, which endow them with applications in the fields such as catalysis, medicine, analytical chemistry and photochemistry. Contemporarily, POMs are found to be extremely versatile inorganic building blocks for constructions of organic–inorganic hybrid materials with new structures and unusual properties [1].

Anion coordination chemistry and molecular recognition of anionic substrates are of great interest for analytical and inorganic chemist [2]. Interest in the coordination chemistry of anionic substrates continues to attract the attention of the supramolecular chemistry community.

In this work we interest to study the interaction between dawson as a polyoxometallate anion and some amino acids including alanine, aspargine. glycine and glutamine in binary and ternary systems potentiometrically.

Materials and methods:

The concentration of each of amino acids was 0.002 M, for the potentiometric *p*H titrations of alone and binary of them in the absence and presence of 0.002 M Wells-Dawson. A standard carbonate-free NaOH solution (0.09435 M) was used in all titrations. The protonation constants of ligands and stability constants of proton transfer and their metal complexes were evaluated using the BEST program.

Apparatus:

A Model 794 Metrohm Basic Titrino was attached to an extension combined glass-calomel electrode mounted in an air-protected, sealed, thermostated jacketed cell maintained at 25.0 ± 0.1 °C by circulating water, from a constant-temperature bath Fisherbrand model FBH604, LAUDA, Germany, equipped with a stirrer and a 10.000-mL-capacity Metrohm piston burette.

Result and discussion:

In preliminary experiments, the fully probability protonated forms of amino acids and dawson as the building blocks of binary and ternary hybrids , were titrated with a standard NaOH aqueous solution to obtain some information about their protonation constants. The protonation constants of amino acids and Wells-Dawson were calculated by fitting the pH-volume data by using BEST program. The evaluation of the equilibrium constants for the reactions of amino acids with each other in different protonation forms, was accomplished through comparison of the calculated and experimental *p*H profiles, obtained with both of them. In order to determine the stoichiometry and stability of Wells-Dawson binary and ternary hybrid with amino acids in aqueous solution, solutions of amino acids alone and 1:1 mixture of alanine/glycine, alanine/glutamine, aspargine/glutamine and glycine/glutamine in the absence and presence of Wells-Dawson were titrated with 0.09435 M solution of NaOH.

Conclusion:

Potentiometric study results for inorganic-organic hybrids including Dawson-aminoacids was comparable with solid state results.

Reference:

[1] M.H. Alizadeh etal . ; " Triprolinium 12-phosphomolybdate: Synthesis, crystal structure and properties of $[C_5H_{10}NO_2]_3[PMo_{12}O_{40}] \cdot 4.5H_2O$ " ; Polyhedron ; 25, 1567-1570, 2006.

[2] R.J. Motekaitis etal . ; " Molecular recognition by protonated O-BISDIEN and its metal complexes " ; inorganic chemical ; 31, 5534-5542, 1992.

Co-adsorption effect of oleic immidazoline and thiourea on the corrosion of carbon steel inCO2-saturated solution

S.M.A.Hosseini, A.Azimi, M.J.Bahrami
Department of Chemistry,Faculty of Science,Shahid Bahonar University of Kerman
Email : Ahmad.azimy@gmail.com

Keywords: Corrosion inhibitor; Synergistic effect; adsorption; CO2 corrosion

Introduction:

Carbon steels are the most commonly used construction materials for pipelines in the oil and gas industry. They are, however, very susceptible to corrosion in environment containing CO2 [1]. Carbon dioxide corrosion of carbon steel pipelines and equipment in the oil and gas industry has been given much attention in recent years because of an increased tendency to inject CO2 into oil wells to reduce the viscosity of oil and increase its production [2, 3]. An important fact is that when CO2 dissolves in water, carbonic acid (H2CO3) is produced with the characteristic that is more aggressive than hydrochloric acid at the same pH [4]. The problems arising from CO2 corrosion have led to the development of various method of corrosion control which includes the injection of corrosion inhibitors that has proven to be a practical and economical method to control CO2 corrosion [5]. These organic compounds inhibit the corrosion of mild steel by adsorption on the metal-solution interface thereby creating a barrier that prevents the active ions in the corrosion reactions to get to the surface [6]. Thiourea (TU) and its derivatives have been studied for more than four decades because they inhibit the corrosion of steels and are superior to amine-based inhibitors in acidic media [7–9]. However, thiourea is seldom used in a neutral medium because of its inefficiency [10]. In this research the adsorption and inhibition effect of two corrosion inhibitor (OI and TU) on carbon steel surface in CO2-saturated 3% NaCl solution were studied and then, co-adsorption effect of them investigated.

Experimental:

The OI inhibitor was synthesized using analytical grade of diethylene triamine and oleic acid. Fresh solutions of the 3% NaCl were prepared for each experiment using analytical grade of

NaCl and distilled water. Testing solution was deaerated by purging CO2 until the pH was constant (1 hour prior to experiment). Before each test, the open circuit potential was stabled within 30 min. CO2 gas was allowed to bubble into the solution at a low flow rate to ensure entire saturation during the test. Working electrode was prepared from a cylindrical rod cut from a 1018 carbon steel rod. The concentration range of inhibitor was 1-10 ppm for OI and 5-100 ppm for TU. Before each experiment the carbon steel samples were abraded using emery papers (grades 800-2000), washed with distilled water and mixture of methylen chloride and acetone, and finally dried at room temperature [11]. Measurements were carried out using IVUIM ELECTROCHEMICAL ANALYSIS SYSTEM equipped with a tree-electrode cell. A saturated calomel electrode was used as a reference electrode and a Pt electrode as a counter. Working electrodes were prepared in such a way that the exposed area was 1cm2. The impedance measurements were carried out under potentiostatic conditions at corrosion potential.

Conclusions :

The IR and 1HNMR results indicated that the OI inhibitor was prepared correctly. The EIS results show a decrease in the double layer electrochemical capacitance values (Cdl), and an increase in the charge transfer resistant (Rt) and inhibition efficiency values (IEEIS%) with increasing in concentration of compounds. Both OI and TU inhibitors act as anodic inhibitors and the mixture acts as a mixed-type inhibitor. Presence of TU can improve the inhibition efficiency of OI inhibitor on the carbon steel surface in CO2-saturated 3% NaCl solution. The IE% values obtained from polarization measurements are consistent with those obtained from EIS and LPR methods.

References:

[1] D. A. Lopez, S. N. Simison, S. R. de Sanchez, Electrochim. Acta 48 (2003) 845.
[2] X. Jiang, Y. G. Zheng, D. R. Qu, W. Ke, Corr. Sci. 48 (2006) 3091.
[3] F. Farelas, A. Ramirez, Int. J. Electrochem. Sci., 5 (2010) 797 – 814
[4] G. Zhang, C. Chen, M. Lu, C. Chai, Y. Wu, Mater. Chem. Phys. 105 (2007) 331.
[5] S. Ramachandran, V. Jovancicevic, Corrosion 55 (1999) 259.
[6] X. Liu, P. C. Okafor, Y.G. Zheng, Corr. Sci. 51 (2009) 744–751.

[7] B. G. Ateya, B. E. El-Anadouli, F. M. El-Nizamv, Corr. Sci. 24 (1984) 509-515.

[8] R. Agrawal, T. K. G. Namboodhiri, Corr. Sci. 30 (1990) 37-52.

[9] S. S. Abdel-Rehim, K. F. Khaled, N. S. Abd-Elshafi, Ele. Chim. Acta 51 (2006) 3269–3277.

[10] J. C. LIN, H. C. Shih, Corr. Sci. 27 (1987) 839-858.

[11] ASTM. G 5 – 87, 1987.

Fabrication of nickel and Pt-Ni particle/carbon paper electrocatalysts for electrooxidation of methanol in alkaline medium

Rasol AbdullahMirzaii*[a], Mohammad Safi Rahmanifar [b],AbolfathEshghi [a]
[a]*Department of Chemistry, ShahidRajaee Teacher Training University, Tehran, Iran*
[b]*Shahed University, Tehran, Iran*
*(Email:*ra.mirzaei @ srttu.edu*)*

Keywords: Nickel, Carbon paper, Platinum, Electro-catalysis, direct methanol fuel cell

Introduction:

The development of alternative power sources is an important issue at present. Fuel cells are attractive sources of electrical power since they realize the direct conversion of chemical into electrical energy. Direct methanol fuel cells (DMFC) are expected to be the first fuel cells to provide a power source for portable electronic devices, such as mobile phones, laptop computers and advanced mobile electronic devices. Since it requires little additional equipment compared to the extensive gas process technology for methanol reforming, the fuel is best transported and converted into energy from the liquid state [1, 2]. However, the fuel cells could not reach the stage of commercialization due to the high cost which was mainly associated with the noble. Nowadays, all pre-commercial, low-temperature fuel cells use supported Pt and Pt alloys as electro-catalysts. Critical properties to consider when choosing an electro-catalyst support include its electrical conductivity, surface area, microstructure, corrosion resistance and cost. In order to reduce the amount of noble metal loading and also for enhancement of electro-catalytic activity of electrodes, there have been considerable efforts to increase the dispersion of the metal particles on the support. In the present study, we pretreated carbon paper and prepared electro-catalysts, and then characterized these supporting nickel and Pt-Ni electro-catalysts in order to find out better catalysts for DMFC. The electro-activity of these electro-catalystsfor the methanol oxidation in alkaline solutions was studied by different electrochemistry methods.

Materials, methods and Apparatus:

Methanol (Merck, 99.8% purity) and KOH (Merck, 84% purity) were used as received. All other chemicals were of analytical grade and used without further purification. Distilled water was used throughout. The electrochemical experiments were performed in a three-electrode cell arrangement. A platinum sheet was used as counter electrode, while all potentials were measured with respect to Ag/AgClelectrode. Electrochemical experiments were carried out using Zahner and EG&G PARSTAT 2263 Advanced Electrochemical systems.

Result and discussion:

Nickel and Pt-Ni particles were deposited on the carbon paper by cyclic voltammetry and electrodeposition method. SEM images of new electro-catalysts show that the nickel and Pt–Ni particles are distributed on the surface of the carbon paper. In order to compare Ni/carbon paper with Pt-Ni/carbon paper, the CV method was used to estimate the behavior of the electro-catalysts. The results indicate these improve the electro-catalytic activity for methanol oxidation greatly and confirmed the good electro-catalytic activity and stability of these electro-catalysts.

Conclusion:

Ni/carbon paper with Pt-Ni/carbon paper with good electro-catalytic property has been successfully fabricated. The morphology and surface analysis of electro-catalysts were investigated by SEM and EDX, respectively. The electro-catalytic activity oftheseelectro-catalysts for methanol oxidation was evaluatedby various electrochemical methods. These electro-catalysts showed high currents formethanol oxidation and good electro-catalytic activity. So it can be said that this electro-catalysts show great prospect in the applications of alcohol fuel cells.

Reference:

[1] Y. Wang, C.Y. Wang, K.S. Chen; " Elucidating differences between carbon paper and carbon cloth in polymer electrolyte fuel cells". ElectrochimActa; 3965-3975, 52, 2007

[2] L.R. Jordan, A.K. Shukla, T. Behrsing, N.R. Avery, B.C. Muddle, M. Forsyth; "Effect of diffusion-layer morphology on the performance of polymer electrolyte fuel cells operating at atmospheric pressure". J ApplElectrochem ;641-646, 30, 2000
[3] Paganin VA, Ticianelli EA, Gonzalez ER. Development of electrochemical studies of gas diffusion electrodes for polymer electrolyte fuel cells. J ApplElectrochem 1996;26:297–304.

The inhibition effect of a new Schiff base on mild steel in 2 M HCl. A complete study: Adsorption, temperature, duration and quantum chemical aspects

N. Soltani*, H. Salavati, M. Paziresh, N. Rasouli
Department of Chemistry, Payame Noor University, PO Box 19395-3697 Tehran, IRAN.
* E-mail: nasrin_soltani2056@yahoo.com

Key words: Mild steel, EIS, Polarisation, Acid corrosion

Introduction:

Iron and its alloys are widely used in industry. Mild steel is one of the important iron containing alloy used in different applications and is susceptible to corrosion due to its thermodynamic instability especially in aggressive media [1]. In order to reduce the degree of metal attack and rate of consumption of the acid, corrosion inhibitors are added to the pickling solutions. Most of the well known acid inhibitors are organic compounds containing nitrogen, sulphur and/or oxygen atoms, which allow an adsorption on the metal surface [2, 3]. In this study, The inhibition of corrosion of mild steel in 2 M HCl by a Schiff base (Fig. 1) have been investigated using weight loss method, electrochemical techniques (potentiodynamic polarization and electrochemical impedance spectroscopy (EIS)). Effect of temperature on the mechanism and also on the efficiency of the corrosion inhibition process was studied using the Arrhenius approximation of the rate law. Polarization experiments were performed at different solution temperatures. Thermodynamic parameters for the corrosion process were obtained and interpreted. The adsorption of the inhibitor, on the steel surface in the acid medium (2 M HCl) obeyed the Langmuir adsorption isotherm.

Materials and methods:

The employed working electrodes were prepared from a mild steel plate with the chemical composition (wt.%) of: C (0.027), Si (0.0027), P (0.009), Al (0.068), Mn (0.340), S (0.007), Nb (0.003), Cu (0.007), Ni (0.030), Ti (0.003), Cr (0.008), V (0.003) and Fe (balance). The aggressive solution of 2 M HCl was prepared by dilution of analytical grade HCl purchased from Merck. AR grade HCl (37%) and distilled water was used for preparing test solutions for all experiments.

Apparatus:

Electrochemical experiments were carried out using AUTOLAB model PGSTAT 35. The three-electrode cell consists of the mild steel sample as working electrode, a platinum as counter electrode, and saturated Ag/AgCl as reference electrode. Working electrode was first immersed into the test solution for 30 min to establish a steady state open circuit potential.

Result and discussion:

Anodic and cathodic polarization curves and Nyquist curves for mild steel in 2M HCl with and without various concentrations of Schiff base are shown in Fig 2. Potentiodynamic polarisation results revealed that Schiff base in HCl solution acted as a mixed-type inhibitor, which decreases the cathodic, anodic, and corrosion currents to a great extent. EIS measurement results indicate that the resistance of the mild steel electrode increases greatly and its capacitance decreases by increasing the inhibitor concentration.

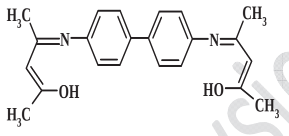

Fig. 1 Chemical structures of Pyrimidine-2-thione derivatives

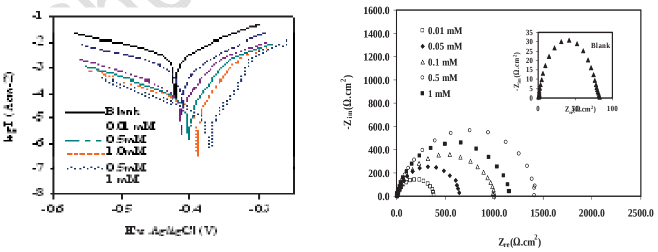

Fig. 2. Right:Polarization curves for mild steel in 1 M HCl in the absence and presence of different concentrations of Schiff base and left Nyquist curves at

Conclusion:

The effect of temperature on corrosion inhibition efficiency of Schiff base has been investigated, showing that the inhibition efficiency decreases with increasing temperature. The SEM analyses indicate that copper corrosion can be inhibited evidently due to the adsorption of Schiff base on the copper surface. The quantum chemical study shows that the nitrogen and oxygen atoms in the Schiff base molecule are the main active sites that result in adsorption of Schiff base on the steel surface.

Reference:

[1] M.K. Pavithra, T.V. Venkatesha, K. Vathsala, K.O. Nayana, Corros. Sci. 52 (2010) 3811–3819.

[2] Y. Tang, X. Yang, W. Yang, R. Wan, Y. Chen, X. Yin, Corros. Sci., 52 (2010) 1801–1808.

[3] X. Li, Sh. Deng, H. Fu, Corros. Sci. 52 (2010) 3413–3420.

Electrochemical study on the effect of a double Schiff base and its cobalt complex on the acid corrosion of carbon steel

N. Soltani*, H. Salavati, M. Paziresh, N. Rasouli
Department of Chemistry, Payame Noor University, PO Box 19395-3697 Tehran, IRAN.
* E-mail: nasrin_soltani2056@yahoo.com

Key words: Schiff base, Complex, Corrosion inhibition, Carbon steel

Introduction:

The use of inhibitors is one of the most practical methods to secure metals against acid corrosion. Most of the well known acid inhibitors are organic compounds containing nitrogen, sulphur, and oxygen atom [1, 2].Schiff bases generally become effective corrosion inhibitors due to the presence of an imine (–CH=N) group and conjugated double bonds. Besides the imine group, substitution of different groups also affects the inhibition properties [3]. The ability of donor-molecules to form stable complexes closely packed in the coordination sphere of metal ion introduces another class of compounds for corrosion inhibition. However, studies about the effect of metal complexes as corrosion inhibitor for steel in acid solution appeared in the literature are extremely limited. The aim of the present work is to study the corrosion behaviour of carbon steel in 2 M hydrochloric acid in the presence of a Schiff base-[4-((1E)-2-(2-pyridil)-1 azaviniyl)phenyl](1Z)-2-(2-pyridil)-1-azaethene and its corresponding cobalt complexes.

Materials and methods:

Tests were performed on Q235 C-steel specimens with the composition (in wt.%) C 0.17%, Mn 0.46%, Si 0.26%, S 0.017%, P 0.005%, and Fe balance. The aggressive solution (2 M HCl) was prepared by dilution of analytical grade 37% HCl with distilled water.

Apparatus:

The electrochemical measurements were carried out using AUTOLAB model PGSTAT 35. The electrochemical cell consisted of a conventional three-electrode configuration with a platinum sheet as the counter electrode and a saturated silver–silver chloride (Ag/AgCl) electrode as the reference electrode. The working electrode was cut from a Carbon steel rod with cross-section area of 1 cm^2 and embedded in an epoxy resin holder. Before the potentiodynamic polarization and EIS measurements, the working electrode was immersed in the test solution at open circuit potential (OCP) for 1 h until a steady state was reached. The polarization curves were obtained from -0.50 V (vs. OCP) to +0.50 V (vs. OCP) at a sweep rate of 0.5 mV s^{-1}.

Result and discussion:

The potentiodynamic polarization curves and Nyquist plots for steel in 2.0 M hydrochloric acid solution containing different concentration of complex are shown in Fig. 1. The Nyquist plots (Fig. 1-a) indicate that the dissolution process occurs under activation control. The potentiodynamic polarization curves indicate that complex can be classified as mixed type inhibitor. The same results were obtained for Schiff base, but the inhibition efficiency complex is higher than ligand.

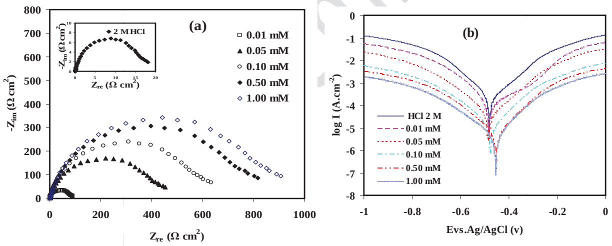

Fig. 1: (a) Nyquist plots for steel and (b) polarization curves in 2.0 M hydrochloric acid solution containing different concentration of complex

Conclusion:

Potentiodynamic and EIS measurements indicated that Schiff base and Co(Schiff base) complex are predominantly mixed-type inhibitors. The inhibitive effect of Schiff base and Co(Schiff base) complex was attributed to the adsorption over the metal surface via the free adsorption centers in the molecule. Theoretical fitting of different isotherms, Langmuir, Flory–Huggins and the kinetic–thermodynamic model were tested to clarify the nature of adsorption. The best fit for inhibitors adsorption is obtained using the Langmuir isotherm model.

Reference:

[1] M. Behpour, S.M. Ghoreishi, N. Soltani, M. Salavati-Niasari, Corros. Sci. 51 (2009) 1073–1082.

[2] R.A. Prabhu, T.V. Venkatesha, A.V. Shanbhag, G.M. Kulkarni, R.G. Kalkhambkar, Corros. Sci. 50 (2008) 3356–3362.

[3] Y. Tang, X. Yang, W. Yang, R. Wan, Y. Chen, X. Yin, Corros. Sci. 52 (2010) 1801–1808

Fe(III) ion selective electrode based on a new macrocyclic ionophore as a neutral carrier

M. H. Fekri[a,] , R. Aminameli[b*] ,H. Shafie[c] ,M. Darvishpour[d] ,H.Khanmohammadi[e]

[a] Department of Chemistry, Islamic Azad University, Khorramabad Branch, Khorramabad, Iran.
[b]Department of Chemistry, Islamic Azad University, Saveh Branch, Saveh, Iran.
[c]Department of Chemistry, Islamic Azad University, Arak Branch, Arak, Iran.
[d] Department of Chemistry, Razi University, Kermanshah, Iran.
[e]Department of Chemistry, Arak University, Arak, Iran.
[*]E-mail: raminameli@yahoo.com

Keywords: Ion selective electrode, PVC membrane, Fe(III) determination

Introduction:

Ion selective electrodes (ISE$_s$) are membrane electrodes that respond selectively to ions in the presence of others. These include probes that measure specific ions and gasses in solution. The most commonly used ISE is the pH probe. For this type of electrodes, the formation constant of the ion-ionophore complex within the membrane phase is very important parameter that dictates the practical selectivity of the sensor [1].

The ion selective electrode (ISE) approach to trace analysis is advantageous because of the speed and ease of ISE procedures in which little is required. Further, ISEs possess wide dynamic ranges, and are relatively low in cost. Ion selective electrodes based on neutral carrier ligands are well established for alkali and alkaline-earth metal cations [2].

Materials and methods:

All of reagents and solvents involved in synthesis were of analytically grade a received without further purification. Tetrahydrofuran (THF), acetophenone (AP), oleic acid (OA), high relative molecular weight PVC were obtained from Aldrich and Merck. a new macrocyclic ionophore (Fig.1).

Chloride and nitrate salts of all other cations and detergent used (all from Merck or Fluka) were of the highest purity available and used without any further purification.

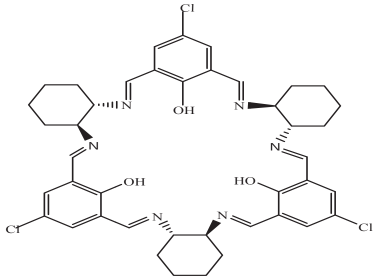

Figure 1. Structure of H_3L.

Apparatus:

Potentiometric and pH measurements were carrid out using a metrohm digital pH/mV meter ion analyzer in stirred solution. In all instances, an Ag-AgCl / KCl (sat.) electrode (Azar electrode company, Urmia, Iran) was used in conjucation with the respective indicator electrode. A Haoke model FK2 circulation water bath was used control the temperature of the test solution.

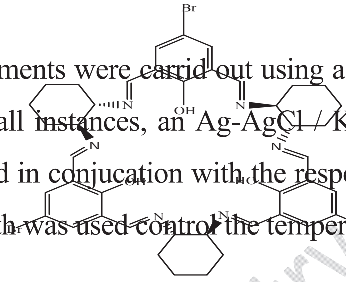

Result and discussion:

It is well Known that the sensitivity and selectivity of the ion-selective sensors not only depend on the nature of ionophore used, but also significantly on the membrane composition and the properties of plasticizers and additives used [3]. Thus, the influences of the membrane composition, the nature and amount of plasticizers and amount of oleic acid as an additive on the potential response of the Fe(III) sensor were investigated.

Among the different composition studied, incorporating 28.5 % PVC, 62.9 % AP, 5.7 % OA and 2.9 % ionophore shows the best sensitivity. The calibration plot is shown in Fig. 2, which indicates a linear range from 1.0×10^{-5} to 1.0×10^{-1} M Fe(III) with a Nernstian slope of 19.4 ± 0.5 mV/decade of Fe(III) concentration.

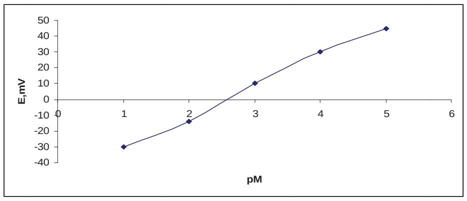

Fig. 2. Calibration plot of the Fe(III)-ISE based on H_3L.

Conclusions:

The membrane sensor incorporating H_3L as the electroactive phase can be used to determine Fe(III) in the wide concentration range. The sensor exhibited good reproducibility over a useful lifetime about 2 months.This electrode is supervior to the existing electrodes with regard to the slope, pH range, response time and selectivity over a number of cation.

References:

[1]. M. Oehme, W.Simon, Anal. Chim. Acta, 86 (1976) 21.
[2]. P.C. Meier, W.E. Morf, M. Laubli, W. Simon, Anal. Chim. Acta, 156 (1984) 1.
[3]. S. Kamata, A. Baliale, Y. Fukonaga, A. Murata, Anal. Chem., 60 (1988) 2464.

Investigation of inhibition effect of 3-(2-Chlorophenyl)-4-(4-nitrophenyl)-1H-1,2,4-triazole-5(4H)-thione against copper corrosion in ZnO nanofluid

Z.Shahri[a*] ,S. Asgharrezaei [a], A.Hassanzadeh[b]
[a] Payamnor University, Urmia Branch, Urmia, Iran
[b] Department of Chemistry, Faculty of Science, Urmia University, Urmia, Iran
Email: shahri_zeinab@yahoo.com

Key words: Nanofluid, Corrosion, Copper, Inhibitor.

Introduction:

Nanofluids are new engineered materials with great potential to handle thermal limitation of common thermal fluid (such as water, industrial oil and so on) for using in heat transfer equipments and electrical devices. An important overlooked practical feature of nanofluids is how these nanoparticles in the fluid impact on the corrosion rates of the metals that are in contact with the nanofluids. Corrosion inhibitors are widely used in industry to reduce the corrosion rate of metals and alloys incontact with aggressive. Most of the corrosion inhibitors are synthetic chemicals, expensive and very hazardous to environments. Therefore, it is desirable to source for environmentally safe inhibitors. There are some reports on the inhibition effects of non-toxic compounds on the corrosion of metals.

In the present work, the inhibition effect of 3-(2-Chlorophenyl)-4-(4-nitrophenyl)-1H-1,2,4-triazole-5(4H)-thione (Cl-ph) as non-toxic compounds on the copper corrosion in ZnO nanofluid was studied. ZnO nanoparticles synthesized then potentiodynamic polarization method and weight-loss measurement were used to evaluate the inhibition efficiencies.

There is not any report of this view that to investigation of copper corrosion and inhibition effect of (cl-ph) against copper in ZnO nanofluid so far [1-5].

Materials and methods:

Potassium hydroxide, zinc acetate dehydrate from Merck Chemical Co.(Germany) and methanol from Applichem Co.(Germany) were used to produce nanofluids. The 3-(2-

Chlorophenyl)-4-(4-nitrophenyl)-1H-1,2,4-triazole-5(4H)-thione were provided by the Research Institute of Nano (Urmia, Iran).

Apparatus:

The particles size of the synthesized particles of ZnO were examined by Scanning Electron Microscope (SEM) [Model:JSM5610LV,version 1.0, made by Jeol, Japan] and XRD [Model: X PERTPRO, made by PANalitical company].The current-potential curves were recorded using a potentiodynamic apparatus [Autolab-Metrohm, Model:PGSTA12,version 49, made by Netherlands] connected to a personal computer.

Result and discussion:

The SEM images of the ZnO nanoparticle shows the average size of nanoparticles around 54.65 nm. Polarization curves for the effect of different concentration of inhibitor and the different agitation speed on the potentiodynamic behavior of copper in ZnO nanofluid were recorded. Corrosion data were determined by extrapolation of the cathodic and anodic Tafel region.The result shows that with increasing inhibitor concentration and agitation speed, the corrosion current density and corrosion rate decrease, respectively. Therefore inhibitor adsorption to metal surface increases and protects metal from corrosion.The weight loss of copper samples in ZnO nanofluid in the presence of different concentrations of inhibitor for 30 days was determined. When the inhibitors concentration are increased the part of copper surface that covered by inhibitor molecules increases, leads to an increase in IE.

Conclusion:

It was found that 3-(2-Chlorophenyl)-4-(4-nitrophenyl)-1H-1,2,4-triazole-5(4H)-thione largely inhibits copper corrosion, due to the formation of a protective layer on the copper surface. For the effect of stirring, the polarization measurements showed that increasing stirring from 0 to 1000 rpm accelerated the corrosion current density of the metal from 0.65 to 0.23 $\mu A/cm^2$. The thermodynamic functions of corrosion indicate that of the investigated compound adsorbs on the copper surface by a physisorption-based mechanism involving a spontaneous and exothermic process.

Reference:

[1] M.Kamal-Ahmadi etal;" MWCNT nanofluid enhancement of copper corrosion "

[2] H.Ashassi-Sorkhabi and etal;" Investigation of inhibition effect of some amino acids against steel corrosion in HCl solution; "Applied Surface Science ; 225,176–185, 2004.

[3] H.Ashassi-Sorkhabi1 and etal;" The inhibition of steel corrosion in hydrochloric acid solution by juice of Prunus cerasus"; Int. J. Electrochem. Sci.; 1,92-98, 2006

[4] M.Scendo etal;"Inhibition Effect of 1-Butyl-4-MethylpyridiniumTetrafluoroborate on the Corrosion of Copper in Phosphate Solutions" ;International Journal of Corrosion; Volume 2011, Article ID 761418, 12 pages.

[5] Dazhi Sun and etal;" Purification and stabilization of colloidal ZnO nanoparticles in methanol "; J Sol-Gel Sci Technol ;43,237–243,2007.

Electrochemical ozone generation on the Ti/Sn-Sb-Ni as anode and improvement of electrocatalytic properties *via* carbon nano tube

Jalal BasiriParsa[a],Mahmoud Abbasi[a.b*] and Ann Cornell[b]
[a] Applied Chemistry Department, Faculty of Chemistry, Bu-Ali Sina University, Hamedan, 65178, Iran
[b]Applied Electrochemistry, Department of Chemical Engineering and Technology, KTH Royal Institute of Technology, SE-100 44 Stockholm, Sweden
[*] E-mail address: mahabbasi79@yahoo.com

Keywords: Carbon nano tube, Electrochemical ozone generation, Electrocatalytic

Introduction:

Electrochemical ozone production (EOP) has advantages over the classic corona method for ozone production, for examplehigh concentrations in the gas and liquid phases, simple system design and low voltage operation**.** In the electrochemical process, ozone is generated at the anode surface. However, ozone generation severely competes with O_2 evolution which is thermodynamically favorable. (seeEqs. 1 and 2):

$$3H_2O \rightarrow O_3 + 6H^+ + 6e^- \quad , \quad E^\circ = 1.52\ V\ vs.NHE \qquad (1)$$

$$2H_2O \rightarrow O_2 + 4H^+ + 4e^- \quad , \quad E^\circ = 1.23\ V\ vs.NHE \qquad (2)$$

Various anode materials have been studied for electrochemical ozone production such as platinum,PbO_2,Si/TiO_x/Pt/TiO_x,Pt-TaO_x, boron doped diamond (BDD),andglassy carbon.Recent reports on mixed oxide electrodes of Sn, Sb and Ni prepared by thermal decomposition on titanium show high current efficiency, depending on operating conditions, at moderate temperatures and anode potentials. The goal of the present work is to improve the electrocatalytic activity and efficiency of anodes for electrochemical ozone generation by using CNTs as a dopant in a Sn-Sb-Ni-CNT composite coating on a Ti substrate [1-3].

Materials and methods:

A titanium mesh (20 mm× 20mm) was degreased with acetone, rinsed in Millipore water, contacted with boiling oxalic acid for 1 hour and cleaned in an ultrasonic bath in Millipore water for 1 hour. Metal salts, $SnCl_4 \cdot 5H_2O$, $SbCl_3$ $NiCl_2 \cdot 6H_2O$ were dissolved in 99.5%

ethanol. In the case of CNT-composite preparation multi walled CNT with O.D:10-15nm, I.D:2-6nm and length 0.1-10µm were then added, and the solution was sonicated for 2 hours**.** The titanium mesh was coated by dipping, followed by drying at 110 ºC for 15 min, and then annealing at 520 ºC for 30 min. The molar ratio of Sn-Sb-Ni-CNT was controlled to be 500/8/1/10 in the coating solution. AnAg/AgCl (KCl sat.) electrode was used as the reference electrode and platinized titanium as counter electrode. Electrogeneration of ozone was performed galvanostatically in a jacketed undivided cell with volume 250 ml. Electrolysis experiments were carried out with potentiostat/galvanostat AUTOLAB PGSTAT 302N. The concentration of dissolve ozone was determined using a UV/Vis spectrophotometer.For the spectrophotometer 1 mg/ L dissolved ozone corresponds to an absorbance of 0.098 at the wavelength of 258 nm.X-ray diffraction (XRD) patterns of the coating films were recorded on a XRD instrument.Surface morphology was characterized using a Ultra-High Resolution FE-SEM Hitachi S-4800.

Result and discussion:

Nanocrystalline coatings of a Sn-Sb-Ni-CNT composite were applied on titanium mesh using a dip coating and annealing procedure, and investigated as anode material for ozone generation in perchloric acid. X-ray diffraction (XRD) and scanning electron microscopy (SEM) were used to reveal the electrode composition and morphology, and voltammetry and current efficiency measurements for electrochemical characterization. Addition of CNT resulted in coatings with a higher loading, a higher onset potential for oxygen evolution and in a higher current efficiency for ozone generation. A long term test of the CNT-containing electrodes at a constant current density (53.5 mA/cm^2) for 17 h indicated a stable anode potential.

Conclusion:

The addition of CNT resulted in coatings with a higher loading, a higher onset potential for oxygen evolution and in a higher current efficiency for ozone generation. The largest effect of CNT-addition on current efficiency was seen at low temperature and at high current density. Current efficiencies well over 20% were obtained for the CNT-containing coatings also which also indicated a relatively stable anode potential for at least 17 h at 53.5 mA/cm^2.

Reference:

[1]J. BasiriParsa and M. Abbasi, J. Solid State Electrochem.,16:1011–1018(2012).

[2]Y.H. Wang, S. Cheng, K.-Y. Chan and X.Y. Li, J. Electrochem. Soc., 152, D197 (2005).

[3]F. Hu, X. Cui, W.Chen, Electrochem.Solid-State.Let., 13, F20 (2010).

Electrochemical Noise Analysis of Pitting Corrosion of Aluminum 7075

R. Moshrefi, M. G. Mahjani*, M. Jafarian , A. Sharify
Department of Physical chemistry, K.N.T University, Tehran, Iran
Email: mahjani@kntu.ac.ir

Keyword: corrosion, electrochemical noise, pitting, wavelet transforms, Aluminum

Introduction:

Various concepts developed in the framework of wavelet transforms have been adapted to the analysis of electrochemical noise measurements (ENM). Wavelet transforms are proposed as an alternative tool to overcome the limitations of FFT in the analysis of ENM data.[1]

Wavelet analysis has been used as an indicator of specific corrosion mechanisms; different timescales of the current and potential signal could be attributed to diffusion, activation or mixed controlled processes. A relatively fast or slow process corresponds to smaller or larger timescales, respectively. The occurrence of metastable pitting is a small timescale process associated with initiation and growth of a pit embryo. This is generally assumed to occur prior to other types of localized corrosion, and therefore may be a considerably faster process than processes associated with larger timescales such as general corrosion, anodic dissolution, ion diffusion or removal of corrosion products. In addition, the relative energy distribution of medium timescale crystals may be associated with pitting propagation and growth.[2]

Materials and methods:

In this context, Electrochemical noise (EN) was measured during pitting corrosion in 3.5% NaCl solutions prepared using analytical reagents and distilled water at 23±1 temperature for type 7075 Aluminum for 10000 second. thereafter we examine application of time-frequency method as wavelet transforms to the analysis of stochastic signals of electrochemical noise. Test.

Apparatus:

The EN was monitored as a function of time between the working electrode and a saturated calomel electrode (SCE, reference) using a micro Autolab type II apparatus, which was controlled by GPES version 4.9 software using the Windows XP operating system. The analytical results for wavelet were obtained by specific data techniques Matlab R2011a software.

Result and discussion:

The EN data were analyzed by wavelet transform in terms of the energy contribution, Standard deviation and Entropy of smooth crystal and detail crystals. In the early stage of the tests, larger timescales such as general corrosion was prevailing, and contribution of smooth crystal to the total energy was greater than that of low frequency detail crystal, but with passing of time, localized corrosion got dominant.

Conclusion:

These results demonstrate that the onset of detailed processes in pitting can be sensitively detected by wavelet analysis in terms of the ED, SPDS or Entropy curves of smooth crystal and low and high frequency detail crystals.

Reference:

[1] Aballe, M. Bethencourt, F.J. Botana, M. Marc, ; "Using wavelets transform in the analysis of electrochemical noise data" ; Electrochimica Acta ; 44, 4805 -4816, 1999

[2] A.M. Homborg, T. Tinga, X. Zhang, E.P.M. van Westing, P.J. Oonincx, J.H.W. de Wit, J.M.C. Mol, ; " Time–frequency methods for trend removal in electrochemical noise data " ; Electrochimica Acta ; 70, 199- 209, 2012

[3] M.T. Smith, D.D. Macdonald, ; " Wavelet Analysis of Electrochemical Noise Data" ; Corrosion ; 438 – 448, 2009

[4] J.A. Wharton, R.J.K. Wood, B.G. Mellor, ; " Wavelet analysis of electrochemical noise measurements during corrosion of austenitic and superduplex stainless steels in chloride media" ; Corrosion Science ; 45, 97- 122, 2003

[5] J. J. Kim, ; " Electrochemical Noise Analysis of Localized Corrosion by Wavelet Transform"; Met. Mater. Int. ; 16, 747 – 753, 2010

[6] O. Duran, E. Vera, C. A. Ortiz and A. Heyn, ; " Use of the wavelet method for analyzing electrochemical noise data" ; Materials and Corrosion ; 58, 997 - 999 ,2007

[7] Chao Cai, Zhao Zhang, Fahe Cao, Zuoning Gao, Jianqing Zhang, Chunan Cao, ; " Analysis of pitting corrosion behavior of pure Al in sodium chloride solution with the wavelet technique" ; Electroanalytical Chemistry ; 578, 143 -150, 2005

Electrochemical removal of ammonium using carbon nanotube-carbon black-PTFE-coated cathode

R. DarvishiCheshmehSoltani[a*],A. Rezaee[a], A. R. Khataee[b]
[a]Department of Environmental Health, Faculty of Medical Sciences, Tarbiat Modares University, Tehran, Iran
[b]Department of Applied Chemistry, Faculty of Chemistry, University of Tabriz, Tabriz, Iran.
Email: rezadarvish86@yahoo.com

Keywords: Electrochemistry, Carbon black, Carbon nanotube, Ammonium

Introduction:

Ammonium generated from several industries exerts harmful effects on aqueous environments such as rivers and lakes[1]. Electrochemical conversion has been considered as a promising technique for the removal of ammonium from different wastewaters.By indirect transformation, oxidants are produced in an electrochemical reactor containing NaCl as an electrolyte. To enhance the efficiency of the electrochemical process, effective modification of electrodes can be performed with a suitable electronic conductor such as carbon black (CB) and carbon nanotubes (CNTs)[2]. Therefore, in the present study, the abilities of carbon black and carbon nanotubes to enhance the electrochemical properties for oxidation of ammonium were utilized. To achieve valuable results regarding the efficiency of the combined system for ammonium removal, response surface methodology (RSM) based on central composite design (CCD) was used due to its advantages over the conventional "one-at-a-time" method

Materials and Methods:

Multi-walled carbon nanotubes were provided by the Research Institute of Petroleum Industry, Iran. The carbon black (CB) used in this study was obtained from Vulcan XC72R (Cabot Co., USA). The coating materials (CB and CNT) were bonded to the surface of the graphite used as a cathode by a polytetrafluoroethylene (PTFE) binder purchased from ElectroChem Co., USA.The reactor was a glass cylinder equipped with a water jacket and appropriately installed devices for the recirculation of the solution throughout the reactor.

The electrochemical process was conducted using a DC power supply to produce an electric current between a Pt anode and CNT-CB-PTFE-coated graphite cathode. Recirculation of the solution and water jacket was carried out with two identical peristaltic pumps.

Result and discussion:

The results showed that the current of the CNT-CB-PTFE-coated cathode was significantly higher than that of the non-coated graphite cathode under the same cathodic potential. Comparatively, the cathodic currents at -2 V were -100 and -500 for the non-coated and CNT-CB-PTFE-coated cathode, respectively. The high coefficients (R^2=0.976 and adjusted R^2=0.954) obtained by analysis of variance (ANOVA) demonstrated closely fitted predicted and experimental values. For 79% ammonium removal, the optimal initial ammonium concentration, reaction time, current intensity and initial pH were 148 mg NH_4-N/L, 97 min, 577 mA and 6.5, respectively.

Conclusion:

Compared to the non-coated graphite cathode, the CNT-CB-PTFE-coated graphite possessed a significantly higher activity according to the cathodic polarization plot.The results indicate that the present process can be applied for the efficient removal of ammonium from aqueous solutions.

References:

[1] K.-W. Kim, Y.-J. Kim, I.-T. Kim, G. Park, II, E.-H. Lee, Electrochemical conversion characteristics of ammonia to nitrogen, Water Research, 40, 1431-1441, 2006.
[2] R. Dominko, M. Gaberscek, J. Drofenik, M. Bele, S. Pejovnik, J. Jamnik, The role of carbon black distribution in cathodes for Li ion batteries, Journal of Power Sources, 119-121, 770-773, 2003.

Evaluation of mild carbon steel corrosion in cooling systems in the presence of Fe_2O_3 Nanofluid and Comparison with the corrosion caused by different concentrations of ethylene glycol

S.Asgharrezaei[a*], Z.Shahri[a], A.Hassanzadeh[b]
[a]Payamnor University, Urmia Branch,Urmia,Iran
[b]Department of Chemistry , Faculty of Science , Urmia University, Iran
E-mail: S.Rezaei58@yahoo.com

Keywords: Nanofluid, Carbon Steel, Ethylene glycol, Corrosion

Introduction:

Ethylene glycol used as a heat transfer fluid in chiller applications, This chemical can degrade and causing corrosion and increasing costs[1]. Nowaday, nanofluid is used in industry to solve this problem. They exhibit enhanced thermal conductivity that make them potentially useful in many applications in heat transfer, including microelectronics, fuel cellsand pharmaceutical processes, Engine cooling/vehicle thermal management, chiller, heat exchanger[2]. Ferrofluids are composed of nanoscale particles of magnetite, hematite or some other compound containing iron [3]. In the present work, Fe_3O_4 magnetic nanofluids have been synthesized and their size in powder, were investigated through a X-ray diffraction (XRD) by using the Scherrer approximation. Scanning electron microscopy (SEM) was used to measure their diameter. An important overlooked practical feature of nanofluids is how these nanoparticles in the fluid impact on the corrosion rates of the metals that are in contact with the nanofluids. Research on Corrosion of copper in nanofluids ontaining MWCNT (Multi Wall Carbon Nano Tubes) began by Ahmadi, Baghalha[4]. Carbon steel finds wide application as a construction material for heat transport system , petrochemical, and chemical process industries. However, this material is highly prone to corrosion in various environment. Corrosion of carbon steel were containing Fe_3O_4 nanofluids studied by potentio-dynamic polarization method and comparison with the corrosion caused by different concentrations of ethylene glycol.

Experimental:

1. Materials and nanofluids preparation:

The synthesis of nanofluids has two main steps: the preparation of nano-sized magnetic particles and the subsequent dispersion-stabilization of the nano-particles in various non-polar and polar carrier liquids (i. e. ethylene glycol). The magnetic nanofluids based on magnetite Fe_3O_4 and mineral oils or organic solvents are prepared by coprecipitation technique from aqueous salt solutions Fe (II) and Fe (III) in alkaline medium and suspended in the carrier liquid [5-6]. The magnetite obtained is stabilized by Oleic acid surfactant.

2. Measurement of potentiodynamic polarization:

Corrosion measurements were performed on Mild Carbon Steel electrods. A (Ag/AgCl 3M KCL) electrode and Pelatinum electrode were used as the reference and the auxiliary electrodes, respectively. The current-potential curves were recorded using a AutoLab apparatus (PGSTA12,version 49) connected to a personal computer. For these measurements, the working electrode potential was linearly changed from -1500 mV to +1000 mV (relative to Ag/AgCl) with a scan rate of 1mV/s. All the experiments were performed at 25±1°C. The particles size of the synthesized particles of Fe_3O_4 were examined by (SEM) [Model: JSM5610LV, version 1.0, Japan] and XRD [Model: X PERTPRO, PANalitical company].

Result and discussion:

Fe_3O_4 nanoparticles size about 2.7 nm is estimated to help X-ray diffractogram. The SEM images of the Fe_3O_4 nanoparticle shows the average size of nanoparticles around 27.34 nm. In the present work,to study the effect of Fe_3O_4 nanofluids and the agitation speed on the corrosion rate of the mild Carbon steel working electrode, potentiodynamic polarization method were used. Polarization curves determined for mild Carbon steel at 0 and100 and 1000 rpm, respectively. Curve fitting and Tafel analysis were carried out to obtain values of corrosion currents and corrosion potentials, Icor and Ecor, respectively. The effect of rotational velocity on potentiodynamic polarization curves shows the corrosion current density of metal decreases with increasing electrode rotation speed. Polarization curves generated for mild carbon sreel in a Fe_3O_4 nanofluid and different concentrations of ethylene glycol shows the corrosion rate of metal in Fe_3O_4 nanofluid toward corrosion rate of metal in mixture of Water / Ethylene glycol decreases.

Reference:

[1] K .Wheeler, Technical Insights into Uninhibited Ethylene Glycol, Heat Transfer Fluids, (2002).

[2]P Keblinski and et al, Nanofluids for thermal transport, materialstady ,2005.

[3] J. A. Lopez1 and et al, Synthesis and characterization of Fe_3O_4 magnetic nanofluid, Revista Latinoamericana de Metalurgia y Materiales, vol.30 .NO.1, (2010),pp. 60-66.

[4] M .Kamal.A and et al , Department of Chemical and Petroleum Engineering, MWCNT nano-fluids enhancement of Copper corrosion, (2011), 11365-9465 .

[5] A.L .Kholmetskiia and et al, Materials Letters, (2005), 59: 1993 –1996.

[6] R.Y Hong and et al, Powder Technology, (2006), 170: 1 –11.

Degradation rate variance quantity from the anode to the cathode in polymer electrolyte layer in PEM fuel cells

S.Yasami[*a], M. Karimkhani[b]
[a, b] Department of Chemistry, Faculty of Science, Islamic Azad University, Central Tehran branch, Tehran, Iran
E-mail: saharyasami@yahoo.com

Keywords: PEMFC, Chemical degradation, COOH, •OH radicals

Introduction:

Basically, a polymer electrolyte membrane fuel cell converts hydrogen and oxygen electrochemically into electrical power, heat and water. A proton exchange membrane (PEM) serves as a solid electrolyte in a fuel cell, separating the anode (hydrogen) from the cathode (oxygen/air) compartments. The most important property of ionomeric membranes employed in polymer electrolyte fuel cells, is the high protonic conductivity that they provide under humidification conditions and at current densities typically required in PEM fuel cells [1, 2]. The degradation of perfluorinated sulfonic acid membrane (PFSA) in fuel cells is one of the critical factors for fuel cells' life time. It is clear from the literature studies that chemical degradation of membrane is mainly due to the attack of radicals formed during the operation of a PEM fuel cell. Chemical degradation of Nafion® involves the attack of •OH radicals formed by the decomposition of peroxide generated in the fuel cell. It was proposed that chemical attack occurs at the –COOH groups at the chain ends [3].

Methods:

Fuel cell modeling is helpful for fuel cell developers because it can lead to fuel cell design improvement, as well as cheaper, better, and more efficient fuel cells. In this paper degradation rate simulated in electrolyte layer. The main mechanisms of radical attack to the membrane are including four following steps [4]:

$\mathrm{R\text{-}CF_2\text{-}COOH + \bullet OH \rightarrow R\text{-}CF_2\bullet + CO_2 + H_2O}$ (1)

$\mathrm{R\text{-}CF_2\bullet + \bullet OH \rightarrow CF_2OH \rightarrow R\text{-}COF + HF}$ (2)

$\mathrm{R\text{-}COF + H_2O \rightarrow R\text{-}COOH + HF}$ (3)

Results and Discussion:

Degradation rate compared in two various areas of membrane.

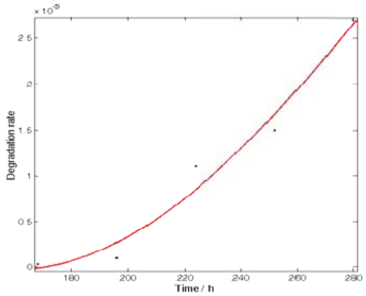

Degradation rate vs. time at y = 0.225 mm [5]

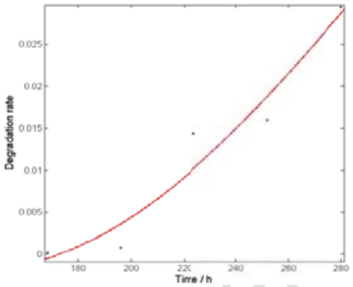

Degradation rate vs. time at y = 0.235 mm [5]

The profiles show that degradation rate at y = 0.235 mm is more than degradation rate at y = 0.225 mm. because •OH radicals increase at y = 0.235 mm.

Conclusions:

The paper describes modeling of a degradation rate in proton exchange membrane in PEM fuel cell. •OH radicals form during anode and cathode electrodes reactions and attack to the membrane structure. Degradation rate is different in various areas of membrane.

References:

[1] BD. Cahan, JS. Wainwright, AC impedance investigations of proton conduction in Nafion^{TM}. J ElectrochemSoc140, L185, 1993.

[2] MK. Kadirov, A. Bosnjakovic, S. Schlick . Membrane-derived fluorinated radicals detected by electron spin resonance in UVirradiated Nafion and Dow ionomers: effect of counterions and H_2O_2. J Phys Chem B 109(16), 7660–4, 2005.

[3] D.E. Curtin, R.D. Lousenberg, T.J. Henry, P.C. Tangeman, M.E. Tisack, Advanced materials for improved PEMFC performance and life, J. Power Sources 131, 41–48,2004.

[4] Healy J, Hayden C, Xie T, Olson K, Waldo R, Brundage M. Fuel Cell 5(2), 302-308,2005.

[5] Sahar Yasami. M.Sc Thesis. 2011.

The effect of PVP (Polyvinylpyrrolidone) on the electrochemical synthesis of Sn nanoparticles for lithium ion batteries

A. Sadeghi, S. Javadian*
Department of Chemistry, Tarbiat Modarres University
E-mail: Javadian_S@modares.ac.ir

Key words: lithium ion battery, nanoparticle, pulse electrodeposition

Introduction:

Lithium ion secondary batteries have the highest energy density in commercialized batteries. The increasing demand for higher capacity batteries in electronics devices has promoted an intensive research effort to develop new materials suitable for new high energy capacity lithium batteries. For the anode materials, there is an increasing interest in alternative anode materials for rechargeable lithium batteries because the graphite, which is used currently in commercialized lithium batteries, has only 10% (372 mAh/g) of the theoretical capacity of metallic lithium (3860 mAh/g). Many alloy anode materials have been studied to overcome the limited capacity of graphite [1]. For example, tin-based materials have been considered as alternative anode materials for the higher energy density and they have almost doubled the capacity of graphite [1]. Although tin have much higher capacities than that of graphite, they undergo severe volume expansion/contraction and pulverization. These limit the life-cycle of the anode [2-4]. In this work, to improve the performance of tin anode, nano-sized tin electrodes were prepared using electrodeposition in the presence of PVP.

Experimental:

Electrodeposition of Sn film were carried out on copper foils (area = 1cm^2) in a bath containing $SnSO_4$ 0.14M, H_2SO_4 0.98M, CTAB (Cetyl trimethyl ammonium bromide) 1mM and different concentration of PVP. A Graphite foil was usedas the counter electrode. The Cu substrate was treated with 30% HNO_3 aqueous solution for 60 s before the electroplating. A bath temperature of 25 ◦C, a current density of 76mAcm^{-2}, a pulse period of 1 ms, a pulse of duty ratio 0.25, and a deposition time of 5.0 min were employed. The three-electrode cell, which consisted of the electrodeposited Sn film electrode as working electrode, a Li foil as reference and counter electrodes, and a 1.0M solution of LiClO4 in EC: DEC (50:50 vol.%) were used for the electrochemical measurements. The cells were assembled in a glove box filled with dry argon at room temperature. Cyclic voltammograms (CVs) were measured with SAMA 500 models and electrochemical impedance spectroscopy (EIS) was carried out using EG&G 2710. The applied alternative voltage signal was 5mV (root mean square) and the frequency range was from 200 kHz to 200mHz.

Results and discussion:

Figure 1 shows CV for all electrodes which prepared in different concentrations of PVP. All these curves posses the same set of quasi-reversible peaks. These peaks relate to insertion and extraction of Li ions. According to figure 1, the current goes through a maximum as the amount of PVP is increased from 0.5 to 15g/L scan rate ν=1mV/s. These results are discussed in terms of the diffusion, interfacial charge transfer, and migration of Li ions through the solid-electrolyte interface. In addition, the impedance spectra showed that the interfacial capacitance and charge transfer resistance (including those related to Li+ migration through the surface films) should be related to the amount of PVP was used. The CV and EIS findings demonstrates the influence of PVP on electrode’s morphology.

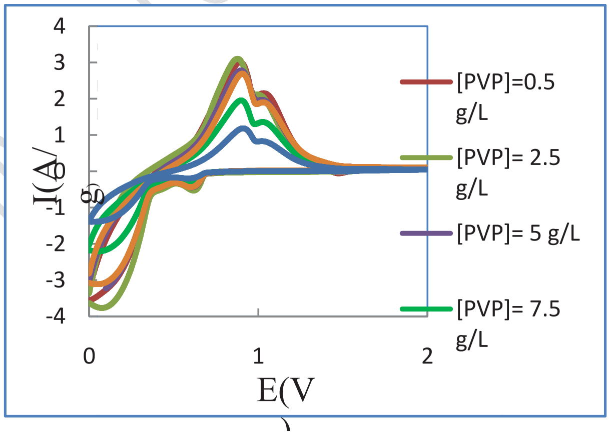

Fig. 1. Cyclic voltammograms of Sn film electrodes prepared by pulse electrodeposition method in presence of various concentrations of PVP. Potential range: 0.0–2.00V *vs*. Li/Li+, scan rate: $1 mVs^{-1}$

References:

[1] M. Winter, J.O. Besenhard, Electrochim. Acta 45 (1999) 31.

[2] I.A. Courtney, J.R. Dahn, J. Electrochem. Soc. 144 (1997) 2045.

[3] L.Y. Beaulieu, S.D. Beattie, T.D. Hatchard, J.R. Dahn, J. Electrochem. Soc. 150 (2003) A419.

[4] A. Sivashanmugam, T.P.Kumar,N.G.Renganathan, S.Gopukumar,M.Wohlfahrt-Mehrens, J. Garche, J. Power Sources 144 (2005) 197.

Study of complexation process between 15-crown-5 with Mg^{2+} cation in binary mixed non-aqueous solvents using conductometric method

S. Alizadeh , M. Mohajeri*, G.H.Rounaghi
Department of chemistry, Faculty of sciences, Mashhad Branch, Islamic Azad university, Mashhad, Iran
Email: mahmoh10@yahoo.com

Key words: 15-crown-5, Mg^{2+} cation, Mixed non-aqueous solvents, Conductometry.

Introduction:

Crown ethers have drawn much attention because of their ability to selectively bind various cations present in solutions. With this unique property, potential applications of crown ethers have been found in many diverse and practical areas[1].The stability and selectivity of crown ether complexes with metal ions depend on several molecular factors. These include the cavity size of the legend, the character of the heteroatoms in the polyether ring, the spatial distribution of ring binding sites, the charge density and polarizability of the cation and the cation diameter. One of the major factors is also the type of solvent used in complexation reactions[2]. The effect of solvent on the complexation of crown ethers with metal cations has been a subject of interest during recent years and has been studied by means of several different techniques.The nature and composition of the solvent system has been found to strongly influence the stoichiometry, selectivity, thermodynamic stability and exchange kinetics of metal ion–crown ether complexes [1-2].

Materials and methods:

15-crown-5 (Merk) and $Mg(NO_3)_2.6H_2O$ and the solvents; acetonitrile, ethanol, methanol, ethyl acetate and methyl acetate all from Merck were used with the highest purity and without further purification. The experimental procedure to obtain the formation constant of the complex was as follows: a solution of metal salt (1.0×10^{-4} M) was placed in a titration cell and the conductance of the solution was measured, then the crown ether concentration was increased by adding crown ether solution in the same solvent (2.0×10^{-3} M) to the titration cell, using a microburette and the conductance of the resulted solution was measured after each step at the desired temperature.

Apparatus:

The conductance measurements were performed on a digital Metrohm conductivity apparatus (model 160) in a thermostated water-bath with a constant temperature maintained within ±0.03 °C. The electrolytic conductance was measured using a cell consisting of two platinum electrodes to which an alternating potential was applied. A conductometric cell with a cell constant of 0.864 cm^{-1} was used throughout the studies.

Result and discussion:

The changes of molar conductivity (Λ_m) versus the ligand to the cation molar ratio, ($[L]_t/[M]_t$), for complexation of 15-crown-5 with Mg^{2+} cation were measured in pure MeOH, EtOH, AN, and also in AN–MeOH, AN–EtOH, AN–EtOAc, AN–MeOAc different temperatures. $[L]_t$ is the total concentration of the ligand and $[M]_t$ is the total concentration of the metal. The molar conductivity data show that in all solvent systems, the stoichiometry of the complex formed between 15-crown-5 and Mg^{+2} cation is 1:1 (M:L) The values of thermodynamic parameters ($\Delta H°c$ and $\Delta S°c$) for formation of $(15\text{-crown-}5.Mg)^{2+}$ complex were obtained from temperature dependence of the stability constant using the van't Hoff plots. The results show that in most cases, the $(15\text{-crown-}5.Mg)^{2+}$ complex is enthalpy and entropy stabilized and the values and also the sign of thermodynamic parameters are influenced by the nature and composition of the mixed solvents.

Conclusion:

A non-linear behaviour was observed for changes of log K_f of $(15\text{-crown-}5.Mg)^{2+}$ complex versus the composition of the binary mixed solvents, which was explained in terms of solvent–solvent interactions and also the heteroselective solvation of the species involved in the complexation reaction. The obtained results show that the stability of $(15\text{-crown-}5.Mg)^{2+}$ complex is sensitive to the mixed solvents composition .

References:

[1] G.H. Rounaghi , M. Mohajeri , S. Tarahomi , R. Rahmanian ;"Study of Complex Formation of Dibenzo-18-Crown-6 with Ce^{3+}, Y^{3+}, UO_2^{2+} and Sr^{2+} Cations in Acetonitrile–Dioxane Binary Solvent Mixtures"; G.H.J. Solution Chem., (2011) 40:377–389.

[2]G.H. Rounaghi , S. Tarahomi , M, Mohajeri ;"A conductometric study of complexation reaction between dibenzo-24-crown-8 with yttrium cation in some binary mixed non-aqueous solvents"; J. Incl Phenom. Macrocycl Chem., (2009) 63:319–32.

A new cluster model based descriptor for quantitative structure-inhibition relationship: Study of imidazole and its derivatives on copper corrosion in NaCl media

Mehdi Mousavi *, Neda Pirouznejad
Department of Chemistry, Faculty of Sciences, Shahid Bahonar University of Kerman, Kerman,
P.O. Box 76175-133, Iran
Email: mmousavi@mail.uk.ac.ir

Keywords: Copper corrosion, Imidazole derivatives, Cluster model, DFT calculation, QSIR.

Introduction:

Corrosion is an electrochemical destructive process of a metal or alloy with its environment which leads to loss of useful properties of materials. The working mechanism of corrosion inhibitors is a crucial problem for anti-corrosion researchers, but it has not been managed to consensus up to now. Theoretical and computational chemistry such as QSIR and cluster model are useful and powerful means in choosing the most appropriate and effective inhibitor by understanding the inhibition mechanism prior to any experiment [1, 2]. Both methods suffer from some restrictions originated from their fundamental. Therefore, in the present work, effort is taken to join these theoretical methods to overcome some of their limitations. This could be done through considering the calculated cluster model based interaction energy of some imidazoles and copper surface, as a new descriptor for a QSIR modeling.

Methods:

The method of calculation began with selecting a series of seven imidazole compounds as data set with their known experimental corrosion inhibition efficiencies on copper in NaCl solution [3]. Geometry optimization and all other quantum chemical calculations were carried out at B3LYP/LANL1MB DFT level implemented in Gaussian 09 package. The interaction energy ($E_{Interaction}$) of the inhibitor molecules in chloride solution with a 13 atoms copper cluster were calculated according to Eq. 1 as follow:

$$E_{Interaction} = E_{Cluster-Inhibitor} + 2E_{Cl^-} - (E_{Cluster-Cl^-} + E_{Inhibitor-Cl^-}) \qquad (1)$$

Where E_{Cl^-} represent electronic energy of the chloride ion and $E_{Cluster-Inhibitor}$,

$E_{Cluster-Cl^-}$, $E_{Inhibitor-Cl^-}$ are electronic energies of the cluster-inhibitor, the cluster-chloride and the inhibitor-chloride systems, respectively. The equation 1 is established based on a competitive behavior of chloride ion and inhibitor molecule for adsorption on the copper cluster surface. Also, the three dimensional structures of the imidazoles were applied to calculate other structural descriptors (including quantum chemical parameters) using Dragon software version 2.1.

Results and discussion:

To find out which descriptor is mostly in favor of corrosion inhibition, stepwise multiple linear regression (MLR) method is used to build the linear model. The most satisfactory model and its statistics are shown in Eq. 2:

$$IE\% = 42.315 - 1948.414E_{Interaction} + 4699.893X4Av - 24.029Mor15u$$

(2) R=0.997 R^2=0.993 F=148.5 S.E. = 1.91 Q^2_{LOO} = 0.929

Where *IE%* is inhibition efficiency percent, *X4Av* is average connectivity index that accounts for the presence of heteroatoms and double and triple bonds and *Mor15u* is among the 3D-MoRSE descriptors that are derived from Infrared spectra simulation using a generalized scattering function. In addition to high values of R^2 and F statistics, high amount of leave one out cross validation (Q^2_{LOO}) test indicates reliability of the derived model.

Conclusions:

It is concluded that the newly proposed inhibition scheme and $E_{Interaction}$ satisfactorily described the corrosion inhibition behavior of the imidazole derivatives on copper in NaCl solution so that more than 99% of experimentally inhibition is described. This may be due to the facts that, in contrast to many descriptors which is used in QSAR studies, in the cluster model all participants of an electrochemical reaction are taken into account. Also, in the DFT method applied here, it is possible to calculate energy of the system more accurately and more precisely.

References:

[1] M. Mousavi et al; "Theoretical investigation of corrosion inhibition effect of imidazole and its derivatives on mild steel using cluster model"; Corrosion Science; 53,3086-3091,2011.

[2] M.A. van Daelen, M. Neurock, R.A. van Santen; "Reactivity of diatomic molecules on Cu(100)"; Surface Science; 417,247-260,1998.

[3] H. Otmacˇic´, E. Stupnišek-Lisac; "Copper corrosion inhibitors in near neutral media"; Electrochimica Acta; 48,985-991,2003.

Cluster model based descriptor for quantitative structure-corrosion inhibition study of benzenethiol and its derivatives on copper

M. Mousavi *, T. Baghgoli
Department of Chemistry, Faculty of Sciences, Shahid Bahonar University of Kerman, P.O. Box 76175-133 ,
Kerman, Iran
*Email: mmousavi@mail.uk.ac.ir

Key words: Cluster model, DFT method, Corrosion inhibition, QSIR study.

Introduction:

Various attempts have been made to prevent the destructive effect of corrosion on metals and alloys. Corrosion control can be achieved by several methods, from which the use of corrosion inhibitors is one of the most effective alternatives [1]. Theoretical and computational chemistry are useful and powerful means in choosing the appropriate and effective inhibitor by understanding the inhibition mechanism prior to any experiment. In the present work, cluster model is used to calculate interaction energy of inhibitor molecules and copper surface [2]. Then, interaction energy in conjunction with other structural parameters is applied in a QSIR study to consider other influencing aspects on the inhibition process. It is believed that these methods could be complementary in describing the inhibition process.

Methods:

In the present work, the inhibition mechanism of benzenethiol and eight of its derivatives on copper surface in acid media [3] were modeled via a combination of cluster model and QSIR methods. The quantum chemical study was focused on the calculation of interaction energy between the inhibitor molecule and the copper cluster, upon which the adsorption is directly tacking place. The Cu cluster which was applied in the calculation is consisting of 13 copper atoms. The interaction energy were calculated based on Eq. (1) and all the geometry optimizations were carried out at B3LYP/LANL1MB DFT level using Gaussian 09 package. The energies were corrected for ZPE, BSSE, deformation energy and solvent effect [4, 5].

$$E_{int} = E_{inhibitor\text{-}cluster} - (E_{cluster} + E_{inhibitor}) + E_{def} \qquad (1)$$

$$E_{def} = [(E_{cluster})_c - E_{cluster}] + [(E_{inhibitor})_c - E_{inhibitor}]$$

Where, $E_{inhibitor}$, $E_{cluster}$ and $E_{inhibitor\text{-}cluster}$ are electronic energies of the inhibitor molecule, the copper cluster and of the inhibitor-copper system, respectively. Also $(E_{cluster})_c$ and $(E_{inhibitor})_c$ are electronic energies of cluster and inhibitor in the complex forms.

With the exception of E_{int} and electronic parameters such as highest occupied and lowest unoccupied molecular orbitals, dipole moment and etc, many structural parameters were calculated by using Dragon software version 2.1 for all the inhibitors. These descriptors were entered in the statistical analysis to obtain a suitable mathematical equation for describing the inhibition phenomena.

Results and discussion:

It is concluded that when using deformation energy in Eq. 1, satisfactory correlation between interaction energy and experimental inhibition efficiencies is found (0.999). To find out which descriptor is mostly in favor of corrosion inhibition, stepwise multiple linear regression (MLR) method is used to build the linear model. The most satisfactory model and its statistics are shown in Eq. 2:

$$\%IE = -4169.831\,(E_{int}) - 827.101(X2A) + 56.932\,(BEHv3) + 437.405 \qquad (2)$$

R^2=0.998 F=593.069 Standard error =0.71619

Where, *X2A* is average connectivity index chi-2, Connectivity Indices are calculated from the hydrogen-depleted molecular graph and it is belong to the topological descriptors, *BEHv3* is among the *BCUT* descriptors, the *BCUT* descriptors are the eigenvalues of a modified connectivity matrix known as the Burden matrix.

Conclusion:

The interaction energy of inhibitor molecules with metal cluster is successfully utilized as an effective, useful and interpretable descriptor in QSIR method. By using this descriptor in an MLR equation, an excellent agreement between the experimental and calculated inhibition efficiencies is found so that almost 99.8% of inhibition imposed by benzenethiol and its derivatives on copper is described.

References:

[1] R.M. Issa, M.K. Awad, F.M. Atlam. Applied Surface Science 255 (2008) 2433–2441.

[2] M. Mousavi, M. Mohammadalizadeh, A. Khosravan. Corrosion science 53(2011)3086-3091.

[3] Y.S. Tan, M.P. Srinivasan, S.O. Pehkonen, Simon Y.M. Chooi. Corrosion science 48(2006)840-862.

[4] M. Lashkari, M. R Arshadi. Chemical physics 82(1985)299-310.

[5] D.M. Chipman. Chemical physics 112(2000)5558-5565.

Er^{3+}-PVC Membrane Sensor Based on 3-hydroxy-N'-((pyridin-2-yl)methylene)naphthalene-2-carbohydrazide

B. Hatamluyi*, H.A. Zamani
Department of Chemistry, Mashhad branch, Islamic Azad University, Mashhad, Iran
Email: behnazhatamluyi@yahoo.com

Key words: Sensor, Ion-Selective Electrode, Potentiometry, PVC Membrane.

Introduction:

Erbium has no biological role but is said to stimulate the metabolism All erbium compounds should be regarded as highly toxic, although initial evidence would appear to suggest that the danger is limited [1]. Solvent polymeric membrane based ISEs, together with the incorporation of ion carriers, have shown to be a very useful tool for clinical, environmental, and chemical analyses as well as for process monitoring. Potentiometric detection based on ion-selective electrodes (ISEs) offer the advantages of speed and ease of preparation and procedures, relatively fast response, reasonable selectivity thorough judicious choice of the membrane active materials, wide linear dynamic range, and low cost [2,3]. In this research, we wish to report the preparation a Er^{3+} PVC-based membrane electrode based on 3-hydroxy-N'-((pyridin-2-yl)methylene)naphthalene-2-carbohydrazide (L) as an neutral ion carrier.

Materials and methods:

The Merck and the Aldrich Chemical Co. were the providers of the following reagent grades: benzyl acetate (BA), nitrobenzene (NB), Dibutyl phthalate (DBP), acetophenone (AP), high relative molecular weight PVC, sodiumtetraphenyl borate (NaTPB), tetrahydrofurane (THF) and chloride and nitrate salts of the cations used. Triply distilled deionized water was used throughout.

Apparatus:

All electromotive force (emf) measurements were carried out with the following cell assembly; Ag/AgCl| internal solution, (1×10^{-3} M $ErCl_3$)|PVC membrane|test solution|Hg_2Cl_2, KCL (saturated). A Corning ion analyzer 250 pH/mV meter was used for the potential measuremrnts at 25.5 ± 0.1 ºC. The activities were calculated according to the Debye-Huckel procedure.

Result and discussion:

In this study, a plasticizer/PVC ratio of about 2.2 was found to be the most suitable ratio. The obtained data revealed that, the membrane incorporating 67% DBP, 30% PVC, 2% ligand, in the presence of 1% sodium tetraphenyl borate (NaTPB) as a suitable lipophilic additive considerably improved the sensitivity of the erbium sensor and showed the best sensitivity, with a good Nernestian slope of 20.5±0.4 mV/decade of Er^{3+} concentrations (1.0×10^{-6}–1.0×10^{-2} M) and a detection limit 5.3×10^{-7} M. The pH dependence of the responses of the membrane was investigated by the sensor behavior in a 1.0×10^{-3} M Er^{3+} solution. The potential response of the sensor is independent of pH, in the pH range of 2.8–9.5. The dynamic response time of the membrane was measured at various concentrations (1.0×10^{-6} to 1.0×10^{-2} M) of the test solutions and the results exhibited that the sensor has a fast response time of ~5 s. To investigate the membrane electrode selectivity, its potential response was monitored in the presence of various interfering foreign cations using the matched potential method (MPM) [2]. The electrode shows a very good selectivity towards Er^{3+} ions over a wide variety of cations, including alkali, alkaline earth, transition and heavy metal ions. The proposed sensor was successfully applied as an indicator electrode for the potentiometric titration of 1.0×10^{-4} M of Er^{3+} ions with a 1.0×10^{-2} M EDTA.

Conclusion:

The results obtained from the above mentioned study reveal that a potentiometric PVC-based membrane sensor based on 3-hydroxy-N'-((pyridin-2-yl)methylene)naphthalene-2-carbohydrazide (L) functions as an excellent Er^{3+} selective sensor and can be used for the determination of this ion in the presence of considerable concentrations of common interfering ions. The short response time, applicable pH range, lower detection limit, and potentiometric selectivity coefficients of the proposed sensor make it a superior device for the determination of this ion.

References:

[1] R.E.Kirk, and etal; "Encyclopedia of Chemical Technology"; Wiley; Chichester; 1982.

[2] E. Bakker etal. ; "Carrier-based ion-selective electrodes, bulk optodes. 1. General characteristics" ; Chemical Review ; 97,3083-3132,1997.

[3] E. Pretsch etal. ; "Carrier-based ion-selective electrodes and bulk optodes. 2. Ionophores for potentiometric and optical sensors" ; Chemical Review ; 98,1593-1687,1998.

Determination of 4-hydroxybenzoic acid with cyclic voltammetry and differential pulse method using the electrode modified with carbon nanotubes

T.Nazemi[a,*] ,M.Ghoreyshi[b]
[a]Department of Chemistry, Islamic Azad University, Center Tehran Branch, Tehran, Iran.
[b]Department of Chemistry, Kashan Branch, Kashan, Iran.
Email:tahere.nazemi@gmail.com

Key words : Carbon paste electrode, DifferentialpluseVoltammetry, Cyclicvoltammetry, Reformer species

Introduction:

Measurement of drugs in the pharmaceutical industry, medical and biological applications is extensive. Among the electrochemical methods, application methods Voltammetry with modified carbon paste electrodes due to high sensitivity and ability to detect very low quantities and high-speed operation and low cost and ease of electrode preparation, the level of renewable and low residual flow in The more recent analytical chemistry has attracted scholars. [1] The most important principle for the use of electrochemical methods as an analytical tool, capable of oxidation and reduction of the desired species is relatively lowpotentials. Many compounds in high potentialoxidation or decrease, or on the no modification electrode surface poor responseagainst the oxidation - reduction of the show, and this leads to a decrease in the sensitivity and selectivity are electrochemical methods of analysis. A reasonable way to reduce voltage electrochemical reaction, the species is a reformer. Reformer of the electrode surface causes a significant improvement in sensitivity and selectivity of electrochemical methods can reduce the detection limit. [2]

Methods:

In the studyis used voltammetry methods including cyclic Voltammetry and Voltammetry Differential pulse. cyclic Voltammetry is a method that has most application in qualitative information about electrochemical reactions. causes the capacitive currents that largely eliminated and be close to zero Differential pulse voltammetry. In this research, all the chemical techniques has been done usedaAutolab(Model:30 PGSTAT that build Netherlands Chemie Eco) and connected to a computer. In all experiments is used the electrode Ag / AgCl as reference electrode from Metrohm company and a platinum electrode as auxiliary electrode. And was used apH-meter(Model 691 Metrohm) equipped with glass electrode(Model6/020/000)toadjust buffer solutionspH,and a ultrasonic generator devices(HF BANDLIN, KHz 35) to disperse multi-walled carbon nanotube.

Result and discussion:

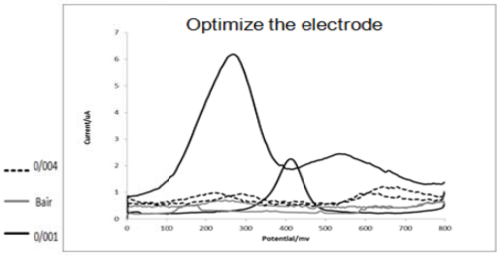

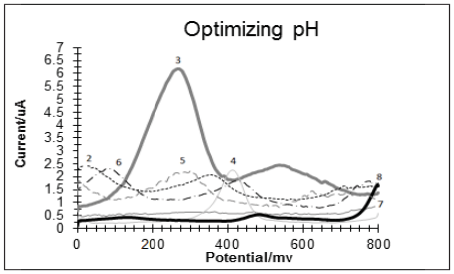

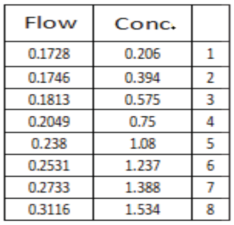

Flow	Conc.	
0.1728	0.206	1
0.1746	0.394	2
0.1813	0.575	3
0.2049	0.75	4
0.238	1.08	5
0.2531	1.237	6
0.2733	1.388	7
0.3116	1.534	8

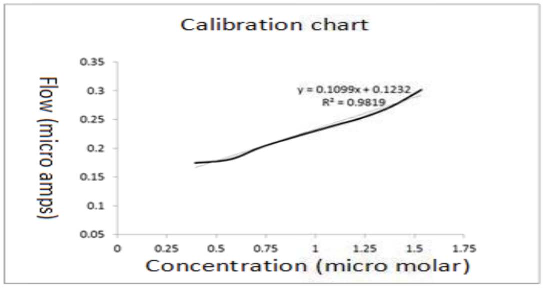

For obtain a detection limit Need to the standard deviation of the peak value of differential pulse Voltammetry That it is 0/015002.and also we need the slope of the calibration curve, which equalsis the amount of0/1099. Therefore, our detection limit is obtained:

$$\frac{3\times\delta}{M} = \frac{3\times 0/015022}{0/1099} = 0/4100637\mu M = 4/1\times 10^{-7}\ M$$

Conclusion:

Carbon paste electrode modified with multi-walled carbon nanoparticlesis used to measure the 4-hydroxybenzoic acid withhigh sensitivity. The advantages of this electrodeisIncludes easypreparation method, low cost and good stability.andthe renewalpossible of surface is easily. This study represents a new method for measuring 4-hydroxybenzoicacidwith high choosing and sensitivity in a short time with the detection limit is comparable to other research.

Reference:

[1]. Agy,L., Fena-Farafal C., Yenz-Sade no P., Pingarron J.M., Talanta, 185, 228 **2007**.

[2].Bard, A.J. ,FaulknerT, L.R.; Electrochemical methods fundamentals and applications. Wiley, New York**2001**.

Study of complexation of cesium(I) and cerium(III) metal cations with 1,13-bis(8-quinolyl)-1,4,7,10,13-pentaoxatridecane in binary mixed non-aqueous solvents

G.H. Rounaghi*, S. Akbari, M. Fakhri, A.R. shams
Department of Chemistry, Mashhad Branch, Islamic Azad University, Mashhad, Iran
E-mail: ronaghi0970i@mashdiau.ac.ir

Key words: Kryptofix5, Cs^+ and Ce^{3+}, Mixed non-aqueous solvents, Conductometry

Introduction:

Studies of complexation of open-chain ligands in various solvents, show that the thermodynamic and kinetic parameters for complexation processes and even the stiochiometry of crown ether complexes are affected by the nature and composition of the solvent system [1,2]. Conductometry offers a simple and an inexpensive experimental arrangement for such investigations. The advantage of conductometry is that the measurements can be carried out with high precision at very low concentration in solution systems [3]. The goal of this investigation is to study the effect of the nature and composition of the mixed non-aqueous solvents on stability,selectivity and thermodynamic parameters of 1,13-bis(8-quinolyl)-1,4,7,10,13-pentaoxatridecane ligand with cesium(I) and cerium(III) cations in acetonitrile-methanol(AN-MeOH) and acetonitrile-ethylacetate (AN-EtOAc) using the conductometric technique.

Materials and methods:

A solution of metal salt (1.0×10^{-4} mol.L^{-1}, 20 ml) was placed in a titration cell, thermostated at a given temperature, and the conductance of the solution was measured. Then the solution of the ligand (2×10^{-3} mol.L^{-1}) was transferred step-by-step to the titration cell using a precalibrated microburette and the conductance of the solution was measured after each transfer.

Apparatus:

All conductance titrations were performed using a digital Metrohm conductometer (model 712). The temperature of all solutions was thermostated at a constant temperature that was maintained within ±0.01°C by circulation of thermostated water through the outer jacket of the cell.

Results and discussion:

Addition of kryptofix5 ligand to Cs^+ and Ce^{3+} cations solutions,shows an increase in molar conductivity, which indicates that the complexes are more mobile than free solvated cations. As an example , a typical molar conductance-mole ratio on plots for complexation of kryptofix5 with Ce^{3+} in acetonitrile-ethylacatate (AN-EtOAc) is shown in Figure1. In all cases, the slope of each curve changes at $[L]_t/[M]_t = 1$, which is an evidence for formation of a relatively stable 1:1 complex. The change of stability constants (log K_f) of complexes versus the composition of the binary mixed solvents shows a non-linear profile in all solvent systems. This behavior can be explained on the basis of the solvent-solvent intractions between the two constituent solvent molecules which result in changing the structure of the solvent systems with their composition. The thermodynamic data show that in most cases,the complexation processes are exothermic (favorable) ,and also the $(kryptofix5.Cs)^+$and $(kryptofix5.Ce)^{3+}$ are stabilized from entropy viewpoint.

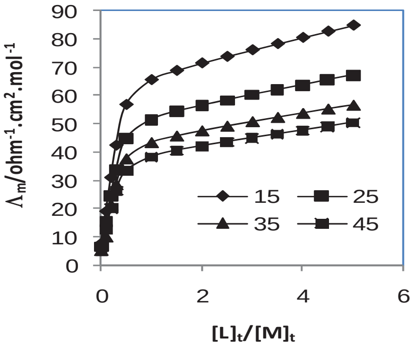

Fig 1. Molar conductance–mole ratio plots for the (kryptofix 5.Ce)$^{+3}$ complexes in AN–EtOAc (mol%AN=40).

Conclusion:

The conductometric measurements reveal that the selectivity and thermodynamic of the complexes formed between kryptofix5 and Cs^+ , Ce^{3+} metal cations changes with the nature of and the composition of the nonaqueous solvents.

Reference:

[1]. G. H. Rounaghi etal. *J. Incl. Phenom. Chem*. 73, 279-286, (2012)

[2]. G. H. Rounaghi etal. *J. Incl. Phenom. Chem*. 72, 113-119, (2012)

[3]. Y. Takeda etal. *J. Incl. Phenom. Chem. 11*, 159–170, 1991.

Solvent influence upon complexation of kryptofix5 with Ce^{3+} cation in binary mixed non-aqueous solvents

G.H. Rounaghi*, M. Fakhri, S. Akbari, A.R. shams
Department of Chemistry, Mashhad Branch, Islamic Azad University, Mashhad, Iran
E-mail:ronaghi0970i@mashdiau.ac.ir

Key words: Kryptofix5, Ce^{3+}, Mixed non-aqueous solvents,Conductometry

Introduction:

The binding ability and selectivity of crown ethers to metal ions depend on several factors: such as the size of the macrocycle ligand cavity, metal ion radius, type of donor atom, conformation of the ligand, the nature of the solvent and etc. Solvent plays a crucial role in the binding selectivity of the ligandes for metal ions [1]. Studies of ligand complexation with the metal cations in different solvents show that the thermodynamic and kinetic parameters are affected by the nature and the composition of the solvent system [2,3].In this work,we report the results of complexation reaction between kryptofix5 with Ce^{3+} cation in acetonitrile-methanol(AN-MeOH),acetonitrile-dichloroethan(AN-DCE).

Materials and methods:

A solution of metal salt (1.0×10^{-4} $mol.L^{-1}$, 20 ml) was placed in a titration cell, thermostated at a given temperature, and the conductance of the solution was measured. Then the solution of the ligand (2×10^{-3} $mol.L^{-1}$) was transferred step-by-step to the titration cell using a precalibrated microburette and the conductance of the solution was measured after each transfer at the desired temperature.

Apparatus:

All conductance titrations were performed using a digital Metrohm conductometer (model 712). The temperature of all solutions was thermostated at a constant temperature that was maintained within ±0.01°C by circulation of thermostated water through the outer jacket of the cell. The electrolytic conductance was measured using a double-walled glass conductivity cell consisting of two platinum electrodes to which an alternating potential was applied.

Results and discussion:

The complexation reaction of kryptofix5 with Ce^{3+} cation was studied in acetonitrile–methanol(AN–MeOH),acetonitrile–dichloroethan(AN–DCE) binary solvent solutions,at different temperatures by conductometry method. The stability constant of the resulting 1:1 complex at each temperature was determined using a computer fitting conductance-mole ratio data.The corresponding standard thermodynamic parameters (ΔH°_{c}, ΔS°_{c}) were obtained from temperature dependence of the stability constant. The results show that the values of these parameters are influenced by the nature and composition of the mixed solvents.

Table 1. Log K_f values of $(kryptofix5.Ce)^{3+}$ complex in AN–MeOH

Medium	**%AN**	**log K_f ± SD^a**			
		288.15 K	**298.15 K**	**308.15 K**	**318.15 K**
AN–MeOH					
	100	4.85±0.08	4.80±0.08	4.77±0.10	4.72±0.07
	80	3.07 ± 0.14	3.34 ± 0.08	3.40 ± 0.06	3.44± 0.08
	60	5.65 ± 0.12	3.97 ± 0.13	2.81 ± 0.11	2.80± 0.15
	40	2.84 ± 0.11	2.83 ± 0.11	2.66 ± 0.12	2.65± 0.14
	20	2.90 ± 0.11	2.83± 0.13	2.79 ± 0.14	2.74± 0.19
	0	2.77 ± 0.14	2.77 ± 0.14	2.72 ± 0.15	2.77± 0.22

Conclusion:

In all cases, the slope of each curve changes at $[L]_t/[M]_t = 1$,which is an evidence for formation of a relatively stable 1:1 complex.The results revealed that, the stability constant of $(kryptofix5.Ce)^{3+}$ complex in pure organic solvents varies in the order: AN>MeOH. A non–linear relationship was observed for changes of log K_f of $(kryptofix5.Ce)^{3+}$complex versus the composition of the binary mixed solvents. The thermodynamic data reveal that complexation process between kryptofix5 and Ce^{3+}cation is exothermic (favorable). In most cases, the $(kryptofix.Ce)^{3+}$ complex is stabilized from entropy viewpoint.

Reference:

[1] G. H. Rounaghi etal. *J. Incl. Phenom. Chem*. 73, 435-441, (2012)

[2] R.M. Izatt etal. Chem. Rev. 95, 2529–2586, 1991.

[3] G.H. Rounaghi etal. *J. Incl. Phenom. Chem*. 73, 67-73, (2012)

Electrochemical study of Catalase Modified Electrode in the Presence of Compatible and Non-Compatible Osmolytes using Carbon Nanotubes

Hessam Sepassi Tehrani, Hedayatollah Ghourchian, Ali Akbar Moosavi-Movahedi
Institute of Biochemistry and Biophysics, University of Tehran, Tehran, Iran
Email: sepasi@ibb.ut.ac.ir

Abstract:

Catalase is an important antioxidant enzyme that converts H_2O_2 into water an O_2. Since H_2O_2 is important both clinically and environmentally, numerous efforts have been done in order to reduce the detection limit of nanosensors for H_2O_2. Catalase modified electrodes have been used for such a detection with promising results. Osmolytes play an influential role in various stresses and also in the protein stabilization. They are generally categorized in two major groups, those that do not perturb the normal catalytic activity and structural stability of enzyme i.e. compatible osmolytes such as proline, and the others which adversely affect structure and function to various degrees such as histidine.

An enzyme modified electrode using multi-walled carbon nanotube and RTIL showed satisfactory results in terms of electrode stability and response. Effect of proline and hisitidine on various electrochemical parameters was investigated. The formal potential ($E°'$) was found to be -0.457 which showed good agreement with the values reported previously. In the presence of proline, $E°'$ was increased and therefore ΔG decreased, which presents protein stabilization at the surface of electrode and enhanced electron transferring whereas in the presence of histidine $E°'$ was pronouncedly decreased and (ΔG increased) which bear testimony to protein destabilization. In both cases the peak currents were decreased; however such a decrease was much more prominent in the presence of histidine rather than proline. The stabilization effect could be utilized in designing new nano-biosensors for numerous applications.

Keywords: Catalase, Proline, Histidine, Osmolyte, Electrochemistry, Carbon nanotube

References:

[1] A.A. Moosavi-Movahedi, J. Chamani, H. Ghourchian, H. Shafiey, C.M. Sorenson, N. Sheibani, J Protein Chem 22 (2003) 23-30.

[2]I. Haque, R. Singh, A.A. Moosavi-Movahedi, F. Ahmad, Biophys Chem 117 (2005) 1-12.

[3]N.K. Poddar, Z.A. Ansari, R.K. Singh, A.A. Moosavi-Movahedi, F. Ahmad, Biophys Chem 138 (2008) 120-129.

[4]I. Haque, R. Singh, F. Ahmad, A.A. Moosavi-Movahedi, FEBS Lett 579 (2005) 3891-3898.

Study of Point of zero charge effect on oxygen reduction reaction at gas diffusionelectrode in PEMFCs

Rasol AbdullahMirzaie[1*], Mohammad Safi Rahmanifar[2], Samaneh Sajedineia[1]
[1]Fuel cell research laboratory, Dep. of chemistry, Faculty of science, ShahidRajaeeteacher training university, Tehran, Iran
[2]Faculty of Basic Sciences, ShahedUniversity,Tehran, Iran
Email: ra.mirzaei@srttu.edu

Key words: Point of zero charge, Electrode performance, Fuel cell, Oxygen reduction reaction

Introduction:

The point of zero charge (pzc) is a concept relating to the phenomenon of adsorption, and it describes the condition when the electrical charge density on a surface is zero. In other words, pzc is (usually) the pH value at which a solid submerged in an electrolyte exhibits zero net electrical charge on the surface[1].

A catalyst in fuel cell is a special material that facilitates the reaction of oxygen and hydrogen and is usually made of platinum powder. The catalyst is rough and porous so that the maximum surface area of the platinum can be exposed to the hydrogen or oxygen[2].In this work, the effect of pzc on synthesizing process of platinum and cobalt on carbon electrocatalyst for Oxygen reduction reaction(ORR) were investigated. The prepared electrocatalysts can be used in low temperature fuel cell systems.

Experimental:

The Pt–Co electrocatalyst obtained in two steps, first by seeding 10 %(v/v) of the Pt–Co solution in graphite slurry and then by reduction of remaining Pt–Co solution (90%) in second step. After preparation of electrocatalyst, it was pasting on a carbon paper (CP)and used as electrode. The pzc was determined by acid-base titration.Liner Sweepvoltammograms(LSV)were obtainedunder O_2, at room temperature, at a scan rate of 1 mV/s in a 0.5M H_2SO_4 solution from 0.8 to -0.2 vs. Ag/AgCl.

ElectrochemicalImpedanceSpectroscopy (EIS)was taken in the frequency range of 100 KHz to 10 mHz.

Results:

In order to evaluationofpzc effect on evaluation ofPt-Co/Celectrocatalyst, two electrodes were prepared,one with the control of electrocatalystpH and the other without the control of pH (blank). The electrodes performance was evaluated by means of LSVand EIS, with three electrode system with an Ag/AgCl electrode as the reference electrode and a Pt electrode as a counter electrode.

The pzcs of Pt-Co/Celectrocatalyst and CP were determinedat pH values of 5 and 13 respectively.Therefore the pzc for CP coating with Pt-Co/C electrocatalystwas adjusted to pH equal to 8.5. On the other hand, it can be expected that in 5 < pH < 13 the surface of the Pt-Co/C is negatively charged while the one that of the CP is positively charged so in pH=8.5 CP and electrocatalysthad opposite charge.

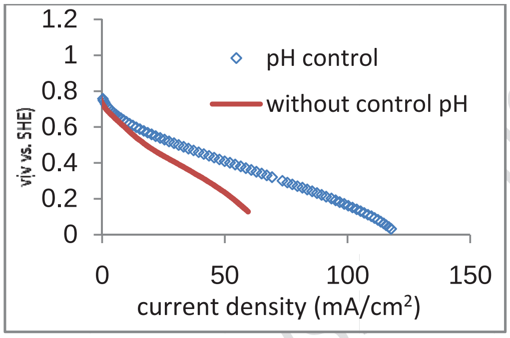

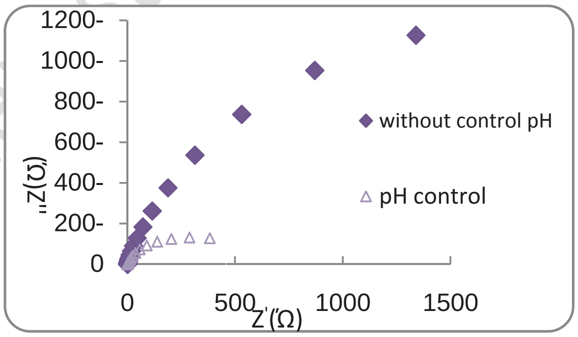

Fig. 1– LSV of prepared electrodes for ORRFig.2 Niquistplotsofprepared electrodes for ORR at OCV.

The LSV of two types of electrocatalyst are shown in the fig.1. As it was seen, the ORR current is increase with decreasing the potential, for both electrodes.But the electrode withthe pH control has higher current in all potential than blank sample(without pH control),i.e, the electrode has higher performancewhen the pH of electrocatalyst is adjusted to 8.5. Fig. 2 is shown the Niquist plots of the two samples. Both of them indicate an incomplete semi circle.But the diameter of electrode with control of pH is lower than the electrode without control of it. Since, the diameter of the semi circle is equal to the polarization resistance, so lowering the polarization resistanceshows better ORR activity and therefore, higher performanceachieved for electrode.According our results, we can say the preparation condition of electrocatalyst influence on performance of prepared electrodes for ORR. In this work, the effect of pzc as a one of preparation parameter was studied.

Reference:

[1] Chip Appel, Lena Q. Ma, R. Dean Rhue,ElizabethKennelley, "Point of zero charge determination in soils andminerals via traditional methods and detection of electroacoustic mobility" Geoderma 113,
77– 93(2003)
[2]H. Gharibi,R. Abdullah Mirzaie, E. Shams, "Preparation of platinum electrocatalysts using carbon supports foroxygen reduction at a gas-diffusion electrode"Journal of Power Sources139, 61-65(2005)

Preparation of carbon paste electrode modified with m-tuloidine in presence surfactant containing Platinum nano particles and its application for electrocatalytic reduction of oxygen

R. Ojani*, J.B. Raoof, M. Gheibi Panbehzari
Electroanalytical Chemistry Research Laboratory, Department of Analytical Chemistry, Faculty of Chemistry,
University of Mazandaran, Babolsar, Iran
Email: Fer-o@umz.ac.ir

Key words: Platinum, Oxygen, Reduction, m-tuloidine .

Introduction:

The electrochemical reduction of oxygen is one of the most important reactions in electrochemistry due to its central role in fuel cells, metal-air batteries and in the electrosynthesis of hydrogen peroxide[1]. Finding a low-cost electrocatalyst for oxygen reduction reaction(ORR) is an important issue in view of its practical application in clean energy generation systems[2]. Although non-noble metals catalysts have been investigated and used for oxygen reduction, Pt and its alloys are one of the best electrocatalysts for use towards the oxygen reduction. In order to enhance the electrocatalytic activity, the use of Pt seems inevitable, but its price is high. An effective way to decrease the cost is lowering the amount of Pt by making high dispersed Pt particles on carbon supports. Carbon materials are of special interest due to their outstanding properties, such as their tunable shape, size, porosity, corrosion resistance, chemical stability, low cost, electrical conductivity, and good thermal resistance. The combination of all these characteristics has promoted the use of these materials as electrode supports. It is well known that conducting polymers (CPs) with porous structures and high surface areas have been proved to be suitable host materials for dispersion of Pt particles. The reason for the incorporation of Pt particles into the porous matrixes is to increase the specific surface areas of them and thus improve their electrocatalytic activity[3]. Recently, we have reported Platinum/CTAB-m-tuloidine carbon paste electrode for electrocatalytic oxygen reduction in acid medium.

Materials and methods:

The solvent used in this work was distilled water. Sulfuric acid (from Fluka) was used as supporting electrolyte. The m-tuloidine (MT) monomer was purchased from Merck. $PtCl_4$ from Merck were used as received. High purity (99.999%) nitrogen was used for deaeration of the solution.

Apparatus:

Electrochemical experiments were carried out using a Electrochemical Analysis System, Ivium coupled with a pentium II personal computer connected to a HP Laser Jet 6 L printer. A platinum wire was used as the auxiliary electrode. A carbon paste electrode as working electrode and a double junction Ag|AgCl|KCl (3 M) electrode as reference electrode were used.

Result and discussion:

In this work, we studied the electropolymerization of m-toluidine in presence of CTAB as surfactant in 0.5 M sulfuric acid at the surface of carbon paste electrode (CPE) by cyclic voltammetry method. This prepared modified electrode was investigated as a matrix for platinum (Pt) particles deposited electrochemically. It has been found that in the optimum conditions, the reduction of oxygen at the surface of Pt/MT(CTAB)-CPE occurs at potential about +580 mV in sulfuric acid O_2-saturated
solution at scan rate 10 mV s^{-1}.

Conclusion:

In this work, poly m-tuloidine have been prepared and investigated as a matrix for Pt dispersion and used for electrochemical reduction of oxygen. Platinum /poly m-tuloidine deposited at the surface of carbon paste electrode acts as a catalyst for the electroreduction of O_2 in acidic solutions.

Reference:

[1] M. Khorasani-Motlagh , M. Noroozifar, A. Ghaemi, N. Safari, Anal. Chem. 565 (2004) 115–120

[2] V.G. Khomenko, V.Z. Barsukov, A.S. Katashinskii, Electrochimica Acta 50 (2005) 1675–1683

[3] R. Ojani, J.B. Raoof, S.R. Hosseini, international journal of hydrogen energy 36 (2011)52-63

Modification of electrode surface with sulfonated polyaniline

S. Hajizadeh*[a], F. Masdarolomoor [a] M. Arab Chamgangali [a]
a Department of chemistry, Shahrood University of Technology, Shahrood, Iran
Email: s.hajizade2011@gmail.com

Key words: Conducting polymer,polyaniline,dopant, sulphonated poly aniline.

Introduction:

The dopant incorporated into inherently conducting polymers during synthesis is known to have a substantial effect on the physical and chemical properties of the resultant material. There has been considerable interest in the incorporation of polyelectroyte as dopants for conducting polymers. Fully sulfonated polyaniline, poly(2-methoxyaniline-5-sulfonic acid) (PMAS), is a conductive and electroactive polyelectrolyte that has been recently used for synthesis of polyaniline with improved properties [1, 2]. As an acidic polyelectrolyte PMAS provides counterions, an acidic microenviroment and a template for electrostatic alignments of aniline monomers for producing the conducting form of polyaniline. A new approach is described for synthesis of poly aniline (PAn) on poly elecrtrolyte modified electrode. The electrode was modified with PMAS.

Materials and methods:

Aniline purchased from Aldrich was distilled and then stored at −4 ◦C (freezer) prior to use. PMAS with a molecular weight about 10 kDa was prepared according to reference 1. Hydrochloric acid (32%, w/v) was purchased from Merck. A METROHOM electrochemical instrument MODEL746 was employed for voltammetric experiments. A three-electrode system was used consisting of a glassy carbon(GC) working electrode, a platinum auxiliary electrode and an Ag/AgCl (3M kCl) reference electrode. The electrode surface was modified either by applying a constant potential in the rage -0.2 to 1.0 V or a potential sweep between −0.2 and 1.1V (vs.Ag/AgCl) in an aqueous solution of PMAS. This PMAS modified electrode was then used for electropolymerisation of aniline using cyclic voltammetry technique [2].

Results and discussion:

Due to negatively charged solfonate groups of PMAS, the PMAS modified electrode is capable of electrostatic interaction with positively charged groups and cab be used as a template for absorbtion and preconcentration of molecules with positive charges such as anilinum ions in polymerization of aniline. Potentiodynamic polymerization of aniline was carried out on the PMAS modified GC electrode. An increase in current density was observed during subsequent scans, indicating the formation of conductive polyaniline (Figure 1). Post-growth cyclic voltamograms of the composite showed the switching between different oxidation states of electroactive polyaniline. The monomer concentration can be lowered to less than 0.01 M where the anilne is not effectively polymerized (Figure 1 A).

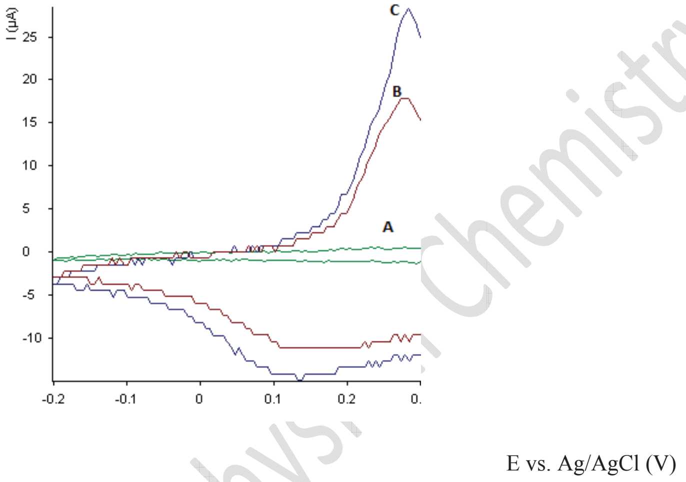

Figure 1: Potentiodynamic polymerisation of 0.01 M aniline in aqueous 1.0 M HCl (15th cycle). A) on bare GC, B) on PMAS modified GC using potentialsweep, C) on PMAS modified GC electrod using constant potential at 0.8 V.

Conclusion:

The method has the advantage of minimizing the amount of PMAS and monomer for deposition of an electroactive and conducting polyaniline film.

Reference:

[1] F. Masdarolomoor, et al., "Nanocomposites of Polyaniline/Poly(2-methoxyaniline-5-sulfonic acid)", Macromol. Rapid Commun. 27 (2006) 1995.

[2]F.Masdarolomoor, etal., “Electrochemical synthesis and characterization of polyaniline/poly(2-methoxyaniline-5-sulfonic acid) composites", Electrochimica Acta, 53,12 (2008) 4146

modification of electrode surface with sulphonated poly aniline and Electrosynthesis of polyaniline

S. Hajizadeh*, F. Masdarolomoor b M. Arab Chamgangalia
a Department of chemistry, Shahrood University of Technology, Shahrood, Iran
b 1 Department of chemistry, Shahrood University of Technology, Shahrood, Iran
Email: s.hajizade2011@gmail.com

Key words: Conducting polymer,polyaniline,dopant, sulphonated poly aniline.

Introduction:

The dopant incorporated into inherently conducting polymers during synthesis is known to have a substantial effect on the physical and chemical properties of the resultant material. There has been considerable interest in the incorporation of polyelectroyte as dopants for conducting polymers. Fully sulfonated polyaniline, poly(2-methoxyaniline-5-sulfonic acid) (PMAS), is a conductive and electroactive polyelectrolyte that has been recently used for synthesis of polyaniline with improved properties [1, 2].As an acidic polyelectrolyte PMAS provides counterions, an acidic microenviroment and a template for electrostatic alignments of aniline monomers for producing the conducting form of polyaniline. electro chemical polymerisation of aniline in the presence of PMAS has been recently reported to give a water insoluble film [2]. The electrodeposition of the polyaniline material is enhanced by the presence of the electrically conducting PMAS polyelectrolyte dopant, which functions as a molecular template providing supramolecular pre-ordering as well as simultaneously facilitating charge transport during electrodeposition. The present paper an alternate electrochemical synthesis route of PAn in modification of electrode surface by polyelecrtrolyte which PMAS acts as an electroactive and electrically conductive dopant polyelectrolyte.The electrode was modified with constant potential or potentiodynamic techniques in an aqueous solution of PMAS resulted in Adsorption of PMAS which was stable in polymerisation solution of aniline.

Materials and methods:

Aniline purchased from Aldrich was distilled and then stored at −4 ◦C (freezer) prior to use. PMAS with a molecular weight > and 10 kDa Hydrochloric acid (32%, w/v) was purchased from Merck. Potentiodynamic polymerisation was carried out on glassy carbon electrode modified of PMAS solution by applying a potential sweep between −0.2 and 1.1V (vs.Ag/AgCl). The monomer concentration can be lowered to less than 0.01 M.

Apparatus:

Cyclic voltammetry (CV) was carried out in a METROHOM MODEL746 CONSTANT three-electrode cell using a glassy carbon(GC) working electrode with a platinum auxiliary electrode and Ag/AgCl (3M kCl) reference electrode.

Result and discussion:

increase in current density was observed during subsequent scans, indicating the formation of conductive polyaniline composite (Figure 1). Post-growth cyclic voltamograms of the composite showed the switching between different oxidation states of electroactive polyaniline composite. The first anodic peak at 0.22 V is a sharp peak characteristic of highly conductive polyaniline. The second anodic peak at 0.52 V can be attributed to the electroactive PMAS.

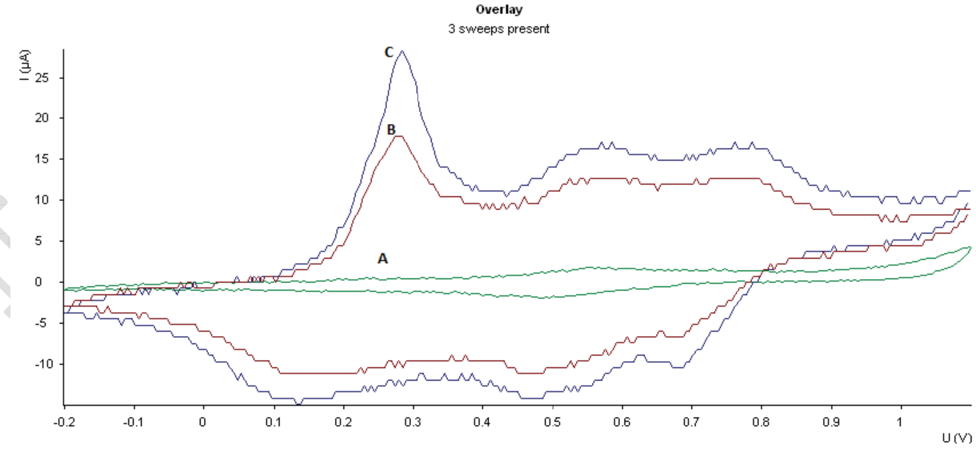

Figure 1: Potentiodynamic polymerisation of 0.01 M aniline in aqueous 1.0 M HCl (15th *cycle). A) on bare GC, B) on PMAS modified GC* with potentiodynamic*, C) on PMAS modified GC electrod* with constant potential =0.8v .

Conclusion:

The method has the advantage of minimizing the amount of PMAS and monomer for deposition of a desirable conducting polymer film.

Reference:

[1] F. Masdarolomoor, et al., "Nanocomposites of Polyaniline/Poly(2-methoxyaniline-5-sulfonic acid)", Macromol. Rapid Commun. 27 (2006) 1995.
[2] F. Masdarolomoor, etal., “Electrochemical synthesis and characterisation of polyaniline/poly (2-methoxyaniline- 5-sulfonic acid) composites", Electrochimica Acta, 53,12 (2008) 4146

Electrooxidation of ethanol using synthesized zeolite modified carbon paste electrode

M.Abrishamkar[a], K.Varnasri[b*]

[a] Department of chemistry, Science and Research Branch, Islamic Azad University, Khouzestan, Iran;
[b]Young Researchers Club, Khouzestan Science and Research Branch, Islamic Azad University, Ahvaz, Iran.
E-mail: Kobra.parto@yahoo.com

Keywords: Zeolite modified electrodes, ZSM-5, electrooxidation, ethanol, cyclic voltammetry

Introduction:

Direct alcohol fuel cells (DAFCs), identified as an important power source in applications ranging from portable electronic devices to fuel cell vehicles. Among various alcohols, ethanol is considered most attractive, because it has less toxicity, higher energy density and boiling point relative to other alcohols, and can be produced with great quantities by the fermentation of sugar containing raw materials [1]. Zeolite-modified electrodes (ZMEs) from a sub-category of the so-called chemically modified electrodes (CME). The use of zeolites as supported electrodes represents one of the solutions overcome the problem of catalytic oxidation of ethanol [2].

Materials and methods:

0.5 g of ZSM-5 zeolite was lightly ground and immersed to 10 ml 1 M $NiCl_2$ solution for 5 h. Then the solide was dried in oven at 373 k for 8 h. The 30% (W/W) zeolite loading Ni^{2+} was made by mixing the given quantity of zeolite loading Ni^{2+} in diethyl ether and hand mixing with 70 times its weight of graphite powder. The paste was inserted in the bottom of a glass tube modified electrode was immersed in 1 M Ni solution for 15 min. Then, this modified electrode (Ni/NiZSM-5/CPE) was washed to remove surface-adsorbed species.

Apparatus:

Electrochemical experiments were carried out using a potentiostat/galvanostat (sama 500-c Electrochemical Analysis system, sama, Iran). An $Hg|Hg_2Cl_2|KCl$ (4.6M) electrode as